

## X-Ray and NMR Measurements on Irradiated Polytetrafluoroethylene and Polychlorotrifluoroethylene

W. M. PEFFLEY, V. R. HONNOLD, and D. BINDER, *Ground Systems  
Group, Hughes Aircraft Company, Fullerton, California*

### Synopsis

The effects of  $^{60}\text{Co}$   $\gamma$ -radiation on polytetrafluoroethylene (PTFE) and polychlorotrifluoroethylene (PCTFE) have been studied for radiation doses up to 940 Mrad. The dependence of per cent crystallinity upon irradiation level has been determined from x-ray analysis. An initial increase in crystallinity in PTFE, attributable to chain scission in the amorphous phase of the material, was found, followed (above 300 Mrad) by a gradual decrease associated with a disordering of the crystallites. No initial increase was observed for annealed samples of PCTFE due to the large initial value of the per cent crystallinity. Above 200 Mrad the crystallinity was found to decrease with accumulated dose. Nuclear magnetic resonance measurements on PTFE have indicated a radiation-induced broadening of the amorphous component of the NMR line appearing to maximize above 700 Mrad. Similar measurements on PCTFE have shown a narrowing of the crystalline component of the NMR line and subsequent appearance of the amorphous component at approximately 200 Mrad. The data indicate that the radiation-induced behavior of PTFE and PCTFE is similar above 200 Mrad.

### Introduction

It is well known<sup>1-3</sup> that radiation has a marked effect upon the physical properties of polytetrafluoroethylene (PTFE). Density and infrared techniques<sup>4</sup> have shown the per cent crystallinity to increase from approximately 60 to 85% for a total irradiation dose of 100 Mrad. Nishioka et al.<sup>2</sup> have related the radiation-induced increase in the principal x-ray diffraction peak height at doses to 10 Mrad to an increase in crystallinity. Licht and Kline<sup>5</sup> have reported a decrease in specific volume with doses to 100-300 Mrad, followed by a subsequent increase with doses up to 890 Mrad. The effects of radiation upon polychlorotrifluoroethylene (PCTFE), which is similar in chemical structure to PTFE,<sup>6</sup> have been studied to a lesser extent. The radiation resistance of PCTFE, in terms of certain physical properties, has been compared to that of PTFE.<sup>3,7</sup>

Initial studies<sup>8,9</sup> of the effect of radiation on the nuclear magnetic resonance line of PTFE have indicated an increase in the width of the amorphous component. While a study of the effect of radiation on the magnetic resonance line does not, in general, lead to a determination of per cent

crystallinity,<sup>10</sup> but rather to an indication of freedom of motion, a study of the dependence of the line width on irradiation level does provide information compatible with that obtained by other techniques. It is the purpose of this paper to report and discuss the effects of <sup>60</sup>Co  $\gamma$ -radiation upon PTFE and PCTFE, subjected to doses up to 940 Mrad, as determined by x-ray diffraction analysis and a study of the nuclear magnetic resonance line.

### Experimental

The samples of PTFE (E. I. du Pont de Nemours and Company, Inc.) and PCTFE (Minnesota Mining and Manufacturing Company) were irradiated in air at an exposure rate of approximately 1.3 Mrad/hr. The thickness of the samples subjected to x-ray analysis was <sup>3</sup>/<sub>32</sub> in. The NMR samples were in the form of <sup>3</sup>/<sub>8</sub>-in. diameter rods.

The x-ray diffraction patterns of the polymers were obtained by using Ni-filtered copper radiation. The crystallinity was determined by comparing the area under the principal crystalline diffraction peak to the area of the broad amorphous background. In order to produce well defined diffraction peaks for PCTFE, the x-ray (and NMR) samples were heated, prior to irradiation, to 206°C. for 1 hr. and annealed. The per cent crystallinity was determined from the expression, developed by Ryland:<sup>11</sup>

$$\% \text{ Crystallinity} = 100/[1 + (A_a/KA_c)] \quad (1)$$

$A_a$  and  $A_c$  are the amorphous and crystalline areas, respectively. The factor  $K$  corrects the areas for polarization, diffraction angle, temperature effects, and density.  $K$  is equal to 1.8 for PTFE.<sup>11</sup> A value of the per cent crystallinity of annealed, unirradiated PCTFE, in agreement with results obtained by infrared and specific heat methods,<sup>12</sup> is obtained by setting  $K = 1.8$  in eq. (1).

The nuclear magnetic resonance line width measurements were made at a frequency of 10.6 Mc./sec. A transistorized marginal oscillator, which could be operated at a radiofrequency level low enough to reduce saturation effects greatly, was employed together with phase-sensitive detection. The modulating field was approximately 0.005 gauss at 500 cps. As determined by a narrow hydrogen resonance line, the line width due to field inhomogeneity was 0.50 gauss. All irradiations and measurements were made at room temperature.

### Results

Per cent crystallinity as a function of accumulated  $\gamma$ -ray dose is shown in Figure 1 for both materials. The value of the per cent crystallinity of PTFE was found to experience an initial rapid increase. At approximately 300 Mrad a maximum value of 88% was observed, followed by a gradual decrease. This crystallinity behavior is in good agreement with results obtained by Licht and Kline<sup>5</sup> from specific volume measurements. The

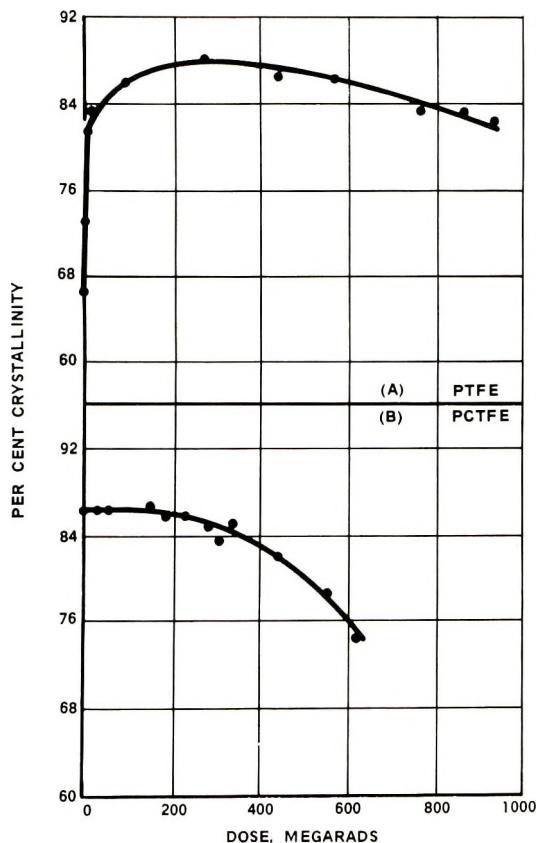


Fig. 1. Per cent crystallinity as a function of  $^{60}\text{Co}$   $\gamma$ -ray dose for PTFE and PCTFE.

per cent crystallinity of PCTFE has an initial value of 86%, remains constant to about 200 Mrad, and then decreases. Above 600 Mrad the surface of the material becomes tacky and is no longer entirely suitable for x-ray analysis. The maximum value of the crystallinity ratio in PTFE was found to be approximately equal to that of PCTFE.

Traces of the derivative of the NMR absorption curves at several irradiation levels are shown in Figures 2A and 2B. The  $^{19}\text{F}$  resonance measurements of PTFE did not reveal the broad component of the resonance line associated with the crystalline phase of the material, which is 10 gauss wide.<sup>13</sup> The absence of this component is due to room temperature saturation of the spin-lattice relaxation time in that phase.<sup>13</sup> The width of the resonance line of unirradiated PTFE, corrected for field inhomogeneity effects, was 0.85 gauss. The radiation-induced line broadening (Fig. 3A) appears to maximize above 700 Mrad at a line width of about 3.1 gauss. The line width of unirradiated PCTFE (Fig. 3B) was determined to be 6.7 gauss. An initial decrease in this line width was observed. Upon continued irradiation a second component appeared at approximately 200

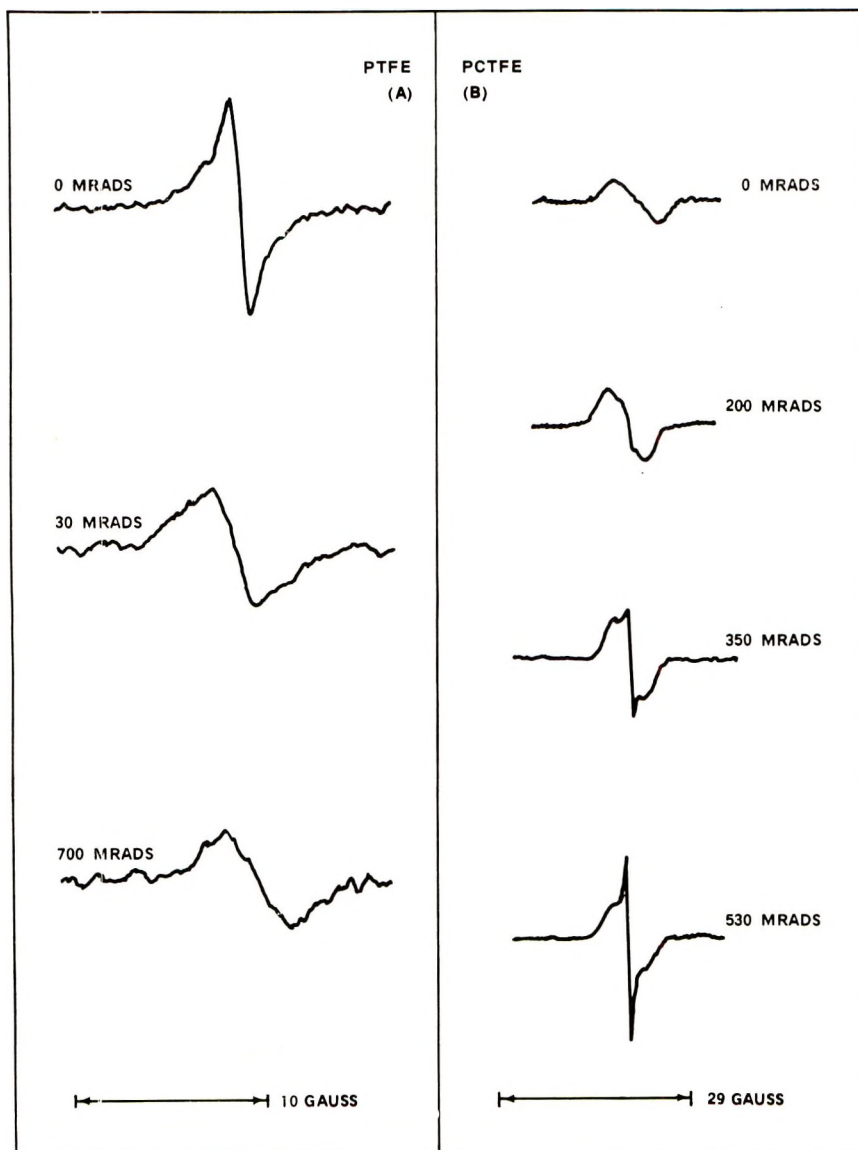


Fig. 2. Traces of derivatives of NMR absorption curves for PTFE and PCTFE at various radiation doses.

Mrad, as may be seen in Figure 2B. This narrow component is associated with the amorphous phase of PCTFE. Further irradiation resulted in an additional, slight decrease of the crystalline line width, accompanied by a marked growth of the NMR signal associated with the amorphous region, as seen in Figure 2B. It should be noted that the irradiation level at which the amorphous component of the PCTFE NMR line appears is that at which the per cent crystallinity begins to decrease.



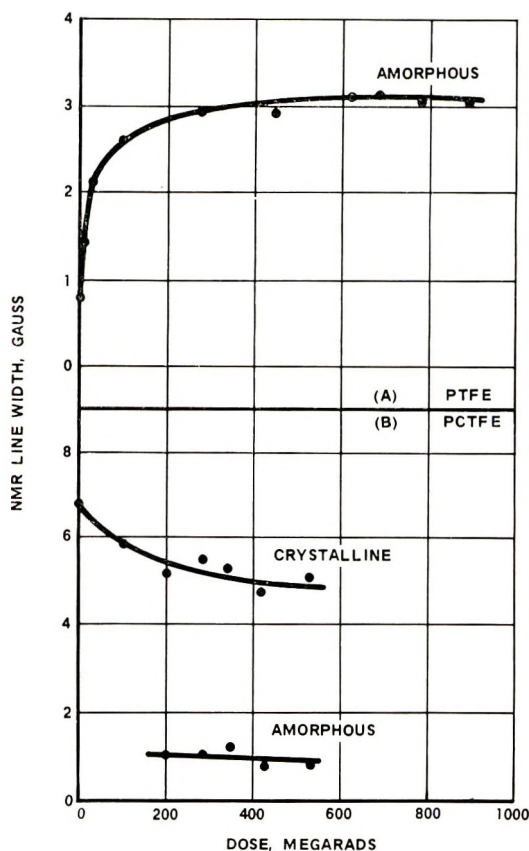


Fig. 3. NMR line width as a function of  $^{60}\text{Co}$   $\gamma$ -ray dose for PTFE and PCTFE.

### Discussion

Correlation in the results of an investigation of radiation effects on PTFE and PCTFE is expected due to the similarities in their chemical structure. Both materials undergo scission when exposed to radiation.<sup>3</sup> Therefore, the suggestion by Nishioka et al.<sup>2</sup> and others that the increase in crystallinity in PTFE is due to chain scission in the amorphous regions appears quite reasonable. This scissioning would relieve strains and permit further alignment of chains, producing a more ordered system and thus a higher crystallinity.

The present work does indeed show an initial radiation-induced increase in the crystallinity of PTFE. In the case of annealed PCTFE, the large initial value of per cent crystallinity minimizes the possibility of a further increase. The subsequent decrease observed for both materials can probably be considered to be due to gas evolution and eventual disordering processes in the crystalline phase. The similarities in response of these two polymers to continued irradiation is apparent above 200–300 Mrad. Both

experience a decrease in crystallinity ratio from a maximum value of approximately 87%.

Calculations based on a  $G$  (scission) value of 0.3 for PTFE<sup>5</sup> and an initial molecular weight of  $5 \times 10^6$  show that the dose at which one scission per chain occurs is 0.7 Mrad. At this irradiation the crystallinity has increased significantly. Similar calculations based on a  $G$  value of 0.67 for PCTFE<sup>3</sup> and a molecular weight of  $2 \times 10^5$  indicate that at 300 Mrad enough scissions have occurred to produce chains short enough to cause x-ray line broadening. This is also true for PTFE.

The observed broadening of the amorphous component of the NMR line in PTFE indicates an increase in the hindrance of molecular motion in the amorphous phase. This greater width, which implies that the chains have become more closely packed, is to be expected in view of the radiation-induced increase in order in that region as suggested by Nishioka. The subsequent saturation of the amorphous line width suggests that the eventual disordering processes take place predominantly in the crystalline phase of the material. The initial decrease in the width of the crystalline component of the NMR line of PCTFE indicates an increase in freedom of polymer motion in that phase. Above 200 Mrad the appearance and growth of the NMR signal due to chain motion in the amorphous region, accompanied by a further decrease in the crystalline line width, provides further evidence of the effect of the disordering processes, in agreement with the decrease in per cent crystallinity found from x-ray analysis.

### References

1. Charlesby, A., *Nucleonics*, **12**, No. 6, 18 (1954).
2. Nishioka, A., K. Matsumae, M. Watanabe, M. Tajima, and M. Owaki, *J. Appl. Polymer Sci.*, **2**, 114 (1959).
3. Florin, R. E., and L. A. Wall, *J. Res. Natl. Bur. Std.*, **65A**, 375 (1961).
4. Kline, D. E., and J. A. Sauer, *J. Polymer Sci. A*, **1**, 1621 (1964).
5. Licht, W. R., and D. E. Kline, *J. Polymer Sci. A*, **2**, 4673 (1964).
6. Geil, P. H., *Polymer Single Crystals*, Interscience, New York, 1963.
7. Bringer, R. P., paper presented at the National Symposium on the effects of space environment on materials, Society of Aerospace Materials and Process Engineers, St. Louis, May 7-9, 1962.
8. Kusumoto, H., *J. Phys. Soc. Japan*, **12**, 826 (1957).
9. Burget, J., and J. Sacha, *Czechoslov. J. Phys.*, **9**, 749 (1959).
10. Slichter, W. P., and D. W. McCall, *J. Polymer Sci.*, **25**, 230 (1957).
11. Ryland, A. L., *J. Chem. Educ.*, **35**, 80 (1958).
12. Matsuo, H., *J. Polymer Sci.*, **25**, 234 (1957).
13. Wilson, C. W., and G. E. Pake, *J. Chem. Phys.*, **27**, 115 (1957).

### Résumé

Les effets de l'irradiation  $\gamma$  provenant d'une source de  $\text{Co}^{60}$  sur du polytétrafluoroéthylène (PTFE) et du polychlorotrifluoroéthylène (PCTFE) ont été étudiés pour des doses de radiation jusqu'à 940 Mrads. La dépendance du pourcent de cristallinité en fonction du niveau d'irradiation a été déterminée par analyse aux rayons-X. Un accroissement initial de cristallinité dans PTFE, attribuable à une scission de chaîne dans la phase amorphe du matériau a été trouvé; cette augmentation est suivie d'une

diminution graduelle, (au-dessus de 300Mrads), associée avec un désordre des cristallites. Aucune augmentation initiale n'a été observée pour des échantillons recuit de PCTFE, par suite de la valeur initiale élevée du pourcentage de cristallinité. Au-dessus de 200 Mrads, la cristallinité décroissait avec une augmentation de dose. Des mesures de résonance nucléaire magnétiques sur PTFE ont indiqué un élargissement du composant amorphe induit par radiation dans la bande NMR qui apparaît être maximale au delà de 700 Mrads. Des mesures semblables sur le PCTFE se manifestent par une ligne NMR plus étroite du composant cristallin et apparition subéquente du composant amorphe à environ 200 Mrads. Les résultats indiquent que le comportement induit par radiation du PTFE et du PCTFE sont semblables au delà de 200 Mrads.

### Zusammenfassung

Der Einfluss der  $\text{Co}^{60}$ - $\gamma$ -Strahlung auf Polytetrafluoräthylen (PTFE) und Polychlorotrifluoräthylen (PCTFE) wurde mit Strahlungsdosen bis zu 940 Mrad untersucht. Die Abhängigkeit des kristallinen Anteils vom Strahlungsniveau wurde durch Röntgenanalyse bestimmt. Anfanglich trat bei PTFE eine Kristallinitätszunahme auf, welche auf Ketenspaltung in der amorphen Phase des Materials zurückzuführen ist; darauf folgte (oberhalb 300 Mrad) eine graduelle Abnahme, die mit einer Desorientierung der Kristallite verknüpft ist. Keine anfängliche Zunahme wurde, offenbar wegen des grossen Anfangswerts des kristallinen Anteils, bei getemperten PCTFE-Proben beobachtet. Oberhalb 200 Mrad nahm die Kristallinität mit Zunahme der Dosis ab. Kernmagnetische Resonanzmessungen an PTFE liessen eine strahlungsinduzierte Verbreiterung der amorphen Komponente der NMR-Linien erkennen, die oberhalb 700 Mrad einem Maximum zuzustreben schien. Ähnliche Messungen an PCTFE zeigten eine Verengung der kristallinen Komponente der NMR-Linien und ein darauffolgendes Auftreten der amorphen Komponente bei etwa 200 Mrad. Die Daten zeigen, dass das strahlungsinduzierte Verhalten von PTFE und PCTFE oberhalb 200 Mrad ähnlich ist.

Received August 13, 1965

Revised September 16, 1965

Prod. No. 4890A

## Polymerization of Methyl Acrylate in Aqueous Media

CAROLYN E. M. MORRIS, A. E. ALEXANDER, and A. G. PARTS,  
*Department of Physical Chemistry, The University of Sydney, Sydney,  
N.S.W., Australia*

### Synopsis

The polymerization of methyl acrylate in water and in dilute, aqueous, soap solutions, initiated by potassium peroxydisulfate, has been investigated, a dilatometric method being used to follow the conversion. It has been shown that small amounts of an anionic soap increase the rate of reaction while a cationic soap has the reverse effect. The change of molecular weight with conversion has also been examined as well as the effect of the exclusion of oxygen from the system.

### INTRODUCTION

In earlier studies the polymerization of vinyl acetate in aqueous solution was examined in the absence and presence of certain soaps (anionic, non-ionic, and cationic), with the use of potassium peroxydisulfate,  $K_2S_2O_8$ , as initiator.<sup>1,2</sup> The kinetic behavior and the particle sizes of the resulting latices were interpreted in terms of a theory for systems in which monomer and polymer are intersoluble. To test the applicability of the theory to other monomers, methyl acrylate appeared to be the obvious choice, being isomeric with vinyl acetate, having a similar water solubility, and being intersoluble with its polymer. The results presented here show that the broad features of the theory also hold for methyl acrylate, although certain differences are apparent. The influence of oxygen on the reaction has also been examined.

### EXPERIMENTAL

The materials used were purified in the following manner.

Methyl acrylate, obtained from the Rohm and Haas Company, was doubly distilled under nitrogen immediately before use under a pressure of about 160 mm. Hg, at which pressure the boiling point is 37°C. Monomer so purified gave very reproducible kinetic results.

Potassium peroxydisulfate was recrystallized twice and dried *in vacuo*. Water distilled from alkaline permanganate was used throughout. Benzene was distilled twice. The soaps were those used previously.<sup>2</sup> All the buffers and other chemicals were of analytical reagent quality.

A dilatometric technique was used to follow the kinetics of the polymerization reaction. By stopping a series of reactions at different stages

and weighing the formed polymer, the contraction was found to be 0.150 cc./g. This may be compared with that predicted from the bulk densities<sup>3</sup> of monomer and polymer, 0.250 cc./g. The discrepancy between these two figures can be explained by the different values of the partial specific volume of the monomer in bulk and in aqueous solution.

To determine the number of latex particles, runs were stopped at various conversions by pouring into iced water. A drop of this diluted latex, dried down on a nitrocellulose film, was examined in a Siemens Elmiskop Ia electron microscope. The average particle diameter was determined from measurements on the electron micrographs and thence the number of particles per cubic centimeter of the original system calculated.

Samples for molecular weight determinations were obtained as follows. A 300-cc. portion of reaction mixture was allowed to polymerize in a vessel swept out by nitrogen, (oxygen content less than 13 ppm). The nitrogen passed first through a tower of distilled water and then through a tower of pure monomer thermostatted at a temperature giving a monomer vapor pressure equal to that of the monomer in the aqueous solution. Change in the composition of the reaction mixture was thus avoided. At intervals the nitrogen pressure was increased and a sample of latex forced out into a large volume of cold, aqueous, hydroquinone-quinone solution. The extent of reaction was ascertained gravimetrically. Molecular weight determinations of the dried polymer were made by viscosity measurements of benzene solutions using an Ostwald viscometer at 30.0°C. Five concentrations in the range 0.03-0.20 g./dl. were used, and the limiting viscosity number was obtained by linear extrapolation. The constants given by Sen et al.<sup>4</sup> were used to calculate the molecular weight.

To examine the influence of oxygen on the reaction, studies were made under deaerated conditions. The deaeration process was as follows. The buffer-peroxydisulfate solution was placed in the dilatometer thermostatted at 40.0°C. Monomer was dissolved in boiled-out distilled water and the solution (500 cc.) placed in a 500 cc., three-necked flask which could be heated with a hot-plate. Nitrogen (oxygen content less than 13 ppm) was then bubbled through the solution at the rate of approximately 7 ml./min., passing first through a tower of distilled water and then through a tower of pure monomer in the manner described above. At the same time, nitrogen was swept through the dilatometer, passing first through a tower of distilled water at 40.0°C. All connecting tubes could also be swept out. For effective deaeration, it was necessary to pass the nitrogen for about 7 hr. After this time elapsed, the aqueous monomer solution was heated to about 45°C. by the hotplate, the nitrogen pressure increased and the solution forced over into the dilatometer. This was filled and the reaction followed in the usual way.

## RESULTS

All the experiments were performed at 40.0°C. with an initial monomer concentration of 0.36 molal. Two initiator concentrations were used, 6.0



$mM$  and  $1.0 mM$ . Reactions were maintained at pH 4.05 by an acetate buffer of concentration  $0.02M$ . Where no attempt was made to eliminate oxygen from the system, the runs were preceded by an induction period.

The commencement of polymerization was readily observed: obvious turbidity coincided with a fall in the capillary meniscus. The system was not stirred during polymerization because of increased coagulation of the latex. It was shown however, that the rate of reaction was unaffected by stirring. The shape of the dilatometer ensured an adequate rate of heat dissipation.

All experiments were performed at least twice, reproducible results being obtained in all cases.

### Behavior in the Absence of Added Soaps

Where no attempt was made to exclude air from the system, reactions were preceded by a long and quite reproducible induction period, the times being 230 and 120 min. with initiator concentrations of  $1.0$  and  $6.0 mM$ , respectively. Figure 1 presents the kinetic data as the per cent conversion versus time.

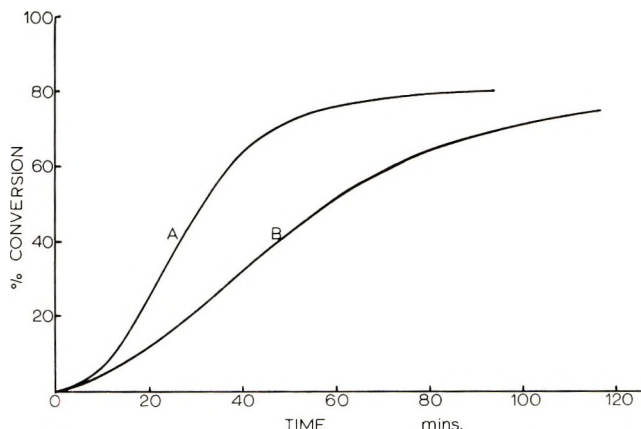


Fig. 1. Conversion vs. time curves with different initiator concentrations: (A)  $6.0 mM$  potassium peroxydisulfate; (B)  $1.0 mM$   $K_2S_2O_8$ . Methyl acrylate  $0.36$  molal.

The latex formed under these conditions was not very stable and tended to aggregate. Stirring the system increased the degree of aggregation but had no discernible effect on the rate of reaction.

Determination of the number of latex particles at various stages was rendered difficult by the instability of the latex. The results obtained from electron microscopy are shown in Table I.

The molecular weight of the formed polymer at various conversions is given in Figure 2 and Table II. At higher conversions, the polymer was visibly aggregated, and a random sample could no longer be obtained by the method used.

TABLE I  
Number of Particles per Unit Volume at Different Conversions<sup>a</sup>

Conversion, %	Average radius, cm. $\times 10^5$	No. of particles/cc. $\times 10^{-12}$
12.0	0.57	3.9
21.2	0.87	1.9
44.7	1.48	0.96
84.5	1.87	0.78

<sup>a</sup> Initial monomer concentration 0.36 molal, initiator concentration 6.0 mM.

TABLE II  
Integral Average Molecular Weight at Different Conversions<sup>a</sup>

Conversion, %	Limiting viscosity no., cm. <sup>3</sup> /g. $\times 10^{-2}$	Molecular weight $\times 10^{-6}$
5.2	5.23	2.84
9.7	6.27	3.69
17.0	5.46	2.97
25.6	4.66	2.43
36.7	3.50	1.67
45.9	2.91	1.26

<sup>a</sup> Initial monomer concentration 0.36 molal, initiator concentration 6.0 mM.

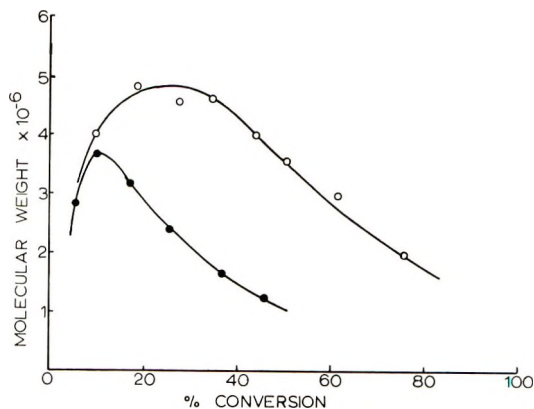


Fig. 2. Integral average molecular weight vs. conversion: (●) 6.0 mM  $K_2S_2O_8$ , no added soap; (○) 1.0 mM  $K_2S_2O_8$  and 0.10 mM sodium cetyl sulfate. Methyl acrylate 0.36 molal.

### Behavior in the Presence of Added Soaps

The kinetic data obtained in the presence of various concentrations of two synthetic soaps, sodium cetyl sulfate and cetyltrimethylammonium bromide, are shown in Figure 3, the curve for no added soap being included for comparison. The critical micellar concentration of sodium cetyl sulfate in water<sup>5</sup> is 0.4 mM and of cetyltrimethylammonium bromide<sup>6</sup> is 0.8 mM.

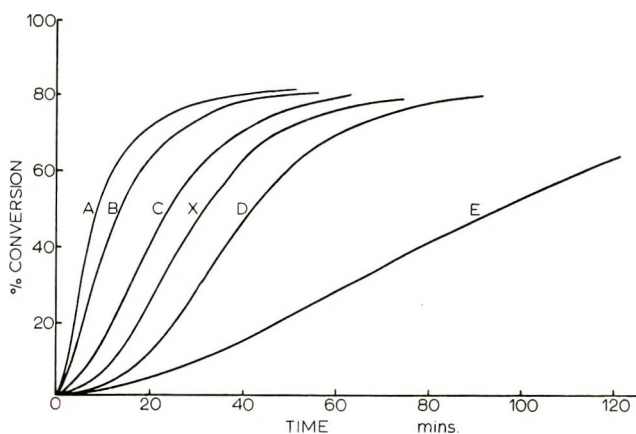


Fig. 3. Effect of surface-active agents on conversion-time curves: (A) 1.0 *mM* sodium cetyl sulfate (SCS); (B) 0.10 *mM* SCS; (C) 0.01 *mM* SCS; (D) 0.01 *mM* cetyltrimethylammonium bromide (CTAB); (E) 0.10 *mM* CTAB; (X) no added soap. Methyl acrylate 0.36 molal.  $K_2S_2O_8$  6.0 *mM*.

With the anionic soap, the rate of polymerization increased with increasing soap concentration, as did the stability of the resulting latex. It was obvious from the increasing blue opalescence of the latex that the size of the latex particles decreased with increasing soap concentration, although no precise measurements could be made.

With the cationic soap the reverse effects were found, namely, decreased rate of reaction and stability of the latex with increasing soap concentration.

The change in molecular weight with per cent conversion was studied for the system sodium cetyl sulfate 0.10 *mM*, initiator concentration, 1.0 *mM*, by the same method as before. The results are shown in Figure 2 and Table III.

TABLE III  
Integral Average Molecular Weight in the Presence of an Anionic Soap at Different Conversions<sup>a</sup>

Conversion, %	Limiting viscosity no., cm. <sup>3</sup> /g. $\times 10^{-2}$	Molecular weight $\times 10^{-6}$
9.8	6.70	4.04
18.4	7.58	4.81
27.3	7.30	4.55
34.7	7.38	4.62
43.7	6.75	4.07
50.2	6.13	3.56
61.4	5.36	2.94
75.5	3.92	1.91

<sup>a</sup> Initial monomer concentration 0.36 molal, sodium cetyl sulfate concentration 0.10 *mM*, initiator concentration 1.0 *mM*.

### Effect of Oxygen

The experiments were performed with an initiator concentration of 6.0 *mM* buffered to pH 4.05. The effect of the deaeration process described above was to reduce the induction period from 120 to 7 min. Hence, it appears that at least 95% of the induction period can be ascribed to the influence of oxygen. It is possible that a more vigorous deaeration process would have shortened the induction period still further.

Once the polymerization began, its rate was little different from that in the presence of oxygen. However, the latex formed was far less stable towards agitation and very readily coagulated. This readiness to aggregate rendered a study of particle number by electron microscopy effectively impossible, although it was obvious that the particles were considerably larger than those formed in the presence of oxygen.

### DISCUSSION

The aqueous polymerization of methyl acrylate in the absence and presence of soap appears to resemble, in its broad features, that previously found for vinyl acetate.<sup>1,2</sup> In the latter system, the kinetic behavior was accounted for by assuming the interior of the latex particles to be the locus of polymerization, the rate being given by the usual expression.<sup>7</sup>

$$-d[M]/dt = k_p C_M N \bar{n}$$

where  $[M]$  is the monomer concentration,  $k_p$  the propagation constant,  $C_M$  the concentration of monomer in the latex particles,  $N$  the number of latex particles per unit volume, and  $\bar{n}$  the average number of radicals per particle.

The following processes are thought to occur. Initially, the system consists of a single phase. Radicals formed by the decomposition of the initiator react with dissolved monomer molecules and thus initiate the chain process. The coiled chain thus formed, or several such chains intertwined, together with its absorbed monomer constitute a latex particle, a large number of these particles being formed in a very short time. Since the monomer concentration in the aqueous phase is rapidly depleted by polymerization and by absorption into the latex particles, the contribution of the aqueous phase reaction to the overall polymerization rate quickly becomes small. The interior of the latex particles then becomes the principal site of reaction.

For small latex particles, where  $\bar{n} = 1/2$ , the rate of reaction is proportional to the number of particles. However, for large particles the rate of polymerization becomes independent of the number of particles and depends only on the total polymer volume.<sup>7,8</sup> It is thought that the very early stages of the polymerization of methyl acrylate in aqueous systems in the absence of surface-active agents corresponds to the first case (i.e.,  $\bar{n} = 1/2$ ) but that, as the particles grow, the possibility of coexistence of radicals within a particle increases (i.e.,  $\bar{n} > 1/2$ ). Thus the rate of reac-

tion increases, reaching a maximum rate, in the case illustrated in Figure 1 at about 30% conversion or after about 20 min. Thereafter the rate of polymerization decreases because of the diminishing monomer concentration. These conclusions are supported by observations on the effect of stirring the reaction mixture; stirring obviously considerably increased the degree of aggregation of the polymer but produced no discernible influence on the overall rate of polymerization, indicating that the rate was dependent not so much on the number of latex particles but rather on the total polymer volume.

The kinetic behavior in the presence of soaps is essentially the same as that previously reported for vinyl acetate. The mechanism by which soaps affect the rate of reaction is considered to be the following; as the polymer chains grow or aggregate to form a latex particle, soap is adsorbed onto the particle surface. Electrophoretic measurements show that the latex formed in the absence of soap carries a negative charge. Adsorption of an anionic soap leads to an increase in charge thus stabilizing the particles at a smaller size. In this way a larger number of smaller particles is formed than in the case where no soap is present. An increase in charge also leads to a diminution in the amount of aggregation and hence enhanced latex stability. On the other hand, for a cationic soap adsorption onto the particle surface reduces the charge and thus aids aggregation. Hence, in the presence of an anionic soap, for example, the production of a latex of smaller particle size than when no soap is present, brings the system into closer agreement with the first case mentioned above (i.e., rate of reaction proportional to particle number) and thus gives an increased rate of polymerization compared with the rate in the absence of such soap. From Figure 3 it is seen that the rate of polymerization in the various systems is different from the very beginning of the reaction. Evidently, the presence of the anionic soap causes a change in the number of radicals present at the time when the inhibiting effect of the oxygen ceases. Thus, the effect of low concentrations of soaps on the rate of polymerization is closely associated with the charge they carry.

The polymerization of vinyl acetate is characterized by the linearity of the plot of  $(\text{conversion})^{1/2}$  versus time over a wide range of experimental conditions and by the stability of the polymer latex. The polymerization of methyl acrylate differs from that of vinyl acetate chiefly in that the  $(\text{conversion})^{1/2}$  versus time curve is not linear and the poly(methyl acrylate) latex formed in the absence of soaps is much less stable. Evidently that combination of factors which resulted in the linearity of the  $(\text{conversion})^{1/2}$  versus time plots in the vinyl acetate case is not achieved with methyl acrylate.

Particle sizes in the two systems were very similar, as were the electrophoretic mobilities, indicating little difference in zeta potentials. However, recent results obtained in this laboratory indicate that the equilibrium uptake of methyl acrylate by poly(methyl acrylate) in water is greater than the corresponding uptake of vinyl acetate by its polymer in water. Hence,



it might be expected that the latex particles in the former case would be softer than those in the latter system thus giving more ready fusion of particles on collision. This would also lead to a decrease in the number of latex particles with time (see Table I).

As discussed above, polymerization begins under conditions where the growing chain has but few monomer molecules associated with it. In this very early stage of reaction, the concentration of monomer at the reaction site approximates to the concentration of monomer in the aqueous phase. At a later stage, the monomer concentration available is its concentration in the polymer, which is always greater than the concentration in the aqueous phase. Hence, the polymer formed in the very early stages of the reaction would be of lower molecular weight than that formed at higher conversions, as found experimentally.

Another consideration which leads to a similar conclusion concerning the molecular weight in the initial stages of reaction concerns the particle size. The concentration of monomer in the polymer is governed by the partition of the monomer between the aqueous and polymer phases. This, in turn, is dependent to some extent on the degree of subdivision of the polymer, since, because of interfacial energy considerations, small latex particles tend to take up less monomer than large ones.<sup>9</sup> This effect has the biggest influence in the initial stages of a polymerization reaction when the particles are extremely small. As the particles grow by reaction and aggregation, the impedance to monomer entry into particles is removed. Thus, the polymer produced in the very small particles is formed under less favorable conditions as regards the supply of monomer.

A decrease in the integral average molecular weight with increasing conversion has been found with other initially homogeneous, aqueous systems in this laboratory, namely acrylonitrile initiated by iron(III)/hydrogen peroxide<sup>10</sup> and also vinyl acetate initiated with potassium peroxydisulfate.<sup>11</sup> Since there is no separate monomer phase, or drops, in these systems to act as reservoirs, the total monomer concentration must decrease continuously from the commencement of polymerization. At higher conversions, where the overall rate of reaction is lower, chain transfer may become increasingly important, and there is also the possibility of degradation of the high molecular weight product formed in the earlier stages of the reaction. The relative importance of these effects is difficult to determine without more extensive experimental data, but further work is being carried out.

### Effect of Oxygen

It seems to be established that the presence of oxygen in a polymerizing system leads to the formation of peroxidic compounds.<sup>12,13</sup> In some cases the compound has been shown to be a 1:1 copolymer of oxygen and monomer of molecular weight about 1800.<sup>14,15</sup> A compound of this type has been detected in the bulk polymerization of methyl acrylate.<sup>12</sup> That such

compounds could form under the experimental conditions prevailing in this work is shown by the following calculations. The maximum amount of oxygen which could be present is given by the saturation solubility of oxygen at 0.2 atm. pressure in water at 40.0°C., namely  $1.1 \times 10^{17}$  molecules/ml. of water. Assuming that a 1:1 compound is formed, the same number of monomer molecules would be used. Since the initial monomer concentration is 0.36 molal, i.e.,  $1.8 \times 10^{20}$  molecules/ml. of water, the amount of monomer used during the induction period is less than 0.1% of the initial monomer concentration, an effect below the sensitivity of the apparatus.

In view of the enhanced stability of the latex formed in the presence of oxygen over that formed in its absence, it is proposed that the oxygen-monomer compound possesses some surface activity. Adsorption of this compound onto the particle surface evidently increases the stability of the particle in the manner described above. The feasibility of this proposal is illustrated by a simple calculation. At 80% conversion, the average radius of the particles formed in the presence of oxygen as shown in the electron microscope is  $1.85 \times 10^{-5}$  cm. Assuming the monomer:polymer ratio in the living particle to be 1:4, the radius of such a particle would be  $2.0 \times 10^{-5}$  cm. Since there are  $7 \times 10^{11}$  particles/ml. of emulsion at this conversion, the total surface area per milliliter of emulsion is  $3.5 \times 10^{19}$  A.<sup>2</sup>. For a molecular weight of 1800 (that is, about 15 monomer-oxygen repeating units) and at  $10^{17}$  oxygen molecules/ml. initially, the number of these peroxidic chains is thus about  $7 \times 10^{15}$ /ml. of emulsion. Hence, if all these are adsorbed on the particle surface, the area occupied by each molecule is approximately 5000 A.<sup>2</sup>. This adsorption would lead to an increase in the hydrophilic nature of the particle surface. Alternatively, the oxygen compound may be actually bound onto the polymer particle surface. If after several monomer-oxygen linkages were formed, normal polymerization then proceeded, a polymer chain with a polar section at one end would be produced. This could be expected to remain at the particle-water interface and hence to increase the hydrophilic nature of the surface. The effect evidently produces an insufficient change in the number of particles formed for an observable change in the rate of polymerization.

The oxygen-monomer compound, being of a peroxidic nature, may not be very stable, and hence the possibility arises of decomposition products having an effect on the polymerization reaction and on the storage stability. However, in view of the fact that the rate of reaction in a deaerated system was found to be effectively the same as in systems containing oxygen, the effect upon the former can only be small.

An attempt has been made to analyze the kinetics of the reactions taking place during the induction period, resulting in the formation of the peroxidic compound. By using effectively the same kinetic scheme as that of Kice<sup>16</sup> and of Schulz and Henrici,<sup>15</sup> and also the Bodenstein stationary-state approximation for radicals present in small concentration, the following results are obtained. The rate of disappearance of oxygen is essentially constant over a wide oxygen concentration range, say  $10^{17}$ - $10^{12}$

molecules/ml. The rate of consumption of monomer during this period is very small but constant, being undetectable by volume change with the present apparatus. In a very short time interval, of the order of a fraction of a second, the remaining oxygen (ca.  $10^{12}$  molecules/ml.) is removed, and the consumption of monomer and formation of polymer then proceeds at a measurable rate. There is thus a sharp demarcation between the inhibited reaction and the true polymerization. There is no intermediate stage of a partly inhibited or retarded reaction. Substitution of the known values<sup>3</sup> of the rate constants for bulk propagation and termination and assuming reasonable values for the other rate constants involved leads to an induction period in agreement with that determined experimentally. The same values of the rate constants also give an initial rate of polymerization in agreement with that found experimentally.

There is one important point, however, which has to be considered, namely, the rate of decomposition of peroxydisulfate ions in the presence of monomer and emulsifying agents. Experiments carried out in this laboratory on the influence of the various organic substances present during polymerization indicate that the rate of decomposition of peroxydisulfate may very well be increased compared with that in the pure solvent.<sup>17</sup> These experiments were performed with initial peroxydisulfate concentrations of approximately  $0.1M$ , and the disappearance of peroxydisulfate followed by volumetric analysis. Other work in this field, using radio-tracer techniques and  $S^{35}$ -labeled peroxydisulfate in much smaller concentrations, approximately that used in polymerization, has shown no increase in the rate of decomposition of peroxydisulfate.<sup>18</sup> Further investigations of this matter are in progress.

### References

1. Napper, D. H., and A. G. Parts, *J. Polymer Sci.*, **61**, 113 (1962).
2. Napper, D. H., and A. E. Alexander, *J. Polymer Sci.*, **61**, 127 (1962).
3. Matheson, M. S., E. E. Auer, E. B. Bevilacqua, and E. J. Hart, *J. Am. Chem. Soc.*, **73**, 5395 (1951).
4. Sen, J. N., S. R. Chatterjee, and S. R. Palit, *J. Sci. Ind. Res. (India)*, **11B**, 90 (1952).
5. Corrin, M. L., H. B. Klevens, and W. D. Harkins, *J. Chem. Phys.*, **14**, 480 (1946).
6. Scott, A. B., and H. V. Tartar, *J. Am. Chem. Soc.*, **65**, 692 (1943).
7. Smith, W. V., and R. H. Ewart, *J. Chem. Phys.*, **16**, 592 (1948).
8. Stockmayer, W. H., *J. Polymer Sci.*, **24**, 314 (1957).
9. Morton, M., S. Kaizerman, and M. W. Altier, *J. Colloid Sci.*, **9**, 300 (1954).
10. Moore, D. E., and A. G. Parts, *Makromol. Chem.*, **37**, 108 (1960).
11. Napper, D. H., M.Sc. Thesis, University of Sydney, 1960.
12. Barnes, C. E., R. M. Eloffson, and G. D. Jones, *J. Am. Chem. Soc.*, **72**, 210 (1950).
13. Bovey, F. A., and I. M. Kolthoff, *J. Am. Chem. Soc.*, **69**, 2143 (1947).
14. Strause, S. F., and E. Dyer, *J. Am. Chem. Soc.*, **78**, 136 (1956).
15. Schulz, G. V., and G. Henrici, *Makromol. Chem.*, **18-19**, 437 (1956).
16. Kice, J. L., *J. Am. Chem. Soc.*, **76**, 6274 (1954).
17. Kolthoff, I. M., and I. K. Miller, *J. Am. Chem. Soc.*, **73**, 3055 (1951).
18. Hawke, J. C., Department of Pharmacy, University of Sydney, private communication.

### Résumé

On a étudié la polymérisation de l'acrylate de méthyle dans l'eau et dans des solutions diluées aqueuses de savon, initiée par du peroxydisulfate de potassium; une méthode dilatométrique a été utilisée pour suivre le degré de conversion. On a montré que de faibles quantités de savons anioniques augmentent la vitesse de réaction, tandis qu'un savon cationique a l'effet inverse. Le changement du poids moléculaire avec le degré de conversion a également été examiné, de même que l'effet d'exclusion de l'oxygène du système.

### Zusammenfassung

Die durch Kaliumperoxydisulfat angeregte Polymerisation von Methylacrylat in Wasser und in verdünnten wässrigen Seifenlösungen wurde mittels einer dilatometrischen Methode zur Verfolgung des Umsatzes untersucht. Kleine Mengen einer anionischen Seife erhöhen die Reaktionsgeschwindigkeit während eine kationische Seife den umgekehrten Effekt hat. Weiter wurde die Abhängigkeit des Molekulargewichts vom Umsatz sowie der Einfluss des Ausschlusses von Sauerstoff aus dem System untersucht.

Received April 26, 1965

Revised September 17, 1965

Prod. No. 4892A



## Stability of Styrene-Maleamic Acid Interpolymers

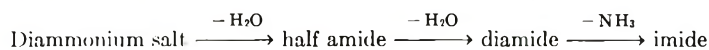
L. M. MINSK and K. R. DUNHAM, *Research Laboratories,  
Eastman Kodak Company, Rochester, New York*

### Synopsis

The response to heat and water of copoly(styrene-maleamic acid, ammonium salt), prepared by treatment with ammonia of the anhydride polymer in toluene suspension, is described. This polymer except for the ammonia bound by salt formation, is stable to heat within the range studied, i.e., to 100°C. The behavior of water solution is determined by the ammonia concentration. Above pH 9, the bound nitrogen remains as amide. If the pH is low, i.e., about 5, as occurs when a dried sample is dissolved in water, then rapid imidization occurs with concurrent hydrolysis. In the early stages of this conversion, imidization occurs mainly through loss of ammonia. This requires that two amide groups be adjacent. Classical imidization by loss of water also occurs, indicating that the normal-amic acid structure is also present.

In the course of an investigation of the interpolymer of styrene and maleic anhydride and its reactions, the ammonium salt of the styrene-maleamic interpolymer was prepared. In this paper are described chemical changes that occur in the polymer, dry at 43°C. and at 103°C., and in water solution.

Heiligmann and McSweeney<sup>1</sup> studied, by weight loss, the response of films of the ammonium salt of the styrene-maleic acid interpolymer to heating. The ammonium salt was prepared by dissolving the anhydride polymer in water containing a 10% excess of ammonia over that required to neutralize the carboxyl groups. They concluded that at temperatures below 93°C., the diammonium salt was stable. Results at temperatures between 90 and 120°C. indicated a transition through the half-amide structure, and at temperatures above 120°C., a diamide-imide structure. They postulated a mechanism involving the following steps:



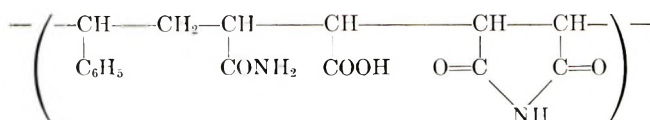
## EXPERIMENTAL

### General

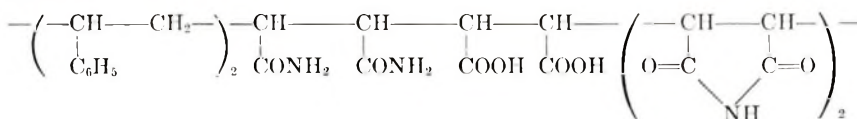
The unequivocal analysis of these -amic acids had not been accomplished hitherto. It is essential that analyses be made on the polymer as it is obtained from the reaction, i.e., as the ammonium salt, in order to avoid any possibility of a structural change which might occur during the process for the removal of the ammonium ion. Conditions for handling the prod-



uct, such as clean-up and drying, were as mild as possible. The polymer contains styrene, amide and/or imide, and carboxyl groups, both free and combined with ammonia. Total nitrogen may be determined by any of the classical methods. If the ammonium nitrogen can be determined separately, then the nitrogen involved in amide and/or imide formation ("bound" nitrogen) can be obtained by difference. For the study of composition, the usual structure for such a polymer being assumed, carboxyl may be calculated as maleic acid, ammonium carboxyl as ammonium maleate, imide nitrogen as maleimide, and amide nitrogen as maleic diamide, as shown in the formula. It is imperative that the methods of analysis be so designed that structural changes do not occur during the determination.



analytically equivalent to



In the determination of ammonium nitrogen, an aqueous system appeared out of the question because of the possible instability of this polymer in water. A method was therefore sought which did not involve water. The Palit<sup>2</sup> procedure involving the titration of a sodium salt of a carboxy acid in ethylene glycol-alcohol solution by perchloric acid in the same solvent appeared to give values which were reasonable for the ammonium salt of the maleamic acid interpolymer. The end point, obtained by using a pH meter to observe the deflection point, was sharp, as seen in Figure 1.

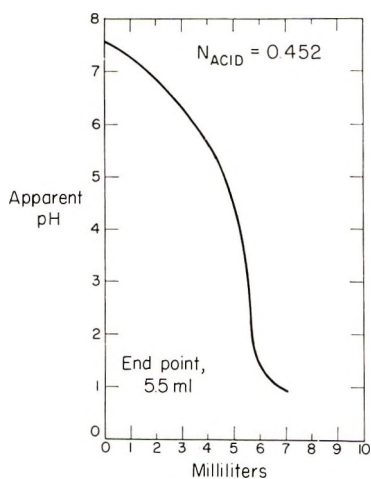


Fig. 1. Titration for ammonium carboxyl.

In the carboxyl determination, the considerations against the use of water are still valid. The method developed for carboxyl was a modification of the sodium bromide-sodium hydroxide method for determination of carboxyl, with the carboxyl-bearing compound as a second phase in a nonsolvent.<sup>3</sup> In this case, the titration was made in an essentially alcohol system. The values obtained could be duplicated and appeared to be reasonable and to comprise both free and ammonium carboxyl. The free carboxyl may be obtained by subtracting from the total the ammonium carboxyl procured by the Palit titration.

The bound nitrogen may be either amide or imide, or both. As yet, no method has been found in the literature or devised in these laboratories which will determine both, or one in the presence of the other. They may be calculated, however, if the ratio of styrene to maleic anhydride in the intermediate is known and if it is assumed that the ratio remains constant through subsequent reactions of the intermediate.

The intermediate interpolymer of styrene and maleic anhydride was made in toluene. Attempts to determine the combined maleic anhydride in the interpolymer by the classical procedures gave unreliable results. Hydrolysis, by water, followed by titration with base, or saponification by base, followed by titration of excess base with acid, was not satisfactory since the end point was uncertain. The addition of pyridine<sup>4</sup> did not improve the end point. The aniline treatment in the usual method for determining anhydride appeared to involve free carboxyl as well as anhydride. The Smith and Bryant procedure<sup>5</sup> yielded a value of 1.08:1 for the styrene-maleic anhydride ratio. Garrett and Guile<sup>6</sup> report a ratio of 1.12:1 for a polymer made from a 1:1 mixture of the monomers. A single titration of this type can only give an approximate ratio, since it is assumed that no maleic acid is present. Actually, it is extremely difficult to prepare the interpolymer absolutely free of maleic acid. For a correct analysis, two titrations, one for total available carboxyl and one for carboxyl involved in anhydride formation, are necessary.

The effect of storage on the dry polymer was studied at 43°C. and accelerated by heating at 100°C. in open containers. The effect of storage in solution was studied at room temperature and accelerated by heating in closed flasks in a constant-temperature water bath at 50°C.

#### **Preparation of the Ammonium Salt of Poly(styrene-Maleic Acid)**

The polymer used in this investigation was of low viscosity and was prepared as follows:

A mixture consisting of 114 g. of distilled styrene, 98 g. of maleic anhydride (Eastman Grade), 4 g. of benzoyl peroxide and 3000 ml. of sulfur-free dry toluene was heated on a steam pot in a 5-liter flask equipped with a reflux condenser, a calcium chloride tube, and a motor-driven stirrer which, while agitating the mixture, did not beat air into the solution. The reaction was heated for 2 hr. after the solution had become cloudy. After

cooling, the suspension was collected on a Büchner funnel by suction and washed on the funnel with dry, sulfur-free toluene.

The polymer was slurried twice with two 1-liter portions of fresh toluene and filtered after each one. A small portion was removed and dried for measuring the viscosity. The main portion was returned to the reaction vessel, toluene was added to a total volume of approximately 3100 ml., and dry ammonia gas was bubbled, with stirring, into the reaction mixture. The temperature rose spontaneously to 42–43°C. and then dropped. When the temperature of the mixture returned to 30°C., the polymer was collected on a Büchner funnel. The precipitate was slurried twice with 1-liter portions of toluene, filtered after each one, and dried at 40°C. for 72 hr. in an air oven. The yield was 208 g. The inherent viscosity in acetone was 0.21 at a concentration of 0.25 g./100 ml. of solution at 25°C.

### Determination of Ammonium Carboxyl

A 1-g. portion of sample of the -amic acid polymer was dispersed in 100 ml. of ethylene glycol (Eastman Grade). Usually, solution of the polymer occurred easily at room temperature, although some samples, particularly those heated for long periods at 100°C., required warming on a steam-bath. To this was added 20 ml. of 99% isopropyl alcohol (Eastman Kodak Company), and the solution, constantly stirred, was titrated with standard (0.4*N*) perchloric acid, in 5:1 by volume ethylene glycol-isopropyl alcohol. The apparent pH of the solution was followed with a Beckman Model G pH meter and glass electrodes. The reading on the meter was taken 1 min. after each addition of acid when the pH appeared to have stabilized. A typical titration curve is shown in Figure 1. The correction for the blank was negligible. The titer was calculated as ammonium maleate and as ammonium nitrogen.

### Total Nitrogen

Total nitrogen content was determined by the micro-Dumas procedure.

### Determination of Total Carboxyl

A 1-g. sample of the -amic acid polymer was suspended in 133 ml. of absolute ethyl alcohol, and 2 g. of sodium bromide was added, followed by 10 ml. of distilled water. After 2 min. stirring, the pH was read and the solution titrated, with the pH meter, with 0.25*N* aqueous potassium hydroxide. The solution was stirred for 2 min. after each alkali addition before the apparent pH reading was taken. The correction for the blank was negligible. A typical titration curve is given in Figure 2. The titer, less that found for ammonium maleate, was calculated as maleic acid.

### Effect of Aqueous Solution

**Solution in Water.** A 100-g. portion of -amic acid polymer was dispersed in 850 ml. of distilled water. When solution was complete, the

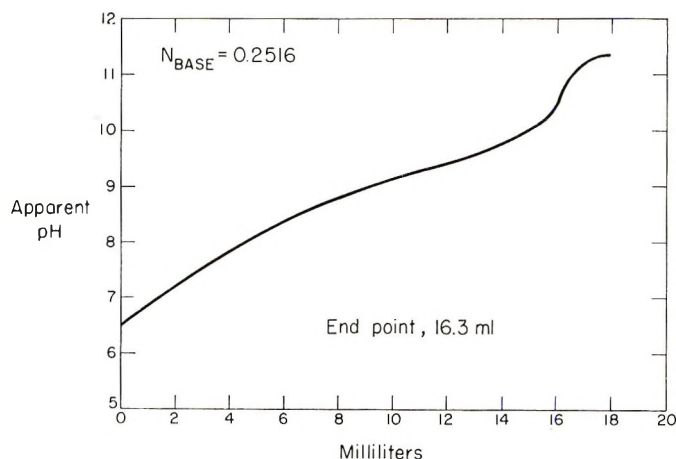


Fig. 2. Titration for total carboxyl.

total weight was adjusted to 1000 g., and the solution was stored at room temperature to allow the foam to settle. About 6 hr. was required. Then, 75-g. portions of the solution were placed in 250-ml. glass-stoppered Erlenmeyer flasks, which were immersed in a 50°C. water bath. At intervals, the samples of solution in the bath were removed, the pH was read, and the solid polymers were isolated by precipitation in 1,4-dioxane. The precipitates were collected, washed with fresh dioxane, and dried in an air oven at 40°C. No attempt was made to prevent the volatilization of the ammonium nitrogen during drying. The results of the analyses of these samples are given in Table I, together with the ratios of styrene to maleic anhydride that were found by calculating all the bound nitrogen as amide and as imide. In view of what is known about the intermediate, these calculated ratios appear to be too high when the bound nitrogen is calculated as amide and to approach a reasonable value of 1.17 when the bound nitrogen is calculated as imide. This was very close to that found by direct determination of the anhydride in the intermediate by single titration procedures. The ratio of 1.17 to 1 was therefore used to calculate the amide and imide content according to the following simultaneous equations:

$$\frac{(100 - M - A - X - Y)/104}{(M/116) + (A/150) + (X/114) + (Y/97)} = 1.17$$

$$(14X/57) + (14Y/97) = N$$

where  $M$  = weight per cent combined maleic acid (mol. wt. 116),  $A$  = weight per cent ammonium maleate (mol. wt. 150),  $X$  = weight per cent maleic diamide (mol. wt. 114),  $Y$  = weight per cent maleimide (mol. wt. 97),  $N$  = weight per cent bound nitrogen (total, less ammonium nitrogen).

In Table II are given the complete compositions of the samples listed in Table I, calculated as mole fractions.

TABLE I  
Effect of Water Solution on -Amic Acid Polymer

Sample no.	Time, hr.	pH	Total carboxyl, ml. N/g.	NH <sub>4</sub> carboxyl, ml. N/g.	Maleic acid, wt.-%	NH <sub>4</sub> maleate, wt.-%	Total nitrogen, wt.-%	NH <sub>4</sub> nitrogen, wt.-%	Bound nitrogen, wt.-%	Styrene/maleic acid with N calcd. as	
										Amide	Imide
0	Before solution	—	4.42	1.77	15.4	13.3	7.25	2.48	4.77	1.26	0.65
1	0	5.57	4.58	2.13	14.3	16.0	6.20	2.98	3.20	1.59	1.00
2	17	6.23	6.28	2.82	20.1	21.2	5.35	3.95	1.40	1.40	1.14
3	41	6.41	6.31	2.96	19.4	22.2	5.60	4.14	1.46	1.37	1.11
4	137	6.76	6.42	2.87	20.6	21.5	5.35	4.02	1.33	1.37	1.13
5	305	7.03	6.37	2.82	20.6	21.2	5.20	3.95	1.25	1.41	1.17

TABLE II  
Effect of Water Solution on the -Amic Acid Polymer Composition  
Calculated on Styrene/Maleic Anhydride Ratio of 1.17

Sample no.	Time, hr.	Diamide, wt.-%	Imide, wt.-%	Mole fraction						Total bound nitrogen, mole	ΔN, mole	ΔN + ΔAcid	
				Maleic acid	NH <sub>4</sub> maleate	Amide	Imide	ΔImide	Styrene				Total COOH, mole
0	—	17.0	4.1	0.148	0.099	0.166	0.048	—	0.539	0.494	0.380	—	—
1	0	4.6	14.4	0.135	0.118	0.044	0.164	+0.116	0.539	0.506	0.252	-0.129	-0.117
2	17	0.7	8.5	0.196	0.159	0.007	0.099	+0.051	0.539	0.710	0.113	-0.268	-0.052
3	41	1.6	7.4	0.190	0.168	0.016	0.089	+0.041	0.539	0.716	0.121	-0.260	-0.038
4	137	1.1	7.4	0.201	0.163	0.011	0.086	+0.038	0.539	0.724	0.118	-0.263	-0.023
5	305	0	8.7	0.200	0.159	0.00	0.101	+0.053	0.540	0.718	0.101	-0.280	-0.056



In view of the extensive conversion of the amide to imide that appears to have occurred during the solution and degassing of the polymer at room temperature, this portion of the experiment was repeated, with more frequent sampling starting as soon as solution appeared to be complete. To hasten solution, mechanical stirring was used, and the concentration of the polymer was reduced to 5% by weight. The results, on a mole fraction basis, are given in Table III.

**Solution in Water in the Presence of Excess Ammonia.** A 50-g. portion of styrene-ammonium maleamic acid copolymer was added, portionwise, with mechanical stirring, to a solution of 15 ml. of 28% aqueous ammonia in 350 ml. of distilled water. The vigor of stirring was such that the solution was kept well agitated, yet air was not beaten into the solution. The glass electrodes of a pH meter were immersed in the solution during the solution process and the pH was followed. The pH of the ammoniacal water before addition of the polymer was 11.5. When all the polymer was in solution, the pH was 9.13. A portion of the solution was poured immediately into dioxane and the precipitate was treated as already described. Another sample was precipitated after 7 days at room temperature. The results are given in Table IV.

#### **Effect of Drying at 40°C. on Ammonium -Amic Acid Salt**

To check drying conditions, samples of toluene-wet polymer, as isolated, were dried at 40°C. in an air oven for the time indicated and then analyzed. The results are given in Table V.

#### **Effect of Heating the Dry -Amic Acid Polymer at 100°C.**

Approximately 8-g. samples of low viscosity -amic acid polymer were heated at 100°C. in an oven in open weighing dishes. At intervals, the dish and the contents were removed from the oven, sealed until cooled to room temperature, and the polymer was analyzed. The results are given in Table VI.

#### **Response of the Imide to Ammonia**

Two samples of the styrene-maleamic acid polymer (sample A, Table VII) were dissolved in water (1 g./10 ml.), and left for different lengths of time (sample B for 20 hr. and sample E for 2 hr.). They were then precipitated in 1,4-dioxane. Each was dried. One portion of sample B was redissolved in water (1 g./10 ml.) maintained at pH 9 by the portionwise addition of 28% ammonium hydroxide and left in solution for 18 hr. (sample C), and one portion was dissolved in 28% aqueous ammonia (1 g./8 ml.) and left for 20 hr. (sample D). The polymers were isolated by precipitation in 1,4-dioxane in the regular manner. Dry sample E was suspended in toluene and dry ammonia was passed through the suspension for 3 hr. The product was collected on a Büchner funnel, washed with toluene, and dried at 40°C. (sample F). All were analyzed. The results are given on a mole fraction basis in Table VII.

TABLE III  
Effect of Room Temperature Solution and Storage on the -Amic Acid Polymer

Time, hr.	Mole fraction						Total bound N, mole	$\Delta_{\text{COOH}}$ , mole	$\Delta_{\text{N}}$ , mole	$\Delta_{\text{Imide}}$ , mole	$\Delta_{\text{COOH}}$ , mole	$\Delta_{\text{N}} + \Delta_{\text{COOH}}$ , mole
	Maleic acid	NH <sub>4</sub> maleate	Amide	Imide	Total COOH, mole	Total bound N, mole						
0	0.111	0.131	0.195	0.024	0.484	0.414	—	0.000	0.000	0.000	0.000	0.000
1/2	0.138	0.109	0.142	0.071	0.494	0.355	+0.010	-0.059	+0.047	-0.049	-0.049	-0.049
1	0.141	0.081	0.122	0.115	0.444	0.359	-0.040	-0.055	+0.091	-0.095	-0.095	-0.095
2	0.139	0.080	0.089	0.152	0.438	0.330	-0.046	-0.084	+0.128	-0.130	-0.130	-0.130
4	0.120	0.086	0.070	0.185	0.412	0.325	-0.072	-0.089	+0.161	-0.161	-0.161	-0.161

TABLE IV  
Effect of Solution at pH 9.13 on Composition of the -Amic Acid Polymer

Sample no.	Keeping time	pH of dope	Total			Bound			Maleic acid, wt.-%			NH <sub>4</sub> maleate, wt.-%			Imide, wt.-%		
			carboxyl, ml. N/g.	NH <sub>4</sub> carboxyl, ml. N/g.	Total nitrogen, wt.-%	nitrogen, wt.-%	Maleic acid, ml. N/g.	Maleic acid, wt.-%	Maleic acid, wt.-%	NH <sub>4</sub> maleate, wt.-%	Imide, wt.-%	Amide, wt.-%	Imide, wt.-%				
Before doping		—	4.11	2.03	7.75	4.91	2.1	12.1	15.3	16.4	6.1						
7B	0	9.13	4.22	1.64	7.35	5.05	2.6	15.0	12.3	18.0	4.4						
7C	7 days	9.16	4.36	1.48	6.95	4.88	2.9	16.7	11.1	17.3	4.4						

TABLE V  
Effect of Drying at 40°C.

Drying time, hr.	Total carboxyl, ml. N/g.	Ammonium carboxyl, ml. N/g.	Total nitrogen, wt.-%	Bound nitrogen, wt.-%	Maleic acid, wt.-%	NH <sub>4</sub> maleate, wt.-%	Amide, wt.-%	Imide, wt.-%
16 <sup>a</sup>	4.11	2.50	7.8	4.3	9.3	18.8	11.5	10.3
43.5 <sup>b</sup>	4.11	2.03	7.75	4.91	12.1	15.2	16.4	6.1
158	4.45	1.54	6.90	4.74	16.9	11.6	16.4	4.7

<sup>a</sup> Residual toluene present. This will cause the imide to appear high.

<sup>b</sup> Very slight amount of residual toluene present.

TABLE VI  
Effect of Heating Copolymer of Styrene and -Amic Acid at 100°C.

Time, hr.	Total carboxyl, ml. N/g.	NH <sub>4</sub> carboxyl, ml. N/g.	Total nitrogen, wt.-%	NH <sub>4</sub> nitrogen wt.-%	Bound nitrogen, wt.-%	Maleic acid, wt.-%	NH <sub>4</sub> maleate, wt.-%	Calcd. from ratio styrene/maleic acid = 1.17	
								Amide, wt.-%	Imide, wt.-%
0	4.42	1.77	7.25	2.48	4.77	15.4	13.3	17.0	4.1
1	4.58	1.45	6.80	2.06	4.72	18.2	10.9	17.3	3.3
4	4.83	0.96	5.75	1.34	4.41	22.5	7.2	15.8	3.7
8 <sup>1</sup> / <sub>3</sub>	4.75	0.83	5.20	1.17	4.03	22.7	6.2	11.8	7.9
16	5.03	0.56	4.55	0.78	3.77	25.9	4.2	11.1	7.2
24	5.11	0.47	4.80	0.60	4.12	26.9	3.5	14.6	3.7

TABLE VII  
Response of Imide to Ammonia

Sample	Mole fraction			Total nitrogen, mole	Total acid, mole	$\Delta_{\text{Nitrogen}}$ , mole	$\Delta_{\text{Acid}}$ , mole
	Maleic acid	NH <sub>4</sub> maleate	Imide				
A	0.149	0.104	0.159	0.367	0.506	0.00	—
B	0.127	0.126	0.00	0.229	0.506	-0.138 <sup>a</sup>	0.00 <sup>a</sup>
C	0.129	0.129	0.00	0.213	0.516 <sup>b</sup>	-0.016 <sup>b</sup>	+0.010 <sup>b</sup>
D	0.236	0.099	0.133	0.273	0.670	+0.045 <sup>b</sup>	+0.144 <sup>b</sup>
E	0.126	0.101	0.020	0.253	0.454	-0.114 <sup>a</sup>	-0.062 <sup>a</sup>
F	0.180	0.101	0.168	0.336	0.562	+0.080 <sup>c</sup>	+0.108 <sup>c</sup>

<sup>a</sup> Compared to sample A.

<sup>b</sup> Compared to sample B.

<sup>c</sup> Compared to sample E.

## DISCUSSION

The data indicate that, except for the loss of ammonia which is associated with carboxyl in salt formation, the dry styrene-maleamic acid interpolymer appears to be reasonably stable (see Tables V and VI) at moderate temperatures and in the absence of atmospheric moisture. The bound nitrogen is essentially amide and remains as such. This is partly in agreement with the findings of Heiligmann and McSweeney.<sup>1</sup> The half-amide is quite stable at 100°C. However, at temperatures as low as 40°C., the ammonium salt of the -amic acid loses a considerable portion of its salt-held ammonia.

In water, the behavior is dependent on the ammonia concentration. If sufficient ammonia is present, the polymer is reasonably stable. When the amount of ammonia is inadequate, as undoubtedly is the case of a polymer that has lost the major portion of its salt-bound ammonia through drying, the conversion from amide to imide is rapid and, in time, is complete. In time, a major hydrolysis of the imide to the diacid apparently occurs. On the other hand, if the imide, once formed in water, is subjected to a sufficiently high concentration of ammonia, conversion to diamide occurs.

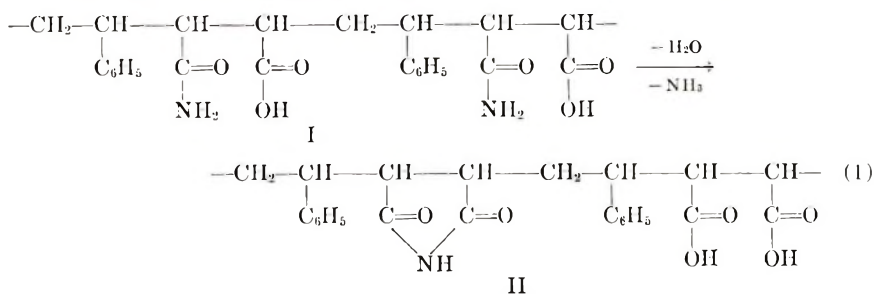
As shown in Tables II and III, imide formation is accompanied by a loss in ammonia, at first without a concomitant loss of a carboxyl and later by a loss of a carboxyl accompanied by a loss of ammonia. There appears to be some concurrent hydrolysis, but during the early stages the major portion of the loss of bound nitrogen and of carboxyl appears to be associated with the formation of imide. It is this apparent formation of imide by the loss of ammonia that must be explained. Formation of imide by carboxyl loss follows classical lines.

The loss of bound nitrogen and temporary removal of carboxyl, later recoverable in the carboxyl analysis, would occur in the formation of anhydride by the removal of the elements of ammonia. The existence of this reaction would necessitate an acid-anhydride equilibrium in water well in favor of the anhydride at the operating pH. The presence of measurable amounts of anhydride could not be demonstrated for styrene-maleic acid interpolymer at pH 4 by the pH stat method employed by Ebersson<sup>8</sup> for  $\alpha,\alpha'$ -dimethylmaleic anhydride. Examination of imidized -amic acid, isolated from the water solutions, by infrared radiation showed absorptions at 5.65 and 5.8  $\mu$ . Copoly(styrene-maleimide) and copoly(styrene-maleic anhydride), the latter isolated from the toluene suspensions, washed with toluene, and dried in a vacuum, had absorptions at 5.65 and 5.8  $\mu$  and 5.4 and 5.6  $\mu$ , respectively. It does not appear that anhydride formation plays a significant role in the observed behavior of styrene-maleamic acid interpolymer.

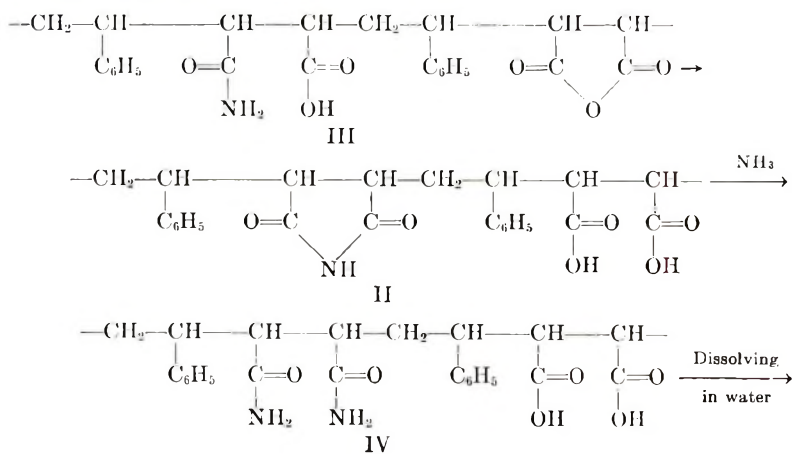
At least two mechanisms are possible for the conversion of amide to imide in water solution with loss of ammonia. If the structure of the polymer is normal for -amic acid [see eq. (1)], then there must occur (a) a

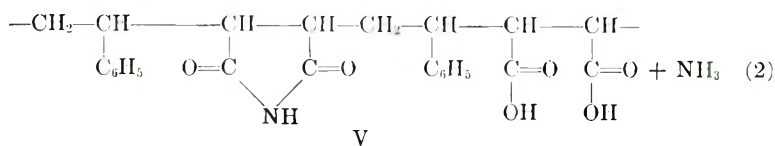


rapid imidization with the loss of water, (b) a rapid hydrolysis of amide with the loss of ammonia and formation of carboxyl, and (c) a slow rate of hydrolysis of the imide. Since there is little change in total carboxyl (see Table I) during the early stage when imide is forming rapidly, the hydrolysis of the amide (b) must be about as rapid as the formation of imide (a).



The other mechanism requires that a substantial portion of the dry -amic acid polymer have a structure with two amides [eq. (2), IV] and, necessarily, two carboxyls adjacent. Imide is formed by the loss of ammonia. The total carboxyl would thus remain substantially unchanged during this imidization. The formation of the intermediate with amide groups adjacent to each other could be accounted for in the following manner. An anhydride group in the intermediate polymer reacts with ammonia to form the -amic acid. Since, in this work, the -amic acid polymer is prepared under dehydrating conditions in toluene, ring formation occurs to form the imide with the loss of one molecule of water which, in turn, hydrolyzes the anhydride to two adjacent carboxyls. In the presence of an excess of ammonia, the imide ring opens to form two adjacent amides. This would yield a polymer whose apparent analysis is similar to that of structure in I [eq. (1)], except that now amide and carboxyl are each present in pairs, with each member on adjacent carbons. It has been demonstrated<sup>7</sup> that the ethylene-ammonium maleamate interpolymer can be converted to the diamide by heating under pressure with ammonia. Here, the imide II may be the intermediate.





A closer examination of the data presented in Table III lends further support to a polymer having a proportion of its amide groups adjacent. The concept of the formation of imide by the loss of the elements of ammonia from two adjacent amide groups requires that for each imide formed, two amide groups be lost. The data given in Table III comply very rigidly with this requirement. The mole fractions of maleamide and maleimide in the zero sample were 0.195 and 0.024, respectively. The mole fraction maleamide and maleimide in the  $1/2$ -hr. sample were 0.142 and 0.071 mole, respectively, a net change of 0.053 mole loss of maleamide and 0.047 mole gain of maleimide, per unit polymer mole. Since each maleamide involves two amide groups, the change in amide group content is 0.106 mole. Of the 0.106 mole, Table III indicates that 0.010 mole was converted to carboxyl, leaving a net loss of amide, involved in imide formation through the loss of ammonia, of 0.096 mole. The ratio of amide lost to imide formed is 0.096/0.047 or 2.04.

Beyond the  $1/2$ -hr. sample the calculation is complicated by the loss of carboxyl and by the reaction with amide to form imide, but the data still fit the requirement of a 2-mole loss of amide for each mole of imide formed by loss of ammonia. For example, the 1-hr. sample had an amide group loss of  $2(0.195 - 0.122)$  or 0.146 mole. Of this 0.146-mole loss of amide, 0.040 mole was involved in the formation of imide by reaction with carboxyl, leaving a net of 0.106 mole involved in the formation of imide by ammonia loss. The total imide formed is 0.091 mole, of which 0.040 mole came from the reaction of carboxyl with amide, leaving a net of 0.051 mole of imide whose origin is attributed to loss of ammonia. The ratio of lost amide to gained imide is 0.106/0.051 or 2.08. By the same calculation, the 2- and 4-hr. samples yield ratio of lost amide to formed imide by ammonia loss of 2.07 and 2.0, respectively.

Such a polymer will meet the behavior requirements. The loss of ammonia should be catalyzed by hydrogen ion and should be suppressed by excess ammonia. The postulate that the imide ring opens in the presence of a large excess of ammonia, particularly under the conditions of these experiments, is supported by the data in Table VII. Since it is very unlikely that reaction rates of imidization and hydrolysis would be of the correct magnitudes to make the first suggested mechanism the correct one, it follows that the second suggested mechanism must apply and the "-amic" acid polymer as here obtained, consists, to a substantial extent, of a quaterpolymer of styrene, maleamic acid, maleic acid, and maleic diamide.

### References

1. Heiligmann, R. G., and E. E. McSweeney, *Ind. Eng. Chem.*, **44**, 113 (1952).
2. Siggia, S., *Quantitative Organic Analysis via Functional Groups*, Wiley, New York, 1959, p. 21.

3. Unruh, C. C., P. A. McGee, W. F. Fowler, and W. O. Kenyon, *J. Am. Chem. Soc.*, **69**, 349 (1947).
4. Minsk, L. M., G. P. Waugh, and W. O. Kenyon, *J. Am. Chem. Soc.*, **72**, 2648 (1950).
5. Smith, D. M., and W. M. D. Bryant, *J. Am. Chem. Soc.*, **58**, 2452 (1936).
6. Garrett, E. R., and R. L. Guile, *J. Am. Chem. Soc.*, **73**, 4534 (1951).
7. Fields, J. E., and J. H. Johnson, U.S. Pat. 2,921,928 (Nov. 29, 1957).
8. Ebersson, L., *Acta Chem. Scand.*, **18**, 1276 (1964).

### Résumé

On décrit la réponse à la chaleur et à l'eau d'un copolymère de styrène-acide maléamique et son sel ammonique, préparé par traitement à l'ammoniac du polymère anhydride en suspension toluénique. Ce polymère, sauf pour l'ammoniac lié sous forme de sel, est stable à la chaleur dans le domaine de température étudié, c'est à dire jusque 100°C. Le comportement en solution aqueuse est déterminé par la concentration en ammoniac. À pH égal à 9, l'azote lié y est présent sous forme d'amide. Si le pH est bas, c'est-à-dire environ 5, ce qui se présente lorsqu'un échantillon séché est dissous dans l'eau, une immidisation rapide se passe concomitamment à une hydrolyse. Dans les premières étapes de cette transformation, l'immidisation se passe essentiellement avec élimination d'ammoniac. Ceci requiert que deux groupes amides adjacents réagissent entre eux. Une immidisation classique par élimination d'eau se passe également, ce que indique que une structure normale et amique-acide se présente dans le copolymère.

### Zusammenfassung

Das Verhalten von Kopoly (styrolmaleinsäure, Ammoniumsalz), welches durch Behandlung des Anhydridpolymeren in Toluolsuspension mit Ammoniak dargestellt worden war, gegen Hitze und Wasser wird beschrieben. Dieses Polymere ist mit Ausnahme des durch Salzbildung gebundenen Ammoniaks gegen Hitze innerhalb des untersuchten Bereichs, nämlich bis zu 100°C, beständig. Das Verhalten in wässriger Lösung wird durch die Ammoniakkonzentration bestimmt. Bei einem pH von 9 verbleibt der gebundene Stickstoff als Amid. Bei niedrigem pH, d.h. etwa 5, wie es bei der Lösung einer getrockneten Probe in Wasser auftritt, tritt rasche Imidierung mit gleichzeitiger Hydrolyse ein. Im frühen Stadium dieser Umwandlung erfolgt die Imidierung hauptsächlich durch Ammoniakverlust. Dies erfordert zwei benachbarte Amidgruppen. Klassische Imidierung durch Verlust von Wasser tritt ebenfalls auf, was beweist, dass auch die normale Amidsäurestruktur vorhanden ist.

Received June 7, 1965

Revised September 22, 1965

Prod. No. 4905A

# Molecular Vibrations of Irregular Chains. I. Analysis of Infrared Spectra and Structures of Polymethylene Chains Consisting of CH<sub>2</sub>, CHD, and CD<sub>2</sub> Groups

M. TASUMI and T. SHIMANOUCI, *Department of Chemistry, Faculty of Science, The University of Tokyo, Bunkyo-ku, Tokyo, Japan*, and H. KENJO and S. IKEDA, *Research Laboratory of Resources Utilization, Tokyo Institute of Technology, Meguro-ku, Tokyo, Japan*

## Synopsis

Various samples of irregularly deuterated polyethylene were prepared and their infrared spectra were studied. The results support the previously proposed view that poly-*trans*-CHD=CHD or -*cis*-CHD=CHD obtained with Al(*i*-Bu)<sub>3</sub>-TiCl<sub>4</sub> is an irregularly deuterated chain consisting of the CH<sub>2</sub>, CHD, and CD<sub>2</sub> groups. A simplified calculation of the CHD scissors and CDH rocking vibration frequencies has been made for various model chains. The assignments of the CDH rocking vibration bands in the region of 700–500 cm.<sup>-1</sup> have been given on this basis.

## Introduction

In earlier papers<sup>1,2</sup> we reported that polyethylene samples obtained in the polymerization of *cis*- or *trans*-1,2-dideuteroethylene with a Ziegler catalyst, Al(*i*-Bu)<sub>3</sub>-TiCl<sub>4</sub>, showed several infrared absorptions in the region of 700–500 cm.<sup>-1</sup> (Fig. 1). These bands have been taken to be due to irregularities in the distribution of the deuterium atoms in the polymer chain. In other words, it has been concluded that the hydrogen–deuterium exchange reaction in monomers as well as the polymerization is promoted by the catalyst. On the other hand, such is not the case for the polymerization with another Ziegler catalyst, AlEt<sub>3</sub>-TiCl<sub>4</sub>, having an Al/Ti molar ratio of about 2. Polymers of *cis*-CHD=CHD and *trans*-CHD=CHD obtained with this catalyst show simplified spectra in the same region; only a doublet at ca. 590 cm.<sup>-1</sup> is observed.

In the present study we have tried to relate the bands characteristic of the polymer obtained by Al(*i*-Bu)<sub>3</sub>-TiCl<sub>4</sub> with local structures of the polymer both experimentally and theoretically.

## Experimental

We prepared various model samples of irregularly deuterated polyethylene by changing composition of monomers. Four species of mono-

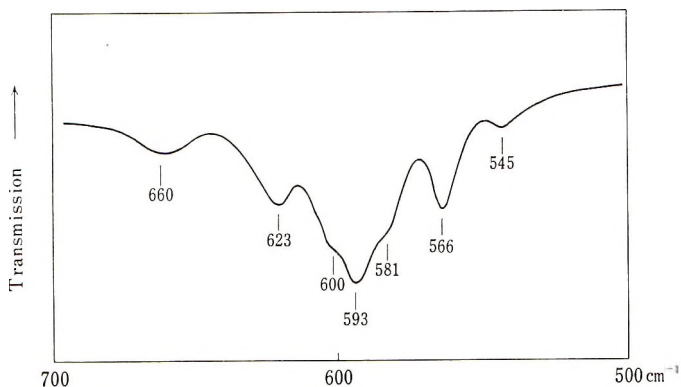


Fig. 1. Infrared spectrum of poly-*trans*-CHD=CHD obtained with  $\text{Al}(i\text{-Bu})_3 + \text{TiCl}_4$  (Sample I). The polymer of *cis*-CHD=CHD obtained with the same catalyst (sample II) shows a similar spectrum.

mers, viz., A, B, C, and D of Table I, were used. The polymer samples obtained from these monomers are listed in Table II. The procedure of polymerization was similar to that described in a previous paper.<sup>3</sup>

Infrared spectra shown in Figures 2 and 3 were recorded by use of a Japan Spectroscopic Co. Model 402G grating spectrometer.

#### Analysis of the Spectra

As is shown in Figures 1 and 2, samples IV and V show the bands at about 660 and 620  $\text{cm}^{-1}$ , which correspond well to the bands at 660 and 623  $\text{cm}^{-1}$  of samples I and II. Similarly, the 567 and 545  $\text{cm}^{-1}$  bands of samples VII and VIII have corresponding bands in the spectra of samples I and II.

From these facts it seems reasonable to consider that the bands at 660, 623, 566, and 545  $\text{cm}^{-1}$  of samples I and II are due to irregularities in the distribution of the deuterium atoms in these polymers. Accordingly, it is evident that the hydrogen-deuterium exchange reaction is promoted by the catalyst  $\text{Al}(i\text{-Bu})_3\text{-TiCl}_4$ .

Our next problem is to make the assignments of these bands clearer than proposed in our earlier paper.<sup>1</sup> Before doing this, we examine the vibrational modes corresponding to the bands at about 725, 590, and 520  $\text{cm}^{-1}$  of  $-(\text{CH}_2)_n-$ ,  $-(\text{CHD})_n-$ , and  $-(\text{CD}_2)_n-$ , respectively. These are the rocking vibrations of the methylene groups. Figure 4 illustrates the modes of these vibrations. It is noted that all the H and D atoms move in phase to one side of the skeletal plane. We call this type of vibration the in-phase mode. It is well known that for an infinite chain only the in-phase modes may interact with light and give rise to optical absorptions. All the other modes, e.g., the modes shown in Figures 5b and 5c, are infrared-inactive. However, for finite-chain molecules like *n*-paraffin homologs and their derivatives, the normal vibrations which are close to the modes of Figure 5b and 5c may become active, and in fact this is



TABLE I  
 Monomers Used in the Polymerization

Monomer	Molar percentage						
	$\text{CH}_2=\text{CH}_2$	$\text{CH}_2=\text{CHD}$	<i>cis</i> - $\text{CHD}=\text{CHD}$	<i>trans</i> - $\text{CHD}=\text{CHD}$	$\text{CHD}=\text{CD}_2$	$\text{CD}_2=\text{CD}_2$	
A	100	0	0	0	0	0	
B	0	3	96	1	0	0	
C	0	3	0	97	0	0	
D		<1 <sup>a</sup>	3	0	25	71	

<sup>a</sup> The total amount of  $\text{CH}_2=\text{CH}_2$  and  $\text{CH}_2=\text{CHD}$  is less than 1%.

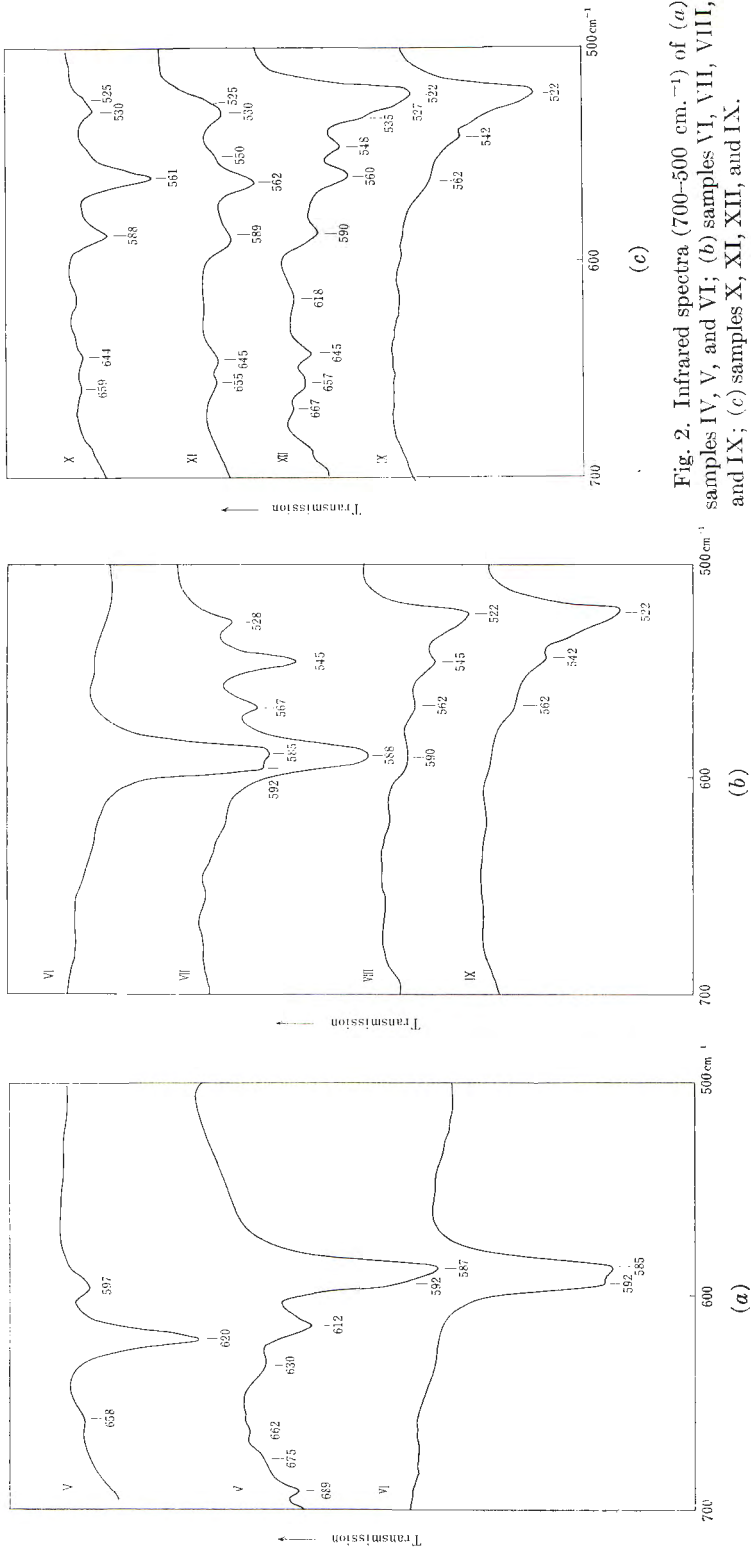


Fig. 2. Infrared spectra ( $700\text{--}500\text{ cm}^{-1}$ ) of (a) samples IV, V, and VI; (b) samples VI, VII, VIII, and IX; (c) samples X, XI, XII, and IX.

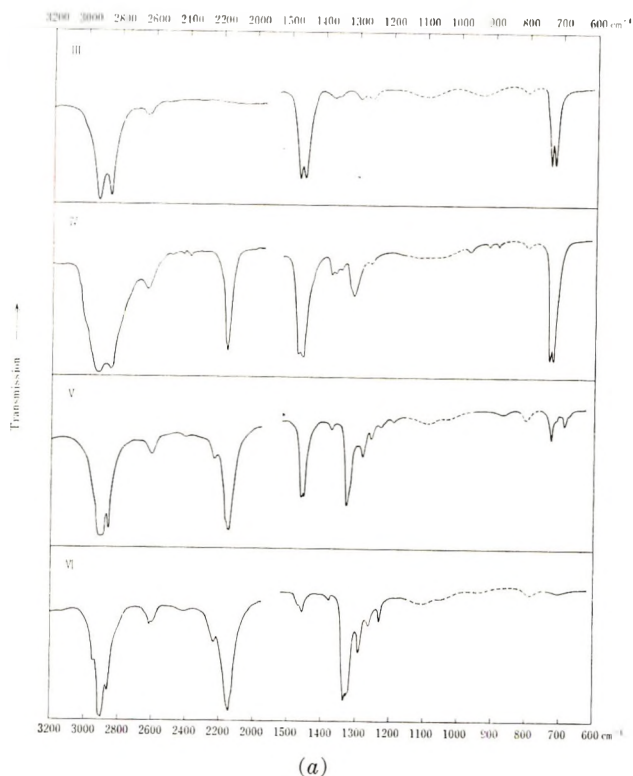
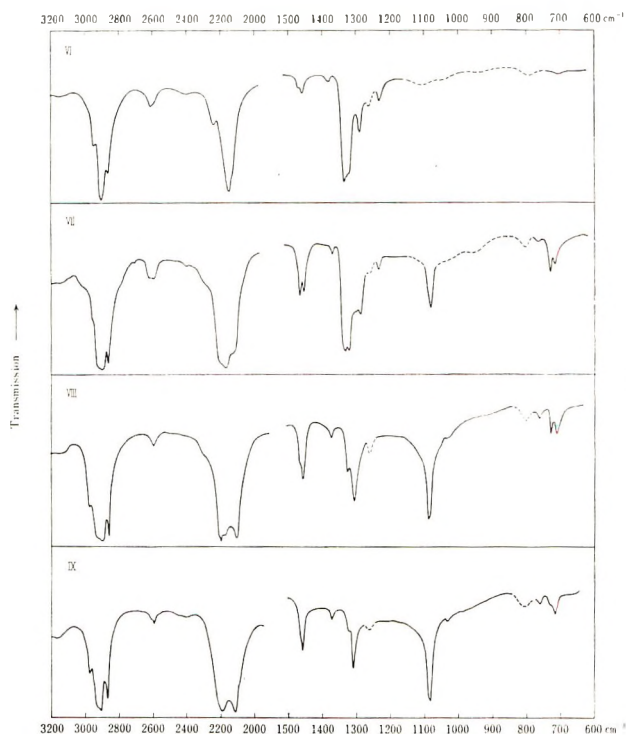


Figure 3. See caption, p. 1017

observed as the so-called band progression. It must be pointed out here that, as far as the methylene rocking modes are concerned, the frequency has the order of  $(a) < (b) < (c) < (d)$  of Figure 5, and the absorption intensity

TABLE II  
Samples of Irregularly Deuterated Polyethylene

Polymer sample	Monomer ratio, %				Catalyst
	A	B	C	D	
I	0	100	0	0	Al( <i>i</i> -Bu) <sub>3</sub> + TiCl <sub>4</sub> , Al/Ti = 2.3
II	0	0	100	0	
III	100	0	0	0	
IV	70	30	0	0	
V	30	0	70	0	AlEt <sub>2</sub> Cl + TiCl <sub>4</sub> , Al/Ti = 2.5
VI	0	0	100	0	
VII	0	0	67	33	
VIII	0	0	30	70	
IX	0	0	0	100	
X	75	0	0	25	
XI	50	0	0	50	
XII	26	0	0	74	



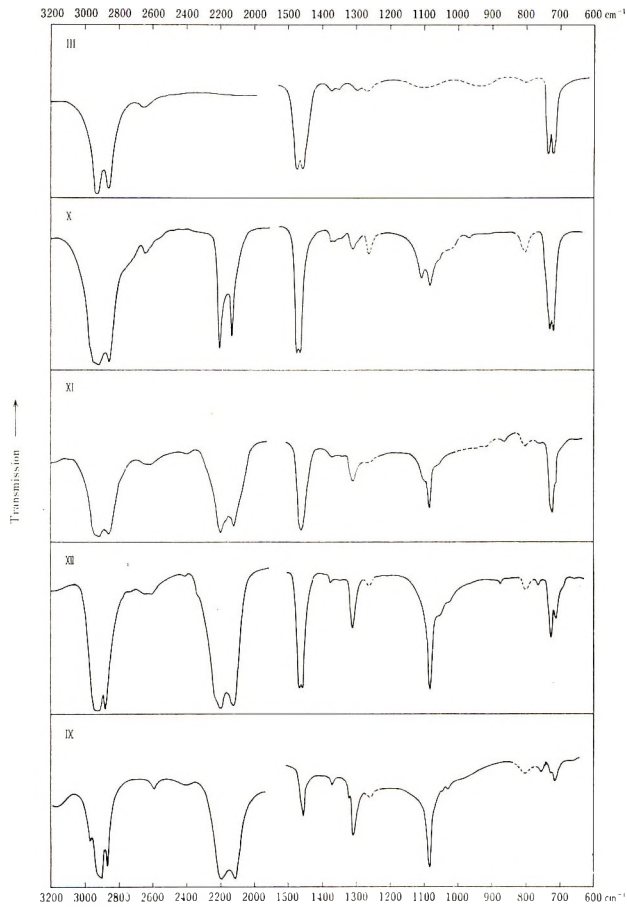
(b)

Figure 3. (continued)

for a long-chain  $n$ -paraffin molecule has, on the contrary, the order of  $(a) > (b) > (c) > (d)$ ; i.e., the in-phase mode has the lowest frequency and the strongest intensity.<sup>4-6</sup> The frequencies of the  $\text{CH}_2$  rocking modes spread over ca.  $400 \text{ cm}^{-1}$ ; the highest frequency corresponding to the  $(d)$  mode is  $1168 \text{ cm}^{-1}$ . The intensity seems to increase sharply when the normal vibration of a  $n$ -paraffin molecule approaches the in-phase one.

For an irregular chain consisting of  $\text{CH}_2$ ,  $\text{CHD}$ , and  $\text{CD}_2$  groups, a case somewhat similar to a finite chain may be expected. For instance, we take a block or a portion of chain made up of  $\text{CHD}$  and  $\text{CD}_2$  groups, such as  $-\text{CHDCHDCHDCD}_2\text{CD}_2\text{CD}_2\text{CHDCHD}-$ . From what we have discussed above, we may expect that the mode shown in Figure 5e would be active in the infrared absorption and it would have a frequency higher than  $520 \text{ cm}^{-1}$ , the frequency corresponding to the in-phase mode of  $-(\text{CD}_2)_n-$ . We call such a mode the locally in-phase mode. Now if we can predict the frequency of this mode, we may establish one-to-one correspondence between the bands observed in the spectra of samples I-XII with the various chain portions.

The method of calculating the normal vibration frequencies of high polymers by the **GF** matrix method<sup>7</sup> has been worked out,<sup>8-10</sup> and the



(c)

Fig. 3. Infrared spectra (3200–600  $\text{cm}^{-1}$ ) of samples III, IV, V, and VI; (b) samples VI, VII, VIII, and IX; (c) samples III, X, XI, XII, and IX. The broken lines indicate the bands arising from impurities.

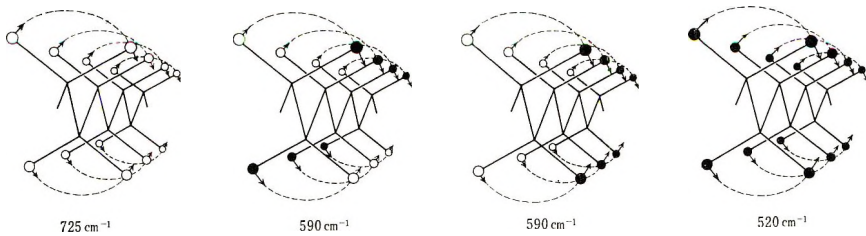


Fig. 4. In-phase methylene rocking modes, (O) = H, (●) = D: (a)  $-(\text{CH}_2)_n-$ , (b) erythro-diisotactic  $-(\text{CHD})_n-$ ; (c) threo-diisotactic  $-(\text{CHD})_n-$ , (d)  $-(\text{CH}_2)_n-$ .



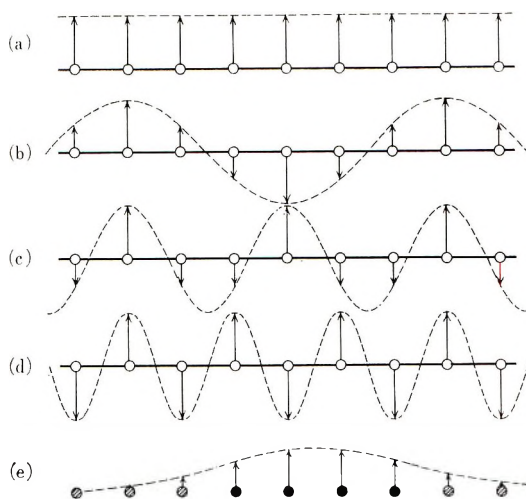


Fig. 5. Schematic representation of the methylene rocking modes, (O) = CH<sub>2</sub>, (⊗) = CHD, (●) = CD<sub>2</sub>: (a) infrared-active in-phase mode; (b), (c) spectroscopically inactive modes; (d) Raman-active mode; (e) locally in-phase mode of  $-(\text{CHD})_3(\text{CD}_2)_4(\text{CHD})_2-$ .

TABLE III

Simplified **G** and **F** Matrices of the Chain having Repeating Unit Made up of Six Methylene Groups<sup>a</sup>

	$\Delta\delta_1$	$\Delta\delta_2$	$\Delta\delta_3$	$\Delta\delta_4$	$\Delta\delta_5$	$\Delta\delta_6$	$\Delta\alpha_1^r$	$\Delta\alpha_2^r$	$\Delta\alpha_3^r$	$\Delta\alpha_4^r$	$\Delta\alpha_5^r$	$\Delta\alpha_6^r$
<b>G</b> =	$g_{a1}^\delta$											
	$g_b^\delta$	$g_{a2}^\delta$										
	$g_c^\delta$	$g_b^\delta$	$g_{a3}^\delta$									
	0	$g_c^\delta$	$g_b^\delta$	$g_{a4}^\delta$								
	$g_c^\delta$	0	$g_c^\delta$	$g_b^\delta$	$g_{a5}^\delta$				(symmetric)			
	$g_b^\delta$	$g_c^\delta$	0	$g_c^\delta$	$g_b^\delta$	$g_{a6}^\delta$						
	$g_1^{\delta r}$	0	0	0	0	0	$g_{a1}^r$					
	0	$g_2^{\delta r}$	0	0	0	0	$g_b^r$	$g_{a2}^r$				
	0	0	$g_3^{\delta r}$	0	0	0	$g_c^r$	$g_b^r$	$g_{a3}^r$			
	0	0	0	$g_4^{\delta r}$	0	0	0	$g_c^r$	$g_b^r$	$g_{a4}^r$		
	0	0	0	0	$g_5^{\delta r}$	0	$g_c^r$	0	$g_c^r$	$g_b^r$	$g_{a5}^r$	
	0	0	0	0	0	$g_c^{\delta r}$	$g_b^r$	$g_c^r$	0	$g_c^r$	$g_b^r$	$g_{a6}^r$
<b>F</b> =	$f_a^\delta$											
	$f_b^\delta$	$f_a^\delta$										
	0	$f_b^\delta$	$f_a^\delta$									
	0	0	$f_b^\delta$	$f_a^\delta$								
	0	0	0	$f_b^\delta$	$f_a^\delta$							
	$f_b^\delta$	0	0	0	$f_a^\delta$	$f_a^\delta$			(symmetric)			
	0	0	0	0	0	0	$f_a^r$					
	0	0	0	0	0	0	$f_b^r$	$f_a^r$				
	0	0	0	0	0	0	0	$f_b^r$	$f_a^r$			
	0	0	0	0	0	0	0	0	$f_b^r$	$f_a^r$		
	0	0	0	0	0	0	0	0	0	$f_b^r$	$f_a^r$	
	0	0	0	0	0	0	0	0	0	0	$f_b^r$	$f_a^r$
	0	0	0	0	0	0	$f_b^r$	0	0	0	$f_b^r$	$f_a^r$

<sup>a</sup> Only the elements  $g_a^\delta$ ,  $g_a^r$ , and  $g^{\delta r}$  change their values with the replacement of the CH<sub>2</sub> group by a CHD or CD<sub>2</sub> group. For the CH<sub>2</sub> and CD<sub>2</sub> groups the element  $g^{\delta r}$  is equal to zero.

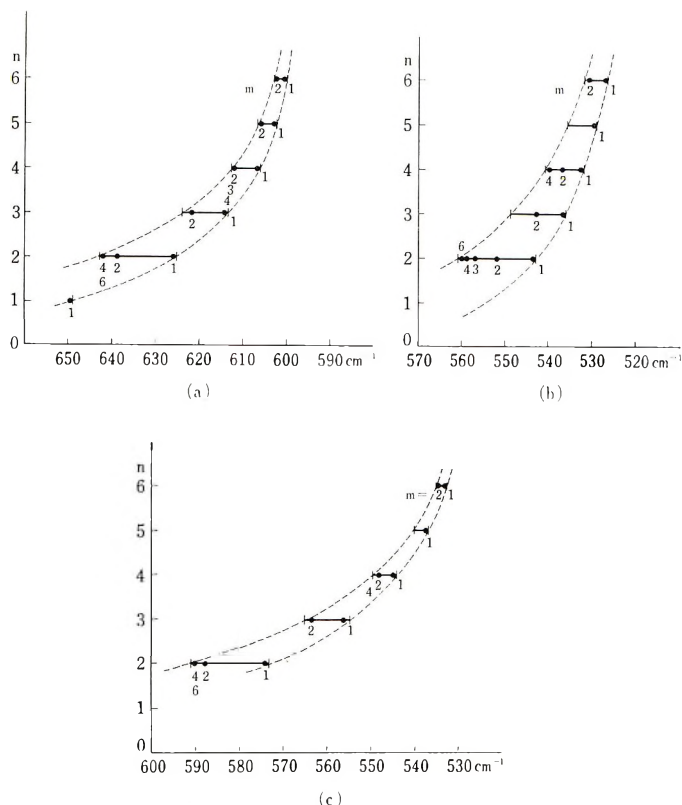


Fig. 6. Locations of the calculated frequencies (indicated by dots) of locally in-phase methylene rocking modes: (a) repeating unit is  $(\text{CH}_2)_m(\text{CHD})_n$ ; (b) repeating unit is  $(\text{CHD})_m(\text{CD}_2)_n$ ; (c) repeating unit is  $(\text{CH}_2)_m(\text{CD}_2)_n$ . The number under the dot indicates the  $m$  value. The frequency range for an  $n$  value is indicated by the horizontal bar.

calculation has been carried out for several high polymers with the aid of electronic computers. However, these calculations are based on the assumption of regularity and infinity. There seems to have been no attempt at all to calculate the frequencies of an irregular chain. It would not be feasible to make this calculation without any simplification or approximation. Here we have made an approach to this problem by calculating the frequencies of spectroscopically active modes of various infinite chains whose repeating units are made up of various combinations of four to eight  $\text{CH}_2$ ,  $\text{CHD}$ , and  $\text{CD}_2$  groups. Furthermore, we take only the methylene scissors ( $\Delta\delta$ ) and rocking ( $\Delta\alpha'$ ) coordinates<sup>5</sup> into account. This would not diminish the reliability of the results of calculation, since our previous calculations<sup>1,5</sup> have shown that the methylene scissors and rocking coordinates do not mix greatly with the other ones, particularly for the in-phase and locally in-phase modes. The inverse kinetic energy matrix  $\mathbf{G}$  and the potential energy matrix  $\mathbf{F}$  constructed on such simplification have the forms of Table III, in which the case of repeating unit made up of six methylene groups is given. The elements of the  $\mathbf{G}$  matrix may be

TABLE IV  
Assignments of the Bands Observed in the Spectra  
of Irregularly Deuterated Polyethylene Samples

Band, cm. <sup>-1a</sup>	Assignment
	Rocking vibration of
660 (I, II, IV, V)	CHD isolated in CH <sub>2</sub> chain
630 (V)	(CHD) <sub>2</sub> between CH <sub>2</sub> groups
620 (I, II, IV)	(CHD) <sub>3</sub> between CH <sub>2</sub> groups
612 (V)	(CHD) <sub>4</sub> between CH <sub>2</sub> groups
600 (I, II)	(CHD) <sub>n</sub> ( <i>n</i> = 5-ca. 8) between CH <sub>2</sub> groups
590 (I, II, IV, V, VI, VII, VIII)	Longer CHD sequences
581 (I, II)	CD <sub>2</sub> isolated in CHD chain
566 (I, II, VII, VIII, IX)	(CD <sub>2</sub> ) <sub>2</sub> between CHD groups
545 (I, II, VII, VIII, IX)	(CD <sub>2</sub> ) <sub>3</sub> and (CD <sub>2</sub> ) <sub>4</sub> between CHD groups
528 (VII, VIII)	(CD <sub>2</sub> ) <sub>5</sub> and (CD <sub>2</sub> ) <sub>6</sub> between CHD groups
522 (VIII, IX)	Longer CD <sub>2</sub> sequences
667 (XII)	These would be due to some complex modes other than the locally in-phase ones
657 (X, XI, XII)	
645 (X, XI, XII)	
618 (X, XII)	
589 (X, XI, XII)	CD <sub>2</sub> between CH <sub>2</sub> and CHD groups <sup>b</sup>
561 (X, XI, XII)	(CD <sub>2</sub> ) <sub>2</sub> between CH <sub>2</sub> groups
548 (X, XI, VII)	(CD <sub>2</sub> ) <sub>3</sub> between CH <sub>2</sub> and CHD groups <sup>c</sup>
535-525 (X, XI, XII)	(CD <sub>2</sub> ) <sub>4</sub> between CH <sub>2</sub> groups
	(CD <sub>2</sub> ) <sub>n</sub> ( <i>n</i> = 5-ca. 8) between CH <sub>2</sub> and CHD groups
522 (XII, IX)	Longer CD <sub>2</sub> sequences

<sup>a</sup> Numbers in parentheses indicate the samples for which the band is observed.

<sup>b</sup> The vibration arising from the portion CH<sub>2</sub>CD<sub>2</sub>CHDCII<sub>2</sub> is most likely assigned to this frequency.

<sup>c</sup> The locally in-phase frequency calculated for the chain whose repeating unit is CH<sub>2</sub>CD<sub>2</sub>CD<sub>2</sub>CD<sub>2</sub>CHD is 554 cm.<sup>-1</sup>.

computed from the geometrical arrangements and the masses of the C, H, and D atoms in the usual manner, and for the elements of the **F** matrix the values which we obtained previously<sup>1,11</sup> may be used. The numerical computation of solving the secular equations  $|\mathbf{GF} - \mathbf{E}\lambda| = 0$  and getting the frequency in wavenumber  $\nu_i = \sqrt{\lambda_i}/2\pi c$  was carried out by the PC-2 computer of the Computation Center of the University of Tokyo.

We have calculated the frequencies for a good number of complex irregular chains, and the results may be most effectively demonstrated as in Figure 6. Comparison of this figure with Figures 2a, 2b, and 2c leads to the assignments given in Table IV. This table contains the final conclusion of this study.

### References

1. Tasumi, M., T. Shimanouchi, H. Tanaka, and S. Ikeda, *J. Polymer Sci. A*, **2**, 1607 (1964).
2. Ikeda, S., and R. Tsuchiya, *J. Polymer Sci. B*, **3**, 39 (1965).

3. Ikeda, S., A. Yamamoto, and H. Tanaka, *J. Polymer Sci. A*, **1**, 2925 (1963).
4. Snyder, R. G., *J. Mol. Spectry.*, **4**, 411 (1960).
5. Tasumi, M., T. Shimanouchi, and T. Miyazawa, *J. Mol. Spectry.*, **9**, 261 (1962); *ibid.*, **11**, 211 (1963).
6. Snyder, R. G., and J. H. Schachtschneider, *Spectrochim. Acta*, **19**, 85, 117 (1963).
7. Wilson, E. B., Jr., *J. Chem. Phys.*, **7**, 1047 (1939); *ibid.*, **9**, 76 (1941).
8. Shimanouchi, T., and S. Mizushima, *J. Chem. Phys.*, **17**, 1102 (1949).
9. Tadokoro, H., *J. Chem. Phys.*, **33**, 1558 (1960).
10. Miyazawa, T., *J. Chem. Phys.*, **35**, 693 (1961).
11. Tasumi, M., and T. Shimanouchi, *J. Chem. Phys.*, **43**, 1245 (1965).

### Résumé

Divers échantillons de polyéthylène irrégulièrement deutéré ont été préparés et leurs spectres infra-rouges ont été étudiés. Les résultats indiquent comme prévu précédemment que le poly-*trans*- ou *cis*-CHD=CHD obtenu avec l'aluminium-triisobutyl et tétrachlorure de titane est irrégulièrement deutéré et contient des groupes CH<sub>2</sub>, CHD et CD<sub>2</sub>. Un calcul simplifié des fréquences de vibrations CHD et CDH ont été effectués pour des chaînes de différents modèles. L'attribution des bandes de vibrations CDH dans la région de 700 à 500 cm<sup>-1</sup> a été effectuée sur cette base.

### Zusammenfassung

Verschieden Proben unregelmässig deuterierten Polyäthylens wurden dargestellt und ihre Infrarotspektren untersucht. Die Ergebnisse bestätigen die frühere vorgeschlagene Annahme, dass mit [Al(*i*-Bu)<sub>3</sub>-TiCl<sub>4</sub>] erhaltenes Poly-*trans*-CHD=CHD oder *cis*-CHD=CHD eine unregelmässig deuterierte, aus CH<sub>2</sub>-, CHD- und CD<sub>2</sub>-Gruppen bestehende Kette bildet. Eine vereinfachte Berechnung der CHD-Spreiz- und CDH-Pendel-Schwingungsfrequenzen wurde für verschiedene Modellketten durchgeführt. Die Zuordnung der CDH-Pendel-Schwingungsbanden im Bereich von 700 bis 500 cm<sup>-1</sup> wurde auf dieser Grundlage durchgeführt.

Received September 3, 1965  
Prod. No. 4909A

## Molecular Vibrations of Irregular Chains. II. Configurations of Polydeuteroethylene

M. TASUMI and T. SHIMANOUCI, *Department of Chemistry, Faculty of Science, The University of Tokyo, Bunkyo-ku, Tokyo, Japan,*  
and S. IKEDA, *Research Laboratory of Resources Utilization, Tokyo Institute of Technology, Meguro-ku, Tokyo, Japan*

### Synopsis

A simplified calculation of the CHD scissors vibration frequencies has been made for  $-(\text{CHD})_n-$  of various configurations. The correlation between the CHD scissors frequency and the local configuration has been established. On this basis the infrared absorption bands of poly-*trans*-CHD=CHD and poly-*cis*-CHD=CHD appearing in the region of 1350-1280  $\text{cm.}^{-1}$  have been interpreted in greater detail.

### Introduction

In earlier papers<sup>1,2</sup> we discussed the stereo structures of the *cis*- and *trans*-polydeuteroethylenes obtained with  $[\text{Al}(\text{ethyl})_3 + \text{TiCl}_4]$ . It has been concluded that poly-*cis*-CHD=CHD and poly-*trans*-CHD=CHD have erythro and threo structures, respectively. This conclusion has been drawn from the calculation of the normal vibration frequencies of the erythro-diisotactic and threo-diisotactic structures. In the present study we wish to give further confirmation to this conclusion by calculating the frequencies of more realistic models.

### Calculations and Results

The calculation of all the normal vibration frequencies of the erythro-diisotactic (e-DI) and threo-diisotactic (t-DI) structures was revised by a more refined set of force constants<sup>3</sup> than that used in the earlier paper,<sup>1</sup> and the results are given in Table I. It is noted that the CHD scissors frequencies of 1310  $\text{cm.}^{-1}$  ( $B_u$  of e-DI), 1281  $\text{cm.}^{-1}$  ( $A_1$  of t-DI), and 1329  $\text{cm.}^{-1}$  ( $B_1$  of t-DI) explain the observed values more reasonably than the earlier results<sup>1</sup> (see Fig. 1). In the earlier calculation these values were, respectively, 1304, 1295, and 1323  $\text{cm.}^{-1}$ .

As it is expected that poly-*cis*-CHD=CHD is an irregular mixture of the two erythro units, *dd* and *ll*, and poly-*trans*-CHD=CHD is an irregular mixture of the two threo units, *dl* and *ld*, it is desirable to calculate the normal vibration frequencies of more irregular chains. For this purpose the same type of calculation as described in the preceding paper<sup>4</sup>



TABLE I  
Calculated Normal Vibration Frequencies of the Erythro-Diisotactic  
and Threo-Diisotactic Structures

Erythro-diisotactic			Threo-diisotactic		
Species	Calculated frequency, cm. <sup>-1</sup>	Assignment	Species	Calculated frequency, cm. <sup>-1</sup>	Assignment
<i>A<sub>g</sub></i>	2860	CH stretch.	<i>A<sub>1</sub></i>	2874	CH stretch.
	2088	CD stretch.		2095	CD stretch.
	1303	CHD scissors		<b>1281<sup>a</sup></b>	CHD scissors
	1129	skeletal		1101	skeletal
	995	CHD rock.		585	CDH rock.
<i>B<sub>u</sub></i>	1372	CDH wag.	<i>A<sub>2</sub></i>	1340	skeletal
	1146	skeletal		1048	CHD wag.
<i>A<sub>u</sub></i>	856	CDH twist.	<i>B<sub>1</sub></i>	777	CDH twist.
	1127	CHD wag.		2880	CH stretch.
<i>B<sub>u</sub></i>	802	CDH twist.	<i>B<sub>2</sub></i>	2116	CD stretch.
	2893	CH stretch.		<b>1329<sup>a</sup></b>	CHD scissors
	2122	CD stretch.	1032	CDH rock.	
	<b>1310<sup>a</sup></b>	CHD scissors	1238	CHD wag.	
	592	CDH rock.	900	CDH twist.	

<sup>a</sup> The boldface indicates an infrared-active CHD scissor vibration.

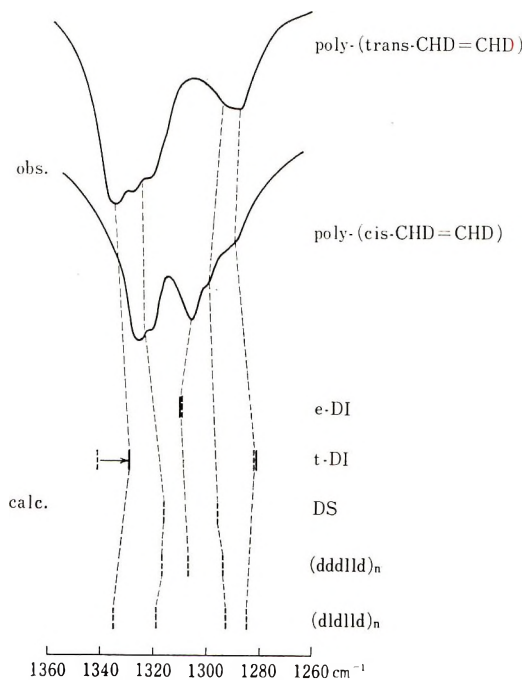


Fig. 1. Observed and calculated CHD scissors frequencies: (—); exact calculation; (---); approximate calculation.

TABLE II  
 Calculated CHD Scissors Frequencies of the Erythro-Diisotactic,  
 Threo-Diisotactic, Disyndiotactic, and Complex Structures

Chain configuration <sup>a</sup>	CHD scissors frequency, cm. <sup>-1</sup> , and mode <sup>b</sup>	
	Approximate calc.	Exact calc.
$(dddd)_n$ or $(llll)_n$ (e-DI)	1319 ( $A_g$ )	1303 ( $A_g$ )
	<b>1310</b> ( $B_u$ )	<b>1310</b> ( $B_u$ )
$(dldl)_n$ or $(ldld)_n$ (t-DI)	<b>1340</b> ( $B_1$ )	<b>1329</b> ( $B_1$ )
	<b>1282</b> ( $A_1$ )	<b>1281</b> ( $A_1$ )
$(dlld)_n$ or $(lddl)_n$ (DS)	1330 ( $B_g$ )	
	<b>1316</b> ( $B_u$ )	
	<b>1296</b> ( $A_u$ )	
	1289 ( $A_g$ )	
$(dlld)_n$ or $(lddl)_n$	<b>1333</b> ( $B_1$ type of $ddd$ or $lll$ )	
	<b>1307</b> ( $B_u$ type of $dld$ or $ldl$ )	
	1302 (Intermediate mode)	
	<b>1288</b> ( $A_1$ type of $ddd$ or $lll$ )	
$(dddlld)_n$ or $(lllddl)_n$	1328 ( $A_g$ type of $dlld$ or $lddl$ )	
	<b>1317</b> ( $B_u$ type of $dlld$ or $lddl$ )	
	<b>1307</b> ( $B_u$ type of $dddd$ or $llll$ )	
	1307 ( $A_g$ type of $dddd$ or $llll$ )	
	<b>1294</b> ( $A_u$ type of $dlld$ or $lddl$ )	
	1291 ( $A_g$ type of $dlld$ or $lddl$ )	
$(dldlld)_n$ or $(ldlddl)_n$	<b>1335</b> ( $B_1$ type of $dldl$ or $ldld$ )	
	<b>1319</b> ( $B_u$ type of $dlld$ or $lddl$ )	
	1312 (Intermediate mode)	
	1296 (Intermediate mode)	
	<b>1293</b> ( $A_u$ type of $dlld$ or $lddl$ )	
	<b>1285</b> ( $A_1$ type of $dldl$ or $ldld$ )	

<sup>a</sup> See Figure 3.

<sup>b</sup> The boldface indicates the infrared-active mode.

would be convenient. In the first place we have treated the three regular structures, viz.,  $(dddd)_n$  or  $(llll)_n$  (e-DI),  $(dldl)_n$  or  $(ldld)_n$  (t-DI), and  $(dlld)_n$  ( $lddl$ )<sub>n</sub> (disyndiotactic, DS), by that method, and the results are given in Table II and Figures 1 and 2. It is clearly seen that the results of the approximate calculation are in good agreement with those of the exact one.

Next we have calculated the frequencies of more complex and realistic models,  $(dlld)_n$  or  $(lddl)_n$ ,  $(dddlld)_n$  or  $(lllddl)_n$ , and  $(dldlld)_n$  or  $(ldlddl)_n$  (see Table II and Fig. 3). From these calculations the frequency regions for the infrared active modes have been established as follows:  $B_1$ -type vibrations of the fractions of t-DI chain ( $dld$  or  $ldl$ ,  $dldl$  or  $ldld$ ) = 1340–1330 cm.<sup>-1</sup>;  $B_u$ -type vibration of the DS part ( $dlld$  or  $lddl$ ) = 1319–1316 cm.<sup>-1</sup>;  $B_u$ -type vibrations of the fractions of e-DI chain ( $ddd$  or  $lll$ ,  $dddd$  or  $llll$ ) = 1310–1307 cm.<sup>-1</sup>;  $A_u$ -type vibration of the DS part ( $dlld$  or  $lddl$ ) = 1296–1293 cm.<sup>-1</sup>;  $A_1$ -type vibrations of the fractions of t-DI chain ( $dld$  or  $ldl$ ,  $dldl$  or  $ldld$ ) = 1288–1282 cm.<sup>-1</sup>. This structure–frequency correlation can explain excellently the observed spectra of the *cis*- and

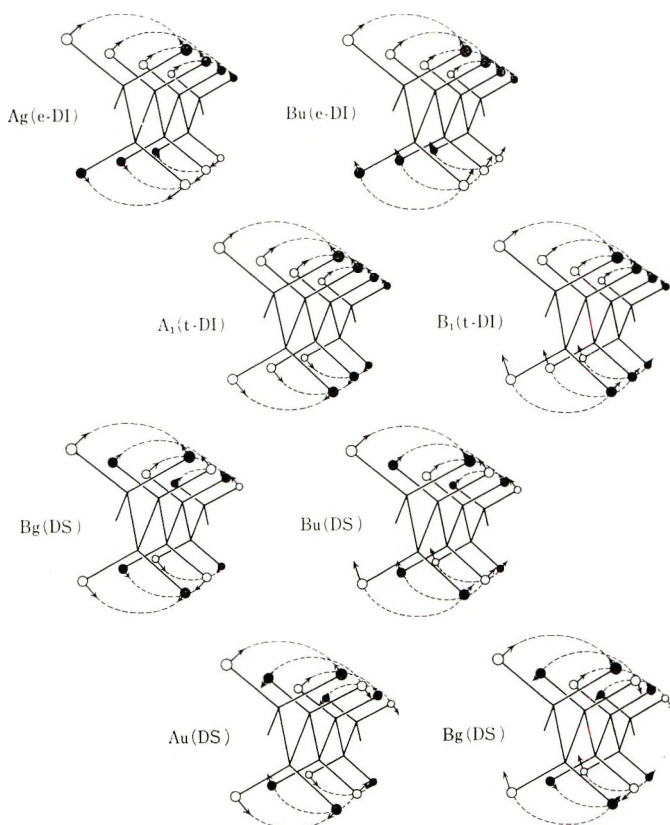


Fig. 2. Vibrational modes of CHD scissors of the three regular model structures: (O) = H; (●) = D.

*trans*-polydideuteroethylenes, giving strong confirmatory evidence to the previous conclusion that poly-*cis*-CHD=CHD and poly-*trans*-CHD=CHD have erythro- and threo-structures, respectively.

Finally we proceeded to the treatment of more sophisticated models, *viz.*,  $(\text{CH}_2\text{CHDCHDCHDCHDCH}_2)_n$ ,  $(\text{CH}_2\text{CHDCHDCHDCHDCHD}_2)_n$ , and  $(\text{CD}_2\text{CHDCHDCHDCHDCHD}_2)_n$ , where all the different configurations with respect to the portion  $-\text{CHDCHDCHDCHD}-$  were taken into account. These would follow the models for samples IV, V, VII, and VIII of the preceding paper.<sup>4</sup> The results of calculation are collected in Table III (only the infrared active modes are listed). For such complex chains also the frequency ranges mentioned above hold clearly:  $B_1$ -type vibrations of the fractions of t-DI chain = 1333–1323  $\text{cm}^{-1}$ ;  $B_u$ -type vibration of the DS part = 1317  $\text{cm}^{-1}$ ;  $B_u$ -type vibrations of the fractions of e-DI chain = 1309–1306  $\text{cm}^{-1}$ ;  $A_u$ -type vibration of the DS part = 1294  $\text{cm}^{-1}$ ;  $A_1$ -type vibrations of the fractions of t-DI chain = 1292–1285  $\text{cm}^{-1}$ . This is in agreement with the experimental results shown in Figures 3a and 3b of the preceding paper.<sup>4</sup> Sample IV, which is regarded roughly as

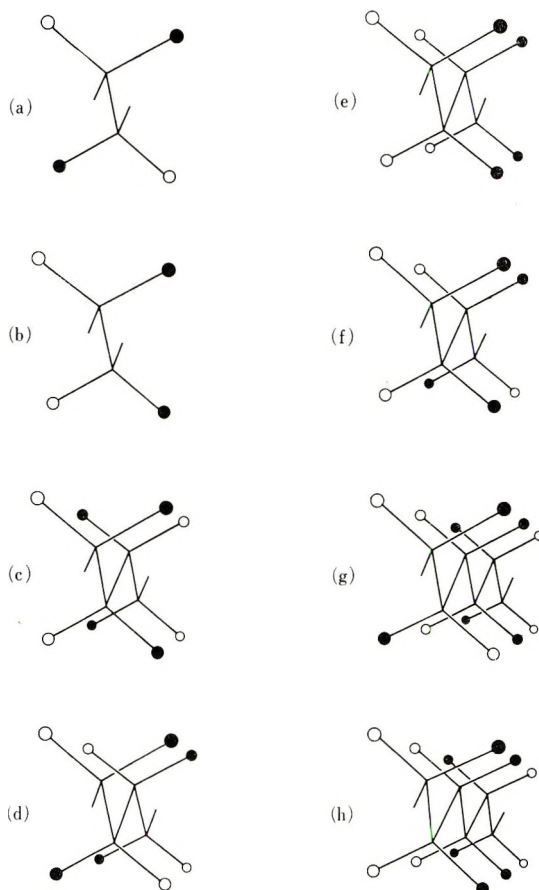


Fig. 3. Configurations of  $-(\text{CHD})_n-$ . (a) erythro unit ( $dd$ ) or ( $ll$ ); (b) threo unit ( $dl$ ) or ( $ld$ ); (c) DS unit ( $dlll$ ) or ( $lldl$ ); (d) ( $dddd$ ) $_n$  or ( $llll$ ) $_n$  (e-DI); (e) ( $dldl$ ) $_n$  or ( $lldl$ ) $_n$  (t-DI); (f) ( $dlld$ ) $_n$  or ( $ldll$ ) $_n$ ; (g) ( $dddlll$ ) $_n$  or ( $llldll$ ) $_n$ ; (h) ( $dldlll$ ) $_n$  or ( $ldllld$ ) $_n$ .

a copolymer of  $\text{CH}_2=\text{CH}_2$  and *cis*- $\text{CHD}=\text{CHD}$ , shows a band at  $1310\text{ cm.}^{-1}$ , whereas sample V which is a copolymer of  $\text{CH}_2=\text{CH}_2$  and *trans*- $\text{CHD}=\text{CHD}$  shows two bands at  $1328$  and  $1287\text{ cm.}^{-1}$ . These spectra are similar to those of poly-*cis*- $\text{CHD}=\text{CHD}$  and poly-*trans*- $\text{CHD}=\text{CHD}$  of Figure 1. Therefore it is apparent that the erythro and threo units are, respectively, abundant in samples IV and V. A similar case is found for samples VII and VIII, the former being a copolymer of  $\text{CD}_2=\text{CD}_2$  and *cis*- $\text{CHD}=\text{CHD}$  and the latter being a copolymer of  $\text{CD}_2=\text{CD}_2$  and *trans*- $\text{CHD}=\text{CHD}$ .

In conclusion we may say that we could confirm satisfactorily the earlier results<sup>1,2</sup> concerning the relationship between the monomer species and the stereo structure of resultant polymer, and the type of double-bond opening in the polymerization with Ziegler catalysts.

TABLE III  
 Calculated Frequencies of the Infrared-Active CHD Scissors  
 Vibrations of Complex Irregular Chains,  $\text{cm.}^{-1}$

Chain configuration	Calculated frequency, $\text{cm.}^{-1}$ , and mode
$(\text{CH}_2\text{CHDCHDCHDCHDCH}_2)_n$	
<i>dddd</i> or <i>llll</i>	1308 ( $B_u$ of <i>dddd</i> or <i>llll</i> )
<i>dldd</i> or <i>lldl</i>	1330 ( $B_1$ of <i>dld</i> or <i>ldl</i> ) 1307 ( $B_u$ of <i>dd</i> or <i>ll</i> ) 1288 ( $A_1$ of <i>dld</i> or <i>ldl</i> )
<i>llll</i> or <i>lddd</i>	1324 ( $B_1$ of <i>dl</i> or <i>ld</i> ) 1306 ( $B_u$ of <i>ddd</i> or <i>lll</i> ) 1292 ( $A_1$ of <i>dl</i> or <i>ld</i> )
<i>dlld</i> or <i>lldd</i>	1323 ( $B_1$ of <i>dl</i> or <i>ld</i> ) 1309 ( $B_u$ of <i>dd</i> or <i>ll</i> ) 1292 ( $A_1$ of <i>dl</i> or <i>ld</i> )
<i>dldl</i> or <i>ldld</i>	1333 ( $B_1$ of <i>dldl</i> or <i>ldld</i> ) 1285 ( $A_1$ of <i>dldl</i> or <i>ldld</i> )
<i>dlld</i> or <i>ldld</i>	1317 ( $B_u$ of <i>dlld</i> or <i>ldld</i> ) 1294 ( $A_u$ of <i>dlld</i> or <i>ldld</i> )
$(\text{CH}_2\text{CHDCHDCHDCHDCHD}_2)_n$	
<i>dddd</i> or <i>llll</i>	1308 ( $B_u$ of <i>dddd</i> or <i>llll</i> )
<i>dldd</i> or <i>lldl</i>	1329 ( $B_1$ of <i>dld</i> or <i>ldl</i> ) 1307 ( $B_u$ of <i>dd</i> or <i>ll</i> ) 1288 ( $A_1$ of <i>dld</i> or <i>ldl</i> )
<i>llll</i> or <i>lddd</i>	1323 ( $B_1$ of <i>dl</i> or <i>ld</i> ) 1307 ( $B_u$ of <i>ddd</i> or <i>lll</i> ) 1292 ( $A_1$ of <i>dl</i> or <i>ld</i> )
<i>dlld</i> or <i>lldd</i>	1323 ( $B_1$ of <i>dl</i> or <i>ld</i> ) 1309 ( $B_u$ of <i>dd</i> or <i>ll</i> ) 1292 ( $A_1$ of <i>dl</i> or <i>ld</i> )
<i>dldl</i> or <i>ldld</i>	1333 ( $B_1$ of <i>dldl</i> or <i>ldld</i> ) 1285 ( $A_1$ of <i>dldl</i> or <i>ldld</i> )
<i>dlld</i> or <i>ldld</i>	1317 ( $B_u$ of <i>dlld</i> or <i>ldld</i> ) 1294 ( $A_u$ of <i>dlld</i> or <i>ldld</i> )
$(\text{CD}_2\text{CHDCHDCHDCHDCHD}_2)_n$	
<i>dddd</i> or <i>llll</i>	1309 ( $B_u$ of <i>dddd</i> or <i>llll</i> )
<i>dldd</i> or <i>lldl</i>	1329 ( $B_1$ of <i>dld</i> or <i>ldl</i> ) 1307 ( $B_u$ of <i>dd</i> or <i>ll</i> ) 1288 ( $A_1$ of <i>dld</i> or <i>ldl</i> )
<i>llll</i> or <i>lddd</i>	1323 ( $B_1$ of <i>dl</i> or <i>ld</i> ) 1307 ( $B_u$ of <i>ddd</i> or <i>lll</i> ) 1292 ( $A_1$ of <i>dl</i> or <i>ld</i> )
<i>dlld</i> or <i>lldd</i>	1323 ( $B_1$ of <i>dl</i> or <i>ld</i> ) 1308 ( $B_u$ of <i>dd</i> or <i>ll</i> ) 1292 ( $A_1$ of <i>dl</i> or <i>ld</i> )
<i>dldl</i> or <i>ldld</i>	1333 ( $B_1$ of <i>dldl</i> or <i>ldld</i> ) 1285 ( $A_1$ of <i>dldl</i> or <i>ldld</i> )
<i>dlld</i> or <i>ldld</i>	1317 ( $B_u$ of <i>dlld</i> or <i>ldld</i> ) 1294 ( $A_u$ of <i>dlld</i> or <i>ldld</i> )



### References

1. Tasumi, M., T. Shimanouchi, H. Tanaka, and S. Ikeda, *J. Polymer Sci. A*, **2**, 1607 (1964).
2. Ikeda, S., and R. Tsuchiya, *J. Polymer Sci. B*, **3**, 29 (1965).
3. Tasumi, M., and T. Shimanouchi, *J. Chem. Phys.*, **43**, 1245 (1965).
4. Tasumi, M., T. Shimanouchi, H. Kenjo, and S. Ikeda, *J. Polymer Sci. A*, **4**, 1011 (1966).

### Résumé

Un calcul simplifié des fréquences de vibrations des groupes CHD a été effectuée pour  $(\text{CHD})_n$  de configurations différentes. La corrélation entre la fréquence de CHD et la configuration locale a été établie. Sur cette base les bandes d'absorption infrarouges de poly-*trans*-CHD=CHD et poly-*cis*-CHD=CHD apparaissant dans la région de 1350 à 1280  $\text{cm}^{-1}$  ont été interprétées en plus grand détail.

### Zusammenfassung

Eine vereinfachte Berechnung der CHD-Spreiz-Schwingungsfrequenzen wurde für  $(\text{CHD})_n$ - von verschiedener Konfiguration durchgeführt. Eine Korrelation zwischen der CHD-Spreiz-Frequenz und der lokalen Konfiguration wurde aufgestellt. Auf dieser Grundlage wurden die im Bereich von 1350 bis 1280  $\text{cm}^{-1}$  auftretenden Infrarotabsorptionsbanden von Poly-*(trans-CHD=CHD)* und Poly-*(cis-CHD=CHD)* eingehender diskutiert.

Received September 3, 1965

Prod. No. 4910A

## Grafting Vinyl Monomers to Starch by Ceric Ion.

### I. Acrylonitrile and Acrylamide

ZOILA REYES, *Stanford Research Institute, Menlo Park, California*, and  
C. E. RIST and C. R. RUSSELL, *Northern Regional Research Laboratory,  
Agricultural Research Service, U. S. Department of Agriculture, Peoria,  
Illinois*

#### Synopsis

Studies were carried out on the grafting of acrylonitrile (AN) and acrylamide (AA) to starch by ceric ion. The variables affecting the grafting of AN and AA were investigated with granular wheat starch dispersed in aqueous *N,N*-dimethylformamide and ceric ammonium nitrate as catalyst. Results showed that the concentrations of monomer and catalyst are the major factors influencing the grafting of AN; thus the monomer content of the grafts can be regulated by these variables. The grafting of AA is also influenced by these variables, but to a much less degree. Increasing concentrations of monomer promote homopolymerization and increasing concentration of catalyst inhibit grafting. The extent of grafting of this monomer can best be controlled by reaction time. Under the most favorable conditions, maximum grafting efficiency (ratio of amount of grafted monomer to total amount of monomer converted to polymer) was 87% for AN and 43.8% for AA. Although the monomer content of the AN grafts was higher than that of AA grafts prepared under identical conditions, the number of branches in the grafts was almost the same; only the length of the branches was different. The AN-starch grafts have branches of higher molecular weight.

#### INTRODUCTION

An investigation of graft copolymerization of wheat starch with a variety of vinyl monomers was undertaken as part of a research program designed to expand the industrial markets for wheat starch and starch-based products. In a preliminary evaluation of initiating systems for grafting vinyl monomers to starch, ceric ion and high-energy irradiation proved the most efficient and were selected for a more intensive study. The redox method with ceric salts, particularly ceric ion-alcohol systems, has been used for initiation of polymerization and grafting of vinyl monomers, and the kinetics and mechanism of the reaction have been studied.<sup>1-10</sup> Results from model experiments designed to elucidate the mechanism of grafting to cellulose by ceric salts<sup>10</sup> indicate that grafting is initiated by free radicals either at the  $\alpha$ -carbon atom of the primary alcohol or at a carbon atom of the 1,2-glycol in the glucose unit. The same mechanism should apply also to the starch-ceric ion system. Preliminary electron spin resonance (ESR) studies conducted at Stanford Research Institute with dry samples of

starch treated with a solution of ceric ammonium nitrate (CAN) showed that the spectrum of the free radicals produced by treatment of starch with CAN was similar to that of  $\gamma$ -irradiated starch. Both the dry CAN-treated starch powder and  $\gamma$ -irradiated starch can initiate graft copolymerization of vinyl monomers when dispersed in vinyl monomer-solvent mixtures. This paper describes a study on the grafting of acrylonitrile (AN) and acrylamide (AA) to starch by ceric ion.

## EXPERIMENTAL

### Materials

Wheat Starch (Hercules No. 120) and the ceric salts (Matheson, Coleman and Bell), CAN, and ceric ammonium sulfate (CAS), were used without further purification. Amylose was obtained by butanol fractionation of wheat starch (prepared by Roy A. Anderson of the Northern Regional Research Laboratory, Peoria, Illinois). AN, vinyl acetate (VAc), methyl methacrylate (MMA), and styrene (Matheson, Coleman and Bell) were twice distilled under vacuum before use. MMA and styrene were washed with dilute alkali before distillation to remove the inhibitor. AA (Eastman Kodak) was recrystallized from benzene and dried under vacuum at room temperature for 24 hr.

The ceric solutions, 0.1*N* CAN in 1*N* nitric acid solution and 0.1*N* CAS in 1*N* sulfuric acid solution, were standardized with arsenic trioxide by using osmium tetroxide as catalyst.<sup>11</sup> No change in the concentration of the solutions was observed in several months of storage in the dark in well-stoppered bottles.

### Grafting Procedure

The reactions were carried out under nitrogen in four-necked flasks equipped with stirrer, thermometer, and reflux condenser and immersed in a constant temperature bath. Granular starch was used in this work, except in a few experiments specifically described below. The procedure was to disperse starch in the solvent medium (water-*N,N*-dimethylformamide, 1:1 by vol.), and, after flushing with nitrogen for 30 min., the monomer and the ceric solution were added. Unless otherwise noted, 100 ml. of solvent was used per 0.05 unit mole of starch (anhydroglucose unit, AGU). Variations in the sequence of addition of monomer and catalyst were tested, but unless otherwise specified, the monomer was added before the catalyst. Hydroquinone was added at the end of the reaction to stop polymerization. The products were separated by filtration and were washed with water, aqueous methanol, and methanol. When viscous solutions were obtained, they were treated with methanol to precipitate the products, which were then separated by filtration, followed by washing with methanol. The resulting products were then extracted with appropriate solvents to remove any homopolymer produced. *N,N*-Dimethyl-

formamide-acetic acid mixture (1:1 by vol.) was used for extraction of polyacrylamide (PAA).

### Proof of Grafting

The infrared spectra of the main products and by-products of the reactions were determined, and, if these spectra indicated grafting, nitrogen analysis of the products was made. In addition, grafting was confirmed by analysis of the products of acid hydrolysis of the grafts.

The hydrolysis procedure was simple and rapid. A sample of the graft (1.0 g.) was dispersed at room temperature in 5 ml. of water, 5 ml. of concentrated HCl was added, and after stirring and warming on a steam bath for 2 min., the products were isolated. The method of isolation varied with the nature of the grafted polymer. For the AN-starch grafts, the warm mixture was filtered and the solid product was washed with the following solvents: water, 2.5% aqueous NaOH, water, 50% aqueous acetic acid, water, and methanol. The resulting product was dissolved in DMF, and after filtering, the polymer was precipitated by addition of isooctane-ethanol (1:1 by vol.). The evidence for a grafted product was the presence of the bands of glucose and those of PAN in the infrared spectrum of this DMF-soluble hydrolysis product. Elementary analysis of some hydrolysis products of the various grafts gave an approximate composition of 90-95% PAN and 5-10% glucose.

A clear solution was obtained from acid hydrolysis of the AA-starch grafts. In order to isolate the grafted PAA, the solution was cooled in an ice bath and treated with an excess of methanol. The precipitate formed was collected, washed with methanol, and redissolved in a small amount of water. After a second precipitation with methanol, the solid was extracted with DMF to remove starch hydrolysis products and was washed with methanol. The product was again dissolved in water, reprecipitated by addition of methanol, filtered, and dried. When the original product was a graft, the dried product was soluble in formamide-acetic acid, and its infrared spectrum showed the bands of PAA and of glucose.

### Molecular Weight Determinations

The molecular weight of the grafted PAN was determined viscometrically in DMF by using the purified water-insoluble acid hydrolyzate of the graft. Viscosity-average molecular weight  $\bar{M}_v$  was calculated from the equation relating intrinsic viscosity and molecular weight, with the constants reported for PAN in DMF:<sup>12</sup>

$$[\eta] = 2.43 \times 10^{-4} \bar{M}_v^{0.75} \quad (1)$$

For the determination of the molecular weight of the grafted PAA, the viscosity of the polymer isolated from acid hydrolysis of the graft was measured in 1*N* sodium nitrate, and the weight-average molecular weight was calculated with eq. (2):<sup>13</sup>

$$[\eta] = 3.73 \times 10^{-4} \bar{M}_w^{0.66} \quad (2)$$

## RESULTS AND DISCUSSION

### Comparison of Monomer Reactivity

In a preliminary study of ceric ion-induced grafting to starch, monomers of different polarity were used in order to assess their relative reactivity toward grafting. The results of a series of experiments conducted with CAS starch and AN, AA, MMA, VAc, and styrene are shown in Table I. Any homopolymer produced was removed by extracting the products with suitable solvents. PAN and PAA solvents were given above. Acetone was used to extract poly(methyl methacrylate), and benzene was used for extraction of poly(vinyl acetate) and polystyrene.

TABLE I  
Ceric Ion-Induced Grafting of Vinyl Monomers to Starch  
(Reaction time, 3 hr. at 50°C.)<sup>a</sup>

Monomer	Monomer wt., g. (0.1 mole)	Homopolymer, g.	Starch graft, g.	Nitrogen, %	Monomer in graft, %
AN <sup>b</sup>	5.3	0.26	8.49	2.93	11.09
AA	7.1	1.91	7.33	0.82	4.17
MMA	10.0	0.52	10.91	—	25.70 <sup>c</sup>
VAc	8.6	1.00	—	—	—
Styrene	10.4	Trace	—	—	—

<sup>a</sup> In each experiment 0.16 g. ceric ammonium sulfate dihydrate in 2.5 ml. 1*N* H<sub>2</sub>SO<sub>4</sub> was used; 8.1 g. (0.05 unit mole) granular starch dispersed in 100 ml. of water-DMF (1:1 by vol.) used, except in No. 1, where 50 ml. was used.

<sup>b</sup> Reaction performed at room temperature.

<sup>c</sup> Calculated from the increase in weight of the original starch and the weight of the graft.

Grafted products, along with varying amounts of homopolymer, were obtained with AN, MMA, and AA, the relative activity of these monomers toward grafting being in the order listed. VAc and styrene yielded small amounts of homopolymer; monomer was recovered from the experiments with AA, VAc, and styrene. Some increase in the degree of grafting was achieved with AN, AA, and MMA by working with swollen or gelatinized instead of granular starch. Swollen starch was prepared by heating the aqueous DMF dispersion to 65°C. for 1 hr., and for the gelatinized starch the dispersion was heated at 85°C. for 1 hr. These preliminary studies on grafting to starch by ceric ion indicated that polar monomers such as AN, AA, and MMA can be grafted readily, but less polar ones, VAc and styrene, are difficult to graft or require different experimental conditions.

### Ceric Ammonium Nitrate vs. Ceric Ammonium Sulfate

In all the experiments described above, CAS was used as catalyst. The regular practice was to prepare a fresh solution of the salt for each experiment. However, to avoid errors resulting from variations in the concen-



tration of the catalyst, standard solutions were prepared. In addition, it was considered important to compare the catalytic efficiency of CAS with that of CAN, in order to use the more satisfactory salt in future experiments.

The results obtained in reactions conducted for 1 hr. at 30°C. with standard solutions of CAS and CAN (0.1*N* CAS in 1*N* H<sub>2</sub>SO<sub>4</sub> and 0.1*N* CAN in 1*N* HNO<sub>3</sub>), starch (0.05 unit mole), and 0.1 mole of either AN or AA in 100 ml. of aqueous DMF are shown in Table II.

TABLE II

Monomer	Catalyst ( $2.5 \times 10^{-3}$ mole/l.)	Monomer in graft, %
AN	CAS	9.92
AN	CAN	11.46
AA	CAS	4.51
AA	CAN	3.75

To judge from the degree of grafting achieved, CAN was a better catalyst for grafting AN, and CAS was slightly more effective in the grafting of AA. However, since the sulfate ion has a stronger tendency than the nitrate ion to form complexes with ceric ion,<sup>14</sup> and since the complexes are so stable that at certain concentration the sulfate inhibits formation of alcohol-ceric ion complexes,<sup>15</sup> CAN was used in subsequent studies.

### Grafting Acrylonitrile and Acrylamide

The variables affecting the ceric ion-induced grafting of AN and AA to starch were studied.

**Effect of Concentration of Catalyst.** The effect of the concentration of CAN on the grafting of AN and AA to starch is shown in Figure 1. It can be seen that a significant increase in the degree of grafting was achieved with AN when the CAN concentration was  $5.0 \times 10^{-3}$  mole/l. At higher concentrations the degree of grafting slightly decreased. The amount of homopolymer produced increased slightly (from 10% to 14% of the original amount of AN present in the reaction) as catalyst concentration was increased from  $2.5 \times 10^{-3}$  to  $1.0 \times 10^{-2}$  mole/l.

In grafting AA, increasing the concentration of CAN from  $2.5 \times 10^{-3}$  to  $1.0 \times 10^{-2}$  mole/l. brought a substantial increase in the amount of homopolymer produced, but little change in the degree of grafting. The amount of polyacrylamide (PAA) produced ranged from 6.5 to 20.7% of the original weight of AA in the reaction.

**Effect of Delayed Addition of the Monomer.** Because ceric salts can initiate the polymerization of certain vinyl monomers,<sup>14,15</sup> such as AN and MMA, and can form complexes with both starch and the monomer, the effect of mode of addition of the catalyst was investigated. The reactions were carried out with identical concentrations of CAN and under identical

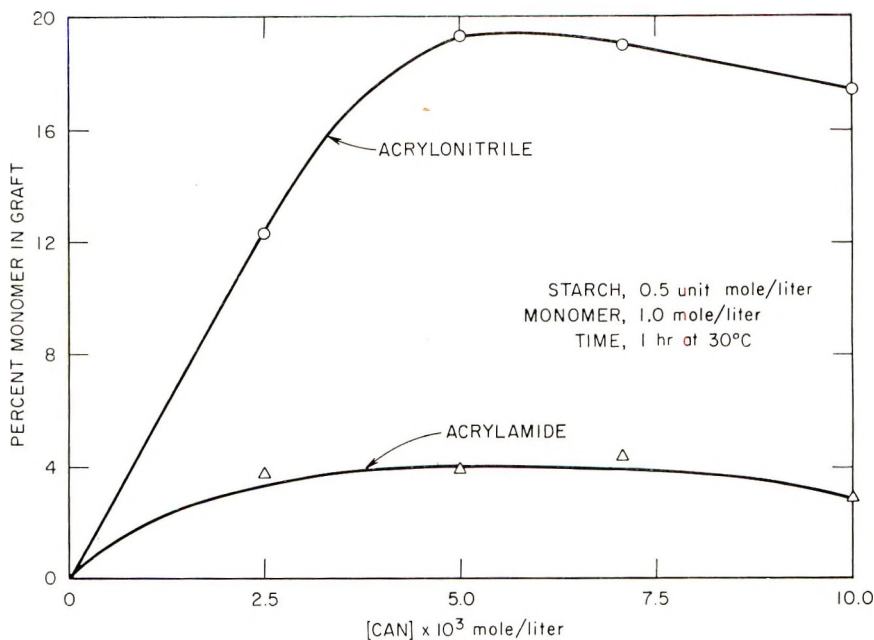


Fig. 1. Effect of catalyst concentration on grafting.

conditions to those of Figure 1, except that the catalyst was added to the dispersed starch 30 min. before addition of the monomer (Tables III and IV). For comparison, the values obtained from the normal addition (immediately after the monomer) of CAN are presented. As can be observed in grafting AN (Table III), the degree of grafting was considerably lowered when the catalyst was added before the monomer, and there was a slight decrease in the amount of PAN produced. However, for AA (Table IV), delayed addition of the monomer brought a slight increase in the degree of grafting but a large increase in the amount of homopolymer produced.

**Effects of Portionwise Addition of the Catalyst.** The effect of portionwise addition of the catalyst in the grafting of AN and AA was evaluated in two sets of experiments conducted with each monomer and two different concentrations of CAN (Tables V and VI). Regardless of the number of portions used in these experiments, the monomer was added before the catalyst. In the first set, the catalyst ( $4.87 \times 10^{-3}$  mole/l.) was added in two equal portions at 1-hr. intervals, and the total reaction time was 2 hr. For comparison, a control experiment was run in which the catalyst was added in one portion and the reaction was allowed to proceed for 2 hr. In the second set, the catalyst ( $7.1 \times 10^{-3}$  mole/l.) was added in three equal portions at 1-hr. intervals; the total reaction time was 2 hr. In the control experiment, the catalyst was added in one portion at the beginning of the reaction, which was run for 3 hr.

TABLE III  
Effect of Delayed Addition of Acrylonitrile (AN) in  
Ceric Ion-Induced Grafting to Starch  
(Reaction Time, 1 hr. at 30°C.)<sup>a</sup>

Catalyst concentra- tion, mole/l.	CAN added 30 min. before monomer			CAN added immediately after monomer		
	PAN, g. <sup>b</sup>	Graft, g.	AN in graft, % <sup>c</sup>	PAN, g. <sup>b</sup>	Graft, g.	AN in graft, % <sup>c</sup>
$2.5 \times 10^{-3}$	0.50	7.45	2.38	0.53	8.10	12.26
$5.0 \times 10^{-3}$	0.65	8.58	11.85	0.63	8.25	19.27
$1.0 \times 10^{-2}$	0.58	9.08	12.40	0.78	8.88	17.43

<sup>a</sup> In each experiment 5.3 g. (0.1 mole) of monomer and 8.1 g. (0.05 unit mole) Hercules wheat starch No. 120 in granular form dispersed in 100 ml. aqueous *N,N*-dimethylformamide (1:1, water:DMF), minus volume of CAN standard solution were used.

<sup>b</sup> Polyacrylonitrile.

<sup>c</sup> Calculated from nitrogen analysis of the graft.

TABLE IV  
Effect of Delayed Addition of Acrylamide (AA)  
in Ceric Ion-Induced Grafting to Starch  
(Reaction Time, 1 hr. at 30°C.)<sup>a</sup>

Catalyst concentra- tion, mole/l.	CAN added 30 min. before monomer			CAN added immediately after monomer		
	PAA, g. <sup>b</sup>	Graft, g.	AA in graft, % <sup>c</sup>	PAA, g. <sup>b</sup>	Graft, g.	AA in graft, % <sup>c</sup>
$2.5 \times 10^{-3}$	1.10	7.78	4.14	0.45	7.35	3.76
$5.0 \times 10^{-3}$	1.65	7.93	3.55	0.69	7.53	3.91
$1.0 \times 10^{-2}$	1.79	8.56	4.32	1.47	8.04	2.89

<sup>a</sup> In each experiment 7.1 g. (0.1 mole) monomer and 8.1 g. (0.05 unit mole) Hercules wheat starch No. 120 in granular form dispersed in 100 ml. aqueous *N,N*-dimethylformamide (DMF) (1:1 water:DMF), minus volume of CAN standard solution were used.

<sup>b</sup> Polyacrylamide.

<sup>c</sup> Calculated from nitrogen analysis of the graft.

Portionwise addition of the catalyst caused a considerable decrease in the degree of grafting in the reactions with AN (Table V), and a slight increase in the amount of PAN produced was observed at the higher CAN concentration. Consequently, CAN should be added in one portion. The results obtained with AA (Table VI) showed that larger amounts of PAA were produced when the catalyst was added in portions. An increase in the degree of grafting was observed in the first experiment, but not in the second one, where larger amounts of catalyst appeared to inhibit the grafting reaction. Therefore, addition of the catalyst in one portion is preferable with both AN and AA.

**Effect of Grafting Time.** The grafting of AN and AA as a function of time is shown in Figure 2. As can be observed, with both monomers, the rate of grafting increases with time first, but as polymerization proceeds,

TABLE V  
Effect of Portionwise Addition of Catalyst in Grafting  
Acrylonitrile (AN) to Starch  
(Reaction Temperature 30°C.)<sup>a</sup>

Expt. no.	Catalyst concentrations, mole/l.	No. of portions added at 1-hr. intervals	PAN, g.	Starch graft, g.	AN in graft, % <sup>b</sup>
1 <sup>c</sup>	$4.87 \times 10^{-3}$	2	0.31	9.85	10.30
Control	$4.87 \times 10^{-3}$	1	0.33	10.73	19.42
2 <sup>d</sup>	$7.1 \times 10^{-3}$	3	0.97	8.47	13.01
Control	$7.1 \times 10^{-3}$	1	0.37	10.65	19.60

<sup>a</sup> In each experiment 5.3 g. (0.1 mole) AN and 8.1 g. (0.05 unit mole) Hercules wheat starch No. 120, in granular form, dispersed in aqueous DMF (100 ml. minus volume of standard CAN solution) were used.

<sup>b</sup> Calculated from nitrogen analysis of the graft.

<sup>c</sup> Reaction time 2 hr.

<sup>d</sup> Reaction time 3 hr.

TABLE VI  
Effect of Portionwise Addition of Catalyst in Grafting  
Acrylamide (AA) to Starch  
(Reaction temperature 30°C.)<sup>a</sup>

Expt. no.	Catalyst concentration, mole/l.	No. of portions added at 1-hr. intervals	PAA, g.	Starch graft, g.	AA in graft, % <sup>b</sup>
1 <sup>c</sup>	$4.87 \times 10^{-3}$	2	3.73	7.52	9.99
Control	$4.87 \times 10^{-3}$	1	2.81	7.64	5.73
2 <sup>d</sup>	$7.1 \times 10^{-3}$	3	4.54	7.67	4.16
Control	$7.1 \times 10^{-3}$	1	2.90	7.77	4.42

<sup>a</sup> In each experiment 7.1 g. (0.1 mole) AA and 8.1 g. (0.05 unit mole) Hercules wheat starch No. 120, in granular form, dispersed in aqueous DMF (100 ml. minus volume of standard CAN solution) were used.

<sup>b</sup> Calculated from nitrogen analysis of the graft.

<sup>c</sup> Reaction time 2 hr.

<sup>d</sup> Reaction time 3 hr.

the rate decreases, and a maximum grafting level is soon reached. However, AN grafts at a much faster rate than AA; the maximum grafting value was achieved with AN in 30–40 min., whereas a longer period, 100–110 min., was needed for AA to reach a maximum grafting value, and this was considerably lower than that achieved with AN.

**Effect of Monomer Concentration.** The effect of monomer concentration on the grafting of AN and AA was evaluated in a series of polymerizations in which the concentration of the monomers was varied from 1 to 8 moles per unit of starch. The results are shown in Figure 3, where the degree of grafting, expressed as percentage of monomer in the graft, was plotted as a

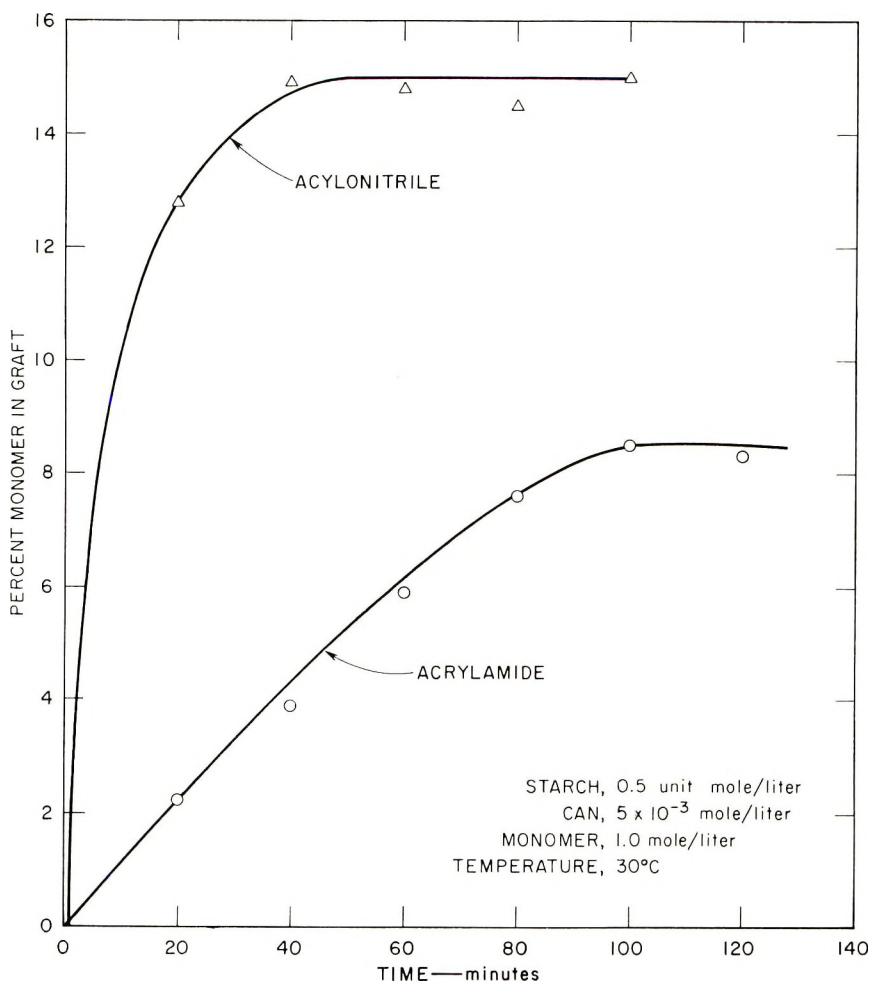


Fig. 2. Grafting as a function of time.

function of the concentration of monomer. In grafting AN, increasing its concentration increased the degree of grafting, and although total conversion was low (24–35%), the amount of AN converted to homopolymer was always lower than the amount grafted. Consequently, the grafting efficiency (ratio of amount of grafted monomer to total amount of monomer converted to polymer) was higher than 50% in all reactions. Actually, the grafting efficiency increased with the concentration of AN and showed a maximum (62.5%) at an AN concentration of 1 mole/l. However, a higher grafting efficiency (87%) was attained at this AN concentration by using the optimum CAN concentration ( $5 \times 10^{-3}$  instead of  $2.5 \times 10^{-3}$  mole/l.). For AA, the degree of grafting also increased with increasing concentrations of AA, but the percentage of monomer grafted was significantly lower than that attained in the reactions with AN. In addition, the amount of AA converted to homopolymer was larger than the amount grafted; therefore,



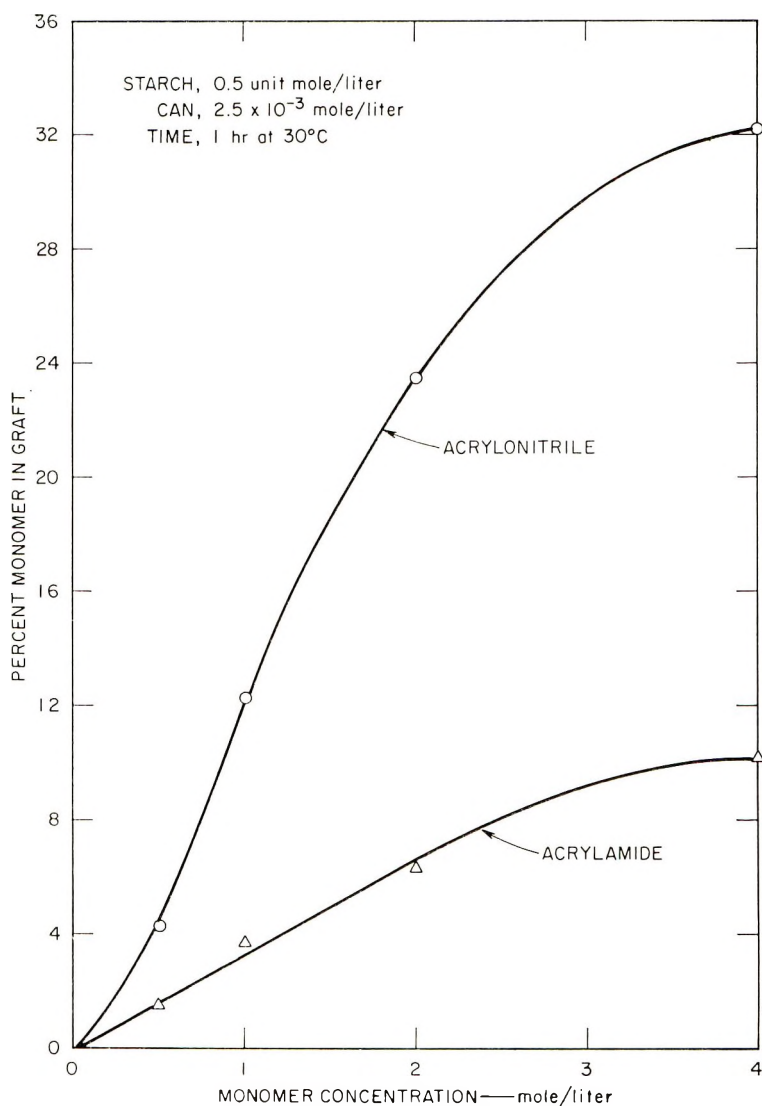


Fig. 3. Effect of monomer concentration on grafting.

grafting efficiency was lower than 50% in these experiments with AA. A maximum grafting efficiency (43.8%) was observed at an AA concentration of 1 mole/l.

In general, it can be concluded that in grafting AN to starch by CAN, the concentrations of monomer and of catalyst are the major factors influencing the degree of grafting. The grafting of AA is also affected by these variables, but is largely dependent on the time of reaction. Low concentrations of AA and CAN are more satisfactory, since large concentrations of AA favor homopolymerization and a high CAN concentration inhibits grafting. Under the conditions of this study, CAN-AA appeared

to be a more efficient redox system than CAN-starch, since larger amounts of AA are converted to PAA than are grafted to starch.

Other factors influencing the grafting of AN and AA are the rate of diffusion of the monomers into starch, the reaction medium, and the state of the starch, i.e., granular, swollen, or gelatinized. Swollen and gelatinized starch yielded starch grafts of higher monomer content than granular starch. These results indicate that starch in swollen and gelatinized forms is more accessible to both monomer and catalyst than granular starch. Such a reasoning is supported by the results obtained in an experiment conducted with amylose, the linear fraction of starch, which is isolated in nongranule form. The reaction was performed with 8.1 g. of amylose and 5.3 g. of AN in 100 ml. of aqueous DMF at a CAN concentration of  $5 \times 10^{-3}$  mole/l. Conversion was 89% and only traces of homopolymer were produced. The AN-amylose graft obtained, 12.9 g., contained 36.2% AN. This high degree of grafting was not achieved with whole starch granules under similar conditions.

AA-starch grafts prepared with gelatinized starch could hardly be separated from the PAA produced in the reaction. Both AN and AA graft at a faster rate when water alone is used as a solvent for the reaction. The kinetics of grafting AN to starch by ceric ion in water dispersions will be presented in a forthcoming paper.

### Molecular Weight of the Grafted Polymer

For molecular weight determinations, larger samples of the AN-starch and AA-starch grafts were prepared in reactions conducted with a 2:1 mole ratio of monomer to starch in aqueous DMF at a CAN concentration of  $5 \times 10^{-3}$  mole/l. The concentration of the monomers in the reaction medium was 1 mole/l., and that of starch, 0.5 anhydroglucose units (AGU)/l. After extraction of the homopolymer produced, the AN graft contained 18.8% grafted AN and the AA graft contained 3.5% AA. The intrinsic viscosity of the PAN and PAA obtained by hydrolysis of the grafts was determined in DMF and 1N sodium nitrate respectively. The molecular weights of both polymers were calculated according to eqs. (1) and (2).  $\bar{M}_v$  for the grafted PAN was 48,900 or 51,900 expressed as weight-average molecular weight,  $\bar{M}_w$ . The  $\bar{M}_w$  for the grafted PAA was 7900. The number of AGU/branch calculated from the  $\bar{M}_w$  and the monomer content of the grafts was 1380 AGU/PAN branch and 1347 AGU/PAA branch, which shows that despite the higher degree of grafting achieved with AN, the number of branches in the two grafts (AN and AA) is about the same. However, the length of the chains is different; the AN-starch graft has longer branches than the AA graft.

This research was done by Stanford Research Institute, Menlo Park, California, under contract with the U. S. Department of Agriculture and authorized by the Research and Marketing Act of 1946. The contract was supervised by the Northern Regional Research Laboratory, Agricultural Research Service, U. S. Department of Agriculture, Peoria, Illinois.

### References

1. Mino, G., and S. Kaizerman, *J. Polymer Sci.*, **31**, 242 (1959).
2. Mino, G., and S. Kaizerman, *J. Polymer Sci.*, **31**, 393 (1959).
3. Mino, G., S. Kaizerman, and E. Ramussen, *J. Polymer Sci.*, **39**, 523 (1959).
4. Mino, G., S. Kaizerman, and E. Ramussen, *J. Am. Chem. Soc.*, **81**, 1494 (1959).
5. Kimura, S., and M. Imoto, *Makromol. Chem.*, **42**, 140 (1960).
6. Schwab, E., V. Stannett, and J. J. Hermans, *Tappi*, **44**, 251 (1961).
7. Richards, G. N., *J. Appl. Polymer Sci.*, **5**, 539 (1961).
8. Katai, A. A., V. K. Kulshrestha, and R. H. Marchessault, *J. Polymer Sci. C*, **2**, 403 (1963).
9. Richards, G. N., and E. F. T. White, paper presented at International Symposium of Macromolecular Chemistry, Paris, July 1-6, 1963.
10. Iwakura, T., Y. Kurosaki, and N. Nakabayashi, paper presented at International Symposium of Macromolecular Chemistry, Paris, July 1-6, 1963.
11. Gleu, K., *Z. Anal. Chem.*, **95**, 305 (1933).
12. Cleland, R. L., and W. H. Stockmayer, *J. Polymer Sci.*, **17**, 473 (1955).
13. *Polyacrylamide*, *New Products Bulletin*, American Cyanamid Co., 1955.
14. Hardwick, T. J., and E. Robertson, *Can. J. Chem.*, **29**, 828 (1951).
15. Ardon, M., *J. Chem. Soc.*, **1957**, 1811.
16. Saldick, J., *J. Polymer Sci.*, **19**, 73 (1956).
17. Venkatakrisnan, S., and M. Santapa, *Makromol. Chem.*, **27**, 51 (1958).

### Résumé

Des études ont été effectuées concernant le greffage de l'acrylonitrile et l'acrylamide sur l'amidon au moyen d'ions cériques. Les variables affectant le greffage de l'acrylonitrile et de l'acrylamide ont été étudiées avec l'amidon de froment granulé dispersé dans le diméthylformamide aqueux et en présence de nitrate acérique ammoniacal comme catalyseur. Les résultats montrent que les concentrations en monomère et catalyseur sont les facteurs principaux influençant le greffage de l'acrylonitrile; par conséquent, la teneur en monomère des produits greffés peut être réglée par ces deux variables. Le greffage de l'acrylamide est également influencé par ces deux variables, mais toutefois à un degré moindre. Des concentrations croissantes en monomères favorisent l'homopolymérisation et des concentrations décroissantes de catalyseurs inhibent le greffage. Le degré de greffage de ce monomère peut le mieux être contrôlé par le facteur temps. Dans les conditions les plus favorables l'efficacité maximum de greffage (rapport de la quantité de monomère greffé à la quantité totale de monomère converti en polymères) s'élève à 87% pour l'acrylonitrile et à 43% pour l'acrylamide. Bien que la teneur en monomère des produits greffés d'acrylonitrile était plus élevée que celle des produits à l'acrylamide préparés dans des conditions identiques, le nombre de ramifications dans les polymères greffés était pratiquement le même; uniquement la longueur des branches était différente. Les produits greffés d'acrylonitrile sur l'amidon ont des branches de poids moléculaire plus élevé.

### Zusammenfassung

Eine Untersuchung der Aufpfropfung von Acrylnitril (AN) und Acrylamid (AA) auf Stärke mittels Cerionen wurde ausgeführt. Die Variablen, welche die Aufpfropfung von AA und AN beeinflussen, wurden an granulierter, in wässrigem *N,N*-Dimethylformamid dispergierter Weizenstärke mit Cerammoniumnitrat als Katalysator untersucht. Die Ergebnisse zeigen, dass die Monomer- und Katalysatorkonzentration den Haupteinfluss auf die Aufpfropfung von AN besitzt; der Monomergehalt der Aufpfropfungen kann daher durch diese Variablen reguliert werden. Auch die Aufpfropfung von AA wird, jedoch zu einem viel geringeren Grad, durch diese Variablen beeinflusst. Steigende Monomerkonzentration fördert die Homopolymerisation und steigende Katalysatorkonzentra-

tion behindert die Aufpfropfung. Das Ausmass der Aufpfropfung dieses Monomeren kann am besten durch die Reaktionsdauer kontrolliert werden. Unter den günstigsten Bedingungen betrug die maximale Pfropfungsausbeute (Verhältnis der Menge des aufgefropften Monomeren zur Gesamtmenge des in Polymeres ungewandelten Monomeren) für AN 87% und für AA 43,8%. Obgleich der Monomergehalt von AN-Aufpfropfungen höher als derjenige der unter identischen Bedingungen hergestellten AA-Aufpfropfungen war, war doch die Anzahl der Zweige in den Aufpfropfungen fast die gleiche; nur die Länge der Zweige war verschieden. Die AN-Stärke-aufpfropfungen besitzen Zweige mit höherem Molekulargewicht.

Received August 9, 1965

Prod. No. 4917A

## Analysis of the Base-Catalyzed Phenol- Epichlorohydrin Condensation\*

GEORGE L. BRODE and JOHN WYNSTRA, *Plastics Division, Union Carbide Corporation, Bound Brook, New Jersey*

### Synopsis

The amount of abnormal addition of phenoxide to epichlorohydrin and phenyl glycidyl ether was determined as a function of reaction conditions. The isomer distribution resulting from attack at either position of these unsymmetrical epoxides was quantitatively measured by vapor phase chromatography of the resulting product mixtures. While both epoxides reacted predominantly in the expected normal fashion, small quantities of abnormal addition products were found whose concentrations were temperature-dependent. The analytical method also permitted a study of the effect of temperature on side reactions involving hydrolytic solvents.

### INTRODUCTION

Various workers<sup>1,2</sup> have demonstrated that anions generally add to the least-substituted carbon atom of the oxirane ring. While this mode of addition (normal) is often predominant, a careful product analysis of several reactions thought to proceed exclusively in this direction revealed the presence of small but measurable concentrations of (abnormal) products arising from attack at the more substituted carbon atom.<sup>3-5</sup> In the case of the base-catalyzed condensation of a diphenol with epichlorohydrin to prepare either epoxy resins with a theoretical functionality of two or high molecular weight polymeric condensates,<sup>6-8</sup> the isomeric product distribution is of primary importance. The selectivity of this reaction was studied as a function of temperature in model systems, where phenol was substituted for the diphenol, and the results are the subject of this paper. In addition to obtaining the required data on selectivity, observations were also made on solvent participation and the relative potential of phenyl glycidyl ether versus epichlorohydrin to add phenoxide ion abnormally.

The product distribution was measured after having first synthesized the products related to those of the polymer system (Fig. 1) and then developing analytical techniques, based on vapor-phase chromatography, for their accurate detection in complex mixtures. Compound VI of

\* Paper presented at the 148th Meeting of the American Chemical Society, September 1964.



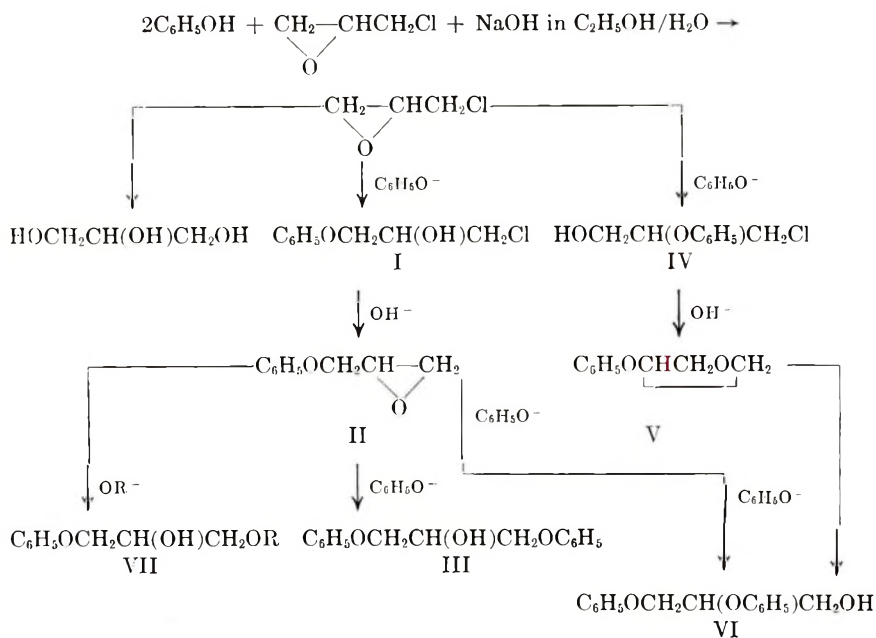
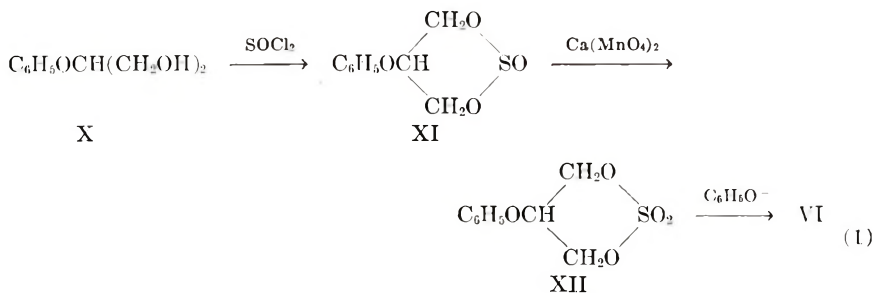
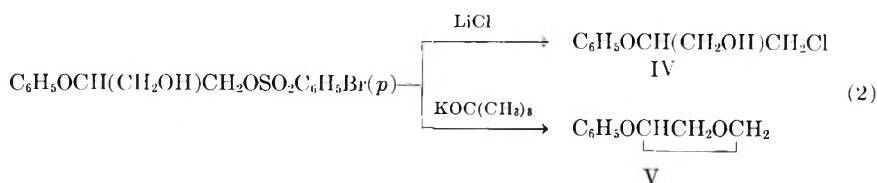


Fig. 1. Potential products from the base-catalyzed condensation of phenol with epichlorohydrin.

Figure 1 was unambiguously synthesized as shown in eq. (1),\* while eq. (2) illustrates the unambiguous synthesis of compounds IV and V. All other products listed in Figure 1 have been previously reported in the literature.



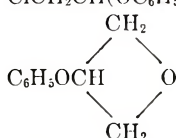
\* Compound XI, 2-phenoxypropylenesulfite-1,3 has been reported by Ben Ishay<sup>9</sup> and later recorded<sup>10</sup> as arising from a rearrangement on treatment of 3-chloropropylene sulfite with sodium phenoxide. The material prepared in these laboratories exhibits quite different physical properties from those cited in the above references. That our material is in fact the six-membered cyclic sulfite is based on physical data summarized in the experimental part, as well as our ability to separate compound XI into geometrical isomers, either of which could be oxidized to the same cyclic sulfate, compound XII, or hydrolyzed back to the starting diol, X. A future publication will deal with the conformational assignments of these isomers.



## RESULTS AND DISCUSSION

The product distribution as a function of reaction conditions is shown in Table I with the mole per cent calculations based on a minimum average of two separate experiments per set of reaction conditions. The reaction was studied under essentially three different sets of reaction conditions summarized as follows: (A) reactants maintained at 30°C. for several

TABLE I  
Product Distribution as a Function of Reaction Conditions

Compound	Isolated product, mole-%			
	Expt. A (yield 98%)	Expt. B (yield 98%)	Expt. C (yield 93%) <sup>a</sup>	Expt. D (yield 92%) <sup>a</sup>
$\text{C}_6\text{H}_5\text{OCH}_2\text{CH}(\text{OH})\text{CH}_2\text{OC}_6\text{H}_5$	97.2	96.5	99.3	99.4
$\text{C}_6\text{H}_5\text{OCH}_2\text{CH}(\text{OC}_6\text{H}_5)\text{CH}_2\text{OH}$	0.48	0.68		
$\text{ClCH}_2\text{CH}(\text{OC}_6\text{H}_5)\text{CH}_2\text{OH}$	0.11	0.29	0.31	0.11
	0.03	0.04	0.02	0.15
$\text{C}_6\text{H}_5\text{OCH}_2\text{CH}(\text{OH})\text{CH}_2\text{OC}_2\text{H}_5$	2.2	2.4	—	—
$\text{HOCH}_2\text{CH}(\text{OH})\text{CH}_2\text{OH}$	—	—	0.37	0.30

<sup>a</sup> The yields in experiments C and D were always low as a result of volatilization of epichlorohydrin before and during removal of water.

hours prior to reflux in ethanol solvent (85°C.); (B) reactants immediately heated to reflux in ethanol solvent (85°C.); (C, D) reactants immediately heated to reflux and eventually subjected to forcing conditions without the use of solvent (C = 120°C.; D = 168°C.). To avoid working with very reactive products such as 1-chloro-3-phenoxypropanol or phenyl glycidyl ether, a 2:1 mole ratio of phenol to epichlorohydrin was used. The presence of glycerol in experiments A and B was obscured by the proximity in retention time of it with ethoxy phenoxypropanol. In C and D where this problem did not exist (no solvent employed), glycerol was found in relatively small concentration and it can be reasonably concluded that its concentration is also small in experiments A and B. The concentration of the hydrolysis product of phenyl glycidyl ether, phenoxypropanediol-1,2, is not listed because of the uncertainty involved in its measurement.

In addition to the major components present in the reaction products as summarized in Table I, the chromatograms of experiments A and B showed two identical trace components (area per cent less than that of oxetane, V) of unknown origin or identity, one of which was also common to experiments C and D. Experiments C and D also contained a second trace component which appeared in the chromatogram of the products from an independent rate study on the addition of phenoxide to 2-phenoxy-3-chloropropanol, IV, indicating this component was due to a side reaction directly involving abnormal chlorohydrin. Other than these, no component of unassigned structure was observed in the chromatograms.

A number of conclusions can be drawn from the data in Table I. First, side reactions resulting from abnormal addition of the phenoxy anion to epoxide occur under all conditions studied, but a prior low temperature reaction effectively reduces the amount of abnormal addition, as measured by the concentrations of 2,3-diphenoxypropanol, 2-phenoxy-3-chloropropanol, and 3-phenoxyoxetane in experiments A and B, respectively. The data also reveal the presence of solvent-terminated products, appearing in the first two experiments as ethoxy phenoxypropanol and in the last two as glycerol. The effect of a prior low-temperature reaction on reducing solvent participation is minimal and is in accord with the theory that solvent termination is a characteristic "late" reaction, independent of initial reaction conditions, occurring to the greatest extent after the buffer system is destroyed (i.e., beyond the 90% reaction mark, where alkoxide begins to replace phenoxide in the reaction mixture). This interpretation is further demonstrated by the kinetic experiments summarized in Figure 2, in which the base-catalyzed addition of phenol to phenyl glycidyl ether was studied as a function of phenol concentration. As can be seen, the reaction obeys pseudo first-order kinetics with change in slope only after phenol is consumed, i.e., where the reactive species changes from phenoxide to alkoxide.

The effect of forcing conditions on the concentration of 2-phenoxy-3-chloropropanol also bears mention and is apparent from comparison of experiments C and D. The use of high temperature is effective in further reacting the abnormal chlorohydrin; however, as shown by the increase in oxetane concentration, a substantial amount is converted to this equally unreactive species by hydroxide ion present at the end of the reaction. Brief rate studies showed that under experimental conditions similar to A or B, more than 90% unreacted 2-phenoxy-3-chloropropanol or 3-phenoxyoxetane could be recovered.

The sluggish reactivity of abnormal chlorohydrin, and similarly the unreactivity of oxetane toward phenoxide ion, leads to the conclusion that the major portion of 2,3-diphenoxypropanol, VI, arises from abnormal addition to phenyl glycidyl ether and implies that phenyl glycidyl ether is slightly more prone to abnormal addition than epichlorohydrin (cf. concentration of 2,3-diphenoxypropanol with 2-phenoxy-3-chloropropanol plus 3-phenoxyoxetane in Table I). This implication is rather surprising

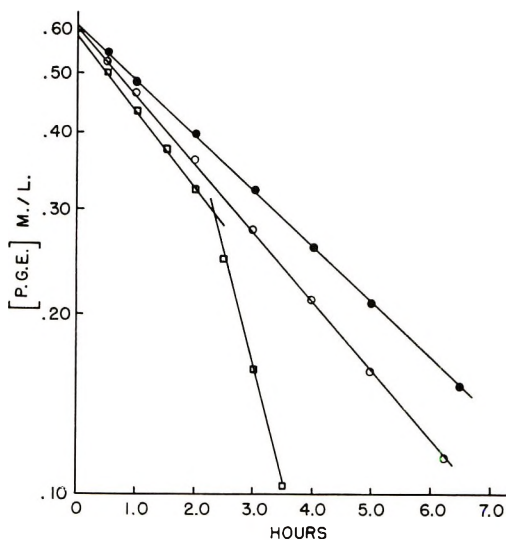


Fig. 2. Plot of base-catalyzed addition of phenol to phenyl glycidyl ether (PGE) in ethanol solvent at 75.0°C.: (●) 1.219 mole phenol, 0.5900 mole PGE; (○) 0.6051 mole phenol, 0.5885 mole PGE; (□) 0.3001 mole phenol, 0.5782 mole PGE. Each experiment contains 0.0235 mole NaOH and 0.55 mole H<sub>2</sub>O per 100 ml. solution.

since the polar substituent constant  $\sigma^*$  for a chloromethylene group is, reportedly, 1.050 whereas that for a phoxymethylene group is only 0.850.<sup>11</sup> Considering that the steric requirements for addition to either epoxide would be about equal, that neither material would be expected to exhibit any conjugation factor to influence the site of attack and that the mechanism of phenoxide to either epoxide must be essentially identical, i.e., largely  $S_N2$  character, one would have predicted epichlorohydrin to be slightly more disposed to abnormal addition. The absence of strongly electron-withdrawing substituents in either epoxide explains the minimal amount of reaction at the secondary carbon of these materials and is responsible for their utility in preparing epoxy resins of high functionality and molecular weight.

## EXPERIMENTAL

### Preparations

**1,3-Diphenoxypropanol (III).** Phenol (94.0 g., 1.0 mole), phenyl glycidyl ether (152.1 g., 1.0 mole), Cellosolve solvent (150 g.), and potassium hydroxide (1.0 g.) were mixed and carefully warmed to effect solution. After gradually raising the temperature, the reactants were refluxed for 16 hr., cooled, and poured with stirring into 300 ml. of water. The yellowish precipitate was recrystallized several times from 95% ethanol to yield a white crystalline product, m.p. 80.4–81.0°C. (lit.:<sup>12</sup> m.p. 80–

81°C.). A 3,5-dinitrobenzoate ester melted 119.3–120.2°C. after recrystallization from 90/10 methanol–water.

ANAL. Calcd. for  $C_{22}H_{18}N_2O_8$ : C, 60.27%; H, 4.14%; N, 6.43%. Found: C, 60.06%; H, 3.92%; N, 6.43%.

**2,3-Diphenoxypropanol (VI).** A solution of 2.1 g. (0.0087 mole) of 2-phenoxypropylene sulfate-1,3 (XII) in 4.0 ml. dioxane was added dropwise with stirring to a solution containing 0.36 g. (0.0087 mole) NaOH, 0.82 g. (0.0087 mole) phenol, 3.0 ml. dioxane, and 1.0 ml.  $H_2O$  heated at 80°C. under an argon blanket. The mixture was permitted to stir overnight at 90°C. after which the dioxane was removed in a nitrogen stream and the resulting slurry was extracted with ether. The ether extract was washed with water and 5% NaOH, dried over  $MgSO_4$ , filtered, and evaporated to yield 1.0 g. (94%) of 2,3-diphenoxypropanol, b.p. 135°C./0.5 mm.

ANAL. Calcd. for  $C_{15}H_{16}O_3$ : C, 73.75%; H, 6.60%. Found: C, 73.60%; H, 6.71%.

A 3,5-dinitrobenzoate ester (from methanol–water) had m.p. 120–120.5°C.

ANAL. Calcd. for  $C_{22}H_{18}N_2O_8$ : C, 60.27%; H, 4.14%; N, 6.39%; O, 29.20%. Found: C, 60.41%; H, 4.06%; N, 6.24%; O, 29.08%.

A mixed melting point with the 3,5-dinitrobenzoate of 1,3-diphenoxypropanol-2(III) was depressed 23°C.; m.p. (50/50 mixture) 97–105°C.

An NMR spectrum of 2,3-diphenoxypropanol in  $CHCl_3$  shows the methyne quintet centered at 270 cps, the phenoxymethylene doublet at 238 cps, and the hydroxymethylene doublet at 225 cps. The NMR spectrum of 1,3-diphenoxypropanol, on the other hand, shows the doublet characteristic of four equivalent methylene protons and the single methyne proton to be the same order of magnitude as the spin coupling constant existing between the groups. Therefore, it closely matches a spectrum for an  $A_4B$  system having all  $J_{AB}$ 's equal with the difference in chemical shift and coupling constant  $\gamma_A - \gamma_B/J_{AB} = 3$ .

**2-Phenoxypropylenesulfate-1,3 (XII).** An 8-g. portion (0.37 mole) of phenoxypropylenesulfite-1,3 (XI a or b) was dissolved in 25.0 ml. glacial acetic acid and while maintaining a temperature of 10–12°C., 15.0 g.  $Ca(MnO_4)_2 \cdot 4H_2O$  (0.043 mole) dissolved in 12.0 ml. of water was added dropwise over a period of 2 hr. Vigorous stirring and an ice–salt bath were required to control this very exothermic reaction. The resultant viscous mixture was poured with stirring onto 43 g. of  $Na_2CO_3$  plus 30 g. crushed ice, contained in a large beaker, to reduce frothing. After adding 2.0 g.  $NaHSO_3$ , the then brown slurry was extracted with ether by a decantation technique; the ether layer was dried over  $MgSO_4-Na_2CO_3$  and evaporated to yield 3.5 g. (40%) of crude product, m.p. 96–104°C. Recrystallization from benzene–petroleum ether yielded white crystalline needles, m.p. 118–119°C.



ANAL. Calcd. for  $C_9H_{10}O_3S$ : C, 46.95%; H, 4.38%; S, 14.19%. Found: C, 47.12%; H, 4.30%; S, 14.19%.

An infrared spectrum taken as a KBr pellet showed, among others, the following major bands ( $\text{cm.}^{-1}$ ): 1603(s), 1495(s); 1244(s); 1005(s) and 871(s) (S-O); 1405(s) and 1205(s) (O-SO<sub>2</sub>-O-).<sup>13</sup>

**2-Phenoxypropylenesulfite-1,3 (XI).** Phenoxypropanediol-1,3<sup>14</sup> (35.0 g., 0.21 mole) was dissolved in 100 ml. methylene chloride, and 29.5 g. (0.25 mole, 20% excess) of thionyl chloride was added dropwise over a period of 2 hr. Addition completed, the mixture was refluxed for 15 min. and the excess thionyl chloride decomposed with 5.0 ml. of water. The organic layer was rapidly extracted with cold 5% K<sub>2</sub>CO<sub>3</sub> solution, dried over MgSO<sub>4</sub>, and the solvent removed under reduced pressure. Distillation of the crude product yielded three fractions.

XIa: 6.3 g., b.p. 118–124°C./14 mm., solidified on standing, m.p. 36–44°C.; recrystallization from ethanol–water produces white fibrous needles, m.p. 58–59.4°C.

ANAL. Calcd. for cyclic sulfite,  $C_9H_{10}O_4S$ : C, 50.47%; H, 4.71%; S, 14.97%. Found: C, 50.66%; H, 4.97%; S, 15.11%.

XIb: 9.00 g., b.p. 124–128°C./0.14 mm., eventually solidifies, m.p. 36–42°C.

XIc: 23.5 g., b.p. 128–130°C./0.14 mm., solidifies immediately; recrystallization from ethanol–water yields white needles, m.p. 68.5–69.5°C.

ANAL. Calcd. for cyclic sulfite,  $C_9H_{10}O_4S$ : C, 50.47%; H, 4.71%; S, 14.97%. Found: C, 50.42%; H, 4.71%; S, 15.12%.

That fractions XIa and XIc are geometrical isomers and not, for example, merely different crystalline forms of the same material was ascertained from a study of both solid and solution spectra, the differences being observed in either state. In addition, a molecular weight determination on compound XIc was in accord with the theoretical value; m.w. IXc = 219 (theory = 214), indicating the XIc is not a dimorphic form of XIa. Also ruled out is the possibility that either XIa or XIc is the rearranged five-membered cyclic sulfite, both on the basis of chemical reactions and infrared analysis. With regard to the latter, examination of 1,2- and 1,3-cyclic sulfites\* has shown that compounds possessing the 1,3-structure have two absorption bands in the 600–400  $\text{cm.}^{-1}$  region attributed to vibrations of the six-membered ring, and in addition, the characteristic S-O stretching frequency customarily appearing at 1214  $\text{cm.}^{-1}$  in 1,2 sulfites<sup>15–18</sup> is seen to be displaced by about 25  $\text{cm.}^{-1}$  in 1,3-sulfites. Both of these spectral phenomena were observed with materials XIa and XIc.

\* De La Mare et al.<sup>15</sup> observed the phenomenon of geometrical isomerism in the case of 2-chloropropylenesulfite-1,3, while, more recently, Pritchard and Lauterbur<sup>16</sup> reported on geometrical isomerism in five-membered cyclic sulfites.

**2-Phenoxy-3-chloropropanol (IV).** Phenoxypropanediol-1,3-monobrosylate (XIII) (10.0 g., 0.025 mole) and lithium chloride, 5.0 g. (0.12 mole) were heated in 100 ml. absolute ethanol at 65°C. for 24 hr. After removal of most of the ethanol, the semisolid residue was partitioned between chloroform-water, the chloroform layer dried over  $\text{MgSO}_4$ , and the solvent removed to yield 2.48 g. (51%) of 1,3-chlorohydrin, b.p. 114–116°C./1.8 mm.,  $n_D^{19}$  1.5399.

ANAL. Calcd. for  $\text{C}_9\text{H}_{11}\text{O}_2\text{Cl}$ : C, 57.91%; H, 5.94%; Cl, 19.00%. Found: C, 58.07%; H, 6.07%; Cl, 19.20%.

**3-Phenoxyoxetane (V).** Phenoxypropanediol-1,3-monobrosylate (XIII) (17.0 g., 0.044 mole) was dissolved in 70 ml. of *tert*-butyl alcohol (distilled from calcium hydride), and 58 ml. of 1.07M (0.062 mole) potassium *tert*-butoxide solution was added dropwise over a period of 2 hr. while maintaining a temperature of 25°C. After stirring an additional hour, 200 ml. of pentane was added and the mixture cooled in a Dry Ice-acetone bath. The solid *tert*-butyl alcohol and inorganic salts were rapidly removed by filtration, washed with an additional 200 ml. of cold pentane, and the pentane removed to yield 4.7 g. (71%) of oxetane, b.p. 110°C./13.5 mm.

ANAL. Calcd. for  $\text{C}_9\text{H}_{10}\text{O}_2$ : C, 71.98%; H, 6.71%. Found: C, 71.76%; H, 6.53%.

In addition to having the required infrared absorption bands characteristic of monosubstituted phenyl, ether, etc., a strong band at 980  $\text{cm}^{-1}$  was also observed, attributed to a four-membered cyclic ether.<sup>19</sup>

**2-Phenoxypropanediol 1,3-Monobrosylate (XIII).** Phenoxypropanediol-1,3 (X) (20.0 g., 0.12 mole) was dissolved in 80 ml. anhydrous pyridine and cooled to 0°C. *p*-Bromobenzenesulfonyl chloride (30.15 g., 0.12 mole) was then added in portions over a 3-hr. period, and the resulting mixture was stirred at 0°C. for 2 days. The mixture was poured on cracked ice containing 130 ml. of concentrated hydrochloric acid, and the oil that resulted was immediately taken up in  $\text{CCl}_4$  and dried over  $\text{MgSO}_4$ . Removal of  $\text{CCl}_4$  yielded 30 g. of a viscous oil (66% yield) which eventually solidified and exhibited a wide melting point. This solid was dissolved in a 50/50 mixture of methanol-isopropyl alcohol, seeded with phenoxypropanediol 1,3-dibrosylate (XIV), and fractionally crystallized to produce 19.8 g. of crude monobrosylate ester, m.p. 60–70°C. Recrystallization from isopropyl alcohol yielded pure monobrosylate, m.p. 68–70°C.

ANAL. Calcd. for  $\text{C}_{15}\text{H}_{15}\text{O}_5\text{SBr}$ : C, 46.52%; S, 8.28%; Br, 20.64%. Found: C, 46.44%; S, 8.52%; Br, 20.46%.

**2-Phenoxypropanediol 1,3-Dibrosylate (XIV).** This was prepared from phenoxypropanediol-1,3 (X) and two moles of brosyl chloride in 48% yield by the same procedure as above. Recrystallization from methanol yielded pure dibrosylate, m.p. 113–114°C.

ANAL. Calcd. for  $C_{21}H_{18}O_3S_2Br_2$ : C, 41.60%; S, 10.58%; Br, 26.36%. Found: C, 41.46%; S, 10.55%; Br, 26.42%.

### Reaction Conditions and Experimental Procedure

The product mixtures obtained from the following four sets of reaction conditions were examined: (A) reactants mixed and stirred at 30°C. for 12–14 hr. and then refluxed (85°C.) for 3 hr. to complete the reaction; (B) reactants mixed and immediately heated to reflux and maintained there for 3 hr. (within 10 min. after addition of the last component, a temperature of 85°C. had been reached); (C) epichlorohydrin added to a water solution of phenol and sodium hydroxide at 70°C.; after subsidence of the exotherm, water was removed by direct distillation with an eventual pot temperature of 110°C. being developed and comprising a total reaction time of 50 min.; (D) conditions similar to C except that on reaching a pot temperature of 110°C., xylene was added to azeotrope the last traces of water, a maximum temperature of 168°C. being reached within a total reaction time of 36 min.

The experimental procedure involved mixing phenol (23.54 g., 0.25 mole), absolute ethanol (in A and B) (28.8 g., 0.625 mole), and 23.73% sodium hydroxide solution (23.0 g., 0.136 mole) in a 250-ml. flask equipped with mechanical stirrer and condenser, cooling the resulting mixture to 23–30°C., and then adding 11.59 g. (0.125 mole) of epichlorohydrin. In experiments C and D, a Dean-Stark trap was used in series with the condenser. After completion of the reaction, 50 ml. of absolute ethanol was added to prevent premature crystallization of 1,3-diphenoxypropanol (III), and the excess caustic was carefully neutralized with hydrochloric acid, a pH meter being used for endpoint control. Most of the ethanol and water was then removed under a nitrogen stream at ambient temperatures and the vapors condensed in a series of traps for eventual examination by gas phase chromatography. Fresh ethanol was added to the reaction mixture and most of the major product (normally about 80%) 1,3-diphenoxypropanol, was fractionally crystallized after filtration of sodium chloride, with subsequent concentration of all other side products in a single fraction of suitable concentration for quantitative gas-phase analysis.

### Product Analysis

The product analysis was accomplished by vapor-phase chromatography after having first determined relative retention times of the various model compounds, and area-per cent to weight-per cent conversion factors for each component in synthetic mixtures of concentrations approximately equal to those found in the actual product mixtures. Only in the case of 3-phenoxypropanediol-1,2 (compound VII, R = H), was the accuracy sufficiently poor to make questionable any conclusions regarding its absolute concentration; in the cases of oxetane (V), abnormal chlorohydrin (IV).

ethoxyphenoxypropanol (VII), and the diphenoxypropanols (III and VI), the relative maximum error in absolute concentration was found to be respectively,  $\pm 7.2$ ,  $\pm 6.8$ ,  $\pm 6.8$ , and  $< \pm 1\%$  on the column used.\* Unfortunately, the accurate determination of the isomer distribution of the diphenoxypropanols (III and VI) on this column was complicated by the close proximity of retention times (about 2 min.) and tailing of the first isomer eluted (1,3-diphenoxypropanol (III)). Much better results were obtained in the resolution of these isomers on a modified polyphenyl ether column,† and this permitted calculation of the isomer distribution as summarized in Table I. The calculations recorded in Table I were based on a minimum average of two separate experiments per set of reaction conditions stated above.

The authors wish to acknowledge the efforts of Mr. George P. Hellerman, Dr. R. B. Hanselman, and Dr. W. F. Beach in the analytical phases of this problem.

### References

1. Eliel, E. L., in *Steric Effects in Organic Chemistry*, M. S. Newman, Ed., Wiley, New York, 1956, pp. 106–114.
2. Winstein, S., and R. B. Henderson, in *Heterocyclic Compounds*, Vol. I, R. C. Elderfield, Ed., Wiley, New York, 1950, pp. 22–46.
3. Chitwood, H. C., and B. J. Freure, *J. Am. Chem. Soc.*, **68**, 680 (1946).
4. Chapman, N. B., N. S. Isaacs, and R. E. Parker, *J. Chem. Soc.*, **1959**, 1925.
5. Bartlett, P. D., and S. D. Ross, *J. Am. Chem. Soc.*, **70**, 926 (1948).
6. Reinking, N. H., A. E. Barnabeo, and W. F. Hale, *J. Appl. Polymer Sci.*, **7**, 2135 (1963).
7. Reinking N. H., A. E. Barnabeo, and W. F. Hale, *J. Appl. Polymer Sci.*, **7**, 2145 (1963).
8. Reinking, N. H., A. E. Barnabeo, W. F. Hale, and J. H. Mason, *J. Appl. Polymer Sci.*, **7**, 2153 (1963).
9. Ben Ishay, D., *J. Org. Chem.*, **23**, 2013 (1958).
10. Van Woerden, H. F., *Chem. Rev.*, **63**, 564 (1963).
11. Taft, R. W., Jr., *J. Am. Chem. Soc.*, **75**, 4231 (1953).
12. Stephens, D. W., *Chem. Ind. (London)*, **1932**, No. 51, 375.
13. Garner, H. K., and H. J. Lucas, *J. Am. Chem. Soc.*, **72**, 5497 (1950).
14. Charkin, S. W., *J. Am. Chem. Soc.*, **70**, 3522 (1948).
15. De La Mare, P. B. D., et al., *J. Chem. Soc.*, **1956**, 1813.
16. Pritchard, J. G., and P. C. Lauterbur, *J. Am. Chem. Soc.*, **83**, 2105 (1961).
17. Barnard, D., J. Fabian, and H. Koch, *J. Chem. Soc.*, **1949**, 2442.
18. Vogel-Hogler, *Acta Phys. Austriaca*, **1**, 328 (1948).
19. Barrow, G. M., and S. Searles, *J. Am. Chem. Soc.*, **75**, 1175 (1953).

\* F and M, Model 500; 2 m., 0.15% Carbowax-4M on 30–60 mesh glass beads. Column temperature 75°C. for 1 min., programmed to 200°C. at 7.5°C./min. Injection port and detector block temperature 300°C.; flow 60 cc./min., 5  $\mu$ l. sample size with helium as carrier gas.

† F and M Model 500; 3 m., 0.15% modified polyphenyl ether on 140–170 mesh glass beads. Column temperature 250°C. Injection port and detector block, 300°C.; 1  $\mu$ l. sample size with helium as carrier gas.

### Résumé

L'importance de l'addition anormale de phénoxyde à l'épichlorhydrine et à l'éther phényl-glycidique a été déterminée en fonction des conditions de réaction. La distribution des isomères résultant de l'attaque à l'une des positions de ces époxydes asymétriques a été mesurée quantitativement par chromatographie en phase vapeur du mélange des produits formés. Tandis que les deux époxydes réagissent principalement de la façon normale attendue, de faibles quantités de produits d'addition anormale ont été trouvées; leurs concentrations est fonction de la température. La méthode analytique permet également une étude de l'effet de la température sur des réactions secondaires d'hydrolyse par solvant.

### Zusammenfassung

Der Betrag an abnormaler Addition von Phenoxyd an Epichlorhydrin und Phenylglycidyläther wurde als Funktion der Reaktionsbedingungen bestimmt. Die sich aus dem Angriff auf die beiden Stellungen dieser unsymmetrischen Epoxyde ergebende Isomerenverteilung wurde durch Gaschromatographie der entsprechenden Reaktionsgemische quantitativ bestimmt. Während beide Epoxyde vorwiegend in der erwarteten normalen Weise reagierten, wurden doch auch kleine Mengen abnormaler Additionsprodukte gefunden, deren Konzentrationen sich als temperaturabhängig erwiesen. Die analytische Methode erlaubte schliesslich eine Untersuchung des Einflusses der Temperatur auf Nebenreaktionen unter Beteiligung hydrolytischer Lösungsmittel.

Received July 21, 1965

Prod. No. 4918A



## Efficiencies of Some Ethyl Acrylate Chain Terminators

LEON B. LEVY and GENE J. FISHER, *Celanese Chemical Company,  
Research and Development Department, Clarkwood, Texas*

### Synopsis

A group of substituted phenols, quinone, and tropone were used to retard AIBN-initiated ethyl acrylate polymerization in ethyl propionate solution at 44.7°C. in the absence of oxygen. It was concluded that the efficiency of retardation depended upon the ability of the terminator to stabilize a positive charge on its reaction site in the transition state. Tropone was found to be a particularly good retarder. The radical-trapping efficiency of 2,2-diphenyl-1-picrylhydrazyl in this system was found to be 50-60%.

### INTRODUCTION

It has been noted<sup>1,2</sup> that polymerization chain terminators which are efficient for monomers like styrene and vinyl acetate are often not nearly so effective for acrylates and methacrylates.

The generally accepted kinetic scheme for free-radical polymerization in the absence of oxygen<sup>1</sup> is shown in eqs. (1)-(7):

Initiator decomposition:



Propagation:



Addition:



Chain transfer (or copolymerization):



Radical-radical combination

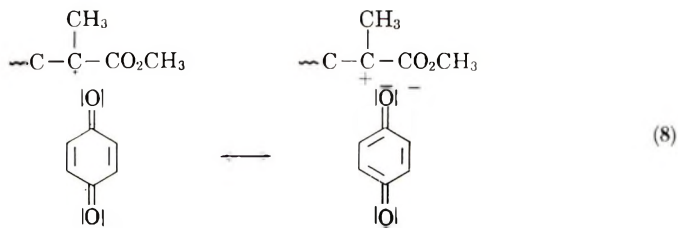


Here I represents initiator;  $R\cdot$  is initiator or polymer chain radical; M is monomer; X is chain terminator; and  $Z\cdot$  is the terminator radical.

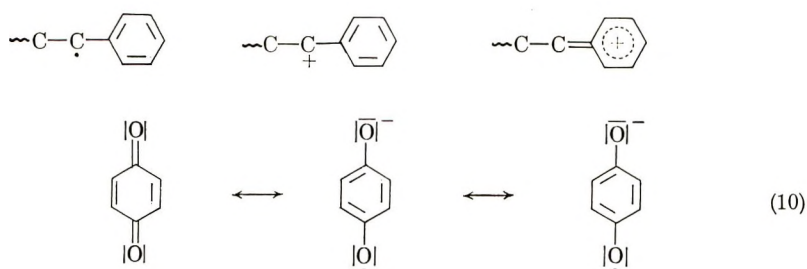
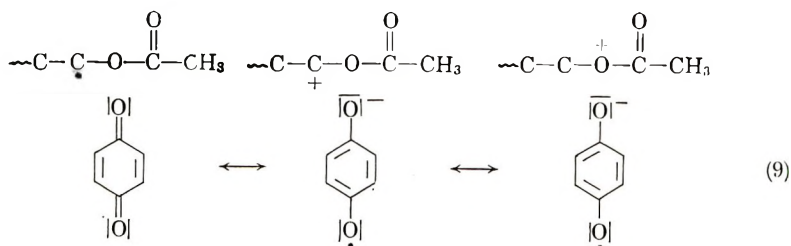
Generally speaking, termination (retardation or inhibition) is a process wherein  $R\cdot$  is replaced by a less reactive radical in the addition step. Moreover, the higher the ratio  $k_z/k_p$ , the more efficient the retardation. The rate of the addition step will be greater, the greater the thermodynamic stability of  $Z\cdot$  (since the transition state for the process presumably possesses some of the character of  $Z\cdot$ ). In addition, the value of  $k_z$  will be influenced by polar contributing structures in the addition transition state.<sup>3</sup>

The suggestion that polar influences played significant roles in homolytic reactions was reviewed by Walling<sup>4</sup> to explain cases where copolymerization of a pair of monomers was possible, even though the monomers could not be polymerized individually. There is also a tendency for a copolymer radical to grow in steps alternating between the addition of one monomer unit and then the other. This was explained by considering the nucleophilic or electrophilic properties of each type of polymer radical and each monomer double bond. A growing polymer radical ending in a maleic anhydride fragment (which is quite electrophilic) would be much more likely to add to an electron-rich molecule of styrene than another electron-deficient maleic anhydride molecule. The relative reactivity of a given monomer has been expressed in terms of two parameters.<sup>5</sup> One parameter is a function of the general reactivity of the monomer molecule and reflects such factors as steric hindrance to the double bond and resonance stabilization of the double bond in the ground state and of the odd electron in the transition state. The second parameter is a function of the polar environment in the vicinity of the olefinic double bond of the monomer. When the values of these parameters are determined for a group of monomers by examining the relative reactivity for copolymerization of certain pairs in the group, these parameters can be used to predict the relative reactivity for a novel pair of monomers, and the values obtained are fairly close to those experimentally determined.

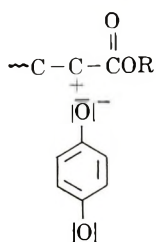
The process of the inhibition of radical polymerization is quite analogous to that of copolymerization. Instead of the polymer radical reacting with one of two monomers it either reacts with monomer or inhibitor, and here again polar factors must certainly play an important role in determining which reaction will occur more readily. It has been suggested that the transition state in the chain termination step of methyl methacrylate polymerization inhibited by benzoquinone consists of the canonical forms<sup>2</sup> shown in eq. (8).



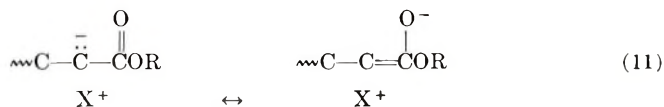
Similar situations may obtain when monomers like vinyl acetate or styrene are inhibited with compounds which cause electron withdrawal from the polymer chain radical.



Now in the case of an acrylate monomer, it will be seen that an analogous polar contribution to the transition state would place a partial positive charge on a carbon atom  $\alpha$  to a carboxyl group, i.e.,



This electronic arrangement is of a relatively higher energy because of the destabilization of the carbonium ion by the carboxyl group. This may account in part for the fact that monomers like vinyl acetate and styrene are generally easier to inhibit than the acrylates. However, if an electron-donating inhibitor were employed, the corresponding ionic canonical form would be as shown in eq. (11),



and it will be seen that this system is resonance-stabilized, and hence favored, especially if the inhibitor moiety  $\text{X}^+$  also possesses resonance stabilization.

By choosing a terminator with an electron-rich active site, it may also be expected that the value of  $k_t$  will be enhanced, since the terminator radical  $Z\cdot$  will be relatively electron-donating, and as stated before  $M\cdot$  is electron-accepting. The possibility exists, however, that because of the electron-donating nature of  $Z\cdot$ , chain transfer will be facilitated as well, thus reducing the apparent efficiency of the terminator. The screening of various model compounds in this investigation will show the effect of the relative electron-donating tendency of  $X$  on the overall rate of AIBN-initiated polymerization of ethyl acrylate.

### EXPERIMENTAL

The reagents used in this work were purified by distillation or by successive recrystallization until the melting point remained unchanged (usually to within  $2^\circ\text{C}$ . of the reported values).

The method used to determine the rates of polymerization of ethyl acrylate in this study was a modification of the dilatometric procedure used by Bartlett and Kwart.<sup>6</sup> The dilatometer used is schematically represented in Figure 1. The "legs" of the dilatometer were charged with

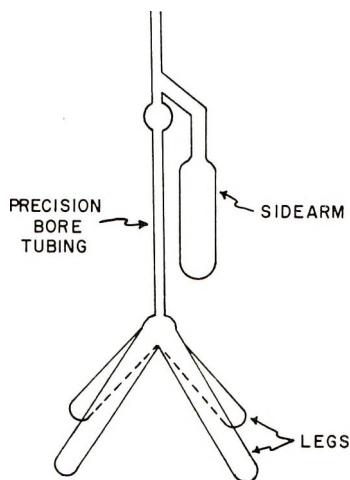


Fig. 1. Dilatometer.

ethyl acrylate solution in ethyl propionate containing the azobisisobutyronitrile (AIBN) used as initiator. The "arm" of the instrument was charged with the terminator to be employed dissolved in 2.0 ml. of ethyl propionate. The amounts of materials used were such that when the contents of the arm were mixed with the monomer solution, the concentration of ethyl acrylate was  $4.57M$  and that of AIBN,  $1.21 \times 10^{-3}M$ .

The contents of the dilatometer were exhaustively degassed by the usual freeze-thaw vacuum technique until the pressure above the solution at liquid nitrogen temperature was not reduced by additional degassing (this

pressure was usually less than  $5\mu$ ). The dilatometer was sealed and immersed in a bath at  $44.7 \pm 0.01^\circ\text{C}$ . The amount of solution in the dilatometer legs was such that on warming to bath temperature the meniscus was somewhere in the precision bore tubing. The monomer solution was allowed to polymerize to the extent of ca. 0.5% (this usually occurred in less than 15 min. from time of immersion in the bath), at which point the terminator solution in the sidearm was thoroughly mixed with the monomer solution. The meniscus was readjusted to be in the precision bore tubing by returning some solution to the sidearm.

The prepolymerization process insured that the last traces of oxygen were removed from the monomer solution. When this procedure was omitted, the synergism between the trace of oxygen left after the degassing procedure and the retarder used was often strong enough to give spurious induction periods. It was found<sup>7</sup> that the per cent shrinkage of these solutions of ethyl acrylate could be converted to per cent polymerization by multiplication by a factor of 9.90. (This had been determined by finding the specific gravities of ethyl acrylate solutions partially polymerized by ultraviolet irradiation in the presence of biacetyl.) Polymerization was allowed to proceed to ca. 3.5% in each kinetic run, during which time the concentration of monomer, AIBN, and terminator remained essentially unchanged, and plots of per cent polymerization versus time were linear. The rate constants reported are calculated from the least-square slopes of these plots. Several of the rate constants are average values obtained from two or three experiments.

## RESULTS AND DISCUSSION

### Phenolic Terminators

The rate constant for the uninhibited polymerization of ethyl acrylate under the experimental conditions used here is given at the head of Table I. It is the average of values obtained from 10 kinetic runs. The standard deviation in these runs was  $0.1 \times 10^{-4}$  mole/l.-sec. at the 68% confidence level.

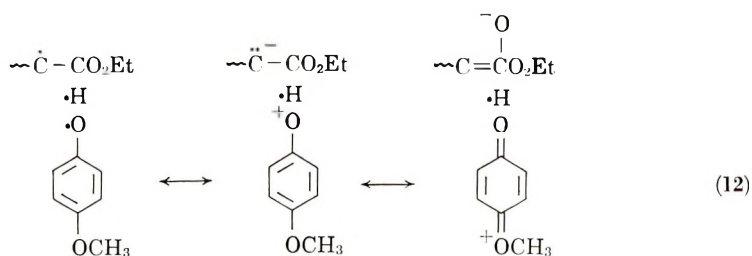
First it will be seen that although phenol itself is not a retarder, its *p*-methoxy derivative is measurably active as a chain terminator. This could be the result of any of the following factors: (a) an intrinsic radical-trapping ability of the methoxy group; (b) resonance stabilization of the terminator (phenoxy) radical by the methoxy group; (c) less chain transfer due to the methoxy group; (d) stabilization of a partial positive charge on the phenolic oxygen atom in the addition transition state by the methoxy group; (e) enhancement of the rates of radical-radical combination reactions by the methoxy group. Factor (a) can be ruled out due to the inefficiency of anisole as a terminator. The only resonance stabilization of a phenoxy radical possible with a *p*-methoxy group involves charge separation and is probably not important. Factor (c) probably does not



TABLE I  
Over-all Rate Constants for the Polymerization of Ethyl Acrylate in the  
Presence of Some Phenols

Compound	Terminator		Induction period, min.	Pseudo zero-order rate constant, mole/l.-sec. $\times 10^4$
	Concentration			
	ppm	Molarity $\times 10^4$		
None			0	1.6
Phenol	100	9.61	1	1.6
Anisole	114	9.52	0	1.6
Hydroquinone monomethyl ether	131	9.54	14	1.3
2,6-Dimethoxyphenol	168	9.52	2	0.73
2,6-Di- <i>tert</i> -butylphenol	217	9.52	0	1.2
2,4,6-Tri- <i>tert</i> -butylphenol	277	9.52	0	1.1
<i>m</i> -Methoxyphenol	131	9.54	0	1.5
Methyl <i>p</i> -hydroxybenzoate	162	9.58	0	1.5
Hydroquinone	99	8.15	0	1.2
Pyrocatechol	99	8.15	0	0.72
Resorcinol	100	8.16	0	1.5
Methyl 2,5-dihydroxybenzoate	152	8.18	0	1.4
Pyrogallol	100	7.12	4	0.78
Phloroglucinol	99	7.11	2	1.0

obtain, because the *p*-methoxyphenoxy radical is more nucleophilic than the phenoxy radical and would be expected to be more reactive toward monomer. Factor (*d*) was mentioned previously and should apply in this case.



The electron-transfer contributing structures shown in eq. (12) for hydrogen donation are analogous to those invoked by Russell<sup>8</sup> for the side-chain chlorination of *p*-substituted toluenes. Finally, factor (*e*) must be considered. It has been found<sup>4</sup> in copolymerization studies that the most favored radical-radical combinations are usually those involving two unlike radicals. In the system at hand this would involve a combination between Z· and R·. Since the acrylate polymer chain radical is electron-accepting, the process will be favored by the presence of electron-releasing substituents on the phenoxy radical.

The conclusion reached by comparing the overall retarding efficiency of phenol with that of hydroquinone monomethyl ether is that the enhance-

ment of  $k_x$  and  $k_c$  by the electron-donating *p*-methoxy group evidently outweighs any enhancement of  $k_0$ , the chain-transfer rate constant. In the case of 2,6-dimethoxyphenol the overall effect of two methoxy groups on the retarding efficiency of phenol is even more evident.

The introduction of *tert*-butyl groups to the *ortho* positions of phenol results in several effects, including an electron enrichment of the ring, steric hindrance to hydrogen abstraction,<sup>9</sup> and a reduction in the amount of chain transfer by the phenoxy radical.<sup>10</sup> Since the retarding efficiencies of 2,6-di-*tert*-butylphenol and 2,4,6-tri-*tert*-butylphenol are of the same order of magnitude as most of the other phenols tested, the multiplicity of effects mentioned above makes an interpretation of the overall polymerization rate constant difficult.

The addition of a *p*-*tert*-butyl group to 2,6-di-*tert*-butylphenol would be expected to increase its retarding ability if chain transfer through the *para* carbon atom were important, and because of its inductive effect. The fact that the efficiencies of the di- and tri-*tert*-butylphenols are very similar indicates that chain transfer at the *para* carbon is not occurring to any great extent, and it suggests the possibility that the steric hindrance of the two *ortho* substituents "swamps out" the inductive effect of the *para* *tert*-butyl.

The last two monofunctional compounds in Table I, *m*-methoxyphenol and methyl *p*-hydroxybenzoate are phenols which contain electron-withdrawing substituents<sup>11</sup> and are both about as active in retardation as phenol.

When the dihydroxybenzenes are compared for terminating efficiency, it will be seen that when the hydroxyl groups are *ortho* or *para* to one another the compounds have measurable retarding properties. If they are *meta* to one another, there is hardly any retardation. As in the case of the methoxy groups, an *ortho* or *para* hydroxy group is electron-donating and a *meta* hydroxy group electron-withdrawing.<sup>11</sup> The presence of an electron-withdrawing carbomethoxy group is seen to decrease measurably the retarding ability of hydroquinone. The same general situation obtains in the trihydroxybenzenes studied. When the hydroxy groups are vicinal (and the overall effect on each hydroxy group by the others is electron-releasing) the compound (pyrogallol) is a better retarder than phloroglucinol, in which each hydroxy group experiences the electron-withdrawing effect of two *meta* hydroxy groups.

It can be concluded from this survey of phenolic retarders that nuclear substituents which can delocalize a positive charge on the phenolic oxygen atom in the transition state of the addition reaction enhance the chain-terminating ability of the retarder, despite the possibility that they might promote copolymerization.

### Quinones

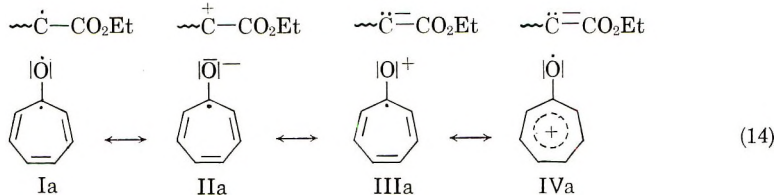
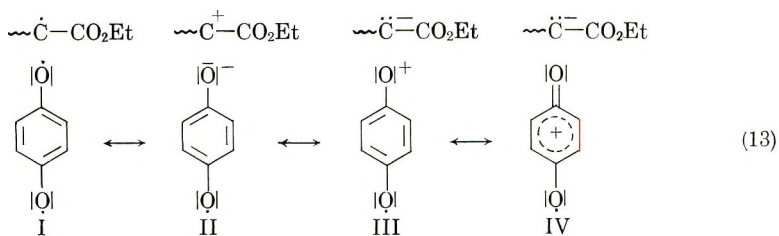
Table II presents the data obtained from ethyl acrylate polymerization retarded by several quinoidal substances.

TABLE II  
Overall Rate of Constants for the Polymerization of Ethyl Acrylate in the  
Presence of Some Quinones

Terminator Compound	Concentration		Induction period, min.	Pseudo zero-order rate constant, mole/l.-sec. $\times 10^5$
	ppm	Molarity		
None			0	16
Quinone	197	$1.64 \times 10^{-3}$	0	0.49
Quinone	68	$5.63 \times 10^{-4}$	0	0.94
Tropone	193	$1.64 \times 10^{-3}$	0	0.16
Tropone <sup>a</sup>	20	$1.69 \times 10^{-4}$	0	6.6
Quinone	43	$3.57 \times 10^{-4}$	0	2.3
2,5-Dihydroxyquinone	88	$5.63 \times 10^{-4}$	8	0.52

<sup>a</sup> The AIBN concentration in this run was  $7.1 \times 10^{-3}M$ .

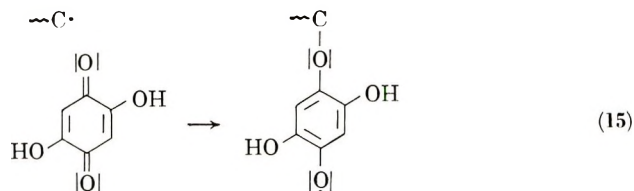
From Table II it can be seen that tropone is three times as efficient a retarder as quinone at a concentration of  $1.64 \times 10^{-3}M$ . Actually, the factor should probably be greater than three, because tropone allegedly has only one active radical-trapping site compared with quinone's two. The transition states for termination with quinone and tropone may be represented as shown in eqs. (13) and (14).



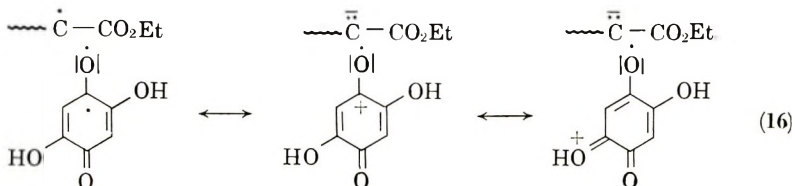
Structures II and IIa represent a complete electron transfer from polymer radical to terminator. As stated before, these structures are probably not favored because of the destabilization of the positive charge by a neighboring carbonyl group in the chain. In structures III and IIIa the negative charge on the chain is resonance-stabilized by the carbonyl group, but the positively charged oxygen atoms render these structures highly energetic. In structures IV and IVa, the positive charges on the oxygen atoms have been delocalized into the rings. In the case of quinone, this delocalization

reduces the aromaticity of the ring. In the case of tropone (IVa), the number of  $\pi$ -electrons in the ring is reduced from seven to six, and full aromaticity is approached. Thus, from all points of view, structure IVa should be a significant contributor to the stability of the transition state in chain termination by tropone, thus making it a better terminator than quinone. This was found to be the case.

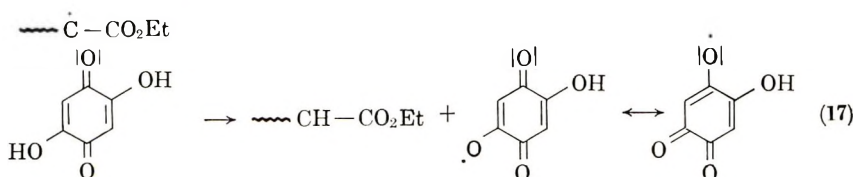
2,5-Dihydroxyquinone was screened as a terminator at concentration of  $5.63 \times 10^{-4}M$ , giving a rate constant of  $5.2 \times 10^{-6}$  mole/l.-sec. This value may be compared to that obtained with an equimolar concentration of quinone,  $9.4 \times 10^{-6}$  mole/l.-sec. 2,5-Dihydroxyquinone can trap radicals like quinone by forming carbon-oxygen bonds.



The transition state for this process would be favored over that for quinone due to delocalization of the partial charge on oxygen by the hydroxyl group.



But in addition, 2,5-dihydroxyquinone can act as a hydrogen donor, forming a resonance-stabilized radical.



Not enough information is at hand to determine which of these two factors makes the 2,5-dihydroxyquinone a better retarder than quinone.

### 2,2-Diphenyl-1-Picrylhydrazyl (DPPH)

Like most stable radicals, DPPH is a relatively efficient radical trap, although its efficiency has sometimes been found to be low enough to preclude its use as a radical counter.<sup>12</sup>

Under the experimental conditions used in this investigation, the induction period for ethyl acrylate polymerization caused by a known concen-

tration of DPPH can be calculated, assuming 100% radical-trapping efficiency for the DPPH.

$$\text{Induction period} = [\text{DPPH}]/(2ek_{\text{AIBN}}[\text{AIBN}])$$

where  $e$  is the efficiency of AIBN in generating free radicals (accounting for cage recombination of radicals), and  $k_{\text{AIBN}}$  is the first-order rate constant for the decomposition of AIBN at the temperature of the run ( $7.6 \times 10^{-5}$  min.<sup>-1</sup> at 44.7°C.<sup>13</sup>). The efficiency of AIBN has not been measured at this temperature in the medium used here. However, most measurements of  $e$  made previously in various solvents at 60–80°C. have given values ranging from 0.5 to 0.8. The value of  $e$  used here as a first approximation is that found by Bevington<sup>14</sup> in styrene at 60°C., namely 0.6.

Three kinetic runs were carried out with DPPH to calculate its approximate efficiency. The results are listed in Table III.

TABLE III

Compound	Terminator		Induction period, min.		DPPH efficiency	Pseudo zero-order rate constant, mole/l.-sec $\times 10^4$
	Concentration	Molarity $\times 10^5$	Obsd.	Caled.		
None			0	0	—	1.6
DPPH	48	1.10	64	100	0.6	1.3
DPPII	48	1.09	54	100	0.5	1.4
DPPII	96	2.19	119	198	0.6	1.3

The length of the observed induction periods are 50–60% of those calculated, indicating an inefficiency in the radical-trapping ability of DPPH in this system.

## References

1. Kice, J. L., *J. Am. Chem. Soc.*, **76**, 6274 (1954).
2. Kice, J. L., *J. Polymer Sci.*, **19**, 123 (1956).
3. Bagdasar'ian, Kh. S., and Z. A. Sinitsina, *J. Polymer Sci.*, **52**, 31 (1961).
4. Walling, C., *Chem. Rev.*, **46**, 191 (1950).
5. Alfrey, T., Jr., and C. C. Price, *J. Polymer Sci.*, **2**, 101 (1947).
6. Bartlett, P. D., and H. Kwart, *J. Am. Chem. Soc.*, **72**, 1051 (1950).
7. Cooper, W. D., Celanese Chemical Co., Clarkwood, Texas, unpublished data.
8. Russell, G. A., *J. Am. Chem. Soc.*, **78**, 1047 (1956).
9. Davies, D. S., H. L. Goldsmith, A. K. Gupta, and G. R. Lester, *J. Chem. Soc.*, **1956**, 4926.
10. Bickel, A. F., and E. C. Kooyman, *J. Chem. Soc.*, **1956**, 2215.
11. McDaniel, D. H., and H. C. Brown, *J. Org. Chem.*, **23**, 420 (1958).
12. Hammond, G. S., J. N. Sen, and C. E. Boozer, *J. Am. Chem. Soc.*, **77**, 3244 (1955).
13. Tobolsky, A. V., and J. P. van Hook, *J. Am. Chem. Soc.*, **80**, 779 (1958).
14. Bevington, J. C., *Trans. Faraday Soc.*, **51**, 1392 (1955).



### Résumé

Un groupe de phénols substitués, la quinone et la tropone, ont été utilisés pour retarder la polymérisation de l'acrylate d'éthyle initiée par l'AIBN en solution dans le propionate d'éthyle à 44.7°C en absence d'oxygène. L'efficacité du retardement dépend de la capacité du réactif à stabiliser la charge positive au site de réaction dans l'état transitoire. La tropone a été trouvée être un retardateur particulièrement adéquat. L'efficacité de radicaux de 2,2-diphényl-1-picrylhydrazyl dans ce système a été trouvée être de 50 à 60%.

### Zusammenfassung

Eine Gruppe substituierter Phenole, Chinon und Tropon wurde zur Verzögerung der AIBN-gestarteten Äthylacrylatpolymerisation in Äthylpropionatlösung bei 44,7°C in Abwesenheit von Sauerstoff verwendet. Man kam zu dem Schluss, dass die Verzögerungswirksamkeit von der Fähigkeit des Verzögerers, eine positive Ladung an seinem Reaktionsort im Übergangszustand zu stabilisieren, abhängt. Tropon erwies sich als besonders guter Verzögerer. Die Radikal-Abfangausbeute von 2,2-Diphenyl-1-picrylhydrazyl betrug in diesem System 50–60%.

Received January 28, 1965

Revised October 5, 1965

Prod. No. 4919A

## Reaction of *n*-Butyllithium with Poly(vinyl Chloride)

K. SHIINA and Y. MINOURA, *Research Institute for Atomic Energy, Osaka City University, Kita-Ku, Osaka, Japan*

### Synopsis

The reactions of poly(vinyl chloride) and butyllithium in tetrahydrofuran were investigated. A deep purple color developed at first with addition of butyllithium to the THF-PVC solution, and a spontaneous color change of the mixture occurred successively to blue, green, and finally pale yellow. In these reaction stages, the PVC might be butylated, dehydrochlorinated, and partially lithiated by BuLi. These facts were substantiated by the results of successive reactions with various substances such as Michler's ketone, carbon dioxide, and styrene.

### INTRODUCTION

Reactions of polystyrene (PSt) have been widely investigated, and it is reported in the literature that both the main chain<sup>1</sup> and benzene ring<sup>2</sup> of PSt can be metallated. Of the polymer reactions, that with poly(vinyl chloride) (PVC) is a relatively pronounced one. Although several reactions between organometallic reagents, such as diethylzinc,<sup>3</sup> trityllithium and its analogs,<sup>4</sup> sodium naphthalene and living polymers,<sup>5,6</sup> with PVC or poly(vinyl bromide) (PVBr) were investigated, no details were published.

We have investigated the possibility of anionic grafting on PVC and tried to elucidate the polymer reactions of PVC by using a more reactive organometallic reagent, such as butyllithium.

### EXPERIMENTAL

#### Materials

The solvent, tetrahydrofuran (THF) was refluxed with sodium wire, distilled, and stored in a bottle containing sodium wire. By refluxing on and distilling from lithium aluminum hydride before use, completely anhydrous THF was obtained. Michler's ketone, benzyl chloride, styrene, and other reagents may be obtained from several commercial sources. They may be purified by distillation or recrystallization from a suitable solvent. Commercial BuLi solution in *n*-heptane was used. A commercial PVC having a degree of polymerization of 1450 was used, after reprecipitation and drying.

#### General Method

In all experiments, a 100-200 ml. three-necked flask equipped with stirrer, reflux condenser, and thermometer was used. After reprecipitation

and vacuum drying, PVC was more completely dried on standing over phosphorus pentoxide for a week. In all experiments, the oven-dried apparatus was flushed with nitrogen several times before addition of 50–100 ml. absolutely dried tetrahydrofuran (THF) and PVC with stirring. To this transparent clear PVC solution maintained at room temperature was injected a given amount of *n*-butyllithium in *n*-heptane from a syringe under stirring and flushing with nitrogen. Immediately, the reaction mixture became deep purple, and heat was evolved due to the reaction and solvation of BuLi. This color persisted for a long time, depending upon the clearness of the systems and the quantity of BuLi used. Successive changes of the color from deep purple to dark blue, green, and finally yellow occurred, the changes being more rapid when the active species in the mixture is destroyed by contact with impurity, probably moisture and oxygen. The transparent, slightly yellow reaction mixture which finally resulted contained no gel. The extent and course of the final stage of the reaction were followed by the color change of the mixture and by using Gilman's test,<sup>7</sup> which is known to detect active C—Li. Hydrolysis, carbonation, or addition of Michler's ketone, styrene, or benzyl chloride to the mixture were carried out at an appropriate time. After these treatments, the resulting polymer was precipitated by pouring into methanol or water and washed repeatedly with methanol and water. All polymers, except grafted styrene, were yellow or pale yellow, brittle substances and insoluble in benzene, toluene, alcohol, cyclohexane, carbon tetrachloride, and chloroform; they swelled in THF, DMF, nitrobenzene, dichloroethane, and dimethyl sulfoxide.

#### Reaction of Michler's Ketone with the Mixture of PVC and BuLi in THF

An amount of BuLi equimolar with the Cl in PVC was added to a solution of 0.62 g. PVC (0.01 mole) in 100 ml. THF, and after 10 min. a solution of 4 g. (0.015 mole) Michler's ketone in THF was added to the mixture with stirring. After standing for 20 min. at room temperature, the mixture was warmed at 50°C. for 10 min. The mixture was then hydrolyzed by adding 1 g. of water. Characteristic Malachite green developed when the mixture was poured into 100 ml. acetic acid containing 1 g. of iodine. The dark green precipitate was filtered and washed repeatedly with water. Low molecular weight Malachite green was eluted smoothly by washing with methanol. The green polymeric residue was then transferred into THF after methanol washings became colorless. The polymer was swelled in THF, and the occluded low molecular weight Malachite green, which is formed by a reaction of free BuLi and Michler's ketone and successive treatment with iodine, was eluted into the solvent. Elution in THF was repeated until the THF supernatant became colorless. On drying *in vacuo*, 0.58 g. of an insoluble, deep green polymer was obtained.

#### Reaction of PVC with "Living" Polystyrene Initiated by BuLi

In a 300-ml. three-necked flask, under nitrogen, 30 g. styrene (0.29 mole) in 150 ml. THF was polymerized by adding 4 mmole of BuLi. To this

reddish "living" polystyrene solution was added a solution of PVC (0.64 g.) in 30 ml. THF under stirring. Heat was not evolved. The system gradually decolorized and finally became brownish red again. After 30 min. stirring, the contents were poured into 500 ml. of methanol, washed, and dried. The polymer was separated into two parts by extraction three times with 100 ml. of boiling acetone; 1 g. of soluble polymer (I) was obtained. The insoluble residue gradually became soluble in large amounts of acetone on prolonged heating and is more easily soluble in cyclohexane. This grafted polymer (II) amounted to 29 g.

## RESULTS AND DISCUSSION

Although the course of the reaction of organic lithium compounds and organic halides is influenced to some extent by halogen organic groups, solvent, and reaction conditions, it is well known that coupling of organic groups and/or halogen-metal interconversion result. It has been found that the dehydrochlorination occurs especially in the reaction of a secondary or tertiary alkyl halide with an alkyl lithium compound other than the coupling of organic groups. In a recent investigation,<sup>8</sup>  $\alpha$ -elimination and successive reaction of the carbene with organic lithium compound or rearrangement of the carbene were reported. From this evidence, it seems probable that in the reaction of PVC and BuLi, various types of reaction will occur.

### Reaction of PVC and BuLi

When BuLi was added to PVC solution, deep purple color developed immediately, and the temperature rose about 10–15°C. The amount of BuLi added was related to the persistence and depth of the purple color. This color changes continuously to transparent yellow through dark blue, blue, and green as shown in Table I. The addition of over two equivalents of BuLi per mole PVC monomer led to the existence of the purple color for as long as 3 days. Although the polymer was neither gelled nor coagulated in the flask, it became insoluble in all solvents once precipitated in methanol. In Table I is shown the color change and results of following the active component by Gilman's test when various proportions of BuLi were added. The polymers obtained were yellowish, brittle lumps in the form of small particles which only swelled in THF, DMF, DMSO, and cyclohexanone; the analyses are listed in Table II. Unexpectedly, the chlorine content of insoluble polymers was markedly decreased, and C=C absorption at 1640 and 990  $\text{cm}^{-1}$  together with OH absorption at 3400  $\text{cm}^{-1}$  in the infrared spectrum were observed (Fig. 1). From this evidence, it appears likely that dehydrochlorination occurs simultaneously with alkylation by BuLi on PVC.

Cristol<sup>9</sup> has reported that coupling and  $\beta$ -elimination occur simultaneously in the reaction of linear primary alkyl halide and organolithium compound, while with *tert*-butyl chloride only the elimination product is obtained. Although no investigation with respect to the reaction of 2,4-

TABLE I  
Color Change and Gilman's Test of the Reaction Mixture of PVC and BuLi

Sample no.	Equiva- lents of BuLi	Mixture	Color at various intervals after the addition of BuLi						
			10 min.	30 min.	1 hr.	2 hr.	3 hr.	20 hr.	
M1	1.0	Reaction mixture	Dark blue	Green	Yellow	Yellow	Yellow	Yellow	Yellow
		Gilman's test	Green	Pale green	Pale greenish blue	Pale greenish blue	Pale greenish blue	Pale greenish blue	Yellow
M2	1.3	Reaction mixture	Dark blue	Dark blue	Dark blue	Dark green	Dark green	Greenish brown	Yellow
		Gilman's test	Dark green	Green	Pale green	Pale green	Pale green	Pale green	Yellow
M3	1.5	Reaction mixture	Dark violet	Dark violet	Dark violet	Dark violet	Dark violet	Dark violet	Yellow
		Gilman's test	Deep green	Deep green	Green	Green	Green	Green	Blueish green



TABLE II  
Analyses of Polymers

Sample no. or polymer	C, %	H, %	Cl, %	N, %
M 1	71.62	9.915	11.33	
M 2	78.25	10.46	3.29	
M 3	76.85	10.61	2.22	
BC 1	47.39	5.74	23.06	
BC 2	62.98	7.81	25.03	
BC 3	64.92	8.09	22.11	
St 2	89.98	7.81	1.11	
St 4	58.76	7.16	30.28	
St 5 <sup>a</sup>	89.43	8.54	1.85	
St 6 <sup>a</sup>	88.74	8.53	3.00	
St 7 <sup>a</sup>	85.29	8.35	0.71	
St 7 <sup>b</sup>	90.46	8.45	0.82	
Malchite green polymer	68.84	7.72	—	0.20
Carbonated polymer	77.81	10.60	—	—
	77.91	10.54	3.29	—
Phenyllithium polymer	54.12	5.45	19.10	—
Sodium naphthalene polymer	78.12	7.55	9.35	—
"Living" polystyrene-grafted polymer (soluble in acetone)	91.18	7.90	—	—
"Living" polystyrene-grafted polymer (insoluble in acetone)	91.14	8.25	—	—

<sup>a</sup> Cyclohexane-soluble polymer.<sup>b</sup> Cyclohexane-insoluble polymer.

dichloropentane as a model substance for PVC or isopropyl chloride with BuLi has been reported, in our study it seems likely that elimination is also predominant over coupling of organic groups. Moreover, once the carbon-carbon double bond in the PVC main chain is formed by dehydrochlorination, the C—Cl bond and the methylene group adjacent to the double bond would become more susceptible to attack of BuLi due to allyl-

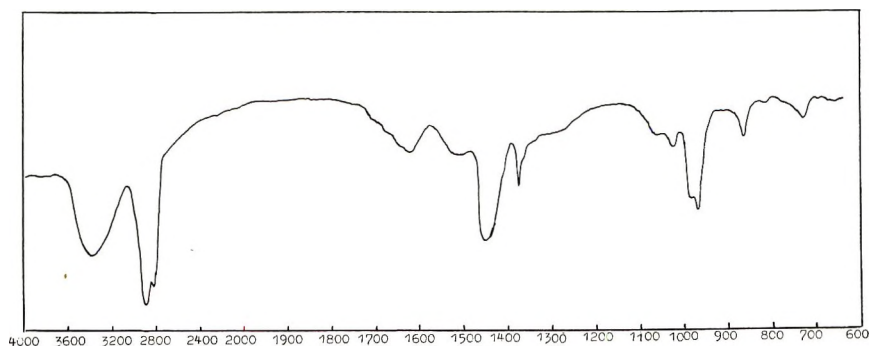
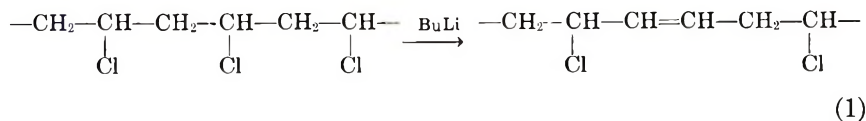


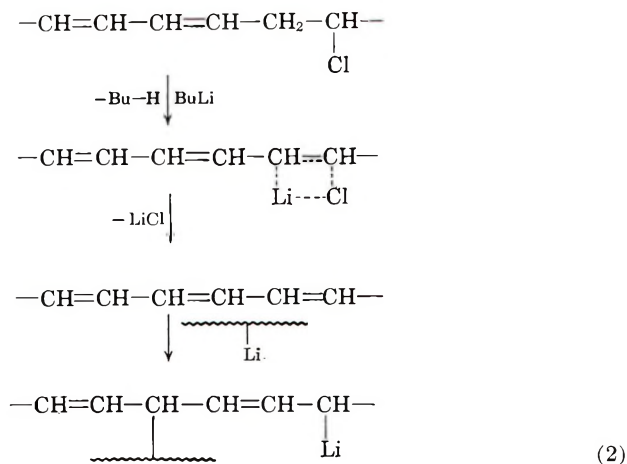
Fig. 1. Infrared spectrum of PVC reacted with BuLi.

type conjugation. The latter methylene hydrogen will be more positive due not only to the resonance effect of the double bond, but also to the electron withdrawing effect of chlorine attached to the adjacent methylene carbon.



The slight yellow color of polymer in spite of low chlorine content suggests that not only dehydrochlorination, but also butylation by BuLi could be responsible. Dehydrochlorination might also be brought about by a small amount of lithium butoxide or lithium hydroxide produced by decomposition of BuLi in storage.

The insolubility of polymers in various solvents would account for the crosslink formation. It may be supposed that polymeric lithium compounds would be formed by addition of BuLi to a conjugated double bond, and the crosslinking reaction takes place by a subsequent 1,4-addition of polymeric lithium groups to the conjugated double bond in same fashion, as shown in eq. (2).



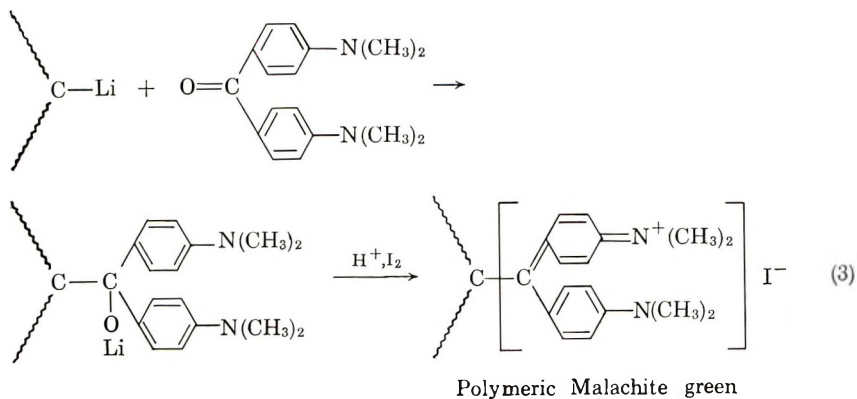
It may also be possible that there is coupling of the polymeric lithiated chain with another polymer chain bearing a chlorine atom by elimination of LiCl.

Although the color of the reaction mixture and its change can not be explained sufficiently, the organolithium complex on the polymer chain such as alfin type catalyst would be expected to be present and to exhibit a characteristic color. This would consist of polymeric lithium group, lithium chloride, and lithium butoxide; the latter two produced by the reaction of BuLi with PVC and oxygen.

#### Reaction of Michler's Ketone with a Mixture of BuLi and PVC in THF.

Deep green (Malachite green) brittle polymer was obtained from the reac-

tion of Michler's ketone with the reaction mixture of BuLi and PVC. Unexpectedly, this polymer shows a low nitrogen content (Table II). These results should afford evidence for existence in the reaction mixture of polymeric lithium component by which Michler's ketone was attacked as shown in eq. (3).



**Carbonation of a Mixture of BuLi and PVC in THF.** The carbonation reaction and isolation of a derived carboxylic compound is a most useful and familiar method for identifying organoalkali compounds. This method was applied to our complex lithiated polymer. A reaction mixture of BuLi and PVC in THF was poured into a slurry of Dry Ice-THF 10 min. after the addition of BuLi, and by treatment in usual way, a pale yellow, insoluble polymer was obtained. Infrared spectral studies of a KBr disk containing this polymer showed a band characteristic of carbonyl at  $1725 \text{ cm.}^{-1}$  and a OH absorption at  $3400 \text{ cm.}^{-1}$  (Fig. 2). Results of analysis are given in Table II.

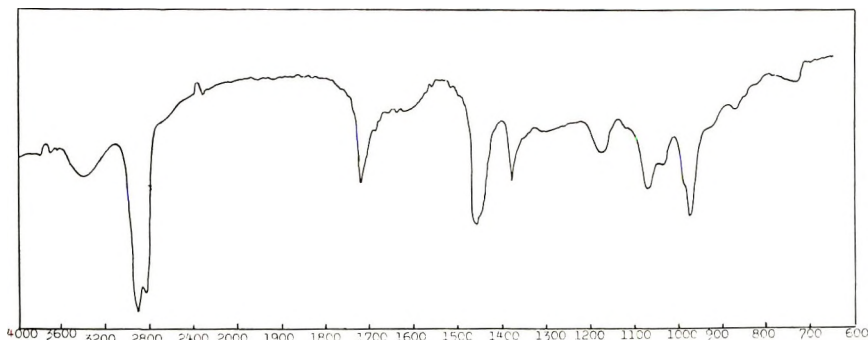


Fig. 2. Infrared spectrum of carbonated PVC polymer after reaction with BuLi.

**Reaction of Benzyl Chloride and a Mixture of BuLi and PVC in THF.** Benzyl chloride, in general is used to consume some alkyl lithium compound according to the reactions, shown in eq. (4), which proceeds quantitatively and is utilized in quantitative analysis of alkyl lithium.



We have intended to introduce benzyl groups into the polymer by the reaction of benzyl chloride and the complex lithiated polymer. Reactions were carried out as shown in Table III. At 5, 10, and 15 min. following

TABLE III  
Relation of Color of the Mixture and Time

Sample no.	Time for changes in color					Polymer obtained, g.
	Deep purple	Dark blue	Blue	Green	Yellow	
BC1	—10 min. <sup>a</sup> —→		BC <sup>b</sup>	—Immediately—→		0.74
BC2	—15 min.—→			BC	—Immediately—→	0.54
BC3	—5 min.—→		BC	—Immediately—→		0.52

<sup>a</sup> Indicates that deep purple color of the mixture at the addition of BuLi to PVC solution, changes spontaneously to blue at the interval of 10 min.

<sup>b</sup> BC denotes the addition of a large excess of benzyl chloride (with respect to BuLi) at this point.

the addition of BuLi to PVC solution in THF, benzyl chloride was injected into the mixture. Immediate decolorization was observed when benzyl chloride was added, and yellow, insoluble polymer was obtained. Infrared spectra of these polymers show no peaks characteristic of aromatic nuclei. It may be concluded that there is a low concentration of lithiated groups in the polymer chain and some of them participate in metal-halogen interconversion.

### Polymerization of Styrene by Lithiated Polymer

There remains the possibility that vinyl monomers may be anionically grafted to PVC at lithiated position, analogous to the reaction of Michler's ketone and carbon dioxide. To study this further, styrene was introduced into a mixture of BuLi and PVC at a given interval of time from the addition of BuLi, depending on the mixture, which would correspond to the reaction stage.

The concentration of active lithiated groups seemed to be sensitive to many factors, such as purity of solvent, dryness of apparatus, purity of atmosphere, and degree of stirring. Results are listed in Table IV. When the system was even slightly contaminated before addition of BuLi, the extent of color change and the evolution of heat at the time of addition of BuLi is large, and no grafted polymer was obtained (St4, Table IV). Heat was not evolved by the addition of styrene, and the characteristic color of living polystyrene was not developed. The order of change of color was similar to that observed in the absence of styrene, but the changes did not take place as rapidly. The resulting polymers were largely soluble in cyclohexane. The infrared spectra are similar to that of styrene in the

TABLE IV  
 Styrene Polymerization by the Lithiated Polymer

Sam- ple no.	Heat evolved at BuLi addition, °C.	Time for changes of color <sup>a</sup>				Polymer obtained, g.	Separation of polymer by cyclohexane extraction, g.
		Deep purple	Dark blue	Blue	Green		
St2	16	—10 min.	→St	→30 min.	→	2.51	1.25 <sup>b</sup>
St4	20	—5 min.	→St	→St	→0.5 min.	0.69	— <sup>c</sup>
St5	11	→20 min.	→St	→90 min.	→Overnight	2.9	Soluble 2.86 Insoluble 0.01
St6	14	—30 min.	→St	→5 min.	→Overnight	2.9	Soluble 2.65 Insoluble 0.03
St7	12	—50 min.	→St	→180 min.	→Overnight	3.5	Soluble 2.44 Insoluble 0.84

<sup>a</sup> Soluble polymer successively extracted by benzene, methyl ethyl ketone, and cyclohexane.

<sup>b</sup> Notation is similar to that of Table III, except that St denotes the addition of 3 g. styrene at the indicated time.

<sup>c</sup> Polymer insoluble in all solvents.



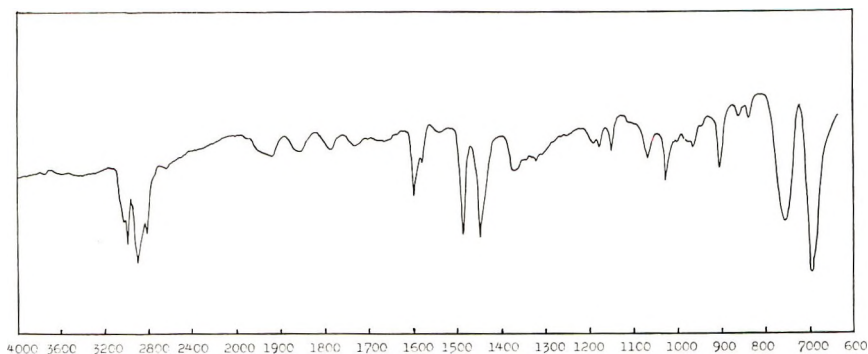


Fig. 3. Infrared spectrum of styrene-grafted PVC after reaction with BuLi.

case of both soluble and insoluble polymers, and the band attributable to the carbon-carbon double bond at  $990\text{ cm.}^{-1}$  was not apparent (Fig. 3). Results of analysis of these polymers are shown in Table II. The small differences in results of analysis between soluble and insoluble polymers suggest that these polymers consisted of partially butylated, dehydrochlorinated, and styrene-grafted PVC, and that the cyclohexane-insoluble polymer seems to be the more crosslinked polymer.

### Reaction of PVC and Other Organometallic Compounds

**Reaction of PVC and Phenyllithium.** One mole equivalent of phenyllithium, which was synthesized in ether from lithium and bromobenzene in usual manner and of which the concentration was determined by acid titration, was injected into PVC solution in THF at room temperature. The reaction began at once and the mixture soon darkened. Gel was formed immediately. After 1 hr., no organolithium component was detected by Gilman's test. The polymer was a brown powder. Results of analysis are given in Table II.

**Reaction of PVC and Sodium Naphthalene.** Addition of only one-third mole equivalent of sodium naphthalene to PVC was sufficient to cause the mixture to darken and gel to form immediately. The polymer obtained after precipitation in methanol, filtration, and drying *in vacuo* was a brown powder. Table II shows analytical data.

**Reaction of PVC and "Living" Polystyrene.** Recently Greber and Egle<sup>5</sup> have investigated the reaction of living polymer with PVC or PMMA. We obtained a cyclohexane-soluble polymer, which was separated with acetone into two parts, soluble, and insoluble, from the reaction of PVC and BuLi-initiated "living" polystyrene. The two polymers were identical in analysis (Table II) and infrared spectrum.

### References

1. A. A. Morton and L. D. Taylor, *J. Org. Chem.*, **24**, 1167 (1959).
2. D. Braun, *Makromol. Chem.*, **30**, 85 (1959).
3. H. Staudinger, M. Brunner, and W. Feisst, *Helv. Chim. Acta*, **13**, 805 (1930).

4. J. P. Roth, P. Rempp, and J. Parrod, *Compt. Rend.*, **251**, 2356 (1960).
5. G. Greber and G. Egle, *Makromol. Chem.*, **53**, 200 (1962).
6. Y. Gallot, P. Rempp, and J. Parrod, *J. Polymer Sci. B*, **1**, 329 (1963).
7. H. Gilman and Schulze, *J. Am. Chem. Soc.*, **47**, 2002 (1925).
8. J. F. Eastham and G. W. Gibson, *J. Org. Chem.*, **28**, 280 (1963).
9. S. J. Cristol, *J. Am. Chem. Soc.*, **73**, 810 (1951).

### Résumé

Les réactions du chlorure de polyvinyle et du butyl-lithium dans le tétrahydrofurane (THF) ont été étudiées. Une couleur pourpre foncé se développe au début lors de l'addition du butyl-lithium à la solution de chlorure de polyvinyle dans THF et spontanément la couleur change, variant successivement du bleu au vert et finalement au jaune pâle. Dans ces différentes étapes de la réaction, le PVC peut être butylé, déshydrohalogéné et partiellement lithié par le BuLi. Ces faits sont confirmés par les résultats des réactions successives avec diverses substances telles que l'acétone de Michler, le CO<sub>2</sub> et le styrène.

### Zusammenfassung

Die Reaktionen zwischen Polyvinylchlorid und Butyllithium in Tetrahydrofuran wurden untersucht. Beim Zusatz von Butyllithium zur THF-PVC-Lösung entwickelte sich zuerst eine tiefe Purpurfarbe und dann trat eine spontane Farbänderung der Mischung über blau und grün zu schliesslich blassgelb auf. Bei diesen Reaktionsstufen konnte PVC durch BuLi butyliert, dehydrochloriert und teilweise lithiiert werden. Dies wurde durch die Ergebnisse aufeinanderfolgender Reaktionen mit verschiedenen Substanzen wie Michler's Keton, Kohlendioxyd und Styrol bestätigt.

Received September 14, 1964

Revised October 1, 1965

Prod. No. 4921A

## Silicon-Containing Schiff Base and Benzimidazole Derivatives\*

H. NAGY KOVACS, A. D. DELMAN, and B. B. SIMMS,  
*U. S. Naval Applied Science Laboratory, Naval Base,  
Brooklyn, New York*

### Synopsis

Investigations were undertaken to obtain information for use in the development of new heat-stable polymers. Model silicon-containing Schiff base and benzimidazole derivatives were synthesized by reaction of *p*-(triphenylsilyl)-benzaldehyde with phenylenediamines. The structure and thermal stability of the products were studied. The reaction of *p*-(triphenylsilyl)benzaldehyde and *o*-phenylenediamine yielded *N*-*p*-(triphenylsilyl)benzylidene-*o*-phenylenediamine which readily oxidizes to form 2-*p*-(triphenylsilyl)phenylbenzimidazole. The di-Schiff bases, which most probably exist in *trans-trans* configurations, were obtained from reaction of the aldehyde derivative with *m*- and *p*-phenylenediamine. In contrast to similar Schiff bases without silicon, the products are soluble in organic solvents. The good resistance of the di-Schiff base and benzimidazole derivatives to thermal decomposition suggests that polymers with repeating units of such structures would also be heat-stable and might possess useful properties.

### INTRODUCTION

In recent years, the search by many investigators for heat-resistant macromolecular substances has been intensified. Marvel and co-workers have shown that Schiff bases<sup>1,2</sup> and benzimidazole derivatives<sup>3-5</sup> are suitable building blocks for preparing thermally stable polymers. The relation of molecular structure to the thermal resistance of aromatic Schiff bases and acid amides has been studied at this laboratory.<sup>6</sup> The products reported in the latter paper are powders that generally exhibit good resistance to degradation by heat, but are insoluble in organic solvents.

It is known that commercially available polysiloxanes possess good mechanical and electrical properties and are useful for short time periods when heated at 300°C. At higher temperatures, the polysiloxanes are rapidly decomposed.

Several investigators<sup>7-10</sup> have attempted to improve the heat stability of polysiloxanes by substituting Si—C bonds such as in silarylene groups for some, or all, of the Si—O linkages in the chains. However, unless they can be crosslinked, such materials generally are fusible at temperatures below 200°C.

\* Presented at the Second International Symposium on Organometallic Chemistry, Madison, Wisconsin, August 30–September 3, 1965.

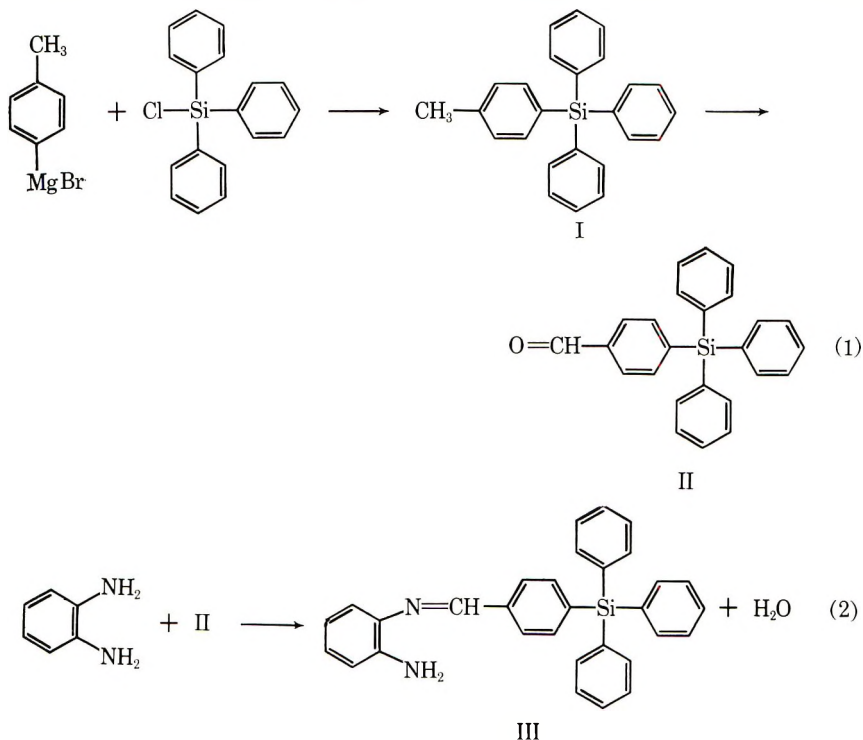
To improve the thermal stability and increase the temperature at which silicon-containing polymers melt or fuse, studies were undertaken at this laboratory to prepare model compounds having aromatic Schiff base or benzimidazole units attached to silicon atoms. It may be expected that such model compounds would have properties that could be related to those of the Schiff base and silarylene units. It is intended that the characteristics of the model compounds serve as a guide for the preparation of high molecular weight polymers with such structures.

This paper reports the results of studies of the reactions of *p*-(triphenylsilyl)benzaldehyde with phenylenediamine compounds and of the heat stability of the products. To obtain information about the influence of molecular structure on thermal stability, model compounds with related structures were synthesized.

### SYNTHESIS AND STRUCTURE OF MODEL COMPOUNDS

Initially, triphenyl(*p*-tolyl)silane (I) was prepared by Grignard reaction of triphenylchlorosilane and *p*-tolylmagnesium bromide. The method is somewhat more convenient than that described by Gilman and Clark.<sup>11</sup> The silane (I) was converted to *p*-(triphenylsilyl)benzaldehyde (II) following the method of Gilman et al.<sup>12</sup> with some modifications. The aldehyde derivative II was then interacted with phenylenediamine compounds.

The reaction of II with *o*-phenylenediamine in benzene or ethyl alcohol solution at room temperature produced the bright yellow, crystalline *N*-*p*-

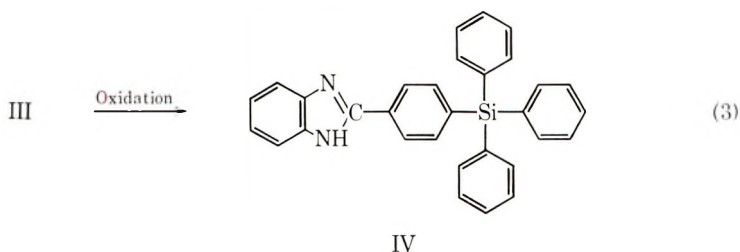


(triphenylsilyl)benzylidene-*o*-phenylenediamine, m.p. (uncorr.) 183–185°C.

Though several attempts were made to prepare the di-Schiff base under different experimental conditions, only the mono derivative was obtained. Because of the steric hindrance of the bulky triphenylsilyl group, the formation of a di-Schiff base with *o*-phenylenediamine appears to be highly improbable. This is supported by molecular scale model studies with Fisher-Hirschfelder-Taylor atom models. The infrared spectrum of III is consistent with its structure.

According to molecular scale models, the most probable structure of the mono-Schiff base is that in which the two phenylene groups are in *trans* position. The *cis* isomer appears to be less probable because of steric hindrance.

Although III is stable in crystalline form, it is gradually oxidized by air when slowly evaporated at room temperature under atmospheric pressure from ethyl alcohol solution to form white, crystalline 2-*p*-(triphenylsilyl)-phenylbenzimidazole (IV), m.p. (uncorr.) 268–269°C.



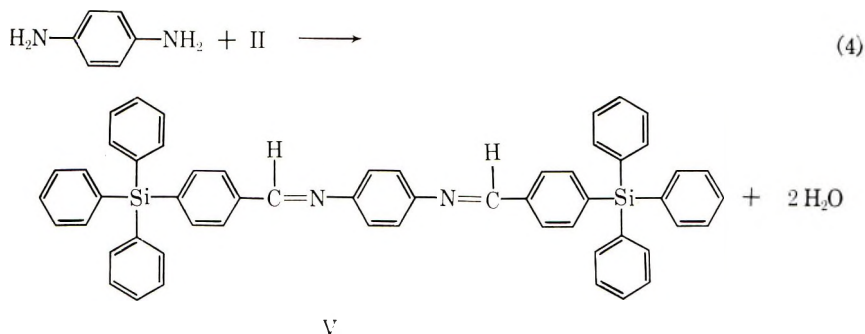
The infrared spectrum of IV in Nujol mull does not have absorption bands at 2.90 and 2.99 $\mu$  that are assignable to NH stretching vibrations from free amino groups. These bands are present in the spectrum of the mono-Schiff base compound. The absorption peak at 6.18  $\mu$  in the spectrum of III, which is attributed to the CH=N bond,<sup>13</sup> is absent in the spectrum from the benzimidazole derivative. Instead, several weak vibration frequencies appear around 6.40  $\mu$ . Morgan<sup>14</sup> reports similar bands in this region for substituted benzimidazole derivatives.

Additional evidence of the conversion of III to IV was obtained by oxidizing the mono-Schiff base with lead tetraacetate<sup>15</sup> to form the benzimidazole. The reaction of II and *o*-phenylenediamine in the presence of cupric acetate<sup>16</sup> also gave IV.

The reaction of *p*-phenylenediamine and II yielded bright yellow *N,N'*-di-*p*-(triphenylsilyl)benzylidene-*p*-phenylenediamine (V), in two crystalline forms melting (uncorr.) at 242–244 and 284–286°C. after recrystallization from ethyl acetate and benzene, respectively. The lower-melting product was converted to the higher-melting form by heat.

Figure 1 shows the x-ray diffraction patterns made from samples of the two crystalline forms. Each ring in the patterns represents the interplanar distance between planes of a set (*hkl*), where *hkl* represents the direction of the set and  $d_{hkl}$  is the interplanar spacing for the set. Several rings that are present in the lower melting sample are absent in the pattern of the





higher melting specimen, indicating a difference in the structure of the two forms. The crystal cell size of the sample which melts at 242–244°C. is about 30% (by vol.) smaller than that of the higher melting form. The two forms showed almost identical x-ray patterns and similar cell sizes after the lower-melting product was heated to 250°C.

The infrared spectra from Nujol mulls (2.5–7.5  $\mu$ ) and carbon disulfide solutions (7.5–15.0  $\mu$ ) of the two different melting forms were identical and consistent with the structure of the molecule. These data, together with the x-ray patterns, suggest that the difference between the two forms may be due to polymorphism.

The possibility that the difference in the crystalline specimens may be attributed to geometric isomerism was also considered. Curtin and Haussner<sup>17</sup> show that *N*-alkyl ketimines may exist in *cis* and *trans* forms,

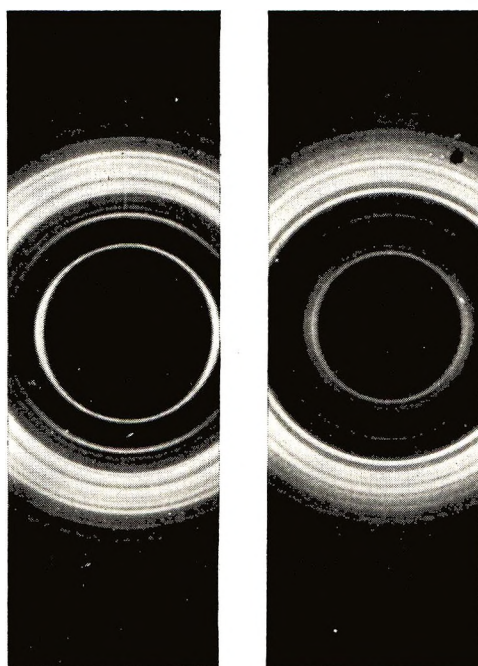


Fig. 1. X-ray diffraction patterns of two forms of *N,N'*-di-*p*-(triphenylsilyl)benzylidene-*p*-phenylenediamine: (a) m.p. 242–244°C.; (b) m.p. 284–286°C.

although recent literature<sup>18</sup> indicates that stereoisomerism has not as yet been found in aldimine compounds.

Three geometric forms can be postulated: *cis-cis*, *cis-trans*, and *trans-trans*. The apparent overcrowding of the molecule makes the existence of *cis-cis* and *cis-trans* geometric structures unlikely. The *trans-trans* isomer, which is less crowded, would seem to be more probable.

NMR and ultraviolet spectra of the two melting forms were essentially identical. This suggests that the difference between the two fractions of V is due to polymorphism rather than geometric isomerism. The NMR spectra indicate that the principal types of hydrogen bonding are phenyl and aldimine hydrogens. The CH=N groups of the molecules are in the same magnetic field, probably exist in the same plane, and are equidistant from the phenyl groups.

Curtin et al.<sup>19</sup> studied the NMR spectra of several pairs of *cis-trans* isomers in which the stereoisomerism involves phenyl substituent groups. In the case of stilbene, the *trans* isomer is found to be coplanar, and the NMR spectrum<sup>20</sup> shows a multiplicity of peaks, while the *cis* isomer is not coplanar and exhibits only a single sharp peak that is assigned to phenyl hydrogens. If one considers the product synthesized in this study in an analogous manner, then the coplanarity of the CH=N—C<sub>6</sub>H<sub>4</sub>—N=CH unit in the molecule and the multiplicity of peaks in the NMR spectra suggest that *trans-trans* stereoisomerism is favored for V.

The reaction of the aldehyde derivative II and *m*-phenylenediamine produced pale yellow *N,N'*-di-*p*-(triphenylsilyl)benzylidene-*m*-phenylenediamine (VI), m.p. (uncorr.) 219–221°C. Molecular scale model studies indicate that the most probable stereoisomeric form for the product is *trans-trans*. The infrared spectrum is consistent with its structure.

### THERMAL STABILITY OF MODEL COMPOUNDS

The heat resistance of the silicon-containing Schiff bases III, V, and VI and the benzimidazole derivative IV was studied by thermogravimetric analysis.

Figure 2 illustrates the weight loss of the model compounds with increasing temperature. The thermograms of the Schiff base compounds derived from *m*- and *p*-phenylenediamine showed no weight loss at temperatures below 350°C. At more elevated temperatures, the *meta* Schiff base derivative was somewhat more heat-resistant than the corresponding *para* compound; the weight loss at 500°C. for the *meta* and *para* derivatives was 14.9 and 31.7%, respectively. The residues from these experiments were comprised of SiO<sub>2</sub> in amounts corresponding to the theoretical silicon values calculated for the products. This indicates that the volatile pyrolysis products were composed of molecular fragments that did not contain silicon atoms. The relative order of heat resistance of these products was similar to that generally found in thermal stability studies of aromatic Schiff bases without silicon.<sup>6</sup>

The thermogram of the *ortho* Schiff base III derivative indicates that the compound is less heat stable than the analogous *meta* and *para* products.

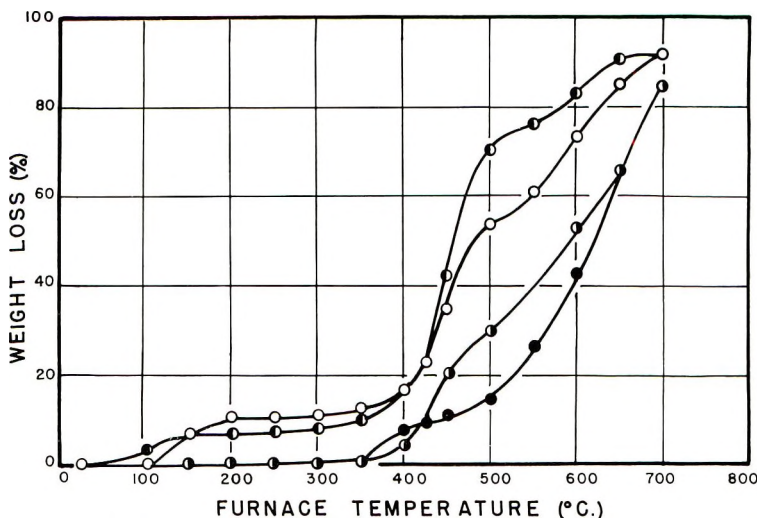


Fig. 2. TGA thermograms of model compounds: (○) III; (◐) IV; (○) V; (●) VI.

The residue obtained after thermogravimetric analysis contained less than the theoretical amount of  $\text{SiO}_2$ . This suggests that some of the substance was volatilized without decomposition, or that the pyrolysis fragments contained silicon atoms.

The thermogram from the benzimidazole derivative IV was very similar to that from the *ortho* Schiff base III. This can be explained by the fact that III is a precursor of IV. As in the case of the *ortho* Schiff base derivative, the quantity of  $\text{SiO}_2$  found after heating the substance to  $700^\circ\text{C}$ . was less than the calculated value. Evidence that IV volatilizes without decomposition when heated below  $400^\circ\text{C}$ . was given by unchanged melting points and infrared spectra of the distillate and residue obtained from another experiment. The benzimidazole derivative decomposed when heated above  $400^\circ\text{C}$ .

## EXPERIMENTAL

### Synthesis

**Triphenyl(*p*-tolyl)silane.** To a mixture of 5.35 g. (0.22 g.-atom) of magnesium chips, 20 ml. of dry ether, and a few crystals of iodine at  $50^\circ\text{C}$ . under a nitrogen atmosphere was added 5.5 g. (0.032 mole) of *p*-bromotoluene to initiate the reaction. The heating of the mixture was interrupted and a solution containing 30.08 g. (0.176 mole) of *p*-bromotoluene dissolved in 160 ml. of ether was added within 1 hr. with stirring. Instantaneous boiling started and the mixture was refluxed for 30 min. Then 49 g. (0.17 mole) of triphenylchlorosilane dissolved in 110 ml. of dry toluene was added dropwise to the stirred reaction mixture within 25 min. The solvents were slowly distilled off and the residue was maintained at  $180\text{--}185^\circ\text{C}$ . for an additional 19 hr. To the residue was added 100 ml. of dilute hydrochloric

acid and 1 liter of benzene while stirring vigorously. The benzene layer was separated and washed successively with water, sodium bicarbonate solution, and water, and then dried over anhydrous magnesium sulfate. The solvent was removed by evaporation under vacuum and the residue was dissolved in 1250 ml. of boiling ethyl alcohol. The solution was cooled to room temperature and the crystalline material was separated to give 41 g. (71% yield) of crude product, m.p. 130°C., which was recrystallized from ethyl acetate to product triphenyl(*p*-tolyl)silane (I), m.p. (uncorr.) 136–137°C. (lit.:<sup>11</sup> 134–135°C.).

***p*-(Triphenylsilyl)benzaldehyde(II).** This compound was prepared in a two-step reaction as described by Gilman et al.<sup>12</sup> with some modifications. The silane I was brominated with *N*-bromosuccinimide by using benzoyl peroxide instead of ultraviolet light as the reaction initiator to obtain an 89% yield of *p*-(triphenylsilyl)benzal bromide, m.p. (uncorr.) 180–182°C. (lit.:<sup>12</sup> 184–184.5°C.). The benzal bromide derivative was converted to the aldehyde II with silver nitrate under nitrogen atmosphere to prevent oxidation. The crude product was isolated by diluting the reaction mixture with water and extracting with ethyl acetate. The ethyl acetate layer was evaporated under reduced pressure to an oily residue which crystallized immediately when ethyl alcohol was added. Yield 63%; m.p. 110–112°C. after recrystallization from ethyl alcohol (lit.:<sup>12</sup> 110–112°C.).

***N-p*-(Triphenylsilyl)benzylidene-*o*-phenylenediamine (III).** To a solution containing 1.21 g. (0.011 mole) of *o*-phenylenediamine dissolved in 60 ml. of benzene was added 3.65 g. (0.01 mole) of II in 20 ml. of benzene. After 2 hr. at room temperature, yellow crystals were formed. The mixture was allowed to stand overnight at room temperature and filtered to recover 3.65 g. of insoluble residue. An additional 0.57 g. was obtained by concentrating the filtrate under reduced pressure to give a 93% yield of crude product, m.p. (uncorr.) 174–176°C., which was recrystallized from *n*-hexane-tetrahydrofuran mixture (10:1) to produce III, m.p. (uncorr.) 183–185°C. The product is soluble in ether, ethyl acetate, and tetrahydrofuran.

ANAL. Calcd. for C<sub>31</sub>H<sub>26</sub>N<sub>2</sub>Si: C, 81.91%; H, 5.76%; N, 6.16%; Si, 6.17%. Found: C, 82.12%; H, 5.67%; N, 6.52%; Si, 6.26%.

**2-*p*-(Triphenylsilyl)phenylbenzimidazole (IV).** A. When *o*-phenylenediamine and twice the stoichiometric quantity of aldehyde II required to produce the mono-Schiff base III was similarly treated, the yellow color of the reaction mixture faded and a white precipitate formed. After a week, the crude product was separated by filtration, washed with cold benzene, and dried, m.p. (uncorr.) 265–268°C. A 69% yield of white, fine needle crystals of IV, m.p. (uncorr.) 268–269°C. was obtained after recrystallization from hot benzene.

ANAL. Calcd. for C<sub>31</sub>H<sub>24</sub>N<sub>2</sub>Si: N, 6.19%; Si, 6.20%. Found: N, 5.97%; Si, 6.19%.

B. A mixture of 0.50 g. (0.0011 mole) of Schiff base derivative III in 25 ml. of benzene was refluxed with 0.50 g. (0.0011 mole) of lead tetraacetate



for 5 min. The reaction mixture was allowed to stand for 1 hr. at room temperature and the lead salt was removed by filtration. The filtrate was evaporated to dryness under reduced pressure and the residue was dissolved in ethyl alcohol. The solution was treated with charcoal, filtered, and evaporated to dryness as before to produce 0.420 g. (84% yield) of IV, m.p. (uncorr.) 265–267°C. Further recrystallizations raised the melting point to 268–269°C.

C. To a mixture of 0.54 g. (0.005 mole) of *o*-phenylenediamine, 10 ml. of methyl alcohol, 2 g. (0.01 mole) of cupric acetate monohydrate, and 25 ml. of water was added 2 g. (0.0055 mole) of aldehyde II suspended in 25 ml. of methyl alcohol. The reaction mixture was refluxed for 1 hr. and filtered. The greenish residue was washed with methyl alcohol and then ether and suspended in 130 ml. of a water–ethyl alcohol (1:1) mixture. Hydrogen sulfide was bubbled for 25 min. through the suspension on a steam bath, and the reaction mixture was filtered. The residue was washed with 200 ml. of hot ethyl alcohol. The insoluble fraction was suspended in 50% aqueous alcohol and, after another hydrogen sulfide treatment, was worked up as before. The filtrates were combined and evaporated to dryness under vacuum and the residue was dissolved in hot ethyl alcohol. The solution was filtered and evaporated to dryness under reduced pressure to produce 2.033 g. (90% yield) of IV, m.p. (uncorr.) 268–269°C. after recrystallization from ethyl acetate–petroleum ether mixture (1:3). Mixed melting points of the products prepared by the different methods showed no depression. Slow volatilization was observed when IV was heated at 280–360°C. The unchanged infrared spectrum and melting point of the volatile product indicated that decomposition did not occur at these temperatures. The darkening of the molten material showed that decomposition started at 400°C.

ANAL. Calcd. for  $C_{31}H_{24}N_2Si$ : C, 82.27%; H, 5.34%; N, 6.19%; Si, 6.20%. Found: C, 82.10%; H, 5.87%; N, 6.06%; Si, 5.87%.

***N,N'*-Di-*p*-(triphenylsilyl)benzylidene-*p*-phenylenediamine (V).** A solution of 1.08 g. (0.01 mole) of *p*-phenylenediamine and 7.28 g. (0.02 mole) of the aldehyde derivative II dissolved in a mixture of 50 ml. of dry toluene and 20 ml. of absolute ethyl alcohol was slowly distilled within 2.5 hr. to evaporate 40 ml. of solvent; after the first 15 min., bright yellow crystals separated. The reaction mixture was cooled to room temperature and filtered. The residue was washed with petroleum ether and dried to produce 7.82 g. (98% yield) of crude crystals which sinter at 232–235°C. and melt at 284–285°C. (uncorr.). Recrystallization of the crude material from ethyl acetate gave yellow, long needle crystals of V, m.p. (uncorr.) 242–244°C. after drying under vacuum at 56°C.

ANAL. Calcd. for  $C_{56}H_{44}N_2Si_2$ : C, 83.95%; H, 5.53%; N, 3.49%; Si, 7.01%. Found: C, 83.92%; H, 5.50%; N, 3.57%; Si, 6.76%.

Recrystallization of the crude product from benzene produced yellow, short needle crystals of V, m.p. (uncorr.) 284–285°C. after drying for 2 hr. over boiling water.



ANAL. Calcd. for  $C_{56}H_{44}N_2Si_2$ : C, 83.95%; H, 5.53%; N, 3.49%; Si, 7.01%. Found: C, 83.92%; H, 5.50%; N, 3.57%; Si, 6.76%.

When the higher-melting compound was recrystallized again from ethyl acetate or acetone, the lower-melting product was recovered. After the latter substance was heated to 250°C. and cooled to room temperature, it showed only one melting point at 282–284°C. (uncorr.) when reheated.

***N,N'*-Di-*p*-(triphenylsilyl)benzylidene-*m*-phenylenediamine (VI).** A solution of 0.108 g. (0.001 mole) of *m*-phenylenediamine and 0.80 g. (0.0022 mole) of the aldehyde derivative II dissolved in 20 ml. of ethyl alcohol was refluxed for 1 hr.; yellow crystals started to precipitate after 10 min. The reaction mixture was filtered and the residue was washed with boiled ethyl alcohol and dried under reduced pressure to obtain 0.730 g. (91% yield) of VI, m.p. (uncorr.) 219–221°C. Recrystallization from ethyl acetate did not change the melting point.

ANAL. Calcd. for  $C_{56}H_{44}N_2Si_2$ : C, 83.95%; H, 5.53%; N, 3.49%; Si, 7.01%. Found: C, 84.50%; H, 5.42%; N, 3.66%; Si, 7.42%.

### Infrared Spectrophotometry

Spectra from Nujol mulls and carbon disulfide solutions of the products were recorded in the 2.5–15.0  $\mu$  region with a Perkin-Elmer model 21 double-beam spectrometer equipped with sodium chloride optics.

### Ultraviolet Spectrophotometry

The spectra were made on a Beckman model DK-2 recording spectrophotometer from cyclohexane and chloroform solutions.

### NMR Spectrophotometry

The spectra from carbon disulfide solutions of the different melting products from the *p*-di-Schiff base derivative V were prepared by Simon Research Laboratory, Elgin, Illinois. Pertinent absorption peaks are shown in Table I.

TABLE I  
NMR Spectra of Different Melting Fractions of V

Melting point, °C.	Shifts relative to tetramethylsilane, ppm	
	CH=N	Phenyl
242–244	8.50	7.93, 7.81, 7.68, 7.52, 7.41, 7.30, 7.20
284–285	8.50	7.93, 7.81, 7.68, 7.52, 7.40, 7.27, 7.20

### X-Ray Diffraction

The diffraction patterns from samples of the two melting forms of V were made with a Norelco Co. Debye-Scherrer powder camera (360/2 $\pi$ ).

### Thermogravimetric Analysis

The weight loss and temperature of about 0.1 g. samples of the products were continuously and simultaneously recorded on an Ainsworth model BYR-AU semimicro recording balance while heating at 3°C./min. in air to 700°C.

### Elemental Analysis

The products were analyzed by the Schwarzkopf Microanalytical Laboratory, Woodside, N. Y.

### CONCLUSION

The reaction of the silylbenzaldehyde derivative II and the phenylenediamines produced new heat-resistant aromatic Schiff base and benzimidazole model compounds containing silicon atoms.

Molecular scale model studies indicate that the model aldimine compounds probably exist as *trans* stereoisomers rather than in *cis* geometric forms.

The model compounds show relatively high melting points and good thermal stabilities, as well as good solubility in a number of conventional organic solvents. This suggests that polymers with repeating units of chains having structures such as in the model compounds may also exhibit good heat resistance and have useful properties.

The authors wish to thank E. A. Buzkin and W. B. Shetterly of the Bureau of Ships, Washington, D. C., for sponsoring this work; Dr. W. Simon of Simon Research Laboratory for his interpretations of the NMR spectra; and to the following Naval Applied Science Laboratory staff members: I. Canner and G. DiGiacomo for the preparation and interpretation of the x-ray powder patterns and J. M. McGreevy, Associate Technical Director for his interest and encouragement.

The opinions or assertions contained in this paper are the private ones of the authors and are not to be construed as official or reflecting the views of the Naval Service at large.

### References

1. C. S. Marvel and N. Tarkoy, *J. Am. Chem. Soc.*, **79**, 6000 (1957).
2. C. S. Marvel and N. Tarkoy, *J. Am. Chem. Soc.*, **80**, 832 (1958).
3. H. Vogel and C. S. Marvel, *J. Polymer Sci.*, **50**, 511 (1961).
4. H. Vogel and C. S. Marvel, *J. Polymer Sci. A*, **1**, 1531 (1963).
5. L. Plummer and C. S. Marvel, *J. Polymer Sci. A*, **2**, 2559 (1964).
6. A. D. Delman, A. A. Stein, and B. B. Simms, paper presented at The Western Regional Meeting, American Chemical Society, Los Angeles, Calif., 1965.
7. F. P. Price, *J. Polymer Sci.*, **37**, 71 (1959).
8. G. Baum, *J. Org. Chem.*, **23**, 480 (1958).
9. M. Sveda, U. S. Pat. 2,562,000, July 24 (1951).
10. J. E. Mulvaney and C. S. Marvel, *J. Polymer Sci.*, **50**, 541 (1961).
11. H. Gilman and R. N. Clark, *J. Am. Chem. Soc.*, **68**, 1675 (1946).
12. H. Gilman, C. G. Brannen, and R. Ingham, *J. Am. Chem. Soc.*, **78**, 1689 (1956).
13. L. E. Clougherty, J. A. Sousa, and G. M. Wyman, *J. Org. Chem.*, **22**, 462 (1957).
14. K. J. Morgan, *J. Chem. Soc.*, **1961**, 2343.

15. F. F. Stephens, *Nature*, **164**, 243 (1949).
16. R. Weidenhagen, *Ber.*, **69**, 2263 (1936).
17. D. Y. Curtin and J. W. Hausser, *J. Am. Chem. Soc.*, **83**, 3474 (1961).
18. H. A. Staab, F. Vogtle, and A. Mannschreck, *Tetrahedron Letters*, **12**, 697 (1965).
19. D. Y. Curtin, H. Gruen, and B. A. Shoulders, *Chem. Ind. (London)*, **1958**, 1205.
20. N. S. Bhacca, D. P. Hollis, L. F. Johnson, E. A. Pier, and J. N. Shoolery, *NMR Spectra Catalog*, Vol. 1 and 2 Combined, Varian Associates, 1964.

### Résumé

Des études ont été entreprises pour obtenir des informations utiles au développement de nouveaux polymères thermostables. On a ainsi synthétisé des bases de Schiff modèles contenant du silicium et des dérivés benzimidazoliques par réaction de *p*-triphénylsilyl-benzaldéhyde avec les phénylène-diamines. La structure et la stabilité thermique de ces produits ont été étudiées. La réaction du *p*-triphénylsilyl-benzaldéhyde et *o*-phénylène diamine fournit la *N-p*-triphénylsilyl-benzilidène-*o*-phénylène-diamine qui s'oxyde facilement pour former le 2-*p*-triphénylsilyl-phénylbenzimidazole. Les bases de Schiff doubles qui existent probablement en configuration *trans-trans* sont obtenues par réaction de dérivés aldéhydiques avec une diamine *m*- et *p*-phénylène. Contrairement aux bases de Schiff semblables sans silicium les produits sont solubles dans les solvants organiques. La bonne résistance de ces bases de Schiff doubles et dérivés du benzimidazole à la décomposition thermique suggère que les polymères avec des unités périodiques de structure semblable seraient également thermostables et pourraient présenter des propriétés très utiles.

### Zusammenfassung

Untersuchungen zur Gewinnung von Informationen wurden unternommen, die bei der Entwicklung neuer, hitzebeständiger Polymeren verwendet werden können. Schiff'sche Basen und Benzimidazolderivate mit Silikongehalt wurden als Modelle durch Reaktion von *p*-(Triphenylsilyl)benzaldehyd mit Phenylendiaminen synthetisiert. Die Struktur und die thermische Stabilität der Produkte wurde untersucht. Die Reaktion von *p*-(Triphenylsilyl)benzaldehyd mit *o*-Phenylendiamin lieferte *N-p*-(Triphenylsilyl)benzyliden-*o*-phenylendiamin, welches sich leicht unter Bildung von 2-*p*-(Triphenylsilyl)phenylbenzimidazol oxydierte. Die Di-Schiff'schen Basen, welche mit grosser Wahrscheinlichkeit in der *trans-trans*-Konfiguration vorliegen, wurden durch Reaktion des Aldehydderivats mit *m*- und *p*-Phenylendiamin erhalten. Im Gegensatz zu ähnlichen Schiff'schen Basen ohne Silikon sind die Produkte in organischen Lösungsmitteln löslich. Die gute Beständigkeit der Di-Schiff'schen Basen und der Benzimidazolderivate gegen thermische Zersetzung sprechen dafür, dass Polymere mit Bausteinen von solcher Struktur ebenfalls hitzebeständig sein werden und brauchbare Eigenschaften besitzen könnten.

Received September 17, 1965

Revised October 11, 1965

Prod. No. 4922A

## Non-Newtonian Behavior of Polymers with Log-Normal Molecular Weight Distribution

W. CONTI and I. GIGLI, *Rumianca S.p.A., Borgaro Torinese, Italy*

### Synopsis

By choosing suitable approximations to Bueche's function, it is possible to calculate the viscosity versus shear stress for log-normal molecularly distributed linear polymers. For bulk polymers the mixing rules  $\bar{M}_v$ ,  $\bar{M}_w$ ,  $\bar{M}_z$  are considered. For values of  $\eta/\eta_0 > 0.1$  and heterogeneities with  $\bar{M}_w/\bar{M}_n > 1.5$  the result obtained with any mixing rule is  $\eta/\eta_0 = \text{erfc} [(1/\delta) \log (M_0 Q^h/aK)]$ , where  $a = \pi^2/6\rho RT$  and where the  $\delta$  and  $K$  values are dependent on the heterogeneity ratio  $Q = \bar{M}_w/\bar{M}_n$ , and on the type of mixing rule; on the other hand, the  $h$  value is independent of the heterogeneity, but depends on the mixing rule. Most experimental data should fit the  $\bar{M}_w$  mixing rule as one would expect from the zero shear stress mixing rule. Experimental data are compared with the theoretical results.

### INTRODUCTION

Rouse's theory<sup>1</sup> predicts the variation of dynamic viscosity as a function of frequency, temperature, and molecular weight of linear homogeneous polymers.

Bueche<sup>2</sup> has developed an analogous theory which predicts the variation of apparent viscosity as a function of shear rate, temperature, and molecular weight.

Mencfee and Peticolas,<sup>3</sup> extending Rouse's theory to heterogeneous polymers, have developed a method which allows the determination of the molecular weight distribution through the investigation of the dynamic viscosity.

In this paper, by choosing suitable approximations to Bueche's function, we will show how it is possible to calculate the viscosity versus shear stress for linear polymers having a log-normal molecular weight distribution.

### THEORY

The values of Bueche's function and those of Rouse's, are practically equal, when referred to the same values of the argument.<sup>4</sup> Therefore we shall use the values of Rouse's equation,<sup>5</sup> substituting, of course, the argument  $\dot{\gamma}\tau_1$  for the argument  $\omega\tau_1$ , where  $\tau_1$  is maximum relaxation time and  $\omega$  is frequency. Takemura<sup>6</sup> has shown that this substitution is theoretically acceptable.

In consequence, for undiluted polymers, Bueche's equation may be expressed by the function:

$$\eta(\dot{\gamma}) = \eta_0 F(\eta_0 M \dot{\gamma} / a) \quad (1)$$

where  $a = (\pi^2/6) \rho R T$  and  $\eta(\dot{\gamma})$  is viscosity at  $\dot{\gamma}$  shear rate,  $\eta_0$  is zero shear rate viscosity,  $M$  is molecular weight,  $\rho$  is density,  $R$  is the gas constant, and  $T$  is absolute temperature.

The apparent viscosity may be calculated also with reference to the shear stress  $\tau$ , and, in this case, Bueche's equation can be written:

$$\eta(\tau) = \eta_0 f(\tau M / a) \quad (2)$$

In passing from a monodisperse polymer to a polydisperse, various mixing rules may be considered. Several such will be considered below.

### Weight-Average Mixing Rule

The most probable mixing rule<sup>7</sup> is

$$\eta = \left( \sum_{i > i_e} w_i \eta_i^{1/b} \right)^b + X \quad (3)$$

for  $b = 3.5$ . The sum is extended to all viscosities greater than the viscosity ( $\eta_{i_e}$ ) at the critical molecular weight ( $M_e$ );  $\eta$  is the viscosity of the whole polymer;  $w_i$  is the weight fraction of species  $i$  with viscosity  $\eta_i$ ;  $X$  is the contribution of the fractions with molecular weight lower than the critical molecular weight. We will only consider cases for which  $X$  is negligible. For example, when  $\bar{M}_w \geq 10M_e$ .

$$X/\eta_0 \ll \eta_{i_e}/\eta_0 = (M_e/M_w)^{3.5} \leq 10^{-3.5} \quad (4)$$

and  $X/\eta_0$  is negligible as long as  $\eta/\eta_0 > 0.01$ . Expression (3) then becomes

$$(\eta)^{1/b} = \sum_{i > i_e} w_i \eta_i^{1/b} \quad (5)$$

For homogeneous polymers, according to Bueche,<sup>8</sup>

$$\eta_0 = A M^b \quad (6)$$

For zero shear stress viscosity, by introducing eq. (6) into eq. (5) it follows that

$$\eta_0 = A \bar{M}_w^b \quad (7)$$

where  $\bar{M}_w$  is the weight-average molecular weight. Thus this mixing rule may be denoted the  $\bar{M}_w$  mixing rule.

We assume that eq. (5) is valid for every shear stress. After introduction of eq. (2) into eq. (5), and conversion of the sum over  $M_i$  to an integral, eq. (5) becomes

$$\eta^{1/3.5} = A^{1/3.5} \int_{M_e}^{\infty} M w(M) [f(\tau M / a)]^{1/3.5} dM$$



and division by  $\eta_0$  gives

$$(\eta/\eta_0)^{1/3.5} = \int_{M_e}^{\infty} (M/\bar{M}_w) w(M) [f(\tau M/a)]^{1/3.5} dM \quad (8)$$

In order to integrate eq. (8) it is necessary to find an approximate function for

$$[f(x)]^{1/3.5} \quad (9)$$

where

$$x = \tau M/a$$

The function

$$h(x) = \sum_1^N \alpha_n \operatorname{erfc} [(1/\gamma) \log (x/x_n)] \quad (10)$$

where

$$\alpha_n = 2^{-n}$$

$$\gamma = 0.5$$

$$\log x_n = 0.086 + 1.03 (n - 1)$$

$\log x$  denotes the common logarithm, and

$$\operatorname{erfc} [(1/\gamma) \log (x/x_n)] = (1/\sqrt{\pi}) \int_{(1/\gamma) \log (x/x_n)}^{\infty} e^{-v^2} dv \quad (11)$$

may be considered as an approximation to the function (9) as shown in Table I. Equation (10) provides a close fit to eq. (9), even if  $N$  is less than 5, if unity is substituted for the other  $\operatorname{erfc}$  function. Increasing the value of  $N$  enhances the fit of eq. (10) to equation (9) when the values of the argument are high (Table II).

Introducing function (10) into eq. (8) and inverting the sums we have

$$\left(\frac{\eta}{\eta_0}\right)^{1/3.5} = \sum_1^N \alpha_n \int_{M_e}^{\infty} \frac{M}{\bar{M}_w} w(M) \operatorname{erfc} \left[ \frac{1}{\gamma} \log \left( \frac{x}{x_n} \right) \right] dM \quad (12)$$

where

$$x = \tau M/a$$

The integration of eq. (12) for polymers with log-normal molecular weight distribution is given in the appendix. The result is as shown in eq. (13).

$$\frac{\eta}{\eta_0} = \left\{ \sum_1^N \alpha_n \operatorname{erfc} [(1/\epsilon) \log (\bar{x}/x_n)] \right\}^{3.5} \quad (13)$$

where

$$\bar{x} = \tau M_0 Q/a = \tau \bar{M}_w Q^{1/2}/a$$

$$Q = \bar{M}_w/\bar{M}_n$$

$$\epsilon = [\gamma^2 + (\beta/2.3)^2]^{1/2} \quad \beta = (2 \ln Q)^{1/2}$$

TABLE I<sup>a</sup>

log $x$	$h(x)$	$[f(x)]^{1/3.5}$
-0.6	0.986	0.993
-0.4	0.955	0.973
-0.2	0.892	0.904
0.0	0.806	0.794
0.2	0.704	0.695
0.4	0.589	0.608
0.6	0.519	0.532
0.8	0.464	0.466
1.0	0.409	0.407
1.2	0.350	0.356
1.4	0.302	0.312
1.6	0.266	0.273
1.8	0.232	0.239
2.0	0.208	0.209
2.2	0.179	0.183
2.4	0.154	0.160
2.6	0.130	0.140
2.8	0.120	0.123
3.0	0.106	0.107
3.2	0.092	0.094
3.4	0.079	0.082

<sup>a</sup> As explained in the text, we have considered  $\eta_0 M \dot{\gamma} / a$  as the argument of the Rouse's (or Bueche's) function. Therefore we have:  $\omega_R = 1/a\eta_0 M \dot{\gamma} = \eta_0/\eta \eta \dot{\gamma} M/a = (\eta_0/\eta)x$ . By means of this expression it is possible to correlate the values of Rouse's function and the argument  $x$ . This conversion has been applied to the values of Rouse's function reported by Ferry.<sup>5</sup> The data of function  $[f(x)]^{1/3.5}$  reported in this table have been obtained by means of interpolations or extrapolations from the calculated values.

and  $M_n$  is the number-average molecular weight. The values of  $\eta/\eta_0$  versus  $\tau$  calculated by means of eq. (13) plotted on log-probability paper fall on a straight line when  $\eta/\eta_0 > 0.1$  and  $Q > 1.5$  (cf. Fig. 1).

Therefore eq. (13) may be replaced by

$$\eta/\eta_0 = \operatorname{erfc} [(1/\delta)\log(\bar{x}/K)] \quad (14)$$

where  $\delta$  and  $K$  are functions of  $Q$ .

Function (10) or its 3.5 power, and hence Bueche's equation, are very far from an  $\operatorname{erfc}$  function, because the  $\gamma$  value of the  $\operatorname{erfc}$  functions of the series is small. However as the heterogeneity increases, the corresponding value of  $\gamma$  in eq. (13), i.e.,  $\epsilon$ , increases, and the result is that the function  $\eta/\eta_0$  tends toward an  $\operatorname{erfc}$  function.

When

$$\tau M_0 Q / a x_1 = 1$$

the viscosity has a well-defined value which we denote by  $(\eta/\eta_0)_0$ . The value of  $\delta$  and  $(\eta/\eta_0)_0$  versus  $Q$  are related in Figures 2 and 3. From the graphs of Figure 2 and 3 it is theoretically possible to calculate the weight-average molecular weight and the ratio  $Q$ .

TABLE II

log $x$	$h(x)$	
	$N = 4$	$N = 3$
-0.6	0.986	0.986
-0.4	0.955	0.955
-0.2	0.892	0.892
0.0	0.806	0.806
0.2	0.704	0.704
0.4	0.589	0.589
0.6	0.519	0.519
0.8	0.464	0.464
1.0	0.409	0.409
1.2	0.350	0.350
1.4	0.302	0.302
1.6	0.266	0.266
1.8	0.232	0.232
2.0	0.208	0.208
2.2	0.179	0.179
2.4	0.154	0.154
2.6	0.130	0.137
2.8	0.120	0.129
3.0	0.106	0.126
3.2	0.092	0.125
3.4	0.079	0.124

### Z-Average Mixing Rule

At every shear stress the following mixing rule may be considered:

$$\eta^{1/b} = \frac{\sum_{i > i_c} w_i \eta_i^{2/b}}{\sum_{i > i_c} w_i \eta_i^{1/b}} \quad (15)$$

At zero shear stress this mixing rule yields

$$\eta_0 = A M_z^b \quad (16)$$

so it may be denoted the  $\bar{M}_z$  mixing rule. As stated above the contribution of molecular weights lower than the critical molecular weight can be omitted. In this case, in order to make possible the previous calculation, it is necessary to find an approximation to the function

$$[f(x)]^{2/3.5} \quad (17)$$

(see Table III)

This is given by

$$v(x) = \sum_1^N \alpha_n \operatorname{erfc} \left[ \frac{1}{\gamma'} \log (x/x'_n) \right] \quad (18)$$

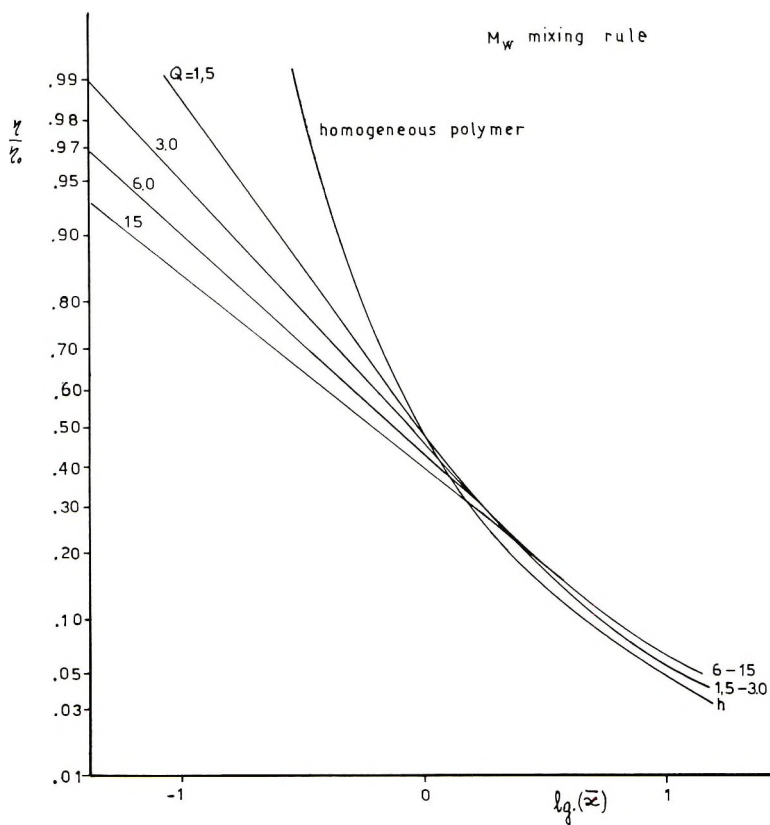


Fig. 1.  $\eta/\eta_0$  vs.  $\log(x)$  for heterogeneous polymers according to the  $M_w$  mixing rule.  
 $\bar{x} = \eta_0 M_0 Q/a$ .

TABLE III

$\log x$	$v(x)$	$[f(x)]^{2/3,6}$
-0.6	0.997	0.986
-0.4	0.965	0.946
-0.2	0.819	0.817
0.0	0.605	0.631
0.2	0.474	0.483
0.4	0.367	0.370
0.6	0.275	0.283
0.8	0.215	0.217
1.0	0.161	0.166
1.2	0.124	0.127
1.4	0.097	0.097
1.6	0.071	0.074
1.8	0.056	0.057
2.0	0.042	0.044

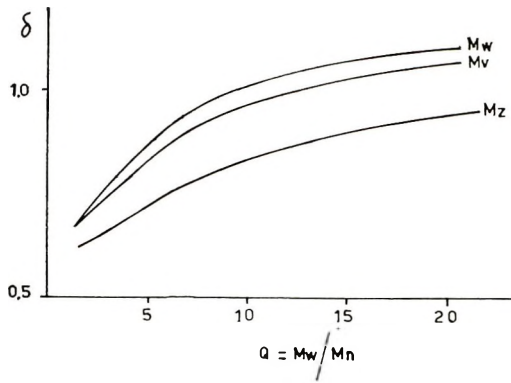


Fig. 2.  $\delta$  vs. the heterogeneity ratio for several mixing rules.

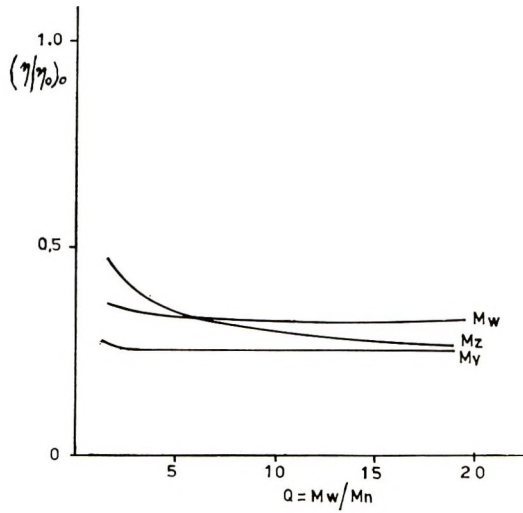


Fig. 3.  $(\eta/\eta_0)_o$  vs. the heterogeneity ratio for several mixing rules.

where

$$\gamma' = 0.25$$

$$\log(x'_n) = 0.13 + 0.52(n - 1)$$

As for the  $\bar{M}_w$  mixing rule, analogous calculations can be made and the final equation will be

$$\frac{\eta}{\eta_0} = \frac{\sum_1^N \alpha_n \operatorname{erfc}[(1/\epsilon') \log(\bar{x}/x'_n)]}{\sum_1^N \alpha_n \operatorname{erfc}[(1/\epsilon) \log(\bar{x}/x_n Q)]} \quad (19)$$



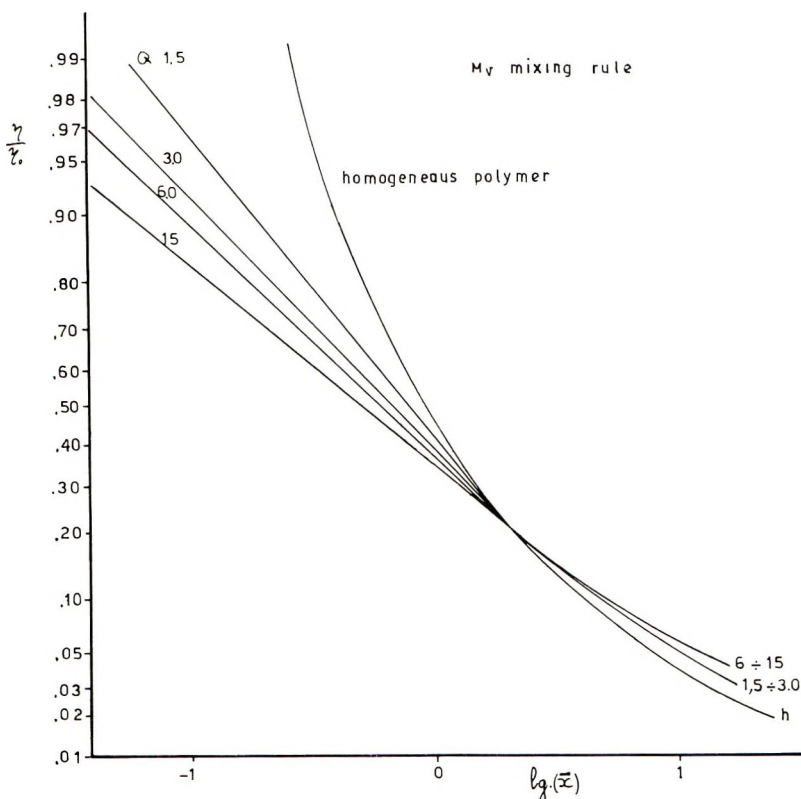


Fig. 4.  $\eta/\eta_0$  vs.  $\log(x)$  for heterogeneous polymers according to the  $M_z$  mixing rule.  
 $\bar{x}' = \eta_0 M_0 Q^2/a$ .

where

$$\bar{x} = \tau M_0 Q^2/a = \tau M_z Q^{1/2}/a$$

$$\epsilon' = [(\gamma')^2 + (\beta/2.3)^2]^{1/2}$$

$$\epsilon = [(\gamma)^2 + (\beta/2.3)^2]^{1/2}$$

In this case also  $\eta/\eta_0$  is very close to an erfc function (Fig. 4), and one may determine  $(\eta/\eta_0)_0$  values for which

$$\tau M_0 Q^2/a x'_1 = 1$$

Figures 2 and 3 show parameters  $\delta$  and  $(\eta/\eta_0)_0$  versus  $Q$ .

### Viscosity-Average Mixing Rule

Another mixing rule can be assumed which generalizes the weight-average mixing law

$$\eta^{\alpha/\beta} = \sum w_i \eta_i^{\alpha/\beta} \quad (20)$$

In fact, for polypropylene, van der Vegt<sup>9</sup> has found

$$\eta_0 = A \bar{M}_v^\alpha$$

$$\alpha = 0.78$$

where  $\bar{M}_v$  denotes the viscosity-average molecular weight. The mixing rule (20), which gives the result of van der Vegt, may be denoted the  $\bar{M}_v$  mixing rule.

In order to proceed as in the previous calculations it is necessary to find an approximation to the function:

$$[f(x)]^{0.78/3.5} \quad (21)$$

This function is given by

$$w(x) = \sum_1^N \alpha_n \operatorname{erfc}[(1/\gamma^n) \log(x/x''_n)] \quad (22)$$

where

$$\gamma^n = 0.65$$

and

$$\log(x''_n) = 0.21 + 1.34(n - 1)$$

(see Table IV). As for the  $\bar{M}_w$  mixing rule, the necessary integrations can be performed, the final equation being given by

$$\eta/\eta_0 = \left\{ \sum_1^N \alpha_n \operatorname{erfc}[(1/\epsilon^n) \log(\bar{x}''/x''_n)] \right\}^{3.5/0.78} \quad (23)$$

TABLE IV

$\log x$	$w(x)$	$[f(x)]^{0.78/3.5}$
-0.6	0.982	0.995
-0.4	0.956	0.980
-0.2	0.908	0.925
0.0	0.837	0.836
0.2	0.752	0.754
0.4	0.666	0.680
0.6	0.591	0.610
0.8	0.534	0.550
1.0	0.491	0.497
1.2	0.450	0.447
1.4	0.408	0.403
1.6	0.363	0.363
1.8	0.319	0.327
2.0	0.282	0.294
2.2	0.260	0.266
2.4	0.239	0.239
2.6	0.219	0.216
2.8	0.197	0.194
3.0	0.174	0.175
3.2	0.154	0.158
3.4	0.138	0.142

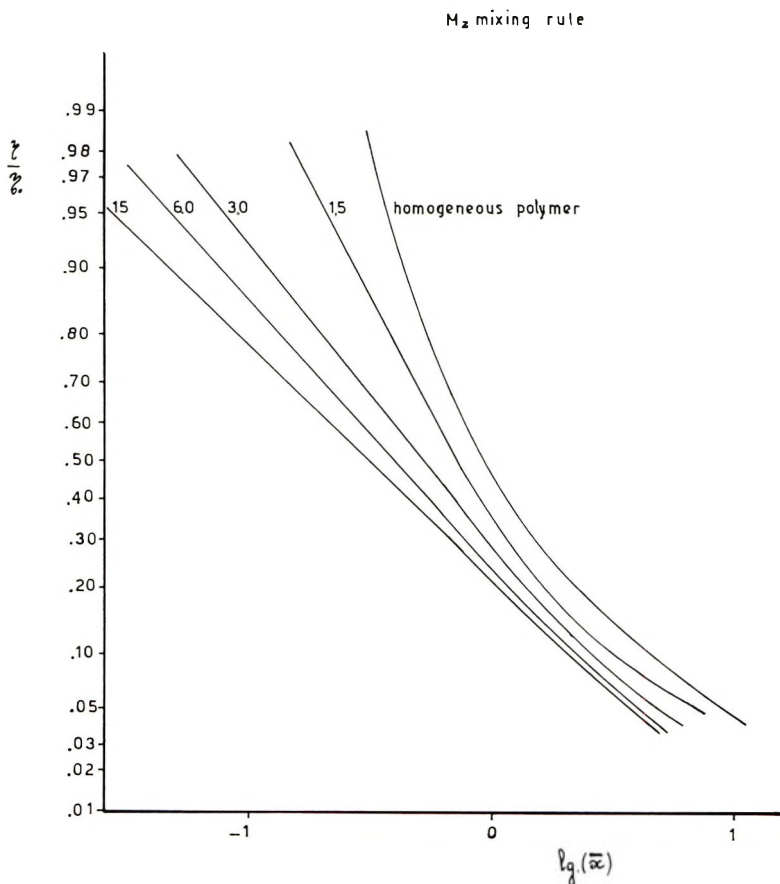


Fig. 5.  $\eta/\eta_0$  vs.  $\log(x)$  for heterogeneous polymers according to the  $M_v$  mixing rule,  $\bar{x} = \eta_0 M_0 Q^{0.78}/a$ .

where

$$\bar{x}'' = \tau M_0 Q^{0.78}/a$$

$$\epsilon'' = [(\gamma'')^2 + (\beta/2.3)^2]^{1/2}$$

As seen previously,  $\eta/\eta_0$  is very close to an erfc function (Fig. 5). In this case the  $(\eta/\eta_0)_0$  values are the values for which

$$\tau M_0 Q^{0.78}/a x'' = 1 \quad (24)$$

The  $\delta$  and  $(\eta/\eta_0)_0$  values versus  $Q$  are shown in Figures 2 and 3.

### COMPARISON BETWEEN THEORETICAL AND EXPERIMENTAL DATA

In order to find an experimental proof of our theory, the data provided by van der Vegt<sup>9</sup> for polypropylene and by Mendelson<sup>10</sup> for high-density polyethylene may be considered. In addition, our experimental data on

polypropylene are considered. It is very likely that both of these polymers have a log-normal molecular weight distribution.

Among Mendelson's data only the data relating to sample 1 may be used to prove our theory. We have chosen for  $\eta_0$  the value  $2.8 \times 10^5$ . In this case the  $\eta/\eta_0$  values versus shear stress, plotted on log-probability paper, are on a straight line. Then we obtain by means of Figure 2 ( $\bar{M}_w$  mixing rule) a value for  $Q$  of 6.2 which is exactly the value calculated by Mendelson from osmotic and light-scattering techniques.

TABLE V

Heterogeneity ratio $Q^a$	Zero shear stress viscosity		Calculated heterogeneity ratio	
	$\eta_0 \times 10^{-1b}$	$\eta_0^\dagger \times 10^{-4c}$	$Q_\delta^d$	$Q'_\delta^e$
3.5	2.7	2.7	3.5	3.0
5	6.3	6.3	5	4.5
9	6.3	6.3	9	7.5
10	3.0	3.0	10	8
11	47	53	7	6
25	16	19	20-25	17-20
9	16	16	9	7.5

<sup>a</sup> Calculated by van der Vegt.<sup>9</sup>

<sup>b</sup> Taken from viscosity-shear stress curves of van der Vegt.<sup>9</sup>

<sup>c</sup> Chosen to fit van der Vegt's data to a straight line on log-probability paper.

<sup>d</sup> Calculated from the  $\delta$  value according to the  $\bar{M}_w$  mixing rule.

<sup>e</sup> Calculated from the  $\delta$  value according to the  $\bar{M}_w$  mixing rule.

The data of van der Vegt plotted on log-probability paper are not exactly on a straight line. However, by choosing suitable values of  $\eta_0$  (see Table V) and by introducing the Rabinowitsch<sup>11</sup> correction, the data of van der Vegt plotted on log-probability paper can also be considered to fall on a straight line. According to van der Vegt, it is the viscosity-average molecular weight, which is linked to  $\eta_0$  by the 3.5 power law. We have therefore obtained the heterogeneity ratio by means of Figure 2 using the curve of the  $\bar{M}_v$  mixing rule. The values of  $Q$  calculated from our theory are very close to those calculated by van der Vegt. We observe, however, that the  $Q$  values obtained by means of the  $\bar{M}_w$  mixing rule also agree fairly well with those of van der Vegt.

The four polypropylene samples investigated by us, are samples of commercial polypropylene. The number-average molecular weight and the weight-average molecular weight were calculated by osmotic and light-scattering techniques.

Melt viscosities were determined by means of a capillary viscometer. Capillaries with different length/diameter ratios were used in order to determine the end correction. For all samples the viscosity measurements were carried out at 160, 190, or 210°C. and reduced to 190°C. by means of the WLF method.<sup>12</sup> The Rabinowitsch correction was applied.

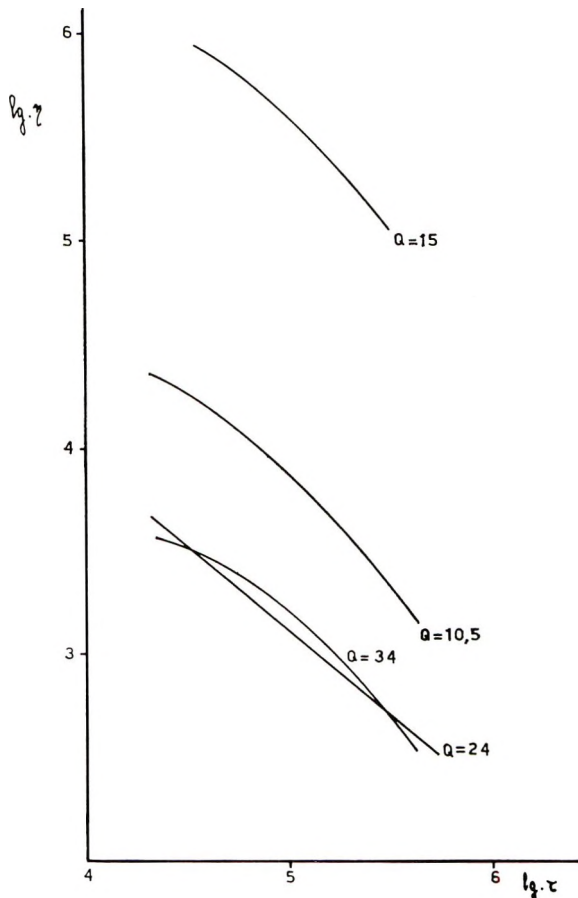


Fig. 6. Viscosity-shear stress master curves at 190°C.

In Figure 6 the viscosity versus shear stress master curves at 190°C. are plotted. The  $\eta_0$  viscosities were calculated in order to obtain (on log-probability paper) the  $\eta/\eta_0$  values versus  $\tau$  along a straight line (Fig. 7). The  $\eta_0$  values and the weight-average molecular weight are related by a 3.5 power law (Fig. 8). The results of our analysis are reported in Table VI. The agreement between  $Q$  calculated by the conventional method and  $Q_s$  calculated by means of Figure 2 ( $\bar{M}_w$  mixing rule) is fairly good.

According to our theory the  $Q$  value can be calculated also from the position of the straight line drawn through the experimental data on log-probability paper. According to our preceding statements we can write (with limitation:  $Q > 1.5$  and  $\eta/\eta_0 > 0.1$ ):

$$\eta/\eta_0 = \operatorname{erfc}[(1/\delta) \log(\tau M_0 Q^h / aK)]$$

where the  $\delta$  and  $K$  values are dependent upon the heterogeneity ratio  $Q$  and upon the type of mixing rule; the  $h$  value is independent of the heterogeneity, but dependent on the mixing rule. Calling  $\tau_{0.5}$  the shear stress



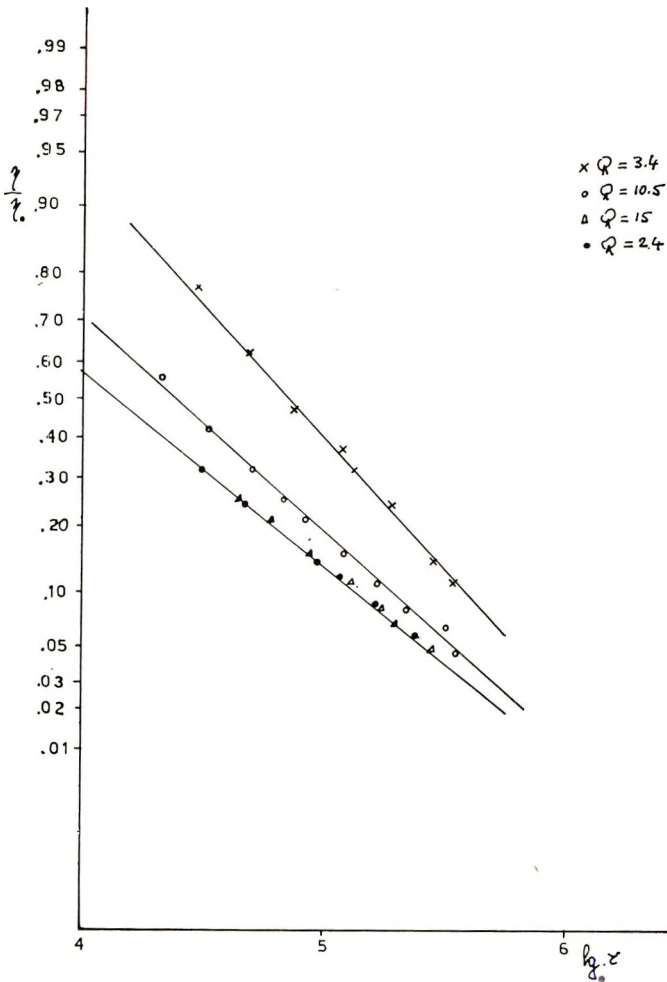


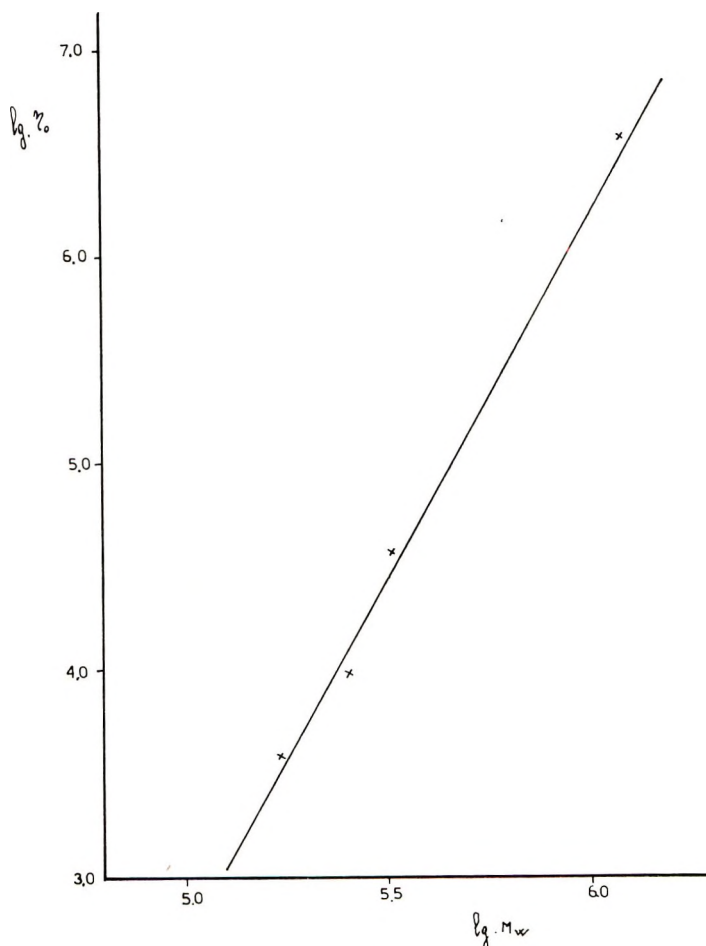
Fig. 7.  $\eta/\eta_0$  vs. shear stress curves plotted on log-probability paper.

for which  $\eta/\eta_0 = 0.5$ , we have  $a/M_0\tau_{0.5} = Q^h/K$ , where  $a/M_0\tau_{0.5}$  depends on both the  $Q$  ratio and the mixing rule. The theoretical  $a/M_0\tau_{0.5}$  value as a function of  $Q$  for the three mixing rules together with the data of van der Vegt, Mendelson, and our data are reported in Figure 9.

Mendelson's and our data agree well with the  $\bar{M}_w$  mixing rule. The data of van der Vegt fit the  $\bar{M}_v$  mixing rule when  $Q$  is higher than 9; for lower  $Q$  values a different mixing rule must be assumed for better agreement. We observe that the van der Vegt samples with narrow distribution were made either by fractionation or by thermal breakdown, so this fact may be a possible explanation of the disagreement.

## DISCUSSION

From this theory the following conclusion can be drawn. When the  $Q$  values are not too low ( $Q > 1.5$ ), a straight line results when the values of

Fig. 8.  $\eta_0$ - $\bar{M}_w$  graph.

$\eta/\eta_0$  versus  $\tau$  are plotted on log-probability paper as long as  $\eta/\eta_0 > 0.1$ , regardless of the mixing rule chosen. The slope and position of the straight line depend both on the heterogeneity and on the mixing rule.

The determination of the  $Q$  values from the  $\delta$  values is somewhat un-

TABLE VI

$\bar{M}_w \times 10^{-5a}$	$\bar{M}_n \times 10^{-5b}$	$\eta_0 \times 10^{-4}$	$Q$ ( $= \bar{M}_w / \bar{M}_n$ )	$Q_\delta^c$
1.78	0.52	0.40	3.4	3.4
3.30	0.31	4.0	10.5	9
12.3	0.82	40	15	15-25
2.60	0.11	1.0	24	15-25

<sup>a</sup> Calculated by light scattering.

<sup>b</sup> Calculated by osmometry.

<sup>c</sup> Calculated from the  $\delta$  value ( $\bar{M}_w$  mixing rule).

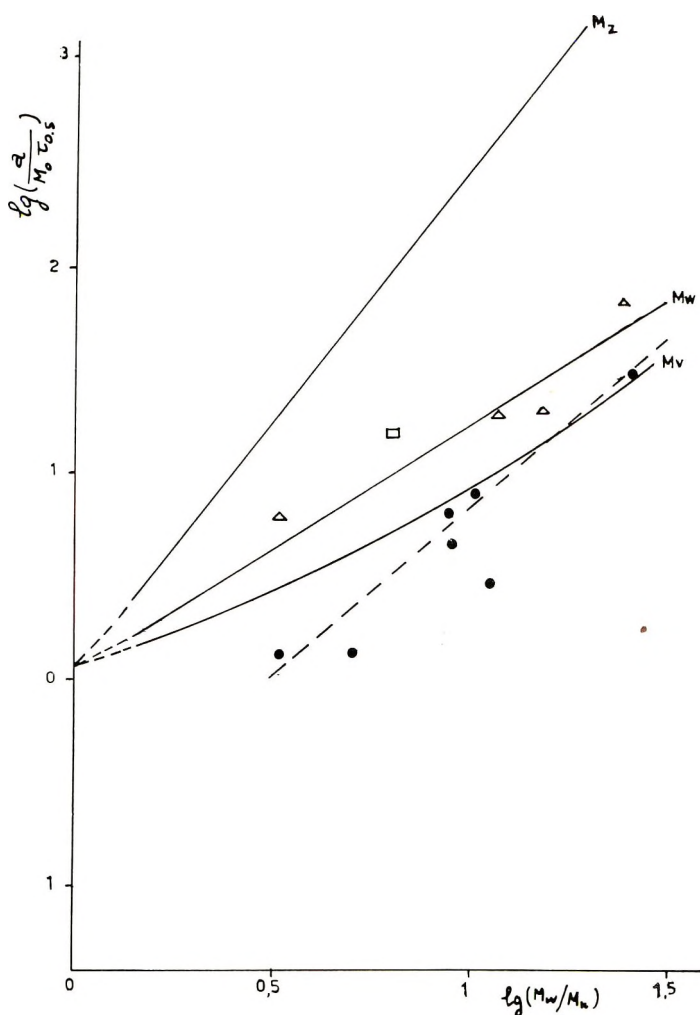


Fig. 9.  $a/(M_0\tau_{0.5})$  vs. heterogeneity ratio for several mixing rules (lines): (●) data of van der Vegt;<sup>9</sup> (□) data of Mendelson;<sup>10</sup> (Δ) our data.

reliable because the  $\delta$  values do not change a great deal as a function of  $Q$  and, besides, strongly depend on the  $\eta_0$  value chosen. The determination of the  $Q$  values by the  $(\eta/\eta_0)_0$  or the  $\tau_{0.5}$  values is more reliable, but on the other hand, the importance to know the right mixing rule is predominant; moreover, it is necessary to know an average molecular weight. The average molecular weight may be calculated from the  $\eta_0$  value by means of the 3.5 power law. In any event, it is indispensable for the application of the theory to know which average molecular weight is linked to  $\eta_0$  by means of the 3.5 power law.

By trial and error it is possible to calculate the  $\eta_0$ ,  $M_0$ , and  $Q$  values by means of rheological data alone if we have viscosity versus shear stress

curves for several samples of different average molecular weights. If we assume that the same mixing rule is valid for the different values of heterogeneity, the present theory provides some functional expressions involving  $M_0$ ,  $\eta_0$ ,  $Q$ , and experimental data. These functional expressions are sufficient to determinate  $M_0$ ,  $\eta_0$ ,  $Q$  from the experimental data. In fact:  $\eta_0$  has to be so chosen that  $\eta/\eta_0$  versus  $\tau$  is a straight line on log-probability paper; the  $Q$  ratio is obtainable from the  $\delta$  value by means of Figure 2 (by choosing a mixing rule); the  $M_0$  average molecular weight may be determined by the  $(\eta/\eta_0)_0$  or the  $\tau_{0.5}$  value; the correct choice of the mixing rule may be checked by means of the 3.5 power law.

By trial and error it is thus possible to determine the right mixing rule, the zero shear stress viscosity, an average molecular weight, and the heterogeneity. If  $\eta_0$  can be experimentally determined the whole procedure is simplified.

Unfortunately from van der Vegt's experimental data it seems that the mixing rule has to be changed, while from our data this does not appear necessary. In the case of polypropylene it can not be explained why different mixing rules are obtained according to van der Vegt's experimental data and ours.

More experimental data are required before this method can be considered reliable. The treatment is valid only for linear polymers with log-normal molecular weight distribution, but can be applied also to other distributions, provided that they can be expanded in terms of a series of log-normal functions. Obviously the treatment will result in more complicated forms.

## APPENDIX

According to Wesslau,<sup>13</sup> the log-normal molecular weight distribution may be expressed by the equation:

$$w(M)dM = \frac{1}{\sqrt{\pi}} e^{-[(1/\beta) \ln (M/M_0)]^2} d \left( \frac{1}{\beta} \ln \frac{M}{M_0} \right) \quad (\text{A-1})$$

where  $w(M)$  is the weight of the fraction of the polymer with molecular weight between  $M$  and  $M + dM$ .

Putting  $y = (1/\beta) \ln (M/M_0) - \beta/2$

we transform eq. (A-1) into

$$(M/M_w)w(M) dM = (1/\sqrt{\pi}) e^{-y^2} dy$$

Setting

$$Q = \bar{M}_w/\bar{M}_n = e^{+\beta^2/2}$$

we write eq. (8) in the form

$$(\eta/\eta_0)^{1/3.5} = (1/\pi) \sum_1^N \alpha_n \int_{y_e}^{\infty} e^{-y^2} \int_{v_e}^{\infty} e^{-v^2} dv dy \quad (\text{A-2})$$

where

$$y_e = -(1/\beta) \ln (\bar{M}_w Q^{1/2}/M_e)$$

$$v_e = (1/2.3\gamma) [\ln(\bar{x}/x_n) + \beta y]$$

$$\bar{x} = \tau M_0 Q/a = \tau \bar{M}_w Q^{1/2}/a$$

By differentiating eq. (A-2) with respect to  $\ln(\bar{x})$ , we have

$$\frac{d(\eta/\eta_0)^{1/3.5}}{d \ln \bar{x}} = \frac{-1}{2.3\gamma\pi} \sum_1^N \alpha_n \int_{y_e}^\infty \exp \left\{ -y^2 - \left[ \frac{1}{2.3\gamma} \left( \ln \frac{\bar{x}}{x_n} + \beta y \right) \right]^2 \right\} dy \tag{A-3}$$

Also we have

$$y^2 + \left[ \frac{1}{2.3\gamma} \left( \ln \frac{\bar{x}}{x_n} + \beta y \right) \right]^2 = z^2 + \frac{1}{2.3} \left[ \frac{1}{\epsilon} \ln \left( \frac{\bar{x}}{x_n} \right) \right]^2$$

where

$$z = (\epsilon/\gamma)y + (\beta/2.3\epsilon) \ln (\bar{x}/x_n)$$

$$\epsilon = [\gamma^2 + (\beta/2.3)^2]^{1/2}$$

By converting the natural logarithms into common logarithms, we obtain

$$\frac{d(\eta/\eta_0)^{1/3.5}}{d \log \bar{x}} = \frac{-1}{\sqrt{\pi}} \sum_1^N \alpha_n \frac{1}{\epsilon} e^{-[(1/\epsilon) \log \bar{x}/x_n]^2} \left\{ 1 - I \left( \log \frac{\bar{x}}{x_n} \right) \right\} \tag{A-4}$$

where

$$I[\log(\bar{x}/x_n)] = (1/\sqrt{\pi}) \int_{-\infty}^{z_{en}} e^{-v^2} dv$$

$$z_{en} = -\frac{\epsilon\beta}{4\gamma} - 2.3 \frac{\epsilon}{\beta\gamma} \log \frac{\bar{M}_w}{M_e} + \frac{1}{2.3} \cdot \frac{\beta}{\epsilon\gamma} \log \frac{\bar{x}}{x_n}$$

The values of  $I[\log(\bar{x}/x_1)]$  and of  $I[\log(\bar{x}/x_2)]$  for  $x = 10$  and  $\bar{M}_w = 10 M_e$  are reported in Table VII. We observe that the value 10 for  $\bar{x}$  is not low, because  $\eta/\eta_0$  is approximately equal to 0.05 when  $\bar{x}$  is equal to 10. The maximum contribution of  $I[\log(\bar{x}/x_1)]$  to  $(\eta/\eta_0)^{3.5}$  is 0.6% (it must be con-

TABLE VII

Q	$\frac{-\epsilon\beta}{4\gamma}$	$-\frac{2.3}{\beta\gamma} \epsilon$	$\frac{+\beta}{2.3\gamma\epsilon}$	$z_{e1}$	$z_{e2}$	$I \left[ \log \left( \frac{\bar{x}}{x_1} \right) \right]$	$I \log \left( \frac{\bar{x}}{x_2} \right)$
1.5	-0.28	-3.22	1.24	-2.34	-3.37	$<10^{-4}$	$<10^{-4}$
3.0	-0.64	-2.71	1.48	-1.95	-2.98	0.0003	$<10^{-4}$
6.0	-0.90	-2.34	1.71	-1.61	-2.64	0.002	$<10^{-4}$
15	-1.31	-2.23	1.79	-2.33	-3.36	$<10^{-4}$	$<10^{-4}$



sidered that its coefficient  $\alpha_1$  is equal to 0.5); therefore the maximum contribution of  $I[\log(\bar{x}/x_1)]$  is  $\simeq 2\%$ . The contribution of  $I[\log(\bar{x}/x_2)]$  is always negligible; consequently the term  $I[\log(\bar{x}/x_n)]$  may be neglected as long as  $\eta/\eta_0 > 0.05$ . Equation (A-4) may be integrated between  $-\infty$  and  $\log(\bar{x})$  to obtain:

$$(\eta/\eta_0)^{1/3.5} = \sum_n^N \alpha_n \operatorname{erfc}[(1/\epsilon) \log(\bar{x}/x_n)] \quad (\text{A-5})$$

where

$$\operatorname{erf}[(1/\epsilon) \log(\bar{x}/x_n)] = (1/\sqrt{\pi}) \int_{(1/\epsilon) \log(\bar{x}/x_n)}^{\infty} e^{-v^2} dv$$

and

$$\bar{x} = \tau M_0 Q/a$$

### References

1. P. E. Rouse, *J. Chem. Phys.*, **21**, 1272 (1953).
2. F. Bueche, *J. Chem. Phys.*, **22**, 1570 (1954).
3. E. Menefee and W. L. Peticolas, *J. Chem. Phys.*, **35**, 946 (1961).
4. J. M. McKelvey, *Polymer Processing*, Wiley, New York, 1962, p. 36.
5. J. D. Ferry, *Viscoelastic Properties of Polymers*, Wiley, New York, 1961, p. 462.
6. T. Takemura, *J. Polymer Sci.*, **27**, 549 (1958).
7. W. L. Peticolas and E. Menefee, *J. Chem. Phys.*, **35**, 951 (1961).
8. F. Bueche, *J. Chem. Phys.*, **25**, 599 (1956).
9. A. K. van der Vegt, *Plastic Inst. (London) Trans. J.*, **32**, No. 97, 165 (1964).
10. R. A. Mendelson, *Trans. Soc. Rheol.*, **9**:1, 53-63 (1965).
11. B. Rabinowitch, *Z. Physik. Chem.*, **A145**, 1 (1929).
12. M. L. Williams, R. F. Landel and J. D. Ferry, *J. Am. Chem. Soc.*, **77**, 3701 (1955).
13. H. Wesslau, *Makromol. Chem.*, **20**, 111 (1956).

### Résumé

En choisissant des approximations convenables pour la fonction de Bueche, il est possible de calculer la viscosité en fonction de la tension de cisaillement pour des polymères linéaires a distribution moléculaire normale. Pour des polymères préparés en bloc les règles de mélanges  $M_w$ ,  $M_w$ ,  $M_z$  ont été prises en considérations. Pour les valeurs de  $\eta/\eta_0 > 0.1$  et des hétérogénéités de  $M_w/M_n > 1.5$  le résultat obtenu avec n'importe quelle règle de mélange est  $\eta/\eta_0 = \operatorname{erfc} [(1/\delta) \log(M_0 Q^b/aK)]$   $a = \pi^2/6 RT$ , où les valeurs de  $\delta$  et  $K$  sont dépendantes du rapport d'hétérogénéité  $Q = M_w/M_n$  et dépendent du type de la règle de mélange; d'autre part, le valeur est indépendant de l'hétérogénéité, mais dépend de la règle de mélange. La plupart des résultats expérimentaux s'accordent avec la règle de mélange  $M_w$  ainsi, que l'on s'y attendrait au départ de la règle de mélange pour des tensions de cisaillement nulles. Les résultats expérimentaux sont comparés avec les résultats de la théorie.

### Zusammenfassung

Durch Wahl geeigneter Näherungen für die Funktion von Bueche ist es möglich, die Abhängigkeit der Viskosität von der Schubspannung für lineare Polymere mit einer log-normalen Molekülverteilung zu berechnen. Für Polymere in Substanz wird die Mittelwertbildung entsprechend  $M_v$ ,  $M_w$  und  $M_z$  in Betracht gezogen. Für Werte von  $\eta/\eta_0 >$

0,1 und Heterogenitäten mit  $M_w/M_n > 1,5$  wird für eine beliebige Mittelwertbildung das Ergebnis  $\eta/\eta_0 = \operatorname{erfc} [(1/\delta) \log (M_w Q^h/aK)]$ ,  $a = (\pi^2/6) \delta RT$ , erhalten, wo die Werte für  $\delta$  und  $K$  von Heterogenitätsquotienten  $Q = M_w/M_n$  und von Typ des Mittelwerts abhängen; andererseits ist der  $h$ -Wert von der Heterogenität unabhängig, hängt jedoch von der Mittelwertbildung ab. Die meisten Versuchsergebnisse entsprechen einer Mittelwertbildung  $M_w$ , wie man aus der Mittelwertbildung für die Schubspannung  $O$  erwarten sollte. Die Versuchsdaten werden mit den theoretischen Ergebnissen verglichen.

Received May 21, 1965

Revised September 30, 1965

Prod. No. 4923A

## Oleophilic Ion-Exchange Resins. IV. Swelling of Quaternary Ammonium Polymers in Mixed Solvents

MITSUZO SHIDA\* and HARRY P. GREGOR, *Department of Chemistry, Polytechnic Institute of Brooklyn, Brooklyn, New York*

### Synopsis

The swelling characteristics of an oleophilic anion-exchange resin in methanol-benzene and ethanol-chloroform mixed solvent systems were compared with those of a conventional anion-exchange resin. The oleophilic resin was prepared by amination of chloromethylated polystyrene 1% DVB with *N,N*-dimethyldodecylamine. It showed a large shift of the swelling peak from polar to less polar solution compositions in both methanol-benzene and ethanol-chloroform systems as compared with the swelling of conventional resins. Total solvent uptake and solvent distribution between resin and solvent phases were also determined. The less polar solvent (benzene or chloroform) was sorbed preferentially by the oleophilic resin over a wide range of composition, while preference for the more polar solvent (methanol or ethanol) by the conventional resin was shown over the entire composition of the mixed solvent systems. The Newman-Krigbaum treatment of mixed solvents was applied to swelling data on the ethanol-chloroform-oleophilic resin system, where the volume of the gel network plus the solvent imbibed was relatively constant over the entire range of composition. The result suggests a strong similarity of the liquid-liquid interaction terms in this gel phase compared with those in the pure binary liquid phase.

### INTRODUCTION

Several investigators have studied ion exchange in nonaqueous and aqueous mixed solvents using ordinary ion-exchange resins. The preparation of oleophilic ion-exchange resins and their swelling characteristics in a variety of pure solvents has been described.<sup>1</sup> In this paper the swelling behavior of a quaternary ammonium oleophilic resin is compared with that of a conventional resin in two mixed solvent systems which contained one polar constituent. A thermodynamic study of these resin systems is presented. It makes use of the work of Newman and Krigbaum,<sup>2</sup> who have shown that for mixtures of solvent molecules, one of which is polar, the contribution to the free energy of mixing due solely to pair formation and association of solvents (1) and (2) can be written by an appropriate power series in concentration as,

$$\Delta G_M = V_T(A_1v_1 + A_2v_2 + A_3v_1v_2 + \dots)v_1v_2$$

where  $v_1$  and  $v_2$  are the volume fractions of corresponding solvents in the

\* Present address: W. R. Grace and Co., Clifton, New Jersey.

binary phase of total volume  $V_T$  and  $A_1$ ,  $A_2$ , and  $A_3$  are the interaction coefficients. If the chemical potentials are written in their usual form for a binary system,

$$\begin{aligned}\mu_1 - \mu_1^\circ &= RT[\ln v_1 + (1 - p)v_2 + X_{12}v_2^2] \\ \mu_2 - \mu_2^\circ &= RT[\ln v_2 + (1 - p^{-1})v_1 + X_{21}v_1^2]\end{aligned}$$

where  $p = V_1/V_2$  is the molar volume ratio,  $X$  is the usual interaction parameter,

$$X_{12} = (V_1/RT)[A_2 + 2(A_1 - A_2 + A_3 + \dots)v_1 - (3A_3 + \dots)v_1^2 + \dots]$$

$$X_{21} = (V_2/RT)[A_1 - 2(A_1 - A_2 - A_3 + \dots)v_2 - (3A_3 + \dots)v_2^2 + \dots]$$

We find then that for a polar solvent system the interaction parameters are no longer concentration-independent, and also that  $X_{12} \neq pX_{21}$ .

### Experimental

The detailed preparation of the polymer studied is described elsewhere.<sup>1</sup> Starting with 1% (DVB - 1) crosslinked polystyrene, chloromethylation followed by amination with *N,N*-dimethyldodecylamine or trimethylamine yielded an oleophilic anion-exchange resin (designated OA) of capacity 2.06 meq./g. in the chloride form and the conventional type I anion-exchange resin A of capacity 3.07 meq./g., respectively. The latter is comparable to Dowex 1-X1; the designations of these resins in the earlier work of Gregor et al.<sup>1</sup> are CA1-1 and CA1-2, respectively.

For the swelling measurement, approximately 0.7 g. of accurately weighed dry chloride state resin was placed in a weighed 1 cm. glass tube having 100 mesh stainless steel wire gauze supported by a Teflon ring at one end. This tube was inserted in a slightly larger one which could be sealed at the top. A measured amount of mixed solvents was added. Rate experiments showed that equilibrium was reached in 48 hr. After one week at 24-26°C. the solvent was withdrawn and its composition measured by an Abbe-3L refractometer (Bausch & Lomb) with an accuracy of  $\pm 0.1\%$  (in mole fractions) of the benzene-methanol and  $\pm 0.2\%$  for the chloroform-ethanol system. The inner tube with swollen resin was then centrifuged for 3 min. at 2600 rpm and weighed. These data allow one to calculate the amount and composition of sorbed solvent. With a larger amount of resin (1.5 g.) and a large excess of solvent (300 ml.), the solvent composition in the resin phase was also measured by vacuum distillation of the solvent from the resin.<sup>3</sup>

The density of the dry resin was determined by a pycnometric technique.<sup>4</sup> Resin A swells but a few per cent in hexane and only 6% in benzene; therefore, its density is determinable with reasonable accuracy. Since all common solvents swell the oleophilic resin somewhat, *n*-hexane was used as the pycnometric fluid, and the assumption was made that the solvent density in the resin was the same as that of pure solvent. The error here is small, for even the oleophilic resin swelled less than 20% in hexane but

more than 200% in chloroform, methanol, and ethanol and 45% in benzene. Scatchard and Raymond<sup>5</sup> measured the density of chloroform-ethanol mixtures and Williams et al.<sup>6</sup> that of benzene-methanol mixtures. Both mixtures usually showed such small deviations from ideality ( $\bar{V}_i = V_i^\circ$  within  $\pm 0.5\%$ ) that they were treated as ideal with regard to volumes. The partial molar volume of a solvent in the resin phase was similarly set equal to its molar volume. An error may result, but it is undoubtedly quite small because of the large degree of swelling and the small deviations from ideality observed by Gregor et al.<sup>7</sup> for water in sulfonated polystyrene resins. There are no direct means (outside of visual observation, which is inaccurate) to determine swollen resin volumes.

### Results and Discussion

The results of the phase analyses for the methanol-benzene-resin and ethanol-chloroform-resin systems are shown in Figures 1 and 2, which are ternary diagrams in terms of volume fractions in the resin phase. The same data in terms of the volume fractions of solvents in the solvent phase are also given. Plots of the volume swelling ratio (the volume of swollen resin/volume of dry resin) or  $v_3^{-1}$  with pure solvents of a wide range of cohesive energy density (CED) with both oleophilic cation and anion-exchange resins showed two peaks, one at relatively low CED and the other at high CED values. The former peak is much smaller with conventional ion-exchange resins, as expected. The analogous effects of the long alkyl chains of the oleophilic resin in mixed solvents can also be seen from Figures 1 and 2; resin OA also shows a swelling peak in equilibrium with benzene or chloroform-rich liquid phases, while resin A has a peak in the methanol- or ethanol-rich phases only.

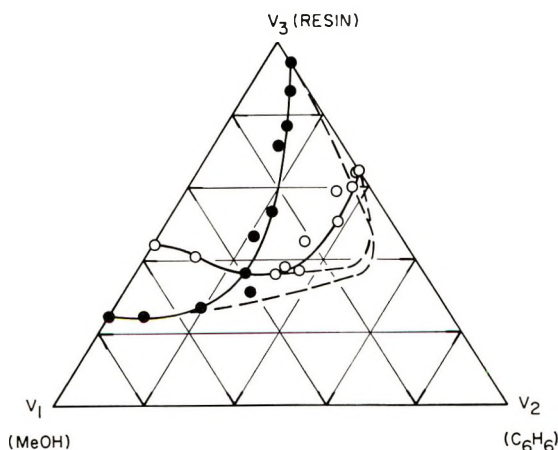


Fig. 1. Volume fraction of (O) oleophilic and (●) conventional resins as a function of the volume fraction of methanol ( $v_1$ ) and of benzene ( $v_2$ ). Dotted line shows the composition of the corresponding solution phases designated on the horizontal lines of constant resin volume fraction ( $v_3$ ).



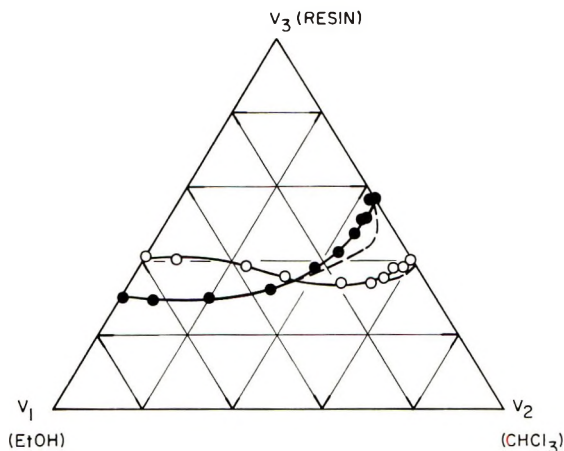


Fig. 2. Volume fraction of (O) oleophilic and (●) conventional resin as a function of volume fraction of ethanol ( $v_1$ ) and of chloroform ( $v_2$ ).

The selectivity coefficient for solvent distribution in a resin phase is  $K_2^1 = (\bar{N}_1/\bar{N}_2)(N_2/N_1)$ , where  $\bar{N}$  is the mole fraction and the superscript bar designates the resin phase. The oleophilic resin showed a selectivity for benzene of about 100 when the solvent mole fraction of methanol in the resin was 0.2; the A resin had a selectivity of several hundred, but the absolute amount sorbed was quite small. The selectivity of the oleophilic resin for ethanol (from ethanol-chloroform) was 3 at an ethanol mole fraction of 0.1, with the other resin showing a selectivity of about 10 at the same gel phase composition. The absolute amounts sorbed are more comparable here (see Fig. 2).

Further thermodynamic studies were made on the ethanol-chloroform-resin system by using the activity data of Scatchard and Raymond<sup>8</sup> for this binary liquid system. These authors determined partial vapor pressures at 35 and 45°C. On assuming the latent heats were constant, the activity of ethanol and chloroform at 25°C. were computed.

In this contribution, we are dealing with a material made by substitution into a preformed polymer network. Braun<sup>8</sup> has described numerous analogous polymers. The molecular weight between crosslinks  $M_c$  is defined by Flory and Rehner.<sup>9</sup> The question arises whether pendant groups are effective or not in exercising constraint against network swelling and should be excluded from the  $M_c$  calculation. Kwei<sup>10</sup> has chosen to neglect this constraint in dealing with a crosslinked polymer with  $M_c \cong 250$ .

A modification of the terms expressing chain configurational entropy change in Flory's theory<sup>11</sup> for a type of substituted networks is now described. The following two systems may be considered. The first is a network formed after a substitution reaction, i.e., formed in the relaxed state in the absence of solvent. Consequently, there is no strain in the dry network. The entropy change associated with swelling is obtained by the usual method, provided the Gaussian form is followed for the distri-

bution of displacement lengths of chain elements. The partial molar free energy of dilution  $\Delta\bar{G}_1$  for the network is,

$$\Delta\bar{G}_1 = RT[\ln(1 - v_3) + v_3 + X_{13}v_3^2 + (V_1/\bar{v}M_c)(1 - 2M_c/M)(v_3^{1/3} - v_3/2)]$$

where  $v_3$  is the volume fraction of polymer in the swollen network,  $X_{13}$  is the interaction parameter for the network and solvent,  $V_1$  the molar volume of the solvent,  $\bar{v}$  the specific volume of the (dry) network, and  $M$  the primary molecular weight. Here the contribution of side chains to  $M$  must be included though they do not exercise constraint against network swelling.

A network may also be formed before the substitution reaction, and will have strain even in its dry state. It is, therefore, necessary to consider the entropy change of the network from its original state to the substituted dry state before swelling. Since the entropy of mixing due to the substitution reaction is essentially negligible, only the entropy change associated with the volume change must be considered.<sup>12</sup> Let  $V_3'$  be the volume of the original network,  $V_3^\circ$  the volume of the substituted network and  $V_3$  that of the swollen network. The total elastic entropy change is that corresponding to the volume change from  $V_3'$  to  $V_3$ . The internal pressure is now that resulting from the original strain plus that due to the swelling process. Letting  $v_3' = V_3'/V_3$  and  $v_3 = V_3^\circ/V_3$ , we have

$$\Delta\bar{G}_1 = RT \{ \ln(1 - v_3) + v_3 + X_{13}v_3^2 + (V_1/\bar{v}M_c')[(v_3')^{1/3} - v_3'/2] \}$$

where  $M_c'$  is the value before the substitution.

The oleophilic resin was prepared from crosslinked polystyrene; accordingly, its volume increased considerably upon chloromethylation and subsequent amination. In ethanol,  $v_3^{-1} = 2.43$  and in chloroform the value is 2.45;  $v_3' = 0.175$  in ethanol and 0.177 in chloroform. Using the data obtained by Boyer and Spencer<sup>13</sup> for polystyrene (1% DVB) for  $M_c'$  ( $8.5 \times 10^3$ ), the interaction parameters were calculated from the above equation.

The corresponding expressions for the chemical potentials in the ternary phase can be written as,

$$\Delta\bar{G}_1 = RT \{ \ln v_1 + (1 - p)v_2 + v_3 + X_{12}'v_2^2 + X_{13}'v_3^2 + (X_{12}' + X_{13}' - pX_{23}')v_2v_3 + [(v_3')^{1/3} - (v_3')/2](V_1/\bar{v}M_c') \}$$

$$\Delta\bar{G}_2 = RT \{ \ln v_2 + (1 - p^{-1})v_1 + v_3 + X_{21}'v_1^2 + X_{23}'v_3^2 + (X_{21}' + X_{23}' - p^{-1}X_{13}')v_1v_3 + [(v_3')^{1/3} - (v_3')/2](V_2/\bar{v}M_c') \}$$

where the subscripts 1, 2, and 3 indicate ethanol, chloroform, and the resin, respectively. The calculated  $X_{13}'$  (0.68) and  $X_{23}'$  (0.68) values were used to obtain  $X_{12}'$  and  $X_{21}'$  from the above equations. The calculated  $X_{12}$  and  $pX_{21}$  for the binary solvent system versus volume fraction of ethanol are shown in Figure 3 by solid lines. The calculated interaction parameters in the gel phase are shown by  $X_{12}'$  and  $pX_{21}'$  versus  $v_1/(v_1 + v_2)$ .

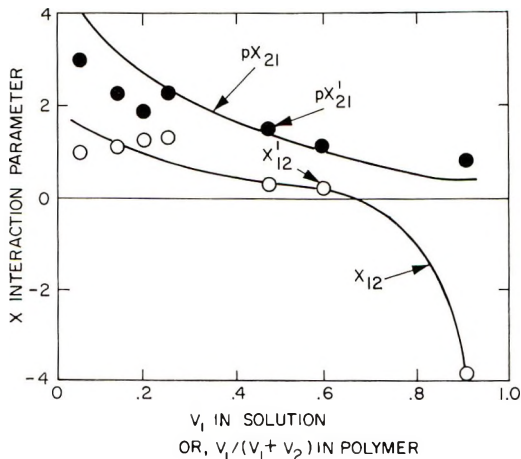


Fig. 3. Calculated and experimentally determined interaction parameters of ethanol (1) and chloroform (2) in the solution phase ( $X$ ) and in the gel phase ( $X'$ ) of the oleophilic resin as a function of the volume fraction of ethanol in the solution phase or of the imbibed solvent in the gel phase: (—) calculated; (O) experimental  $X_{12}$ ; (●) experimental  $pX_{21}$ .

The assumption that  $X_{13}'$  and  $X_{23}'$  are constant over a wide range of polymer concentration is not correct. However, in the present experiment the value of  $v_3$  stayed within 0.35–0.41; furthermore, the calculated values of  $X_{13}'$  and  $X_{23}'$  were identical (0.68) for this system.

In the case when the network swells more than 2.5 times its dry volume the "free" solvent molecules in the gel phase may far outnumber the "bound" solvent molecules. The interaction parameters in the gel phase ( $X_{12}'$  and  $pX_{21}'$ ) should then exhibit the same changes with volume fraction which they exhibit in the solution phase ( $X_{12}$  and  $pX_{21}$ ). From Figure 3 it can be seen that the dependence of  $X_{12}'$  and  $pX_{21}'$  on the concentration follows that of  $X_{12}$  and  $pX_{21}$  as shown by the solid lines, except in the range of a small volume fraction of ethanol in the gel phase. This fact corroborates the validity of the equations used.

Taken from the dissertation of Mitsuzo Shida, presented in partial fulfillment of the requirements for the degree of Doctor of Philosophy in Chemistry, Polytechnic Institute of Brooklyn, New York, June 1964.

## References

1. H. P. Gregor, G. K. Hoeschele, R. Potenza, A. G. Tsuk, R. Feinland, M. Shida, and Ph. Teyssie, *J. Am. Chem. Soc.*, **87**, 5525 (1965).
2. S. Newman and W. R. Krigbaum, *J. Polymer Sci.*, **18**, 107 (1955).
3. M. H. Gottlieb, Ph.D. Dissertation, Polytechnic Institute of Brooklyn, Brooklyn, N. Y., 1953.
4. H. P. Gregor, F. Gutoff, and J. I. Bregman, *J. Colloid Sci.*, **6**, 245 (1951).
5. G. Scatchard and C. L. Raymond, *J. Am. Chem. Soc.*, **60**, 1278 (1938).
6. G. C. Williams, S. Rossenberg, and H. A. Rothenberg, *Ind. Eng. Chem.*, **40**, 1273 (1948).

7. H. P. Gregor, B. R. Sundheim, K. M. Heid, and M. H. Waxman, *J. Colloid Sci.*, **7**, 511 (1952).
8. D. Braun, *Kunststoffe*, **50**, 375 (1960).
9. P. J. Flory and J. Rehner, *J. Chem. Phys.*, **11**, 521 (1943).
10. T. K. Kwei, *J. Polymer Sci., A*, **1**, 2977 (1963).
11. P. J. Flory, *J. Chem. Phys.*, **18**, 108 (1950).
12. P. J. Flory, *J. Chem. Phys.*, **18**, 112 (1950).
13. R. F. Boyer and R. S. Spencer, *J. Polymer Sci.*, **3**, 97 (1948).

### Résumé

Les caractéristiques de gonflement d'une résine oléophile échangeuse d'anions dans des mélanges méthanol-benzène et éthanol-chloroforme comme systèmes de solvants mixtes, ont été comparées avec celles d'une résine conventionnelle échangeuse d'anions. La résine oléophile a été préparée par amination du polystyrène chlorométhylé (DVB 1%) avec la *N,N*-diméthyl dodécylamine. On constate un large glissement du pic de gonflement en passant de systèmes polaires à des compositions moins polaires dans les deux systèmes méthanol-benzène et éthanol-chloroforme, ainsi qu'ils résultent d'une comparaison avec le gonflement d'une résine conventionnelle. L'absorption totale de solvant et la distribution du solvant entre la résine et le solvant ont également été déterminées. Le solvant moins polaire (benzène ou chloroforme) était absorbé préférablement par la résine oléophile dans un large domaine de composition tandis que l'on constate une préférence pour le solvant plus polaire (méthanol ou éthanol) pour la résine conventionnelle sur l'entière composition des systèmes de solvants mixtes. Le traitement de Newman-Krigbaum des solvants mixtes a été appliqué aux données de gonflement du système résine-oléfine-éthanol-chloroforme où le volume du réseau-gel plus le solvant d'inhibition était relativement constant sur le domaine entier des compositions. Ce résultat suggère une grande similitude d'interaction liquide-liquide dans cette phase gel comparée à celle de la phase binaire liquide.

### Zusammenfassung

Die Quellungscharakteristik eines oleophilen Anionenaustauscherharzes in Methanol-Benzol und Athanol-Chloroform als Mischlösungssystemen wurde mit derjenigen eines konventionellen Anionenaustauscherharzes verglichen. Das oleophile Harz wurde durch Aminierung eines chloromethylierten Polystyrols (DVB-1%) mit *N,N*-Dimethyldodecylamin dargestellt. Es zeigte im Vergleich zur Quellung von konventionellen Harzen eine grosse Verschiebung des Quellungsmaximums von einer polaren zu einer weniger polaren Lösungszusammensetzung sowohl in Methanol-Benzol als auch in Athanol-Chloroformsystemen. Weiters wurde die gesamte Lösungsmittelaufnahme sowie die Lösungsmittelverteilung zwischen Harz- und Lösungsmittelphase bestimmt. Das weniger polare Lösungsmittel (Benzol oder Chloroform) wurde über einen weiten Zusammensetzungsbereich vom oleophilen Harz präferentiell sorbiert, während die konventionellen Harze eine über den gesamten Zusammensetzungsbereich der Mischlösungsmittelsysteme eine Bevorzugung des stärker polaren Lösungsmittels (Methanol oder Athanol) zeigte. Die Behandlung von Lösungsmittelgemischen nach Newman-Krigbaum wurde auf die Quellungsdaten im Athanol-Chloroform-oleophiles-Harz-System angewandt, bei welchem das Volumen von Gelnetzwerk plus imbibiertem Lösungsmittel über den gesamten Zusammensetzungsbereich verhältnismässig konstant blieb. Das Ergebnis lässt eine starke Ähnlichkeit der Flüssig-flüssig-Wechselwirkungsterme in dieser Gelphase mit denjenigen in der reinen binären Flüssigkeitsphase erkennen.

Received September 9, 1965

Revised October 8, 1965

Prod. No. 4924A



## Base-Catalyzed Polymerization of Maleimide and Some Derivatives and Related Unsaturated Carbonamides

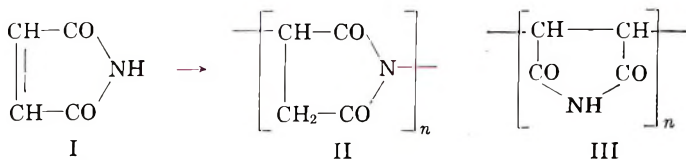
KUNIHARU KOJIMA,\* N. YODA,† and C. S. MARVEL, *Department  
of Chemistry, University of Arizona, Tucson, Arizona*

### Synopsis

Basic catalysts in dimethylacetamide solution initiated the polymerization of maleimide to yield a low molecular weight polymer which has a copolymer structure. Approximately 75–85% of the recurring units are formed by hydrogen transfer and 15–25% by vinyl polymerization, as shown by hydrolysis, to yield aspartic acid on the one hand and ammonia and polymaleic acid on the other. Several maleimide derivatives have been prepared, but none has given a high molecular weight polymer by basic catalysis. Some unsaturated carbonamides such as *p*-vinylbenzamide, mono-*N*-acrylyl-hexamethylenediamine, and mono-*N*-acrylyl-*p*-phenylenediamine have been synthesized and polymerized by basic catalysts. Polymers with low molecular weights were obtained, but the complete structures of all these polymers were not established.

Since Breslow et al.<sup>1</sup> showed that acrylamide would yield poly-β-alanine by hydrogen-transfer polymerization, this general reaction has received considerable attention.<sup>2–5</sup> It has been shown by Tawney and co-workers<sup>6</sup> that maleimide can be polymerized by free-radical initiation and they have mentioned that it can be polymerized by basic catalysts but have not investigated this in detail. Joshi<sup>7</sup> has also studied this polymer.

We have now investigated the base-catalyzed polymerization of maleimide (I) and found that two recurring units (II and III) are formed during the formation of the copolymers which have 75–85% of unit II and 15–25% of unit III in the chain. This was demonstrated by hydrolysis and



\* Postdoctoral Research Associate supported by the Textile Fibers Department, E. I. du Pont de Nemours and Company, Inc., 1963–1965. Present address: Tokyo Medical and Dental University, Bunkyo-ku, Tokyo, Japan.

† Postdoctoral Research Associate supported by the Textile Fibers Department of E. I. du Pont de Nemours and Company, Inc., 1962–1963. Present address: Toyo Rayon Company, Ltd., Basic Research Laboratory, Kamakura, Japan.



the isolation of aspartic acid and ammonia. The latter was determined quantitatively to establish the ratio of recurring units. The base-catalyzed polymer was compared with the radical-initiated polymer and found to differ in solubility, and infrared and NMR spectra. The base-catalyzed polymers showed very little NH absorption in the infrared and NMR spectra.

The following related imides and derivatives have been synthesized and their polymerization by basic catalysts studied: citraconimide, *cis*-4-cyclohexene-1,2-dicarbonimide, 4-methyl-*cis*-4-cyclohexene-1,2-dicarbonimide, *N*-carbonylmaleimide, *N*-4-amino-*p*-phenylenemaleimide, *N*-aminohexamethylenemaleimide, *N*-carbonylcitraconimide, and *N*-carbonyl-*cis*-4-cyclohexene-1,2-dicarbonimide. Citraconimide and *N*-carbonylcitraconimide gave no polymers. The cyclohexene derivatives gave very low yields of very low molecular weight products. *N*-Carbonylmaleimide gave a good yield of a low molecular weight polymer. *N*-4-Amino-*p*-phenylenemaleimide gave a poor yield of polymer which did not completely dissolve in formic acid. *N*- $\omega$ -Amino-hexamethylenemaleimide gave a completely insoluble polymer.

*p*-Vinylbenzamide, when treated with sodium butoxide, gave polymers with inherent viscosities varying from 0.05 to 0.84. Hydrolysis of the polymer indicates it has about 17% of the vinyl structure and 83% of hydrogen transfer structure based on the ammonia liberated. However, no *p*-ethylbenzoic acid was isolated from the hydrolysis mixture. Cinnamamide and crotonamide gave low yields of low molecular weight polymers (29.5%,  $\eta_{inh} = 0.03-0.05$ ). Mono-*N*-acrylhexamethylenediamine gave a completely insoluble product. Mono-*N*-acrylyl-*p*-phenylenediamine gave a product with an inherent viscosity of 0.1 (0.5% in sulfuric acid at 30°C.) which was not further investigated.

## EXPERIMENTAL

### Monomer Synthesis

**Maleimide.** Maleimide (U. S. Rubber Co.) was purified by recrystallization from benzene solution; it melted at 95–96°C.

**Citraconimide.** Citraconic anhydride (11.2 g., 0.1 mole) (Eastman Chemical Co.) was placed in a 500-ml., round-bottomed, three-necked flask and then dissolved in 100 ml. of chloroform. The flask was fitted with a condenser, thermometer, and a gas inlet tube. Then, dry ammonia gas was passed into the solution. After 2 hr. the gas was stopped and the mixture was allowed to stand overnight. The crystalline product was filtered off and dried under reduced pressure; the yield was 15.6 g. crude citraconamide (99%; m.p. 116–118°C.).

Citraconamide (22 g., 0.2 mole) was added to 25 g. of acetic anhydride which had been heated to 90–95°C. The mixture was stirred vigorously at 90–95°C. for 30 min., at which time the solid had dissolved. After hot filtration, the filtrate was allowed to stand overnight at room tem-

perature. The mixture was evaporated under reduced pressure. The residue was recrystallized from benzene solution, yielding 6.5 g. (33% yield) of crystalline product. The material was purified by sublimation above 100°C. The sublimed product melted at 108°C. (lit.<sup>8</sup> 109°C.).

ANAL. Calcd. for  $C_5H_9O_2N$ : C, 54.95%; H, 4.54%; N, 12.61%. Found: C, 54.96%; H, 4.61%; N, 12.83%.

***cis*-4-Cyclohexene-1,2-dicarbonimide.** The general procedure was the same as for citraconimide. In the cyclization step, 0.1 mole of *cis*-4-cyclohexene-1,2-dicarbonamide and 50 ml. of acetic anhydride were used. A 12.6% yield of the sublimed (at 150°C.) material (m.p. 112–113°C.) was realized.

ANAL. Calcd. for  $C_8H_9O_2N$ : C, 63.56%; H, 6.00%; N, 9.27%. Found: C, 63.92%; H, 5.87%; N, 9.76%.

**4-Methyl-*cis*-4-cyclohexene-1,2-dicarbonimide.** In a one-liter, three-necked flask, fitted with a reflux condenser, a thermometer, and a dropping funnel, 9.7 g. (0.1 mole) of maleimide was placed and then dissolved in 250 ml. of dry benzene and heated to 50°C. Next, 7.5 ml. (0.11 mole) of isoprene was added while the mixture was well stirred and heated for 3 hr. After standing overnight, the solvent was evaporated and the precipitate was filtered off. A 21.5% yield of the vacuum oven-dried material (m.p. 105–106°C.) was obtained.

ANAL. Calcd. for  $C_9H_{11}O_2N$ : C, 65.04%; H, 6.69%; N, 8.48%. Found: C, 65.22%; H, 6.76%; N, 8.42%.

***N*-Carbamylcitraconimide.** In a 250-ml., round-bottomed flask, 100 g. of glacial acetic acid, 15 g. (0.25 mole) of urea and 28 g. (0.25 mole) of citraconic anhydride were heated at 50°C. for 12 hr. and then allowed to stand overnight at room temperature. The solid product was filtered off and dried under reduced pressure; the yield was 10.5 g. (24%) of *N*-carbamylcitraconamide (m.p. 144–145°C., dec.). *N*-Carbamylcitraconamide (8.5 g. 0.05 mole) was added to 32 g. of acetic anhydride which had been heated to 90–95°C. The suspension was stirred vigorously at 90–100°C. for 30 min., at which time the solid had dissolved. After a hot filtration, the filtrate was cooled to room temperature and the precipitated solid was filtered off and washed with acetone and dried under reduced pressure. The yield was 7.5 g. (97%) of *N*-carbamylcitraconimide (m.p. 151°C.).

ANAL. Calcd. for  $C_6H_9O_3N_2$ : C, 47.78%; H, 3.92%; N, 18.18%. Found: C, 46.98%; H, 3.93%; N, 18.16%.

***N*-Carbamylmaleimide.** The same procedure as for *N*-carbamylcitraconimide was employed, maleic anhydride and urea being used. The yield was 22.5%. The *N*-carbamylmaleimide melted at 158–159°C. (lit.<sup>9</sup> 157–158°C.).

ANAL. Calcd. for  $C_5H_4O_3N_2$ : C, 42.88%; H, 2.87%; N, 20.00%. Found: C, 43.12%; H, 2.86%; N, 20.13%.

***N*-Carbamyl-*cis*-4-cyclohexene-1,2-dicarbonimide.** The same procedure as for 4-methyl-*cis*-4-cyclohexene-1,2-dicarbonimide was employed with butadiene and maleimide. A 16.8% yield of the product, m.p. 137°C., was obtained.

ANAL. Calcd. for  $C_9H_{10}O_3N_2$ : C, 55.66%; H, 5.19%; N, 14.43%. Found: C, 55.83%; H, 5.11%; N, 14.91%.

***N*-Aminohexamethylenemaleimide.** In a one-liter, three-necked flask, 11.6 g. (0.1 mole) of hexamethylenediamine was dissolved in 200 ml. of dry benzene; 9.7 g. of maleic anhydride in 150 ml. of benzene was dropped into the mixture at 20–30°C., and the mixture was then heated at 50–60°C. for 3 hr. After standing overnight at room temperature, the precipitate was filtered off and dried under reduced pressure. The yield was 19.6 g. (92%) of crude *N*-aminohexamethylenemaleimide, m.p. 55–60°C.

A 10-g. portion of *N*-aminohexamethylenemaleimide was dissolved in 50 ml. of acetic anhydride at room temperature. After a few hours, the precipitate was filtered off and dried under reduced pressure. A 27% yield of recrystallized (acetone) product, m.p. 152–153°C. (dec.) was obtained.

ANAL. Calcd. for  $C_{10}H_{16}O_2N_2$ : C, 61.19%; H, 8.22%; N, 14.58%. Found: C, 60.88%; H, 8.14%; N, 14.10%.

***N*-Amino-*p*-phenylenemaleimide.** The same procedure as for *N*-aminohexamethylenemaleimide was employed with *p*-phenylenediamine and maleic anhydride. A 16.6% yield of the product, m.p. 245°C. (dec.) was obtained.

ANAL. Calcd. for  $C_{10}H_8O_2N_2$ : C, 63.82%; H, 4.29%; N, 14.88%. Found: C, 63.77%; H, 4.83%; N, 13.59%.

***p*-Vinylbenzamide.** In a 500-ml., three-necked flask, were placed 100 ml. of a 5% KOH-ethanol solution, 1.6 ml. of water, and 0.1 g. of metallic copper powder. The mixture was well stirred, and 13.1 g. of *p*-cyanostyrene (W. R. Grace and Co., Research Division) was added; this mixture was heated at 60°C. for 3 hr. After cooling, the reaction mixture was neutralized with 10% hydrochloric acid. The collected precipitate was washed with a small amount of 2% aqueous potassium hydroxide, ethyl alcohol, and ether. The material was recrystallized from acetone. A 24.8% yield of the product, m.p. 172–173°C. was obtained.

ANAL. Calcd. for  $C_9H_8ON$ : C, 73.45%; H, 6.16%; N, 9.53%. Found: C, 73.39%; H, 6.32%; N, 9.43%.

**Cinnamamide.** In a one-liter, three-necked flask, 16.6 g. (0.1 mole) of cinnamoyl chloride (Eastman Org. Chem.) was dissolved in 300 ml. of dry benzene. The solution was well stirred and cooled in an ice-water bath at 10°C. while dry ammonia gas was passed into it. After 2 hr., the white precipitate was filtered off and dried under reduced pressure. The residue

TABLE I  
 Effect of Solvents in the Polymerization of Maleimide<sup>a</sup>

Expt. no.	Solvent	Yield, %	Viscosity ( $\eta_{inh}$ ) <sup>b</sup>	Remarks
1	—	100	0.04	Brown gel
2	Toluene	1.3	0.10	Pink powder
3	Chlorobenzene	88.9	0.05	Pink powder
4	Nitrobenzene	46.4	0.10	White powder
5	Aniline	55.8	0.03	White powder
6	Dimethylaniline	1.6	—	Pink powder
7	Triethylamine	14.7	0.07	Pink powder
8	Dimethylacetamide	86.3	0.08	Pink powder
9	Pyridine	22.3	0.04	Brown powder
10	Dioxane	15.6	0.06	White powder

<sup>a</sup> In each experiment were used: 2.0 g. of maleimide, 0.02 g. of sodium *tert*-butoxide and 0.002 g. of *N*-phenyl- $\beta$ -naphthylamine in 20 ml. of solvent.

<sup>b</sup> Inherent viscosities were determined on 0.05 g./10 ml. of dimethylformamide solutions at 30°C.

 TABLE II  
 Effect of Catalysts in the Polymerization of Maleimide<sup>a</sup>

Expt. no.	Catalyst	<sup>1</sup> Amt. cata-lyst, g.	Solvent	Amt. solvent, ml.	Conversion, %	Viscosity ( $\eta_{inh}$ )
11	<i>n</i> -BuONa	0.009	DMA <sup>b</sup>	2	98.2	0.06
12	<i>tert</i> -BuONa	0.009	DMA	2	98.7	0.07
13	<i>tert</i> -BuOK	0.011	DMA	2	98.6	0.07
14	<i>tert</i> -BuOLi	0.008	DMA	2	93.3	0.08
15	<i>tert</i> -BuONa	0.051	Toluene	20	2.3	0.36
16	<i>n</i> -BuMgCl	0.26 <sup>c</sup>	Toluene	20	4.0	0.08
17	<i>n</i> -Bu <sub>3</sub> B	0.30 <sup>c</sup>	Toluene	20	49.2	0.18
18	<i>n</i> -BuLi	0.13 <sup>d</sup>	Toluene	20	29.0	0.09
19	BF <sub>3</sub> ·(C <sub>2</sub> H <sub>5</sub> ) <sub>2</sub> O	0.14 <sup>e</sup>	Toluene	20	—	—
20	Al( <i>i</i> -Bu) <sub>3</sub> ·TiCl <sub>4</sub> (0.3S:0.16) <sup>d</sup>		Toluene	20	—	—
21	PdCl <sub>6</sub>		Chlorobenzene		3.0	0.12
22	AIBN <sup>e</sup>		Chlorobenzene		98.5	0.24

<sup>a</sup> In each experiment, 2 g. of maleimide and 0.002 g. of *N*-phenyl- $\beta$ -naphthylamine were used. The mixtures were heated at 80°C. for 24 hr.

<sup>b</sup> Dimethylacetamide.

<sup>c</sup> Ml. of 2 mole/l. ether solution.

<sup>d</sup> 3 ml. of 1M hexane solution

<sup>e</sup> Azobisisobutyronitrile.

was recrystallized from benzene solution. A 48.6% yield of sublimed (reduced pressure) product, m.p. 147°C. (lit.: <sup>10</sup> 147°C.) was obtained.

**Crotonamide.** Crotonamide was prepared by the same method described above using crotonyl chloride (Eastman Org. Chem.). A 51.2% yield of the product, m.p. 158°C. (lit.: <sup>11</sup> 158°C.) was obtained.

TABLE III  
Effect of Catalyst Concentration in the Polymerization of Maleimide<sup>a</sup>

Expt. no.	Catalyst Concentration × 10 <sup>2</sup> , mole/l.	Conversion, %	Viscosity ( $\eta_{inh}$ )
31	0	0	—
32	0.05	1.2	—
33	0.10	17.0	0.18
34	0.21	29.3	0.11
35	0.41	48.1	0.10
36	0.62	66.4	0.06
37	1.24	93.4	0.08
38	2.48	95.3	0.07

<sup>a</sup> In each experiment, 2 g. of maleimide, 0.001 g. of *N*-phenyl- $\beta$ -naphthylamine and a catalyst were dissolved in 10 ml. of dimethylacetamide and heated at 100°C. for 8 hr.

TABLE IV  
Effect of Initial Monomer Concentration in the Polymerization of Maleimide<sup>a</sup>

Expt. no.	Initial monomer concentration, mole/l.	Conversion, %	Viscosity ( $\eta_{inh}$ )
41	17.51	44.6	0.09
42	7.01	31.7	0.08
43	3.50	12.3	0.07
44	1.75	7.4	0.05
45	0.88	2.7	—

<sup>a</sup> In each experiment, 2 g. of maleimide was dissolved in a constant amount of dimethylacetamide containing  $4.7 \times 10^{-4}$  mole/l. of *N*-phenyl- $\beta$ -naphthylamine and  $1.2 \times 10^{-2}$  mole/l. of sodium *tert*-butoxide and heated at 100°C. for 1 hr.

***N*-Acrylylhexamethylenediamine.** In a 500-ml., three-necked flask fitted with a mechanical stirrer and dropping funnel, was placed a solution of 11.6 g. (0.1 mole) of purified hexamethylenediamine (Eastman Kodak Company) and 250 ml. of dry benzene. Then 9.6 g. of acrylyl chloride (Borden Chemical Co.) in benzene was added dropwise to the well-stirred solution which was cooled in an ice-water bath at 10–20°C. The mixture was warmed to 40–50°C. for 3 hr. and allowed to stand at room temperature overnight. The precipitate was filtered off and washed with dry benzene and ether. The organic solution was evaporated and the residue recrystallized from a small amount of ether. The crystals of *N,N'*-diacrylylhexamethylenediamine melted at 80–82°C. The residue on the filter was *N*-acrylylhexamethylenediaminehydrochloride.

ANAL. Calcd. for C<sub>9</sub>H<sub>18</sub>ON<sub>2</sub>·HCl: C, 52.28%; H, 9.25%; N, 13.52%. Found: C, 51.97%; H, 9.22%; N, 13.36%.

These crystals of the salt were dissolved in 200 ml. of water and neutralized with 5% sodium bicarbonate aqueous solution. The solution was extracted twice with 250 ml. of chloroform. The chloroform extract was



TABLE V  
Temperature Dependence in the Polymerization of Maleimide<sup>a</sup>

Expt. no.	Temperature, °C.	Time, hr.	Conversion, %	Viscosity ( $\eta_{inh}$ )
51	60	1	6.8	0.12
52	60	2	9.4	0.12
53	60	3	14.5	0.13
54	60	6	25.0	0.12
55	60	12	30.2	0.13
56	60	24	33.4	0.14
57	60	48	38.1	0.14
58	60	72	39.4	0.16
63	80	3	24.8	0.10
64	80	6	29.0	0.11
65	80	12	39.8	0.17
66	80	24	42.2	0.19
67	80	48	46.5	0.19
72	100	2	31.8	0.09
73	100	4	34.9	0.08
74	100	6	37.0	0.08
75	100	24	46.8	0.08
76	100	48	49.4	0.08
83	120	3	61.3	0.06
84	120	6	67.2	0.06
85	120	24	77.8	0.06
86	120	48	84.1	0.07
121	30	35 days	44.9	0.12
122	-25 to 20	35 days	26.8	0.13

<sup>a</sup> In each experiment, 2 g. of maleimide and 0.001 g. of *N*-phenyl- $\beta$ -naphthylamine were dissolved in 2 ml. of dimethylacetamide containing  $1.2 \times 10^{-2}$  mole/l. of sodium *tert*-butoxide and were heated at constant temperature.

dried with anhydrous sodium carbonate and evaporated. The crystals were collected on a filter and again recrystallized from chloroform. They melted at 142–143°C.

ANAL. Calcd. for  $C_9H_{18}ON_2$ : C, 63.49%; H, 10.65%; N, 16.46%. Found: C, 62.66%; H, 9.78%; N, 14.23%.

***N*-Acrylyl-*p*-phenylenediamine.** The same procedure as for *N*-acrylyl-hexamethylenemaleimide was employed with the use of purified *p*-phenylenediamine and acrylyl chloride. The product melted at 118–119°C.

ANAL. Calcd. for  $C_9H_{10}ON_2$ : C, 66.64%; H, 5.05%; N, 17.28%. Found: C, 65.19%; H, 6.15%; N, 18.58%.

### Polymerizations

**Maleimide.** A mixture of maleimide and a small amount of *N*-phenyl- $\beta$ -naphthylamine was placed in a glass tube. The catalyst was added and the tube was sealed in a nitrogen atmosphere. The reaction mixture was heated for 8 hr. at 100°C. After heating, the mixture was poured into

about ten times its volume of methanol. The precipitated polymer was dried in a vacuum oven at 50°C. to constant weight. The results of polymerization in different solvents are shown in Table I and the effect of different catalysts in Table II. In Table III are collected the experiments dealing with the effects of catalyst concentration. In Table IV are the experiments dealing with monomer concentration. In Table V are given the effects of temperature.

**Hydrolysis of Polymaleimide.** A solution of 0.5 g. of polymer in 50% aqueous sodium hydroxide was heated for 48 hr. and the ammonia gas collected and titrated. The results of the hydrolysis of different polymers are shown in Table VI.

TABLE VI  
Hydrolysis of Polymaleimide

Sample no.	Polymerization conditions	Catalyst	NH <sub>3</sub> , mg.	Vinyl polymerization, %
5-2	60°C., 24 hr.	<i>tert</i> -BuONa	12.7	14.6
6-2	80°C., 24 hr.	<i>tert</i> -BuONa	16.2	20.2
7-2	100°C., 24 hr.	<i>tert</i> -BuONa	21.2	24.4
8-2	120°C., 24 hr.	<i>tert</i> -BuONa	21.4	24.8

When the residual alkaline solution was examined by paper chromatography with *n*-butyl alcohol, acetic acid, and water to develop the strip and ninhydrin reagent to test it, aspartic acid up to 30% of the theoretical amount was indicated.

**Infrared and NMR Spectra.** In Figures 1-4 are shown the infrared and NMR spectra of radical-initiated polymaleimide and base-catalyzed polymaleimide. The free radical-initiated polymer shows much more N—H absorption band at 3350 cm.<sup>-1</sup> than does the base-catalyzed polymer.

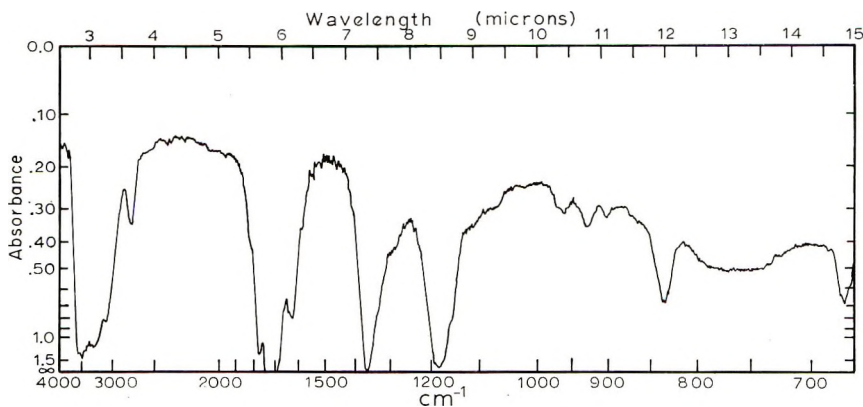


Fig. 1. Infrared spectrum of radical-initiated polymaleimide.

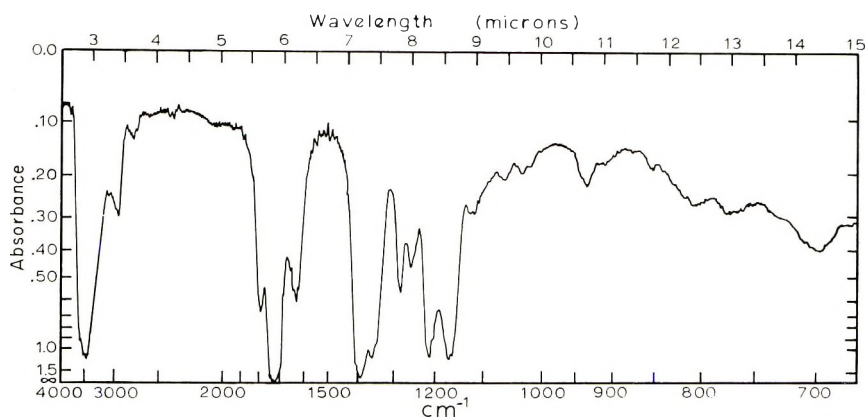


Fig. 2. Infrared spectrum of base-catalyzed polymaleimide.

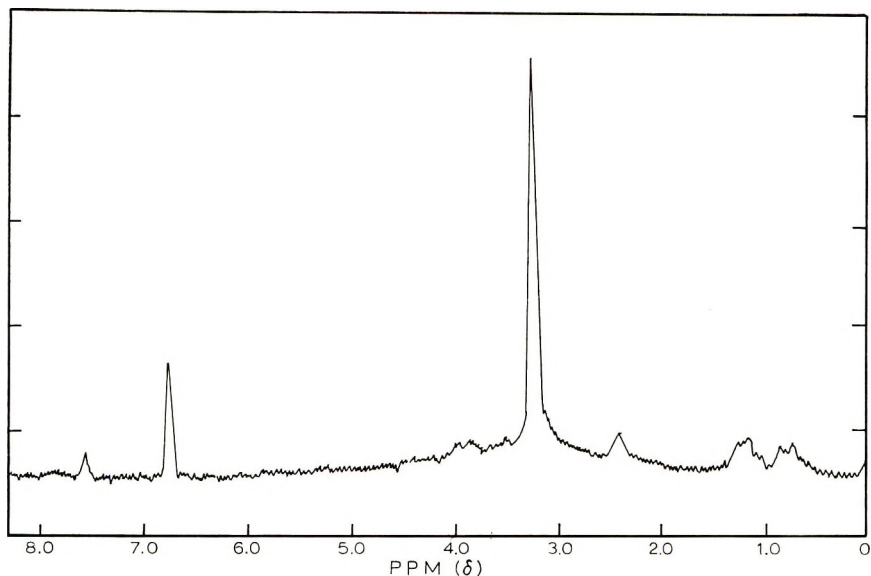


Fig. 3. NMR spectrum of radical-initiated polymaleimide.

The NMR spectra of the two polymers were taken in a 60% dimethyl sulfoxide-D<sub>6</sub> (Merck, Sharp and Dohme of Canada, Ltd.) solution at room temperature with a Varian A-60 NMR spectrometer. Again, the difference in N-H groups showed up markedly.

**Solubility of Polymaleimides.** Base-catalyzed polymers dissolved readily in formic acid, whereas the radical-initiated polymer was insoluble. The radical-initiated polymer was easily soluble in dimethylformamide and the base-catalyzed polymer was only slightly soluble in this solvent.

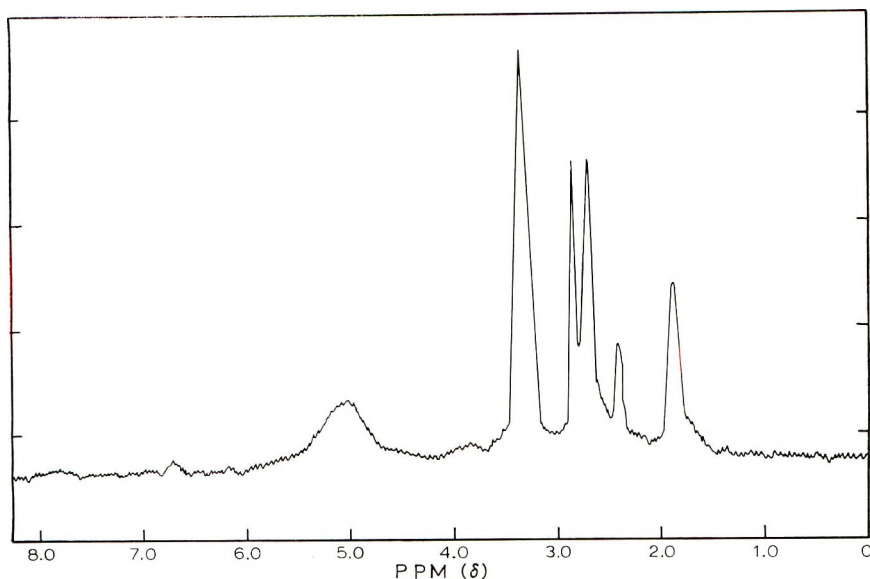


Fig. 4. NMR spectrum of base-catalyzed polymaleimide.

### Polymerization of Maleimide Derivatives

In each case, a solution of the imide in 2 ml. of dimethylacetamide containing 0.01 g. of sodium *tert*-butoxide as catalyst and 0.001 g. of *N*-phenyl- $\beta$ -naphthylamine as inhibitor was heated to 80°C. for 24 hr. The solution was then poured into 100 ml. of methanol and the polymer collected on a filter and dried. The results are summarized in Table VII.

### *p*-Vinylbenzamide and Other Amides

***p*-Vinylbenzamide.** In a 100-ml., round-bottomed flask were placed 1.47 g. (0.01 mole) of *p*-vinylbenzamide, 0.01 g. of sodium *tert*-butoxide and 0.001–0.005 g. of inhibitor. The mixture was dissolved in a constant amount of solvent and heated for 24 hr. The reaction mixture was then poured into a tenfold amount of ether. The precipitate was separated by filtration and dried under reduced pressure at 50°C. until a constant weight was obtained. Then, 0.05 g. of polymer was dissolved in 10 ml. of formic acid and the inherent viscosity of the polymer determined at 30°C. The results are shown in Table VIII.

A solution of 0.5% of poly-*p*-vinylbenzamide ( $\eta_{inh}$  0.43) in 10 ml. of 50% aqueous sodium hydroxide was heated at 100°C. for 72 hr. The ammonia gas evolved was collected and titrated. Altogether 37.5 mg. of ammonia was collected, indicating that the polymer contained about 17–17.5% of vinyl units.

The infrared spectra of radical-initiated poly-*p*-vinylbenzamide and of base-catalyzed polymer are shown in Figures 5 and 6; those figures show that there is a distinct difference and that some hydrogen-transfer polymerization has occurred.

TABLE VII  
 Base-Catalyzed Polymerization of Some Maleimide Derivatives

Imide	Amt.	Yield, g.	Viscosity ( $\eta_{inh}$ )	Caled.			Found		
				C, %	H, %	N, %	C, %	H, %	N, %
Citraconimide	1.11	None							
<i>cis</i> -4-Cyclohexene- 1,2-carbonimide	1.51	0.018	0.04 <sup>a</sup>						
4-Methylcyclohex- ene-1,2-carboni- mide	1.65	Trace							
<i>N</i> -Carbamyl- maleimide	1.40	0.474	0.07 <sup>b</sup>	42.88	2.87	20.00	44.67	3.13	18.01
<i>N</i> -Amino- <i>p</i> -phenyl- enemalimide	1.74	0.620	0.09 <sup>c</sup>	63.82	4.29	14.88	64.45	5.11	14.60
<i>N</i> -Aminohexa- methylene- maleimide	2.12	0.372	Insoluble	61.19	8.22	14.58	62.97	6.50	14.45
Carbamylcitra- conimide	1.54	None							
<i>N</i> -Carbamyl-cyclo- hexene-1,2-dicar- bonimide	1.94	0.035	0.06 <sup>a</sup>						

<sup>a</sup> In dimethylformamide at 30°C.

<sup>b</sup> In dimethylacetamide at 30°C.

<sup>c</sup> In formic acid at 30°C.

**Cinnamamide.** In a 100-ml., round-bottomed flask, 1.47 g. (0.01 mole) of cinnamamide, 0.02 g. of sodium *tert*-butoxide and 0.002 g. of *N*-phenyl- $\beta$ -naphthylamine were dissolved in 5 ml. of dimethylacetamide. The mixture was heated at 100°C. for 24 hr. in a nitrogen atmosphere. The polymer was precipitated by pouring the solution into a tenfold amount of ether. The yield was 0.4331 g. (29.5%) of vacuum oven-dried polymer of inherent viscosity 0.03–0.05 (0.5% in formic acid at 30°C.).

**Crotonamide.** In a 100-ml., round-bottomed flask, 0.85 g. of crotonamide, 0.02 g. of sodium *tert*-butoxide, and 0.001 g. of *N*-phenyl- $\beta$ -naphthylamine were dissolved in 5 ml. of dry pyridine. The mixture was heated at 100°C. for 24 hr. The polymer was precipitated by pouring into a tenfold amount of ether. The polymer weighed 0.0658 g. (7.3%). The inherent viscosity of this polymer was 0.04 (0.5% in formic acid at 30°C.).

***N*-Acrylylhexamethylenediamine.** A mixture of *N*-acrylylhexamethylenediamine (1.170 g.), sodium *tert*-butoxide (0.02 g.) and *N*-phenyl- $\beta$ -naphthylamine (0.002 g.) was dissolved in 50 ml. of dimethylacetamide–chloroform (1:1) and heated at 80°C. for 24 hr. The product was poured in 200 ml. of ether. The yield was 0.9399 g. (51.6%) of vacuum oven-dried insoluble polymer.

***N*-Acrylyl-*p*-phenylenediamine.** A mixture of *N*-acrylyl-*p*-phenylenediamine (1.62 g.), sodium *tert*-butoxide (0.02 g.), and *N*-phenyl- $\beta$ -naphthylamine (0.002 g.) was dissolved in 50 ml. of dimethylacetamide–chloroform



TABLE VIII  
 Polymerization of *p*-Vinylbenzamide

Expt. no.	Solvent (10 ml.) <sup>a</sup>	Catalyst	Amt. catalyst, g.	Inhibitor <sup>b</sup>	Amt. inhibitor, g.	Temp., °C.	Time, hr.	Conversion, %	Viscosity ( $\eta_{inh}$ )
1	DMA	<i>tert</i> -BuONa	0.01	PNA	0.001	80	24	5.3	0.16 (After reprecipitation)
2	DMA	<i>tert</i> -BuONa	0.01	PNA	0.001	90	24	4.9	0.43 0.15
3	DMA	<i>tert</i> -BuONa	0.01	PNA	0.001	100	24	12.9	0.06
4	DMA	<i>tert</i> -BuONa	0.01	PNA	0.001	120	24	15.8	0.05
5	Pyridine	<i>tert</i> -BuONa	0.01	PNA	0.001	100	24	3.3	—
6	Triethylamine	<i>tert</i> -BuONa	0.01	PNA	0.001	100	24	Trace	—
7	Chlorobenzene	<i>tert</i> -BuONa	0.01	SN	0.005	80	24	47.8	—
8	Chlorobenzene	AIBN	0.01	—	—	100	24	78.2	0.24
9	Toluene	<i>tert</i> -BuONa	0.01	PNA	0.001	100	24	64.1	0.04
10	Toluene	Bu <sub>3</sub> B	0.06 (0.01)	—	—	100	24	57.5	0.04

<sup>a</sup> DMA = dimethylacetamide.

<sup>b</sup> PNA = *N*-phenyl- $\beta$ -naphthylamine; SN = sodium nitrite.

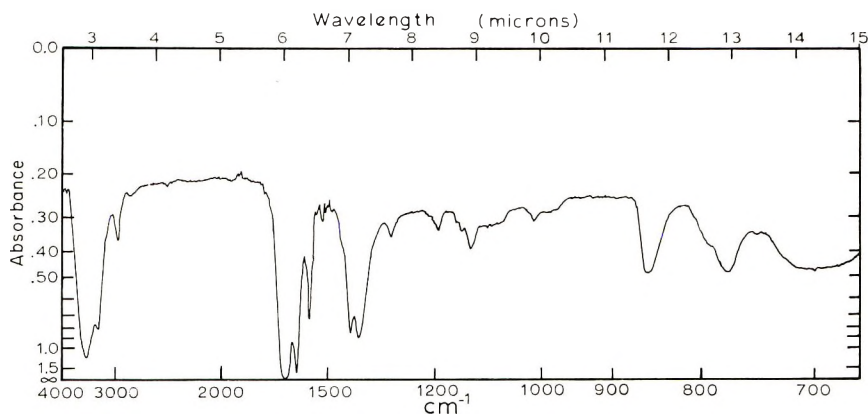


Fig. 5. Infrared spectrum of radical-initiated poly-*p*-vinylbenzamide.

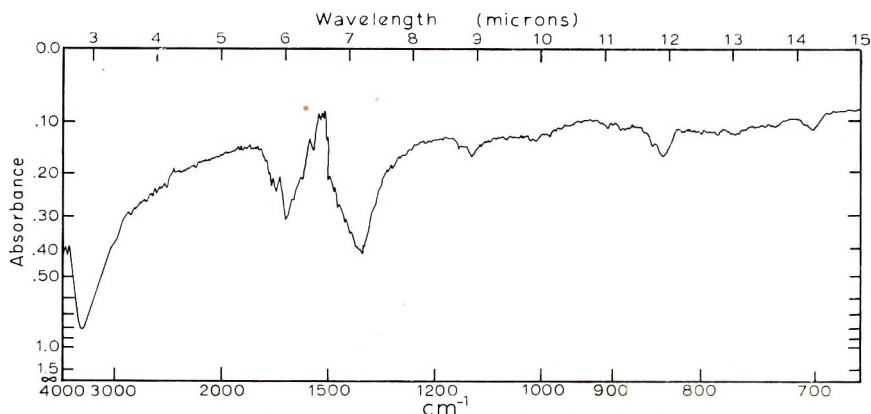


Fig. 6. Infrared spectrum of base-catalyzed poly-*p*-vinylbenzamide.

(1:1) and heated at 100°C. for 24 hr. The product was poured in 200 ml. of ether. The yield was 1.2540 g. (76.5%) of vacuum oven-dried polymer of inherent viscosity of 0.10 (0.5% in formic acid at 30°C.).

We are indebted to Dr. P. O. Tawney (U. S. Rubber Company) for a generous supply of maleimide and to Dr. Thomas R. Steadman of W. R. Grace and Company for the *p*-cyanostyrene used. The financial support of the Textile Fibers Department of E. I. du Pont de Nemours and Company is gratefully acknowledged. One of us (N. Y.) is indebted to the Toyo Rayon Company, Ltd., for permission to do post-doctoral work in the United States.

### References

1. Breslow, D. S., G. E. Hulse, and A. S. Matlack, *J. Am. Chem. Soc.*, **79**, 3760 (1957).
2. Ogata, N., *Bull. Chem. Soc., Japan*, **33**, 906 (1960); *Makromol. Chem.*, **40**, 55 (1960); *J. Polymer Sci.*, **46**, 271 (1960).
3. Tani, H., and J. Takeda, *Ann. Rept. Textile Sci. Inst., Japan*, **13**, 134 (1960).

4. Okamura, S., Y. Oishi, T. Higashimura, and T. Seno, *Kobunshi Kagaku*, **19**, 323 (1962).
5. Yokota, K., M. Shimizu, Y. Yamashita, and Y. Ishii, *Makromol. Chem.*, **77**, 1 (1964).
6. Tawney, P. O., R. H. Snyder, R. P. Conger, K. A. Liebrand, C. H. Stiteler, and A. R. Williams, *J. Org. Chem.*, **26**, 15 (1961).
7. Joshi, R. M., *Makromol. Chem.*, **53**, 33 (1962); *ibid.*, **62**, 140 (1963); *J. Polymer Sci.*, **60**, 56 (1962).
8. Brown, P. M., D. B. Spiers, and M. Whalley, *J. Chem. Soc.*, **1957**, 2882.
9. Kell, R. J., and C. H. Statler, *J. Org. Chem.*, **25**, 56 (1960).
10. Jerzmanowska, Z., and S. Kiewiczowa, *Roczniki Chem.*, **15**, 510 (1935); *Chem. Abstr.*, **30**, 2933 (1936).
11. Phillips, M. A., *J. Chem. Soc.*, **1926**, 2979.

### Résumé

Les catalyseurs basiques, en solution dans le diméthylacétamide, initient la polymérisation du maléimide et fournissent un polymère de bas poids moléculaire qui a une structure copolymérique. Approximativement 75–85% des unités périodiques sont formées par transfert d'hydrogène et 15–25% par polymérisation vinylique tel qu'indiqué par hydrolyse pour former de l'acide aspartique d'une part et de l'ammoniac et de l'acide polymaléique d'autre part. Des dérivés maléimides ont été préparés, et aucun n'a donné de poids moléculaire élevé par catalyse basique. On a synthétisé quelques carbonamides insaturés tels que le *p*-vinylbenzamide, le mono-*N*-acrylylhexaméthylènediamine et le mono-*N*-acrylyl-*p*-phénylènediamine; ces carbonamides ont été polymérisés en présence de catalyseurs basiques. On a ainsi obtenu des polymères de bas poids moléculaire, mais les structures complètes de tous ces polymères n'ont pas pu être établies.

### Zusammenfassung

Basische Katalysatoren führten in Dimethylacetamidlösung zur Polymerisation von Maleinimid unter Bildung eines niedermolekularen Polymeren mit einer Kopolymerstruktur. Etwa 75–85% der Bausteine werden durch Wasserstoffübertragung und 15 bis 25% durch Vinylpolymerisation gebildet, wie die Hydrolyse zu Asparaginsäure einerseits und zu Ammoniak und Polymaleinsäure auf der anderen Seite zeigt. Einige Maleinimid-derivate wurden dargestellt, keines jedoch lieferte durch basische Katalyse ein hochmolekulares Polymeres. Einige ungesättigte Karbonamide wie *p*-Vinylbenzamid, Mono-*N*-acrylylhexamethylendiamin und Mono-*N*-acrylyl-*p*-phenylendiamin wurden synthetisiert und mit basischen Katalysatoren polymerisiert. Es wurden niedermolekulare Polymere erhalten, eine völlige Strukturaufklärung aller dieser Polymerer wurde jedoch nicht durchgeführt.

Received August 17, 1965

Revised September 29, 1965

Prod. No. 4911A

## Some Polymers of High Dielectric Constant

ROBERT ROSEN and HERBERT A. POHL,\* *Departments of Electrical Engineering and Chemistry, Polytechnic Institute of Brooklyn, Brooklyn, New York*

### Synopsis

A class of highly conjugated macromolecules exhibiting extraordinarily high effective dielectric constants ( $DK = 50-900$ ) is described. These polymers are of the polyacene radical quinone type, are highly purified, and exhibit electronic semiconduction. The dielectric constant varies only slightly with pressure (up to 20 Kbar), but strongly with frequency (300-300,000 cps) and moderately with temperature and field strength. The latter effect of field strength on the effective dielectric constant (and on the conductivity) required the development of special measurement techniques which are described. The unusual dielectric behavior can be accounted for assuming the presence of what amounts to a thermally generated plasma of electrons and holes, each locally mobile on extended regions of associated  $\pi$ -orbitals on the molecules. The postulated resulting "hyperclectronic" polarization of the locally mobile charges in external fields fits the observed high magnitude of the polarizability, as well as its field, frequency, and temperature dependence.

Among some of the more recent semiconductors developed are those materials classed as organic solids. Research into the electrical nature of organic compounds goes back to the beginning of the century, but the development of them strictly as semiconducting devices has only been of interest in the last few years. To date, the more interesting types of organic semiconductors can be classed in two groups: (1) crystals of monomeric solid and (2) polymeric bodies. The second group includes a number of compounds called polyacene quinone radical polymers<sup>1,2</sup> (PAQR polymers). A number of characteristic PAQR polymers were studied in order to determine the nature of conduction and the dielectric constant as a function of temperature, pressure and field strength. We were particularly interested in the electric polarization for the following reasons.

Normal electronic polarization is considered to be due to the slight relative shift of the centers of negative and positive charge in atoms. This type of polarizability usually results in a bulk polarization which is linearly proportional to the applied electric field strength for wide range of field strength.

We asked the following questions: In a macromolecular solid in which a dilute plasma of electrons and holes was present (i.e., in an organic semi-

\* Present address: Department of Physics, Oklahoma State University Stillwater, Oklahoma.

conducting solid) could not the separated electrons and holes localized temporarily (trapped) on the long and very polarizable molecules exhibit a very high polarizability? If so, what might be the characteristics of such polarization? In a molecular view, the mobile charges would lie individually on extended regions of near-zero resistance (i.e., within extraordinarily long regions of associated  $\pi$ -orbitals) but with their domain path limited ultimately by a molecular boundary. The mobile charges, arising from inherent and easily thermally excited intermolecular ionization levels of the long conjugated molecules would form a collection of highly polarizable monopoles and thereby possibly exhibit a high bulk polarizability. This collection of highly field sensitive monopoles would then exhibit what might be termed "hyperelectronic" polarization.

### Experimental Materials

The PAQR polymers were prepared as described by Pohl et al.<sup>1</sup> The synthesis involves the reaction of pyromellitic dianhydride (PMA) with several aromatic hydrocarbon derivatives to produce a series of polymers.

In the synthesis process, the PMA and acene were thoroughly mixed with zinc chloride, which acted as a catalyst. The mixture was heated for 24 hr. at 300°C., powdered, and then purified by successive exhaustive extractions with hydrochloric acid, water, alcohol and toluene, at the boiling points. The polymers were then dried at 50°C. for about 12 hr. and stored until used.

Three samples were tested to determine their electrical characteristics. Polymer EHE-76 was a polymer formed by the reaction of 6.0 g. of pyrene, 6.6 g. of PMA and 4.0 g. of zinc chloride and was synthesized by Engelhardt.<sup>2</sup> Polymers IS-1 and IS-2 were synthesized by I. Stillman at the Polytechnic Institute of Brooklyn. Polymer IS-1 was composed of anthraquinone and PMA and IS-2 of pyrene and PMA.

Proposed structure types for typical PAQR polymers are shown in Figure 1. As yet it has not been proven whether these are proper representations.

Table I indicates the ratios of acene and PMA in each sample at synthesis.

### Experimental Procedure

Determinations of the conductivity and dielectric constant for the polymers tested were made by using the bridge circuit shown in Figure 2.

The samples which initially were in the form of a crystalline powder were molded into small pellets between two circular tungsten carbide pistons (Fig. 3). The contact area between the two pistons was surrounded by a Mycalex cylinder in order to prevent sideways slippage of the pistons and also to keep the polymer from being forced out from between as pressure was applied. Mycalex was chosen as the retaining ring because of its good mechanical properties, coupled with the fact that it is a good insulator.



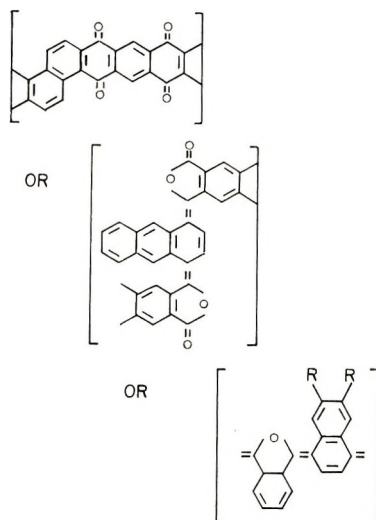


Fig. 1. Proposed structures, of some typical PAQR polymers, as yet unproven.

Lexan sheets,  $\frac{1}{8}$  in. thick, were placed between the load-distributing disks and the hydraulic press to insulate the electrodes of the pressure cell. Lexan is a good insulator and has a relatively constant dielectric constant over the range of temperatures at which the samples were examined.

Each sample was made by placing a small amount of polymer powder in the cell and then molding it at  $125^{\circ}\text{C}$ . and 10,000 atm. into a small pellet. To insure that the sample was properly molded, the pressure was cycled between zero and 10,000 atm. three times.

Prior to making any measurements on any sample, the resistivity and capacity of the pressure cell were checked with a polystyrene spacer between the pistons. The resistivity was checked to see that it was greater than 5–10 megohms and the capacity was noted as a function of frequency and temperature, so that when a polymer sample was substituted for the polystyrene spacer the contribution of capacitance of the pressure cell would be known.

Conductivity was measured as a function of field strength and pressure for constant values of temperature. The temperature was controlled by two thermostatically controlled platens on a Preco hydraulic press, Model

TABLE I  
Ratios by Weight of Acene, PMA, and Zinc Chloride in each Sample.

Polymer	Hydrocarbon	Weight of acene, g.	Weight of pyromellitic anhydride, g.	Weight of $\text{ZnCl}_2$ , g.
EHE-76	Pyrene	6.0	6.6	4.0
IS-1	Anthraquinone	210.22	118.02	136.29
IS-2	Pyrene	101.12	118.02	136.29

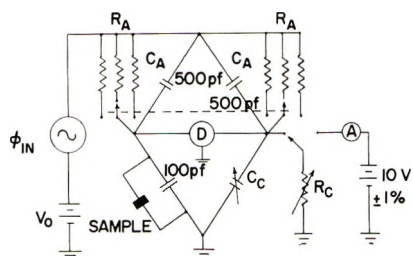


Fig. 2. Circuit for the determination of the parameters of PAQR polymers: (D) Tektronix oscilloscope, Type 536 W/Type D differential amp; (A) Keithley 150 A microvolt ammeter; ( $C_C$ ) Leeds and Northrup variable capacitor, #188, 50–1300  $\mu\mu\text{f}$ ; ( $R_C$ ) Allen-Bradley Type J potentiometers; ( $\phi_{in}$ ) Hewlett-Packard oscillator, Model 200CD; ( $V_0$ ) Harrison Labs Model 856B dc supply; ( $R_A$ ) 2K, 20K, 200K;  $\pm 1\%$  molded carbon resistors.

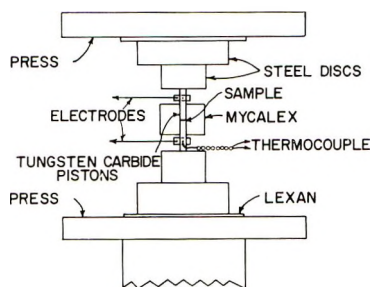


Fig. 3. Pressure cell for the mechanical, thermal and electrical testing of PAQR samples.

RA6, and it was monitored by a Leeds and Northrup temperature-indicating potentiometer system with a copper-constantan thermocouple. The thermocouple was attached to the lower piston about  $\frac{3}{8}$  in. from the sample. This enabled control of the temperature to within  $\pm 1^\circ\text{C}$ ., for the pressure cell lay in a glass wool-jacketed enclosure.

Capacitance measurements were made using a variable-frequency sinusoidal oscillator in the modified Schering bridge of Figure 2. The variation of capacitance as a function of frequency, field intensity, pressure, and temperature was evaluated in the same manner as the conductive measurements were made. The battery and microammeter shown in Figure 2 were used to calibrate  $R_C$  at each measurement.

### Results and Discussion

The experimental variation of conductivity as a function of temperature, pressure, and field strength was observed to be consistent with the theory we shall discuss.

Conduction in a given PAQR polymer is governed principally by three factors: temperature, pressure, and field intensity. In general, the conductivity  $\sigma$  of an intrinsic semiconductor can be written

$$\sigma = |e| \mu n \quad (1)$$

where  $|e|$  is the electronic charge,  $\mu$  is the mean mobility of the carriers, and  $n$  is the number of electronic charge carriers per unit volume.

Pohl et al.,<sup>3</sup> using transition state reaction rate theory, considered that the mobility  $\mu$  of a charge carrier in a molecular solid is governed by the ability of the charge carrier to hop between molecules. The energy required for this hopping process is a function of the external pressure applied. The conductivity will be

$$\sigma_s = \sigma_0 \exp \left\{ -E_0/2kT \right\} \exp \left\{ (p^{1/2}/kT)(b''T + b_0) \right\} \quad (2)$$

where  $p$  is external pressure applied (in atmospheres),  $b''$  and  $b_0$  are constants of proportionality, and  $\sigma_0$  is the conductivity at zero external pressure and infinite temperature.

An expression must now be arrived at which will explicitly take into account the field intensity dependence of the conductivity.

The energy to produce ionization in a molecular solid can arise in several ways, from thermal energies and from electric field energies. The energy available to assist ionization (carrier formation) between like points in a molecular lattice is

$$-\Phi_i = \vec{\epsilon} \cdot \vec{L}_i \quad (3)$$

where

$\epsilon$  is the local average field intensity across the lattice due to an externally applied voltage and  $L_i$  is the lattice spacing for the  $i$ th molecule.

For randomly assembled long, rod-like molecules we may set

$$L_i = L \cos \theta_i = \text{projected length in the direction of the field}$$

where  $L$  is molecular length, including gap distance to next neighbor.

For a semiconducting molecular species of forbidden energy band gap,  $E_0$ , the effective ionization energy is then

$$E = E_0 - |e|\Phi_i \quad (4)$$

in the presence of the electric field, as  $e = -|e|$

$$\begin{aligned} n_i &= n_{0i} \exp \left\{ (-E_0 + |e|\Phi_i)/2kT \right\} \\ &= n_{0i} \exp \left\{ (-E_0 + e\vec{\epsilon} \cdot \vec{L}_i)/2kT \right\} \end{aligned} \quad (5)$$

The total concentration of carriers  $n$  is

$$n = \sum_i n_i \quad (6)$$

$$= \sum_{\theta_i} n_{0i} \exp \left\{ (-E_0 + e\epsilon L \cos \theta_i)/2kT \right\} \quad (7)$$

Assuming a random distribution of orientations,

$$n = \int_{\omega} (\partial n / \partial \omega) d\omega \quad (8)$$

where  $\omega$  is the solid angle,

$$d\omega = \sin \theta d\theta \quad (9)$$

and

$$\partial n / \partial \omega = n_i = n_0 \exp \{ (-E_g + e \epsilon L \cos \theta) / 2kT \} \quad (10)$$

Hence

$$n = (2kT n_0 / |e| \epsilon L) (\exp \{ e \epsilon L / 2kT \} - 1) \exp \{ -E_g / 2kT \} \quad (11)$$

Comparing the ratio of the expected carrier densities with and without a strong applied external field for a typical organic polymer semiconductor and using the assumptions applied here, we see:

$$\text{Ratio} = \frac{N_{\Phi = \Phi}}{N_{\Phi = \Phi_0}} = (2kT / e \epsilon L) (\exp \{ e \epsilon L / 2kT \} - 1) \quad (12)$$

For a molecule extending 1000 Å., average end-to-end distance, and an applied field of 1000 v./cm., the ratio is 1.1, and in a field of 10,000 v./cm. the ratio is 11.7.

Finally, combining eqs. (1), (3), and (12), the conductivity,  $\sigma_s$  can be expressed as

$$\sigma_s = \sigma_0 \exp \left\{ \frac{-E_g}{2kT} \right\} \exp \left\{ \frac{p^{1/2}}{kT} (b''T + b_0) \right\} \frac{2kT}{e \epsilon L} \left( \exp \left\{ \frac{e \epsilon L}{kT} \right\} - 1 \right) \quad (13)$$

Since the potential,  $\Phi_s$ , across an entire sample of width  $w$  is

$$-\Phi_s = \epsilon w \quad (14)$$

and we may define

$$a = 2kT w / |e| L \quad (15)$$

the conductivity in terms of the applied potential becomes

$$\sigma_s = \sigma_0 \exp \left\{ \frac{-E_g}{2kT} \right\} \exp \left\{ \frac{p^{1/2}}{kT} (b''T + b_0) \right\} \frac{a}{\Phi_s} \left( \exp \left\{ \frac{\Phi_s}{a} \right\} - 1 \right) \quad (16)$$

A normalized plot of the calculated conductivity versus field strength is shown in Figure 4.

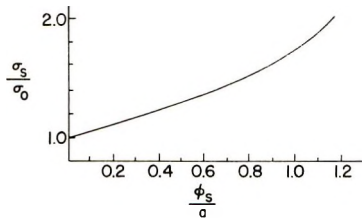


Fig. 4. Normalized plot of the conductivity vs. field strength for a PAQR sample at constant temperature and pressure:  $\sigma_0^* = \sigma_0 \exp \{ -E_g / 2kT \} \exp \{ p^{1/2} / kT \} (b''T + b_0)$ .

Since the conductivity of such molecular solids will vary with field strength we now turn to a discussion of how one may measure their properties by use of alternating current where one deliberately uses large and varying field strengths.

Of interest at this point is the determination of the sinusoidal response of a PAQR sample when the driver is applied to the bridge of Figure 2. Since the conductance of a PAQR polymer is a function of field intensity it will not be possible to completely reduce the difference voltage across the bridge to zero, and therefore a knowledge of the waveshape obtained when the bridge is balanced will be necessary to determine the capacitance of the sample.

If the sample is assumed to be a conductance,  $G_s$ , in parallel with a capacitance,  $C_s$ , the voltage across the sample,  $\Phi_s$ , is

$$\Phi_s = (A \sin \omega t) Y_a / (Y_s + Y_a) \quad (17)$$

where  $A(\sin \omega t)$  is the input voltage  $\Phi$  to the bridge of Figure 2,  $Y_a$  is the admittance function  $G_A \parallel C_A$ ;  $Y_s$  is the admittance function  $G_s \parallel C_s$ .

The voltage across the comparison branch  $\Phi_c$  is

$$\Phi_c = (A \sin \omega t) Y_A / (Y_c + Y_a) \quad (18)$$

where

$Y_c$  is the admittance function  $G_c \parallel C_c$ .

Defining

$$\Delta\Phi = \Phi_s - \Phi_c \quad (19)$$

as the voltage appearing across the detector,

$$\Delta\Phi = (A \sin \omega t) \left\{ Y_A(Y_c - Y_s) / [(Y_s + Y_A)(Y_c + Y_A)] \right\} \quad (20)$$

An attempt at an exact solution of this equation in terms of the conductances and capacitances proves awkward due to the cumbersome mathematics. In order to get around this, the low frequency response will be found, and from that a reasonable explanation for the response at higher frequencies will become evident. Therefore at low frequency, assuming  $\omega C \cong 0$ ,

$$\Delta\Phi = (A \sin \omega t) \left\{ G_A(G_c - G_s) / [(G_s + G_A)(G_c + G_A)] \right\} \quad (21)$$

The conductance of the sample of unit dimensions  $G_s$  can be written

$$G_s = \sigma_s (a / \Phi_s) \left\{ \exp (|\Phi_s|/a) - 1 \right\} \quad (22)$$

and therefore

$$\Delta\Phi = \frac{(A \sin \omega t) G_A}{(G_c + G_A)} \left[ \frac{G_c - \frac{\sigma_s a}{|\Phi_{sp} \sin \omega t|} \left( \exp \left\{ \frac{|\Phi_{sp} \sin \omega t|}{a} \right\} - 1 \right)}{G_A + \frac{\sigma_s a}{|\Phi_{sp} \sin \omega t|} \left( \exp \left\{ \frac{|\Phi_{sp} \sin \omega t|}{a} \right\} - 1 \right)} \right] \quad (23)$$



where  $\Phi_{sp}$  is the peak voltage across the sample.

If  $G_c$  is adjusted to equal to  $G_s$  when  $\Phi_s = \Phi_{sp}$  then

$$G_c = \frac{\sigma_s a}{\Phi_{sp}} [\exp \{ |\Phi_{sp}/a| \} - 1] \quad (24)$$

and finally

$$\Delta\Phi = \frac{(AG_c \sin \omega t)}{G_A + G_c} \times \left[ \frac{(\exp \{ \Phi_{sp}/a \} - 1)(\sin \omega t) - \exp \left\{ \frac{|\Phi_{sp} \sin \omega t|}{a} \right\} + 1}{(\exp \{ \Phi_{sp}/a \} - 1)(\sin \omega t) + \frac{G_s}{G_A} \left( \exp \left\{ \frac{|\Phi_{sp} \sin \omega t|}{a} \right\} - 1 \right)} \right] \quad (25)$$

A normalized plot of  $\Delta\Phi$  versus  $\omega t$  is shown in Figure 5.

At intermediate and high frequency, where the capacitive effect becomes more evident and can no longer be neglected, it can be seen that if there is any capacitive imbalance in the bridge, it will cause  $\Phi_s$  to lead or lag  $\Phi_c$ , thereby causing the symmetric pattern of Figure 5 to lose that symmetry (Fig. 6). This will be evidenced by the fact that instead of the wave-shape having peaks of the same height, as in Figure 5, one peak will be higher than the other. It can be further seen that suitable adjustment of  $C_c$  will cause the heights of the peaks to vary with respect to each other and that the proper value of capacitance,  $C_c = C_s$ , will cause the peaks to have the same magnitude.

The computed values of the energy constants associated with the conductivity equation as found from the measured values are shown in Table

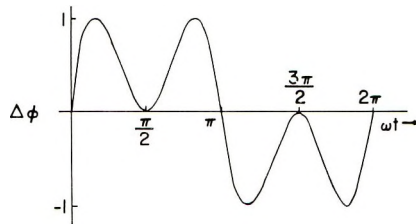


Fig. 5. Differential voltage  $\Delta\Phi$  across bridge for proper bridge balance.

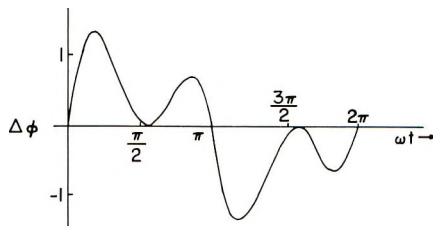


Fig. 6. Differential voltage  $\Delta\Phi$  across detector when bridge is improperly balanced.

TABLE II  
Conductivity Parameters for Some PAQR Polymers

Polymer	$E_g$ , e.v.	$a$ , v.	$b^* \times 10^6$ , e.v./atm. <sup>1/2</sup> °K.	$b_0 \times 10^3$ , e.v./atm. <sup>1/2</sup>	$b'' \times 10^6$ , e.v./atm. <sup>1/2</sup> °K.	$\sigma_{sp} \times 10^6$ , mho/cm.
EHE-76	0.520	1170	2.3	0.5	0.62	13
IS-1	0.332	1300	2.48	0.466	0.91	23
IS-2	0.400	1050	2.46	0.408	1.09	16

II. The specific conductivity  $\sigma_{sp}$  at 24°C. and 1800 atm. is also indicated. Temperature-sensitive parameters are listed for their values at 24°C. Here,  $E_g$  is the energy for formation of carrier pairs,  $a$  is the field-dependence parameter,  $b^*$ ,  $b_0$ , and  $b''$  are the pressure-dependence parameters, and  $\sigma_{sp}$  is the specific conductivity at 1800 atm. and 24°C.

The variation of conductivity versus field strength is seen in Figure 7. A number of curves indicating the variation of  $\sigma/\sigma_0$  versus field strength for different values of average molecular lengths are plotted, and the experimentally observed conductivity ratios are indicated for the various samples tested. The average molecular length can be found by interpolating to the proper  $L$  value between the curves.

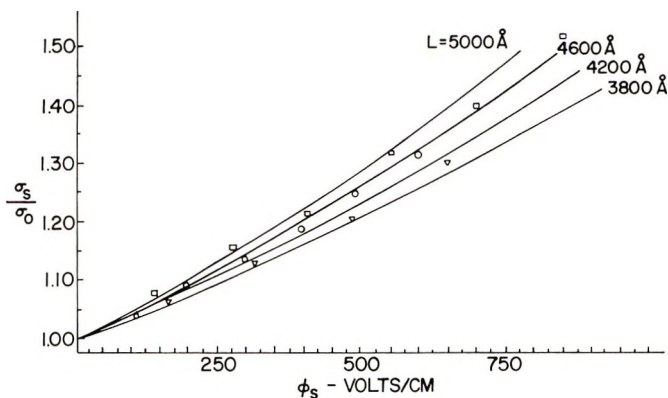


Fig. 7. Variation of the normalized conductivity vs. field strength for various average molecular lengths  $L$ : indicated for (O) EHE-76; ( $\Delta$ ) IS-1; ( $\square$ ) IS-2. Temperature, 24°C.;  $\sigma_0$  is the conductivity at zero field strength.

From the data obtained, the indication is that the molecules are very long in nature and the average molecular lengths are for EHE-76,  $L = 4400$  Å.; for IS-1,  $L = 3950$  Å.; and for IS-2,  $L = 4900$  Å.

Figure 8 shows the variation of the specific conductivities of the samples tested versus the square root of the pressure applied.

The capacitance of the samples under test was determined by adjusting the bridge balance until the waveshape shown in Figure 5 was observed.

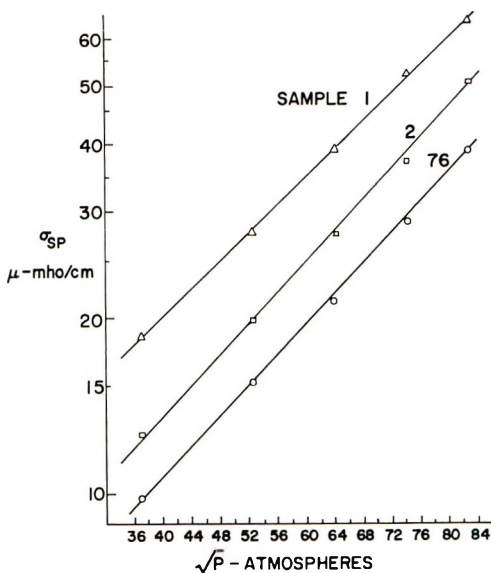


Fig. 8. Variation of the specific conductivity vs. the square root of the pressure at 24°C. for the three samples tested ( $\circ$ ) EHE-76; ( $\Delta$ ) IS-1; ( $\square$ ) IS-2.

The observed waveshape was almost exactly that of the theoretical waveshape computed in the section on the sinusoidal response.

The PAQR polymers appear to exhibit extremely strong dipolar contributions to the dielectric constant, and to require a rather long relaxation time. The polarizability is also sensitive to field strength and the dielectric constant decreases appreciably with increasing field strength.

Figures 9, 10, and 11 show the variation of the relative dielectric constant  $\epsilon_r$  versus frequency for samples EHE-76, IS-1, and IS-2, respectively. The curves are plotted for constant field strength, and it is seen that the greatest decrease in  $\epsilon_r$  for increasing field occurs at low frequency. At higher frequency the effect of variations in the fields magnitude becomes negligible. Therefore it can be seen that the polarization  $a_d$  is a nonlinear function of the field.

Figures 12-14 show the variation of the relative dielectric constant versus frequency for various temperatures.

The effect of increased pressure on the dielectric constant is felt to be relatively negligible. An increase in pressure from 1400 to about 7000 atm. caused an increase of about 10-15% in the PAQR sample cell capacitance. This increase is probably due to the compression and corresponding decrease in the thickness of the sample.

The extremely high dielectric constant observed at low frequency is not an ordinary occurrence in organic solids. Most organic solids exhibit relative dielectric constants of the order of 2-10.<sup>4</sup>

The field sensitivity variation of the conductance of the PAQR polymer samples tested agreed very well with the theoretically assumed variation.

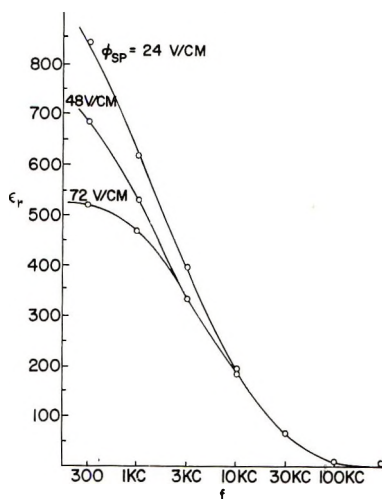


Fig. 9. Variation of the relative dielectric constant  $\epsilon_r$  of sample EHE-76 vs. frequency for constant value of field intensity;  $T = 24^\circ\text{C}$ .

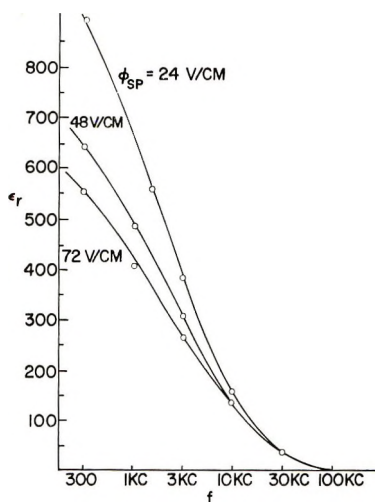


Fig. 10. Variation of the relative dielectric constant  $\epsilon_r$  for sample IS-1, vs. frequency for constant values of field intensity;  $T = 24^\circ\text{C}$ .

Pohl and Engelhardt<sup>2</sup> indicated the same variation for a sample of pyrene and PMA (EHE-39). From their data a molecular length of  $L = 3250$  Å. is indicated.

An order of magnitude check on this molecular length as obtained from field-dependence measurements can be obtained by using the rough relation<sup>2</sup>

$${}^3E \cong h^2/4ml^2z = (38.4/z) \quad (26)$$

where  ${}^3E$  is the activation energy to excite the biradical state (in electron

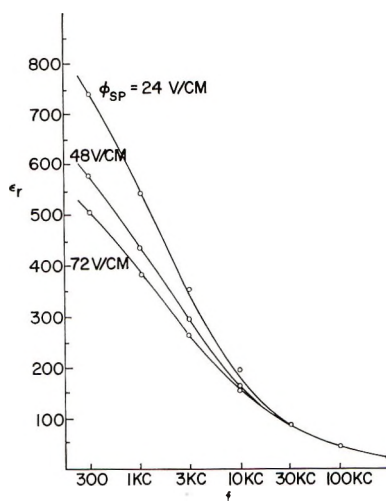


Fig. 11. Variation of the relative dielectric constant  $\epsilon_r$ , for sample IS-2 vs. frequency for constant values of field strength,  $T = 24^\circ\text{C}$ .

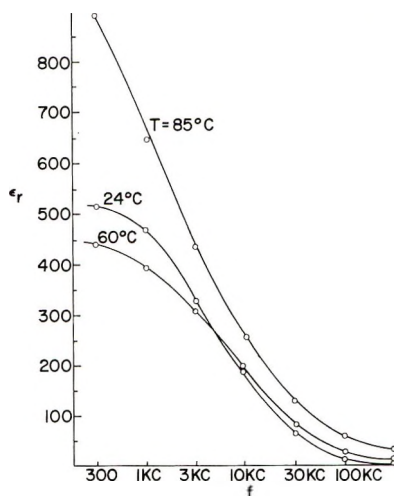


Fig. 12. Variation of the relative dielectric constant  $\epsilon_r$  for sample EHE-76 vs. frequency for constant values of temperature;  $\Phi_{sp} = 72 \text{ v./cm}$ .

volts),  $h$  is Planck's constant,  $m$  is the rest mass of electron,  $l = 1.40 \text{ \AA}$ . is the aromatic carbon-carbon bond length, and  $Z$  is the number of  $\pi$ -bonded carbon atoms in the aromatic ring compound.

The energy increment  ${}^3E$  can be identified closely with  $E_s$ , the observed<sup>5</sup> activation energy for spin states in such polymers.  $E_s$  values observed range from 0.016 to 0.03 e.v. In the polymer<sup>5</sup> EHE-39,  $E_s = 0.016 \text{ e.v.}$ , from which one estimates  $z = 2500$ . If the molecule were a string of fused benzenoid rings, for example, each carbon atom would contribute a projected length of  $2l/\sqrt{3} = 0.8 \text{ \AA}$ . The overall maximum chain length



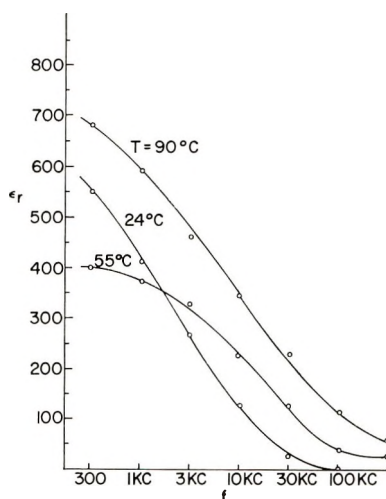


Fig. 13. Variation of the relative dielectric constant  $\epsilon_r$  for sample IS-1 vs. frequency for constant values of temperature;  $\Phi_{sp} = 72$  v./cm.

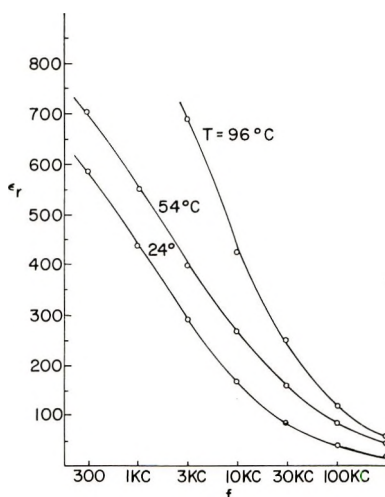


Fig. 14. Variation of the relative dielectric constant,  $\epsilon_r$ , for sample IS-2 vs. frequency for constant values of temperature;  $\Phi_{sp} = 48$  v./cm.

would then be  $L = (0.8 \text{ \AA.})z \cong 2000 \text{ \AA.}$  This agrees roughly with the value of 3250  $\text{\AA.}$  found with the field-dependence method and lends support to the conclusions drawn there.

To explain such behavior in these long molecules we suggest that we are probably observing a newly recognized type of electronic polarization which is the response to an electric field of an assembly of highly mobile charges lying individually in extended regions of near zero resistance (i.e., with extraordinarily long regions of associated  $\pi$ -orbitals) but limited in path ultimately by a molecular boundary.

The charge separation is initially that due to the normal and easily thermally excited intermolecular ionization of the long conjugated molecules. This, it is suggested, creates what is in effect an assembly of highly field sensitive monopoles.

At zero external field, the monopoles would mutually interact to form domains of spiralled and cyclized links of polarization. The collection of domains would exhibit a net near-zero overall moment easily perturbed by external fields. The response would probably be expected to be nonlinear to applied field strength, slight fields being able to accomplish most of the potential electronic shifts. Because of the kinetic and transitory nature of the individual monopoles, a finite rate of domain reorganization should be expected, meaning that one should expect a notable frequency dependence, with low frequencies most effective. Further, since the formation, recombination, and intermolecular transfer rate are obviously temperature-dependent, the degree of hyperelectronic polarization would be expected to be quite temperature dependent.

It appears that in the case of the present highly conjugated long molecules in which appreciable intermolecular charge transfer can occur (as evidenced by the observable semiconduction), that one may indeed have to account for the extraordinarily high polarizabilities in terms of some mechanism other than normal electronic polarization. The possibility of invoking normal atomic polarization associated with shifts of whole ions in a lattice (e.g., NaCl), or of dipole polarization associated with orientations and rotations of molecular dipoles seems to be excluded in the case of these organic molecules, for they are essentially hydrocarbon derivatives in their chemical structure.

The postulated hyperelectronic polarization fits the unusual degree of polarizability observed, the observed field dependence, the observed temperature dependence, and the observed frequency dependence.

There is, however, an alternate explanation possible. The polymers examined here are polycrystalline semiconductors. One could suppose that we had observed the migration and accumulation of carriers at the crystalline boundaries in such a manner as to exhibit a similarly high dielectric constant. In a very real sense, however, hyperelectronic polarization could be regarded as such a Maxwell-Wagner-Sillars<sup>4,6</sup> polarization on a molecular scale. The decision as to the mechanism in the present cases is therefore still an open one.

In conclusion, it appears that the postulated hyperelectronic polarization could exist and could have been observed in the materials examined. Its predicted characteristics fit in the following four respects (*a*) the unusually high dielectric constants for hydrocarbon derivatives ( $\epsilon_r = 50-890$ , compared to the  $\epsilon_r = 2-3$  normally observed<sup>4</sup> for hydrocarbon derivatives); (*b*) the observed field dependence; (*c*) the observed temperature dependence; and (*d*) the observed strong frequency dependence of the dielectric constant,  $\epsilon_r$ .

One of us (HAP) expresses his thanks to Professor P. O. Löwdin for the opportunity to finish writing of this paper while at the Quantum Chemistry Group in Uppsala. Thanks are due to the Cancer Institute of the National Institutes of Health and to the Kung Gustav VI Adolf's 70-Years Fund for Swedish Culture—Knut and Alice Wallenberg's Foundation for support during this period.

A portion of this work was done by one of us (R. R.) in partial fulfillment of the requirements for the degree of M.S.E.E.

### References

1. H. A. Pohl, J. A. Bornmann, and W. Ito, in *Organic Semiconductors*, J. J. Brophy and J. W. Buttrey, Eds., MacMillan, New York, 1962, p. 143.
2. H. A. Pohl and E. H. Engelhardt, *J. Phys. Chem.*, **68**, 2085 (1962).
3. H. A. Pohl, A. Rembaum, and A. W. Henry, *J. Am. Chem. Soc.*, **84**, 2699 (1962).
4. A. Von Hippel, Ed., *Dielectric Materials and Applications*, Wiley, New York, 1954.
5. H. A. Pohl and R. P. Chartoff, *J. Polymer Sci. A*, **2**, 2787 (1964).
6. L. K. H. Van Beek, *Physica*, **26**, 66 (1960).

### Résumé

Une classe de macromolécules fortement conjuguées présentant des constantes diélectriques effectives extraordinairement élevées ( $DK = 50$  à  $900$ ) est décrite; ces polymères sont du type quinone-radical polyacène: ils ont été purifiés et ils présentent des propriétés semiconductrices électriques. La constante diélectrique varie faiblement avec la pression (jusque  $20$  Kbars) mais fortement avec la pression ( $300$  à  $300.000$  cps) et modérément avec la température et la force du champ. Ce dernier effet de l'intensité du champ sur la constante diélectrique effective et sur la conductivité nécessite un développement de techniques spéciales de mesures qui sont décrites. Le comportement diélectrique inhabituel peut être expliqué en admettant la présence de ce qui est responsable des électrons et des défauts dans un plasma obtenu thermiquement, ces éléments étant mobiles localement sur des régions étendues par suite des orbitales associées au sein de ces molécules. La polarisation "hyperélectronique" admise et qui en résulte par suite de ses charges locales mobiles sous l'influence d'un champ extérieur s'accorde avec la grandeur observée de la polarisabilité de même que en ce qui concerne son champ, sa fréquence et sa dépendance thermique.

### Zusammenfassung

Eine Klasse hochgradig konjugierter Makromoleküle mit aussergewöhnlich hohen effektiven Dielektrizitätskonstanten ( $DK = 50$  bis  $900$ ) wird beschrieben. Diese Polymeren sind vom Polyacenradikalchinontyp: sie werden gut gereinigt und bilden elektronische Halbleiter. Die Dielektrizitätskonstante hängt nur schwach vom Druck (bis zu  $20$  kBar), jedoch stark von der Frequenz ( $300$  bis  $300.000$  Hz) und nur mässig von der Temperatur und der Feldstärke ab. Der Einfluss der Feldstärke auf die effektive Dielektrizitätskonstante (und auf die Leitfähigkeit) macht die Entwicklung spezieller Messmethoden notwendig, welche beschrieben werden. Das ungewöhnliche dielektrische Verhalten kann durch die Annahme der Anwesenheit sozusagen eines thermisch erzeugten Plasmas von Elektronen und Löchern, die örtlich auf ausgedehnten Bereiche assoziierter  $\pi$ -Orbitale der Moleküle beweglich sind, erklärt werden. Die postulierte resultierende "hyperelektronische" Polarisation der lokal beweglichen Ladungen im äusseren Feld passt zu der hohen beobachteten Polarisierbarkeit und ebenso ihre Feld-, Frequenz und Temperaturabhängigkeit.

Received May 25, 1965

Revised October 9, 1965

Prod. No. 4925

## Anionic Heterogeneous Polymerization of Methacrylonitrile by *n*-Butyllithium

BEN-AMI FEIT,\* ERI HELLER, and ALBERT ZILKHA, *Department of Organic Chemistry, The Hebrew University, Jerusalem, Israel*

### Synopsis

The anionic heterogeneous polymerization of methacrylonitrile by butyllithium in petroleum ether was investigated. The polymerization was of the "living" type, as seen from the linear dependence of the molecular weights on  $[\text{MAN}]/[\text{BuLi}]$ . This behavior was further supported by block polymerization experiments in which the monomer was added in two portions and the molecular weights obtained were directly proportional to the total monomer concentration. The initiator efficiency was low, and initiator consumption was only about 2%. This fact, together with the results of the block polymerizations showed that there was preferential addition of monomer to the growing chain ends rather than to the initiator. The molecular weights were independent of the rate of monomer addition. This as well as the "living" behavior of the polymerization of methacrylonitrile on a wide range of monomer and catalyst concentrations and the absence of chain transfer to monomer was essentially different from that of the similar heterogeneous polymerization of acrylonitrile by butyllithium previously investigated. This is due to the absence of an  $\alpha$ -acidic hydrogen in methacrylonitrile.

### INTRODUCTION

No detailed study of the butyllithium-initiated polymerization of methacrylonitrile has been reported.<sup>1</sup> Alkali metal alkyls and aryls such as triphenylmethylsodium,<sup>2</sup> phenylisopropylpotassium,<sup>3</sup>  $\alpha$ -methylstyrene tetramer,<sup>3</sup> alkali metal amides,<sup>4</sup> alkoxides,<sup>5</sup> and hydroxides,<sup>4</sup> alkali metals in liquid ammonia,<sup>6</sup> and quaternary ammonium hydroxides<sup>7</sup> were used as initiators for the anionic polymerization of methacrylonitrile.

When the monomer was polymerized in dimethylformamide by a methanolic solution of an alkali metal methoxide,<sup>5</sup> a direct initiation by the methoxide anion took place and termination was by transfer to the methanol present. Such a termination by transfer to a proton donor took place also in liquid ammonia.<sup>4</sup>

The anionic heterogeneous polymerization of acrylonitrile in petroleum ether by *n*-butyllithium was investigated in this laboratory.<sup>8</sup> A "living" type polymerization and/or a polymerization involving chain transfer to monomer took place, depending on the momentary concentration of monomer in the polymerization mixture. It was the purpose of the present work to investigate, under the same conditions, for the sake of

\* Present address: Institute of Chemistry, Tel-Aviv University, Israel.

comparison, the mechanism of the polymerization of methacrylonitrile, which has no acidic  $\alpha$ -hydrogen available for chain transfer to monomer.

## RESULTS

### Dependence of Molecular Weight on Monomer Concentration

Two series of experiments were carried out, one in which the monomer was added to the initiator solution (Table I and Fig. 1), and the other in which the initiator was added to the monomer (Table II and Fig. 2).

TABLE I  
Dependence of Molecular Weight on Monomer Concentration:  
Monomer Added to Catalyst<sup>a</sup>

Run no.	[MAN], mole/l.	[MAN] [BuLi]	Yield, %	$[\eta]$ , dl./g.	$\bar{M}_w$	$\bar{DP}$
A15 <sup>b</sup>	0.238	4.9	80	0.230	5,350	80
A16 <sup>b</sup>	0.238	4.9	85	0.292	8,400	125
A17	0.476	9.7	83	0.589	34,800	520
A19	0.716	14.6	80	0.640	41,050	615
A20	0.716	14.6	92	0.704	49,600	740
A9	0.958	19.5	95	0.851	72,300	1080
A21	0.958	19.5	96	0.824	67,800	1010
A22	0.958	19.5	96	0.888	78,700	1175
A10	1.192	24.3	90	0.895	79,950	1195
A23	1.192	24.3	96	0.946	89,250	1330
A24	1.192	24.3	95	0.915	83,500	1245
A26	1.432	29.2	90	1.108	121,600	1815
A27 <sup>c</sup>	1.916	39.1	90	1.318	172,600	2575
A28 <sup>c</sup>	1.916	39.1	94	1.290	165,400	2470

<sup>a</sup> Experimental conditions: monomer was added during 5 sec. to a solution of BuLi (0.049 mole/l.) in petroleum ether.

<sup>b</sup>  $\alpha_{A15} = 4 \times 10^{-2}$ ;  $\alpha_{A16} = 3.8 \times 10^{-2}$ .

<sup>c</sup>  $\alpha_{A27} = 1.56 \times 10^{-2}$ ;  $\alpha_{A28} = 1.63 \times 10^{-2}$ .

In both cases the degree of polymerization increased linearly with the monomer concentration. Deviations from linearity were observed at the lowest and highest monomer concentrations used. With the former the molecular weights were too low, and with the latter too high (Figs. 1 and 2).

The polymerization was fast, and similar yields were obtained after reaction times of 1-30 min. (Table II).

Block polymerization experiments were carried out in which the monomer was added to the butyllithium in two portions, the second portion being added after the first one was polymerized (Table III and Fig. 2). The molecular weights obtained were essentially the same as when the total monomer was added in one portion, except in the case of the relatively high monomer concentrations (runs F7, G23, Table III), where they were higher.



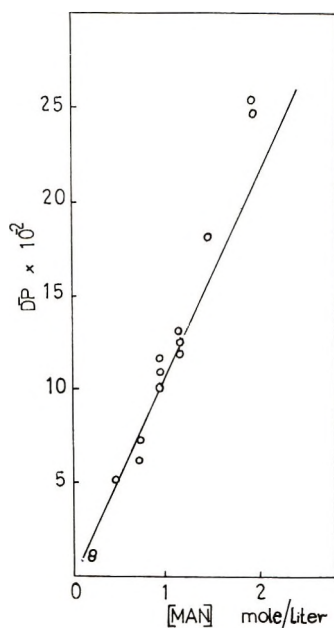


Fig. 1. Dependence of molecular weight on monomer concentration. Monomer added to catalyst.

TABLE II  
Dependence of Molecular Weight on Monomer Concentration:  
Catalyst Added to Monomer<sup>a</sup>

Run no.	[MAN], mole/l.	$\frac{[MAN]}{[BuLi]}$	Yield, %	$[\eta]$ , dl./g.	$\overline{M}_w$	$\overline{DP}$
D1	0.238	3.6	85	0.115	1,350	20
F12	0.358	5.4	87	0.138	1,950	30
D10	0.476	7.1	91	0.280	7,950	120
D11	0.476	7.1	91	0.269	7,350	110
F4 <sup>b</sup>	0.716	10.7	80	0.442	19,650	295
F6 <sup>c</sup>	0.716	10.7	87	0.424	18,100	270
D12	0.958	14.4	95	0.633	40,150	600
D13	0.958	14.4	94	0.603	36,450	545
D7	1.192	17.9	94	0.777	60,350	900
D8	1.192	17.9	90	0.674	45,500	680
D3	1.432	21.5	95	0.849	71,950	1070
D4	1.432	21.5	95	0.828	68,450	1020

<sup>a</sup> Experimental Conditions: BuLi in petroleum ether was added in one portion to a cool solution of MAN in petroleum ether. The concentration of BuLi in the polymerization mixture was 0.0667 mole/l.

<sup>b</sup> Polymerization time 1 min.

<sup>c</sup> Polymerization time 5 min.

### Dependence of Molecular Weight on Butyllithium Concentration

The degree of polymerization was inversely proportional to the butyllithium concentration. This was the case on adding either the monomer to



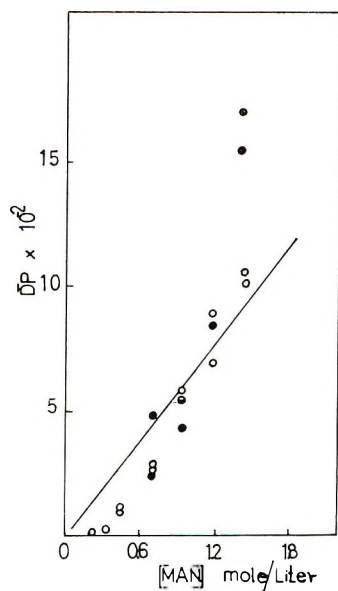


Fig. 2. Dependence of molecular weight on monomer concentration, catalyst added to monomer: (O) monomer added in one portion; (●) monomer added in two portions.

TABLE III  
Dependence of Molecular Weight on Monomer Concentration:  
Block Polymerization<sup>a</sup>

Run no.	MAN, mole		[MAN] (total), mole/l.	Yield, %	[ $\eta$ ], dl./g.	$\bar{M}_w$	$\bar{DP}$
	1st portion	2nd portion					
F10 <sup>b</sup>	0.0179	0.0179	0.716	89	0.405	16,500	245
F11 <sup>b</sup>	0.0179	0.0179	0.716	83	0.573	32,950	490
F8	0.0358	0.0118	0.958	90	0.540	29,250	435
F9	0.0358	0.0238	1.192	91	0.755	57,000	850
F7	0.0358	0.0358	1.432	92	1.075	95,750	1430
G23	0.0358	0.0358	1.432	92	1.025	104,700	1560

<sup>a</sup> Experimental conditions: BuLi (0.0667 mole/l.) was added in one portion to the solution of the first portion of monomer in petroleum ether, followed after 5 min. by the second portion of monomer.

<sup>b</sup> The second portion of monomer was added after 2 min.

the initiator (Table IVA and Fig. 3) or the initiator to the monomer (Table IVB and Fig. 4). Deviations from linearity were observed at the high initiator concentrations.

#### Dependence of Molecular Weight on [Methacrylonitrile]/[BuLi]

From Figure 5, which represents all the results obtained (Tables I-IV) at different  $[MAN]/[BuLi]$  ratios, it is seen that there is a linear dependence of  $\bar{DP}$  on  $[MAN]/[BuLi]$ . The straight line was drawn through

TABLE IV  
 Dependence of Molecular Weight on Initiator Concentration<sup>a</sup>

Run no.	[BuLi] × 10 <sup>2</sup> , mole/l.	[MAN]/[BuLi]	Yield, %	[ $\eta$ ], dl./g.	$\bar{M}_w$	$\bar{DP}$
Series A						
B13	1.63	44.00	83	1.231	150,500	2240
B14	1.63	44.00	80	1.208	145,000	2160
G3	2.37	30.20	95	1.060	111,900	1665
G4	2.37	30.20	95	1.080	116,100	1730
K14	3.29	21.80	95	0.965	92,700	1380
A19	4.92	14.60	82	0.640	41,050	610
A20	4.92	14.60	92	0.701	49,200	735
B8	8.64	8.30	89	0.381	14,650	220
A1	9.50	7.55	80	0.388	15,150	225
B2	9.84	7.30	83	0.502	25,300	375
B9	11.52	6.20	86	0.437	19,200	285
B10	11.52	6.20	81	0.430	18,600	275
B12	14.40	5.00	84	0.228	5,250	80
B16	22.80	3.14	82	0.322	10,550	155
B18	29.40	2.44	80	0.138	1,950	30
Series B						
E3	1.66	43.00	80	1.070	114,000	1700
E4	1.66	43.00	87	1.240	152,800	2275
K16	2.56	27.90	90	0.933	86,800	1295
K18	3.20	22.30	80	0.743	55,200	825
K19	3.20	22.30	85	0.745	55,500	825
K20	3.64	19.70	92	0.675	45,600	680
K21	3.64	19.70	95	0.666	44,400	660
K22	4.27	16.80	95	0.707	50,850	755
K23	4.27	16.80	95	0.690	47,650	710
F4	6.67	10.70	81	0.442	19,650	295
F6	6.67	10.70	86	0.424	18,100	270
E6	9.96	7.20	84	0.308	9,600	145
E7	16.60	4.30	85	0.182	3,350	50

<sup>a</sup> Experimental conditions for series A: monomer (0.716 mole/l.) was added during 5 sec. to a solution of BuLi in petroleum ether. Experimental conditions for series B: BuLi was added in one portion to a solution of monomer (0.716 mole/l.) in petroleum ether.

the points for which the order of addition of reagents was solvent, initiator, monomer. The points for which the initiator was added the last were generally below the line. This is so because for the same [MAN]/[BuLi] ratio, the molecular weights obtained were a little lower on adding the initiator the last.

### Dependence of Molecular Weight on the Rate of Monomer Addition

The molecular weights were independent of the rate of monomer addition to a solution of butyllithium in the range of 0.002–0.700 mole/l.-sec. A small decrease of molecular weights was, however, observed with the highest rate of monomer addition investigated (Table V).

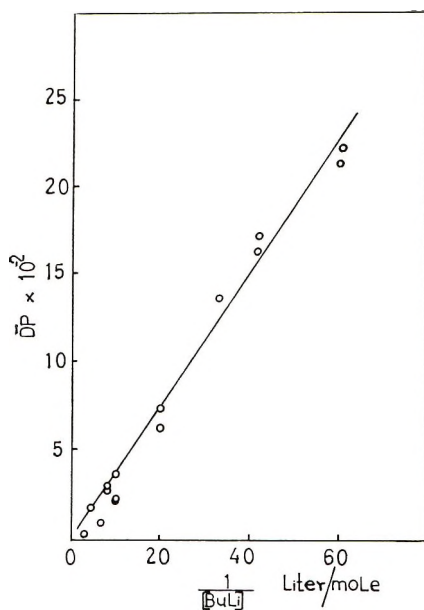


Fig. 3. Dependence of molecular weight on BuLi concentration. Monomer added to catalyst.

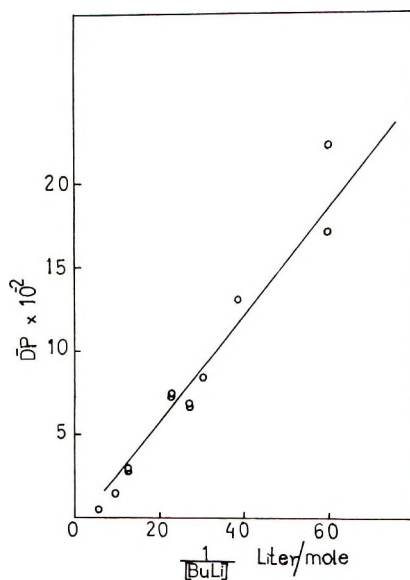


Fig. 4. Dependence of molecular weight on BuLi concentration. Catalyst added to monomer.

### Effect of Temperature on the Molecular Weights

Under otherwise constant conditions, the molecular weights remained practically constant on varying the polymerization temperature from  $-30$  to  $+10^\circ\text{C}$ .

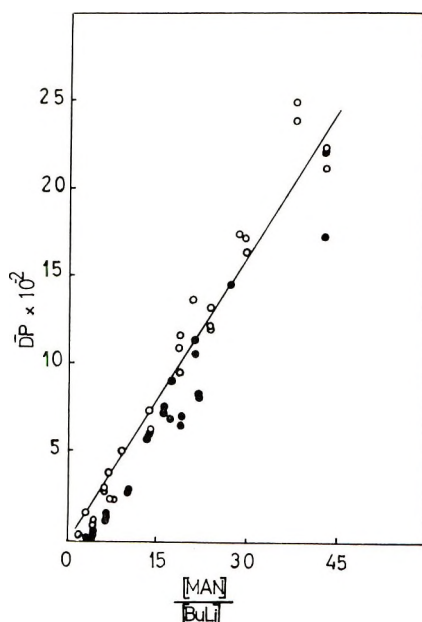


Fig. 5. Dependence of molecular weight on  $[\text{MAN}]/[\text{BuLi}]$ : (O) monomer added to catalyst; (●) catalyst added to monomer.

## DISCUSSION

The linear dependence of the degree of polymerization on monomer concentration (Tables I and II) and on  $1/[\text{BuLi}]$  (Table IV) was in accordance with a "living" mechanism<sup>9-11</sup> for the butyllithium-initiated polymerization of methacrylonitrile in petroleum ether. The formation of block polymers and the linear dependence of their degree of polymerization on the total concentration of monomer (Table III) were also characteristic of a "living" system.<sup>9-12</sup>

TABLE V  
Dependence of Molecular Weight on the Rate of Monomer Addition<sup>a</sup>

Run no.	Rate of addition, mole/l.-sec.	Yield, %	$[\eta]$ , dl./g.	$\bar{M}_w$	$\bar{DP}$
C7	0.002	89	0.448	20,200	300
C6	0.090	88	0.442	19,650	295
C5	0.090	90	0.481	23,240	345
B20	0.143	85	0.446	20,000	300
C4	0.238	80	0.458	21,100	315
C2	0.716	93	0.410	16,950	250
C1	0.716	83	0.391	15,400	230

<sup>a</sup> Experimental conditions: monomer (0.716 mole/l.) was added at different rates to a solution of butyllithium (0.065 mole/l.) in petroleum ether.

TABLE VI  
 Effect of Temperature on the Molecular Weight<sup>a</sup>

Run no.	Temperature, °C.	Yield, %	$[\eta]$ , dl./g.	$\bar{M}_w$	$\bar{DP}$
G19	10	94	0.448	20,200	300
G20	10	92	0.382	14,700	220
F4	0	80	0.442	19,650	295
F6	0	87	0.424	18,100	270
G17	-10	94	0.424	18,100	270
G16	-30	90	0.439	18,620	278

<sup>a</sup> Experimental conditions: butyllithium (0.067 mole/l.) was added in one portion to a solution of monomer (0.716 mole/l.) in petroleum ether.

The present polymerization was of the "living" type, irrespective of the order and the rate of addition of reagents to the polymerization mixture (Tables, I, II, and IV). It was in this respect entirely different from the analogous polymerization system of acrylonitrile,<sup>8</sup> where a "living" mechanism was dominant in the presence of low momentary concentrations of monomer and a polymerization involving chain transfer to monomer was dominant at relatively high ones, as was evident from the independence of  $\bar{DP}$  of both monomer and initiator concentrations. The acidic  $\alpha$ -hydrogen of the acrylonitrile was responsible for this transfer reaction. The absence of a chain transfer reaction in the case of methacrylonitrile was due to the  $\alpha$ -methyl group in this monomer. The experimental results did not support any other chain-transfer reaction, such as that involving hydride ion.<sup>4</sup>

Since no transfer reaction took place during the polymerization which was of the "living" type, the fraction of butyllithium which was effective in the initiation step could be defined by  $\alpha = [\text{MAN}]/\bar{DP}[\text{BuLi}]_{\text{total}}$ . Mean values of  $\alpha$  were accordingly calculated from the slope of the straight lines of Figures 1-5. The  $\alpha$  values thus obtained were:  $1.86 \times 10^{-2}$ ,  $2.33 \times 10^{-2}$ ,  $1.91 \times 10^{-2}$ ,  $2.23 \times 10^{-2}$ , and  $1.9 \times 10^{-2}$ , respectively, indicating that only about 2% of the total amount of the butyllithium introduced was effective in the initiation. These low consumptions of initiator were realized with relatively high  $[\text{MAN}]/[\text{BuLi}]$  ratios. Low efficiencies of the same order were previously found for the butyllithium-initiated polymerization of acrylonitrile.<sup>8,13</sup>

The small consumption of initiator and the formation of block polymers having the same molecular weights as those obtained on addition of the monomer in one portion showed that the rate constant of propagation was much greater than that of initiation, and that monomer reacted preferentially with carbanionic chain ends than with unreacted butyllithium. This was also supported by the independence of the molecular weight of the rate of monomer addition; the molecular weight remained constant even with the lowest rate of addition used (Table V).

The preferential addition of monomer to the active chain ends rather than to the initiator also explains why the molecular weights of polymer

obtained when the initiator was added in one portion in the end to the polymerization mixture were a little lower than those obtained when the monomer was added dropwise to the initiator (Fig. 5). In the second mode of reaction there is a smaller possibility of competition for monomer between the initiator and the active chain ends. That is why the consumption of initiator when monomer was added last was a little lower than when the initiator was added in the end ( $\alpha = 1.9 \times 10^{-2}$  as compared to  $\alpha = 2.3 \times 10^{-2}$ ). This also explains why, at the highest rate of addition of monomer, there was a small lowering in molecular weight (Table V).

The low efficiency of the initiator, the results of the block polymerizations (in which the second portion of monomer was added after several minutes), and the independence of the molecular weight of the temperature of polymerization tend to point out that the position of the equilibrium:  $(\text{BuLi})_n \rightleftharpoons n\text{BuLi}$ , does not critically affect the polymerization under the conditions investigated, even though free BuLi is probably the active initiator.<sup>14</sup>

The "living" chain ends of polymethacrylonitrile were relatively stable as compared to those of polyacrylonitrile.<sup>8</sup> This was evident from the linear dependence of molecular weight on the total concentration of monomer in the block polymerization experiments (Table III), where the second portion of monomer was added 5 min. after the first one. This might be due to the absence of any acidic  $\alpha$ -hydrogens in the monomer and the polymer, in contrast to the case of acrylonitrile. The molecular weight obtained with the highest monomer concentrations investigated (including the block polymerizations at high monomer concentration) were higher than expected for strict linear relation; this might be due in part to partial deactivation of "living" chain ends (by monomolecular cyclization,<sup>15</sup> or otherwise) whose effect would be more pronounced at high monomer concentrations. Thus monomer will be consumed by a relatively smaller number of active ("living") chain ends, leading to the higher molecular weights observed.

At relatively very high BuLi concentrations and low  $[\text{MAN}]/[\text{BuLi}]$  ratios, the molecular weights were below linear (Fig. 5), probably due to a more effective competition of BuLi (initiation) versus the propagation reaction for monomer at such high initiator concentrations. In fact, such a competition for monomer exists during the entire polymerization process. On the other hand, the linear dependence of  $\overline{\text{DP}}$  on  $[\text{M}]$  and on  $1/[\text{BuLi}]$  (excluding the extreme cases) points out that essentially no butyllithium in addition to that required to initiate polymerization was further consumed during the polymerization. This is further substantiated by the block polymerization experiments.

## EXPERIMENTAL

### Materials

Methacrylonitrile (MAN) (Fluka) was purified as previously described.<sup>7</sup> Petroleum ether (b.p. 60–80°C.) analar grade, was refluxed over sodium



wire and distilled under argon. *n*-Butyllithium was prepared in petroleum ether as previously described;<sup>8</sup> only freshly prepared catalyst was used. Liquid reagents and solutions were kept under argon and transferred with hypodermic syringes by applying positive argon pressure.

### Polymerization and Isolation Procedures

The polymerization apparatus and procedure were the same as used before.<sup>5</sup> A high-speed stirrer was employed. The total volume of the polymerization mixture was 50 ml., polymerization temperature was  $0 \pm 2^\circ\text{C}$ ., and polymerization time was 30 min., unless otherwise indicated. On adding the initiator to the monomer solution, a green colored polymer precipitated out. The polymerization was stopped by adding 5% hydrochloric acid (10 ml.), and the polymer was filtered, washed with water, and dried. The polymer was further purified for viscosity measurements by grinding, washing with water, and drying at  $50^\circ\text{C}$ . to a constant weight.

Viscosities were measured in dimethylformamide at  $29.2^\circ\text{C}$ . in an Ubbelohde viscometer. In addition, the following equation<sup>16</sup> was used to determine intrinsic viscosities by measuring the viscosity of the polymer solution at one concentration (0.1 g./100 ml.):  $\eta = \eta_0 e^{[\eta]C}$ , where  $\eta_0$ ,  $\eta$ , and  $[\eta]$  are the viscosity of solvent, the viscosity of polymer solution, and intrinsic viscosity respectively, and  $C$  is the concentration of polymer solution in g./100 ml. This equation was applicable for  $C \leq 0.13$  g./100 ml.

Molecular weights were calculated by using the equation of Overberger et al.:<sup>6</sup>  $[\eta] = 3.06 \times 10^{-3} \bar{M}^{0.503}$ .

### References

1. W. K. Wilkinson, U. S. Pat. 3,087,919 (1963).
2. R. C. Beaman, *J. Am. Chem. Soc.*, **70**, 3115 (1948).
3. P. Rempp and A. Blumstein, *Bull. Soc. Chim. France*, **1961**, 1018.
4. C. G. Overberger, H. Yuki, and N. Urakawa, *J. Polymer Sci.*, **45**, 127 (1960).
5. B. A. Feit, J. Wallach, and A. Zilkha, *J. Polymer Sci. A*, **2**, 4743 (1964).
6. C. G. Overberger, E. M. Pearce, and N. Maves, *J. Polymer Sci.*, **31**, 217 (1958).
7. A. Zilkha, B. A. Feit, and M. Frankel, *J. Polymer Sci.*, **49**, 231 (1961).
8. B. A. Feit, D. Mirelman, and A. Zilkha, *J. Appl. Polymer Sci.*, **9**, 2459 (1965).
9. M. Szwarc, M. Levy, and R. Milkovich, *J. Am. Chem. Soc.*, **78**, 2656 (1956).
10. M. Szwarc, *Nature*, **178**, 1168 (1956).
11. R. Waack, A. Rembaum, J. D. Coombes, and M. Szwarc, *J. Am. Chem. Soc.*, **79**, 2026 (1957).
12. J. Grodzinsky, A. Katchalsky, and D. Vofsi, *Makromol. Chem.*, **44-46**, 591 (1961).
13. M. L. Miller, *J. Polymer Sci.*, **56**, 203 (1962).
14. M. Szwarc and J. Smid, in "Progress in Reaction Kinetics" Vol. 2, Pergamon Press, London, 1964, p. 243.
15. M. Szwarc, *Fortschr. Hochpolymer. Forsch.*, **2**, 281 (1960).
16. D. K. Thomas and T. A. J. Thomas, *J. Appl. Polymer Sci.*, **3**, 129 (1961).

### Résumé

La polymérisation hétérogène anionique du méthacrylonitrile par le butyllithium dans le pétrole, a été étudiée. La polymérisation était du type vivant tel qu'il résulte de la dépendance linéaire du poids moléculaire MAN/BuLi. Ce comportement a été en outre, confirmé par les expériences de polymérisation en block, dans laquelle le monomère était additionné en deux portions et où le poids moléculaire obtenu était directement proportionnel à la concentration totale en monomère. L'efficacité d'initiation était faible et sa concentration était seulement d'environ 2. Ce fait, en même temps que les résultats de la polymérisation en block montre qu'il y a une addition du monomère à la chaîne en croissance plutôt qu'à l'initiateur. Les poids moléculaires sont indépendants de la vitesse d'addition du monomère. De même que le comportement vivant de la polymérisation du polyméthacrylonitrile sur un vaste domaine de concentration en monomère et en catalyseurs et l'absence de transfert de chaînes aux monomères était essentiellement différents de celui de la polymérisation hétérogène similaire de l'acrylonitrile par le butyl-lithium étudiée précédemment. Ceci est dû à l'absence d'un hydrogène  $\alpha$ -acid dans le méthacrylonitrile.

### Zusammenfassung

Die anionische heterogene Polymerisation von Methacrylnitril durch Butyllithium in Petroleum wurde untersucht. Wie man aus der Abhängigkeit des Molekulargewichts vom MAN/BuLi ersehen kann, handelt es sich um eine Polymerisation vom "Lebendtyp." Dies wurde durch Blockpolymerisationsversuche bestätigt, bei welchen das Monomere in zwei Teilen zugesetzt wurde und die erhaltenen Molekulargewichte der gesamten Monomerkonzentration direkt proportional waren. Die Starterausbeute war niedrig, und der Starterverbrauch betrug nur etwa 2%. Dieser Umstand zeigt zusammen mit den Ergebnissen der Blockpolymerisation, dass eine bevorzugte Addition des Monomeren an die wachsenden Kettenenden und nicht an den Starter stattfindet. Die Molekulargewichte waren von der Geschwindigkeit des Monomerzusatzes unabhängig. Dieses Verhalten sowie die Polymerisation vom "Lebend"-typ von Methacrylnitril in einem weiten Bereich von Monomer- und Katalysatorkonzentration und das Fehlen einer Kettenübertragung zum Monomeren bildet einen wesentlichen Unterschied zur früher untersuchten ähnlichen heterogenen Polymerisation von Acrylnitril durch Butyllithium. Dies ist die Folge des Fehlens eines sauren  $\alpha$ -Wasserstoffs im Methacrylnitril.

Received June 23, 1965

Revised October 12, 1965

Prod. No. 4926A

## Polymerization of Olefin Oxides and of Olefin Sulfides

JOGINDER LAL, *Research Laboratories, The Goodyear Tire & Rubber Company, Akron, Ohio*

### Synopsis

Two new catalyst systems, sulfur-diethylzinc and 98% hydrogen peroxide-diethylzinc, have been investigated for polymerizing propylene oxide. The sulfur-diethylzinc catalyst system has a broad range of sulfur/zinc atomic ratio for polymerizing propylene oxide heterogeneously to high molecular weight materials in high yields. The highest polymer yield is obtained at the sulfur/zinc atomic ratio of 3-3.5. Like the water-diethylzinc system, the hydrogen peroxide-diethylzinc system has a narrow range of hydrogen peroxide/diethylzinc molar ratio in the vicinity of 0.57 for optimum polymer yield. Crystallinity measurements by x-ray diffraction of a few polymers prepared with these three catalyst systems showed that they are fairly similar in the extent of their crystallinity. A plot of the per cent of polymer insoluble in acetone against inherent viscosity of the original polymer also showed that the polymers prepared with sulfur-diethylzinc and hydrogen peroxide-diethylzinc catalyst systems have similar amounts of crystallinity. Data are given for the polymerizability of ethylene oxide, 1,2-butene oxide, styrene oxide, propylene sulfide, 1,2-butene sulfide, and a vulcanizable copolymer of propylene oxide and allyl glycidyl ether with the sulfur-diethylzinc catalyst system. The polymers from the olefin sulfides had lower inherent viscosities than the polymers from the corresponding olefin oxides. Aging of the sulfur-diethylzinc catalyst (S/Zn atomic ratio = 3.5) improved the yield of poly(propylene oxide). The yield was essentially unchanged when propylene oxide was polymerized in six different solvents. The formation of  $C_2H_6S_xZnSC_2H_5$  and  $C_2H_6S_xZnS_yC_2H_5$  ( $x$  and  $y$  are integers between 2 and 8) and possibly  $C_2H_6S_xZnC_2H_5$  as the catalytically active species is postulated during the reaction of sulfur and diethylzinc.

### INTRODUCTION

A wide variety of catalysts is capable of polymerizing olefin oxides to high molecular weight materials.<sup>1</sup> More recently, alkylmetals in combination with water have been reported as catalysts for the polymerization of olefin oxides.<sup>2-4</sup> It has been observed, however, that the water to dialkylzinc molar ratio at which polymers are obtained in high yields is limited to a rather narrow range in the vicinity of 1.<sup>3,5</sup> A new catalyst system encompassing a wider range of the ratio of the catalyst components for substantial polymer yields consists of sulfur and diethylzinc. The yields and characteristics of the polymers obtained with this catalyst system are compared with the corresponding data from another newly investigated catalyst system, viz., hydrogen peroxide-diethylzinc, and the water-diethylzinc system.

## EXPERIMENTAL

All operations for purifying monomers and solvents, catalyst preparation, and polymerization were conducted under nitrogen of lamp grade purity.

### Materials

High purity propylene oxide and 1,2-butene oxide were obtained from Union Carbide Chemicals Company. They were distilled over calcium hydride. Styrene oxide (Dow Chemical Company), allyl glycidyl ether (Dow Chemical Company), and epichlorhydrin (Union Carbide Company) were fractionally distilled under reduced pressure and the middle cuts used. Ethylene oxide (Matheson Company) was dissolved in benzene and the solution was dried by passing over alumina. Propylene sulfide (Aldrich Chemical Company) and 1,2-butene sulfide were fractionally distilled over calcium hydride. The latter monomer was synthesized by the reaction of 1,2-butene oxide with aqueous potassium thiocyanate.

Thiophene-free benzene (Baker and Adamson) was distilled over phosphorus pentoxide or calcium hydride. *n*-Heptane (Phillips pure grade), carbon tetrachloride (technical grade) and chlorobenzene (technical grade) were dried by passing through silica gel. Tetrahydrofuran (du Pont) was distilled over lithium aluminum hydride. Anhydrous diethyl ether (Baker and Adamson) was used directly.

Diethylzinc was obtained from Stauffer Chemical Company. It was carefully diluted with benzene to about 2*M* solution. The solution was standardized by measuring ethane evolved on reaction with water. High purity sulfur (Stauffer Chemical Company) was used directly.

### Polymerization

Polymerizations were generally carried out in 4-oz. glass bottles. Through a self-sealing gasket under the screw-cap, the required amount of organometallic compound was injected into the bottle containing solvent, monomer, and cocatalyst. The screw-cap was then replaced by a new one having a polyethylene liner. The bottle was tumbled in a constant temperature bath and the polymerization was allowed to proceed with this catalyst prepared *in situ*. For polymerization with a preformed catalyst, the monomer was injected into the bottle containing the catalyst prepared by reacting diethylzinc with sulfur in benzene solution. The polymerization was stopped by chilling the bottle and adding about 15 ml. methanol containing phenyl- $\beta$ -naphthylamine as a stabilizer. The polymeric material was dried under aspirator vacuum for 24 hr. and then under 2 Torr for about 68 hr. at 40°C. The indicated polymer yields have not been adjusted for catalyst residues.

### Characterization

Inherent viscosity of the polymer was determined at 30°C. on a 0.05% solution in benzene and is expressed in units of deciliters per gram.

Per cent solubility in acetone was determined on a 0.06-in. thick molded specimen at 25°C. after immersion in acetone for 72 hr. The specimens were molded at about 150°C. for 15 min. and allowed to remain at room temperature for 72 hr. before immersion in acetone. The acetone solvent was changed after 24, 48, and 72 hr. The swollen sample was subsequently dried under vacuum before weighing to determine the weight loss.

## RESULTS AND DISCUSSION

The data in Tables I and II show that sulfur acts as a cocatalyst in the polymerization of propylene oxide with diethylzinc. The effect of sulfur/zinc atomic ratio on polymer yield and its inherent viscosity are shown in

TABLE I  
Effect of Sulfur/Zinc Atomic Ratio on Polymer Yield and Properties in Polymerization of Propylene Oxide with Sulfur-Diethylzinc Catalyst Prepared *in Situ*<sup>a</sup>

Wt. of sulfur, g.	S/Zn atomic ratio	Polymer yield, %	Inherent viscosity, dl./g.	Acetone- insoluble, %
0	0	2.0	2.2	—
0	0	4.0	1.6	—
0.037	0.5	2.5	3.1	—
0.074	1	2.0	5.3	—
0.148	2	62.6	10.4	70
0.222	3	91.3	9.0	44
0.296	4	88.0	9.6	48
0.444	6	80.2	9.7	50
0.592	8	74.4	9.0	54

<sup>a</sup> Conditions; 40 ml. benzene, 40 ml. monomer, 1.26 ml. of diethylzinc solution (1.85 *M*) and sulfur as indicated: 50°C., 7.7 hr.

Figures 1 and 2. The inherent viscosities of the polymers obtained at sulfur/zinc atomic ratio of 2–8 are in the range of 7.7–10 dl./g. The highest polymer yield is obtained at the sulfur/zinc atomic ratio of 3–3.5. Above this ratio, there is only a slight decrease in the polymer yield, especially when polymerizations are allowed to continue to longer times as in Figure 1. The sulfur–diethylzinc catalyst system has a broad range of sulfur/zinc atomic ratio for obtaining high molecular weight polymers in high conversion in heterogeneous polymerizations. This is in contrast to the narrow range of water/diethylzinc molar ratio in the water–diethylzinc catalyst system for obtaining poly(propylene oxide) in high yield. Our data on this system as well as on the hydrogen peroxide–diethylzinc catalyst system for polymerizing propylene oxide are given in Tables III and IV, respectively. The effect of cocatalyst/diethylzinc molar ratio on the polymer yield is shown in Figure 3. The hydrogen peroxide–diethylzinc catalyst system has not been reported previously. Like the water–diethylzinc catalyst system, it too has a narrow range of hydrogen peroxide/diethylzinc molar ratio in the vicinity of 0.57 for optimum polymer yield.



TABLE II  
Effect of Sulfur/Zinc Atomic Ratio on Polymer Yield and Properties in Polymerization of Propylene Oxide with Sulfur-Diethylzinc Catalyst Prepared *in Situ*<sup>a</sup>

Wt. of sulfur, g.	S/Zn atomic ratio	Polymerization characteristics	Polymer yield, %	Inherent viscosity, dl./g.	Acetone-insoluble, % <sup>b</sup>
0.0592	1.0	Homogeneous	1.35	5.6	—
0.0888	1.5	Homogeneous <sup>c</sup>	1.95	6.1	—
0.1184	2.0	Heterogeneous	24.0	9.2	41
0.1480	2.5	"	35.0	8.5	44
"	"	"	37.5	8.8	45
0.1776	3.0	"	60.0	9.7	56
"	"	"	59.3	9.4	49
0.2072	3.5	"	62.8	9.4	56
"	"	"	60.7	8.9	50
0.2368	4.0	"	50.0	10.0	51
0.3552	6.0	"	36.0	7.7	41
0.4736	8.0	"	30.4	6.9	39

<sup>a</sup> Conditions; 60 ml. benzene solution of sulfur, 40 ml. propylene oxide, 1.0 ml. diethylzinc solution (1.85*M* in benzene); 50°C., 4.5 hr.

<sup>b</sup> Samples were not molded for this determination.

<sup>c</sup> The catalyst was initially soluble but turbidity developed soon after the bottle was placed in the 50°C. bath.

The data in Table V indicate that the per cent acetone-insoluble fraction of poly(propylene oxide) prepared with the sulfur-diethylzinc catalyst system at the sulfur/zinc atomic ratio of 3.5 is dependent on conversion. There is an initial increase in inherent viscosity up to about 30% conversion. At higher conversions, the inherent viscosity tends to level off. As shown in Table VI, aging of the preformed catalyst at 25°C. up to 1 hr. improved the polymer yield. Although quantitative data are not presented here, it was also found that the polymer yield remained virtually unchanged, whether the catalyst was prepared *in situ* or was freshly preformed.

In Table VII it is seen that the yield of poly(propylene oxide) was essentially unchanged when polymerization with the sulfur-diethylzinc catalyst was carried out in six different solvents (expts. 1-6). Except for the polymer prepared in tetrahydrofuran the remaining polymers had high inherent viscosities and a high percentage of acetone-insoluble material. Presumably, tetrahydrofuran participates in the chain termination mechanism. The polymerizability of ethylene oxide, 1,2-butene oxide, styrene oxide, propylene sulfide, and 1,2-butene sulfide with sulfur-diethylzinc catalyst is also shown in Table VII (expts. 7-11). The polymers obtained from the olefin sulfides had lower molecular weights than the polymers from the corresponding olefin oxides. These olefin sulfides also polymerize faster with sulfur-diethylzinc catalyst than the corresponding oxygen analogs, although data for the comparison are not included in Table VII. The reaction product of sulfur and dimethylcadmium (expt. 12) yielded only traces of a low viscosity polymer from propylene oxide.



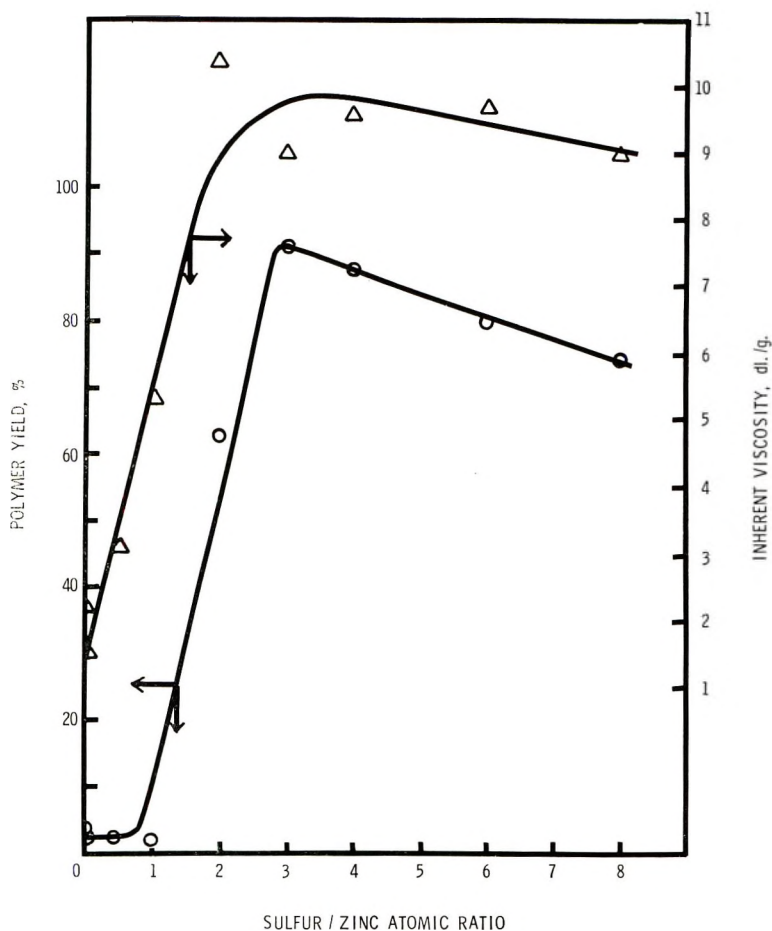


Fig. 1. Effect of sulfur/zinc atomic ratio on (O) yield and ( $\Delta$ ) inherent viscosity of polymer obtained by polymerization of propylene oxide with *in situ* sulfur-diethylzinc catalyst for 7.7 hr. at 50°C. in benzene: 40 ml. benzene, 40 ml. monomer, 2.33 mmole diethylzinc, and varying amounts of sulfur.

Epichlorhydrin gave a slight yield of an oily material with the sulfur-diethylzinc catalyst (expt. 13). The yield of poly(epichlorhydrin) was sharply increased when triisobutylaluminum was employed in place of diethylzinc to form a catalyst with sulfur *in situ*; however, the inherent viscosity of the polymer was still quite low.

As shown in Table VIII, some organic polysulfides as well as selenium act as suitable cocatalysts in conjunction with diethylzinc for polymerizing propylene oxide.

#### Nature of the Catalyst

The reaction of elemental sulfur and dialkylzinc is likely to produce the following compounds:  $RSZnR$ ,  $RS_2ZnR$ ,  $RSZnSR$ ,  $RS_2ZnSR$ , and  $RS_2-$

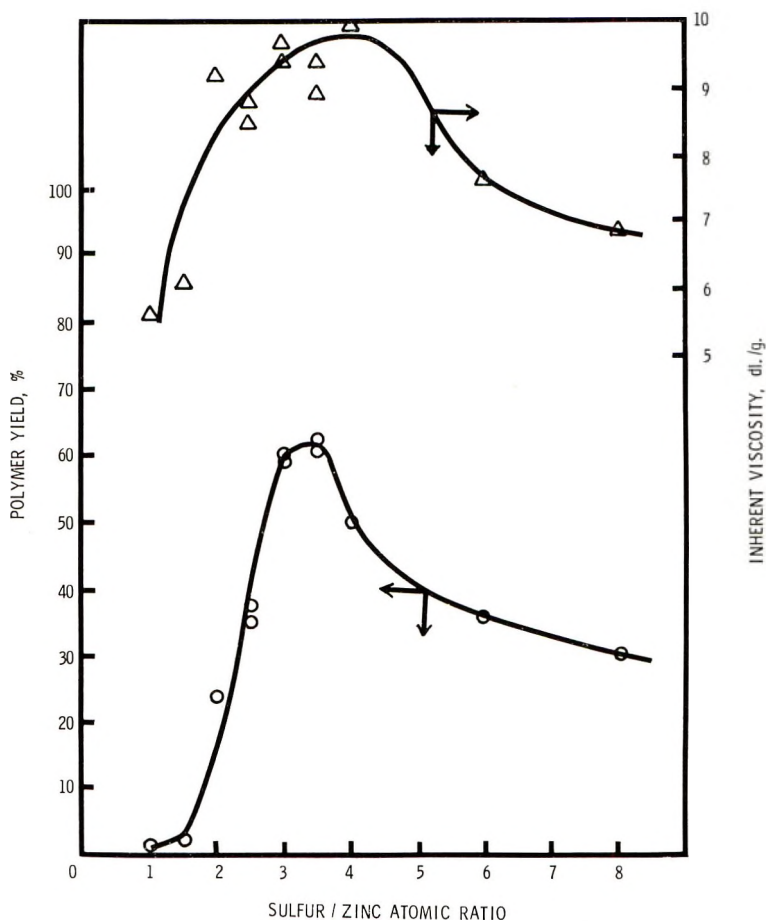


Fig. 2. Effect of sulfur/zinc atomic ratio on (O) yield and ( $\Delta$ ) inherent viscosity of polymer obtained by polymerization of propylene oxide with *in situ* sulfur-diethylzinc catalyst for 4.5 hr. at 50°C. in benzene: 60 ml. benzene, 40 ml. monomer, 1.85 mmole diethylzinc, and varying amounts of sulfur.

$ZnS_xR_y$ , where R is an alkyl group (e.g., ethyl) and  $x$  and  $y$  are integers having values between 2 and 8. The reaction product of sulfur and diethylzinc (sulfur/zinc atomic ratio = 4) which had been aged for several days evolved ethane on treatment with water. This indicates that such a reaction product contains  $C_2H_5-Zn$  bonds, which may be due to the presence of  $RSZnR$  and/or  $RS_2ZnR$ . As shown in Table VI, aging of the catalyst prepared at sulfur/zinc atomic ratio of 3.5 resulted in enhancement of the catalytic activity for propylene oxide polymerization. Another similar catalyst which was aged for several months was also catalytically active.

Compounds of the type  $RSZnR$  are expected to be inactive for polymerizing propylene oxide, by analogy<sup>7</sup> with their oxygen analogs. The reaction product of di-*tert*-butyl disulfide and diethylzinc at the molar ratio of 1:1 (Table VIII), which is expected to have a structure of the

TABLE III

Effect of Water/Diethylzinc Molar Ratio on Polymer Yield and Properties in Polymerization of Propylene Oxide with Water-Diethylzinc Catalyst Prepared *in Situ*<sup>a</sup>

Water/diethylzinc molar ratio <sup>b</sup>	Polymer yield, %	Inherent viscosity, dl./g.	Acetone-insoluble, %
0.21	5.6	6.3	—
0.42	24.8	9.4	71
0.63	79.4	5.8	79
0.74	97.0	5.9	—
0.80	94.5	—	—
0.88	98.0	9.3	85
0.98	99.0	6.75	59
1.05	71.0	6.7	57
1.10	27.0	6.3	—
1.14	22.5	6.15	18
1.20	14.9	5.1	17

<sup>a</sup> Conditions; 40 ml. benzene, 40 ml. monomer, 2.0 ml. diethylzinc (2.23*M* in benzene); 50°C., 18.5 hr.

<sup>b</sup> 1 ml. water  $\equiv$  55.52 mmole.

TABLE IV

Effect of Hydrogen Peroxide/Diethylzinc Molar Ratio on Polymer Yield and Properties in Polymerization of Propylene Oxide with Hydrogen Peroxide-Diethylzinc Catalyst Prepared *in Situ*<sup>a</sup>

Hydrogen peroxide/diethylzinc molar ratio <sup>b</sup>	Polymer yield, %	Inherent viscosity, dl./g.	Acetone-insoluble, %
0	1.0	2.7	—
0.185	4.2	1.9	—
0.37	7.1	6.2	40
0.46	24.4	10.1	60
0.51	35.5	9.8	56
0.555	40.4	7.1	—
0.57	47.0	10.2	71
"	45.5	10.0	—
0.62	37.5	7.3	—
"	35.0	7.7	—
0.67	34.2	7.1	31
0.72	27.4	5.0	36
0.74	21.8	5.2	37
0.83	8.3	4.9	36
0.90	3.2	4.4	—
1.0	1.3	—	—
"	1.4	—	—
1.1	1.5	—	—
1.3	1.3	—	—

<sup>a</sup> Conditions; 40 ml. benzene, 40 ml. monomer, 2.0 ml. diethylzinc (2.23*M* in benzene); 50°C., 18.5 hr.

<sup>b</sup> 1 ml hydrogen peroxide (98%)  $\equiv$  41.3 mmole.

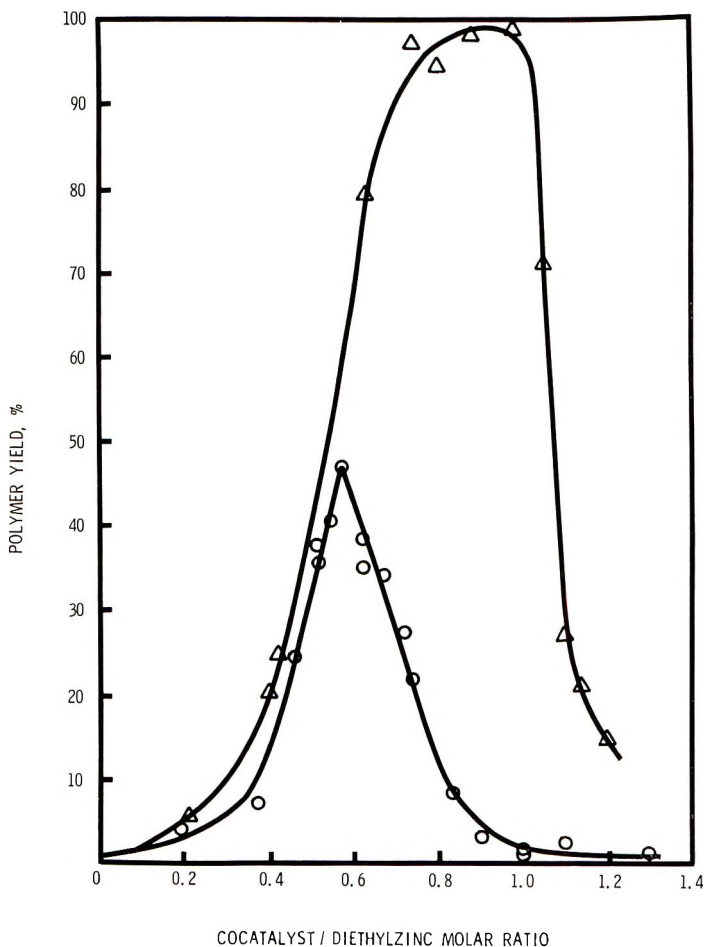


Fig. 3. Effect of cocatalyst/diethylzinc molar ratio on the yield of polymer obtained by polymerization of propylene oxide with (O) *in situ* hydrogen peroxide–diethylzinc catalyst and (Δ) water–diethylzinc catalyst for 18.5 hr. at 50°C. in benzene: 40 ml. benzene, 40 ml. monomer, 4.46 mmole diethylzinc, and varying amounts of cocatalyst.

RSZnR type, was a catalyst of low activity. The data in Table IX show that authentic samples of zinc di(ethyl mercaptide),  $Zn(SC_2H_5)_2$ , either alone or in the presence of added sulfur, and zinc di(phenyl mercaptide),  $Zn(SC_6H_5)_2$ , prepared in our laboratory, are also catalysts of low activity. This might be due to their existence as associated species or to their low solubility. The inactivity of zinc dialkoxides for polymerizing propylene oxide has been interpreted<sup>7</sup> as being due to their existence in associated forms which are stable in the presence of the monomer. In contrast, zinc dialkoxides formed *in situ* by the reaction of diethylzinc and an alcohol in the molar ratio of 1:2 were found<sup>7</sup> to polymerize propylene oxide. An insoluble, white reaction product was obtained when diethylzinc was injected into a solution containing *n*-butyl mercaptan, propylene oxide, and

TABLE V  
Effect of Conversion on Properties of Polymer Obtained in Polymerization of Propylene Oxide with Sulfur-Diethylzinc Catalyst Prepared *in Situ* (Sulfur/Zinc Atomic Ratio = 3.5)<sup>a</sup>

Polymerization time, hr.	Polymer yield, %	Inherent viscosity, dl./g.	Acetone-insoluble, %
0.5	14.2	5.7	26
1	31.0	7.0	33
1.5	43.3	7.8	36
2.0	57.1	7.8	46
3.0	65.3	7.3	45
7.0	94.0	8.8	49

<sup>a</sup> Conditions; 26 ml. benzene solution containing 0.208 g. sulfur, 40 ml. propylene oxide, 1 ml. diethylzinc (1.85*M* in benzene); 50°C.

TABLE VI  
Effect of Catalyst Aging at 25°C. on Yield of Polymer in Polymerization of Propylene Oxide with Preformed Sulfur-Diethylzinc Catalyst (Sulfur/Zinc Atomic Ratio = 3.5)<sup>a</sup>

Aging interval, hr.	Polymer yield, %	Inherent viscosity, dl./g.
0	42	7.0
0.5	52.1	8.0
1	56.4	7.5
19	56.7	10.7

<sup>a</sup> Conditions; 58.5 ml. benzene solution containing 0.208 g. sulfur, 1 ml. diethylzinc (1.85*M* in benzene), 40 ml. propylene oxide; 50°C., 5 hr.

benzene. The molar ratio of the mercaptan to diethylzinc was 2:1 (Table IX). However, the polymerization at 50°C. was homogeneous and the catalyst, presumably  $(C_4H_9S)_2Zn$ , was very mildly active. Based on this assumption, compounds having the structure  $RS_zZnSR$  can have only low catalytic activity when prepared *in situ*. The data in Table VIII suggest that the catalytic activity of the reaction product of diethylzinc and a polysulfide compound may presumably be due to the formation of compounds of the  $RS_zZnR$  type in which the structure of the R group plays an important role. In Figures 1 and 2 it is observed that the catalyst prepared at sulfur/zinc atomic ratio of 2 is reasonably active. On increasing this ratio to 3-3.5, optimum catalytic activity is achieved; it was also observed that the reaction mixtures became more opaque than when the ratio was 2. Compounds of the structures  $RS_zZnSR$  and/or  $RS_zZnS_yR$  which are expected to be formed *in situ* under these conditions presumably contribute to the enhanced activity of the catalysts. The ability of the catalyst prepared at a sulfur/zinc atomic ratio of 4:1 to exhibit catalytic activity even after aging for many months suggests that these structures either do not form associated species to any appreciable extent, or the latter are not stable in the presence of propylene oxide. The reason for the observed decrease in the catalytic activity when the sulfur/zinc atomic ratio



TABLE VII  
 Polymerization of Olefin Oxides and of Olefin Sulfides with Sulfur-Alkylmetal Catalyst System

Expt. no.	Monomer	Vol. monomer, ml.	Solvent	Vol. solvent, ml.	Catalyst variables			Polymerization time, hr.	Polymer yield, % <sup>b</sup>	Inherent viscosity, dl./g.	Acetone insoluble, %	
					Preparation	S/Metal atomic ratio <sup>a</sup>	Merization temp., °C.					
1	Propylene oxide	30	Benzene	30	5 ml., preformed suspension	0.9	3.5	50	3	56.5	9.7	—
2	"	"	n-Heptane	30	"	"	"	"	"	67	9.6	65
3	"	"	Tetrahydrofuran	30	"	"	"	"	"	4.9	52.5	27
4	"	"	Diethyl ether	30	"	"	"	"	"	53.6	10.2	66
5	"	"	Carbon tetrachloride	30	"	"	"	"	"	58	9.3	57
6	"	"	Chlorobenzene	30	"	"	"	"	"	59	8.8	63
7	Ethylene oxide	600	Benzene	200	10 ml., preformed suspension	1.3	4	"	1.3	66	7.0	—
8	1,2-Butene oxide	80	None	—	<i>In situ</i>	3.5	4	"	17	40.4	5.6	—
9	Styrene oxide <sup>d</sup>	600	Benzene	200	Preformed in the entire solvent	17.5	4	"	90	79	3.0	—
10	Propylene sulfide	20	None	—	<i>In situ</i> at -20°C.	0.4	10.6 <sup>e</sup>	-20	8	31	1.7	—
11	1,2-Butene sulfide <sup>f</sup>	20	Benzene	50	<i>In situ</i>	3.5	4	30	67	94	0.8	—
12	Propylene oxide	40	Benzene	40	<i>In situ</i>	3.5	4	50	18	1	<0.1	—
13	Epichlorhydrin	40	Benzene	40	Preformed in the entire solvent	2.1	4	50	16	4	0.05	—
14	Epichlorhydrin	40	None	—	<i>In situ</i>	2	4	50	40	70	0.14	—

<sup>a</sup> Catalysts expts. 1-11 and 13 were prepared with diethylzinc solution in benzene (2.0M), in expt. 12 with dimethylcadmium solution in heptane (1.35M) and in expt. 14 with triisobutylaluminum solution in benzene (1.0M); <sup>b</sup> Polymer yields are not corrected for catalyst residues; <sup>c</sup> 17.6 g. of ethylene oxide in 75 ml. benzene solution; <sup>d</sup> b.p. 54°C./3.8 mm., <sup>e</sup> 1.5304; <sup>f</sup> Calculated for the amount of sulfur added, although it was incompletely soluble in the monomer; <sup>g</sup> b.p. 100.5°C./737 mm., <sup>h</sup> 1.4672.

TABLE VIII  
Polymerization of Propylene Oxide with Sulfur-Bearing Compounds and Diethylzinc<sup>a</sup>

Additive	No. sulfur atoms per molecule of additive	Molar ratio of additive to diethylzinc	S/Zn atomic ratio in catalyst	Polymer yields, %	Inherent viscosity, dl./g.
Di- <i>tert</i> -butyl disulfide	2	1	2	2.4	0.5
“	2	2	4	2.8	1.7
Di- <i>tert</i> -butyl polysulfide	5.5	1	5.5	4.2	0.8
Di- <i>tert</i> -octyl polysulfide	4.6	1	4.6	10	0.16
VA-7 <sup>b</sup>	4.5	1	4.5	21.6	6.35
Sulfur	8	3/8	3	15.6	11.7
None	—	0	0	2.9	0.7
Selenium <sup>c</sup>	—	—	—	25.7	10.4

<sup>a</sup> Preformed catalyst from 60 ml. benzene, 3.0 ml. diethylzinc (1.55*M* in benzene) and sulfur compound as indicated was aged for 60 hr. Subsequent injection of 20 ml. monomer; polymerization at 50°C. for 2 hr.

<sup>b</sup> VA-7 is a product of Thiokol Chemical Company. It is an organic polysulfide, —R—S<sub>*n*</sub>—R—, where R is an aliphatic ether radical and *n*, the sulfur rank, averages 4.5.<sup>6</sup>

<sup>c</sup> Selenium was incompletely soluble in benzene. Atomic ratio of added selenium to zinc was 1:1. Polymerization time was 6 hr.

TABLE IX  
Bulk Polymerization of Propylene Oxide<sup>a</sup>

Expt. no.	Catalyst	Amt. catalyst		Polymer yield, %	Inherent viscosity, dl./g.
		g.	mmole		
1	Zinc di(ethyl mercaptide) <sup>b</sup>	0.3	1.6	1.3	0.3
2	“ “ “	0.6	3.2	1.8	0.3
3	{Zinc di(ethyl mercaptide)	0.3	1.6	1.4	0.3
	{Sulfur	0.1	4.1 <sup>c</sup>		
4	Zinc di(phenyl mercaptide) <sup>d</sup>	0.455	1.6	1.4	0.1
5	“	0.91	3.2	2.24	0.1
6	<i>n</i> -Butyl mercaptan-diethylzinc	<sup>e</sup>	<sup>e</sup>	4.5	—

<sup>a</sup> Conditions; 40 ml. monomer, catalyst as indicated, 50°C., 21 hr.

<sup>b</sup> Prepared by reacting ethyl mercaptan and diethylzinc in benzene solution. Calcd. for C<sub>4</sub>H<sub>10</sub>S<sub>2</sub>Zn; S, 34.17%. Found; S, 33.15%.

<sup>c</sup> Milliatoms of sulfur.

<sup>d</sup> Prepared by reacting thiophenol and zinc oxide according to Verbanc's (8) method.

<sup>e</sup> Monomer, 0.69 ml. *n*-butyl mercaptan, and 1.95 ml. diethylzinc (1.65*M* in benzene) in the order indicated. Mercaptan/diethylzinc molar ratio = 2:1.

exceeds 4 is not clear. The polymerization of propylene oxide with the sulfur-diethylzinc catalyst is expected to be by coordinate polymerization mechanism.

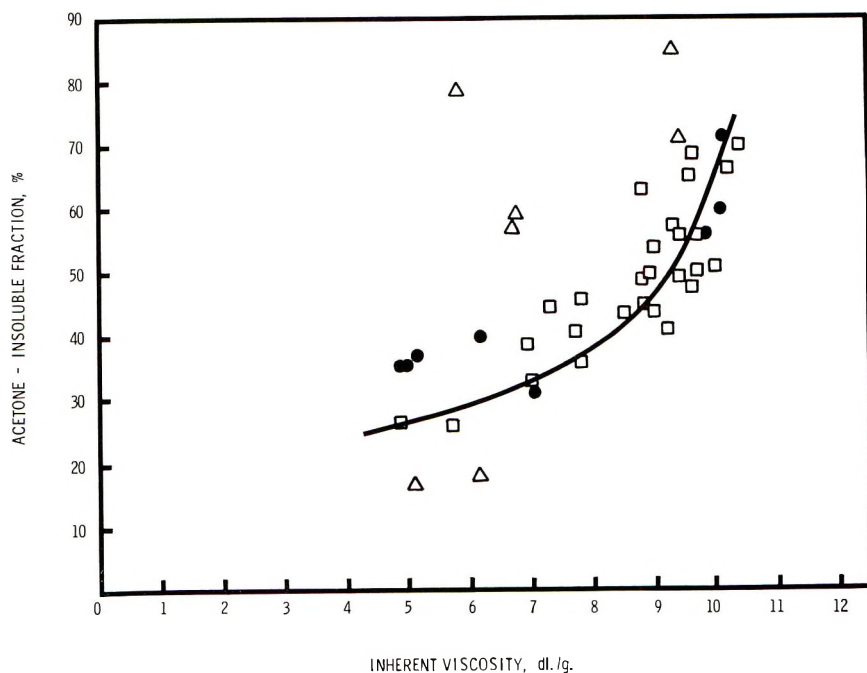


Fig. 4. Relationship between per cent acetone-insoluble fraction of poly(propylene oxide) and inherent viscosity of the original polymer prepared with three polymerization catalysts: ( $\square$ ) S-Et<sub>2</sub>Zn; ( $\bullet$ ) H<sub>2</sub>O<sub>2</sub>-Et<sub>2</sub>Zn; ( $\Delta$ ) H<sub>2</sub>O-Et<sub>2</sub>Zn.

### Solubility of Poly(propylene Oxide) in Acetone

In Figure 4, the various polymers prepared with sulfur-diethylzinc, hydrogen peroxide-diethylzinc, and water-diethylzinc catalyst systems (Tables I-V, VII) are compared by plotting per cent acetone-insoluble fraction against inherent viscosity of the original polymer. The percentage of acetone-insoluble fraction may be taken as an approximate measure of crystallinity of the polymer. The solid line in Figure 4 is drawn for the data points for the polymers prepared with the sulfur-diethylzinc catalysts under a variety of conditions. The data points for the polymers obtained with hydrogen peroxide-diethylzinc catalyst fall around this solid line. However, the data for the polymers prepared with water-diethylzinc catalyst show considerable scatter. Poly(propylene oxide) prepared with sulfur-diethylzinc catalyst (Table VII, expt. 1) was about 15% crystalline by x-ray diffraction; the polymers prepared with water-diethylzinc catalyst at molar ratios of 0.74, 0.98, and 1.1 (Table III) were about 11, 12, and 19% crystalline, respectively; the polymer prepared with hydrogen peroxide-diethylzinc catalyst (molar ratio 0.555, Table IV) showed a corresponding value in range of 20%. Thus, these polymers are fairly similar in the extent of their crystallinity. The data in Figure 4 demonstrate that an increase in the inherent viscosity or molecular weight of the polymers increases the proportion of the acetone-insoluble material. Thus, the molec-

ular weight of the polymer, in conjunction with its isotacticity, is an important factor in determining the amount of crystallinity. Irregularities in the polymer such as head-to-head structures<sup>9</sup> may adversely affect the crystallinity.

### Vulcanizable Copolymer of Propylene Oxide and Allyl Glycidyl Ether

A copolymer was prepared from propylene oxide (160 ml.) and allyl glycidyl ether (8 ml.) by injecting the monomer mixture (molar charge ratio 97.23:2.77) into a suspension of 1.776 g. sulfur and 12 ml. diethylzinc (1.85*M* solution in benzene) (S/Zn atomic ratio = 3:1) in 500 ml. benzene. Polymerization for 21 hr. at 50°C. yielded 74 g. (51%) of a product having an inherent viscosity of 3.8 dl./g. The copolymer was compounded according to the recipe given in Table X and cured for 90 minutes at 143°C. in a press. The vulcanizate exhibited a tensile strength of 1935 psi at 725% elongation at break (Table XI). These stress-strain properties are similar

TABLE X

Vulcanization Recipe for Copolymer of Propylene Oxide and Allyl Glycidyl Ether

	Parts by weight
Rubber	100
Zinc oxide	5
Stearic acid	3
Sulfur	2
Tetramethylthiuram disulfide	1
Tellurium diethyldithiocarbamate	0.5
Cure; 90 min. at 143°C.	

TABLE XI

Stress-Strain Properties and Swelling Data for Propylene Oxide-Allyl Glycidyl Ether Copolymer Vulcanizate<sup>a</sup>

Property	
Tensile strength, psi	1935
Elongation at break, %	725
300% modulus, psi	300
Swelling ratio <sup>b</sup>	8.95
Solubility in benzene, %	11

<sup>a</sup> Stress-strain properties given as average of two values. Dumbbells, having a narrowed cross section of  $0.1 \times \frac{1}{16}$  in. over a length of 0.9 in., were used for stress-strain measurement on an Instron testing machine. The cross-head speed was 2 in./min.

<sup>b</sup> Grams of benzene solvent per gram of the vulcanizate at 25°C.

to those reported for the vulcanizate of a similar copolymer.<sup>10</sup> Our vulcanizate had an inflection temperature of -57°C. in the low-temperature torsion flex test (ASTM D1053-54T) and an estimated<sup>11</sup> glass transformation temperature of -72°C. Other low temperature data were as follows:  $T_2 = -48^\circ\text{C}$ .,  $T_5 = -55^\circ\text{C}$ .,  $T_{10} = -57^\circ\text{C}$ .,  $T_{100} = -60.5^\circ\text{C}$ .

Allen et al.<sup>12</sup> have reported dilatometric  $T_g$  values of  $-72$  to  $-75^\circ\text{C}$ . for high molecular weight polymers of propylene oxide.

The author wishes to express his thanks to Mr. R. S. Thudium for crystallinity measurements and to Mr. J. Hionides for technical assistance.

### References

1. J. Furukawa and T. Saegusa, *Polymerization of Aldehydes and Oxides*, Interscience, New York, 1963.
2. J. Furukawa, T. Tsuruta, R. Sakata, T. Saegusa, and A. Kawasaki, *Makromol. Chem.*, **32**, 90 (1959); *J. Polymer Sci.*, **36**, 541 (1959).
3. R. Sakata, T. Tsuruta, T. Saegusa, and J. Furukawa, *Makromol. Chem.*, **40**, 64 (1960).
4. E. J. Vandenberg, *J. Polymer Sci.*, **47**, 486 (1960).
5. K. T. Garty, T. B. Gibb, Jr., and R. A. Clendinnings, *J. Polymer Sci. A*, **1**, 85 (1963).
6. K. R. Cranker and V. H. Perrine, *Rubber Age*, **81**, 113 (1957).
7. M. Ishimori and T. Tsuruta, *Makromol. Chem.*, **64**, 190 (1963), and discussion of the paper.
8. J. J. Verbanc, U. S. Patent 2,413,531 (Dec. 31, 1946).
9. C. C. Price and R. Spector, *J. Am. Chem. Soc.*, **87**, 2070 (1965).
10. E. W. Madge, *Chem. Ind. (London)*, **1962**, 1806.
11. G. S. Trick, *J. Appl. Polymer Sci.*, **3**, 253 (1960).
12. G. Allen, C. Booth, M. N. Jones, D. J. Marks, and W. D. Taylor, *Polymer*, **5**, 547 (1964).

### Résumé

Deux systèmes catalyseurs nouveaux à base de soufre et diéthylzinc et de 98% de peroxyde hydrogène-diéthylzinc, ont été étudiés pour polymériser l'oxyde de propylène. Le système catalyseur soufre-diéthylzinc a un large domaine de rapport soufre atome de zinc pour polymériser l'oxyde de propylène de façon hétérogène en vue d'obtenir des matériaux de poids moléculaires élevés avec rendements élevés. Le polymère le plus élevé a été obtenu avec le rapport soufre/atome de zinc = 3-3.5. De même qu'avec un système eau-zinc diéthyl le système peroxyde d'hydrogène-diéthylzinc a un domaine étroit de rapport molaire peroxyde d'hydrogène/diéthylzinc au voisinage de 0.57 pour fournir un rendement optimum de polymère. Des mesures de cristallinité par diffraction aux rayons-X pour quelques polymères préparés par ces trois systèmes catalytiques ont montrés qu'ils sont sensiblement équivalents en ce qui concerne la cristallinité. Un diagramme du pourcentage du polymère insoluble dans l'acétone en fonction de la viscosité inhérente du polymère original montre également que les polymères préparés avec le système catalyseur soufre/diéthylzinc et peroxyde hydrogène-diéthylzinc ont des quantités semblables de cristallinité. Les résultats sont donnés en ce qui concerne la polymérisabilité de l'oxyde d'éthylène, de l'oxyde de 1,2-butène, de l'oxyde de styrène, du sulfure de propylène, du sulfure de 1,2-butène, de même que des résultats concernant un copolymère vulcanisable d'oxyde de propylènes et d'éther glycidylallylique utilisant le système catalyseur soufre/diéthylzinc. Les polymères au départ de sulfure d'oléfine ont des viscosités inhérentes plus basses que les polymères provenant d'oxydes d'oléfine correspondants. Par vieillissement du catalyseur soufre/diéthylzinc (S/Zn rapport atomique = 3.5) on améliore le rendement en oxyde de polypropylène. Le rendement était essentiellement inchangé lorsque l'oxyde de polypropylène était polymérisé dans 6 solvants différents. La formation de  $\text{C}_2\text{H}_5\text{S}_2\text{ZnSC}_2\text{H}_5$  et de  $\text{C}_2\text{H}_5\text{S}_2\text{ZnS}_y\text{C}_2\text{H}_5$  où  $x$  et  $y$  sont des nombres entiers entre 2 et 8 et éventuellement  $\text{C}_2\text{H}_5\text{S}_2\text{ZnC}_2\text{H}_5$  comme espèce catalytique active est postulée au cours de la réaction entre le soufre et le diéthylzinc.



### Zusammenfassung

Zwei neue Katalysatorsysteme, Schwefel-Diäthylzink und 98%iges Wasserstoffperoxyd-diäthylzink wurden auf ihre Anwendbarkeit für die Polymerisation von Propylenoxyd untersucht. Das Schwefel-Diäthylzink-Katalysatorsystem besitzt einen breiten Bereich für das Atomverhältnis Schwefel:Zink bei der heterogenen Polymerisation von Propylenoxyd zu hochmolekularen Produkten in hoher Ausbeute. Die höchste Polymerausbeute wird beim Atomverhältnis Schwefel:Zink von 3–3,5 erhalten. So wie das Wasser-Diäthylzink-System besitzt auch das Wasserstoffperoxyd-Diäthylzink-System einen engen Bereich des Molverhältnisses Wasserstoffperoxyd:Diäthylzink in der Nähe von 0,57 für eine optimale Polymerausbeute. Kristallinitätsmessungen durch Röntgenbeugung an einigen mit diesen drei Katalysatorsystemen dargestellten Polymeren zeigten, dass sie in bezug auf das Kristallinitätsausmass ziemlich ähnlich sind. Ein Digramm des Prozentgehalts an unlöslichen Polymeren gegen die Viskositätszahl des ursprünglichen Polymeren zeigte ebenfalls, dass die mit Schwefel-Diäthylzink- und Wasserstoffperoxyd-Diäthylzink-Katalysatorsystemen dargestellten Polymeren einen ähnlichen Kristallinitätsanteil aufweisen. Ergebnisse für die Polymerisierbarkeit von Äthylenoxyd, 1,2-Butenoxyd, Styroloxyd, Propylensulfid, 1,2-Butensulfid und einem vulkanisierbaren Copolymeren von Propylenoxyd und Allylglycidyläther mit dem Schwefel-Diäthylzink-Katalysatorsystem werden mitgeteilt. Die Polymeren der Olefin-sulfide besaßen andere Viskositätszahlen als die Polymeren aus den entsprechenden Olefinoxyden. Eine Alterung des Schwefel-Diäthylzink-Katalysators (S/Zn-Atomverhältnis = 3,5) verbesserte die Ausbeute an Poly(propylenoxyd). Bei der Polymerisation in sechs verschiedenen Lösungsmitteln blieb die Ausbeute im wesentlichen unverändert. Es wird die Bildung von  $C_2H_6S_xZnSC_2H_5$  und  $C_2H_6S_xZnS_yC_2H_6$  ( $x$  und  $y$  sind ganze Zahlen zwischen 2 und 8) und möglicherweise  $C_2H_6S_xZnC_2H_6$  als katalytisch wirksame Spezies bei der Reaktion zwischen Schwefel und Diäthylzink angenommen.

Received September 17, 1965

Revised October 12, 1965

Prod. No. 4927A



## Graft Polymerization Kinetics of Acrylamide Initiated by Ceric Nitrate-Dextran Redox Systems

R. A. WALLACE and D. G. YOUNG, \* *Department of Chemical Engineering  
University of California, Berkeley, California*

### Synopsis

The kinetics of the graft polymerization of acrylamide initiated by ceric nitrate-dextran polymeric redox systems was studied primarily at 25°C. Following an initial period of relatively fast reaction, the rate of polymerization is first-order with respect to the concentrations of monomer and dextran and independent of the ceric ion concentration. The equilibrium constant for ceric ion-dextran complexation  $K$  is  $3.0 \pm 1.6$  l./mole, the specific rate of dissociation of the complex,  $k_d$ , is  $3.0 \pm 1.2 \times 10^{-4}$  sec.<sup>-1</sup>, and the ratio of polymerization rate constants,  $k_p/k_t$ , is  $0.44 \pm 0.15$ . The number-average degree of polymerization is directly proportional to the ratio of the initial concentrations of monomer and ceric ion and increases exponentially with increasing extent of conversion. The initial rapid rate of polymerization is accounted for by the high reactivity of ceric ion with *cis*-glycol groups on the ends of the dextran chains. The polymerization in the slower period that follows is initiated by the breakdown of coordination complexes of ceric ions with secondary alcohols on the dextran chain and terminated by redox reaction with uncomplexed ceric ions.

A number of studies have been made of the mechanism and kinetics of polymerizations initiated by ceric ion-alcohol redox systems.<sup>1-5</sup> Only a limited amount of kinetic information, however, has been obtained by use of polymeric reducing agents. Richards<sup>6</sup> has shown that a true graft copolymer of acrylonitrile and cellulose is formed by using ceric ion-initiation. In addition, Fumio<sup>7</sup> studied the overall polymerization reactions of acrylonitrile and methyl methacrylate initiated by ceric nitrate-cellulose redox systems. No individual rate constants were determined in either of these studies.

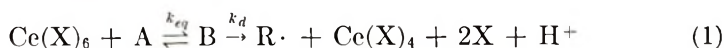
To bridge the kinetic gap between the investigations of Mino et al.<sup>1-4</sup> and the applied studies of Richards and Fumio, a kinetic study of a homogeneous vinyl polymerization with a water-soluble polymeric reducing agent was pursued. Dextran was chosen as the polymeric reducing agent because of its solubility in water and because, like cellulose, it is composed of glucoside units. Acrylamide was used as the monomer, since both acrylamide and polyacrylamide are soluble in water, and also because it has been shown that acrylamide does not react appreciably with ceric nitrate<sup>2</sup> as does acrylonitrile.

\* Present address: Esso Research and Engineering Co., Linden, N. J.

In this paper the dependencies of the rate of polymerization on the concentrations of ceric ion, acrylamide, and dextran are given. The equilibrium constant for the ceric ion-dextran complexation is estimated, as well as the rate constant for complex dissociation and the ratio of rate constants for chain polymerization and termination.

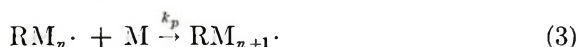
### THEORY

It has been shown that ceric ions complex reversibly with alcohols and glycols and that the dissociation of the complexes is the rate-determining step.<sup>8-10</sup> During the oxidation-reduction, transient free radicals are produced which are capable of initiating vinyl polymerization. The initiation reaction can be written as follows:



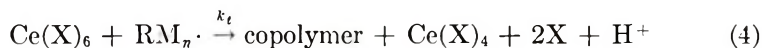
where X is either OH<sup>-</sup> or NO<sub>3</sub><sup>-</sup> ions or water molecules, A represents a hydroxyl or glycol group, B is the complex, and R· is the free radical formed.

Addition of one monomer molecule to the free radical begins the polymerization as shown by eqs. (2) and (3).



No reaction need be written to express initiation of homopolymerization because it has been shown<sup>6</sup> to be negligible for acrylamide under the reaction conditions used.

Termination has been shown<sup>11,12</sup> to be predominantly by redox reaction of the polymeric radical with ceric ion. Thus, the termination step can be written as



It is desirable to relate the rate of polymerization and the chain length of the graft polymer to the variables and parameters which describe the system. By means of careful consideration of the equilibrium relationship for eq. (1),

$$K \equiv \frac{K_{eq}}{[\text{X}]^2} = \frac{[\text{B}]}{[\text{Ce}(\text{X})_6][\text{A}]} \quad (5)$$

and by a ceric ion material balance,

$$[\text{Ce}(\text{X})_6] = [\text{Ce}^{\text{IV}}]_0 - [\text{B}] - \int_0^t - (d[\text{Ce}^{\text{IV}}]/dt)dt \quad (6)$$

the rate of initiation becomes

$$R_i = \frac{d[\text{RM}\cdot]}{dt} = \frac{k_d K [\text{A}]}{1 + K[\text{A}]} [\text{Ce}^{\text{IV}}] \quad (7)$$

The rate expression for the termination step (4) is

$$R_t = \frac{k_t}{1 + K[A]} [\text{RM}_n \cdot] [\text{Ce}^{\text{IV}}] \quad (8)$$

The parameters  $K$ ,  $k_d$ , and  $k_p/k_t$ , which describe the kinetics of the system, can be determined experimentally. The total disappearance of ceric ion is equal to that consumed in the initiation step plus that consumed in the termination step. The assumption is also made that  $1/2$  of the ceric ion is consumed in the initiation step and  $1/2$  in the termination step. Thus,

$$-\frac{d[\text{Ce}^{\text{IV}}]}{2dt} k_d[\text{B}] = \frac{k_d K [\text{A}]}{1 + K[\text{A}]} [\text{Ce}^{\text{IV}}] \quad (9)$$

By rearranging and integrating eq. (9), and assuming that  $[\text{A}]$  is constant, it is seen that

$$-(d \ln [\text{Ce}^{\text{IV}}]/dt)^{-1} = (1/2k_d K)(1/[\text{A}] + K) \quad (10)$$

The values of  $k_d$  and  $K$  can then be determined from the slope and intercept of this latter relationship.

In a similar fashion, again assuming  $[\text{A}]$  to be constant, differentiation with respect to time yields the relationship

$$-d \ln [\text{M}]/dt = (k_p k_d K/k_t) [\text{A}] \quad (11)$$

Thus, if  $k_d$  and  $K$  are obtained as shown previously, the ratio  $k_p/k_t$  can be calculated.

The dependence of the degree of polymerization on the system variables and parameters is given by

$$\bar{P}_n = (k_p/k_t)(1 + K[\text{A}]) [\text{M}]/[\text{Ce}^{\text{IV}}] \quad (12)$$

The dependence of the ratio  $[\text{M}]/[\text{Ce}^{\text{IV}}]$  on the extent of conversion  $x$  is given by

$$[\text{M}]/[\text{Ce}^{\text{IV}}] = ([\text{M}]_0/[\text{Ce}^{\text{IV}}]_0)(1 - x)^{1 - 1/2k_t/k_p(1 + K[\text{A}])} \quad (13)$$

Employing the definition of the overall degree of polymerization  $\bar{P}_n$  given by Bovey et al.<sup>13</sup> that

$$\bar{P}_n = 1/N \int_0^N \bar{P}_n dN \quad (14)$$

where  $N$  is the total number of chains, it is easily shown<sup>14</sup> that

$$\bar{P}_n = 2 \frac{[\text{M}]_0}{[\text{Ce}^{\text{IV}}]_0} \frac{x}{1 - (1 - x) \exp \{2k_t/k_p(1 + K[\text{A}])\}} \quad (15)$$

This result differs from that given by Bovey for emulsion polymerization by a factor of 2 and also the factor  $1/(1 + K[\text{A}])$  in the exponent.

The simple form of eq. (15) is applicable only when a single type of reducing group is present, and  $[\text{A}]$  is relatively large so that it is essentially constant throughout the reaction. It is notable, however, that changing

the reducing agent affects  $\bar{P}_n$  only in that the factor  $1/(1 + K[A])$  would change. For large values of  $[A]$ , this factor becomes significant.

The frequency of grafting of polymer chains onto a substrate is a useful property for characterizing a graft copolymer. This property can easily be calculated for a polyacrylamide-dextran copolymer if the length of the polyacrylamide chains and the nitrogen content of the copolymer are known. If  $n$  is the per cent of nitrogen in a copolymer, then

$$\frac{0.0507n}{1 - 0.0507n} = \frac{\text{g. polyacrylamide}}{\text{g. dextran}} \quad (16)$$

The number-average molecular weights of both the polyacrylamide graft  $\bar{M}_{nAc}$  and the dextran substrate  $\bar{M}_{nD}$  are known. The weight-average molecular weight of the dextran  $M_{wD}$  can be determined by viscosity measurements. To convert this  $\bar{M}_{nD}$ , the relationship for clinical dextran which was published by Ciferri and Daune<sup>15</sup> should be used. On applying these factors in eq. (16), it is found that

$$\frac{0.0507n}{1 - 0.0507n} \left( \frac{\bar{M}_{nD}}{\bar{M}_{nAc}} \right) = \frac{\text{polyacrylamide chains}}{\text{substrate dextran chain}} \quad (17)$$

## EXPERIMENTAL

### Chemicals

Acrylamide (Matheson, Coleman & Bell) was sublimed at 60°C. under a reduced pressure of 0.05 mm. Hg. Clinical dextran was obtained from Cutter Laboratories. The ceric ammonium nitrate (reagent grade, G. Frederick Smith Chemical) was dissolved in 0.5*M* nitric acid, and the stock solution, 0.0625*M* in ceric nitrate, was used to prepare the polymerization solutions.

### Determination of Total Ceric Ion Concentrations

The concentrations of total ceric ion in the reactions were determined volumetrically with ferrous sulfate, ferrous *o*-phenanthroline (ferroin) being used as the indicator. An aliquot of the solution was removed at various time intervals and the unreacted ceric ion was quenched in an excess of 0.0025*N* standard ferrous sulfate. The volume of the aliquot was determined by weighing the container of the ferrous quench immediately before and after adding the sample. By using a micropipet, 50  $\mu$ l. of 0.025*M* ferroin solution was added. The excess ferrous ion was then titrated with a 0.0025*N* standard ceric sulfate solution. A correction was made for the ferrous in the ferroin solution. The ceric solution was standardized by using arsenious oxide catalyzed by a few drops of 0.01*N* osmium tetroxide.<sup>16</sup> Ferrous *o*-phenanthroline was also used as the indicator for the standardization. The maximum error in a ceric ion concentration determination was estimated to be 6%. Ceric ion concentration data for duplicate runs differed by less than 3%.

### Iodometric Determination of Acrylamide Concentrations

The procedure used for the acrylamide concentration determinations was similar to that used by Mino.<sup>2</sup> The same sample which had been quenched in excess ferrous sulfate and titrated with ceric sulfate was flushed into a 500-ml. Erlenmeyer flask containing 15 ml. of 0.250*N* bromate solution (6.960 g. of  $\text{KBrO}_3$  and 30 g. of  $\text{KBr}$  per liter). After adding the sample, the flask was closed with a male ground-glass joint to which was attached a stopcock. The flask and its contents were then cooled in an ice bath and 10 ml. of 2*N* sulfuric acid sucked into it. The flask was placed in a dark place, and the contents were allowed to react for 30 min. with frequent shaking. Once again the flask was cooled and 15 ml. of a 20% solution of potassium iodide added. The free iodine was then titrated to a starch end point by using standard thiosulfate solution.

### Polymerization Procedure

A stock solution of acrylamide was placed in a 100-ml. cone-shaped reaction vessel which had three necks. Normally, a 23-ml. aliquot of the acrylamide solution was used. A 25-ml. aliquot of a stock dextran solution was then added. Depending on the variable being investigated, the concentrations of the above two stock solutions were adjusted accordingly. The acrylamide solution also contained sodium nitrate for the purpose of maintaining the nitrate ion concentration constant at 0.10*M* regardless of the concentration of ceric ammonium nitrate or nitric acid.

The 48 ml. of acrylamide and dextran solution was then frozen, evacuated to 0.02 mm. pressure, and thawed to remove dissolved oxygen. This procedure was repeated. The vessel was pressurized to 2 psig with prepurified nitrogen, and a true-bore stirrer was lowered into a constant-temperature bath. Both solutions were allowed to equilibrate for 30 min. The positive pressure of 2 psig of nitrogen maintained in both vessels aided in removing samples with hypodermic needles, and ensured that no air would enter the vessels.

After the equilibration time was complete, a 2-ml. portion of the stock ceric ammonium nitrate solution was injected by a hypodermic needle, and the timer was started. Samples were withdrawn with hypodermic needles at various times, quenched in standard ferrous solution and analyzed for ceric ion and monomer concentrations.

After all kinetic samples had been removed, the remaining reaction mixture was allowed to continue reacting for a total reaction time of about 3 hr. At that time, the remaining solution was poured into methanol and the copolymer product was precipitated. This precipitate was washed with methanol and acetone, filtered, and vacuum-dried at 40°C.

### Hydrolysis of Dextran Substrate by Acid

Analysis of the copolymer product required hydrolysis of the dextran substrate to allow molecular weight determinations of the grafted poly-



acrylamide chains. The hydrolysis conditions used were the same as used by Shen.<sup>17</sup> A copolymer product was dissolved in water. The solution was made 2*N* in H<sub>2</sub>SO<sub>4</sub> and heated at 75°C. with constant stirring for 48 hr. These hydrolysis conditions were shown by Shen to be adequate to hydrolyze all the dextran. Stronger acid conditions would degrade the dextran, and milder acid conditions require prohibitive amounts of time for hydrolysis.

## RESULTS AND DISCUSSION

The linear dependence of  $R_p$  on monomer concentration is illustrated in Figure 1 for reaction times of 30, 40, and 60 min. For reaction times less than 30 min.,  $R_p$  was found to be significantly higher and exponentially dependent on monomer concentration. Following this period of rapid reaction,  $\ln [M]$  becomes a linear function of time. Both the ceric ion concentration profiles (Fig. 2) and the monomer concentration profiles (Fig. 3) for this system show similar behavior as observed by Mino. For a dextran concentration of 0.0181*M*, the fast initial reaction is barely discernible, and it lasts for only about 10 min. For a dextran concentration of 0.0976*M*,

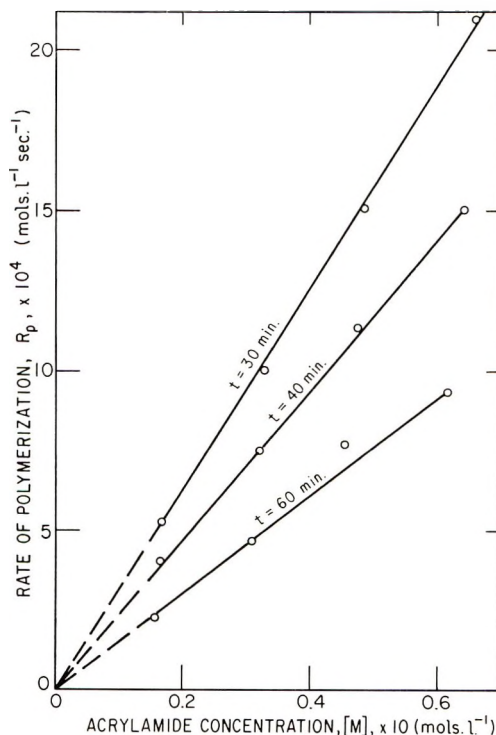


Fig. 1. Linear dependence of instantaneous rate of polymerization on acrylamide concentration. Temperature = 30°C.; pH = 1.7; [NO<sub>3</sub><sup>-</sup>] = 0.10 *M*; [Ce<sup>IV</sup>]<sub>0</sub> = 0.0022 *M*; [A]<sub>0</sub> = 0.061 *M*.



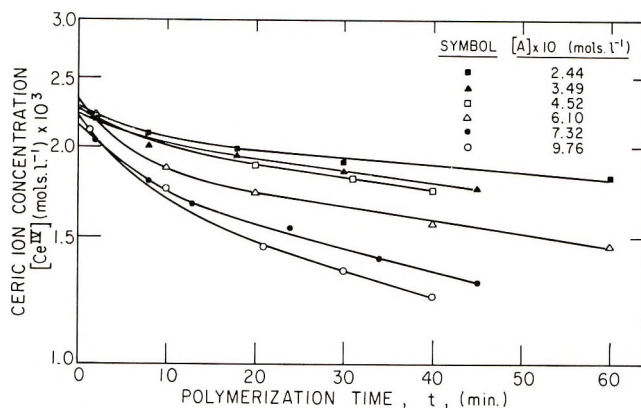


Fig. 2. Ceric ion concentration histories for different dextran concentrations (semilog coordinates). Temperature = 25°C.; pH = 1.7;  $[\text{NO}_3^-] = 0.10M$ ;  $[\text{M}]_0 = 0.60M$ .

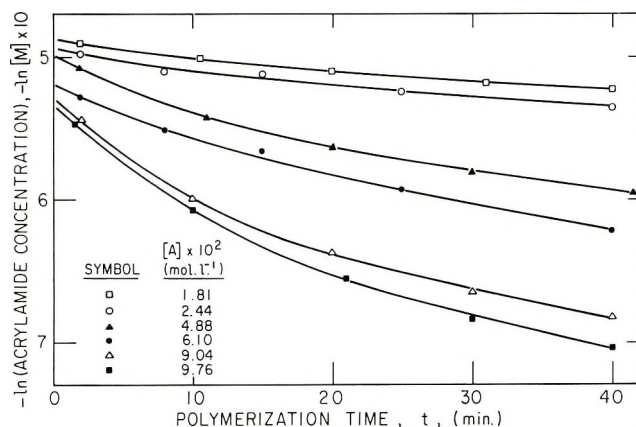


Fig. 3. Acrylamide concentration histories for different dextran concentrations. Temperature = 25°C.; pH = 1.7;  $[\text{NO}_3^-] = 0.10M$ ;  $[\text{Ce}^{\text{IV}}]_0 = 0.0022M$ .

however, the fast initial reaction is pronounced, and it lasts for about 25 min. The proposed rate expression is applicable for reaction times greater than 30 min. for the ranges of concentrations of dextran, ceric ions, and monomer used.

The initial fast reaction observed is accounted for by the high reactivity of ceric ion with *cis*-glycol groups on the ends of the dextran chains. Calculation of the concentration of *cis*-glycols present in clinical dextran, based on the number of moles of ceric ion consumed in the period of relatively fast reaction, shows that about 0.5% of the glucose units contain *cis*-glycols. This explanation is buttressed by Mino's work<sup>3</sup> on the reactivity of ceric ion with poly(vinyl alcohol) containing various amounts of glycol and secondary alcohol groups. Mino found that glycols exhibit a much higher reactivity with ceric ion than do secondary alcohols. This be-

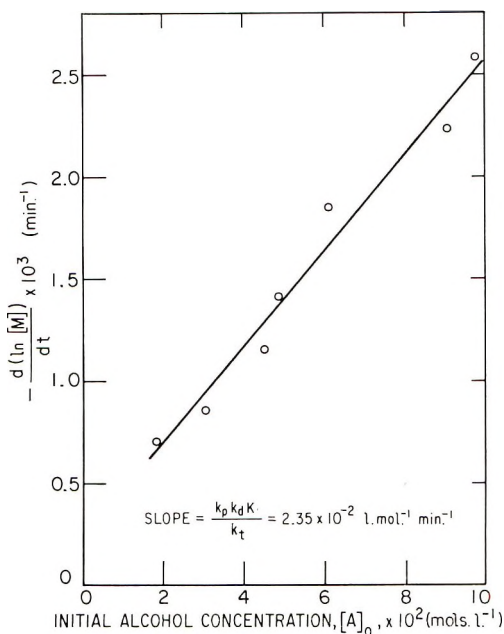


Fig. 4. Graphical determination of the ratio of rate and equilibrium constants  $k_p k_d K/k_t$ . Temperature = 25°C.; pH = 1.7;  $[\text{NO}_3^-] = 0.10M$ ;  $[\text{Ce}^{\text{IV}}]_0 = 0.0022M$ ;  $[\text{M}]_0 = 0.60M$ .

havior caused an initial fast reaction followed by a much slower reaction after all the glycol groups had reacted. The polymerization rate equation was derived assuming that  $R_p$  is a linear function of  $[\text{A}]$ . If this linear relationship is valid, plots of  $\ln [\text{A}]$  versus  $t$  for different values of  $[\text{A}]$  have slopes of  $(k_p k_d K/k_t) [\text{A}]$ . Figure 4 represents the values of these slopes obtained for a range of the  $[\text{A}]$  of 0.018–0.098M. The linear relationship shown confirms the first-order dependence of  $R_p$  on the  $[\text{A}]$ .

Experiments at three different ceric ion concentrations confirmed the predicted independence of the rate of polymerization on ceric ion concentration. Table I gives the results of these experiments evaluated at reaction times of 0, 20, and 30 min.

TABLE I  
Instantaneous Rates of Acrylamide Polymerization at  
Different Initial Ceric Ion Concentrations<sup>a</sup>

$[\text{Ce}^{\text{IV}}]_0 \times 10^3$ , mole/l.	$R_p \times 10^3$ , l./mole-min.		
	Initial	20 min.	30 min.
2.2	6.2	2.20	1.50
1.0	7.4	2.47	1.56
0.4	6.8	2.27	1.43

<sup>a</sup> Conditions:  $[\text{NO}_3^-] = 0.10M$ ,  $[\text{H}^+] = 0.02M$ ,  $T = 30.0^\circ\text{C}$ .

Figure 5 represents the ceric concentration data as a function of dextran concentration. The values of  $d(\ln [\text{Ce}^{\text{IV}}])/dt$  used to obtain the ordinate values in Figure 5 were directly calculated from the slopes of the linear plots of  $\ln [\text{Ce}^{\text{IV}}]$  versus  $t$  for times greater than 30 min.

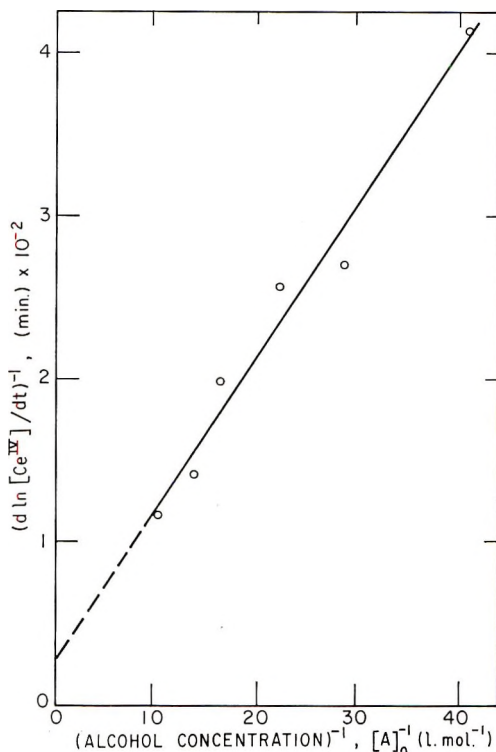


Fig. 5. Determination of  $K$  and  $k_d$  for the complex of ceric ion and dextran. Temperature = 25°C.;  $[\text{NO}_3^-] = 0.10$  mole/l.; pH = 1.7;  $[\text{Ce}^{\text{IV}}]_0 = 0.0022M$ ;  $[\text{M}]_0 = 0.60M$ .

From the slope and intercept of Figure 4, a value of the equilibrium constant for complex formation and also a value for the rate constant for dissociation of the complex at 25°C. are obtained:

$$K = 3.0 \pm 1.6 \text{ l./mole} \quad \text{and} \quad k_d = 3.0 \pm 1.2 \times 10^{-4} \text{ sec.}^{-1}$$

The slope of the line in Figure 4 has been shown to be the ratio of constants  $k_p k_d K / k_t$ . On using the slope of Figure 5, since it has been shown to be  $1/2k_d K$ , the ratio  $k_p / k_t$  is found to be  $0.44 \pm 0.15$  at 25°C.

In comparing the values of the equilibrium and rate constants obtained in this work with those obtained by Mino,<sup>2</sup> inspection of Mino's kinetic development shows that the  $1 + K[A]$  factor does not appear in his reported rate equations. This occurred because Mino considered the rate of termination equal to  $k_t[\text{RM}_n \cdot][\text{Ce}^{\text{IV}}]$  rather than  $k_t[\text{RM}_n \cdot][\text{Ce}(\text{X})_6]$ . Individual rate constants, therefore, could not be directly computed from his polymerization data.

Two values of  $K$  were estimated, however, on the basis of Mino's  $\bar{M}_n$  data. A value of  $K = 1.5$  l./mole best predicted  $\bar{M}_n$  at high conversions, and a value of  $K = 0.5$  l./mole best predicted  $\bar{M}_n$  at low conversions. Thus, a value of  $K = \pm 0.5$  l./mole was used to estimate rate constants from Mino's polymerization data. The values determined at 25°C. are  $k_d = (1.2 \pm 0.7) \times 10^{-3}$  sec.<sup>-1</sup> and  $k_p/k_t = 0.29 \pm 0.03$ . These values cannot be compared directly with the rate constants determined in this work because the equilibrium, dissociation, and termination steps, and therefore  $K$ ,  $k_d$ , and  $k_t$  are strongly dependent on  $[\text{NO}_3^-]$  and  $[\text{H}^+]$ .

The value of  $k_d K$  estimated in these experiments at 25°C. was  $9.0 \times 10^{-4}$  l./mole-sec. Mino's value of  $1.2 \times 10^{-3}$  l./mole-sec. is 33% higher and would be expected to be even higher for the conditions used in these experiments. This difference is understandable, since a much smaller and more mobile molecule (3-chloro-1-propanol) was used in Mino's experiments compared with the dextran used in these experiments.

The ratio  $k_p/k_t$  should be the same for both systems at given  $[\text{NO}_3^-]$  and  $[\text{H}^+]$  values. Although the value found from Mino's data is 34% lower than the value of 0.44 found in this study, the discrepancy is explained above in light of the higher  $[\text{H}^+]$  used in Mino's experiments.

Viscosity measurements were made on a typical copolymer of polyacrylamide and dextran formed in reaction time of 195 min. at 25°C. at initial reactant concentrations of  $[\text{Ce}^{\text{IV}}]_0 = 0.0022M$  and  $[\text{M}]_0 = 0.58M$ . The intrinsic viscosity of the copolymer solution was determined to be  $25.6 \pm 0.4$  cc./g. at 25°C., while that for a comparable dextran solution was  $22.8 \pm 0.4$  cc./g. It was concluded that a chemically bonded graft polymer was formed, as indicated by the 12% increase in intrinsic viscosity of the copolymer solution.

Calculations of  $\bar{p}_n$  and  $\bar{P}_n$  were made for a typical polymerization by using eqs. (12) and (15). The data and results are given in Table II.

TABLE II  
Calculated Instantaneous and Average Degrees of Polymerization  
of Polyacrylamide Graft as a Function of Extent of Conversion<sup>a</sup>

Time, min.	$x$	$\bar{p}_n \times 10^{-2}$	$\bar{P}_n \times 10^{-2}$
0+	0+	1.4	2.7
195	0.345	4.8	

<sup>a</sup> Conditions:  $[\text{Ce}^{\text{IV}}]_0 = 0.0022M$ ,  $[\text{M}]_0 = 0.58M$ ,  $[\text{A}]_0 = 0.061M$ ,  $2k_t/k_p(1 + K[\text{A}])$ .

Thus, although all kinetic factors of the system, other than concentrations, have been assumed to be constant, the instantaneous degree of polymerization would be expected to increase 240% in a reaction time of 195 min. The overall degree of polymerization, however, is only 93% higher than the initial instantaneous value of  $\bar{p}_n$ . This calculated increase of the degree of polymerization with increasing time of reaction is attributable solely to an increase with time of the ratio  $[\text{M}]/[\text{Ce}^{\text{IV}}]$ .

In view of the rather strong trends in the degree of polymerization of the grafted chains, experimental verification was considered highly desirable. Upon hydrolysis of the dextran, using the moderate hydrolysis conditions given in the experimental section, a water-insoluble product was formed which contained 7% nitrogen. It was concluded that at least half of the amide groups of the polyacrylamide had also been hydrolyzed, and also a large amount of polyacrylamide crosslinking had taken place under these hydrolysis conditions.

The number-average degree of polymerization was determined to be 270 for the polyacrylamide formed in a reaction time of 195 minutes. The number-average degree of polymerization of the dextran substrate was determined to be 173. Nitrogen analysis of the copolymer showed that it contained 8.1% nitrogen. On converting the above two degrees of polymerization to number-average molecular weights and by using eq. (17), it was found that the frequency of grafting was 1.1 chains of polyacrylamide per chain of dextran.

The authors wish to thank the National Science Foundation and the Sun Oil Company, Marcus Hook, Pennsylvania, for financial assistance.

### References

1. G. Mino and S. Kaizerman, *J. Polymer Sci.*, **31**, 242 (1958).
2. G. Mino, S. Kaizerman, and E. Rasmussen, *J. Polymer Sci.*, **38**, 393 (1959).
3. G. Mino, S. Kaizerman, and E. Rasmussen, *J. Polymer Sci.*, **39**, 523 (1959).
4. G. Mino, S. Kaizerman, and E. Rasmussen, *J. Am. Chem. Soc.*, **81**, 1494 (1959).
5. A. A. Katai, V. K. Kulshrestha and R. H. Marchessault, in *Proceedings of the Fourth Cellulose Conference (J. Polymer Sci. C, 2)*, R. H. Marchessault, Ed., Interscience, New York, 1963, p. 403.
6. G. N. Richards, *J. Appl. Polymer Sci.*, **5**, 539 (1961).
7. I. Fumio, *Kogyo Kagaku Zasshi*, **62**, 213 (1959).
8. F. R. Duke and A. A. Forist, *J. Am. Chem. Soc.*, **71**, 2790 (1949).
9. F. R. Duke and R. F. Bremer, *J. Am. Chem. Soc.*, **73**, 5179 (1951).
10. M. Ardon, *J. Chem. Soc.*, **1957**, 1811.
11. E. Collison and F. S. Dainton, *Nature*, **177**, 1224 (1956).
12. E. Collison, F. S. Dainton, and G. S. McNaughton, *Trans. Faraday Soc.*, **53**, 489 (1957).
13. F. A. Bovey, I. M. Kolthoff, A. L. Medalia, and E. J. Meehan, *Emulsion Polymerization*, Interscience, New York, 1961, p. 139.
14. D. G. Young, M.S. Thesis, University of California, Berkeley, 1964.
15. A. Ciferri and M. Daune, *J. Polymer Sci.*, **27**, 581 (1958).
16. A. I. Vogel, *Quantitative Inorganic Analysis*, 2nd Ed., Longmans, London, 1955, p. 303.
17. K. Shen, Doctoral Thesis, Polytechnic Institute of Brooklyn, 1959.

### Résumé

La cinétique de polymérisation greffée de l'acrylamide initiée par des systèmes rédox à base de nitrate de cérium et de dextrane polymérique a été étudiée au départ à 25°C. Après une période initiale de réaction relativement rapide, la vitesse de polymérisation a été trouvée de premier ordre par rapport à la concentration en monomère et dextrane et indépendante de la concentration en anions cériques. La constante d'équilibre pour la complexation d'ions cériques-dextrane  $K = 3.0 \pm 1.6 \text{ l-mole}^{-1}$ , la vitesse spécifique de dis-



sociation du complexe,  $k_d$ , est  $3.0 \pm 1.2 \times 10^{-4} \text{ sec}^{-1}$ , et le rapport des constantes de vitesse de polymérisation,  $k_p/k_t$ , est  $0.44 \pm 0.15$ . Le degré de polymérisation moyen en nombre est directement proportionnel au rapport des concentrations initiales de monomère et d'ions cériques et croît exponentiellement avec un degré de conversion croissant. La vitesse initiale rapide de polymérisation est due à la haute réactivité des ions cériques avec les groupes *cis*-glycoliques aux extrémités des chaînes de dextrane. La polymérisation dans la période plus lente qui suit est initiée par la rupture des complexes de coordination des ions cériques avec les alcools secondaires le long de la chaîne du dextrane et terminée par la réaction oxydo-réductrice avec les ions cériques non-complexés.

### Zusammenfassung

Die Kinetik der durch Cernitrat-Dextran-Polymerredoxsysteme gestarteten Pfropfpolymerisation von Acrylamid wurde vorwiegend bei 25°C untersucht. Nach einer Anfangsperiode mit verhältnismässig rascher Reaktion erwies sich die Polymerisationsgeschwindigkeit als von erster Ordnung in bezug auf die Monomer- und Dextrankonzentration und als unabhängig von der Cerionenkonzentration. Die Gleichgewichtskonstante für die Komplexbildung Cerion-Dextran  $K$  ist  $3,0 \pm 1,6 \text{ l. Mol}^{-1}$ , die spezifische Dissoziationsgeschwindigkeit des Komplexes  $k_d$ , ist  $(3,0 \pm 1,2) \times 10^{-4} \text{ sec}^{-1}$  und das Verhältnis der Polymerisationsgeschwindigkeitskonstanten  $k_p/k_t$  beträgt  $0,44 \pm 0,15$ . Der Zahlenmittelpolymerisationsgrad ist dem Verhältnis der Anfangskonzentrationen von Monomerem und Cerion direkt proportional und nimmt mit steigendem Umsatz exponentiell zu. Die anfänglich hohe Polymerisationsgeschwindigkeit wird durch die hohe Reaktivität des Cerions mit *cis*-Glycolgruppen am Ende der Dextranketten erklärt. Die Polymerisation in der darauffolgenden langsameren Periode wird durch die Zerfallsreaktion der Koordinationskomplexe der Cerionen mit sekundären Alkoholen in der Dextrankette gestartet und durch eine Redoxreaktion mit nicht komplexierten Cerionen abgebrochne.

Received August 16, 1965

Revised October 4, 1965

Prod. No. 4930A

**Polymerizations of Some Diene Monomers.  
Preparations and Polymerizations of Vinyl  
Methacrylate, Allyl Methacrylate, *N*-Allylacrylamide,  
and *N*-Allylmethacrylamide**

WASABURO KAWAI, *Government Industrial Research Institute,  
Osaka, Japan*

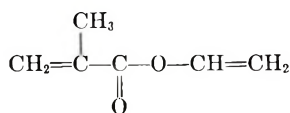
**Synopsis**

Vinyl methacrylate, allyl methacrylate, *N*-allylacrylamide, and *N*-allylmethacrylamide were prepared, and these monomers were polymerized in toluene by  $\alpha, \alpha$ -azobisisobutyronitrile catalyst. Cyclization content of poly(vinyl methacrylate) was estimated by infrared spectroscopy to be 50–60% at low conversions, but at the high conversions, due to gelation the polymers were insoluble in the usual organic solvents. Allyl methacrylate did not produce any soluble polymer, even at a low conversion, in contrast with poly(vinyl methacrylate). Poly-*N*-allylacrylamide and poly-*N*-allylmethacrylamide were also insoluble in common solvents. It was assumed that the polymers from monomers containing the allyl group might form crosslinks as a result of allyl resonance stabilization.

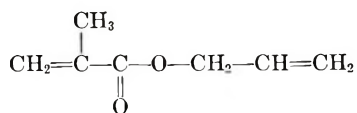
**INTRODUCTION**

In order to investigate the reactivities for polymerization of asymmetrical diene monomers, some diene monomers, i.e., vinyl methacrylate, allyl methacrylate, *N*-allylacrylamide and *N*-allylmethacrylamide were prepared. It is known that the polymerization of diene monomers proceeds generally through 1,2 polymerization, cyclopolymerization, and cross-linking during propagation.

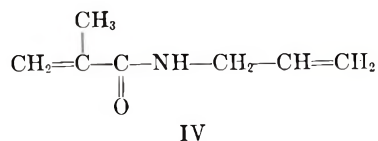
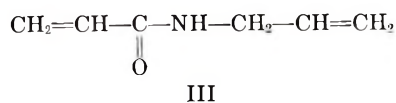
Vinyl methacrylate (I), which is a 1,5-diene monomer, produced a polymer that was soluble in chloroform or acetone at low conversion (below 25%), and the polymerization was accompanied by cyclopolymerization.



I



II



However, allyl methacrylate (II), *N*-allylacrylamide (III), and *N*-allylmethacrylamide (IV), which are 1,6-diene monomers, produced polymers insoluble in such solvents as chloroform, acetone, dimethylformamide, benzene, and dimethyl sulfoxide even at low conversions. It was reported by Schulz<sup>1</sup> that cyclopolymerization occurred in allyl acrylate, but Cohen<sup>2</sup> indicated that allyl methacrylate produced a gelation polymer under ultraviolet irradiation, in agreement with the results of the present paper, in which polymerization of allyl methacrylate catalyzed by  $\alpha,\alpha$ -azobisisobutyronitrile was not accompanied by cyclopolymerization.

## EXPERIMENTAL

### Preparation of Vinyl Methacrylate

Preparation of vinyl methacrylate has been reported in a previous paper<sup>3</sup> and patents.<sup>4-6</sup> In the present work, vinyl methacrylate was prepared from methacrylic acid with vinyl acetate in the presence of mercuric acetate, sulfuric acid, and hydroquinone, according to a literature method.<sup>7</sup>

Thus, 0.5 mole methacrylic acid, 2.5 mole vinyl acetate, 1.1 g. mercuric acetate, 0.3 g. sulfuric acid, and 0.5 g. hydroquinone were mixed in a flask and stirred for 3 days at room temperature. After addition of 5 g. sodium acetate, to the reaction mixture and washing several times with water, the upper layer was separated and dried over magnesium sulfate. The organic layer was distilled at reduced pressure, and the following fractions were collected: (I) recovered vinyl acetate, b.p. 34–39°C./150 mm. Hg; (II) vinyl methacrylate, b.p. 40°C./38 mm. Hg, 33.0 g. (58.3% yield),  $n_D^{25} = 1.4241$ ,  $d_4^{25} = 0.9329$ , MR (found) = 30.70, MR (calcd.) = 30.51. The second fraction was estimated to be of 97.5% purity by double-bond determination.<sup>8</sup> The infrared spectrum is shown in Figure 1.

### Preparation of Allyl Methacrylate

The preparation of allyl methacrylate was previously reported by Rehberg et al.<sup>9</sup> In the present study allyl methacrylate was prepared by a water elimination reaction between 0.47 mole methacrylic acid and 0.86 mole allyl alcohol in the presence of 0.2 g. hydroquinone, 0.5 g. *p*-toluenesulfonic acid, and 100 cc. benzene. After refluxing of the reaction mixture for 6 hr., it was washed with an aqueous solution of potassium carbonate

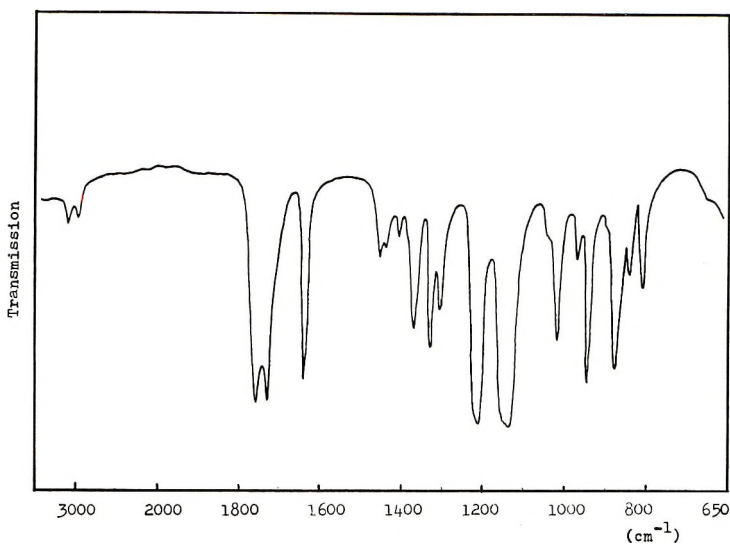


Fig. 1. Infrared spectrum of vinyl methacrylate.

and with water three times, and the upper layer was dried over magnesium sulfate. The fraction boiling at 65–68°C./35 mm. Hg (20.1 g.) was collected by redistillation; yield 34.5%. The refractive index and density of the fraction were observed to be  $n_D^{25} = 1.4338$  (lit.<sup>9</sup>  $n_D^{20} = 1.4358$ ),  $d_4^{25} = 0.9218$ . It was estimated to have MR (found) = 35.59, MR (calcd.) = 35.13 and 99.5% purity by double-bond determination. The infrared spectrum is shown in Figure 2.

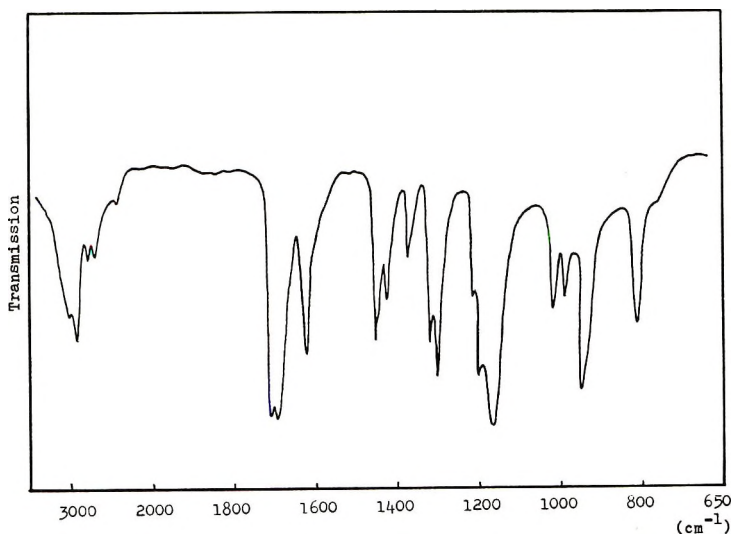


Fig. 2. Infrared spectrum of allyl methacrylate.

### Preparation of *N*-Allylacrylamide

*N*-Allylacrylamide was prepared by *N*-acylation of allylamine with acrylic chloride. Thus, 0.61 mole allylamine was dropped slowly into 0.31 mole acrylic chloride in 60 cc. carbon tetrachloride at ice-water temperature. After stirring for 2 hr. allyl amine hydrochloride was separated by filtering and the reaction mixture was washed with 50 cc. water. The carbon tetrachloride layer was dried over magnesium sulfate, and then the fraction boiling at 107–109°C./3 mm. Hg was collected. On redistillation, the fraction boiled at 107–108°C./3 mm. Hg (12.8 g., 37.2% yield). The refractive index and density of the fraction were observed to be  $n_D^{25} = 1.4850$ ,  $d_4^{25} = 0.9661$ , and the fraction was estimated to have MR (found) = 32.88, MR (calcd.) = 32.58. The infrared spectrum is shown in Figure 3.

ANAL. Calcd.: C, 64.84%; H, 8.16%; N, 12.60%. Found: C, 64.61%; H, 8.14%; N, 12.36%.

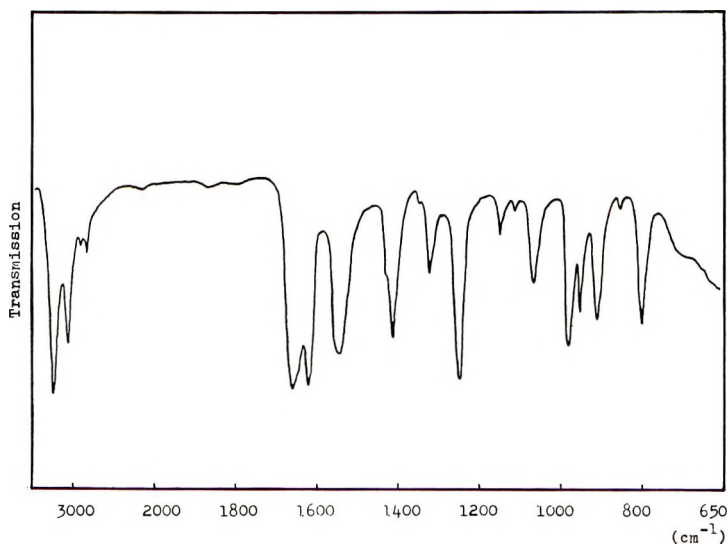


Fig. 3. Infrared spectrum of *N*-allylacrylamide.

### Preparation of *N*-Allylmethacrylamide

By the same procedure as used for preparing *N*-allylacrylamide, *N*-allylmethacrylamide was prepared from 0.23 mole methacrylic chloride in 60 cc. carbon tetrachloride, and 0.44 mole allylamine. It boiled at 97–100°C./3 mm. Hg and was obtained in 28.5% yield (8.9 g). The refractive index and density of the fraction were  $n_D^{25} = 1.4817$ ,  $d_4^{25} = 0.9575$ . The product had MR (found) = 37.18, MR (calcd.) = 37.19. The infrared spectrum is shown in Figure 4.

ANAL. Calcd.: C, 67.17%; H, 8.86%; N, 11.19%. Found: C, 66.94%; H, 8.86%; N, 10.55%.



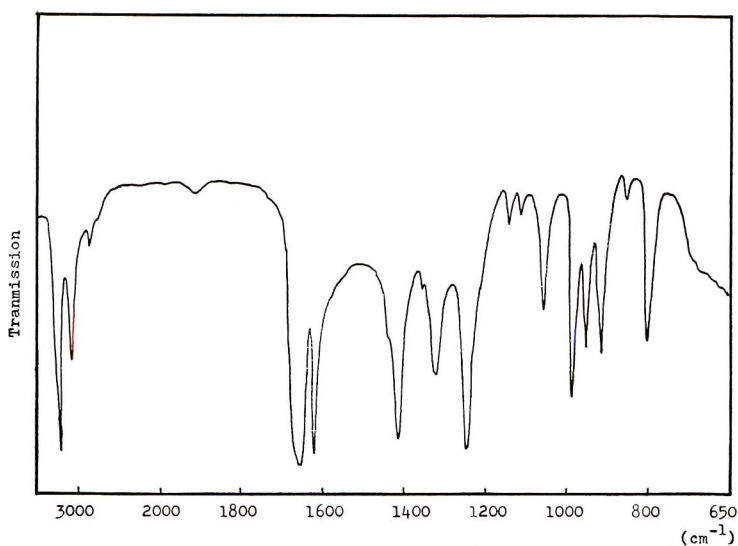


Fig. 4. Infrared spectrum of *N*-allylmethacrylamide.

### Polymerization of Diene Monomers

Diene monomers were polymerized in sealed glass tubes previously flushed with nitrogen gas, with  $\alpha, \alpha$ -azobisisobutyronitrile as catalyst in toluene as solvent. The obtained polymer solutions were poured into methanol, and then the precipitated polymers were collected and washed with methanol several times and then dried in a vacuum oven.

### Infrared Spectra of Polymers

For determination of double-bond content in poly(vinyl methacrylate), a polymer solution in chloroform and a solution cell with a thickness of 0.026 mm. were used. The calibration curve was made by plotting  $\log(I_0/I)$  at  $1630 \text{ cm}^{-1}$  versus vinyl methacrylate concentration as is shown in Figure 5. Considering that one mole of vinyl methacrylate corresponds to two moles of  $-\text{CH}=\text{CH}_2$  group, the cyclization content was estimated by using the equation:

$$\text{Cyclization content (\%)} = 100 - X$$

where

$$\frac{\text{Double-bond content (\%)} \text{ in polymer}}{\text{Double bond content (\%)} \text{ in polymer without cyclization}} = X/100$$

## RESULTS AND DISCUSSION

The results of the polymerization of vinyl methacrylate are given in Table I. At low monomer concentration, the polymerization rate  $R_p$  was proportional to monomer concentration, i.e., first-order with respect to the monomer concentration, as shown in Figure 6. These polymers obtained

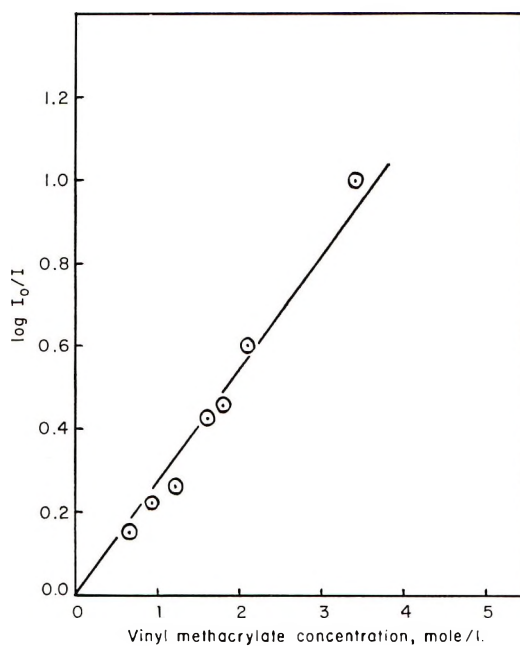


Fig. 5. Plot of  $\log (I_0/I)$  at  $1630 \text{ cm.}^{-1}$  vs. vinyl methacrylate concentration.

TABLE I  
Polymerization of Vinyl Methacrylate Catalyzed by  $\alpha, \alpha$ -Azobisisobutyronitrile<sup>a</sup>

No.	[M] <sub>0</sub> , mole/l.	Vol. toluene, cc.	Conversion, %	Polymerization rate, %/hr.
1	2.11	1.5	32.6 (gel)	13.5
2	3.39	1.2	49.0 (gel)	20.2
3	4.23	1.0	61.0 (gel)	25.2
4	5.51	0.7	68.1 (gel)	28.1
5	6.31	0.5	68.5 (gel)	28.3
6	7.65	0.2	65.5 (gel)	27.0
7	8.50	0.0	74.1 (gel)	30.6
8	2.09	2.0	22.6	10.1
9	1.61	3.0	18.6	8.3
10	1.26	4.0	15.7	7.0
11	1.04	5.0	12.6	5.6
12	0.885	6.0	8.2	3.66
13	1.84	2.5	ca. 25 (gel)	—
14	1.41	3.5	23.3	7.2
15	1.12	4.5	20.0	6.15

<sup>a</sup> Conditions: [Cat.] = 0.08 mole/l., temp. = 65°C.

at below 25% conversion were soluble in chloroform and toluene, although polymers obtained at high conversion, were insoluble in organic solvents due to gelation. Cyclization content of the soluble polymers was calculated from the measurement of infrared spectra and is shown in Table II.

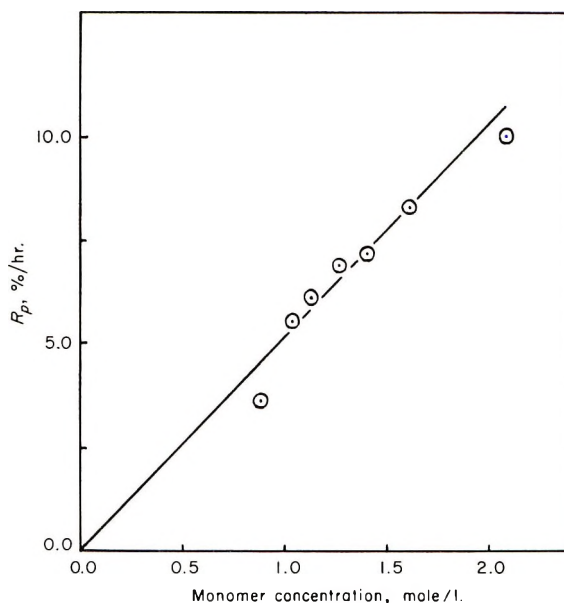
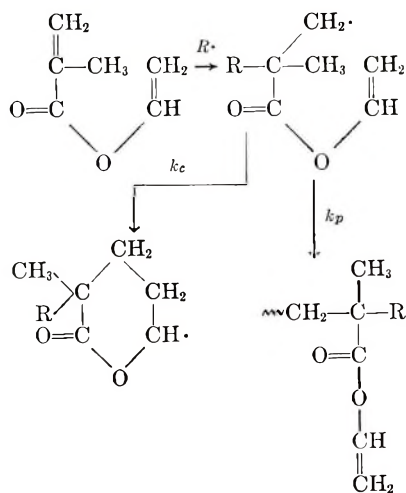


Fig. 6. Polymerization rate of vinyl methacrylate vs. monomer concentration.

It was assumed from the infrared spectrum that the structure of the cyclization unit was a  $\delta$ -lactone (six-membered ring) because poly(vinyl methacrylate) showed the absorption at  $1740 \text{ cm.}^{-1}$  assigned to a  $\delta$ -lactone and not that at  $1760\text{--}1780 \text{ cm.}^{-1}$  assigned to the  $\gamma$ -lactone (five-membered ring), although an absorption appears at  $1735\text{--}1750 \text{ cm.}^{-1}$  which was assigned to the saturated ester group of a noncyclized unit. From these observations, the proposed polymerization scheme would be as shown in eqs. (1).

The polymerization results for allyl methacrylate are shown in Table III. Poly(allyl methacrylates) were insoluble in chloroform, dioxane, dimethyl-



(1)

TABLE II  
 Cyclization Contents of Poly(vinyl Methacrylates)

No.	$\eta_{sp}/c^a$	Cyclization content, %
8	0.135 (CHCl <sub>3</sub> )	54.1
10	0.109 (CHCl <sub>3</sub> )	51.5
14	0.306 ( <i>m</i> -cresol)	61.0

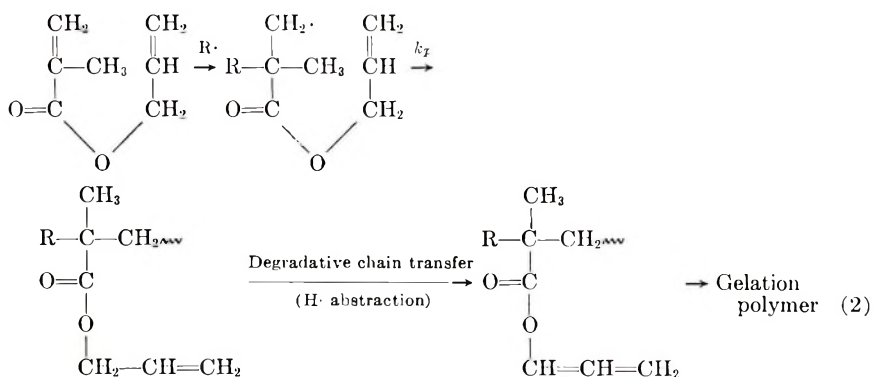
<sup>a</sup> At 20°C.,  $c = 0.20$  g./100 cc.

 TABLE III  
 Polymerization of Allyl Methacrylate Catalyzed by  $\alpha, \alpha$ -Azobisisobutyronitrile<sup>a</sup>

No.	[M] <sub>0</sub> , mole/l.	Solvent	Vol. solvent, cc.	Conversion, %
A-1	1.91	Toluene	2.5	32.0
A-2	1.66	"	3.0	33.2
A-3	1.46	"	3.5	34.4
A-4	1.31	"	4.0	25.9
A-5	1.19	"	4.5	37.0
A-6	1.08	"	5.0	29.7
A-7	0.925	"	6.0	37.2
A-8	1.56	Ethyl acetate	3.0	17.7
A-9	1.23	"	4.0	5.05
A-10	0.865	"	6.0	3.55
A-11	0.750	"	7.0	3.40

<sup>a</sup> Conditions: [Cat] = 0.08 mole/l., temp. = 65°C., polymerization time = 70 min.

formamide, toluene, benzene, and *m*-cresol, even for polymers obtained at low conversion in ethyl acetate. In contrast to poly(vinyl methacrylate), poly(allyl methacrylate) did not give polymer soluble in organic solvents, and it appeared that allyl resonance stabilization [eq. (2)] in the allyl group through degradative chain transfer led to crosslinking of the polymer, which contained almost no residual double bond, as shown in Figure 7*b*; these observations were different from those for poly(vinyl methacrylate) (Fig. 7*a*) and agreed with the results of Cohen, who reported ultraviolet-irradiated polymer of allyl methacrylate to be insoluble in organic solvents due to gelation.



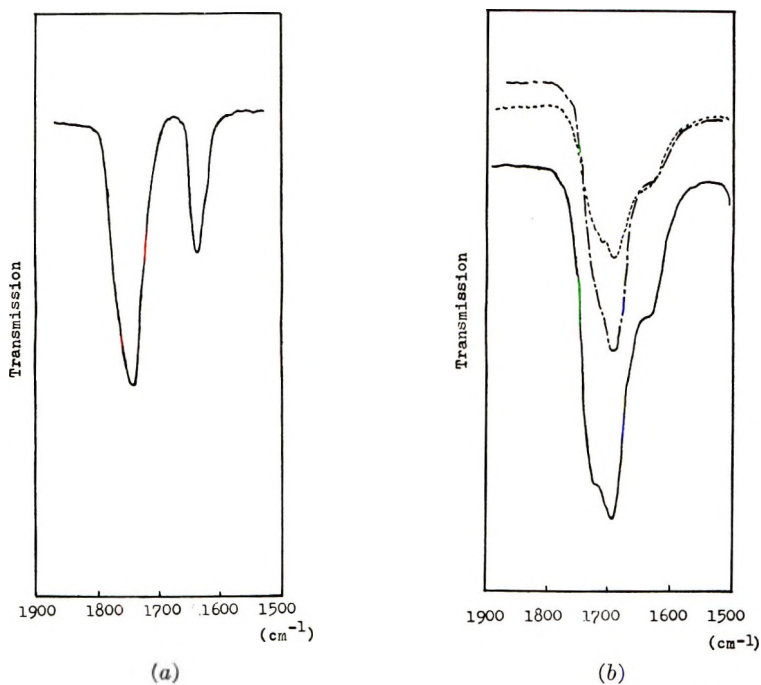


Fig. 7. Infrared spectra of (a) poly(vinyl methacrylate) at 1600–1800  $\text{cm}^{-1}$ ; (b) poly(allyl methacrylate) at 1600–1800  $\text{cm}^{-1}$ .

The results of polymerization of *N*-allylacrylamide and *N*-allylmethacrylamide are shown in Tables IV and V, respectively. The products were not linear polymers, as they were insoluble in such organic solvents as dimethylformamide, *m*-cresol, 80% aqueous formic acid, acetone, chloroform, benzene, and toluene, and were infusible, probably due to cross-linking; this was supported by disappearance of the absorption at 1630  $\text{cm}^{-1}$  assigned to the double bond. As in poly(allyl methacrylate), it appeared that poly-*N*-allylacrylamide and poly-*N*-allylmethacrylamide were crosslinked polymers formed by intermolecular reaction, with allyl

TABLE IV  
Polymerization of *N*-Allylacrylamide<sup>a</sup>

No.	[M] <sub>0</sub> , mole/l.	Vol. toluene, cc.	Conversion, %
1	2.73	2.0	6.3
2	1.32	5.0	6.4
3	1.13	6.0	8.9
4	0.981	7.0	6.2
5	0.870	8.0	12.8

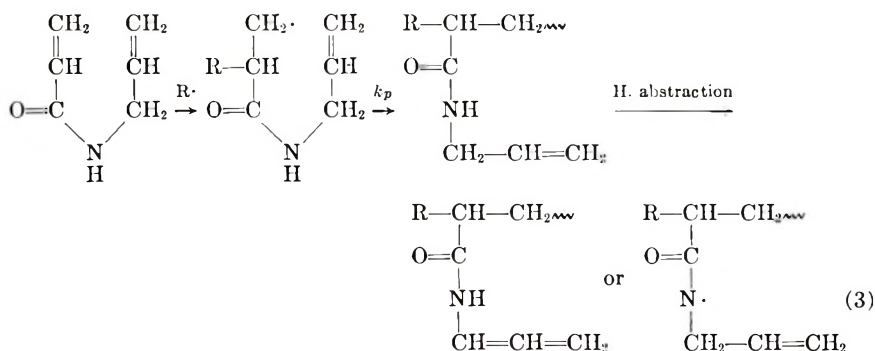
<sup>a</sup> Conditions: [Cat] = 0.08 mole/l., temp. = 60°C., polymerization time = 50 min.

TABLE V  
 Polymerization of *N*-Allylmethacrylamide<sup>a</sup>

No.	[M] <sub>0</sub> , mole/l.	Vol. toluene, cc.	Conversion, %
6	1.63	3.0	16.0
7	1.28	4.0	17.2
8	1.06	5.0	8.2
9	0.786	7.0	5.7
10	0.695	8.0	5.4

<sup>a</sup> Conditions: [Cat] = 0.08 mole/l., temp. = 60°C., polymerization time = 75 min.

resonance stabilization in the allyl group or radical produced from —NH group through hydrogen radical abstraction as shown in eq. (3).



### References

1. R. C. Schulz, M. Marx, and H. Hartmann, *Makromol. Chem.*, **44-46**, 281 (1961).
2. S. G. Cohen, B. E. Ostberg, D. B. Sparrow, and E. R. Blout, *J. Polymer Sci.*, **3**, 264 (1948).
3. A. M. Sladkov and G. S. Petrov, *Zh. Obshch. Khim.*, **24**, 450 (1954).
4. J. H. Broun and J. S. Watt, U. S. Pat. 2,344,798 (1944).
5. C. T. Kantter, Ger. Pat. 728,702 (1942).
6. D. W. Huebner and J. E. Fearey, U. S. Pat. 2,391,162 (1945).
7. D. Swern and E. F. Jordan, Jr., *Organic Synthesis*, **30**, 106 (1950).
8. A. Polgar and J. L. Jungnickel, *Organic Analysis*, **3**, 243 (1956).
9. C. E. Rehberg, C. H. Fisher and L. T. Smith, *J. Am. Chem. Soc.*, **65**, 1003 (1943).

### Résumé

Le méthacrylate de vinyle, le méthacrylate d'allyle, le *N*-allylacrylamide, et le *N*-allylméthacrylamide ont été préparés, et ces monomères ont été polymérisés dans le toluène en présence de  $\alpha, \alpha'$  azobisisobutyronitrile comme catalyseur. La teneur en cycles du polyméthacrylate de vinyle a été évaluée à 50–60% aux faibles degrés de conversion au moyen de la spectroscopie infrarouge, mais aux degrés de conversion élevés, ces polymères sont insolubles dans les solvants organiques usuels par suite de la gélification. Le méthacrylate d'allyle ne produit pas de polymères solubles, même pas aux faibles con-



versions, contrairement au polyméthacrylate de vinyle. Le poly-*N*-allylacrylamide et le poly-*N*-allylméthacrylamide sont également des polymères insolubles dans les solvants usuels. On suggère que les polymères préparés au départ de monomères contenant un groupe allyle, pourraient subir un pontage par suite de la stabilisation par résonance du système allylique.

### Zusammenfassung

Vinylmethacrylat, Allylmethacrylat, *N*-Allylacrylamid und *N*-Allylmethacrylamid wurden dargestellt und in Toluollösung mit  $\alpha,\alpha$ -Azobisisobutyronitril als Katalysator polymerisiert. Die Zyklisierung wurde bei Polyvinylmethacrylat bei niedrigen Umsätzen infrarotspektroskopisch zu 50 bis 60% bestimmt, bei hohen Umsätzen waren aber die Polymeren wegen Gelbildung in den üblichen organischen Lösungsmitteln unlöslich. Im Gegensatz zum Polyvinylmethacrylat lieferte Allylmethacrylat auch bei niedrigem Umsatz kein lösliches Polymeres. Poly-*N*-allylacrylamid und Poly-*N*-allylmethacrylamid waren ebenfalls in den üblichen Lösungsmitteln unlöslich. Es wurde angenommen, dass die Polymeren aus Monomeren mit einer Allylgruppe zur Vernetzung durch Allylresonanzstabilisierung neigen.

Received August 11, 1965

Revised October 11, 1965

Prod. No. 4937A

## Vanadium- or Vanadylacetylacetonate as a Cocatalyst for the Terpolymerization of Ethylene, Propylene, and Dicyclopentadiene

ROBERT E. CUNNINGHAM, *Research Division,  
Goodyear Tire and Rubber Company, Akron, Ohio*

### Synopsis

Vanadium trisacetylacetonate [ $V(C_5H_7O_2)_3$ ] and vanadyl bisacetylacetonate [ $VO(C_5H_7O_2)_2$ ] were found to be satisfactory catalysts (with  $Al_2Et_3Cl_3$  cocatalyst) for the terpolymerization of ethylene, propylene, and dicyclopentadiene to unsaturated, sulfur-curable elastomers. Polymerization solvents of heptane or benzene were used. Best yields of terpolymers were obtained in benzene. Terpolymers with unsaturations of greater than  $\sim 0.20$  mole  $C=C/kg.$  can be cured with a sulfur-based vulcanizing recipe. Both acetylacetonates produced terpolymers, in benzene, with practically equivalent properties. They also appeared to be nearly equal to corresponding terpolymers made with catalysts of  $VOCl_3$  or  $VCl_4$ .

The copolymerization of ethylene and propylene to form amorphous elastomers, and the terpolymerization of ethylene, propylene, and various dienes to form unsaturated, sulfur-curable elastomers have been described in great breadth.<sup>1</sup> The best known transition metal catalysts for such reactions have been the vanadium chlorides. A prior paper dealt with the use of these compounds as catalysts for the terpolymerization of ethylene, propylene, and dicyclopentadiene.<sup>2</sup> The two acetylacetonates of vanadium have not been described in any great detail as catalysts for these reactions, although a few references do appear in the literature.<sup>3-8</sup> Most of these are patents, in which only general examples are given of the use of the acetylacetonates as catalysts for these polymerizations.<sup>4-8</sup> It was thus of interest to study the catalytic activity of vanadium trisacetylacetonate and vanadyl bisacetylacetonate for this terpolymerization reaction, and to compare the results with those obtained with catalysts containing the vanadium chlorides.

### EXPERIMENTAL

#### Materials

The source and purification of all materials used in these studies are the same as described in detail in the previous paper.<sup>2</sup> The exception was the ethylene and propylene, which were used without further purification. It

was found that satisfactory polymerizations could be carried out by using the monomers directly from the cylinders.

Vanadium trisacetylacetonate,  $V(C_5H_7O_2)_3$ , was obtained from Anderson Chemical Division of Stauffer Chemical Company and was a brown powder. Vanadyl bisacetylacetonate,  $VO(C_5H_7O_2)_2$ , was obtained from Union Carbide Metals Company and was a green powder. Both materials were used as received. It might be noted that vanadium trisacetylacetonate is the only common source of hydrocarbon-soluble trivalent vanadium.

### Catalyst Solutions

For all runs,  $Al_2Et_3Cl_3$  was handled as a 1.0M (in Al) solution in heptane (0.50M for the formula weight of  $Al_2Et_3Cl_3$ ). Both acetylacetonates were used as 0.10M solutions in benzene. All solutions were kept under nitrogen in 4-oz. bottles that were capped with self-sealing rubber gaskets and were transferred with hypodermic syringes.

### Polymerizations

The detailed techniques of polymerization were described in a previous paper.<sup>2</sup> These were followed, with few changes, for the experiments described below. Ethylene and propylene were metered into the system through calibrated flow meters at 1200 and 800 cc./min., respectively. Mass spectrographic analysis of the feed gas for each run showed it averaged about 58 mole-% ethylene.

Dicyclopentadiene was added all at the start of a run, before catalyst was added. All catalysts were formed *in situ*, the  $Al_2Et_3Cl_3$  being added first. Its concentration was always 0.010M. The vanadium acetylacetonates were added in sufficient quantity to provide an initial vanadium concentration of 0.0005M. Thus the initial Al/V molar ratio was 20. Polymerizations were allowed to proceed for 15 min. Then another addition of the vanadium compound was made to bring the vanadium concentration to 0.001M, and a final Al/V molar ratio of 10. Polymerizations were allowed to proceed another 15 min. before termination. Reactions proceeded in much the same manner as those described previously, and polymer isolation and evaluation were also carried out by techniques detailed in the prior paper.<sup>2</sup>

### DISCUSSION

Both of the vanadium acetylacetonates, with  $Al_2Et_3Cl_3$  as cocatalyst, were studied as catalysts for the terpolymerization of ethylene, propylene, and dicyclopentadiene, in either heptane or benzene solvent. With each combination of catalyst and solvent, the dicyclopentadiene level in the polymerization mixture was varied over a small range. The complete experimental results are given in Tables I and II.

It was found that all four possible combinations of the acetylacetonates and polymerization solvents gave good yields of elastomeric terpolymer,

TABLE I  
Vanadium Trisacetylacetonate as Cocatalyst for  
Ethylene-Propylene-Dicyclopentadiene Terpolymerization<sup>a</sup>

Solvent	Dicyclo- penta- diene charged, g.	Ter- polymer yield, g.	Inherent viscosity	Insoluble polymer, %	Unsaturation, mole C=C/kg.	Volume swelling, %	
						15 min. cure	60 min. cure
Benzene	0	36	1.43	2.2	—	—	—
	0.5	34.5	1.50	1.9	0.13	No cure	1126
	1.0	30	1.56	8.3	0.23	733	423
	1.5	32	1.73	2.2	0.32	414	314
	3.0	27	1.32	6.3	0.71	286	248
Heptane	0	25	2.13	0.7	—	—	—
	1.0	22.5	2.46	3.9	0.32	503	373
	1.5	22.5	2.33	0.2	0.47	384	309
	3.0	24.5	1.12	48.9	0.91	241	230

<sup>a</sup> Experimental section and previous paper<sup>2</sup> give details of the polymerization conditions and methods of measuring the tabulated quantities. In all runs, 500 ml. of solvent was used, with  $Al_2Et_3Cl_3$  as cocatalyst.

TABLE II  
Vanadyl Bisacetylacetonate as Cocatalyst for  
Ethylene-Propylene-Dicyclopentadiene Terpolymerization<sup>a</sup>

Solvent	Dicyclo- penta- diene charged, g.	Ter- polymer yield, g.	Inherent viscosity	Insoluble polymer, %	Unsaturation, mole C=C/Kg.	Volume Swelling, %	
						15 min. cure	60 min. cure
Benzene	0	38.5	1.37	2.9	—	—	—
	0.5	33.5	1.47	1.3	0.11	No cure	923
	1.0	30.5	1.85	1.3	0.23	758	387
	1.5	29.5	1.80	3.2	0.27	479	318
	3.0	26.5	1.74	3.2	0.72	308	252
Heptane	0	17	3.30	1.7	—	—	—
	0.5	14.5	3.52	0.1	0.28	297	227
	1.0	12.5	2.65	27.7	0.56	193	175
	1.5	11.5	2.63	9.1	0.87	172	167

<sup>a</sup> Experimental section and previous paper<sup>2</sup> give details of the polymerization conditions and methods of measuring the tabulated quantities. In all runs, 500 ml. of solvent was used, with  $Al_2Et_3Cl_3$  as cocatalyst.

which could be cured with a sulfur-based vulcanizing recipe to tight networks (as measured by volume swelling in toluene). An exact comparison cannot be made between terpolymer yields from this work and the previous experiments with vanadium chlorides,<sup>2</sup> since the acetylacetonates were introduced by a two-step addition during a run while the chlorides were added all at the start. The yields from all the systems are of the same order of magnitude, however. Natta's data<sup>3</sup> compared rates of ethylene-propyl-

ene copolymerization, using catalysts of the acetylacetonates with  $\text{AlEt}_2\text{Cl}$ , and also  $\text{VCl}_4$  with  $\text{Al}(\text{C}_6\text{H}_{13})_3$ . They showed that under their reaction conditions, the chloride catalyst was about 25 times as active as the acetylacetonates. The data of this paper, however, show that at least comparable terpolymer yields are obtained with catalysts of the vanadium acetylacetonates,  $\text{VCl}_4$ , or  $\text{VOCl}_3$ , when  $\text{Al}_2\text{Et}_3\text{Cl}_3$  is used as the cocatalyst. Similarly, by making such cross-comparisons as are possible between the data of this and the previous paper,<sup>2</sup> it does not appear that the initial valence of vanadium in the catalyst has any gross effect on such properties of the terpolymer as were tested. There may well be, however, differences in microstructure of the terpolymers made with these various catalysts, which have not been determined as yet.

Another difference may be noted between terpolymers made with chloride and acetylacetonate catalysts, in their content of insoluble polymer (measured in toluene at  $30^\circ\text{C}$ .; see Tables I and II). This insoluble polymer may arise in two ways: from crystalline segments of polyethylene blocks in the chain or from polymerization of the second double bond in the dicyclopentadiene to form true, crosslinked gel. The chloride catalysts, especially in heptane solvent, tend to produce terpolymers with fairly high content of insoluble polymer ( $>20\%$ ).<sup>2</sup> A considerable portion of this insoluble polymer, especially with the system of  $\text{VOCl}_3$  and heptane solvent, is crosslinked gel. The acetylacetonates, however, tend to produce terpolymers with very low insoluble content, even in heptane solvent (with two exceptions, noted in Tables I and II).

Terpolymerizations run in benzene solvent gave much higher polymer yields than those run in heptane; this was also true of the chloride catalysts. A few other points about each combination of catalyst and solvent are as follows.

#### **Vanadium Trisacetylacetonate with Benzene Solvent**

This combination produced good yields of terpolymers with moderate inherent viscosity (averaging about 1.5) and low percentage of insoluble polymer. The polymers cured tightly with the sulfur-based curing recipe.

#### **Vanadyl Bisacetylacetonate with Benzene Solvent**

This system also gave good yields of terpolymers with low per cent of insoluble polymer. Their inherent viscosities averaged slightly higher (about 1.7) than those of the polymers made with vanadium trisacetylacetonate. The polymers also cured tightly with the sulfur-based recipe. From the tests that were made, it appears that the two acetylacetonates produce practically equivalent terpolymers when benzene is used as the polymerization solvent.

#### **Vanadium Trisacetylacetonate in Heptane Solvent**

This system produced moderate yields of terpolymers with high inherent viscosities ( $>2.0$ ). The per cent of insoluble polymer was low, except for



the run with the highest dicyclopentadiene level, and the polymers cured tightly.

### Vanadyl Bisacetylacetonate in Heptane Solvent

This combination gave the lowest terpolymer yields, but they had the highest inherent viscosities ( $>2.5$ ). Insoluble polymer content was low (with one exception), and the polymers cured very tightly. For a given unsaturation level, these terpolymers were more tightly cured than any other. Possibly this reflects the distribution of dicyclopentadiene units in the polymer chains (see below).

In these last two combinations, the polymerization solvent was heptane (500 ml.) but the solvent for the acetylacetonates was benzene (5 ml.). Other unpublished data on other systems indicate that this small amount of aromatic solvent in the aliphatic one does not appear to alter the polymerization from the results obtained with wholly aliphatic solvent.

As the dicyclopentadiene charged in each system increased, terpolymer yield decreased and unsaturation increased. The effect of the diene on the terpolymer's inherent viscosity was erratic. Efforts at determining the propylene content of the terpolymers have given erratic results and are still undergoing calibration studies; hence, these results are not included here. There is definite evidence, however, that within a given series of terpolymers, as the dicyclopentadiene concentration increases, the propylene content of the terpolymer decreases.

The data in Tables I and II for volume swelling of the vulcanized polymers also show that they cured tightly ( $<400\%$  volume swell) after a 60-min. cure with a sulfur-based vulcanizing recipe, except for those polymers with the lowest amount of unsaturation. A number of the polymers with the higher levels of unsaturation were tightly cured with only a 15-min. vulcanization. In the broadest terms, it appeared that terpolymers made with catalysts of tetravalent vanadium, whether chloride or acetylacetonate, cured most tightly, for a given degree of unsaturation. This behavior should be related to the distribution of the dicyclopentadiene (and thus the subsequent crosslinks) through the terpolymer chains. Natta has shown<sup>1</sup> that the reactivity ratios of ethylene and propylene, with vanadium chloride catalysts, depend on the initial valence of the vanadium. It would also seem logical that the reactivity ratios between dicyclopentadiene and ethylene or propylene would show such a dependence. Such studies have not been detailed yet.

The author wishes to thank the Goodyear Tire and Rubber Company for permission to publish these results. Acknowledgments are also due Mrs. V. A. Bittle for determination of the inherent viscosities and percentages of insoluble polymer, E. E. Fauser for the vulcanizing recipe, Frank Chan for the unsaturation analyses, and J. K. Phillips for the mass spectrographic analyses of the ethylene-propylene mixtures. This is contribution number 338 from the Goodyear Research Laboratories.



### References

1. G. Natta, G. Crespi, A. Valvassori, and G. Sartori, *Rubber Chem. Technol.*, **36**, 1583 (1963).
2. R. E. Cunningham, *J. Polymer Sci.*, **A**, **3**, 3157 (1965).
3. G. Natta, G. Mazzanti, A. Valvassori, G. Sartori, and D. Fiumani, *J. Polymer Sci.*, **51**, 411 (1961).
4. Polymer Corporation, Belg. Pat. 632,028 (November 18, 1963)
5. Montecatini S. p. A., French Pat. 1,311,274 (December 7, 1962)
6. Montecatini S. p. A., Belg. Pats. 623,741 (February 14, 1963) and 631,165 (August 16, 1963).
7. Montecatini S. p. A., Italian Pats. 638,953 (April 2, 1962) and 638,656, (April 18, 1962).
8. Farbwerke Hoechst, Brit. Pat. 941,665 (November 13, 1963).

### Résumé

Le trisacétylacétonate de vanadium  $V(C_5H_7O_2)_3$  et le bisacétylacétonate  $VO(C_5H_7O_2)_2$  sont des catalyseurs satisfaisants (avec  $Al_2Et_3Cl_3$  comme cocatalyseur) pour la polymérisation ternaire de l'éthylène, propylène, et dicyclopentadiène en vue d'obtenir des élastomères insaturés, vulcanisables au soufre. On a utilisé comme solvant de polymérisation l'heptane ou le benzène. Le meilleur rendement de terpolymères a été obtenu dans le benzène. Des terpolymères avec des insaturations supérieures à 0.2 mole  $C=C$ /Kg peuvent être vulcanisés par une méthode à base de soufre. Les terpolymères produits au moyen de ces deux acétylacétonates en milieu benzénique, présentent pratiquement des propriétés équivalentes. Ces produits semblent également être équivalents pratiquement avec des terpolymères correspondants préparés avec des catalyseurs de  $VOCl_3$  ou de  $VCl_4$ .

### Zusammenfassung

Vanadintriäcetylacetonat  $[V(C_5H_7O_2)_3]$  und Vanadylbisäcetylacetonat  $[VO(C_5H_7O_2)_2]$  erwiesen sich als brauchbare Katalysatoren (mit  $Al_2Et_3Cl_3$  als Kokatalysator) für die Terpolymerisation von Äthylen, Propylen, und Dicyclopentadien zu ungesättigten, mit Schwefel vulkanisierbaren Elastomeren. Als Lösungsmittel für die Polymerisation wurden Heptan oder Benzol verwendet. Die besten Ausbeuten an Terpolymeren werden in Benzol erhalten. Terpolymere mit einem Doppelbindungsgehalt grösser als  $\sim 0,20$  Mol  $C=C$ /kg können mit einem Vulkanisationssystem auf Schwefelgrundlage vulkanisiert werden. Beide Acetylacetonate lieferten in Benzol Terpolymere mit praktisch gleichen Eigenschaften. Diese schienen auch den entsprechenden mit  $VOCl_3$  oder  $VCl_4$ -Katalysatoren hergestellten Terpolymeren nahezu gleich zu sein.

Received October 14, 1965

Prod. No. 4952A

## Photodegradation of Poly(methyl Methacrylate)

J. P. ALLISON, *General Motors Research Laboratories, Warren, Michigan*

### Synopsis

The vacuum photodegradation at 30°C. of poly(methyl methacrylate) and copolymers with acrylaldehyde, methacrylaldehyde, and methyl acrylate has been studied. The polymers were examined in the form of expanded films as produced by a freeze-drying technique. At least one molecule of carbon monoxide is evolved for each chain scission. It is concluded that chain scission in poly(methyl methacrylate) is primarily the result of photoinduced aldehyde groups.

### INTRODUCTION

Although the vacuum photodegradation of poly(methyl methacrylate) has received considerable attention,<sup>1-6</sup> the mechanisms of reactions at ambient temperatures which lead to chain scission are still speculative. This study is intended to provoke further thought concerning the route of photolytic decomposition, and also introduces a freeze-drying sample preparation as an alternative to film and solution methods. To this end, copolymers of methyl methacrylate with acrylaldehyde, methacrylaldehyde, or methyl acrylate were synthesized. Aldehydes were chosen as comonomers since their participation in the chain-scission reaction was suspected.<sup>7</sup>

### EXPERIMENTAL

#### Materials

Monomers polymerized for the irradiation studies were distilled before use. Polymerizations were conducted either in benzene or toluene solutions under high-vacuum conditions, azobisisobutyronitrile being used as initiator. Recoveries of polymer obtained after heating the monomer mixtures at 60°C. for 24 hr. averaged 70% after two precipitations from benzene into heptane. The weight-average molecular weights of the samples ranged between  $3.6 \times 10^4$  and  $2.95 \times 10^5$ , copolymers containing acrylaldehyde gravitating towards the lower end of the scale (Table I). In the absence of information relating to changes in the constants in the Mark-Houwink equation for copolymers based on methyl methacrylate, the values calculated for poly(methyl methacrylate) were used throughout this investigation.<sup>8</sup> Since the degree of degradation is a relative quantity, no great uncertainty in measurement was introduced. The aldehyde con-

TABLE I  
Number of Molecules of Volatile Fragments Produced per Chain-Scission in Polymers

Polymer composition				Polymer molecular weight $M_w \times 10^{-4}$	Products		
Methyl methacrylate, mole-%	Acrylaldehyde, mole-%	Methacrylaldehyde, mole-%	Methyl acrylate, mole-%		Carbon monoxide	Methyl formate	Methanol
100	0	0	0	20.9	3.0	6.0	10.0
99.71	0.29	0	0	13.7	2.5	0.16	0.45
77.6	22.4	0	0	9.0	2.1	0.05	0.17
88.5	11.5	0	0	10.0	0.9	0.1	0.3
80.0(5)	0	19.9(5)	0	4.0	0.8	0.025	0.088
50	0	0	50	29.5	5.0	6.0	40.0
25	0	0	25	19.6	5.5	10.5	33.0
13	0	0	13	21.2	4.5	7.6	1.0

tent of the copolymers was established by forming the 2,4-dinitrophenylhydrazone in slightly acid tetrahydrofuran, precipitating the polymer into methanol, and eliminating excess reagent by Soxhlet extraction with methanol before analyzing for nitrogen. The maximum acrylaldehyde content was 26.5 mole-%, and the maximum methacrylaldehyde content reached 28.2 mole-%. The concentration of methyl acrylate was approximated to the amount used in the polymerization, the upper limit being 50 mole-% (Table I).

### Actinometry

The nature of the polymer deposit and the geometry of the radiation source<sup>9</sup> (Rayonet photochemical reactor, according to manufacturer's specifications, photons of 2537 Å. =  $1.65 \times 10^{16}$  sec.<sup>-1</sup> cm.<sup>-3</sup>) were such that reproducibility of intensity was a more critical factor than the energy emitted during any given interval. Reassurance was provided by a lack of variation in the degree of degradation of a single polymer sample over the entire duration of this investigation.

### Sample Preparation

Film forming is the most commonly used method of preparing polymers for photolytic studies. However, the retention of solvent and low molecular weight degradation fragments may produce undesirable effects. Accordingly, a freeze-drying technique was developed to surmount this problem. This method reproduces solution procedures but retains macromolecular immobility. A preliminary study with poly(methyl methacrylate) indicated that benzene-insoluble residue (presumed to be cross-linked polymer) was not formed at a sample density of less than 0.09 g./ml. In subsequent experiments, the polymer concentration averaged 0.002 g./ml. However, crosslinking did occur in samples containing methyl acrylate and to a lesser extent with acrylaldehyde copolymers.

Polystyrene and polyisobutene have been reported<sup>10</sup> to degrade severely when solutions in benzene or cyclohexane are frozen. In a control experiment with poly(methyl methacrylate), the change in average molecular weight was less than 3% for two freeze-drying sequences.

The irradiation apparatus is pictured in Figure 1. The outer tube was constructed from quartz, the remainder from Pyrex. Better support for the polymer was obtained by wrapping a glass spiral around the inner tube. The diameter of the quartz tube was 5 cm. and the length below the side-arm, 25 cm. The central tube was approximately 3 cm. in diameter. The cell was maintained at a steady preset temperature (30°C.) by circulating water from a thermostatically controlled bath.

To prepare a sample for photolysis, the polymer (~60 mg.) was dissolved in distilled benzene (30 ml.) in a tube having a diameter (3.4 cm.) slightly greater than that of the inner tube of the irradiation unit. The supporting tube was aligned in the solution to ensure uniform deposition and refrigerant (Dry Ice-ethanol) added. The jacket was detached from the frozen solu-

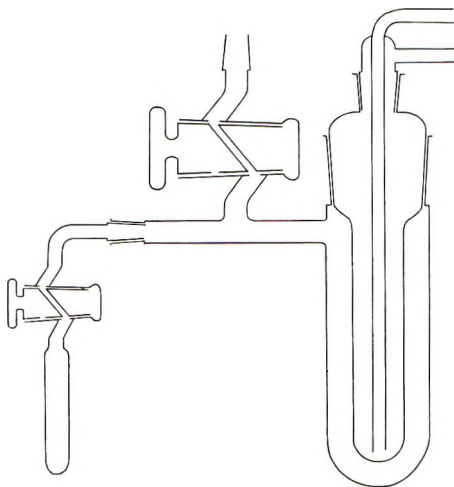


Fig. 1. Irradiation cell.

tion by momentarily immersing in cold water. The sample was inserted in the quartz tube and freeze-dried. The refrigerant was withdrawn after 45 min. This delay minimized the risk of solution melting adjacent to the support which might have served to displace polymer from the glass.

For the removal of solvent, the irradiation cell was connected to a large trap cooled by liquid nitrogen and exposed to an oil-pump vacuum. Once this had been accomplished, the cell was further evacuated at  $1.0 \times 10^{-5}$  torr. Then it was transferred to the irradiation chamber, the water supply connected, and the sample exposed for a given period (0.5–3.0 hr.). The source of ultraviolet light had been switched on 30 min. before the transfer was made to provide a steady flux.

Polymer was recovered by washing down the supporting tube with benzene and concentrating the solution prior to filtration through a 25–50  $\mu$  porosity, sintered glass crucible into a tared 10-ml. volumetric flask. After washing the filter with benzene, the solution was freeze-dried. This approach eased the practical problem of making viscosity measurements with small amounts of polymer. Solutions were prepared in methyl ethyl ketone and the determinations made at 25°C. in an Ubbelohde dilution viscometer. Except for copolymers with methyl acrylate, insoluble material did not exceed 2% of the initial sample weight.

#### Volatile Products

In experiments of long duration, assays of volatile degradation products were not performed. When the analysis of these compounds assumed paramount importance, exposures were of 0.75–3.0 min. in duration, the materials being condensed in the side-arm by liquid nitrogen. The timing became more critical for these short exposures. After the initial warm-up period, the source was extinguished, the sample quickly positioned, and the lamps relit to attain the original intensity. By employing high-vacuum

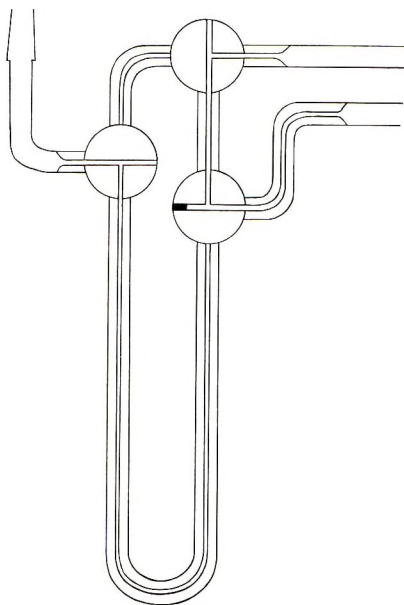


Fig. 2. U-tube for transfer of volatile degradation fragments.

methods, the compounds were transferred to a U-tube (Fig. 2) which could be connected into the carrier-gas line of a vapor fractometer (Perkin-Elmer, Model 154D). This device allowed helium to bypass the sample until equilibrium had been attained, then by suitable juxtaposition of stopcocks, the sample was flushed into the column. The response to carbon monoxide, methyl formate, and methanol was especially noted since they constituted the main degradation fragments. The instrument has been calibrated with respect to these compounds with the use of the same apparatus.

## RESULTS

### Chain Scission

The degree of degradation (number of scissions per polymer chain) was calculated from the formula  $(\bar{M}_{w_0} - \bar{M}_w)/\bar{M}_w$ , where  $\bar{M}_{w_0}$  is the initial weight-average molecular weight and  $\bar{M}_w$  is the weight-average molecular weight of the exposed sample. Theoretically, this value is based upon the number-average molecular weight. However, both quantities may be derived from the intrinsic viscosity, a simple arithmetical operation allowing the transformation from weight-average to number-average molecular weight.<sup>11</sup>

In calculating the extent of chain scission from molecular weights derived from viscosity measurements, certain assumptions have had to be made. Firstly, a "most probable" distribution of molecular weights is assumed for both irradiated and nonirradiated polymer. Secondly, parameters pertaining to homopoly(methyl methacrylate) have been used in calculating the molecular weights of the copolymers.



### Temperature Dependence

Increasing the temperature of the circulating water from 10 to 60°C. produced a twofold increase in the incidence of chain scission for otherwise equivalent exposures. No explanation is offered.

### Copolymers of Methyl Methacrylate with Acrylaldehyde

At longer exposures (3.0 hr.) degradation curves  $[(\bar{M}_{w_0} - \bar{M}_w)/\bar{M}_w]$  versus time] for poly(methyl methacrylate) depart from linearity, the incidence of chain scission being reduced (Fig. 3 and 4). Presumably, this is a direct result of the dilution of carbonyl chromophores during degradation and is not a feature of a concurrent crosslinking reaction, because the capture of insoluble material was negligible. However, copolymers with acrylaldehyde appeared to reach a limiting molecular weight after being exposed for 1 hr. in this system. Copolymers containing methacrylaldehyde began to show the same trend after 2 hr. exposure. This fact may be emphasized by plotting a graph of degree of degradation versus acrylaldehyde content in the copolymer for any selected exposure. An example is shown in Figure 5. The curves extrapolate sharply to the abscissa at an acrylaldehyde content of 28 mole-%. This phenomenon is not reflected by copolymers containing methacrylaldehyde, as seen in Figure 5.

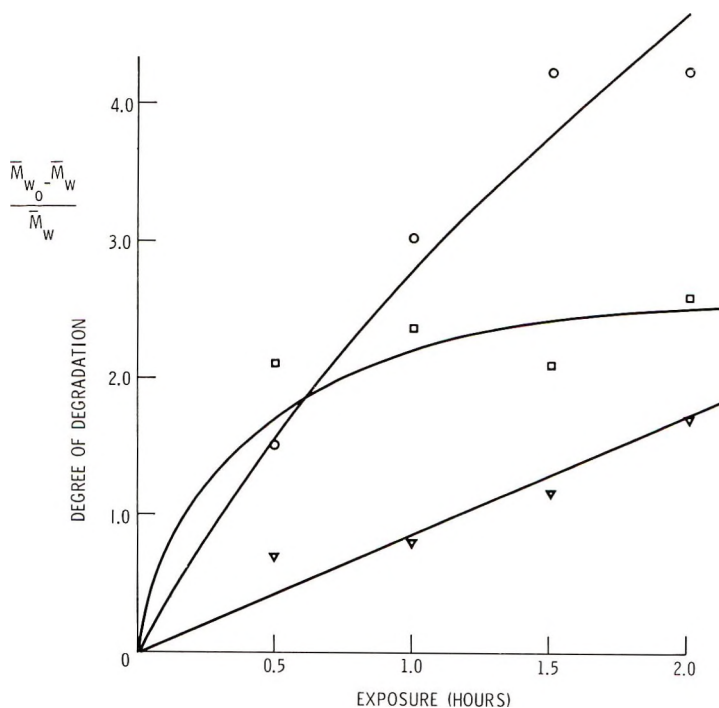


Fig. 3. Degree of degradation vs. exposure at 30°C.: (O) poly(methyl methacrylate); (□) copolymer with 22.4 mole-% acrylaldehyde; (∇) copolymer with 50 mole-% methyl acrylate.

This event may be rationalized by postulating crosslinking simultaneously with chain scission, these two processes equilibrating at an aldehyde concentration of 28 mole-%. It was noted that copolymers of methyl acrylate crosslinked under identical conditions. However, if occurring in

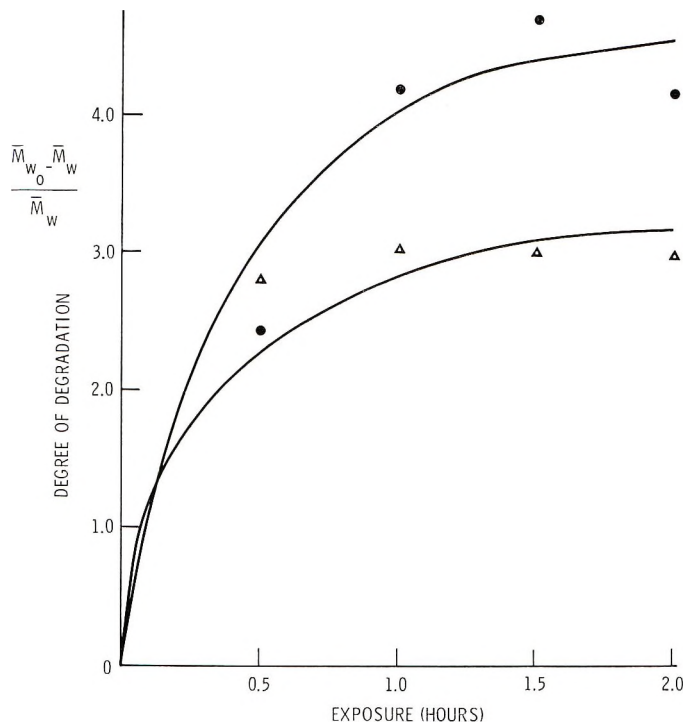


Fig. 4. Degree of degradation vs. exposure at 30°C.; (●) copolymer with 19.5(5) mole-% methacrylaldehyde; (△) copolymer with 11.5 mole-% acrylaldehyde.

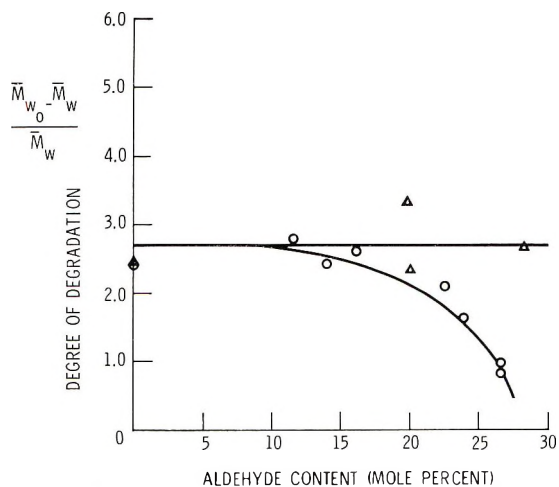


Fig. 5. Degree of degradation vs. aldehyde content at 0.5 hr. exposure and 30°C.: (O) acrylaldehyde copolymer; (△) methacrylaldehyde copolymer.

concert with chain scission, cross linking need not be associated with insolubility. As this pattern of behavior is at variance with that of poly(methyl methacrylate), it is inferred that acrylaldehyde units are responsible for crosslinking. A barely tenable explanation would be that absorption of radiation by an aldehyde chromophore does not automatically lead to scission in the polymer chain.

The tertiary hydrogen atom bound to the polymer backbone is pre-eminent in the cross linking function.<sup>12</sup> When eliminated from the system by the inclusion of methacrylaldehyde, rates of chain scission were comparable with those of poly(methyl methacrylate). This negates the second possibility outlined above. The rate of chain scission in poly(methyl methacrylate) was marginally greater than that in copolymers with methyl acrylate. This suggests a minor crosslinking performance.

### Volatile Products

By far the greater proportion of low molecular weight fragments resulting from the photolysis of poly(methyl methacrylate) consisted of carbon monoxide, methyl formate, and methanol. It is pertinent to point out that the recovery and transfer of carbon monoxide by the rather rudimentary liquid nitrogen trapping system, may have been less than quantitative. Chromatography did not permit analysis of trace amounts of uncondensable gases, and the amounts of methyl methacrylate evolved were too erratic to be of value in subsequent discussion. It is presumed that the presence of this compound is a feature of depolymerization initiated at unsaturated chain ends.<sup>6,13</sup>

Graphs of the rate of formation of volatile products parallel qualitatively the corresponding chain-scission curves (Figs. 6-9). Linear relationships hold true for polymers devoid of aldehyde groups, while a tendency

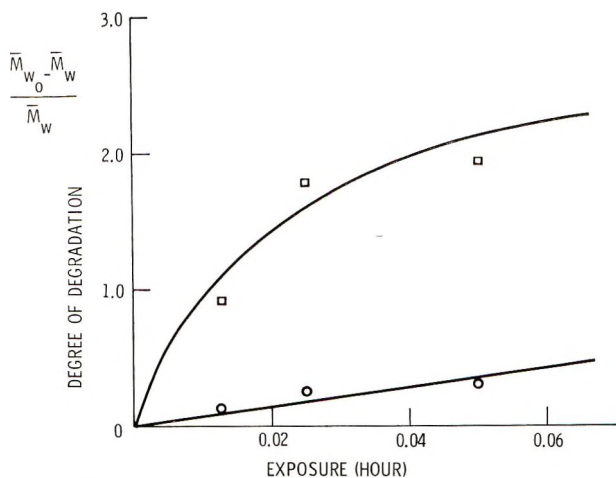


Fig. 6. Degree of degradation vs. exposure at 30°C.: (O) poly(methyl methacrylate); (□) copolymer with 22.4 mole-% acrylaldehyde.

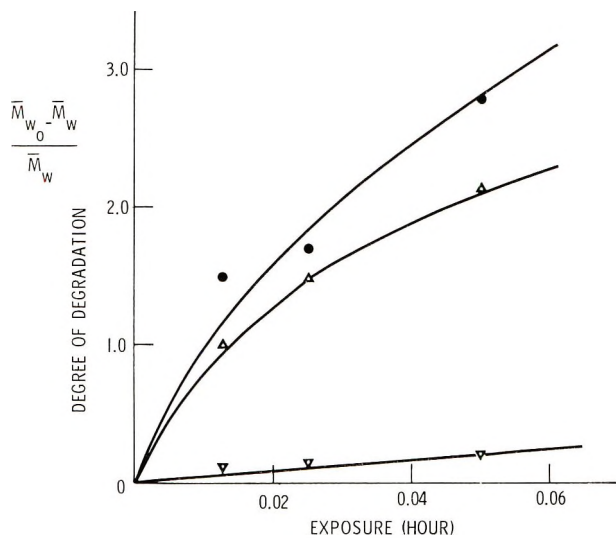


Fig. 7. Degree of degradation vs. exposure at 30°C.: (●) copolymer with 19.9(5) mole-% methacrylaldehyde; (Δ) copolymer with 11.5 mole-% acrylaldehyde; (▽) copolymer with 50 mole-% methyl acrylate.

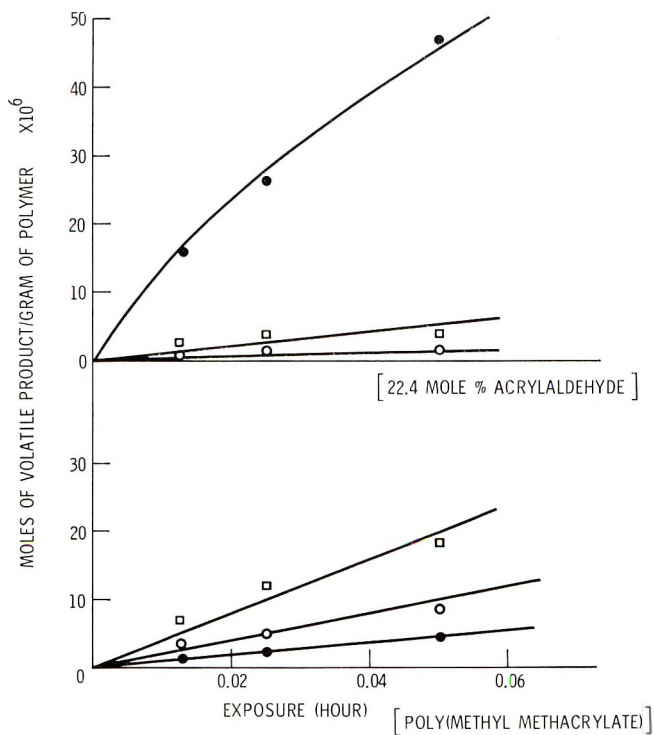


Fig. 8. Volatile fragments per gram of polymer vs. exposure at 30°C.: (●) carbon monoxide; (□) methanol; (○) methyl formate.

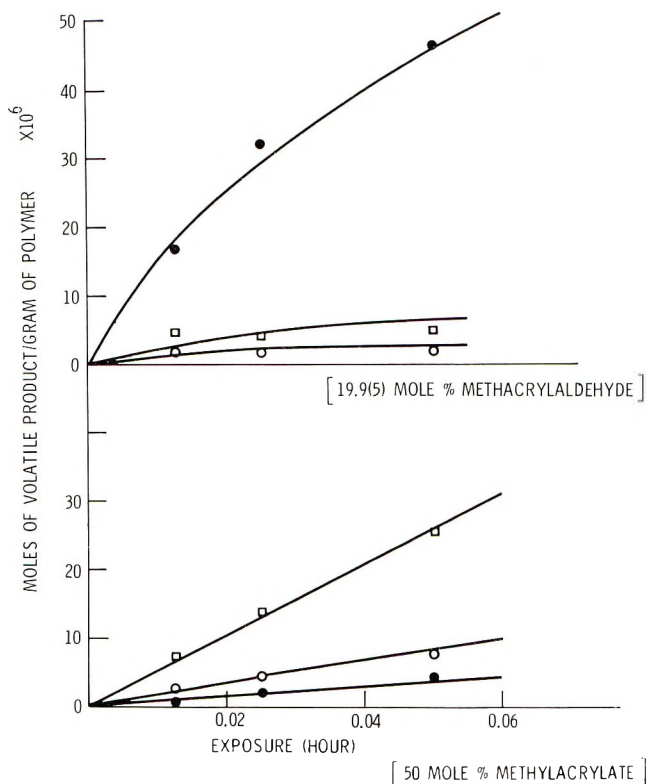


Fig. 9. Volatile fragments per gram of polymer vs. exposure at 30°C.: (●) carbon monoxide; (□) methanol; (○) methyl formate.

towards limiting values is observed for the latter. This may be a misleading impression, since these exposures did not exceed 3 min. At this juncture, it is difficult to escape from associating all volatile fragments with chain scission.

To elucidate this apparent congruence, the number of molecules of each compound presumed to be associated with a break in the polymer chain was determined graphically, i.e.,  $W_v N$  was plotted against  $W_p N \Delta / \bar{M}_{w_0}$ , the gradient of the graph resulting in the desired quantity. Where  $W_v$  is the initial amount of polymer (moles),  $N$  is Avogadro's number,  $W_p$  is the amount of volatile product (moles),  $\bar{M}_{w_0}$  is the weight-average molecular weight of the polymer sample before irradiation, and  $\Delta$  is the number of scissions per polymer chain.

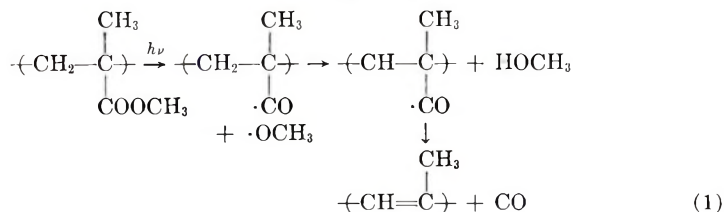
The dominating feature here is the multiplicity of fragments formed per chain scission in specimens free from aldehyde groups. Here prominence may be accorded to copolymers with methyl acrylate, yet this effect must be tempered by the realization that this is a system prone to crosslinking, hence, the disproportionately high ratio. Turning to the aldehyde copolymers, the fractional ratios for methyl formate and methanol indicate that very little volatile material emanates from chain scission. Yet at least one

molecule of carbon monoxide is eliminated during this process. Another interesting feature lies in the constancy of the ratio of methyl formate to methanol. At the same time, there can be no direct correlation between the yields of carbon monoxide and methanol. Here it may be concluded that photolysis of methyl formate produced by a primary act of decomposition to carbon monoxide and methanol occurs to negligible extent. Also, the formation of methanol is directly associated with the initial degradation of the ester group, but not necessarily with scission in the polymer chain.

### DISCUSSION

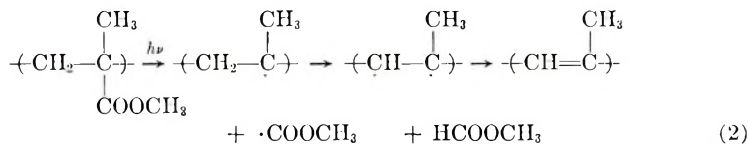
Whether or not polymers based on methyl methacrylate contain aldehyde units, it is plain that at least one molecule of carbon monoxide is evolved for each chain scission. The surplus must arise from photolysis of the carbomethoxy groups which is not a chain-destructive. It must also be distinguished from the amount of methanol realized since there is no correlation between the two quantities. It is no surprise that the ratios of the yields of carbon monoxide to the other compounds are very much greater for the aldehyde copolymers than for the poly(acrylic esters). Yet there is no proportionality existing between this number and the numbers of molecules of methyl formate and methanol calculated to be involved with each chain scission. Therefore, it is concluded that this mode of decomposition occurs independently of other chemical species present in the polymer, and moreover is an efficient chain-breaking process. This effect may be obscured by the propensity of the acrylaldehyde segments to indulge in cross-linking. But when these are replaced by methacrylaldehyde, the objection is no longer valid. In this system, the yield of carbon monoxide per chain-scission is at a minimum. In other words, the degradation mechanism is operating at maximum efficiency.

This reasoning is now extended to the mechanism of photodegradation of polymers prepared from methyl methacrylate and methyl acrylate. It has been noted that disproportionate amounts of methanol are formed for each break in the polymer chain. It is proposed that where carbomethoxy groups do not yield methyl formate, methoxy radicals are expelled which abstract hydrogen atoms to stabilize as methanol.<sup>14</sup> Should this abstraction take place at a neighboring carbon atom in the polymer backbone, the route is open for double-bond formation [eq. (1)].



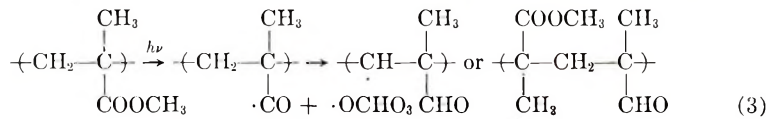
The elimination of a carbomethoxy radical which could either disproportionate to carbon monoxide and methoxy radical or abstract a hydrogen atom would be responsible for an identical effect in the polymer [eq. (2)].



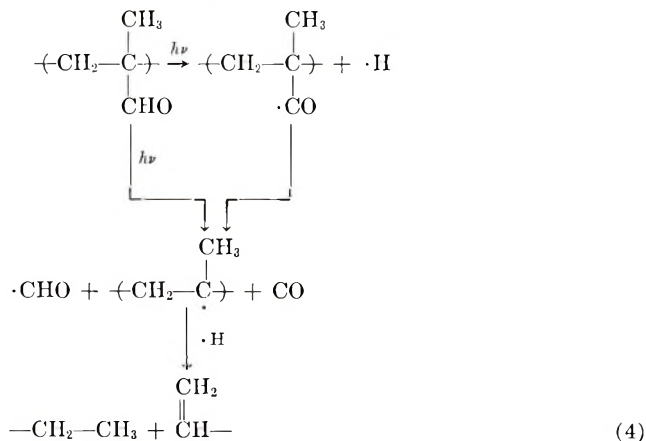


The yellowing of poly(methyl methacrylate), a result of exposure to ultra-violet light, is attributable to the presence of conjugated double bonds. This provides circumstantial evidence for this mechanism.<sup>7</sup>

Reverting to the postulate of methanol being expelled independently of chain scission, the free radical remaining with the polymer chain can stabilize by hydrogen abstraction to form an aldehyde group [eq. (3)].



Absorption spectra at 2850 Å. have been tentatively assigned to aldehyde groups formed in poly(methyl methacrylate) as a result of irradiation.<sup>7</sup> The degradative susceptibility of aldehydes is such that a choice of avenues is available for decomposition.<sup>15-17</sup> Either expulsion of the aldehyde radical, or the release of the hydrogen atom followed by evolution of carbon monoxide results in chain scission [eq. (4)]



Formaldehyde has been observed to form during the photodegradation of poly(methyl acrylate).<sup>12</sup> Hydrogen has been detected in studies with poly(methyl methacrylate).<sup>6</sup> Methane and carbon dioxide are considered to be final products resulting from the decay of free radicals generated by the initial photolytic act.<sup>6</sup>

## CONCLUSION

It is concluded that photolysis of aldehyde groups in copolymers of methyl methacrylate with acrylaldehyde or methacrylaldehyde leads directly to chain scission. Further, it is proposed that the photolytically induced

presence of aldehyde groups in poly(methyl methacrylate) is primarily responsible for chain scission in this polymer.

The author's appreciation is extended to Messrs. T. O. Morgan and J. M. Montgomery of the General Motors Research Laboratories for the determination of viscosities.

### References

1. M. I. Frolova, L. I. Efimov, and I. V. Chekmodeeva, *Plasticheskie Massy*, **1964**, No. 3, 38.
2. A. Charlesby and D. K. Thomas, *Proc. Roy. Soc. (London)*, **A269**, 104 (1962).
3. J. F. Kircher, F. A. Sliemers, R. A. Markle, W. B. Gager, and R. I. Leininger, *J. Phys. Chem.*, **69**, 189 (1965).
4. Y. Hajimoto, N. Tamura, and S. Okamoto, *J. Polymer Sci. A*, **3**, 255 (1965).
5. A. T. Bullock and L. H. Sutcliffe, *Trans. Faraday Soc.*, **60**, 625 (1964).
6. R. B. Fox, L. G. Isaacs, and S. Stokes, *J. Polymer Sci. A*, **1**, 1079 (1963).
7. A. R. Shultz, *J. Phys. Chem.*, **65**, 967 (1961).
8. J. Bischoff and V. Desreux, *J. Polymer Sci.*, **10**, 437 (1953).
9. R. Srinivasan, *J. Phys. Chem.*, **67**, 1367 (1963).
10. F. Patat and W. Hoegner, *Makromol. Chem.*, **75**, 85 (1964).
11. B. Baysal and A. V. Tobolsky, *J. Polymer Sci.*, **9**, 171 (1952).
12. R. B. Fox, L. G. Isaacs, S. Stokes, and R. E. Kagarise, *J. Polymer Sci., A*, **2**, 2085 (1964).
13. S. Bywater, *J. Phys. Chem.*, **57**, 879 (1953).
14. J. W. Linnett, J. R. Gilbert, and I. A. Reed, *Nature*, **201**, 1211 (1964).
15. G. Wettermark, *Arkiv Kemi*, **18**, No. 1, 1 (1961).
16. K. Pfordte and G. Leuschner, *Ann.*, **622**, 6 (1959).
17. S. K. Ho, *Proc. Roy. Soc. (London)*, **A276**, 278 (1963).

### Résumé

La photodégradation sous vide à 30°C du polyméthacrylate de méthyle et de copolymères avec l'acroléine, la méthacroléine et l'acrylate de méthyle a été étudiée. Les polymères ont été examinés sous la forme de films, tels qui obtenus par la technique de lyophilisation. Au moins une molécule de monoxyde de carbone est dégagée par scission de chaîne. On en conclut que la scission dans le polyméthacrylate de méthyle est primariement le résultat de groupes aldéhydes formés par photoinduction.

### Zusammenfassung

Der Photoabbau vom Poly(methylmethacrylat) und Copolymeren mit Acrylaldehyd, Methacrylaldehyd und Methylacrylat im Vakuum bei 30°C wurde untersucht. Die Polymeren wurden in Form von expandierten Filmen, wie sie durch ein Gefriertrocknungsverfahren erhalten werden, untersucht. Wenigstens ein Molekül Kohlenmonoxyd wird für jede Kettenspaltung entwickelt. Man kommt zu dem Schluss, dass die Kettenspaltung bei Poly(methylmethacrylat) primär durch photoinduzierte Aldehydgruppen zustande kommt.

Received July 30, 1965

Revised September 24, 1965

Prod. No. 4931A

## Investigation of Autoacceleration Effects during the Solution Polymerization of Styrene\*

J. E. GLASS and N. L. ZUTTY, *Research and Development Department, Plastics Division, Union Carbide Corporation, South Charleston, West Virginia*

### Synopsis

The possibility of obtaining increases in the rate and degree of polymerization through a decrease in the termination rate in nonviscous, homogeneous solution polymerizations of styrene has been investigated. Decreases in the termination rate were achieved through decreasing segmental diffusion of the propagating macroradical by greater occlusion, on the average, of the radical in the coiled polymeric chain. Coiling of the polymeric chain was effected by polymerizing styrene in thermodynamically poor ( $\theta$ ) solvents near the  $\theta$  temperature for polystyrene. Examples of such systems are diethyl oxalate at 51.5°C. and cyclohexane at 34.6°C. Polymerization under these conditions did lead to a decrease in the  $k_t/k_p^2$  kinetic ratio; this decrease resulted in increases in the degree of polymerization, but changes in the rate of polymerization, in contrast to the marked increases noted in viscous solution or heterogeneous polymerizations, were not observed. Possible explanations for the latter observations are discussed.

### INTRODUCTION

Increases in the rate and degree of polymerization, due to autoacceleration effects during the course of free radical initiated vinyl polymerizations, have been related to three variables; solution viscosity,<sup>1-8</sup> heterogeneous conditions,<sup>9</sup> and chain coiling.<sup>10</sup>

Autoacceleration resulting from an increase in solution viscosity, the Trommsdorff or gel effect, has been studied extensively.<sup>1-8</sup> The autocatalytic effect is ascribed to the increased viscosity of the system (achieved after a certain conversion) which so retards the translational diffusion of the propagating polymer radical that the bimolecular termination reaction becomes diffusion-controlled; however, the propagating macroradicals are not appreciably affected in their continued reaction with the smaller, more mobile, monomer entities, i.e., the propagation rate constant remains constant. As a result of a decrease in the termination rate constant, in a viscous media where diffusion control termination is operative, there is an increase in the overall rate of polymerization, an inversely related property.

$$R_p = \sqrt{fk_d[I]/k_t(k_p)} [M] \quad (1)$$

\* Presented in part at the 150th Meeting of the American Chemical Society, Atlantic City, N. J., September 1965.

where  $R_p$  is the rate of polymerization,  $f$  is efficiency of the initiator,  $k_d$  is the dissociation rate constant of initiator,  $[I]$  is the concentration of initiator (mole/liter),  $k_t$  is the termination rate constant,  $k_p$  is the propagation rate constant, and  $[M]$  is monomer concentration (moles/liter). The resulting increase in the kinetic chain length accompanying the above changes leads to an increase in the degree of polymerization,

$$\frac{1}{\bar{P}_n} = C_M + C_S \frac{[S]}{[M]} + \left(\frac{k_t}{k_p^2}\right) \frac{R_p}{[M]^2} + C_I \left(\frac{k_t}{k_p^2 f k_d}\right) \frac{R_p^2}{[M]^3} + C_P \frac{[P]}{[M]} \quad (2)$$

where  $\bar{P}_n$  is the degree of polymerization,  $C_M$ ,  $C_S$ ,  $C_I$ ,  $C_P$  are transfer constants of polymer radical with monomer, solvent, initiator, and polymer, respectively,  $[S]$  is concentration of solvent (moles/liter), and  $[P]$  is concentration of polymer (moles/liter). The latter two terms in this equation are not important in the present investigation due to employment of an azo initiator<sup>11</sup> and low conversion studies.

Autoacceleration in the rate and degree of polymerization of heterogeneous bulk-polymerized vinyl halide and acrylonitrile is also a well-known phenomenon.<sup>9</sup> The increases, analogous to polymerization in solutions of high viscosity, have been related to a decrease in the termination rate constant. This decrease is a result of the insolubility of the polymer and its occluded radicals in the polymerizing monomer and thus limits termination.

Burnett and Melville<sup>10</sup> have explained a decrease in the termination rate constant, noted in moderate temperature (30°C.) solution (cyclohexane) polymerization of vinyl acetate, as resulting from coiling of the polymer chain. Flory<sup>12a</sup> has criticized this interpretation and noted that the decrease is a result of the heterogeneous experimental conditions employed. Aside from Burnett and Melville's questionable interpretation of their results, literature support of autoacceleration effects resulting from polymeric chain coiling is scarce. Evidence for such phenomena is indirect, namely, the rate and molecular weight correlations to stiffening of the polymer chain noted by North and Hughes<sup>13,14</sup> and to a passing comment, in the viscosity studies by Benson and North.<sup>5</sup> The latter authors noted an increase in the ratio of propagation to termination rate constants in the solution polymerization of methyl methacrylate conducted in diethyl ether (a thermodynamically poor solvent for the resultant polymer) relative to that conducted in ethyl acetate.

Recently, the theory of Kuhn and Kuhn<sup>15</sup> for the diffusion of polymer chain ends has been correlated<sup>16</sup> by Burkhart with the segmental diffusion termination mechanism<sup>1,2</sup> for free-radical polymerizations. An expression was obtained for the termination rate constant in terms of certain hydrodynamic properties of polymer molecules. This equation suggests that polymeric chain coiling in the solution polymerization of vinyl monomers might effect an increase in the rate and degree of polymerization. This study was undertaken, as a result of Burkhart's equation, to investigate the

aspects of solution polymerization in which segmental motion of the polymer chain is reduced through chain coiling.

## EXPERIMENTAL

### Materials

All solvents employed were dried with an appropriate desiccant, filtered, and distilled through a Nester-Faust spinning band column. Calcium chloride was used to dry acetone and methyl ethyl ketone (Union Carbide Corp.), and *n*-butanol, benzene, and diethyl oxalate (Matheson, Coleman, and Bell); calcium hydride was employed for ethyl acetate. Middle fractions of initial distillations were redistilled from  $\alpha, \alpha'$ -azobisisobutyronitrile until vapor-phase chromatographic analysis revealed 100% purity except in the *n*-butanol and diethyl oxalate cases. Boiling points of the accepted fractions were in agreement with literature values. Mass spectral data indicated lower boiling alcohol impurities (0.4%) in both *n*-butanol and diethyl oxalate. Cyclohexane, both Eastman and Matheson, Coleman, and Bell spectro grades and Phillips technical grade, was shown to contain impurities by vapor-phase chromatographic analysis. Time consuming distillations from  $\alpha, \alpha'$ -azobisisobutyronitrile failed to completely remove these impurities. Phillips research grade (99.94%) cyclohexane was shown by vapor-phase chromatographic analysis to be of 100% purity. This latter grade solvent was utilized without further purification in all cyclohexane studies.

$\alpha, \alpha'$ -Azobisisobutyronitrile (Eastman) was recrystallized twice from absolute ethanol. The material was stored under nitrogen and in the dark until utilized. Styrene (Union Carbide Corp.) was prepolymerized in bulk with  $\alpha, \alpha'$ -azobisisobutyronitrile to approximately 5–10% conversion before use. The unpolymerized material was flash distilled from the prepolymerization and stored in the dark at  $-20^{\circ}\text{C}$ . under nitrogen over night. It was redistilled into the dilatometric flasks within 24 hr.

### Procedure

Solutions were prepared by mixing weighed amounts of styrene with solvent at room temperature in 250-ml. volumetric flasks. These prepared samples were employed in calibrating the dilatometers used for the rate measurements. The dilatometers consisted of 125 ml. cylindrical bulbs sealed to  $1/8$  in. precision bore, Pyrex tubing. From the calibrated weights, an appropriate amount of styrene was distilled ( $28^{\circ}\text{C}$ . at 1–2 mm. Hg.) into the dilatometer. Solvent and catalyst ( $\alpha, \alpha'$ -azobisisobutyronitrile) employed at 1 mole-%, based upon and kept constant with respect to monomer concentration, were then added to the flask. The flasks were attached to a vacuum line and the samples frozen in liquid nitrogen. The flasks were evacuated, and the samples were degassed by thawing and refreezing. The dilatometers were sealed at a pressure of  $10^{-5}$  mm. Hg. Polymerizations were carried out at 60, 50, 40, and  $35^{\circ}\text{C}$ . Temperatures



were recorded on Taylor 20°C. range thermometers. A constant temperature of  $\pm 0.002^\circ\text{C}$ . was maintained with a Hallikainen Thermotrol unit. Temperature variations were noted with a Beckman thermometer. Agitation of the dilatometer contents was provided magnetically with a Labline Mag-nestir unit. The polymerizations were held, except in cases cited, to approximately 12% conversion or less. The movement of the meniscus was followed by means of a Gaertner cathetometer ( $\pm 0.05$  mm.). Polymerization rates, based on densities reported by Patnode and Scheiber<sup>17</sup> for monomeric and polymeric styrene, were calculated from the volume change. The polymer was recovered by precipitation in 20 to 30 times its volume of methanol, filtered, and dried under vacuum. The rate of polymerization based on the weight of polymer collected was slightly lower, but in good agreement with initial rates calculated from the volume change. The difference in the volume and weight calculated rates could foreseeably be due to low molecular weight methanol-soluble polymer fractions. No effort was made to ascertain this possibility.

### Viscosity Determinations

Intrinsic viscosities were determined in cyclohexanone at  $30^\circ\text{C}$ . in Cannon viscometers with flow times of approximately 100 sec. Kinetic energy corrections were neglected. Sufficient intrinsic viscosities were determined by graphical means in cyclohexanone to calculate a Huggins constant<sup>18,19</sup>  $k$  of 0.37 for polystyrene in this solvent. Thereafter this constant was used to calculate the intrinsic viscosities from one measurement at 0.2 wt.-% concentration through eq. (3).

$$\eta_{sp}/c = [\eta] + k[\eta]^2c \quad (3)$$

Intrinsic viscosities determined in cyclohexanone were transposed into data applicable to benzene solutions through eq. (4)

$$\log [\eta]_{\text{C}_6\text{H}_6} = 0.029 + 1.01 \log [\eta]_{\text{C}_6\text{H}_{10}\text{O}} \quad (4)$$

derived<sup>20</sup> from selected common viscosity determinations in benzene (Ubbelohde viscometers). Molecular weights were determined from the latter intrinsic viscosities of the unfractionated polymers through Mayo's equation<sup>21</sup> for benzene solutions, i.e., eq. (5):

$$\bar{M}_n = 167,000[\eta]^{1.37} \quad (5)$$

Bulk solution viscosities of the solvents and solvent-monomer-polymer mixtures, indicative of initial conditions in the lower molarity investigations at  $40^\circ\text{C}$ ., were made with a Brookfield viscometer. Intrinsic viscosities determined in order to calculate the root-mean-square end-to-end distance<sup>12b</sup>  $(\bar{r}^2)^{1/2}$  of polymer at various solvent-monomer concentrations were obtained in Ubbelohde (cyclohexane, benzene, and acetone-based solutions) and Cannon (diethyl oxalate-based solutions) viscometers.



## RESULTS AND DISCUSSION

Investigations of styrene polymerizations were undertaken with several different solvents. The approach utilized was simple. The kinetics of the solution polymerizations of styrene were studied at a temperature above the  $\theta$  temperatures of the thermodynamically poor solvents; the temperature of polymerization was then lowered and the  $\theta$  points of the "poor" solvents were approached. A reference, thermodynamically "good" solvent, was employed for comparison with data from the thermodynamically poor solvents. Ethyl acetate was employed as the reference solvent at 60°C. From the results of these initial studies, ethyl acetate was discarded because of its relatively high transfer constant. Later intrinsic viscosity measurements also showed it to be a thermodynamically poor solvent. At the other temperatures investigated benzene was used as the thermodynamically good solvent. The thermodynamically poor solvents<sup>22</sup> utilized were diethyl oxalate, which has a  $\theta$  temperature at 51.5°C. for polystyrene; cyclohexane,  $\theta$  temperature, 34.6°C., and 2-butanone, which is a thermodynamically poor solvent for polystyrene at almost all temperatures<sup>23,24</sup> but which appears unique, in that the polymer is not precipitated from solution over a very wide temperature range. An abundance of data dealing with thermodynamic variables for polystyrene-solvent interactions for benzene, cyclohexane, and 2-butanone are available<sup>22</sup> in the literature. It should be noted at this point that heterogeneity was not noted in studies conducted at, or below, the  $\theta$  temperature of the poor solvents due to the cosolvent action of monomeric styrene. The solvents, 2-butanone, acetone, and ethyl acetate, were noted to produce lower rates and degrees of polymerization, relative to the other solvents studied, due to their greater transferring ability. The data from these investigations are included here because of the lack of literature data in solution polymerizations, and in support of the benzene solution experiments reported below.

Due to the lack of available information on the initial rates and molecular weights involved in heterogeneous polymerizations, *n*-butanol was employed as a solvent in some investigations so that information from solution polymerizations in thermodynamically poor solvents and heterogeneous polymerizations could be compared. This kinetic investigation was aimed primarily at the study of initial rates and molecular weights; however, some high-conversion studies were conducted in an effort to obtain a full spectrum of information.

### Low Conversion Studies

The data from these studies are presented graphically. Four types of graphs, denoting results of low conversion studies, are presented. Steady-state conditions are assumed in calculations of all kinetic data. From the information recorded in these graphs, it is evident that no differences in the rates of polymerization, outside of those due to chain transfer with solvent, are noted, regardless of solvent or temperature of the polymerization

TABLE I  
Transfer Constants for Solvents in Styrene Polymerization

Solvent	$C_s \times 10^3$		
	At 60°C.	At 40°C.	At 35°C.
Ethyl acetate	1.55	—	—
Diethyl oxalate	1.35	— <sup>a</sup>	— <sup>a</sup>
Cyclohexane	0.85	— <sup>a</sup>	— <sup>a</sup>
Benzene	—	0.58	0.39
<i>n</i> -Butanol <sup>b</sup>	—	1.12	—

<sup>a</sup> Nonlinear slope even at high styrene concentrations;  $C_s \cong 0$  at intermediate molarities.

<sup>b</sup>  $C_s$  taken from slope of homogeneous polymerization studies.

studied. However, it is apparent that there is a substantial increase in molecular weight of the polymers recovered from polymerization in the thermodynamically "poor" solvents as the  $\theta$  temperatures for polystyrene in the pure solvent are approached.

The nonlinearity of plots ( $1/\bar{P}_n$  vs.  $[S]/[M]$ , Figs. 1-3) used to determine chain transfer constants has been the subject of several recent investigations.<sup>25-27</sup> Transfer constants were determined from the slopes of the linear portions of these graphs (Table I). Chain transfer constants

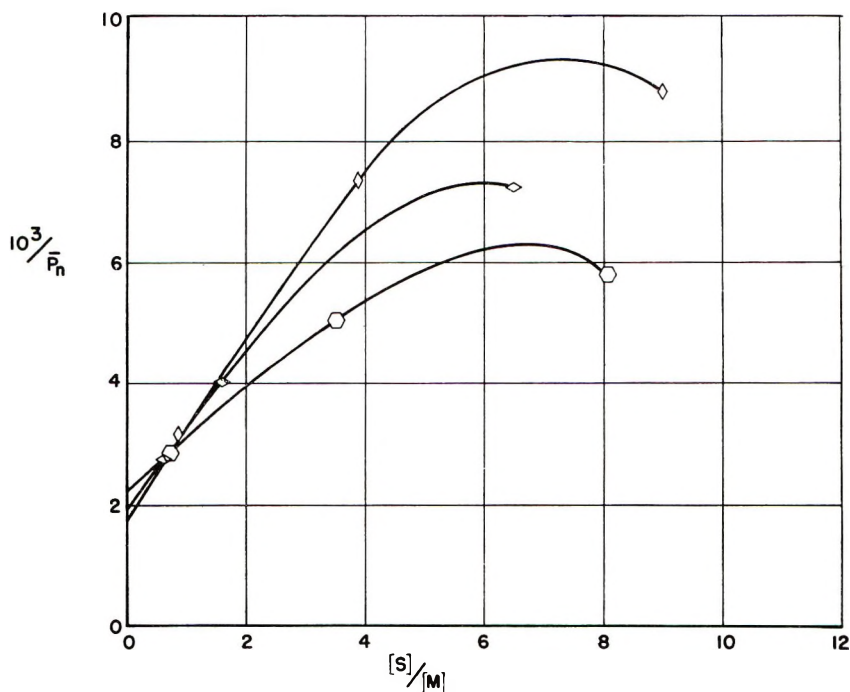


Fig. 1. Reciprocal degree of polymerization vs. solvent/monomer ratio, 60°C.: ( $\diamond$ ) ethyl acetate; ( $\diamond$ ) diethyl oxalate; ( $\circ$ ) cyclohexane.

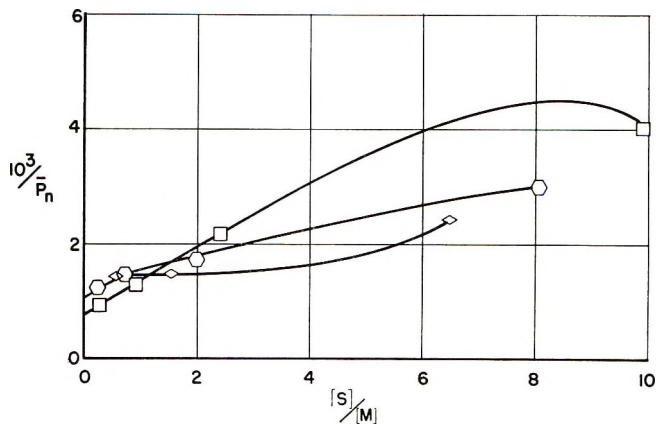


Fig. 2. Reciprocal degree of polymerization vs. solvent/monomer ratio, 40°C.: (□) benzene; (○) cyclohexane; (◇) diethyl oxalate.

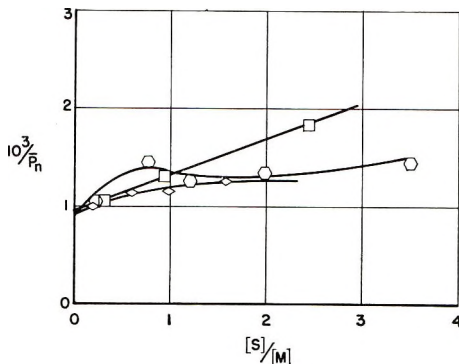


Fig. 3. Reciprocal degree of polymerization vs. solvent/monomer ratio, 35°C.: (□) benzene; (○) cyclohexane; (◇) diethyl oxalate.

for the respective solvents employed in the 60°C. experiments were obtained from Figure 1. The constant determined for cyclohexane is in fair agreement with that reported in the literature.<sup>21</sup> The transfer constant of diethyl oxalate was found to be greater than that of cyclohexane at 60°C.

It is evident from Figures 2 and 3 that the chain transfer constant of diethyl oxalate drastically changes as the  $\theta$  point (51.5°C.) is passed. The chain transfer constant for cyclohexane also can be noted to change rather drastically, relative to benzene, as its  $\theta$  point (34.6°C.) is approached. It is improbable that such drastic changes in the transfer constants of these solvents are due to any property of the solvents themselves that might change with temperature or that these particular solvents would have a smaller transfer constant than benzene. This appears to be the case near the  $\theta$  temperature. These results reflect changes in molecular weight in the polymerizations carried out in the various poor solvents, relative to those

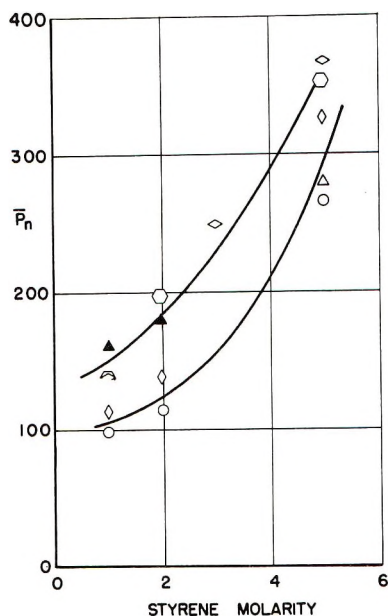


Fig. 4. Degree of polymerization vs. styrene molarity, 60°C.: ( $\Delta$ ) *n*-butanol, homogeneous polymerization; ( $\blacktriangle$ ) *n*-butanol, heterogeneous polymerization; ( $\diamond$ ) diethyl oxalate; ( $\diamond$ ) ethyl acetate; ( $\circ$ ) 2-butanone; ( $\circ$ ) cyclohexane.

conducted in the good solvent, benzene. It is to be emphasized, that no precipitation of polymer, except in cases where *n*-butanol was employed at monomer concentrations below 5*M*, was noted in these experiments.

The change in polymer molecular weight as a function of monomer concentration is shown more vividly in Figures 4–6. Since the molecular weights of polymers isolated from the poor solvents show increases not observed in the good solvent polymerizations, the question arises as to whether this increase is a result of a decreased termination rate constant.

TABLE II  
Variation of  $k_t/k_p^2$  Values with Solvent and Temperature

Solvent	$k_t/k_p^2$ values				
	At 60°C.	At 50°C.	At 40°C.	At 35°C.	At 30°C.
Benzene	—	—	7063	7112	
2-Butanone	1737	4417	—	—	
Acetone	—	—	12,258	—	
Diethyl oxalate	1585	665	<sup>a</sup>	<sup>a</sup>	
Cyclohexane	1434	1144	<sup>a</sup>	<sup>a</sup>	
Bulk styrene	1162 <sup>b</sup>	—	—	—	8260 <sup>b</sup>
	816 <sup>c</sup>	—	3044 <sup>c</sup>	—	

<sup>a</sup> Not constant with monomer concentration variation.

<sup>b</sup> Data of Matheson et al.<sup>28</sup>

<sup>c</sup> Data of Tobolsky and Offenbach.<sup>29</sup>

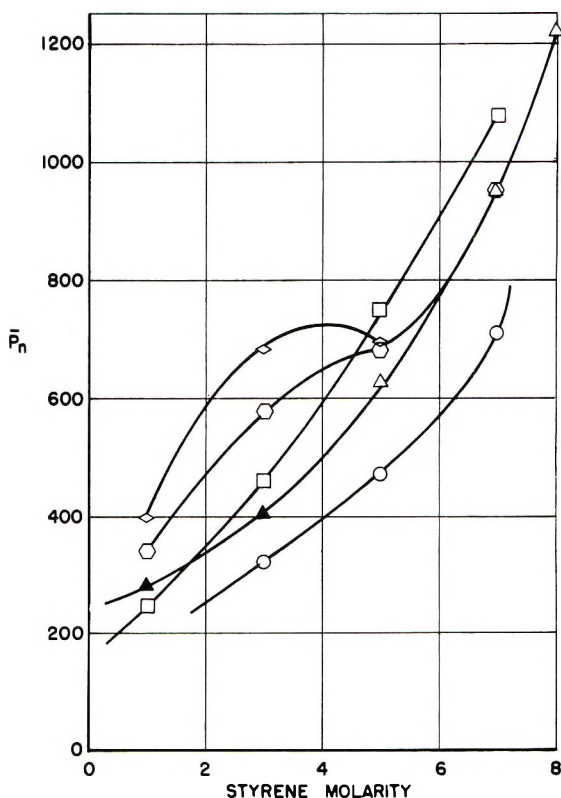


Fig. 5. Degree of polymerization vs. styrene molarity, 40°C.: ( $\Delta$ ) *n*-butanol, homogeneous polymerization; ( $\blacktriangle$ ) *n*-butanol, heterogeneous polymerization; ( $\circ$ ) cyclohexane; ( $\diamond$ ) diethyl oxalate; ( $\square$ ) benzene; ( $\circ$ ) acetone.

The significance of the data shown in Figures 7–9 is evident from eq. (2), the slope being equal to  $k_i/k_p^2$ . From the investigations of Matheson et al.<sup>28</sup> at 30 and 60°C. it is evident that the propagation rate constant increases faster, by at least a factor of two, than the termination rate constant as the temperature is increased. It would be anticipated from Matheson's data that in decreasing the temperature of polymerization an increase in the kinetic ratio,  $k_i/k_p^2$ , would result. This is evident from Matheson's, and also from Tobolsky's data<sup>29</sup> and from the ketonic solvent work shown in Table II. Within experimental error, there is no apparent difference in the  $k_i/k_p^2$  ratio as noted in the benzene studies at 35 and 40°C. (Fig. 7, Table II).

Data from the diethyl oxalate investigations are shown in Figure 8. A decrease in  $k_i/k_p^2$  is noted, in contrast to the literature cited above<sup>28,29</sup> and to the results in the benzene and ketonic solvent studies. Furthermore, the kinetic ratio is noted to depart from linearity in the studies conducted below 50°C. Analogous, contrasting results are noted in cyclohexane (Fig. 9) as the  $\theta$  temperature of the pure solvent (34.6°C.) is approached.

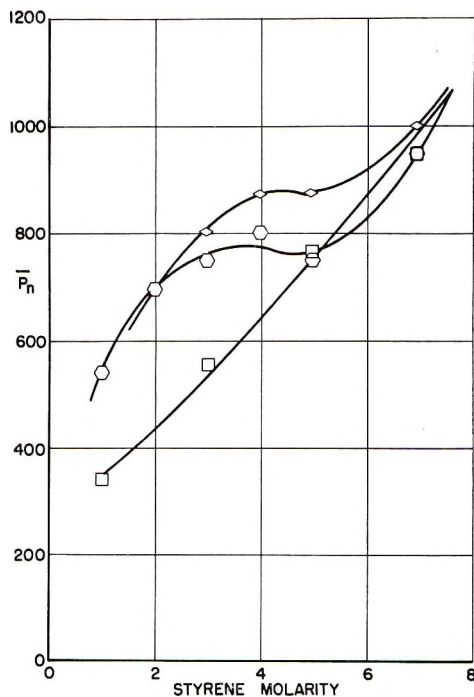


Fig. 6. Degree of polymerization vs. styrene molarity, 35°C.: (□) benzene; (○) cyclohexane; (◇) diethyl oxalate.

The decrease in  $k_t/k_p^2$  noted with decreasing temperature is indicative of a rapidly decreasing termination rate constant; it is evident that  $k_t$  decreases faster than  $k_p^2$  in cyclohexane and diethyl oxalate solvents with decreasing polymerization temperature. Calculated values of  $k_t/k_p^2$  are shown in Table II.

Increases in the degree of polymerization were correlated not only with a decreasing  $k_t/k_p^2$  ratio, but with decreasing chain dimensions for the polymer. The root-mean-square distance,  $(\bar{r}^2)^{1/2}$  between the ends of a given polymer chain were determined through eq. (6) from intrinsic viscosity measurements.

$$(\bar{r}^2)^{1/2} = ([\eta]M/\Phi)^{1/3} \quad (6)$$

Intrinsic viscosity measurements were determined in monomeric styrene-solvent mixtures representative of initial 1, 3, and 5M solutions at 40°C. Three polymers of appropriate molecular weights for the respective molarities were used. The values are listed in Table III; they are intended only to show the correlation of molecular weight changes with polymer chain coiling. The reader is cautioned<sup>30-34</sup> against making comparisons between the data from cyclohexane and diethyl oxalate solutions because of the difference in the chemical nature of the two solvents and the differences in the proximity of their respective  $\theta$  temperatures. Differences in the



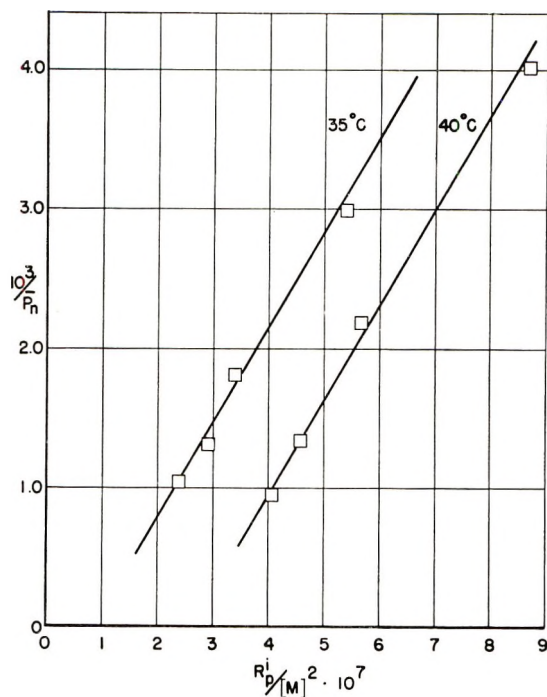


Fig. 7. Benzene solution data.

chemical nature of the solvents employed, and their capability of preferential interactions with polymers of different molecular weights should also serve to admonish any detailed analysis of the data in Table III. The employment of cosolvent systems<sup>35,36</sup> wherein preferential solvation of the polymeric chain by the common solvent, monomeric styrene, may vary as a function of the cosolvent adds further disorder to an already complicated system. Caution is also advised in comparing the thermodynamic data calculated at different concentrations due to possible variance in the value of the Flory constant<sup>20</sup>  $\Phi$  in eq. (6) with concentration. This variance could be caused by the failure, at lower values of  $\bar{M}_n$ , of a linear relationship between the excluded volume of the polymer coil and  $(\bar{r}^2)^{3/2}$ , an assumption used<sup>30</sup> in fixing the value of  $\Phi$  in eq. (6). The temperature required for the thermodynamically poor solutions to produce approximately the same degree of change in the kinetic ratio,  $k_t/k_p^2$ , is not in proportion to the respective  $\theta$  temperatures of the pure solvents, diethyl oxalate (51.5°C.) and cyclohexane (34.6°C.). The above considerations are probably of equal importance, along with the transfer constants of the respective solvents, in producing the difference in the effective temperatures required. Data obtained from ketonic solvent investigations would indicate that the above considerations are of secondary importance to transfer constants, in determining an effective temperature for the production of increased molecular weight polymer from the latter solutions.

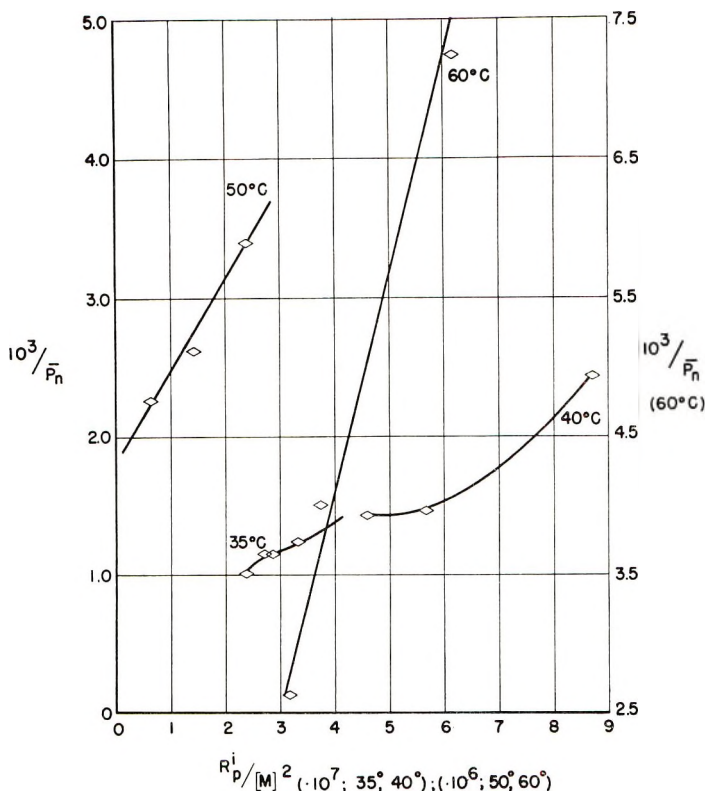


Fig. 8. Diethyl oxalate solution data.

With the achievement of increased polymer molecular weights under certain specified solution conditions, the question arises whether an increase in the rate of polymerization accompanies the changes in the degree of polymerization. From eq. (1), in the specific cases where  $k_t/k_p^2$  was noted to decrease with decreasing temperature, one would expect, provided other kinetic factors in the equation did not vary, an increase in the rates of polymerization.

Figure 10 shows the rates of polymerization found in studies at 40°C., the higher molarity denoting that of bulk-polymerized styrene. It is obvious from these data that the rates of polymerization are not a linear function of monomer concentration. It is also evident that there is no difference, outside of those explainable through relative differences in chain transfer constants, in the rates of polymerization among the various solvents investigated. These two observations were found to hold for plots for  $R_p$  versus  $[M]$  or  $R_p$  versus  $[M][I]^{1/2}$  at the other temperatures studied. It is obvious from Figure 10 that the kinetic ratio,  $(fk_d/k_t)^{1/2}k_p$  is a function of the monomer concentration and is not constant over the dilution range studied. This ratio can be plotted over the intermediate monomer concentrations as a linear function of the molarity; this is also

TABLE III  
Intrinsic Viscosities of Polystyrene in Monomeric Styrene-Solvent Polymerization Mixtures

	At 30°C.			At 60°C.		
	$[\eta]$ , dl./g.	$(\bar{r}^2)^{1/2} \times$ $10^6$ , cm. <sup>a</sup>	Variance from C <sub>6</sub> H <sub>6</sub> solution, %	$[\eta]$ , dl./g.	$(\bar{r}^2)^{1/2} \times$ $10^6$ cm. <sup>a</sup>	Variance from C <sub>6</sub> H <sub>6</sub> solution, %
5M solutions <sup>b</sup>						
Benzene	0.45	2.45	—	0.45	2.45	—
Cyclohexane	0.42	2.39	2.3	0.42	2.39	2.3
Diethyl oxalate	0.41	2.37	3.1	0.41	2.37	3.1
Acetone	0.41	2.37	3.1	—	—	—
3M solutions <sup>c</sup>						
Benzene	0.37	2.03	—	0.37	2.03	—
Cyclohexane	0.30	1.90	6.7	0.36	2.01	0.9
Diethyl oxalate	0.24	1.76	13.4	0.32	1.94	4.7
Acetone	0.29	1.87	7.9	—	—	—
1M solutions <sup>d</sup>						
Benzene	0.20	1.35	—	0.21	1.37	—
Cyclohexane	0.17	1.28	5.6	0.21	1.37	0
Diethyl oxalate	0.15	1.23	9.4	0.19	1.33	3.3

<sup>a</sup> Calculated from eq. (6);  $\Phi = 2.1 \times 10^{21}$ .

<sup>b</sup> Polymer of  $\bar{M}_n = 68,735$  employed.

<sup>c</sup> Polymer of  $\bar{M}_n = 47,756$  employed.

<sup>d</sup> Polymer of  $\bar{M}_n = 25,988$  employed.

true of the kinetic ratio  $k_t/k_p^2$ . Since the latter kinetic ratio varies with solvent at a given temperature (Table II), the catalyst efficiency, dissociation constant, and perhaps the order of dependence upon the catalyst concentration must also vary with solvent in order to maintain the same rate of polymerization in benzene, diethyl oxalate and cyclohexane.

Consideration of the magnitude of the molecular weight changes is of interest with respect to these latter considerations. The differences between polymerizations in benzene and cyclohexane will be examined because kinetic parameters in these solvents have been reported. The variance in the degree of polymerization (at 35°C., Fig. 6) at 3 and 1M is approximately 23 and 35%, respectively. Since the relative difference in contribution, between the two solvents studied, of  $C_M$ ,  $C_S$ , and  $C_P$  terms in eq. 2 to the  $\bar{P}_n$  term will be negligible,  $1/P_n \cong (k_t/k_p^2)R_p/[M]^2$ . Considering the equality of rate and monomer concentration at any particular molarity, the variance in polymer molecular weight between benzene and cyclohexane reflect corresponding differences in  $k_t/k_p^2$  or  $k_t$  if one considers  $k_p$ , in analogy with viscous or heterogeneous polymerization phenomena, essentially constant.

A difference in the dissociation rate of  $\alpha, \alpha'$ -azobisisobutyronitrile has previously been found<sup>37</sup> at 50°C. for three of the solvents employed, benzene ( $2.18 \times 10^{-6}$  sec.<sup>-1</sup>), cyclohexane ( $1.50 \times 10^{-6}$  sec.<sup>-1</sup>), and 2-butanone

( $2.06 \times 10^{-6}$  sec. $^{-1}$ ). Assuming other factors constant, the dissociation constants, through a process defined by eq. (1), produced a substantial difference (17%) in the rate of polymerization. From differences in the calculated and observed rates, an increase in the rate of polymerization from the cyclohexane solution might well be claimed.

Examination of the literature, with respect to variation in the efficiency of  $\alpha, \alpha'$ -azobisisobutyronitrile in initiating vinyl polymerization, reveals an appreciable fluctuation with monomer dilution. A decrease<sup>38</sup> of almost

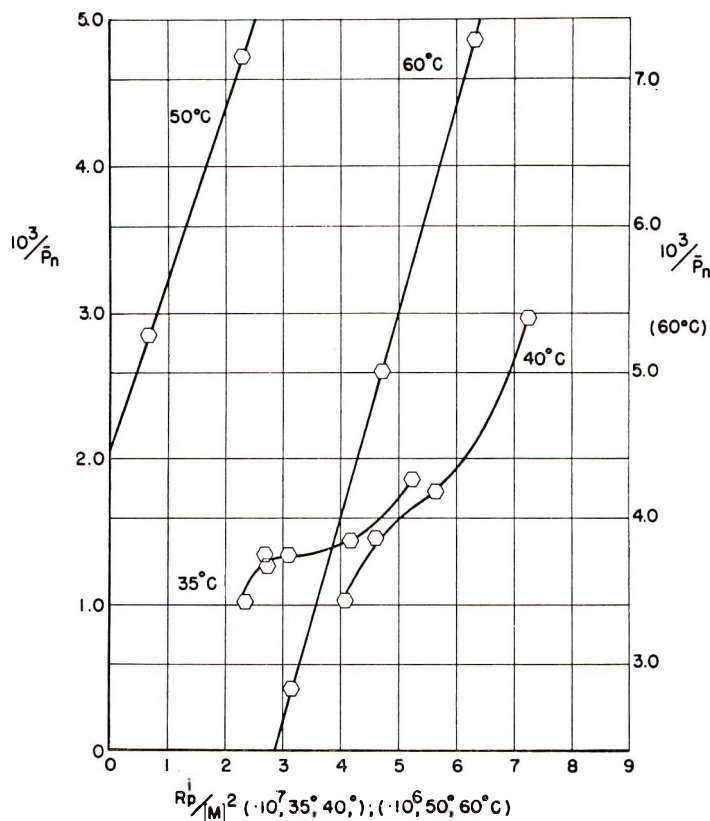


Fig. 9. Cyclohexane solution data.

100% has been noted by Pryor, for the efficiency of the azo catalysts initiating the polymerization of styrene in a 50% dioxane solution ( $f = 0.36$ ) when compared to that in pure styrene ( $f = 0.60$ ). Van Hook and Tobolsky,<sup>39</sup> in styrene-benzene solution polymerization studies, noted a linear dependence for the efficiency of  $\alpha, \alpha'$ -azobisisobutyronitrile in initiating polymerizations at various initiator concentrations above 0.05 mole/l. Below this threshold concentration the efficiency increased nonlinearly; the departure from linearity was attributed to a decrease in secondary combination reactions of the catalyst at low concentrations.

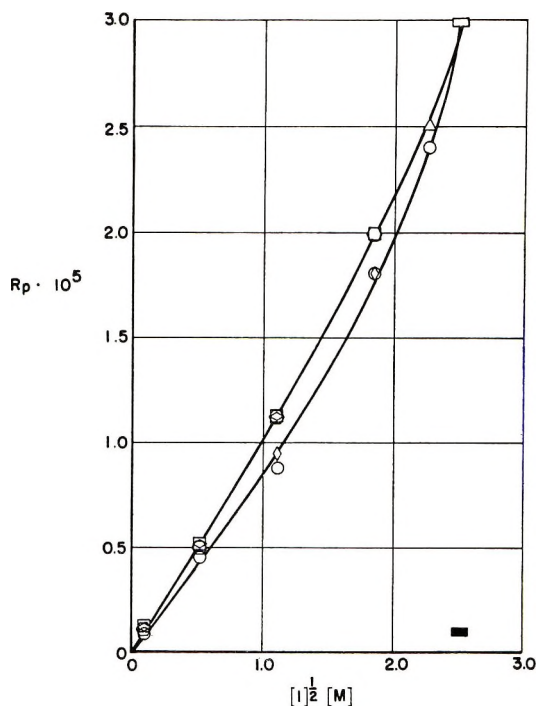


Fig. 10. Rate of polymerization at 40°C.: ( $\square$ ) bulk styrene, azo-initiated; ( $\blacksquare$ ) bulk styrene, thermally initiated; ( $\Delta$ ) *n*-butanol, homogeneous polymerization; ( $\circ$ ) acetone; ( $\diamond$ ) ethyl acetate; ( $\diamond$ ) diethyl oxalate; ( $\square$ ) benzene; ( $\circ$ ) cyclohexane.

The catalyst concentrations employed in these investigations (1 mole-% based upon and kept constant with respect to the monomer molarity) was below the linear dependent concentration defined above by Tobolsky. The question of whether or not this threshold concentration is the same in cyclohexane and diethyl oxalate solutions has not been answered. The differences in the dissociation constants of the azo catalyst in cyclohexane and benzene solutions would suggest the definite possibility of a lower threshold concentration and efficiency values, perhaps due to cage effects,<sup>40</sup> in the cyclohexane solutions.

Employing the different  $k_d$  values noted by Olivé at 50°C. and assuming, as an extreme case, an efficiency difference of two for the azo catalyst in the two solvents,  $f = 0.6(\text{C}_6\text{H}_6)$ ;  $f = 0.3(\text{C}_6\text{H}_{12})$  the calculated difference in rates, through the process defined by eq. (1), amounts to approximately 40%. This is of equivalent magnitude to the relative difference in the degree of polymerization noted in the 1M study at 35°C.; thus the effective changes in  $f$  and  $k_d$ , due to the different solvent media, could conceivably offset the  $k_i/k_p^2$  or  $k_t$  changes noted.

If there is a sufficient difference in catalyst efficiency in the different solvents and this efficiency is dependent upon the catalyst concentration, the rate dependence upon catalyst concentration is also likely to vary with



solvent.<sup>41</sup> At the low catalyst and monomer concentrations employed in these investigations, it has been established that the first-order and half-order dependence of the rate upon monomer and catalyst concentrations, respectively, are not valid.<sup>42</sup> Thus, it can be recognized that the lack of variance in the rates of polymerization observed need not correlate with increases in the degree of polymerization noted between the thermodynamically poor and good solvents if kinetic variables such as  $f$ ,  $k_d$ , and the order of dependence upon the catalyst concentration are dependent upon the nature of the nonpolymerizing medium. Additional experiments, particularly at varying catalyst concentrations, must be conducted in order to determine how the above kinetic factors, independently or collectively, vary as a function of the solvent employed.

It should be pointed out that a similar finding in the solution polymerization of styrene in benzene and dioxane has been noted by Olivé.<sup>43</sup> He found a 6–40% increase, the increase correlating with the increased amount of solvent employed, in the molecular weight of polymer isolated from dioxane relative to that isolated from benzene solutions, while the rates in both solvents were equivalent. The chain-coiling explanation offered for the observations noted in this paper may be applicable to Olivé's observations, since dioxane, denoted by its relative cohesive energy value,<sup>23</sup> is a poorer solvent than benzene for polystyrene.

### High-Conversion Studies

Several polymerizations to high conversions at 40°C. were also carried out. These investigations were conducted by techniques similar to the kinetic studies investigated dilatometrically; however, they were conducted in cylindrical tubes and agitated by rotation in a constant temperature bath. Heterogeneous polymerizations were also conducted in this series of experiments.

Autoacceleration is apparent (Fig. 11) in the heterogeneous polymerization conducted in *n*-butanol at 1*M* styrene concentration. The polymers isolated during the prolonged time periods studied showed substantial increases in molecular weight (50 hr.,  $\bar{M}_n = 56,190$ ; 100 hr.,  $\bar{M}_n = 280,906$ ; 168 hr.,  $\bar{M}_n = 331,400$ ). Polymers isolated from cyclohexane and diethyl oxalate ( $\bar{M}_n = 36,680$ ) were again higher, and of the same initial magnitude, than those isolated from benzene solutions ( $\bar{M}_n = 23,374$ ). Polymers isolated from the poor solvents maintained a constant degree of polymerization over the prolonged time period; they were not noted to increase in molecular weight as a function of time as was the case in the heterogeneous *n*-butanol studies. Analogous results were recorded, except in the *n*-butanol case, in the 3*M* solution studies (Fig. 12). In the 3*M* heterogeneous polymerizations a notable decrease in the autocatalytic effect was noted. The relative difference in the rate accelerations of the 1*M* and 3*M* heterogeneous solutions can be explained by the manner of precipitation noted in the two instances. An even, well distributed, granular precipitate characterized the 1*M* solutions, a solid lump at one end of the



reaction tube, which presumably led to separation of the buried propagation macroradicals and monomer,<sup>9</sup> characterized the 3*M* solution.

The intent of these investigations was to increase the rate and degree of polymerization by limiting segmental diffusion through chain coiling. The degree of success was dependent upon the degree of occlusion provided the macroradical end by the coiled polymer. Dilution of the thermodynamically poor solvents with various concentrations of monomer detracted from true  $\theta$  conditions and possibly dampened observation of the magnitude of the effect. In an attempt to overcome this latter detraction, periodically

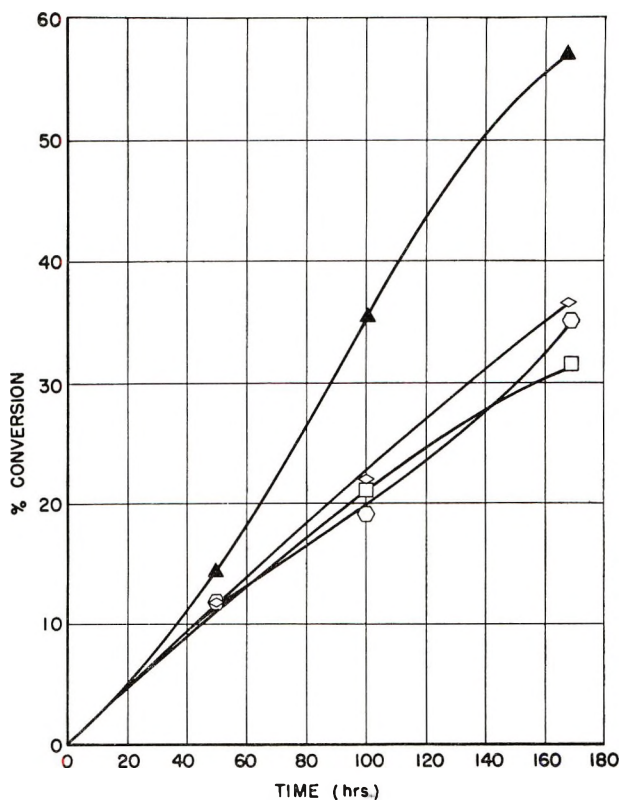


Fig. 11. Conversion of 1*M* styrene solutions at 40°C.: (□) benzene; (○) cyclohexane; (◇) diethyl oxalate; (▲) *n*-butanol, heterogeneous polymerization.

heterogeneous polymerizations in benzene–butanol mixtures were conducted. The differences in the rate and degree of polymerization for the 70:30, 50:50, and 30:70 benzene–butanol mixtures bridged the difference, in order of apparent heterogeneity, between the conversion and molecular weight observed in the thermodynamically “good” and “poor” solvents. Heterogeneity in these mixed solvent systems is best described as a milky liquid partially immiscible with a clearer liquid; no large amount of solid precipitate was noted in such instances.

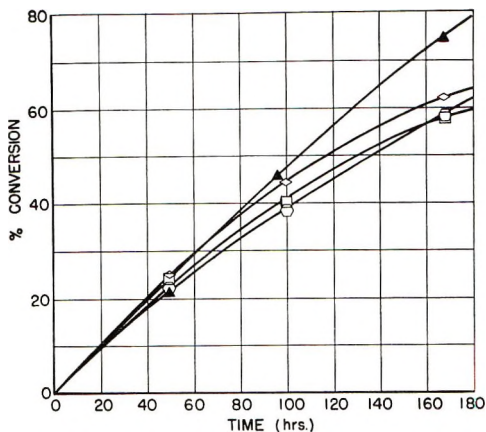


Fig. 12. Conversion of 3*M* styrene solutions at 40°C.: (□) benzene; (○) cyclohexane; (◇) diethyl oxalate; (▲) *n*-butanol, heterogeneous polymerization.

In contrast to the above findings, studies of initial rates (dilatometrically) and molecular weights in these mixed solvent systems did not show any differences with variance of the butanol-benzene ratio. All of the initial studies were terminated while they were still homogeneous (less than 5% conversion). Also, in contrast, differences between the initial and the prolonged heterogeneous investigations in *n*-butanol were noted. In the high-conversion studies in pure butanol, increases in the rate and molecular weight were noted with heterogeneous conditions. In the low-conversion studies in *n*-butanol no increases were noted. The lack of autoacceleration found in the low-conversion, well agitated, heterogeneous experiments was not found to be the case for the initially homogeneous, low-conversion polymerizations conducted in *n*-butanol (5*M* in styrene). In these latter studies, concentrations below 5*M* yielded precipitate instantaneously with polymer formation. At 5*M* or greater the solutions were homogeneous; a 5*M* solution was homogeneous for the first 5 hr. of polymerization at 40°C. At this time a light bluish tinge, indicative of small particle formation, was noted. Between 5 and 11 hr. this tint remained and heterogeneity was evident thereafter. During these first 11 hr. of polymerization at 40°C., there is a gradual and constant increase in the rate of polymerization. These values are listed in Table IV.

TABLE IV

Autoacceleration in the Initial Rate of Polymerization of 5*M* Styrene in *n*-Butanol at 40°C.

Reaction time, hr.	$R_p \times 10^5$ , mole/l. sec.
1.5-3.0	1.02
4.0-6.5	1.07
9.5-11.0	1.14

The increases (9% within 9% conversion) noted in Table IV would not have been noted in comparison of rates between polymerization runs in different solvents. In comparison of rates between solvents these differences would have been within experimental error.

Accessibility of monomer and solvent throughout the macrochain was evident by the swollen nature of the polymer in the mixed solvent studies. No large increases, comparable to those noted in *n*-butanol for prolonged time periods (>50 hr. at 40°C.), in either the rate or degree of polymerization was noted in the mixed solvents investigated. These later observations shed a great deal of light upon the findings of these investigations. The heterogeneous polymerized "swollen" polymers obtained in the mixed benzene-butanol solution polymerizations did not achieve the same high molecular weights noted in the *n*-butanol precipitated polymers because of solvation. Solvation,<sup>12c</sup> probably preferentially by benzene molecules, allowed sufficient mobility to the polymer coil so that termination of the propagating macroradicals was only slightly retarded with respect to that in unswollen heterogeneous polymerizations. Analogously, this preferential solvation was likely provided by monomeric styrene in the  $\theta$ -solvent solution polymerizations. The change in polymerization rate that such a modified termination rate would produce, would likely be minor, particularly in view of possible varying catalyst efficiencies and dissociation constants discussed above.

A degree of variance, comparable with our findings, is noted in the heterogeneous and homogeneous polymerizations, in thermodynamically good and poor solvents, of methyl methacrylate.<sup>8</sup> Analysis of these data, however, is complicated by a predominating gel effect and the wide range of transferring ability exhibited by the solvents employed.

No correlation was noted between the solution viscosities and the degree or, rate squared,<sup>44</sup> of polymerization in the low-conversion studies. This and the high-conversion results eliminate the possibility that increases in polymer molecular weight are due to viscosity effects. Due to the observance of the changes in dilute solutions, at low conversions with decreasing polymerization temperature, the possibility that the increases in molecular weight result from a reaction<sup>43,45-47</sup> between initiator radical and complete polymer molecules can be ruled out.

In summary, it appears that solvation of the polystyrene chain and possibly solvation of the propagating macroradical exist up to the point of precipitation; this provides sufficient mobility to the polymeric radical so that termination of the macrospecies is not greatly dampened.

### References

1. A. M. North and G. A. Reed, *J. Polymer Sci. A*, **1**, 1311 (1963).
2. S. W. Benson and A. M. North, *J. Am. Chem. Soc.*, **84**, 935 (1962).
3. J. N. Atherton and A. M. North, *Trans. Faraday Soc.*, **58**, 2049 (1962).
4. A. M. North and G. A. Reed, *Trans. Faraday Soc.*, **57**, 859 (1961).
5. S. W. Benson and A. M. North, *J. Am. Chem. Soc.*, **81**, 1339 (1959).
6. S. W. Benson and A. M. North, *J. Am. Chem. Soc.*, **80**, 5625 (1958).

7. E. Trommsdorff, Colloquium on High Polymers, Freiburg (1944).
8. R. G. W. Norrish and R. R. Smith, *Nature*, **150**, 336 (1942).
9. C. H. Bamford, W. A. Barb, A. D. Jenkins, and P. F. Onyon, *The Kinetics of Vinyl Polymerization by Radical Mechanisms*, Academic Press, New York, 1958, Chap. 4; see references therein.
10. G. M. Burnett and H. W. Melville, *Proc. Roy. Soc. (London)*, **A189**, 494 (1947).
11. A. V. Tobolsky and J. Offenbach, *J. Polymer Sci.*, **16**, 311 (1955).
12. P. J. Flory, *Principles of Polymer Chemistry*, Cornell Univ. Press, Ithaca, N. Y., 1953, (a) p. 160; (b) Chap. 14; (c) p. 553.
13. J. Hughes and A. M. North, *Proc. Chem. Soc.*, **1964**, 404.
14. J. Hughes and A. M. North, *Trans. Faraday Soc.*, **60**, 960 (1964).
15. W. Kuhn and H. Kuhn, *Helv. Chim. Acta*, **28**, 1533 (1945).
16. R. D. Burkhart, *J. Polymer Sci. A*, **3**, 883 (1965).
17. W. Patnode and W. J. Scheiber, *J. Am. Chem. Soc.*, **61**, 3449 (1939).
18. T. Alfrey, A. Bartovics, and H. Mark, *J. Am. Chem. Soc.*, **64**, 1557 (1942).
19. M. L. Huggins, *J. Phys. Chem.*, **42**, 911 (1938).
20. C. E. H. Bawn, R. F. J. Freeman, and A. R. Kamalliddin, *Trans. Faraday Soc.*, **46**, 1107 (1950).
21. F. R. Mayo, R. A. Gregg, and M. S. Matheson, *J. Am. Chem. Soc.*, **73**, 1691 (1951).
22. G. V. Schulz and H. Baumann, *Makromol. Chem.*, **60**, 120 (1963).
23. D. J. Streeter and R. F. Boyer, *Ind. Eng. Chem.*, **43**, 1790 (1951).
24. R. F. Boyer and R. S. Spencer, *J. Polymer Sci.*, **3**, 97 (1948).
25. M. H. George, *J. Polymer Sci. A*, **2**, 3169 (1964).
26. A. C. Toohey and K. E. Weale, *Trans. Faraday Soc.*, **58**, 2439 (1962).
27. G. Henrici-Olivé and S. Olivé, *Fortschr. Hochpolymer Forsch.*, **2**, 496 (1961).
28. M. S. Matheson, E. E. Auer, E. B. Bevilacqua, and E. J. Hart, *J. Am. Chem. Soc.*, **73**, 1700 (1951).
29. A. V. Tobolsky and J. Offenbach, *J. Polymer Sci.*, **16**, 311 (1955).
30. T. G. Fox, Jr., and P. J. Flory, *J. Am. Chem. Soc.*, **73**, 1904, 1915 (1951).
31. T. A. Orofino and A. Ciferri, *J. Phys. Chem.*, **68**, 3136 (1964).
32. U. Bianchi, *J. Polymer Sci. A*, **2**, 3083 (1964).
33. A. Ciferri, *J. Polymer Sci. A*, **2**, 3089 (1964).
34. T. A. Orofino and J. W. Mickey, Jr., *J. Chem. Phys.*, **38**, 2512 (1963).
35. J. F. Henderson and C. A. Winkler, *Can. J. Chem.*, **37**, 1225 (1959).
36. C. E. H. Bawn and R. D. Patel, *Trans. Faraday Soc.*, **52**, 1669 (1956).
37. G. Henrici-Olivé and S. Olivé, *Makromol. Chem.*, **58**, 188 (1962).
38. W. A. Pryor and G. L. Kaplan, *J. Am. Chem. Soc.*, **86**, 4234 (1964).
39. J. P. Van Hook and A. V. Tobolsky, *J. Phys. Chem.*, **62**, 257 (1958).
40. M. H. George and P. F. Onyon, *Trans. Faraday Soc.*, **59**, 1390 (1963).
41. A. V. Tobolsky and B. Baysal, *J. Polymer Sci.*, **11**, 471 (1953).
42. W. A. Pryor, A. Lee, and C. E. Witt, *J. Am. Chem. Soc.*, **86**, 4229 (1964); see reference 11.
43. G. Henrici-Olivé and S. Olivé, *Makromol. Chem.*, **37**, 71 (1960).
44. A. T. Guertin, *J. Polymer Sci. B*, **1**, 477 (1963).
45. G. Henrici-Olivé and S. Olivé, *Makromol. Chem.*, **27**, 166 (1958).
46. G. Henrici-Olivé and S. Olivé, *Kunststoffe-Plastics*, **5**, 315 (1958).
47. G. Henrici-Olivé and S. Olivé, *Mezhdunarod. Simp. Makromol. Khim., Dokl., Moscow*, **1960**, **3**, 243; *J. Polymer Sci.*, **48**, 329 (1960).

### Résumé

La possibilité d'obtenir un accroissement de vitesse et de degré de polymérisation en diminuant la vitesse de terminaison en solution homogène non visqueuse de styrène a été étudiée. On a obtenu une diminution de la vitesse de terminaison en diminuant la

diffusion des segments au sein du macroradical qui se propage grâce à une occlusion en moyenne plus grande du radical dans la chaîne polymérique enroulée en pelote. L'em-pelotonnement de la chaîne polymérique a été effectué en polymérisant le styrene dans des solvants thermodynamiquement pauvres au voisinage de la température  $\theta$  du poly-styrene. Des exemples de tels systèmes sont l'oxalate d'éthyle à 51.5°C, le cyclohexane à 34.6°C. La polymérisation dans de telles conditions amène à une diminution du rapport cinétique  $k_t/k_p^2$ ; cette diminution entraîne une augmentation du degré de polymérisation mais aucun changement de vitesse de polymérisation, contrairement à l'augmen-tation notoire de vitesse qui se manifeste en solution visqueuse ou en polymérisation hétérogène. Des explications possibles pour ces dernières observations sont discutées.

### Zusammenfassung

Die Möglichkeit, durch eine Herabsetzung der Abbruchgeschwindigkeit bei der Polymerisation von Styrol in nicht viskoser, homogener Lösung eine Zunahme der Polymerisationsgeschwindigkeit und des Polymerisationsgrades zu erhalten, wurde untersucht. Eine Abnahme der Abbruchgeschwindigkeit wurde durch Herabsetzung der Segmentdiffusion des wachsenden Makroradikals durch grösseren mittleren Ein-schuss der Radikals in der geknäuelten Polymerkette erreicht. Die Verknäuelung der Polymerkette wurde durch Polymerisation von Styrol in thermodynamisch schlechten ( $\theta$ ) Lösungsmitteln nahe der  $\theta$ -Temperatur für Polystyrol bewirkt. Beispiele für solche Systeme sind Diäthylloxalat bei 51,5°C und Zyklohexan bei 34,6°C. Polymerisation unter diesen Bedingungen führte zu einer Abnahme des kinetischen Verhältnisses  $k_t/k_p^2$ . Diese Abnahme lieferte eine Erhöhung des Polymerisationsgrades, jedoch wurde im Gegensatz zu der in viskoser Lösung oder bei heterogener Polymerisation auftretenden merklichen Zunahme keine Änderung der Polymerisationsgeschwindigkeit beobachtet. Mögliche Erklärungen für diesen Sachverhalt werden diskutiert.

Received July 23, 1965

Revised October 11, 1965

Prod. No. 4936A



## Untersuchung der Bildung von Polyesteramiden aus Dicarbonsäure-anhydriden und Oxazolidinonen-2

S. BURCKHARDT, K.-H. REICHERT, und K. HAMANN,  
*Forschungsinstitut für Pigmente und Lacke e. V., Stuttgart,  
Germany*

### Synopsis

The well-known reaction of dicarboxylic acid anhydrides with epoxides, catalyzed by bases and yielding linear polyesters, has been extended by a variation of the reactants. The reactions of succinic and phthalic anhydrides with *N*-substituted oxazolidinones-2, which by their tendency to split off CO<sub>2</sub> may be regarded as ethyleneimine derivatives, give in the presence of a few mole percent of LiCl at 200–220°C. within 5–10 hr. polyester amides of molecular weights up to 3.500 in nearly quantitative yield. The polymer yield corresponds to the CO<sub>2</sub> evolution indicating an equal consumption of oxazolidinone and anhydride in the reaction. The experimental activation energies of 22.8 and 20.2 kcal./mole for the reaction of 3-phenyl oxazolidinone-2 with succinic and phthalic anhydrides, respectively, fairly agree with earlier values reported for the corresponding reactions of the cyclic carbonates.

### Einleitung

Die klassische Methode zur Herstellung von linearen Polyestern durch Polykondensation von Dicarbonsäuren mit bifunktionellen Alkoholen erfordert eine möglichst vollständige Entfernung des entstehenden Wassers aus dem Reaktionsgleichgewicht. In wesentlich kürzerer Zeit werden solche Polymere durch ringöffnende Copolymerization aus den entsprechenden cyclischen Verbindungen erhalten. In sehr ausführlichen Arbeiten berichteten Schwenk,<sup>1</sup> Hamann und Mitarbeiter<sup>2–4</sup> sowie Fischer<sup>5</sup> über die Herstellung von Polyestern aus Dicarbonsäureanhydriden und Epoxiden durch basenkatalysierte Copolymerisation mit Metallsalzen. Anstelle der Epoxide konnten auch die entsprechenden cyclischen Carbonate und Sulfite eingesetzt werden, welche unter CO<sub>2</sub>- bzw. SO<sub>2</sub>-Abspaltung mit Dicarbonsäureanhydriden ebenfalls zu linearen Polyestern führen.<sup>1–3</sup>

In ähnlicher Weise können Oxazolidinone-2 als Derivate des Äthylenimins aufgefasst werden. Bei der thermischen Behandlung solcher cyclischen Urethane wurde die Bildung von Polyäthylenimin unter CO<sub>2</sub>-Abspaltung nachgewiesen.<sup>6</sup> Wie auch andere Autoren<sup>7</sup> bereits feststellten, entstehen aus Dicarbonsäureanhydriden und Oxazolidinonen-2 bei erhöhter Temperatur in Gegenwart von Metallsalzkatalysatoren lineare Polyesteramide, deren Bildung in der vorliegenden Arbeit näher untersucht wird.<sup>8</sup>



### Experimenteller Teil

Zur Darstellung der Oxazolidinone-2 wurde die Reaktion von Phenylisocyanat mit den entsprechenden Epoxiden in Gegenwart von LiCl nach Gulbins u.a.<sup>9</sup> herangezogen.

Die Umsetzung von Oxazolidinonen-2 mit Dicarbonsäureanhydriden wurde bei erhöhter Temperatur unter Durchleiten von trockenem, CO<sub>2</sub>-freiem Stickstoff in der Schmelze mit äquimolaren Mengen der Reaktionspartner durchgeführt. Die Polyesterbildung aus cyclischen Carbonaten ist nach Hamann u.a.<sup>2</sup> unabhängig von der Konzentration des Katalysators. Die Versuche wurden daher ebenfalls mit gleichbleibender Katalysatorkonzentration von 1 Mol-%, bezogen auf eingesetztes Oxazolidinon, ausgeführt. Nach beendeter CO<sub>2</sub>-Abspaltung wurde das Reaktionsgemisch 2 h. bei 140°C im Vakuum behandelt, anschliessend heiss in 1,2-Dichloräthan gelöst und aus Petroläther ( $K_p = 60-95^\circ\text{C}$ ) gefällt. Die erhaltenen, meist pulverförmigen, polymeren Produkte wurden bei 40°C im Vakuum bis zur Gewichtskonstanz getrocknet.

Die Umsetzung wurde in Abhängigkeit von der Reaktionszeit durch gravimetrische Bestimmung der Adsorption von freigesetztem CO<sub>2</sub> an Natronasbest verfolgt.

Die optimalen Reaktionsbedingungen wurden durch Variation der Temperatur zwischen 150 und 250°C und durch die Wahl verschiedener Katalysatoren ermittelt. Hierbei gelangten sowohl die für die Herstellung von Polyestern aus Epoxiden beschriebenen salzartigen Katalysatoren,<sup>2</sup> wie LiCl, Natriumbenzoat und Tetraäthylammoniumchlorid, als auch einige saure Katalysatoren, wie *p*-Toluolsulfonsäure, Bernsteinsäure und TiCl<sub>4</sub> bei der optimalen Reaktionstemperatur von 210°C zur Anwendung.

Die Abhängigkeit der Reaktion vom Reinheitsgrad des Anhydrids wurde durch extreme Reinigung (Sublimation) von Bernsteinsäureanhydrid einerseits und durch Zusatz geringer Mengen an freier Bernsteinsäure zum hochgereinigten Anhydrid andererseits untersucht.

Als Reaktionskomponenten wurden auf der einen Seite Phthalsäureanhydrid und Bernsteinsäureanhydrid, auf der anderen Seite 3-Phenylloxazolidinon-2, 3-Phenyl-5-phenoxyethyl-oxazolidinon-2 sowie 3,5-Diphenyl-oxazolidinon-2 in Gegenwart von LiCl bei 210°C eingesetzt.

Die Charakterisierung der erhaltenen Polymeren erfolgte durch C,H,N-Elementaranalyse und Infrarotspektrum, sowie durch Molekulargewichtsbestimmung mit dem Dampfdruckosmometer (Modell 301 A der Firma Mechrolab) in Aceton bei 37°C und nach der kryoskopischen Methode in Benzol.

Zur Untersuchung des chemischen Aufbaus wurde eine Probe in 20%-iger wässriger KOH hydrolytisch abgebaut und 86% des erwarteten Aminoalkohols (*N*-Phenyl-2-aminoäthanol) isoliert und durch Elementaranalyse, Infrarotspektrum und Siedepunkt identifiziert.

Durch Polykondensation wurde ausserdem ein Modell-Polyesteramid aus *N*-Phenyl-2-aminoäthanol und Bernsteinsäure mit geringem Unter-

TABELLE I  
Umsetzung von Dicarbonsäureanhydriden mit 3-Phenylloxazolidinon-2<sup>a</sup>

Vers. Nr.	Anhydrid	Temp., °C	CO <sub>2</sub> -Abspaltung nach 3 h, Mol-%	Reaktionszeit, h	Gesamt CO <sub>2</sub> -Abspaltung, Mol-%	Polymer Ausbeute, Mol-%	$\bar{M}_n^b$
P2	PSA	160	8,0	50,0	80,8	78,0	1500
P4		180	22,9	19,0	87,8	83,0	1480
P6		200	34,5	12,0	93,2	89,0	1200
P7		210	71,9	7,5	97,7	93,0	770
B2		BSA	160	7,7	100,0	93,7	89,0
B3	170		24,2	23,5	89,6	86,0	1110
B4	180		27,2	15,5	91,4	87,0	2100
B5	190		40,8	15,0	97,3	93,0	2200
B6	200		55,7	10,0	98,5	93,0	2400
B7	210		89,8	4,5	98,2	95,5	2500
B8	220		94,5	3,0	94,5	92,0	2250
B9	250		—	1,25	100,0	96,0	2200

<sup>a</sup> 1 Mol-% LiCl.

<sup>b</sup> Molekulargewichte bei 37°C in Aceton mit Dampfdruckosmometer gemessen.

schuss an Bernsteinsäure nach folgendem Temperaturprogramm in der Schmelze unter Stickstoff hergestellt: 24 h/100°C, 3 h/130°C und 2 h/160°C.

### Ergebnisse und Diskussion

Die Ergebnisse der Reaktion von 3-Phenylloxazolidinon-2 mit Bernsteinsäureanhydrid (BSA) und Phthalsäureanhydrid (PSA) bei verschiedenen Temperaturen in Gegenwart von LiCl sind in Tabelle I zusammengefasst.

Die Übereinstimmung der Ausbeute, gemessen an der CO<sub>2</sub>-Abspaltung und an der Polymerenbildung, deutet auf einen gleichmässigen Verbrauch an Oxazolidinon und Anhydrid während der Reaktion. Auch aus der Elementaranalyse der Reaktionsprodukte (P9/250°C),\* kann die Bildung eines äquimolaren Adduktes unter Abspaltung von CO<sub>2</sub> angenommen werden. Weiterhin zeigen die Infrarotspektren der Reaktionsprodukte der Bernsteinsäureanhydridreihe eine weitgehende Identität mit dem Spektrum eines Polyesteramids, welches durch Polykondensation aus Bernsteinsäure und dem entsprechenden Phenylaminoäthanol erhalten wurde (Abb. 1). Da ausserdem beim hydrolytischen Abbau der Probe B10 86% des erwarteten Aminoalkohols isoliert und identifiziert werden konnten und die Molekulargewichte der Substanzen nach Tabelle I höhermole-

\*z.B. Für P9 ber.: C, 71,8%; H, 4,9%; N, 5,3%. Gef.: C, 71,3%; H, 6,5%; N, 5,0%. Für B7 ber.: C, 65,7%; H, 6,0%; N, 6,4%. Gef.: C, 66,2%; H, 6,6%; N, 6,5%.

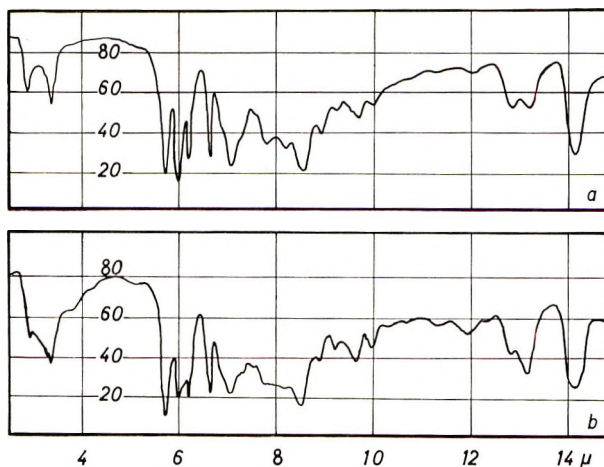
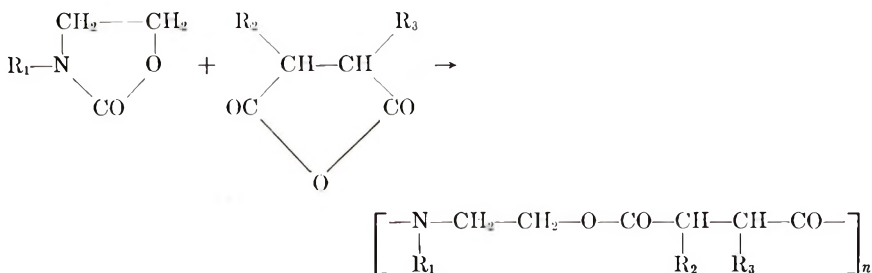


Abb. 1. Infrarot spektren von Polyesteramiden (a) durch Copolymerisation, B9/250°C und (b) durch Polykondensation.

kulare Produkte anzeigen, ist die Bildung von Polyesteramiden aus Oxazolidinonen-2 und Dicarbonsäureanhydriden gesichert:



Wie aus Tabelle I hervorgeht, ist die Reaktionsgeschwindigkeit sehr stark von der Temperatur abhängig und wird im günstigsten Fall (B9, 250°C) so gross, dass schon nach 1 h ein nahezu vollständiger Umsatz erreicht ist. Dies wird besonders aus den in Abb. 2 gezeigten Umsatz-Zeitkurven am Beispiel der Bernsteinsäureanhydridreihe verdeutlicht. Aus dieser Darstellung ist auch ersichtlich, dass die Reaktion innerhalb des gesamten Temperaturbereiches bei ausreichender Reaktionszeit einem 100% igen Umsatz zustrebt. Die innerhalb des Temperaturbereiches von 160-210°C für die Reaktion von 3-Phenylloxazolidinon-2 mit Dicarbonsäureanhydriden gemessenen Aktivierungsenergien ergaben 22,8 kcal/Mol für Bernsteinsäure- und 20,2 kcal/Mol für Phthalsäureanhydrid und sind damit vergleichbar mit dem Wert von 17,3 kcal/Mol, den Hamann u.a.<sup>2</sup> für die entsprechende Reaktion von Glykolcarbonat mit Phthalsäureanhydrid gefunden haben.

Der Einfluss der Reaktionstemperatur auf das Molekulargewicht ist besonders ausgeprägt bei der Bernsteinsäureanhydridreihe. Steigende Temperatur bewirkt die Bildung höhermolekularer Produkte. Oberhalb von

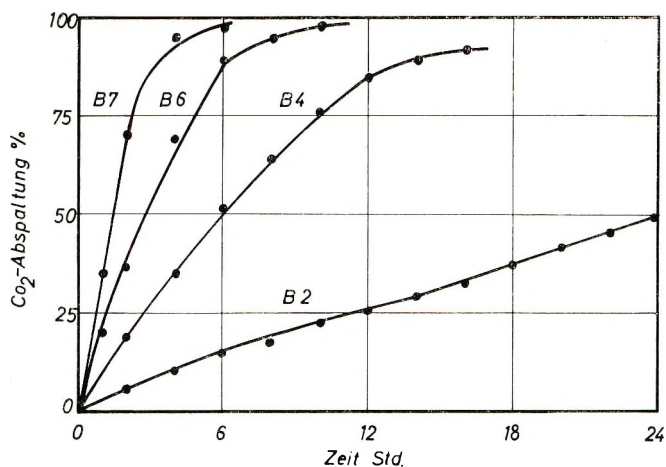


Abb. 2. Ausbeuteverlauf der Reaktion von 3-Phenyloxazolidinon-2 und Bernsteinsäureanhydrid mit 1 Mol-% LiCl bei verschiedenen Temperaturen.

210–220°C werden wieder niedrigere Molekulargewichte erhalten, was mit einem Anhydridverlust durch Sublimation und damit verbundener Verschiebung des äquimolaren Verhältnisses der Komponenten erklärt werden kann. Der optimale Temperaturbereich liegt somit zwischen 200 und 220°C.

Das Molekulargewicht wird durch Feuchtigkeitsspuren, welche wahrscheinlich als Kettenabbrucher wirken, stark beeinflusst. Die Entfernung der letzten Spuren von freier Bernsteinsäure bei extremer Reinigung des Bernsteinsäureanhydrids durch Sublimation, führt daher bei der anschließenden Reaktion mit 3-Phenyloxazolidinon-2 in Gegenwart von LiCl (210°C) zu einem Polymeren (B10) mit beträchtlich höherem Molekulargewicht als bei Verwendung des normal gereinigten Anhydrids (Probe B7):

$$\bar{M}_n = 2500 \text{ (B7) bzw. } 3400 \text{ (B10)}$$

Die Reaktionsgeschwindigkeit ändert sich dabei nicht wesentlich.

Entsprechend wird das Molekulargewicht des erhaltenen Polymeren durch Zugabe kleiner Mengen, z.B. 5 Mol-% Bernsteinsäure (B16) unter sonst gleichen Bedingungen erniedrigt, während die Reaktionsgeschwindigkeit unbeeinflusst bleibt.

$$\bar{M}_n = 3400 \text{ (B10) bzw. } 2650 \text{ (B16)}$$

Tabelle II zeigt den Einfluss von verschiedenen Katalysatoren auf die Reaktionsgeschwindigkeit, sowie auf Gesamtausbeute und Molekulargewicht der erhaltenen Reaktionsprodukte. Salzartige Katalysatoren zeigen in Übereinstimmung mit Hamann u.a.<sup>2</sup> die beste Wirksamkeit. Während jedoch Natriumbenzoat und Tetraäthylammoniumchlorid eine ähnlich rasche CO<sub>2</sub>-Abspaltung bewirken, ist das Molekulargewicht der entstehenden Produkte niedriger als bei der Verwendung von LiCl. Die sauren

TABELLE II

Umsetzung von hochgereinigtem Bernsteinsäureanhydrid mit 3-Phenylloxazolidinon-2 in Gegenwart verschiedener Katalysatoren<sup>a</sup>

Vers. Nr.	Katalysator <sup>b</sup>	CO <sub>2</sub> -Abspaltung nach 3 h, Mol-%	Reaktionszeit, h	Gesamt CO <sub>2</sub> -Abspaltung, Mol-%	Polymer Ausbeute, Mol-%	$\bar{M}_n$ <sup>c</sup>
B15	—	8,5	7	18,2	—	—
B23	TiCl <sub>4</sub>	8,5	7	18,3	—	—
B18	<i>p</i> -Toluolsulfonsäure, 5 Mol-%	21,5	15	41,2	38,0	980
B17	Bernsteinsäure	18,0	28	60,3	57,0	—
B10	LiCl	79,9	8	99,6	96,0	3400
B24	Tetraäthylammoniumchlorid	79,1	7	87,1	84,0	1800
B11	Na-Benzoesäure	70,7	11	96,0	92,0	850

<sup>a</sup> 210°C.

<sup>b</sup> 1 Mol-% Katalysator.

<sup>c</sup> Molekulargewichte durch Kryoskopie in Benzol.

Katalysatoren sind sowohl im Hinblick auf die Reaktionsgeschwindigkeit als auch auf die Molekulargewichte ungeeignet.

TABELLE III

Umsetzung von hochgereinigtem Bernsteinsäureanhydrid mit verschiedenen Oxazolidinonen-2<sup>a</sup>

Vers. Nr.	Oxazolidinon-2	CO <sub>2</sub> -Abspaltung nach 3 h, Mol-%	Reaktionszeit, h	Gesamt CO <sub>2</sub> -Abspaltung, Mol-%	Polymer Ausbeute, Mol-%	$\bar{M}_n$ <sup>b</sup>
B10	3-Phenyl-	79,9	8	99,6	96	3400
B19	3-Phenyl-5-phenoxy-methyl-	6,6	7	7,7	—	—
B20	3,5-Diphenyl-	38,8	12	80,0	77	1190

<sup>a</sup> 1 Mol-% LiCl, 210°C.

<sup>b</sup> Molekulargewichte durch Kryoskopie in Benzol.

Die Variation der Oxazolidinon-Komponente führte unter optimalen Bedingungen (1 Mol-% LiCl/210°C) zu dem in Tabelle III aufgeführten Ergebnis. Unter Verwendung des aromatisch disubstituierten Oxazolidinons (B20 und B21) wurden bei nur wenig verringerter Reaktionsgeschwindigkeit Polymere mit kleinerem Molekulargewicht erhalten.

ANAL. Für B21 ber.: C, 73,3%; H, 5,7%; N, 4,7. Gef.: C, 73,7%; H, 5,7%; N, 5,0%.

Die Reaktion von 3-Phenyl-5-phenoxy-methyl-oxazolidinon-2 mit Bernsteinsäureanhydrid zeigte keine erkennbare Polymerenbildung an.



### References

1. E. Schwenk, Dissertation, TH, Stuttgart, 1957.
2. E. Schwenk, K. Gulbins, M. Roth, G. Benzing, R. Maysenhölder, und K. Hamann, *Makromol. Chem.*, **51**, 53 (1962).
3. A. Hilt, J. Trivedi, und K. Hamann, *Makromol. Chem.*, im Druck.
4. A. Hilt und K. Hamann, in Vorbereitung (Private Mitt.).
5. R. F. Fischer, *J. Polymer Sci.*, **44**, 155 (1960); *Ind. Eng. Chem.*, **52**, 321 (1960).
6. J. I. Jones, *Chem. Ind. (London)*, **1956**, 1454.
7. Fabriek van Chemische Producten Vandelingenplaat N.V., Belg. Pat. 612.000, 15.1.62, Anm. 27.12.61
8. S. Burckhardt, Diplomarbeit, TH Stuttgart, 1963.
9. K. Gulbins u.a., *Chem. Ber.*, **93**, 1975 (1960).

### Résumé

Les réactions bien connues des anhydrides d'acides dicarboxyliques avec des époxydes, catalysées par des bases et fournissant des polyesters linéaires, ont été étendues en variant les réactifs utilisés. Les réactions des anhydrides succiniques et phthaliques avec les oxazolidines-2 substituées à l'azote, qui, suite de leur tendance à perdre du CO<sub>2</sub> peuvent être considérés comme étant des dérivés de l'éthylène-imine, donnent en présence de quelques moles % de chlorure de lithium à 200–226°C endéans les 5–10 heures des polyesters amides en rendement quasi quantitatif de poids moléculaire allant jusque 3500. Le rendement en polymères correspond au dégagement de CO<sub>2</sub> qui indiquent une consommation égale d'oxazolidinone et d'anhydride en cours de réaction. Les énergies d'activation expérimentales de 22,8 et 20,2 Kcal/mole pour la réaction de la 2-oxazolidinone phényle-3 avec les anhydrides succiniques et phthaliques, respectivement, sont en accord suffisant avec la valeur rapportée précédemment pour les réactions correspondantes avec les carbonates cycliques.

### Zusammenfassung

Die bekannte basenkatalysierte Reaktion zwischen Dicarbonsäureanhydriden und Epoxiden, welche zu linearen Polyestern führt, wurde durch Abwandlung der Reaktionspartner erweitert. Die Umsetzung von Bernstein- und Phthalsäureanhydrid mit *N*-substituierten Oxazolidinonen-2, welche infolge ihrer CO<sub>2</sub>-Abspaltungstendenz als Derivate des Äthylenimins aufzufassen sind, führt in Gegenwart von einigen Mol-% LiCl bei 200–220°C innerhalb von 5–10 h in nahezu quantitativer Reaktion zu Polyesteramiden mit Molekulargewichten bis zu 3500. Aus der Übereinstimmung der Polymerausbeute und der CO<sub>2</sub>-Entwicklung ergibt sich ein gleichmässiger Verbrauch an Oxazolidinon und Anhydrid während der Reaktion. Die experimentell ermittelten Aktivierungsenergien von 22,8 und 20,2 kcal/Mol für die Reaktion von 3-Phenyl-oxazolidinon-2 mit Bernstein-bzw. Phthalsäureanhydrid sind gut vergleichbar mit früher beschriebenen Werten für die entsprechende Reaktion der cyclischen Carbonate.

Received September 13, 1965

Revised October 19, 1965

Prod. No. 4940A

## Room Temperature Polymerization of Glycidol

STANLEY R. SANDLER and FLORENCE R. BERG, *Central Research Laboratory, The Borden Chemical Company, Philadelphia, Pennsylvania*

### Synopsis

Glycidol has been shown to be easily polymerized at room temperature in the presence of triethylamine, pyridine, lithium hydroxide, potassium hydroxide, sodium hydroxide, sodium methoxide, sodium amide, and other catalysts. Its reactivity with these catalysts is vastly greater than that of propylene oxide. Evidence is presented to support the structural assignment for polyglycidol and the mechanism of polymerization.

The chance observation that glycidol polymerized vigorously in the presence of excess triethylamine led us to investigate further the effect of catalysts on the rate of polymerization. A literature search indicated that earlier work<sup>1</sup> briefly mentioned that pyridine polymerized glycidol to a water-soluble black tar and that calcium chloride caused it to polymerize exothermically more rapidly with the production of a water-soluble red tar. In addition Frank<sup>2</sup> reported that tin tetrachloride at  $-25^{\circ}\text{C}$ . polymerized glycidol. Frank<sup>2</sup> also mentioned that aluminum chloride mineral acids and alkali are useful catalysts but gave no details as to the type or kind of alkali catalysts that were useful. Daimon et al.<sup>3</sup> recently described the preparation of polymers by polymerization or copolymerization of glycidol in the presence of an organometallic compound of Group II or III metals, or their alkoxide, as a catalyst. Triethylaluminum is given as an example.

During the course of a synthesis problem involving glycidol it was observed that glycidol polymerized exothermically in the presence of triethylamine and on standing in a glass kettle containing some alkali, probably due to residual detergent. The marked difference in polymerization behavior of propylene oxide<sup>4</sup> to that of glycidol and the lack of useful experimental data in the literature on polyglycidol formation led us to initiate this investigation.

### RESULTS AND DISCUSSION

Glycidol was stirred at room temperature with 1% or less by weight of several varieties of bases. In Table I and II are listed some of the catalysts used and the catalytic effects. Whenever the catalysts are insoluble in the glycidol the catalysts were powdered and then continuously stirred during polymerization over nitrogen. Most of the reactions were carried out at room temperature. The degree of conversion was determined by dissolving

TABLE I  
Room Temperature Polymerization Behavior with Inorganic and Organic Bases of  
Glycidol Compared to that of Propylene Oxide

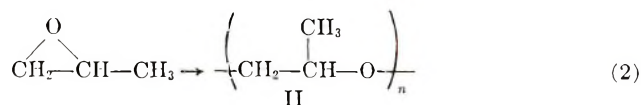
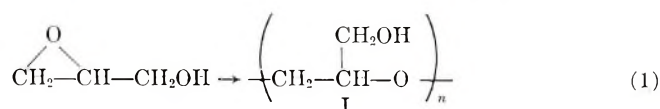
Catalyst	Catalyst, %	Time, hr.	Conversion, % <sup>a</sup>	
			Glycidol	Propylene oxide <sup>b</sup>
KOH	1	27	88	
	10	51		33
NaOCH <sub>3</sub>	1	20	87	
	10	72		0
LiOH	1	72	84	
	10	72		0
NaOH	1	72	81	
	10	72		0
NaNH <sub>2</sub>	1	72	82	
	10	92		1
Et <sub>3</sub> N	1	19.5	73	—
Pyridine	1	25	78	—
CaCl <sub>2</sub>	1	25	38	—

<sup>a</sup> A zero signifies an experiment has been performed and no polymer was obtained; however, a dash indicates that an experiment was not performed.

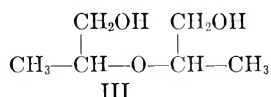
<sup>b</sup> Data of St. Pierre and Price.<sup>4</sup>

the material in dimethyl sulfoxide or methanol and quenching the polymerization by the addition of 3 g. of Amberlite ion-exchange resin IR-120-14. After thorough shaking the solution was filtered and the unreacted material and solvent were removed by heating to 140°C. at 0.5 mm. Hg. Heating a sample of pure glycidol under similar conditions yielded 0.9% of a residue which gave an infrared spectrum identical to that of polyglycidol.

Polyglycidol (I) and poly(propylene oxide) (II) are related structurally, but differ in that I has an OH group substituted on the methyl group.



The infrared spectrum of polyglycidol is similar to that of dipropylene glycol (III).



Polyglycidol obtained in the present work appears from infrared data to be free of large amounts of unsaturation, as will be discussed in the Experimental section.

TABLE II  
 Rate of Polymerization of Glycidol at Room Temperature Catalyzed by Base

Sample	Catalyst	Catalyst, %	Time, hr.	Conver- sion, %	$\eta_{inh}$	Molecular weight
471-30-1	KOH	1.00	$2/3$	28	0.067	
-2			3	53	0.055	
-3			$5\frac{1}{4}$	53	0.072	
-4			$22\frac{1}{2}$	89	0.069	
-5			27	88	0.070	
471-35-1	NaOCH <sub>2</sub>	1.00	$1/3$	22	—	
-2			$2\frac{1}{2}$	58	—	
-3			20	87	—	
-4			27	90	—	
-5			92	89	0.0608	
471-34-1	NaOCH <sub>3</sub>	0.30	2	37	—	
-2			20	53	—	
-3			45	66	—	
-4			116	84	0.056	445 <sup>a</sup>
-5			140	100	0.0667	
471-36-1	Et <sub>3</sub> N	1.00	$19\frac{1}{2}$	73	—	
-2			$26\frac{1}{2}$	79	—	
-3			44	81	—	
-4			70	92	—	
-5			94	90	0.0584	
471-44-1	Pyridine	1.00	6	72		
-2			25	78		
-3			49	81		
-4			73	78		
-5			97	84	0.071	442
-6			2	39		
471-45-1	CaCl <sub>2</sub>	1.00	6	39		
-2			25	38		
-3			49	45		
-4			73	59	0.061	
-5			97	64		
-6			2	26		

<sup>a</sup> Molecular weight determined in methanol at Galbraith Laboratories, Knoxville, Tenn., by a vapor-pressure osmometer (Mecrolab).

The results in Table I indicate the enhanced ability of glycidol to polymerize in the presence of a wide variety of bases. It is interesting to note that propylene oxide is inert toward sodium methoxide, lithium hydroxide, sodium hydroxide, and sodium amide at room temperature, whereas glycidol is quite reactive under similar conditions.

Earlier work<sup>1</sup> indicated quantitatively that calcium chloride was more effective than pyridine; however, the quantitative results in Table II indicate the reverse order. The explanation for the catalytic activity of calcium chloride is not clear at this time. It is possible that some calcium hydroxide or oxide is present and this may be the actual catalyst.

Table II indicates the progress of the polymerization as a function of time. It should be noted that the inherent viscosity remains about the same dur-

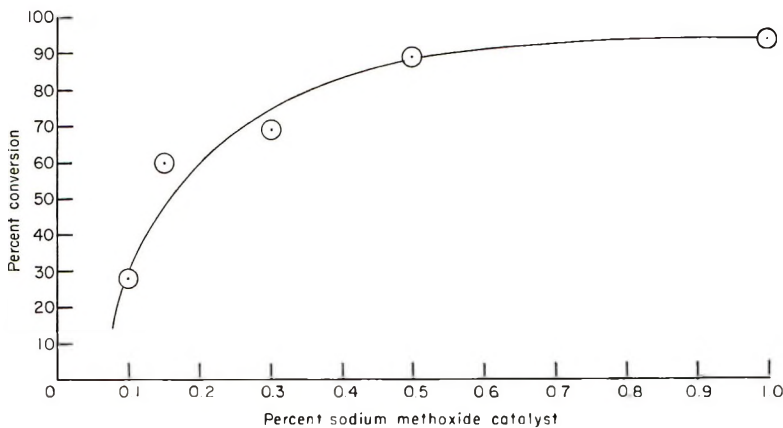


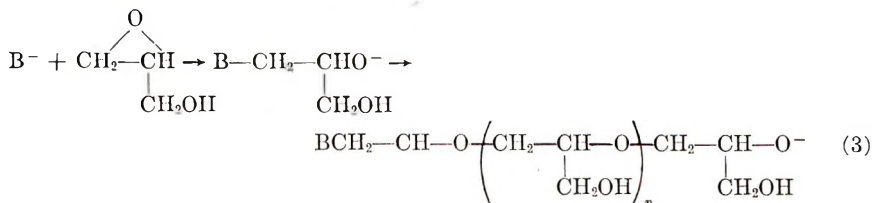
Figure 1.

ing the progress of the polymerization for the isolated polymer in the KOH catalyst system. A similar trend in viscosities was observed earlier for propylene oxide polymerizations with potassium hydroxide.<sup>4</sup> It appears that all the catalysts used at room temperature in Table II give about the same molecular weights as that of the sodium methoxide catalyzed polymerization.

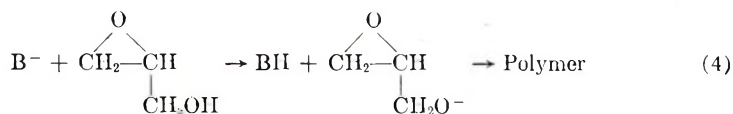
The molecular weight obtained for the 0.3% sodium methoxide-catalyzed polymer is 445 and this agrees well with that calculated for a structure with 6 repeat glycidol units. The latter material is a clear, very viscous liquid having good solubility in water. The preparation of higher molecular weight polymers is in progress.

Surface catalysis may be involved in the sodium methoxide case since the per cent conversion increases from 0.1 to 0.5% catalyst and then slows down as seen in Figure 1. However, Steiner et al.<sup>5</sup> found that the rate of polymerization of propylene oxide with KOH was not compatible with surface catalysis.

A likely course for the polymerization process might be outlined following a similar mechanism as with propylene oxide.<sup>6,7</sup>



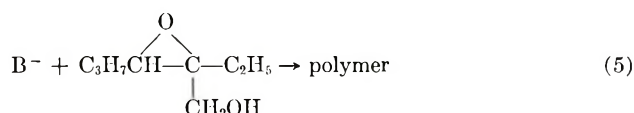
and





The latter path, eq. (4) probably accounts for the low molecular weight polymers, since the hydroxyl group can act as a chain-terminating agent for a growing polymer with a terminal alkoxide group as in eq. (3). The base  $B^-$  in eq. (4) can then be thought of as representing a growing polymer with an alkoxy group. Termination may also occur by an intramolecular path.

The stereochemistry of the monomer is important, since a substituted glycidol, i.e., 2,3-epoxy-2-ethylhexanol, is unreactive towards sodium methoxide or triethylamine



at room temperature or at 50°C., as indicated in Table III.

TABLE III  
Rate of Polymerization of 2-Ethyl-2,3-Epoxyhexanol at Room Temperature Catalyzed by Bases

Sample No.	Catalyst	Catalyst, %	Time, hr.	Conversion, %
471-40-3	$\text{Et}_3\text{N}$	1	52	1
471-49-1	$\text{NaOCH}_3$	1.96	$1/3$	0
-2			$2\frac{1}{2}$	0
-3			20 <sup>a</sup>	30

<sup>a</sup> The inherent viscosity in dimethyl sulfoxide at 32.5°C. is 0.0191.

In an analogous manner Gee<sup>8</sup> has shown that the butene oxides react at a much slower rate compared to propylene oxide.\* For example, the ratio of rate of reaction of *cis*-2-butene oxide with sodium methoxide in methanol at 29.8°C. to that of ethylene oxide is 1.3/21.4. The effect of alkyl substitution retarding the rate of reactions was explained by Gee either as due to the inductive transfer of a fractional negative charge for the adjacent carbon atom and/or steric hindrance of the approaching ion. The available data were insufficient to indicate which effect was more important in the compounds studied.

## EXPERIMENTAL

### Room Temperature Polymerizations

Sodium methoxide, potassium hydroxide, triethylamine, pyridine, and calcium chloride were selected as catalysts for kinetic studies of glycidol polymerization. The glycidol was obtained from The Ott Chemical Company, Muskegon, Michigan, and used as received. The reported boiling point is 59°C. at 15 mm.,  $n_D^{20}$  1.4310. In addition, glycidol is an odorless,

\* These reactions were not polymerizations but the base-catalyzed addition of alcohols to ethylene oxide.

water-clear liquid that is miscible with water and most organic solvents. Heating it at atmospheric pressure causes it to polymerize.

The glycidol was stirred in an Erlenmeyer flask in a water bath at 23°C. The catalyst was added. Samples were removed at intervals, weighed, dissolved in a suitable solvent, and shaken with Amberlite 1R-120-H. The solution was filtered, heated to 140°C. at 0.5 mm. Hg, weighed, and the viscosity determined in dimethyl sulfoxide at 32.5°C. Tetrahydrofuran was used as solvent in the first experiment, but it was found that samples which had undergone more than 50% conversion were not soluble. Some dimethyl sulfoxide was used to dissolve the last two aliquots. In subsequent experiments, methanol was found suitable. The results are listed in Tables II and III.

On removing the solvents before determining the viscosity of the polymer it was shown by vapor-phase chromatography that only the glycidol was recovered and not some rearranged product.

The propylene oxide polymerization data were taken from the literature.<sup>4</sup>

The molecular weights were determined at Galbraith Laboratories, Knoxville, Tenn. The infrared spectra were run by Mr. Glen Doan on a Perkin-Elmer, model 21 spectrophotometer.

### Determination of Unsaturation

The method used was earlier described<sup>4</sup> and the polymers appeared to be saturated within experimental error.

### Volatile Fractions

The isolated volatiles from the polymerization indicated that unreacted glycidol was isolated, and no cyclization product was detected in the vapor-phase chromatographs.

### Polymerization of 2-Ethyl-2,3-Epoxyhexanol

Polymerization of 2,3-epoxy-2-ethylhexanol at 20–22 and 50°C. by 1% triethylamine gave erratic results, and the product obtained was not resinous, but a mixture of liquid and solid. A blank determination—that is, the residue obtained when the starting material alone was heated to 140°C. at 0.5 mm. Hg.—had 9.36% residue. When 1.96% NaOCH<sub>2</sub> was substituted as catalyst, a viscous liquid residue was obtained.\* The results of this determination are listed in Table III.

The inherent viscosity determinations made on pure monomeric glycidol (0.011) and 2,3-epoxy-2-ethylhexanol (0.010) in dimethylsulfoxide indicated that the difference with the polymer is substantial, as shown in Table II.

We would like to thank NASA for support of this work under Contract NAS-8-11518.

\* 1.96% NaOCH<sub>2</sub> is equivalent to 1 g. NaOCH<sub>3</sub> per 1.35 mole of 2,3-epoxy-2-ethylhexanol. This ratio (1 g. NaOCH<sub>3</sub>/1.35 mole glycidol) was used in 471–35.

### References

1. T. H. Rider and A. J. Hill, *J. Am. Chem. Soc.*, **52**, 1521 (1930).
2. G. Frank, Ger. Pat. 575,750 (1933).
3. A. Daimon, K. Kamio, and S. Kojima, Japan. Pat. 5443 (1963).
4. L. E. St. Pierre and C. C. Price, *J. Am. Chem. Soc.*, **78**, 3432 (1956).
5. E. C. Steiner, R. R. Pelletier, and R. O. Truex, *J. Am. Chem. Soc.*, **86**, 4678 (1964).
6. G. Gee, W. C. E. Higginson, K. J. Taylor and M. W. Trenholme, *J. Chem. Soc.*, **1961**, 4298.
7. G. Gee, W. C. E. Higginson, and G. T. Merrall, *J. Chem. Soc.*, **1959**, 1345.
8. G. Gee, W. C. E. Higginson, P. Levesley, and K. J. Taylor, *J. Chem. Soc.*, **1959**, 1338.

### Résumé

Le glycidol peut être polymérisé facilement à température de chambre en présence de catalyseurs tels que la triéthylamine, la pyridine, l'hydroxyde de lithium, l'hydroxyde de potassium, l'hydroxyde de sodium, le méthoxyde de sodium, l'amidure de sodium, et autres catalyseurs. Sa réactivité en présence de ces catalyseurs est beaucoup plus grande que celle de l'oxyde de propylène. On présente une preuve de la structure du polyglycidol de même qu'une preuve pour son mécanisme de polymérisation.

### Zusammenfassung

Glycidol kann bei Raumtemperatur in Gegenwart von Triäthylamin, Pyridin, Lithiumhydroxyd, Kaliumhydroxyd, Natriumhydroxyd, Natriummethoxyd, Natriumamid und anderen Katalysatoren leicht zur Polymerisation gebracht werden. Seine Reaktivität mit diesen Katalysatoren ist bedeutend grösser als diejenige von Propylenoxyd. An Hand der Ergebnisse wird eine Strukturzuordnung für Polyglycidol sowie ein Polymerisationsmechanismus vorgeschlagen.

Received September 9, 1965

Revised October 13, 1965

Prod. No. 4941A

## Polymerization of 1,2:5,6-Di-*O*-Isopropylidene- $\alpha$ -D-Glucofuranose and 1,2-*O*-Isopropylidene- $\alpha$ -D-Glucofuranose\*

ROY L. WHISTLER and PAUL A. SEIB,† *Department of Biochemistry, Purdue University, Lafayette, Indiana*

### Synopsis

A new method for preparing D-glucose polymers is described. Isopropylidene derivatives of D-glucofuranose, particularly the 1,2-mono-*O*-derivative, are treated with Lewis acids, such as boron trifluoride, to eliminate acetone and produce a highly branched polymer with a molecular weight of 12,700. Approximately one isopropylidene unit remains, possibly on the potential reducing end of the glucan. Up to 95% of the polymer units are D-glucopyranoside units indicating that ring expansion occurs during the condensation.

Polymerization of D-glucose and its derivatives has long attracted interest because of the abundance and low cost of D-glucose, obtained by hydrolysis of corn starch. Formation of oligomers from D-glucose in aqueous solution by acid catalysis, sometimes termed "reversion," is well known and has been examined extensively.<sup>1-6</sup> Polymerization conditions have been modified<sup>7</sup> to shift the reaction equilibrium to favor glycan formation, but the number-average degree of polymerization has seldom exceeded 20. Mora and co-workers<sup>8,9</sup> refined the conditions by heating D-glucose with phosphorous acid at 140-170°C. under reduced pressure and reported polymers with number-average molecular weights up to 30,000. Polymers produced from D-glucose by such acid-catalyzed glycoside syntheses are highly branched and of complex structure.

The present work reports a new approach to the methods for making polymers of D-glucose. It embodies condensation of isopropylidene sugars with Lewis acid catalysis to produce glycans with the simultaneous elimination of acetone. The reaction seems generally applicable to sugar 1,2-ketals and very likely to 1,2-acetals as well. With isopropylidene sugars the reaction proceeds without the need for reduced pressure or special conditions to remove by-product acetone. In closed containers polymerization proceeds readily to produce highly branched, water-soluble glycans with molecular weights as high as 12,700.

\* Presented in part at the 149th National Meeting of the American Chemical Society, Detroit, Michigan, April 1965.

† Present address: The Institute of Paper Chemistry, Appleton, Wisconsin.

The polymerization of isopropylidene sugars was first encountered in this laboratory during an investigation of the ring-opening polymerization of 5,6-dideoxy-5,6-epithio-1,2-*O*-isopropylidene- $\alpha$ -L-idofuranose.<sup>10</sup> Here it was observed that under the influence of boron trifluoride the sugar derivative not only polymerized by the expected ring-opening route but also formed an insoluble crosslinked polymer by what appeared to be a type of transglycosylation wherein the isopropylidene group was eliminated as acetone.

Bredtschneider and Beran<sup>11</sup> earlier reported the reactions of 1,2,3,4,6-penta-*O*-acetyl- $\beta$ -D-glucopyranose with phenols and boron trifluoride catalyst to produce aryl D-glucosides. The same reaction was found to proceed with stannic chloride catalyst<sup>12</sup> and was observed to produce either phenyl or methyl D-glucosides. More recently Bonner and co-workers<sup>13</sup> reacted boron trichloride with methyl  $\alpha$ -D-glucopyranoside to form a complex which reacted with alcohols to produce new D-glucosides and disaccharides. These reactions have been explained by assuming elimination of the group attached to carbon C<sub>1</sub> to form a carbonium ion which reacts with an alcohol or phenol to form a D-glucoside.

In this work 1,2:5,6-di-*O*-isopropylidene- $\alpha$ -D-glucofuranose in benzene solution is observed to polymerize at 65°C. with boron trifluoride catalyst. During a 1 hr. reaction, polymer of highest molecular weight is obtained at a monomer:catalyst ratio of 10 (Fig. 1). At higher catalyst concentrations the amount of ether precipitable polymer is greater, but the molecular weight of the polymer and the amount of polymer which does not dialyze through cellulose casing is small, possibly because of the large number of chains which are initiated. At low catalyst concentrations the molecular weight of the polymer and the amount formed are small because of the slow condensation rate.

At a monomer:catalyst ratio of 10 most of the polymer growth occurs during the first 1-2 hr. (Fig. 2). Heating periods longer than 6-8 hr. cause the development of color in the solution. Hydrolysis of the polymer produced during short periods of heating yields only D-glucose, as observed by paper chromatography, but hydrolysis of polymers produced in extended reaction periods yields small amounts of two carbohydrates other than D-glucose. These modified sugar units must result from dehydration of D-glucose during the polymerization reaction. One of these modified sugars is identified chromatographically as 3,6-anhydro-D-glucose while the other is possibly a hexulose since it reacts with resorcinol-hydrochloric acid reagent.

Polymers formed from 1,2:5,6-di-*O*-isopropylidene- $\alpha$ -D-glucofuranose in benzene solution precipitate from the reaction media since condensation eliminates acetone and produces hydrophilic polymers. This heterogeneity, however, is not the cause for the abrupt change in polymer growth as seen during the first 1-2 hr. (Fig. 2). Melt polymerizations of 1,2:5,6-di-*O*-isopropylidene- $\alpha$ -D-glucofuranose at 110°C. give molecular weights in the same range as solution polymerization (Table I). Catalyst concentration is



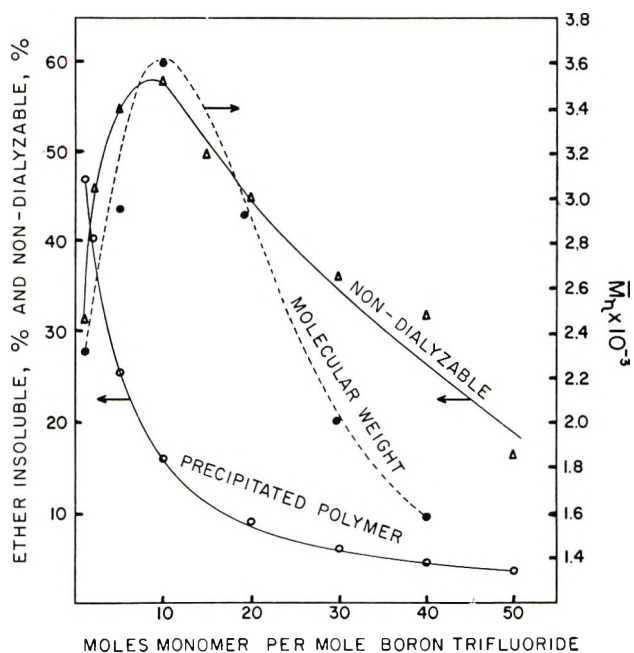


Fig. 1. Polymerization of 1,2:5,6-di-*O*-isopropylidene- $\alpha$ -D-glucufuranose in benzene with boron trifluoride at 65°C. for 1 hr. Molecular weights are of the nondialyzable polymer.

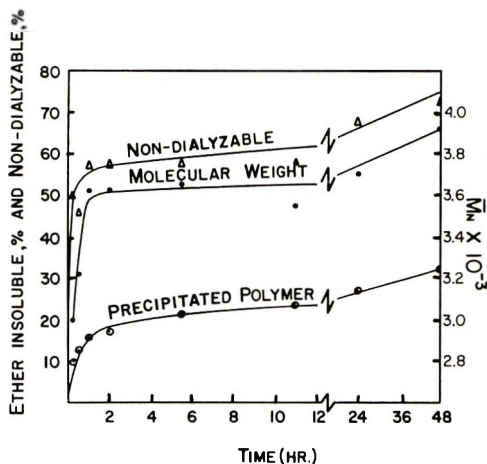


Fig. 2. Polymerization of 1,2:5,6-di-*O*-isopropylidene- $\alpha$ -D-glucufuranose in benzene with boron trifluoride at 65°C. at a monomer catalyst ratio of 10:1.

reduced in the melt because of the higher temperature and because of greater effectiveness of catalyst since it is not combined as a benzene complex. The low limiting viscosity numbers of the polymers indicate branching.

1,2-*O*-Isopropylidene- $\alpha$ -D-glucufuranose, when melt-polymerized at 165–170°C., requires much less boron trifluoride catalyst than the diisopropylidene sugar. Thus, the latter at a monomer:catalyst ratio of 1000 gives

TABLE I  
Melt Polymerization of 1,2:5,6-Di-*O*-Isopropylidene- $\alpha$ -D-Glucufuranose  
at 110°C. with Boron Trifluoride Catalyst

Polymer	Molar ratio monomer catalyst	Reaction time, hr.	Non- dialyzable polymer, %	$\bar{M}_n$	$[\alpha]_D^{25}$ ( $c = 0.5$ , water)	$[\eta]$ , dl./g.
1	10	1	20	3550	+61	0.05
2	100	4	11	2930	+48	0.04
3	100	8	15	3560	+45	0.05
4	100	12	21	5230	—	0.06
5	10,000	168	6	2390	—	0.02

only a trace of polymer in 48 hr., while the monoisopropylidene sugar gives 30% nondialyzable polymer with a number-average molecular weight of 12,700.

The higher rate of condensation of the monoisopropylidene monomer results from its higher functionality and the presence of a reactive primary hydroxyl group. Since it has three hydroxyl groups available for reaction the hydroxyl functionality of the growing polymer increases by three times the number-average degree of polymerization. The diisopropylidene sugar has a hydroxyl functionality of one and the functionality of the growing polymer is equal to the number-average degree of polymerization. When the free hydroxyl group at carbon C<sub>3</sub> is blocked, as for example with a methyl group, or when the three hydroxyls at carbons C<sub>3</sub>, C<sub>5</sub>, and C<sub>6</sub> of the monoisopropylidene sugar are methylated, no polymerization is observed even at high catalyst concentrations. Similarly 1,2:3,5-di-*O*-isopropylidene- $\alpha$ -D-xylofuranose also does not polymerize.

TABLE II  
Melt Polymerization of Isopropylidene Sugars with Boron Trifluoride  
at 165–170°C.

Monomer	Nondialyzable polymer, % <sup>a</sup>			
	Monomer:catalyst 1000:1		Monomer:catalyst 100:1	
	2 hr.	12 hr.	1 hr.	5 hr.
1,2:5,6-Di- <i>O</i> -propylidene- $\alpha$ -D- glucufuranose	0	Trace	8.8 (4860)	6.8 (3040)
1,2:3,4-Di- <i>O</i> -isopropylidene- $\alpha$ -D- galactopyranose	Trace	1.5%	27.6 (8100)	4.2 (3540)
2,3:5,6-Di- <i>O</i> -isopropylidene- $\alpha$ -D- mannofuranose	0	Trace	4.8 (3800)	26.0 (6750)
1,2- <i>O</i> -Isopropylidene- $\alpha$ -D- xylofuranose	16.0 (4660)	18.0 (5060)	2.8 (1200)	0
1,2- <i>O</i> -Isopropylidene- $\alpha$ -D- glucufuranose	26.0 (4350)	31.2 (5900)	14.6 (2540)	4.8 (1600)

<sup>a</sup> Numbers in parentheses are molecular weights.

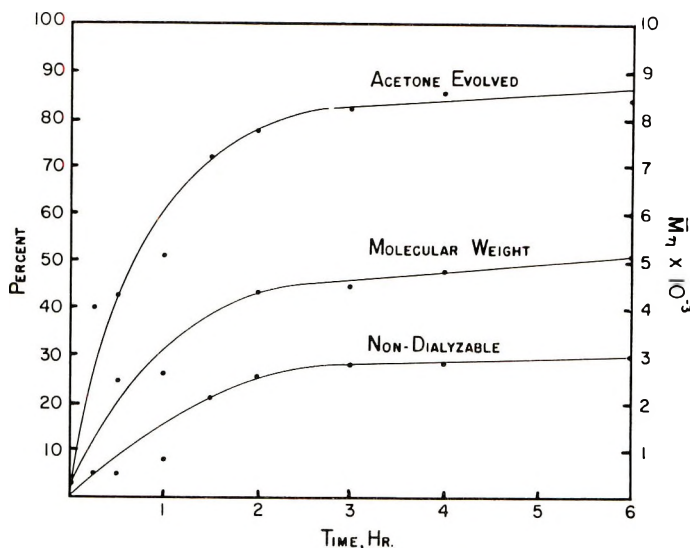


Fig. 3. Melt polymerization of 1,2-*O*-isopropylidene- $\alpha$ -D-glucofuranose at 165–170°C. at a monomer:boron trifluoride ratio of 1000:1.

1,2-*O*-Isopropylidene- $\alpha$ -D-xylofuranose and 1,2:3,4-di-*O*-isopropylidene- $\alpha$ -D-galactopyranose both polymerize in the melt with boron trifluoride as catalyst (Table II). The D-galactopyranose derivative polymerizes faster than the diisopropylidene D-glucose derivative, producing 27.6% polymer in 1 hr. compared to 8.8% polymer from the D-glucose monomer when both are heated at 165–170°C. with a monomer:catalyst ratio of 100. Hence, it is apparent that the polymerization reaction is of a general nature and is not confined to sugar monomers with furanose rings.

The catalyst concentration for the melt polymerization of 1,2-*O*-isopropylidene sugars must be carefully selected. If the monomer has two or three hydroxyl groups, dehydration reactions occur rapidly at 165–170°C. A low concentration of catalyst promotes polymer growth with minimum dehydration side effects. Thus, polymerization of 1,2-*O*-isopropylidene- $\alpha$ -D-glucofuranose or 1,2-*O*-isopropylidene- $\alpha$ -D-xylofuranose gives a high yield of polymer with a high molecular weight when the monomer:catalyst ratio is 1000, but higher catalyst concentrations produce low yields of degraded polymers, as shown in Table II. Monomers with only one hydroxyl group, such as 1,2:3,4-di-*O*-isopropylidene- $\alpha$ -D-galactopyranose, require larger amounts of catalyst to produce a high concentration of activated monomer units needed for moderate rates of polymerization. Under these conditions of high catalyst concentration only short polymerization periods are needed.

In sealed tube reactions the evolution of acetone is clearly visible. The amounts of acetone evolved during the polymerization of 1,2-*O*-isopropylidene- $\alpha$ -D-glucofuranose during different polymerization periods are shown in Figure 3. It is evident that acetone is evolved in proportion to polymer

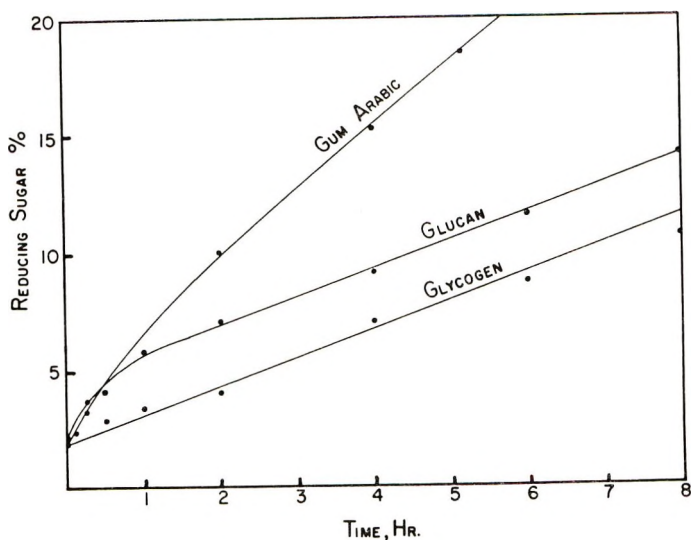


Fig. 4. Rates of increase of reducing sugar at 90°C. for 1% solutions of gum arabic, animal glycogen, and polyglucose in 0.02*N* H<sub>2</sub>SO<sub>4</sub>.

growth. The nondialyzable polymer formed after 6 hr. contains 0.7% isopropylidene groups or about 0.6 groups per polymer molecule. Since the method of analysis for residual acetone in the polymer is not precise, the actual amount of residual acetone might be one molecule per polymer molecule, as expected if isopropylidene groups at other than the potential reducing end of the polymer are lost during the polymerization reaction.

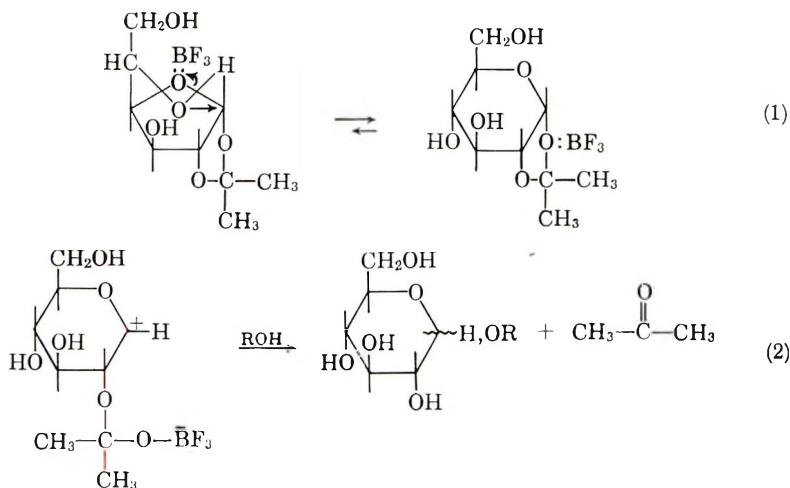
When monoisopropylidene *D*-glucose is polymerized at 165–170°C. with a monomer: catalyst ratio of 1000 the nondialyzable polymer formed in 3 hr. hydrolyses to *D*-glucose. The rate of hydrolysis is similar to that for animal glycogen and dissimilar to the initial rate for gum arabic which contains acid-labile furanosidic linkages. By extrapolation of the rate curves in Figure 4, it can be calculated that approximately 97% of the *D*-glucose units in the polymer must be in a normal *D*-glucopyranose ring form. During polymerization of 1,2-*O*-isopropylidene- $\alpha$ -*D*-glucofuranose the specific optical rotation of the isolated polymer remains nearly constant at +42° for periods up to 12 hr. which suggests that a mixture of  $\alpha$  and  $\beta$  linkages is present, with perhaps a slight predominance of the  $\beta$ .

Periodate oxidation of the polymer consumes 1.37 moles of oxidant per sugar unit and yields 0.45 moles of formic acid per *D*-glucose unit. The large yield of formic acid indicates a large number of *D*-glucopyranoside units which can occur as end units or as 1  $\rightarrow$  6 linked chain units. In addition, periodate oxidation releases 0.05 mole formaldehyde per hexose unit, implying that up to 95% of the repeating units are pyranosidic.

Methanolysis of the methylated polymer gives a complex mixture of methylated methyl *D*-glucosides. By gas-liquid chromatography methyl 2,3,4,6-tetra-*O*-methyl-*D*-glucopyranosides, methyl tri-*O*-methyl-*D*-gluco-

pyranosides, and methyl di-*O*-methyl-*D*-glucopyranosides are found in the ratio 1:2:1. Some indication of methylated *D*-glucofuranosides is also obtained. These data are further evidence of a highly branched polymer. A highly complex polymeric structure can be expected from a random condensation of a monomer containing high hydroxyl functionality.

The polymerization reaction seems to involve cleavage of the alkoxy-carbon bond at carbon atom C<sub>1</sub>, leaving a carbonium ion at carbon C<sub>1</sub> stabilized by the adjacent ether oxygen atom. A stabilized carbonium ion at carbon C<sub>1</sub> seems necessary, since 3,4-*O*-isopropylidene-*D*-glucitol does not polymerize with boron trifluoride. The carbonium ion can react with a hydroxyl oxygen on another monomer unit to produce a glycosidic bond. The boron trifluoride complex with the isopropylidene group accepts a proton to yield a hydroxyl group on the sugar, and acetone is released [eqs. (1) and (2)].



Since *D*-glucopyranoside units predominate in the polymer, a ring expansion probably occurs in the monomer before the polymerization reaction. It is known<sup>14</sup> that tetrahydrofuran is a stronger Lewis base towards boron trifluoride than aliphatic ethers or alcohols. It is reasonable to assume that the catalyst coordinates with the ring oxygen of the monomer allowing attack on carbon C<sub>1</sub> by the oxygen at carbon C<sub>5</sub>, producing a pyranose ring. A similar ring expansion of methyl β-*D*-glucofuranoside to methyl *D*-glucopyranoside was demonstrated by Overend and co-workers.<sup>15</sup> After ring expansion the alkyl oxygen bond involving the isopropylidene group at carbon C<sub>1</sub> opens to allow polymerization with release of acetone.

Theoretically the condensation reaction can produce molecules of very high molecular weight. However, dehydration reactions probably inhibit polymer growth due to hydrolysis of isopropylidene groups and conversion of the catalytic system to a protic type which is inefficient (Table III). Two products resulting from dehydration, 3,6-anhydro-*D*-glucose and a hexulose, are detected chromatographically in the hydrolyzate of a polymer



TABLE III  
Melt Polymerization of 1,2:5,6-Di-*O*-Isopropylidene- $\alpha$ -D-Glucufuranose  
at 110°C. with Various Catalysts

Catalyst	Molar ratio monomer catalyst	Reaction period, hr.	Non- dialyzable polymer, %	$\bar{M}_n$
$\text{SnCl}_4$	1000	12	20	6100
$\text{TiCl}_4$	1000	12	14	2200
$\text{AlCl}_3$	1000	12	13	2650
$\text{BF}_3$	1000	168	1	—
$\text{ZnCl}_2$	1000	12	0	—
$\text{BF}_3$	100	12	21	5230
$\text{BF}_3$	10	1	20	3550
$\text{Cl}_3\text{CCOOH}$	1000	12	0	—
$\text{ClCH}_2\text{COOH}$	1000	168	0	—
$\text{ClCH}_2\text{COOH}$	10	12	2	—
$\text{ClCH}_2\text{COOH}$	10	168	10	1900

from 1,2:5,6-di-*O*-isopropylidene- $\alpha$ -D-glucufuranose. Because of these effects the polymerization proceeds slowly after an initial rapid rate of condensation for both 1,2:5,6-di-*O*-isopropylidene- $\alpha$ -D-glucufuranose (Fig. 2) and 1,2-*O*-isopropylidene- $\alpha$ -D-glucufuranose (Fig. 3). Likewise, methyl  $\alpha$ -D-glucopyranoside and D-glucose give only small amounts of low molecular weight polymers because the condensation by-products, methanol and water, alter the catalytic system. If the water of condensation could be removed from the polymerization system, condensation would be expected to continue. Thus, 2,3:5,6-di-*O*-isopropylidene- $\alpha$ -D-mannofuranose produces good yields of polymer, since the isopropylidene groups on the monomer hydrolyze with consequent removal of water (Table II).

### EXPERIMENTAL

Melting points were taken on a Fisher-Johns apparatus and are corrected. Thin layer chromatography was conducted on 20 × 100 mm. plates coated with silica gel G (Brinkman Instruments, New York, N. Y.). After irrigation, the plates were sprayed with a 5% solution of sulfuric acid in methanol and charred on a hot plate. Paper chromatography was conducted on Whatman No. 1 paper at 25°C., ethyl acetate, acetic acid, formic acid, and water (18:3:1:4 v/v) being used as irrigant. Chromatograms were sprayed with (A) an aqueous acetone solution of silver nitrate, followed by a methanolic sodium hydroxide solution,<sup>16</sup> (B) an aqueous alkaline solution of potassium permanganate and sodium metaperiodate,<sup>17</sup> or (C) resorcinol-hydrochloric acid reagent.<sup>18</sup> Limiting viscosity numbers were determined in water solutions at 25°C. with an Ubbelohde viscometer. Number-average molecular weights were determined in water solution with the use of a Mechrolab vapor pressure osmometer, Model 301 A. Boron trifluoride etherate was purified as previously described.<sup>10</sup> Reagent grade benzene was refluxed and distilled from lithium aluminum hydride and stored over sodium.

### Preparation of Monomers

1,2:5,6-Di-*O*-isopropylidene- $\alpha$ -D-glucofuranose<sup>19</sup> was recrystallized twice from petroleum ether (b.p. 60–68°C.), m.p. 110°C. When it was methylated with dimethyl sulfate<sup>20</sup> 1,2:5,6-di-*O*-isopropylidene-3-*O*-methyl- $\alpha$ -D-glucofuranose was obtained as a syrup; b.p. 105°C./0.02–0.03 mm.;  $[\alpha]_D^{25} = -31.6^\circ$  ( $c = 4.2$ , ethanol) (lit.:<sup>21</sup> b.p. 139–140°C./12 mm.;  $[\alpha]_D^{25} - 32.2^\circ$ ,  $c = 5.05$ , ethanol). 1,2-*O*-Isopropylidene- $\alpha$ -D-glucofuranose was prepared as described by Whistler and co-workers<sup>22</sup> and was recrystallized twice from ethyl acetate, m.p. 160–161°C. It was converted to the tri-*O*-methyl ether of 1,2-*O*-isopropylidene- $\alpha$ -D-glucofuranose with dimethyl sulfate in carbon tetrachloride,<sup>20</sup> followed by two methylations with Purdie<sup>23</sup> reagents. The product was a syrup; b.p. 85–87°C./0.02 mm.;  $[\alpha]_D^{25} - 26.3^\circ$  ( $c = 4.8$ , ethanol), (lit.:<sup>24</sup> b.p. 110–115°C./0.2 mm.,  $[\alpha]_D^{20} - 27.2$ ,  $c = 4.64$ , ethanol). 1,2:3,5-Di-*O*-isopropylidene- $\alpha$ -D-xylofuranose was prepared according to the procedure of Levene;<sup>25</sup> m.p. 44–45°C.;  $[\alpha]_D^{25} + 6.1$  ( $c = 1.0$ , chloroform). 1,2-*O*-Isopropylidene- $\alpha$ -D-xylofuranose was obtained through partial hydrolysis of 1,2:3,5-di-*O*-isopropylidene- $\alpha$ -D-xylofuranose. The monoisopropylidene derivative crystallized after distillation, b.p. 120–125°C./0.02–0.03 mm.;  $[\alpha]_D^{25} + 15.9$  ( $c = 1.0$ , water). 1,2:3,4-Di-*O*-isopropylidene- $\alpha$ -D-galactopyranose<sup>19</sup> distilled with b.p. 126–130°C./0.02–0.03 mm.;  $[\alpha]_D^{25} - 61.0^\circ$  ( $c = 1.1$ , chloroform). 2,3:5,6-Di-*O*-isopropylidene- $\alpha$ -D-mannofuranose<sup>19</sup> was crystallized from a mixture of petroleum ether (b.p. 60–68°C.) and diethyl ether, m.p. 122–123°C.,  $[\alpha]_D^{25} + 32.1 \rightarrow +7.8$  ( $c = 1.0$  chloroform). 3,4-*O*-Isopropylidene-D-glucitol, m.p. 87–88°C., was prepared according to the procedure of Bourne and co-workers.<sup>26</sup>

### Solution Polymerization of 1,2:5,6-Di-*O*-isopropylidene- $\alpha$ -D-glucofuranose

All solution polymerizations were conducted in sealed tubes (25 × 250 mm.) at 65°C. with the use of a 0.2*M* benzene solution of monomer. Before use, each tube was rinsed with hot cleaning solution, washed with water, dried in an oven at 110°C., and stoppered, while hot, with a rubber cap (Aloc Scientific, V 72400). One series of tubes was prepared with different amounts of catalyst and heated for 1 hr. The tubes were placed in a Dry Ice–acetone bath, evacuated, and injected with an appropriate amount of benzene in which was dissolved 2.6 g. of 1,2:5,6-di-*O*-isopropylidene- $\alpha$ -D-glucofuranose (0.01 mole). With the contents frozen, a calculated amount of a 10% solution of boron trifluoride etherate in benzene was injected. The tubes were sealed under reduced pressure, placed in a constant-temperature bath, and mechanically agitated. After 1 hr. the tubes were removed and the polymers precipitated by pouring into four volumes of diethyl ether. The polymers were collected on tared sintered glass funnels, washed well with ether, and dried in a vacuum desiccator for 24 hr. Conversion to crude polymer based on the weight of monomer is shown in Figure 1.

The amount of nondialyzable polymer formed was determined by dissolving 0.3 g. of crude polymer in water and dialyzing in Visking cellulose casing against distilled water for 3 days. A small amount of insolubles, always less than 2%, was removed from the dialyzed solution by filtering through a sintered glass funnel fitted with a Celite-talc pad as a filter aid. After lyophilization, the weight and the molecular weight of the nondialyzable polymer was determined. The molecular weight and per cent nondialyzable obtained with different catalyst concentrations are illustrated in Figure 1.

Since a monomer:catalyst ratio of 10 seemed to produce highest molecular weights within a short time this ratio was used in a series of reactions in which the reaction time was varied. These results are shown in Figure 2. Reactions were examined periodically by thin layer chromatography using ethyl acetate and hexane (80:20 v/v) as irrigant. Visual comparison of the relative intensities of spots showed that after 1 hr. most of the 1,2:5,6-di-*O*-isopropylidene- $\alpha$ -D-glucofuranose was consumed.

Each nondialyzable polymer (20 mg.) was heated at 100°C. with 2 ml. of 1*N* aqueous sulfuric acid solution for 5 hr. The hydrolyzate was cooled and neutralized with barium carbonate. The solution was filtered, concentrated, and examined qualitatively by paper chromatography by using developing sprays A and C. At low catalyst concentrations or after short polymerization reaction times only D-glucose was detected. In polymerizations with high catalyst concentrations or in those whose reaction times were long, two new components appeared in the polymer hydrolyzate. One component had  $R_G = 2.0$ , identical with 3,6-anhydro-D-glucose, while the other with  $R_G = 2.9$  was possibly a hexulose,<sup>27</sup> since it gave a pink color reaction with spray C.

### Melt Polymerizations

1,2:5,6-Di-*O*-isopropylidene- $\alpha$ -D-glucofuranose (2.6 g.) was weighed into each of five test tubes (18 × 150 mm.) which were constricted to facilitate sealing later. The tubes were dried 12 hr. in a vacuum desiccator over phosphorus pentoxide, capped with a rubber stopper, evacuated, and cooled in a Dry Ice-acetone bath. Appropriate amounts of boron trifluoride etherate in 0.13 ml. of benzene were injected, and the tubes sealed under reduced pressure. It is important to anneal and seal the tubes properly because of the high vapor pressure of acetone which is released during the polymerization. The tubes were shaken vigorously while warming to room temperature in order to disperse catalyst and were placed in an oven at 110°C. At intervals, a tube was removed, cooled, and the solid extracted with an aqueous solution of 1% sodium bicarbonate. The solution was filtered through a Celite-talc pad on a sintered glass funnel, dialyzed for 3 days against distilled water, filtered, lyophilized, and weighed. The optical rotation, molecular weight, and limiting viscosity number are given in Table I.

Melt polymerization reactions with 2.2 g. of 1,2-*O*-isopropylidene- $\alpha$ -D-

glucofuranose (0.01 moles) were conducted in sealed tubes in an oil bath at 165–170°C. Each tube was charged with monomer, 0.13 ml. of 1% solution of boron trifluoride etherate ( $1 \times 10^{-5}$  mole) in benzene and treated as described before. At intervals a tube was opened and placed in a boiling water bath for 1 hr. The glassy polymer was crushed and heated 24 hr. under reduced pressure over phosphorus pentoxide at 65°C. Polymer was dissolved in 10.0 ml. of 1% aqueous sodium bicarbonate solution. A 1.0-ml. portion of this polymer solution was diluted to 100 ml., then a 1.0- or 3.0-ml. aliquot of this solution was analyzed for acetone by the method of Reid.<sup>28</sup> 1,2-*O*-Isopropylidene- $\alpha$ -D-glucofuranose was used to obtain a standard curve. Acetone released during the polymerization was calculated by difference and plotted against time in Figure 3. The remaining 9.0 ml. of aqueous bicarbonate polymer solution was diluted to 20 ml. Examination of this solution by paper chromatography by using spray reagent B showed that all 1,2-*O*-isopropylidene- $\alpha$ -D-glucofuranose was consumed after 3 hr. of reaction. Polymer solution was dialyzed against distilled water for 3 days and lyophilized. Per cent nondialyzable polymer and corresponding molecular weights are given in Figure 3. Several tubes were allowed to react for 24 and 48 hr. The yield of nondialyzable polymer remained at 30% for these longer periods, while the molecular weight of the polymer rose from 10,000 at 24 hr. to 12,700 at 48 hr. Polymers formed with polymerization periods up to 12 hr. gave  $[\alpha]_D^{25} + 41.0 \pm 2.1$  ( $c = 0.5$ , water), while the polymer formed after 24 hr. had  $[\alpha]_D^{25} + 64.0$  ( $c = 0.5$ , water). 1,2:5,6-Di-*O*-isopropylidene- $\alpha$ -D-glucofuranose (2.6 g.,  $1 \times 10^{-2}$  mole) was heated also with 0.13 ml. of 1% solution of boron trifluoride etherate ( $1 \times 10^{-5}$  mole) in benzene in a sealed tube at 165–170°C. After 48 hr. the melt was dissolved in 50% acetone–water solution containing 1% sodium bicarbonate. The solution was dialyzed 2 days against 50% acetone–water, 1 day against acetone, and 2 days against distilled water. Lyophilization gave 0.1% yield of polymer.

Elimination of acetone during polymerization was also confirmed as follows. 1,2-*O*-Isopropylidene- $\alpha$ -D-glucofuranose (1.1 g.,  $5 \times 10^{-3}$  mole) was placed in a two-necked 50-ml. round-bottomed flask fitted with a nitrogen inlet and a condenser arranged for downward distillation. The delivery tube was submerged in an acidic alcoholic solution of 1.6 g. of 2,4-dinitrophenylhydrazine cooled in an ice bath. After the flask containing the sugar derivative was heated to 160°C., 0.07 ml. of a 10% solution of boron trifluoride etherate in benzene was injected, and a slow stream of nitrogen passed through the reaction vessel. An immediate precipitate of acetone 2,4-dinitrophenylhydrazone formed in the receiver. After reaction for 1 hr. the hydrazone solution was removed and allowed to stand an additional hour at 0°C., whereupon the precipitate was collected on a tared sintered glass funnel, washed once with a cold solution of 25 ml. of 95% ethanol containing 1.5 ml. of concentrated sulfuric acid, then washed with water, and dried in a vacuum desiccator. The yield of crude acetone derivative was 0.736 g. (62%), and the product had m.p. 122–126°C.



One recrystallization from 95% ethanol gave acetone 2,4-dinitrophenylhydrazone, m.p. and mixed m.p. 126–127°C., (lit.:<sup>29</sup> m.p. 126°C.). In a similar manner 1,2:5,6-di-*O*-isopropylidene- $\alpha$ -D-glucofuranose (0.65 g.) polymerized at 110°C. produced 0.46 g. of 2,4-dinitrophenylhydrazone (76%).

A partial structural analysis was made on the nondialyzable portion of polymer formed from 1,2-*O*-isopropylidene- $\alpha$ -D-glucofuranose on treatment at 165–170°C. for 3 hr. with 1 mole of boron trifluoride per 1000 moles of monomer. The polymer had a number-average molecular weight of 4450 and contained 1.9% acetone as determined by the method of Reid.<sup>28</sup> The theoretical value for one acetone endgroup per chain is 1.3%. Another 0.6 g. portion of polymer was hydrolyzed and the acetone released was trapped as its 2,4-dinitrophenylhydrazone as previously described. Yield of hydrazone was 7 mg. with m.p. 126–127°C. This polymer had a  $[\alpha]_D^{25} + 41.2$  ( $c = 0.5$ , water).

A 10-mg. portion of polymer was hydrolyzed for 12 hr. in 1.0 ml. of 1*N* sulfuric acid solution. After neutralization with barium carbonate the hydrolyzate was examined by paper chromatography with the use of spray A. The hydrolyzate contained D-glucose together with traces of the same reducing spots found in a solution when pure D-glucose (10 mg.) was heated with 1 ml. of 1*N* sulfuric acid solution.

In another hydrolysis the amount of reducing sugar formed was determined by hypiodite oxidation.<sup>30</sup> Polymer (8.90 mg.) was heated with 1 ml. of 1*N* sulfuric acid solution for 12 hr. at 110°C. in a sealed tube. The hydrolyzate was neutralized, and the amount of reducing power determined to be 96.2% of theoretical.

The hydrolysis rate of the polyglucose was measured. Polyglucose (0.5 g.) was added to 50.0 ml. of 0.02*N* sulfuric acid solution and stirred at 90°C. Aliquots of 3.0-ml. size were taken at intervals and neutralized with 4 ml. of a 0.54% aqueous sodium bicarbonate solution. To the solution was added 20 ml. of 0.05*M* borate buffer and 5.0 ml. of 0.1*N* iodine solution. After standing 2 hr. the solution was acidified with 60 ml. of 0.1*N* hydrochloric acid solution, and the liberated iodine was titrated with 0.1*N* sodium thiosulfate solution. The amount of reducing sugar is plotted against hydrolysis time in Figure 4. In the same manner the reducing power was measured at intervals during the hydrolysis of solutions of gum arabic and animal glycogen (Fig. 4). D-Glucose subjected to the same hydrolysis conditions gave 95–97% of the theoretical reducing value.

A 0.203-g. sample of polymer was dissolved in 50 ml. of 0.12*M* sodium metaperiodate, and the mixture was kept in the dark at 25°C. After an appropriate time had elapsed, the residual oxidant was iodometrically titrated in the usual manner, and formic acid was also determined. After 24 hr., oxidation was essentially complete, and periodate consumed and formic acid liberated was 1.37 and 0.45 mole per hexose unit, respectively. In a separate experiment 200 mg. of polymer was oxidized with sodium metaperiodate according to the procedure of Reeves.<sup>31</sup> The oxidation gave 1.86 mg. of formaldehyde or 0.05 mole formaldehyde per hexose unit.



A 0.8-g. portion of polymer was methylated by three successive treatments with potassium hydroxide and dimethyl sulfate.<sup>32</sup> The 0.34 g. of chloroform-soluble polymer was then methylated six times by the Purdie<sup>23</sup> method. The final product of 0.24 g. showed hydroxyl absorption in the infrared  $[\alpha]_D^{25} + 66.5$  ( $c = 1.4$ , chloroform); methoxyl content 42.1% (theoretical 45.6%). This polymer resembles other highly branched glycans, such as glycogen, which are difficult to fully methylate under Purdie conditions.<sup>33</sup>

The methylated polymer (100 mg.) was refluxed 10 hr. with 5 ml. of methanol containing 5% hydrogen chloride. The solution was neutralized with silver carbonate and concentrated to a syrup. The methylated D-glucosides were analyzed by gas-liquid column chromatography. The mixture included methyl 2,3,4,6-tetra-*O*-methyl- $\alpha$ - and - $\beta$ -D-glucopyranosides and anomeric pairs of all the possible tri-*O*-methyl and di-*O*-methyl glucopyranosides.

### Reactions of Some Sugar Derivatives with Boron Trifluoride

Into three separate polymerization tubes were placed 0.01-mole portions of 1,2:5,6-di-*O*-isopropylidene-3-*O*-methyl- $\alpha$ -D-glucopyranose, 1,2-*O*-isopropylidene-3,5,6-tri-*O*-methyl- $\alpha$ -D-glucopyranose, and 1,2:3,5-di-*O*-isopropylidene- $\alpha$ -D-xylofuranose. The monomers were dissolved in 48.7 ml. of benzene, and the tubes were treated as described for the solution polymerization of 1,2:5,6-di-*O*-isopropylidene- $\alpha$ -D-glucopyranose at a molar ratio of monomer to boron trifluoride of 10. After a polymerization period of 1 hr. at 65°C., the solutions were neutralized by vigorously stirring with 25 ml. of 50% aqueous acetone solution containing 2% sodium bicarbonate, and then dialyzed 2 days against 50% aqueous acetone, 1 day against acetone, and 2 days against water. The solutions were concentrated under reduced pressure to 50 ml., and upon lyophilization no residues were present.

Melt polymerization of 3,4-*O*-isopropylidene-D-glucitol (0.22 g.) was examined. The polymerization period was 1 hr. at 110°C. with a molar ratio of monomer to catalyst of 10. The product was dissolved in 5% aqueous sodium bicarbonate solution, dialyzed against distilled water, and lyophilized. No product was present. Examination of the solution of the 3,4-*O*-isopropylidene-D-glucitol melt by thin layer chromatography using as irrigant *n*-butanol, ethanol, water (3:1:1 v/v) and by paper chromatography showed only a trace of 3,4-*O*-isopropylidene-D-glucitol and some unidentified compounds that moved close to the solvent fronts. No oligomers or polymers were detected.

Melt polymerization of D-glucose (1.8 g.,  $1 \times 10^{-2}$  mole) was attempted at 165–170°C. with  $1 \times 10^{-5}$  moles of boron trifluoride. At the end of 3 hr. a 3.9% yield of nondialyzable brown polymer was obtained with a molecular weight 2600. Methyl  $\alpha$ -D-glucopyranoside under the same conditions gave a 2.4% conversion to nondialyzable polymer.

In addition, melt polymerizations were done on a number of sugar

ketals, and the results are given in Table II. In each case a 0.01-mole portion of isopropylidene derivative was treated in a sealed tube at 165–170°C. at either a molar ratio of monomer to catalyst of 1000 or 100.

### Comparison of Catalysts

Since 1,2-*O*-isopropylidene- $\alpha$ -D-glucofuranose polymerized readily, a better comparison of the catalytic activity of Lewis and protic acids was gained by using the more difficultly polymerizable monomer 1,2:5,6-di-*O*-isopropylidene- $\alpha$ -D-glucofuranose. Thus a series of melt polymerizations of 1,2:5,6-di-*O*-isopropylidene- $\alpha$ -D-glucofuranose was conducted to compare boron trifluoride; stannic, aluminum, titanium, and zinc chlorides; chloroacetic and trichloroacetic acids. Each tube was charged with 2.6 g. of 1,2:5,6-di-*O*-isopropylidene- $\alpha$ -D-glucofuranose. Boron trifluoride, stannic chloride, titanium tetrachloride, chloroacetic and trichloroacetic acids were all added by injecting 0.1 ml. of a 0.10*M*, 1.0*M*, or 10.0*M* benzene solution of catalyst. Zinc chloride and aluminum chloride were added as solids. The tubes were sealed as usual and heated in an oven at 110°C. At the end of the reaction periods the products were dissolved by stirring in 25 ml. of 50% aqueous acetone solution containing 2% sodium bicarbonate. The solutions were dialyzed in Visking cellulose casing 2 days against 50% aqueous acetone, 1 day against acetone, and 2 days against distilled water. The polymer solutions were filtered through a Celite-talc filter aid on a sintered glass funnel. The solutions were concentrated to 50 ml. under reduced pressure and lyophilized. Yields of product and molecular weights of polymers are given in Table III.

This study from the Purdue Agricultural Experiment Station, Lafayette, Indiana, was carried out in collaboration under North Central Regional Project NC60.

The authors gratefully acknowledge the grant and support of this work from the Pioneering Research Program of the Institute of Paper Chemistry, Appleton, Wisconsin. The authors also thank Dr. C. T. Bishop, National Research Council, Ottawa, Canada, for gas-liquid chromatographic examination of the methylated methyl-D-glucosides.

### References

1. F. Musculus, *Bull. Soc. Chim. France* [2], **18**, 67 (1872).
2. A. Whol, *Ber.*, **23**, 2084 (1890).
3. E. Fischer, *Ber.*, **23**, 3687 (1890).
4. R. Willstatter and L. Zeichmeister, *Ber.*, **46**, 3401 (1913).
5. H. Fram, *Ber.*, **74**, 622 (1941).
6. H. Fram, *Ann. Chem.*, **555**, 187 (1944).
7. Y. L. Pogosov and Z. A. Rogovin, *Russ. Chem. Rev.*, **30**, 545 (1961).
8. P. T. Mora and J. W. Wood, *J. Am. Chem. Soc.*, **80**, 685 (1958).
9. P. T. Mora, J. W. Wood, P. Maury, and B. G. Young, *J. Am. Chem. Soc.*, **80**, 693 (1958).
10. R. L. Whistler and P. A. Seib, *J. Polymer Sci. A*, **2**, 2595 (1964).
11. H. Bredtschneider and K. Beran, *Monatsh.*, **80**, 262 (1949).
12. R. U. Lemieux and W. P. Shyluk, *Can. J. Chem.*, **31**, 528 (1953).
13. T. O. Bonner, E. J. Bourne, and S. McNally, *J. Chem. Soc.*, **1962**, 761.
14. H. E. Wirth and P. I. Slick, *J. Phys. Chem.*, **66**, 2277 (1962).

15. B. Capon, G. W. Loveday, and W. G. Overend, *Chem. Ind. (London)*, **1962**, 1537.
16. W. E. Trevelyan, C. P. Parker, and J. S. Harrison, *Nature*, **166**, 444 (1950).
17. R. U. Lemieux and H. F. Bauer, *Anal. Chem.*, **26**, 920 (1954).
18. L. Hough, J. K. N. Jones, and W. H. Wadman, *J. Chem. Soc.*, **1950**, 1702.
19. R. L. Whistler and M. L. Wolfrom, *Methods in Carbohydrate Chemistry*, Vol. II, Academic Press, New York, 1963.
20. W. Freudenburg and A. M. Vajda, *J. Am. Chem. Soc.*, **59**, 1955 (1937).
21. J. C. Irvine and J. O. Scott, *J. Chem. Soc.*, **1913**, 564.
22. R. E. Gramera, A. Park, and R. L. Whistler, *J. Org. Chem.*, **28**, 3230 (1963).
23. T. Purdie and J. C. Irvine, *J. Chem. Soc.*, **83**, 1021 (1903).
24. P. A. Levene and G. M. Meyer, *J. Biol. Chem.*, **74**, 701 (1927).
25. P. A. Levene and A. L. Raymond, *J. Biol. Chem.*, **102**, 317 (1933).
26. E. J. Bourne, G. P. McSweeney, M. Stacey, and L. F. Wiggins, *J. Chem. Soc.*, **1952**, 1408.
27. O. Theander, *Acta Chem. Scand.*, **11**, 1557 (1957).
28. R. L. Reid, *Analyst*, **85**, 265 (1960).
29. R. L. Shriner, R. C. Fuson, and K. Y. Curtin, *The Systematic Identification of Organic Compounds*, 4th Ed., Wiley, New York, 1956, p. 316.
30. A. R. Martin, L. Smith, R. L. Whistler, M. Harris, *J. Res. Natl. Bur. Std.*, **27**, 449 (1941).
31. R. E. Reeves, *J. Am. Chem. Soc.*, **63**, 1476 (1941).
32. W. N. Haworth, *J. Chem. Soc.*, **107**, 8 (1915).
33. R. L. Whistler and L. Smart, *Polysaccharide Chemistry*, Academic Press, New York, 1953, p. 440.

### Résumé

Une nouvelle méthode pour préparer des polymères de D-glucose est décrite. Des dérivés isopropyléniques de D-glucosé, particulièrement le dérivé 1,2 sont traités par des acides de Lewis tels que le trifluorure de bore afin d'éliminer l'acétone et produisent un polymère hautement branché d'un poids moléculaire de 12.700. Approximativement une unité isopropylidénique reste vraisemblablement à l'extrémité pseudo-réductrice du glucane. Jusqu'à 95% d'unités du polymère sont de nature D-glucopyranosidique, ce qui indique que l'élargissement de cycles se passe au cours de la condensation.

### Zusammenfassung

Eine neue Methode zur Darstellung von D-Glucosepolymeren wird beschrieben. Isopropylidenderivate von D-Glucosé, besonders das 1,2-Mono-O-derivat werden mit Lewisäuren, wie Bortrifluorid unter Eliminierung von Aceton und Bildung eines hochgradig verzweigten Polymeren mit einem Molekulargewicht von 12.700 behandelt. Näherungsweise eine Isopropylideneinheit bleibt zurück, möglicherweise am potentiell reduzierenden Ende des Glucans. Bis zu 95% der Polymerbausteine sind D-Glucopyranosideinheiten, was beweist, dass während der Kondensation eine Ringerweiterung eintritt.

Received August 17, 1965  
Prod. No. 4947A

## Studies On Poly(aquahydrochromium Diphenylphosphinate)\*

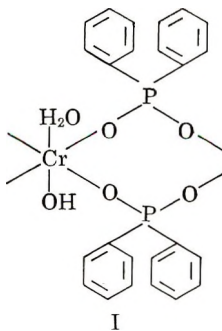
A. D. DELMAN, J. KELLY, J. MIRONOV, and B. B. SIMMS, *Organic Chemistry Branch, U. S. Naval Applied Science Laboratory, Naval Base, Brooklyn, New York*

### Synopsis

The novel inorganic polymer poly(aquahydrochromium diphenylphosphinate) was investigated to obtain information concerning its degree of polydispersity and properties when dissolved in organic solvents. Viscometric, infrared absorption spectroscopic, and electrical conductimetric techniques were employed to ascertain the characteristics of the polymer dissolved in benzene, chlorobenzene, and chloroform. Gel permeation chromatography was used to determine the degree of heterogeneity of the polymer. Results indicate that the polymer, as prepared, is quite polydisperse. The polymer main chains do not undergo radical reactions with the solvents. High values of the Huggins interaction constant  $K'$  suggest that polymer-solvent association reactions involving chain-endgroups are probable. Such reactions are also indicated by association constant values and by the shapes of phoreograms obtained from electrical conductance data. Both "local" and "bulk" solvent properties, such as the dielectric constant, appear to influence the characteristics of the polymer when dissolved in the different solvents.

### INTRODUCTION

Recently, novel coordination polymers having completely inorganic backbones were reported.<sup>1-6</sup> As part of a general study of the properties of new macromolecular substances that might be useful at high temperatures, we have investigated the properties of the aquahydrochromium diphenylphosphinate polymer which is considered to have a double-bridged backbone (I).<sup>5</sup>



\* Presented to Division of Organic Coatings and Plastics Chemistry, 150th National Meeting of the American Chemical Society, Atlantic City, N. J., September 12-17, 1965.



This paper presents the results of studies of the characteristics of the polymer in different solvents. Data are also presented on the degree of polydispersity of the polymer.

## EXPERIMENTAL

### Polymer Preparation

The polymer was synthesized by the method of Saraceno and Block.<sup>4</sup> Essentially, this is a two-step process involving the reaction of freshly prepared chromium(II) acetate and potassium diphenylphosphinate to yield the corresponding chromium(II) diphenylphosphinate which is then oxidized with air in the presence of water to produce the polymer. Several batches (3-4 g.) were thus prepared and combined to form a masterbatch for this study.

### Solution Preparation

An accurately weighed sample of the polymer was dissolved in each of the solvents in a dry nitrogen atmosphere. The solution was filtered and the polymer concentration of the filtrate was determined from the amount of gel removed. The dilution method was then used to obtain solutions with lower polymer concentrations.

The highest purity solvents available from commercial sources were used in this study. Benzene and chlorobenzene were dried over sodium and calcium chloride, respectively. After drying, the solvents were filtered and distilled. The solvent chloroform contained approximately 0.75% of ethyl alcohol as a stabilizer. During the initial stage of the work, the chloroform was dried over calcium chloride and redistilled to remove stabilizer. However, the polymer solutions made with the purified chloroform became cloudy within one week, it was suspected, therefore, that the stabilizer-free solvent was breaking down and that the degradation products were interacting with the polymer. Accordingly, chloroform was dried over calcium chloride, filtered, and used without further purification.

### Polydispersity

The molecular size distribution of the polymer was determined by gel permeation chromatography (GPC) with the use of the Waters Associates, Inc. instrument. This technique has been previously described by Moore<sup>7</sup> and Harmon.<sup>8</sup> In this study a 1% by weight solution of the polymer dissolved in dry reagent-grade tetrahydrofuran was prepared. At room temperature, a 2-ml. sample was pumped at 1 ml./min. through a chromatographic system consisting of two columns packed with crosslinked polystyrene of  $10^4$  and  $10^3$  A. pore size, respectively. The columns were calibrated from narrow molecular weight distribution samples of anionically polymerized styrene and polypropylene glycol having molecular sizes of 6029 and 247 A., respectively. The abscissa of the curve obtained from the GPC instrument recorder was equally divided with index marks which



represented successive 5 ml. portions of solvent flow from the time the sample was injected. Each index mark was converted to angstrom length according to the calibration data.

### Viscosity

Viscometric measurements of the polymer solutions and solvents were made at 30°C. with a Cannon-Ubbelohde dilution viscometer.

### Infrared Spectra

Spectra were obtained over the 2.5–25.0  $\mu$  range on a Perkin-Elmer Model 337, grating infrared spectrophotometer equipped with KBr optics. The polymer spectra were obtained from solutions, solution-cast films, and Nujol or hexachlorobutadiene mulls. Solution and solvent spectra were made with a cell of 0.1 mm. path length and having KBr windows, with and without solvent compensation. Polymer solution concentrations were adjusted by evaporation of dilute solutions at room temperature under a dynamic nitrogen atmosphere or by the addition of known amounts of solvents to concentrated solutions. Polymer concentrations were determined by evaporation of aliquot samples of the solutions to constant weight. Absorbances and half-intensity band widths were measured from tangent baselines.

### Electrical Conductivity

The literature<sup>9–11</sup> gives several examples of the use of dc techniques to measure the electrical conductance of various substances when dissolved in organic solvents. The theoretical basis for the usefulness of such measurements to obtain information on ionic species in nonaqueous solution is described by Gavis.<sup>12</sup>

In this study the electrical conductivity measuring procedure described by Burkin<sup>13</sup> was adopted. Measurements were made with a two-terminal, 20  $\mu\text{f}$ . air capacitance, glass-mounted, 7–10 ml. capacity, type 225P Balsbaugh cell having 0.035 in. spacing between platinum electrodes. The cell constant was determined to be  $4.61 \times 10^{-3} \text{ cm.}^{-1}$  by the method of French and Hart.<sup>14</sup> The current flowing through the cell while applying 10 v. dc from a stabilized power supply was measured with a Keithley 610A electrometer. The usual correction for solvent conductance was made. Molar concentrations of the solutions were calculated on the basis of a number-average molecular weight of 7300 for the polymer, as determined from GPC data.

## RESULTS AND DISCUSSION

### Polydispersity

Figure 1 shows the GPC fractionation curve of the polymer. In general these data indicate that the polymer comprises a broad distribution of molecular weight species with two major fractions at about 10 and 1900 Å. A smaller fraction at 19 Å. also is evident.

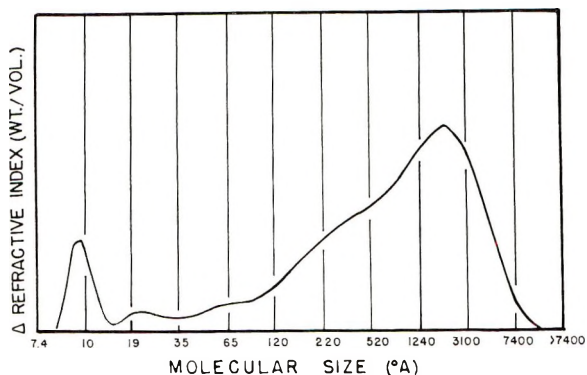


Fig. 1. Gel permeation chromatogram of polymer.

A good approximation to the actual Cr-Cr distance in the polymer is considered to be 5.03 Å.<sup>15</sup> On this basis, the fractions in the GPC chromatogram at 10 and 19 Å. are dimer and tetramer, respectively, while the polymer component at 1900 Å. has a weight-average molecular weight of about 200,000. Tetrahydrofuran solutions of polymer samples which were previously dissolved in benzene or chloroform and evaporated to dryness at room temperature produced similar GPC chromatograms. It would appear from this that polymer molecules, except for possible chain-end effects which could not be determined by this method, were unaffected by solution in benzene and chloroform. Polymer solutions in dimethylformamide gave GPC chromatograms with a negative rather than positive peak at 10 Å. This suggests that the dimer component was altered in some manner by solution in dimethylformamide, or that another substance of comparable size to a dimer fraction was present.

### Viscosity

The intrinsic viscosity values obtained by the least-squares method from  $\eta_{sp}/c$  versus  $c$  plots, wherein  $\eta_{sp}/c$  and  $c$  represent the reduced viscosity and concentration (g./100 ml. of solution), respectively, are shown in Table I.

The  $k'$  constant in the Huggins equation

$$\eta_{sp}/c = [\eta] + k'[\eta]^2c \quad (1)$$

is generally considered to be a complex function of polymer-polymer and polymer-solvent interactions that are influenced by the nature of the

TABLE I  
Intrinsic Viscosities of the Polymer in Various Solvents

Solvent	$[\eta]$	$k'$	$k'[\eta]^2$
Benzene	0.483	0.408	0.095
Chlorobenzene	0.654	0.439	0.188
Chloroform	0.724	0.649	0.340

polymer and of the solvent, and by temperature changes. The value for  $k'$  usually is found in the 0.3-0.4 range, although many exceptions are known.

Table I shows the  $k'$  values obtained for the polymer in each of the solvents are somewhat higher than the usual range, particularly when chloroform is the solvent. According to the method by which the polymer was prepared, it is expected that the molecules contain acetate and/or diphenylphosphinate endgroups. If such polar endgroups do exist in the polymer, association might be expected with the more polar solvents chlorobenzene and chloroform. This could account for the observed variations of the  $k'$  values from the normal range.<sup>16</sup> Departure of  $k'$  from the usual range also may be due to the broad distribution of the molecular weights.<sup>17</sup>

### Infrared Spectra

The infrared spectrum of the polymer masterbatch is identical to one made from a sample prepared at another laboratory. Because of the large average molecular weight of the chains, the expected endgroup vibration frequencies from acetate and/or diphenylphosphinic acid structures are absent.

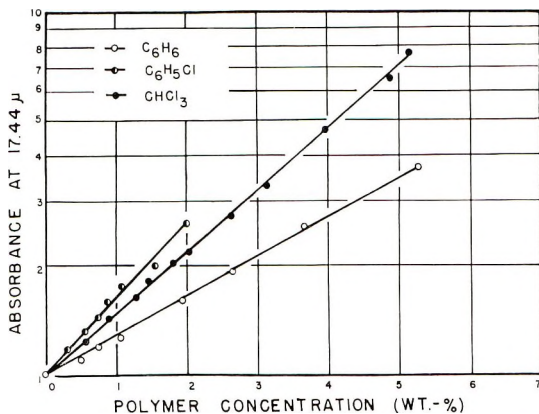
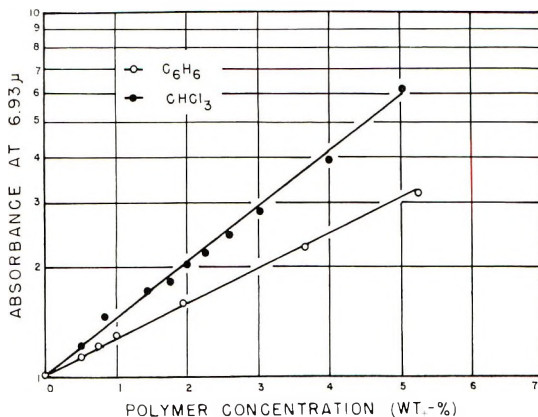
The immediate environment of a molecule can have an appreciable influence on its infrared spectrum. In the case of strong interactions, the development of new spectral vibrations and the disappearance of polymer or solvent bands may be noted. Other variations which may be observed from solvent to solvent are changes in band frequencies, band shape, and band intensities.

A comparison of the polymer spectra prepared from solution-cast films and mulls with those made from solutions in the various solvents gives no evidence of the formation of new vibration frequencies or the disappearance of polymer or solvent absorption bands. These findings indicate that the chemical species of the polymer main chains and the solvent are not appreciably altered, if at all.

The infrared data also show that the polymer and solvent absorption bands do not undergo frequency shifts in the spectra from the various solutions. This apparently shows that the predominant main chain chemical structures are not subject to hydrogen-bonding reactions with the different solvents.<sup>18</sup>

Each of the solution spectra contains a medium absorption mode at 17.44  $\mu$  which is free from interference by solvent vibration frequencies. Coates and Golightly<sup>19</sup> reported the presence of an analogous band near 17.70  $\mu$  in the infrared spectrum of cobalt (II) diphenylphosphinate. From observations reported in the literature<sup>20,21</sup> the 17.44- $\mu$  band is tentatively being assigned to a O-P-O bending mode of the polymer.

The results of peak intensity measurements of the 17.44- $\mu$  band of the polymer in different solvents are shown in Figure 2. It is evident from these data that, within the concentration limits studies, the polymer solutions in the various solvents follow Beer's Law. For any specific polymer

Fig. 2. Effect of concentration on absorbance at 17.44  $\mu$ .Fig. 3. Effect of concentration on absorbance at 6.93  $\mu$ .

concentration, however, the intensities of the band vary moderately from solvent to solvent. The observed variations may be due to local inter- and intramolecular forces acting on the polymer molecules.<sup>22,23</sup> The more marked increase of absorbance with the chlorobenzene and chloroform solutions over that of the benzene solutions is probably due to the greater degree of interaction of the polymers with the more polar solvent molecules at any given concentration. Such interactions are assumed to be rather weak and are not generally considered to be definite molecular associations<sup>24</sup> involving the main chains. Although the intensity of a bending vibration is thought to depend on the magnitude of change produced in the dipole moment of the molecule, the lack of such information at this time about the complex polymer molecule discussed herein precludes the analysis of these intensity data in terms of such bonding properties.

Figure 3 shows the changes of absorbance at 6.93  $\mu$ , associated with P-C<sub>6</sub>H<sub>5</sub> links, which were obtained from spectra of benzene and chloroform solutions of the polymer. Similar data were not obtainable from the

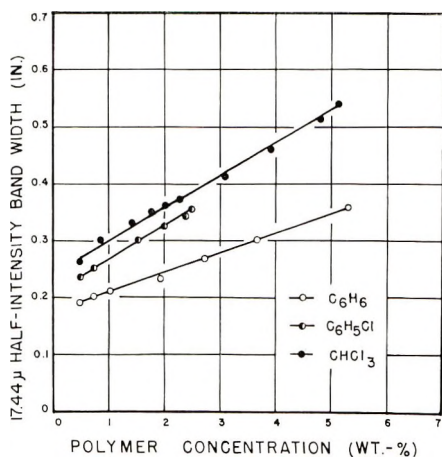


Fig. 4. Effect of concentration on 17.44- $\mu$  half-intensity band width.

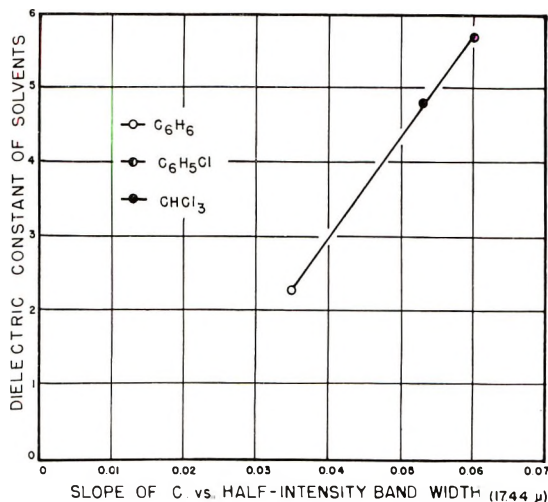


Fig. 5. Influence of solvent dielectric constant on infrared measurements.

chlorobenzene solutions because the 6.93- $\mu$  band was masked by intense solvent absorptions in this region. Results closely parallel the data obtained from the 17.44- $\mu$  band measurements.

Results of half-intensity band width measurements of the 17.44- $\mu$  vibration mode are presented in Figure 4. These data indicate that the 17.44- $\mu$  band from the chloroform solutions of the polymer is broader than the same absorption obtained from the chlorobenzene solutions which, in turn, is broader than the vibration frequency produced from the benzene solutions. It is noteworthy that the order of the half-intensity band widths parallels the sequence of intrinsic viscosities obtained from solutions in the same solvents. This suggests that whatever is influencing the observed broadening of the O-P-O band, may be similarly affecting the in-



trinsic viscosity of the polymer. The 17.44- $\mu$  absorption mode also broadens in a systematic manner as the polymer concentration of the solutions is increased.

Figure 5 shows a plot of the slopes of the straight lines obtained from the concentration versus half-intensity band width measurements against the bulk dielectric constants of the solvents at 30°C. The dielectric constants, determined graphically from literature data<sup>25</sup> for benzene, chlorobenzene, and chloroform are 2.29, 5.71, and 4.81, respectively. It is evident from these data that the changes of vibration mode broadening with polymer concentration is proportional to the dielectric constants of the solvents. This suggests that the observed half-intensity band-width variations, when related to polymer concentration, are probably due to bulk solvent property effects.

### Electrical Conductivity

The polymer solutions prepared from the different solvents all showed low specific conductances which can be attributed to the solute molecules or possible contaminants. Since similar electrical conductivity measurements of chloroform solutions containing individually prepared polymer samples, furnished by the Pennsalt Chemicals Corp., gave almost identical results, it is considered rather unlikely that contamination is a contributing factor in this instance.

Plots of molar conductance  $\Lambda$  versus square root of concentration  $c^{1/2}$  for the polymer solutions are shown in Figures 6–8. The marked curvature exhibited by all of the phoreograms is typical of that given by weakly dissociated electrolytes. Similar shaped phoreograms obtained from solutions of solutes in solvents with low dielectric constants are also re-

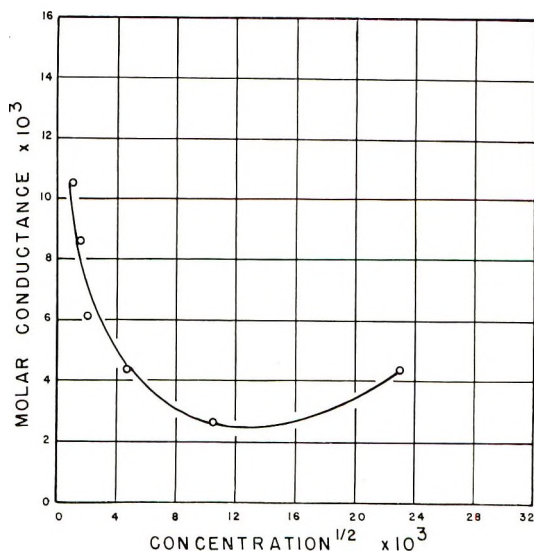


Fig. 6. Phoreogram of polymer in benzene solution.

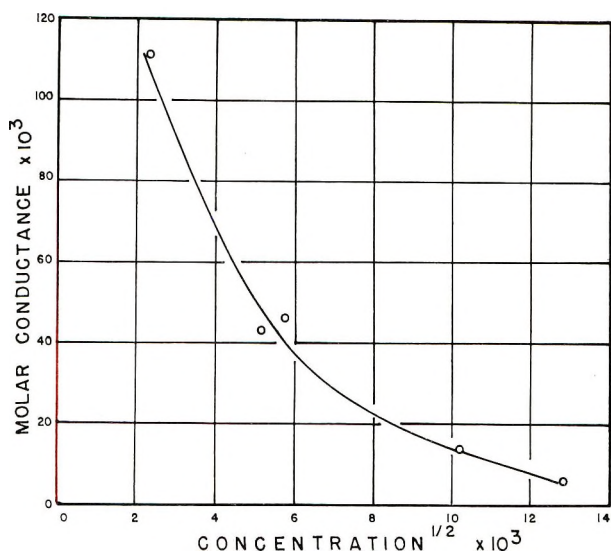


Fig. 7. Phoreogram of polymer in chlorobenzene solution.

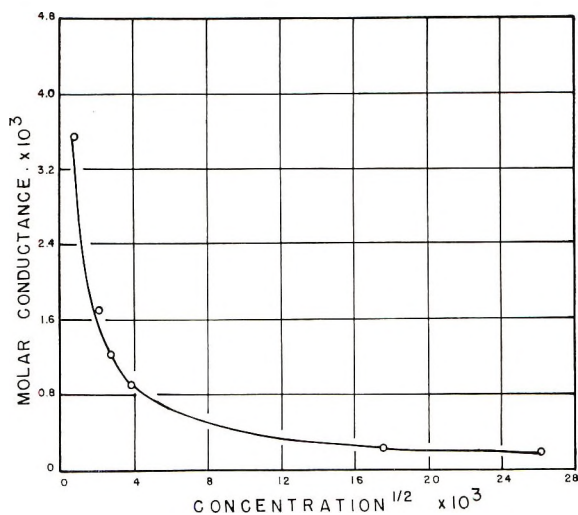


Fig. 8. Phoreogram of polymer in chloroform solution.

ported by other investigators.<sup>26,27</sup> MacFarlane and Fuoss<sup>11</sup> suggest that the minimum shown in the curve of Figure 6 indicates the presence in the benzene solution of free ions, ion pairs, and triple ions in equilibrium, and that the sharp upward curvature with dilution represents a dissociation of ion pairs. Although such minima were not observed from similar measurements of the chlorobenzene and chloroform solutions of the polymer, the linearity of  $\Delta c^{1/2}$  versus  $c$  plots indicates the presence of triple ions in these solutions.<sup>27</sup>

Due to the marked curvature of the phoreograms, extrapolation of the data in Figures 6-8 to zero concentration in order to obtain values for

TABLE II  
 Electrical Conductance Measurements

Solvent	$\Lambda_0$	$K_{A_c=0}$	log Slope ( $K_{A_c=0}$ vs. $c$ )
Benzene	0.45	$1.50 \times 10^{11}$	-16.06
Chlorobenzene	1.2	$1.09 \times 10^7$	11.43
Chloroform	4.1	$3.45 \times 10^5$	10.90

limiting molar conductance,  $\Lambda_0$ , was not attempted. Instead, the Shedlovsky  $\Lambda'_0$  method<sup>28</sup> was used to obtain a close approximation of  $\Lambda_0$ .

Fuoss and Accascina<sup>29</sup> indicate that in the range of solvent dielectric constants where a minimum is observed in the phorogram, as shown in Figure 6, the curve is described by the equation

$$\Lambda c^{1/2} g(c) = \Lambda_0 K_A^{-1/2} + (\lambda_0/kK_A^{1/2})(1 - \Lambda/\Lambda_0)c \quad (2)$$

wherein  $\lambda_0$  represents the limiting molar conductance of the solute corresponding to the triple-ions and counter-ion;  $g(c)$  is a known function of  $\Lambda_0$  which takes into account ion-atmosphere effects;  $k$  is the triple-ion dissociation constant, and  $K_A$  is the association constant. For the benzene solutions of the polymer,  $g(c)$  was determined to be very close to unity. Therefore, the linear  $\Lambda c^{1/2}$  versus  $c$  plot mentioned previously was extrapolated to zero concentration to obtain  $\Lambda_0/K_{A_c=0}^{1/2}$ , from which the limiting association constant  $K_{A_c=0}$  was calculated. The result is shown in Table II.

When association to ion pairs is pronounced enough to produce the phorograms shown in Figures 7 and 8, then the shapes of the curves is described by the equation

$$\Lambda = \gamma(\Lambda_0 - Sc^{1/2}\gamma^{1/2}) \quad (3)$$

wherein  $\gamma$  is the fraction existing as free ions and  $S$  is the Onsager coefficient of the limiting conductance law. After calculating  $\gamma$ , values for  $K_A$  were determined from the mass action equation

$$1 - \gamma = K_A c \gamma^2 f^2 \quad (4)$$

wherein  $f$  is the activity coefficient which was computed by the Debye first approximation for ions of finite size. At very low concentrations,  $f$  has the limiting form

$$-\log f_{\pm} = \beta'' c^{1/2}$$

wherein the constant  $\beta''$  equals  $1.8247 \times 10^6/(DT)^{3/2}$  with  $D$  and  $T$  representing the dielectric constant of the solvent and the absolute temperature of the solution, respectively. The results of  $K_{A_c=0}$  calculations are presented in Table II.

The relatively low order of magnitude of the  $\Lambda_0$  values obtained may indicate that only a small number of ionic species exists in all solvent systems. From indications given by infrared and viscometric data, it seems unlikely that the small amount of ionic species are produced by polymer-

solvent interactions which dissociate main chains of the polymer molecules. The low range of  $\Lambda_0$  values may also imply that movement of the ions in the solutions are retarded by extensive, even if weak solvation in these solvent molecules.<sup>27</sup> Indeed, a high degree of association of the solute ions in the different solvents is plainly evident from the large  $K_{Ac=0}$  values shown for the various systems in Table II. The observed  $K_{Ac=0}$  results also tend to confirm the indications of association given by the higher than normal  $k'$  values computed from viscosity data. Variations from solvent to solvent of the  $K_{Ac=0}$  values parallel the relative order observed from intrinsic viscosity and infrared spectroscopy measurements.

Since a straight line of different slope was obtained from each solvent, it would seem that some property of the solvent, perhaps the dielectric

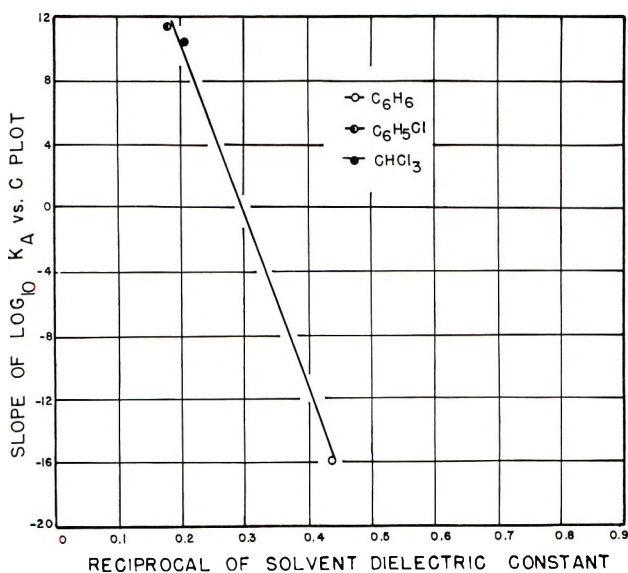


Fig. 9. Influence of solvent dielectric constant on electrical conductance measurements.

constant, is affecting the characteristics of the mass of the polymer molecules. Figure 9 presents a plot of the log of the slope of the  $K_A$  versus  $c$  curves against the reciprocal of the dielectric constants of the solvents. These data show that, as a function of polymer concentration,  $K_A$  values are directly proportional to the dielectric constants of the solvents. These findings parallel the results obtained from infrared measurements of half-intensity band width at  $17.44 \mu$ . It is apparent from this that bulk solvent properties influence the characteristics of the mass of the polymer molecules in solution.

However, at any given polymer concentration, values of  $K_A$ , and also the results of half-intensity band-width measurements at  $17.44 \mu$  show no direct relation to the relative order of dielectric constants of the solvents. This lack of direct relation with polymer concentration suggests that pos-

sible "local" solute-solvent interaction factors influenced these measurements.

Inami, Bodenseh, and Ramsey<sup>30</sup> have indicated that the bulk dielectric constant of ethylene chloride and 1,2-dichloropropane is considerably smaller than the effective "local" value which exists near the ionic and molecular species in solutions of  $n\text{-(C}_4\text{H}_9)_4\text{NClO}_4$  at 25°C. It is entirely possible that the results obtained in the studies described herein can be attributed to similar "local" bulk dielectric constant effects which experimental evidence suggests is due to polymer-solvent interactions at polymer chain ends.

The authors wish to express their appreciation to Dr. L. W. Butz, Office of Naval Research, Washington, D. C., for sponsoring this study, Drs. B. P. Block and A. J. Saraceno, Pennsalt Chemicals Corp., King of Prussia, Pa., for helpful suggestions during the course of the work, and to J. M. McGreevy, Associate Technical Director, U. S. Naval Applied Science Laboratory, Naval Base, Brooklyn, New York, for his continued interest and encouragement.

The opinions or assertions contained in this paper are the private ones of the authors and are not to be construed as official or reflecting the views of the Naval Service at large.

### References

1. B. P. Block, J. Simkin, and L. R. Ocone, *J. Am. Chem. Soc.*, **84**, 1749 (1962).
2. B. P. Block and G. Barth-Wehrenlap, *J. Inorg. Nucl. Chem.*, **24**, 365 (1962).
3. A. J. Saraceno, and B. P. Block, *Inorg. Chem.*, **2**, 804 (1963).
4. A. J. Saraceno, and B. P. Block, *J. Am. Chem. Soc.*, **85**, 2018 (1963).
5. A. J. Saraceno and B. P. Block, *Inorg. Chem.*, **3**, 1699 (1964).
6. V. Crescenzi, V. Giancotti, and A. Ripamonti, *J. Am. Chem. Soc.*, **87**, 391 (1965).
7. J. C. Moore, *J. Polymer Sci. A*, **2**, 835 (1964).
8. D. J. Harmon, paper presented to the Division of Polymer Chemistry, 148th American Chemical Society Meeting, Chicago, Ill., Sept. 1964; *Polymer Preprints*, **5**, No. 2, 712 (1964).
9. J. R. Purdon and M. Morton, *J. Polymer Sci.*, **57**, 453 (1962).
10. J. A. Aukward and R. W. Warfield, *Rev. Sci. Instr.*, **27**, 413 (1956).
11. R. MacFarlane and R. M. Fuoss, *J. Polymer Sci.*, **23**, 403 (1957).
12. J. Gavis, *J. Chem. Phys.*, **41**, 3787 (1964).
13. A. R. Burkin, *J. Chem. Soc.*, **1954**, 71.
14. C. M. French and P. B. Hart, *J. Chem. Soc.*, **1960**, 1671.
15. C. E. Wilkes and R. A. Jacobson, *Inorg. Chem.*, **4**, 99 (1965).
16. D. Cleverdon and P. G. Smith, *J. Polymer Sci.*, **14**, 375 (1954).
17. S. Gundiah, N. V. Viswanathan, and S. L. Kapur, *Makromol. Chem.*, **55**, 25 (1962).
18. L. J. Bellamy, *The Infra-Red Spectra of Complex Molecules*, Wiley, New York, 1958.
19. G. E. Coates and D. S. Golightly, *J. Chem. Soc.*, **1962**, 2523.
20. A. C. Chapman and L. E. Thirwell, *Spectrochim. Acta*, **20**, 937 (1964).
21. K. Nakamoto, *Infrared Spectra of Inorganic and Coordination Compounds*, Wiley, New York, 1963.
22. L. J. Bellamy, *Spectrochim. Acta*, **14**, 192 (1958).
23. F. C. Nachod and W. D. Phillips, *Determination of Organic Structures by Physical Methods*, Vol. 2, Academic Press, New York, 1962.
24. W. R. Ward and A. R. Philpotts, *J. Appl. Chem. (London)*, **8**, 265 (1958).



25. *Handbook of Chemistry and Physics*, 42nd Ed., Chemical Rubber Pub. Co., Cleveland, Ohio, 1964-65.
26. I. N. Klotz, S. F. Russo, S. Hanlon, and M. A. Stake, *J. Am. Chem. Soc.*, **86**, 4774 (1964).
27. C. N. French and R. C. B. Tomlinson, *J. Chem. Soc.*, **1961**, 311.
28. T. Shedlovsky, *J. Am. Chem. Soc.*, **54**, 1405 (1932).
29. R. M. Fuoss and F. Accascina, *Electrolytic Conductance*, Interscience, New York, 1959.
30. Y. H. Inami, H. K. Bodenseh, and J. B. Ramsey, *J. Am. Chem. Soc.*, **83**, 4745 (1961).

### Résumé

On a étudié un nouveau polymère inorganique poly(aquahydroxydiphénylphosphinate de chrome) en vue d'obtenir des informations concernant son degré de polydispersité et ses propriétés lorsque ce polymère est dissous dans des solvants organiques. On a utilisé des méthodes viscosimétriques d'absorption infra-rouge et de conductivité électrique pour déterminer les caractéristiques du polymère dissous dans le benzène, le chlorobenzène et le chloroforme. La chromatographie par perméation sur gel a été utilisée en vue de déterminer le degré d'hétérogénéité du polymère. Les résultats indiquent que le polymère ainsi obtenu, est fort polydispersé. Les chaînes principales polymériques ne donnent pas lieu à des réactions radicalaires avec les solvants. Des valeurs des constantes  $k'$  de Huggins élevées suggèrent que les réactions d'association polymère-solvant faisant intervenir les groupes terminaux sont probables. De telles réactions sont également suggérées par les valeurs des constantes d'association et par la forme des diagrammes obtenus au départ de données de conductance électrique. Lorsque le polymère est dissous dans différents solvants, ses caractéristiques sont influencées à la fois par les propriétés locales et en masse du solvant telle la constante diélectrique.

### Zusammenfassung

Das neue anorganische Polymere, Poly(aquahydroxychromdiphenylphosphinat), wurde auf seinen Polydispersitätsgrad und seine Eigenschaften in organischen Lösungsmitteln untersucht. Viskosimetrische, infrarot absorptionsspektroskopische und elektrische Leitfähigkeitsverfahren wurden zur Ermittlung der Charakteristik des in Benzol, Chlorbenzol und Chloroform gelösten Polymeren verwendet. Der Heterogenitätsgrad des Polymeren wurde mittels Gelpermeationschromatographie bestimmt. Die Ergebnisse zeigen, dass das Polymere, so wie es bei der Darstellung erhalten wurde, polydispers ist. Die Hauptketten des Polymeren gehen keine Radikalreaktionen mit dem Lösungsmittel ein. Hohe Werte für die Huggins-Wechselwirkungskonstante  $k'$  machen das Auftreten von Polymer-Lösungsmittel-Assoziationsreaktionen über die Kettenendgruppen wahrscheinlich. Solche Reaktionen werden auch durch die Werte der Assoziationskonstanten und durch die Gestalt der aus elektrischen Leitfähigkeitsdaten erhaltenen Phoreogramme nahegelegt. Sowohl "lokale" als auch "Bulk"-Lösungsmittelleigenschaften wie die Dielektrizitätskonstante scheinen die charakteristischen Eigenschaften des in verschiedenen Lösungsmitteln gelösten Polymeren zu beeinflussen.

Received October 12, 1965

Revised October 20, 1965

Prod. No. 4948A

## Radiation-Induced Solid-State Copolymerization of Maleic Anhydride and Acenaphthylene

AKIRA SHIMIZU and KOICHIRO HAYASHI, *Osaka Laboratories, Japanese Association for Radiation Research on Polymers, Neyagawa, Osaka, Japan*

### Synopsis

Radiation-induced solid-state copolymerization of the maleic anhydride-acenaphthylene system was carried out for the purpose of studying the solid-state polymerization of vinyl compounds in a binary system. Melting point measurement confirmed that this binary monomer system forms a eutectic mixture in the solid state. The solid-state polymerization of these monomers proceeds at maximum rate at the eutectic composition, and the polymerization products consist of a mixture of polyacenaphthylene and 1:1 maleic anhydride-acenaphthylene alternating copolymer. Since the 1:1 copolymer was obtained in solution polymerization also and maleic anhydride did not homopolymerize in solid state, it is considered that the solid-state copolymerization of maleic anhydride and acenaphthylene occurs in a liquidlike state at the boundary of the two monomer crystals.

### INTRODUCTION

The solid-state polymerization of vinyl compounds in a binary monomer system already has been reported for acrylamide-methacrylamide.<sup>1,2</sup> In this case, the monomer system forms a solid solution, and random copolymerization is possible. On the other hand, it may be possible that a eutectic mixture of vinyl compounds is involved in copolymerization or a block copolymerization, because the solid-state polymerization of vinyl compounds has been known to occur in the disordered crystalline lattice.<sup>3</sup> It was found that maleic anhydride and acenaphthylene formed a eutectic mixture, so the copolymerization of maleic anhydride and acenaphthylene in the solid state was carried out in order to elucidate the solid-state polymerization behavior of vinyl or vinylene compounds in a eutectic mixture.

The radiation-induced homopolymerization of acenaphthylene and maleic anhydride has already been reported. Chen<sup>4</sup> irradiated solid acenaphthylene with x-rays and observed that homopolymerization occurred. Polymerization of molten or dissolved maleic anhydride induced by  $\gamma$ -ray irradiation of molten or dissolved maleic anhydride induced by  $\gamma$ -ray irradiation or radical initiators was reported by Lang and co-workers,<sup>5</sup> but solid-state polymerization has not been reported. Petit<sup>6</sup> reported the photo-induced copolymerization of maleic anhydride and acenaphthylene in benzene solution to yield an alternating copolymer.

## EXPERIMENTAL

### Materials

Acenaphthylene (AcN) and maleic anhydride (MAH) were obtained commercially. AcN was purified by recrystallization from methanol (m.p. 93°C.). MAH was used without further purification of commercial guaranteed grade (m.p. 52°C.). In some experiments MAH recrystallized from chloroform was used, but the results did not differ from those obtained with untreated MAH.

### Polymerization

Monomer mixtures were prepared by carefully weighing out the required amounts, sealing under the presence of air or under vacuum ( $10^{-3}$  mm. Hg) into a glass ampule, melting at 100°C., and crystallizing quickly by immersion of the ampule in Dry Ice-methanol or cooling gradually to room temperature. Unless otherwise stated, the results followed were obtained from gradually cooled monomer. Polymerization in source was carried out at room temperature (15–30°C.) by  $\gamma$ -rays from a 1000-c.  $^{60}\text{Co}$  source. Post-polymerization was carried out at 0°C. after preirradiation at  $-196^\circ\text{C}$ . with an electron beam from a 2 M.e.v. Van de Graaff accelerator. In the electron-beam irradiation, samples were kept 2 mm. under the surface of liquid nitrogen by using a float. In this case, ceric sulfate dosimetry was employed under conditions designed to simulate the experimental arrangement. Polymer from solid-state polymerization was obtained by washing the monomers with methanol after polymerization, and the insoluble residue was dried in vacuum at 50°C. for one night. The overall yield was calculated from the weight of methanol-insoluble product. After extraction of polyacenaphthylene from total polymer with benzene at room temperature, the residue gave a 1:1 copolymer of MAH and AcN. Solution polymerization products were obtained by precipitation of irradiated contents into methanol.

### Composition Analysis

Copolymer composition was analyzed by alkali titration of maleic anhydride unit in dioxane solution<sup>7</sup> and by infrared spectrometry. A calibration curve was drawn between the titration data and the intensity ratio of the infrared absorption band characteristics of MAH (5.59  $\mu$ ) and of AcN (12.2  $\mu$ ); in practice, composition analysis was carried out by infrared spectrum measurement with KBr disks. The possibility of anhydride-ring opening by methanol or water during processing was denied by observation of the infrared spectrum. In some experiments, elemental analysis was used in parallel with the infrared spectrum measurement, and the results were in essential agreement. A phase diagram of MAH and AcN was drawn from the data on melting point measurements.

## RESULTS AND DISCUSSION

## Phase Equilibrium of Monomer System

The phase diagram of the MAH–AcN binary system is given in Figure 1. This diagram shows that in the solid state, the two components form a eutectic mixture, namely a mixture of fine crystalline grains of MAH and AcN. The eutectic mixture is composed of MAH/AcN = 2 (in mole ratio), and has a melting point at 35.5–36.0°C. The solid-state binary system which shifts from the eutectic composition is made up of the eutectic mixture and a pure crystal of the monomer in excess. At higher temperature, the system is liquid and the monomers become completely mixed. The intermediate regions, Liq. + S<sub>AcN</sub> and Liq. + S<sub>MAH</sub>, in Figure 1 are the states in which liquid and solid AcN crystal, and liquid and solid MAH, respectively coexist. An attempt to measure the size of the monomer crystalline grain from the half-width of the x-ray diffraction pattern failed. The half-width did not change regardless of the monomer composition. The reason for this unsuccessful result may mean that the size of crystalline grain was out of the range measurable by x-ray diffraction. It has been reported by Brady<sup>8</sup> that the crystal grain of the eutectic mixture is smaller than that of other compositions. The difference in the crystalline composition between gradually cooled and shock-cooled samples may result from the likelihood that the former treatment gives a closer approach to the true phase equilibrium, in which case the gradually cooled sample contains a higher proportion of eutectic mixture. An examination of this problem was undertaken by the differential thermal analysis method to determine the melting point

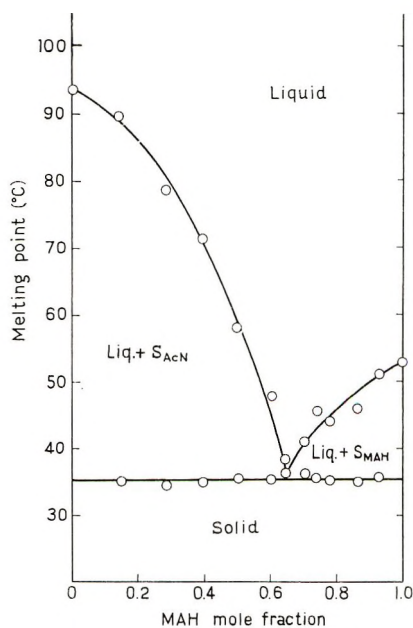


Fig. 1. Phase diagram of MAH–AcN system.

difference for the two kinds of monomer systems, but was unsuccessful because the heat of sublimation of the two monomers was so large.

It is known that a mixture of MAH and styrene forms a complex, and coloration occurs in the liquid state.<sup>9,10</sup> Therefore, a similar phenomenon may be expected to occur in the case of MAH and AcN. However, if such a complex forms also in the solid state, there should be a corresponding melting-point maximum in the phase diagram, but this is clearly not the case.

### Solution and Solid-State Polymerization

Polymeric products were obtained by  $\gamma$ -ray irradiation of the MAH-AcN system in acetone solution and in the solid state. The solid-state homopolymerization of AcN occurred easily at ordinary temperature with  $\gamma$ -ray irradiation doses of about  $10^6$  r as reported by Chen,<sup>5</sup> but MAH did not homopolymerize in the solid state even at the doses exceeding  $10^7$  r. Hence, the polymeric products were treated on the assumption that the homopolymer of MAH was not prepared. The infrared spectrum of the copolymer insoluble in methanol and benzene at room temperature is given in Figure 2*b*. The absorption band at  $5.59 \mu$  indicates MAH units, while the bands at  $12.20$  and  $12.85 \mu$  identify AcN units in the copolymer as deduced from the spectrum of polyacenaphthylene (Fig. 2*a*). Through this spectrum the copolymerization of MAH and AcN was recognized. Further confirmation of copolymerization was performed by extraction of polymer *b* with methanol and benzene at  $50^\circ\text{C}$ . for 12 hr. The infrared spectrum of the insoluble residue given in Figure 2*c* shows the characteristic peaks of maleic acid at  $5.80 \mu$  which represents a shift from  $5.59 \mu$  by methanolysis of MAH unit, and the AcN characteristic peaks at  $12.20$  and  $12.85 \mu$  similar to spectrum 2*b*. The copolymer obtained was a pale yellow powder, soluble in dioxane and dimethylformamide (DMF); it decomposed above  $250^\circ\text{C}$ ., and the intrinsic viscosity in DMF was 0.4 at  $30^\circ\text{C}$ . An extract from benzene was expected to be a homopolymer of AcN, but it actually con-

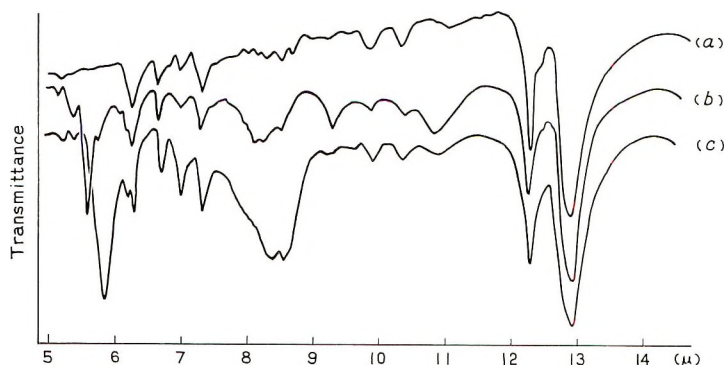


Fig. 2. Infrared spectra of the polymers (KBr disk method): (a) polyacenaphthylene; (b) MAH-AcN copolymer from solid-state polymerization; (c) portion of MAH-AcN copolymer insoluble in benzene, methanol at  $50^\circ\text{C}$ . for 12 hr.



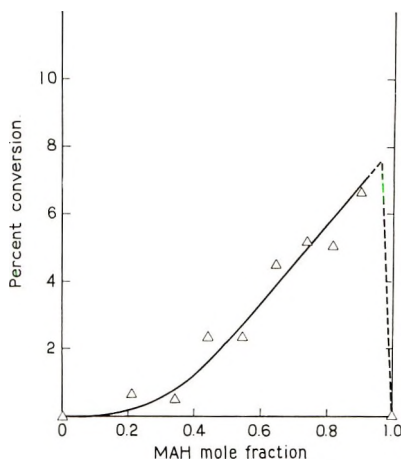


Fig. 3. Radiation-induced copolymerization of MAH-AcN in acetone solution at 16°C. Dose rate,  $8.0 \times 10^4$  r/hr.; polymerization time, 24 hr.; monomer/solvent, 1 g./3 cc.

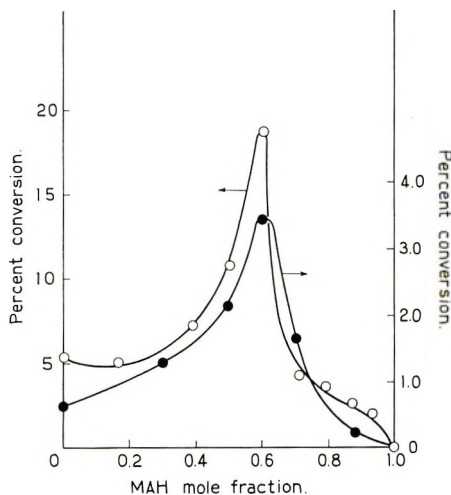


Fig. 4. Effect of the monomer composition on the solid-state polymerization of AcN and MAH: (O) in-source polymerization at 30°C., dose rate  $8.0 \times 10^4$  r/hr., time 120 hr.; (●) post-polymerization at 0°C. for 24 hr., (preirradiation,  $1 \times 10^8$  rad at  $-196^\circ\text{C}.$ ).

tained 5–8% MAH units. The fractional precipitation of this benzene-soluble polymer, using dioxane as solvent and *n*-hexane as precipitant, showed no AcN pure homopolymer but a copolymer containing at least 2% MAH units. This suggests that a small amount of MAH is soluble in the AcN crystalline phase. This result indicates that most of the benzene-soluble polymer was an AcN polymer containing a small amount of MAH, for which the following structures may be reasonable: (a)  $-(\text{AcN})_n-\text{MAH}-$   $(\text{AcN})_{n''}-\text{MAH}-$  or (b)  $-(\text{AcN})_n-(\text{MAH-AcN})_{n'}-(\text{AcN})_{n''}-$ , where  $n'$  is small and  $n, n''$  are large. In the discussion below, the benzene-soluble polymer is termed AcN polymer for expedience.

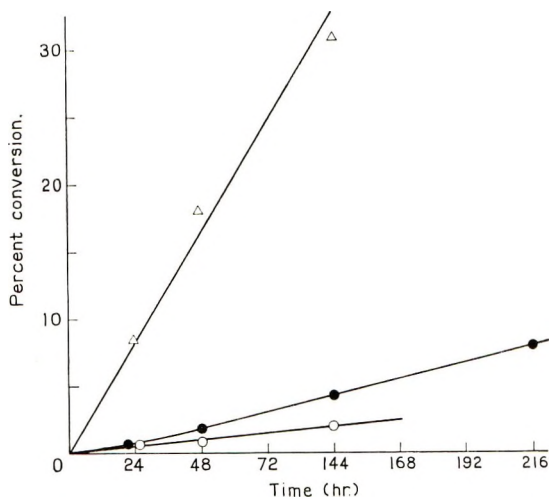


Fig. 5. Time dependence of per cent conversion in solid-state and solution polymerization at 20°C.: ( $\Delta$ ) acetone solution, in air; ( $\bullet$ ) solid state, in air; ( $\circ$ ) solid state, in vacuum. Monomer composition, MAH/AcN = 2; dose rate,  $8.0 \times 10^4$  r/hr.

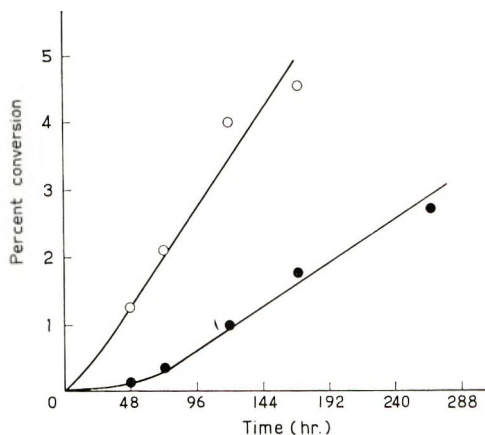


Fig. 6. Effect of sample preparation on the in-source solid-state copolymerization of AcN and MAH at 14°C.: ( $\circ$ ) gradually cooled crystals; ( $\bullet$ ) shock-cooled crystals. Monomer composition, MAH/AcN = 2; dose rate,  $7.7 \times 10^4$  r/hr.; in air.

Figures 3 and 4 show the polymerization rate dependence on the monomer composition in acetone solution and in solid state. In acetone solution, the polymerization was accelerated as MAH content in the monomer increased. In the solid state, however, both for in-source and post-polymerization, the polymer yield reached a maximum point where the monomer composition was identical with the eutectic composition. When the polymerization temperature was just below the melting point and the irradiation dose was high, it was sometimes observed that the system became pastelike at the end of polymerization. This seems to be due to the melting point depression of the monomer crystalline system by formation of poly-

mer. In post-polymerization at 0°C. (35°C. below the eutectic temperature), the maximum yield was also observed at the eutectic composition; therefore this suggests that the increased contact area of the two crystal surfaces at the eutectic point serves to enhance the polymerization. Moreover, the rapid diffusion of oxygen into the monomer crystal may also contribute to the rapid polymerization at the eutectic composition, as mentioned below.

When the polymerization rate in acetone solution and in the solid state were compared at a monomer ratio MAH/AcN = 2, the rate of solution polymerization was found to exceed the rate in the solid state (Fig. 5). Also, in the solid state, the polymerization rate in air was larger than in vacuum, and the effect of air on the polymerization rate was different from that in the usual radical polymerization. Chen<sup>3</sup> reported that the homopolymerization of AcN in the presence of air also occurs faster than that in vacuum, and Ueberreiter<sup>11</sup> reported the same effect for the copolymerization of AcN with styrene.

The following study is concerned with the effect of the crystalline state of the monomer on the polymerization rate in the solid state. Figure 6 gives the polymerization rate for gradually cooled and shock-cooled monomer at the eutectic composition. In both cases, the polymerization was carried out in air. The polymerization rate of gradually cooled monomer was greater than that of shock-cooled monomer. However, it is known that the solid-state polymerization of vinyl compounds occurs more rapidly in a shock-cooled monomer than in a gradually cooled monomer,<sup>12</sup> and this was also confirmed in the homopolymerization of AcN in this work; this has been explained by the hypothesis that the solid-state polymerization of vinyl compounds is inclined to occur in the region of the disordered crystalline lattice. Since this explanation does not apply for the binary system of MAH and AcN, it must be concluded that the rate of polymerization is significantly affected by other factors. As mentioned above, a gradually cooled monomer may form a more complete eutectic mixture, in accordance with the phase diagram, than shock-cooled monomer. So, if it is supposed that the copolymerization in a eutectic mixture is rapid, it may be easily explained why the gradually cooled monomer had a large polymerization rate in comparison with the shock-cooled monomer. It can be considered that this effect results from the larger rate of disordering at the boundary of the eutectic crystalline grains as compared with the other part of the system.

### Polymer Composition

Composition analyses of polymerization products in acetone solution and in the solid state were performed. The results are given in Figure 7. Copolymer from polymerization in acetone solution had an alternating composition of MAH/AcN = 1. This behavior is similar to the copolymerization of MAH and styrene, in which the formation of a colored 1:1 molecular complex causes an alternating copolymerization. Since AcN

has its own yellow color, it was impossible to tell in this instance whether significant coloration occurs or not on mixing of MAH and AcN, and no change was observed in the ultraviolet and visible spectrum when MAH and AcN were mixed. Although the question of complex formation between MAH and AcN in solution is not clear, it is obvious that the copolymer from polymerization in acetone solution represents a 1:1 composition. The content of MAH units in total polymer from solid-state polymerization was smaller than that from solution polymerization. Furthermore, the total polymer from gradually cooled and that from shock-cooled monomer were different in their compositions, that is, the former had about 10% more MAH units than the latter. In solid-state polymerization, some

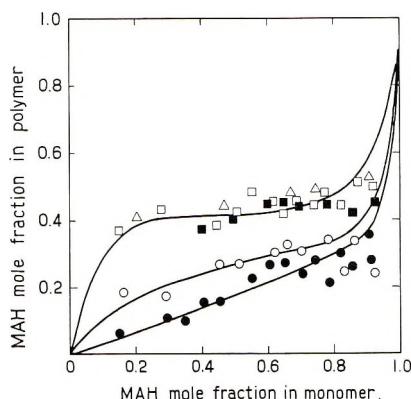


Fig. 7. Polymer composition curves for the solid-state and the solution copolymerization of AcN and MAH: ( $\Delta$ ) polymer from acetone solution; ( $\circ$ ) total composition from gradually crystallized monomer; ( $\bullet$ ) total composition from shock-cooled monomer; ( $\square$ ) copolymer composition from gradually crystallized monomer; ( $\blacksquare$ ) copolymer composition from shock-cooled monomer. In-source polymerization at 25°C.; polymer yield, 5–10%.

homopolymerization of AcN takes place, and as a result, the average content of MAH in total polymer is lower than that of solution polymerization. Figure 7 shows the composition curves for the copolymer from solid-state polymerization which was obtained as the benzene-insoluble part. This composition curve indicates that the copolymer composition in solid-state polymerization agrees well with the copolymer composition in solution polymerization. Therefore, the copolymerization in the solid state seems to occur in the disordered crystalline region. This experimental fact lends some support to the hypothesis that solid-state polymerization of vinyl compounds is likely to take place in the disordered crystalline state. In post-polymerization this was essentially identical. It is also shown in Figure 7 that the dissimilarity of polymer composition between gradually cooled and shock-cooled monomer comes from the difference of AcN homopolymerizability, which was larger in the shock-cooled crystals than in the gradually

cooled ones as shown above. These considerations become more obvious when we observe the dependence of copolymer content in total polymer on conversion (Fig. 8). In the initial stage, the copolymerization rate was greater than that of homopolymerization, and as polymerization progressed, the homopolymerization of AcN seemed to accelerate. At last, when the

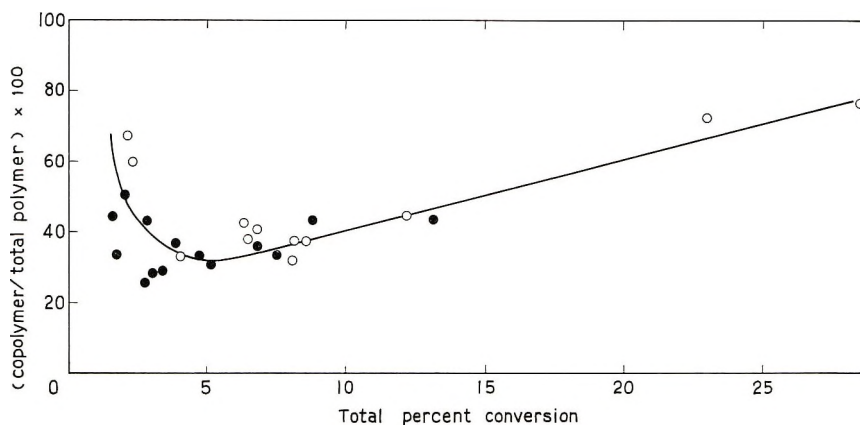


Fig. 8. Total conversion vs. copolymer content: (○) gradually cooled monomer; (●) shock-cooled monomer. Monomer composition, MAH/AcN = 2.

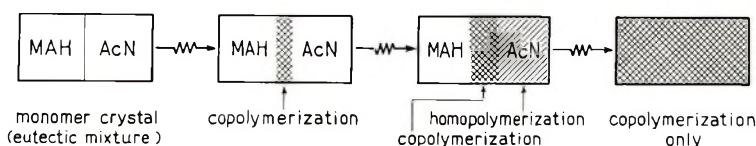


Fig. 9. Radiation-induced polymerization of the MAH-AcN system in the solid state.

polymerization yield became high enough, the entire polymerization system became so disordered that the ratio of copolymerization increased. This is not shown in Figure 8, but at a conversion of 45%, the copolymer content in the total polymer was 95%.

## CONCLUSIONS

In view of the above experimental results, the following four points are summarized: (1) AcN and MAH formed a eutectic mixture in the solid state; (2) the polymerization products in MAH and AcN solid-state copolymerization were a mixture of 1:1 copolymer and polyAcN which contained a small amount of MAH, while in solution polymerization, only the 1:1 copolymer was obtained; (3) The polymerization yield in the solid state reached a maximum at the eutectic composition; (4) the polymerization rate of gradually cooled monomer in solid state was greater than that of shock-cooled monomer.



In order to illustrate these experimental facts, the processes shown in Figure 9 are proposed for the solid state polymerization of MAH and AcN. At first, copolymerization initiates at the boundary of monomer microcrystals and then homopolymerization of AcN gradually occurs in AcN monomer crystal. As the polymerization yield becomes high, the crystalline lattice becomes so disordered that only copolymerization occurs in all monomer crystals.

The authors thank Professor Seizo Okamura of Kyoto University for helpful discussion and Dr. Sanae Tanaka of Mitsubishi Petrochemical Co. for his continuing encouragement during this work.

### References

1. J. Z. Orszagh, paper presented at Symposium on Radiation Chemistry, Hungary, May 1962.
2. M. Nishii, H. Tsukamoto, K. Hayashi, and S. Okamura, *Ann. Rept. Japan, Assoc. Radiation Res. Polymers*, **5**, 115 (1964).
3. G. Adler and W. Reams, *J. Polymer Sci. A*, **2**, 2617 (1964).
4. C. S. H. Chen, *J. Polymer Sci.*, **62**, S38 (1962).
5. J. L. Lang, W. A. Pavelich, and H. D. Clarey, *J. Polymer Sci. A*, **1**, 1123 (1963).
6. J. Petit and L. Strezelecki, *Compt. Rend.*, **253**, 2691 (1961).
7. J. S. Fritz and N. M. Lisicki, *Anal. Chem.*, **23**, 589 (1951).
8. F. L. Brady, *J. Inst. Metals*, **28**, 369 (1922).
9. W. G. Barb, *Trans. Faraday Soc.*, **49**, 143 (1953).
10. C. Walling, E. R. Briggs, K. B. Wolfstirn, and F. R. Mayo, *J. Am. Chem. Soc.*, **70**, 1537 (1948).
11. K. Ueberreiter and W. Krull, *Makromol. Chem.*, **24**, 50 (1957).
12. T. A. Fadner and H. Morawetz, *J. Polymer Sci.*, **45**, 475 (1960).

### Résumé

La copolymérisation à l'état solide induite par irradiation du système anhydride maléique-acénaphthylène a été effectuée en vue d'étudier la polymérisation à l'état solide de composés vinyliques dans un système binaire. En mesurant le point de fusion on a pu confirmer que le système monomérique binaire forme un mélange eutectique à l'état solide. La polymérisation à l'état solide de ces monomères manifeste une vitesse de polymérisation maximum à la composition eutectique et le produit de polymérisation consiste en un mélange de polyacénaphthylène et de copolymères alternant 1:1 anhydride maléique-acénaphthylène. Puisque que par polymérisation en solution, on obtient également un copolymère 1:1, et que par ailleurs l'anhydride maléique n'homopolymérise pas à l'état solide, on considère que la copolymérisation à l'état solide de de l'anhydride maléique et de l'acénaphthylène se passe dans un état analogue à l'état liquide à la surface des cristaux des deux monomères.

### Zusammenfassung

Die strahlungsinduzierte Copolymerisation des Maleinsäureanhydrid-Acenaphthylensystems im festen Zustand wurde durchgeführt, um die Polymerisation von Phenylverbindungen im festen Zustand in einem binären System zu untersuchen. Durch Schmelzpunktmessungen wurde gezeigt, dass dieses binäre Monomersystem im festen Zustand eine eutektische Mischung bildet. Die Polymerisation dieser Monomeren im festen Zustand besass bei der eutektischen Zusammensetzung eine maximale Polymerisationsgeschwindigkeit, und die Polymerisationsprodukte bestanden aus einer Mischung

von Polyacenaphthalen und alternierenden 1:1 Maleinsäureanhydrid-Acenaphthylen-copolymeren. Da bei der Polymerisation in Lösung ebenfalls das 1:1-Copolymere erhalten wurde und da Maleinsäureanhydrid im festen Zustand keine Homopolymerisation zeigt, wird geschlossen, dass die Copolymerisation von Maleinsäureanhydrid und Acenaphthylen in fester Phase in einem flüssigkeitsähnlichen Zustand an der Grenzfläche zweier Monomerkristalle stattfindet.

Received April 16, 1965

Revised October 18, 1965

Prod. No. 4957A

## Polyamides from $\alpha,\omega$ -Oxaalkanedioic Acids Having Long Methylene Chain Units

KAZUO SAOTOME and KENICHIRO SATO, *Technical Research  
Laboratory, Asahi Chemical Industry Company, Ltd.,  
Itabashi-ku, Tokyo, Japan*

### Synopsis

Three series of polyamides were prepared from diamines (hexamethylenediamine, bis-5-aminoamyl ether, *p*-xylylenediamine) and  $\alpha,\omega$ -oxaalkanedioic acids of formula  $\text{HOOC}(\text{CH}_2)_m\text{O}(\text{CH}_2)_n\text{COOH}$ , where  $m = n = 3-10$ , in symmetric structures, but  $m = 3$  or 4 in unsymmetric structures. The melting points of these polymers were plotted against the number of carbon atoms of the oxaalkylene groups. The melting points of polymers from each diamine fell on three different curves according to the structures of the dicarboxylic acids: symmetric  $-(\text{CH}_2)_n\text{O}(\text{CH}_2)_n-$ ; unsymmetric  $-(\text{CH}_2)_3\text{O}(\text{CH}_2)_n-$ , and unsymmetric  $-(\text{CH}_2)_3\text{O}(\text{CH}_2)_n-$ . A minimum melting point is observed at about the same point of the acid structure in every curve of the unsymmetric dicarboxylic acids. The marked depression in the polymer melting points around the minimum point is attributed to the increase of the entropy of fusion.

### INTRODUCTION

The effect of the introduction of ether linkages into polymer chains has been investigated with polyamides of some oxaalkylenediamines.<sup>1</sup> The characteristic features of these polymers are lower melting points and increased water affinity. For example, the polyamide of 1,2-bis(3-aminoethoxy)ethane with adipic acid<sup>2</sup> has a melting point of 160°C. and is soluble in hot water. Polyamides of oxaalkylenediamines with terephthalic acid are found in the patent literature.<sup>3,4</sup>

The synthesis of symmetric  $\alpha,\omega$ -oxaalkanedioic acids having the formula  $\text{O}[(\text{CH}_2)_n\text{COOH}]_2$ , where  $n = 2-5$ , has been reported previously. However, little has been studied regarding the polyamides from them. In a preceding paper,<sup>5</sup> the synthesis of novel  $\alpha,\omega$ -oxaalkanedioic acids having the general formula  $\text{HOOC}(\text{CH}_2)_m\text{O}(\text{CH}_2)_n\text{COOH}$  (where  $m = n = 3-10$  in symmetric acids and  $m = 3$ , or 4 in unsymmetric structures) has been reported. The present work deals with the polyamides prepared from diamines of several different types and these  $\alpha,\omega$ -oxaalkanedioic acids.

### EXPERIMENTAL

#### Materials

The preparation and the characteristics of  $\alpha,\omega$ -oxaalkanedioic acids were reported in the preceding paper.<sup>5</sup> Hexamethylenediamine was obtained

commercially. *p*-Xylylenediamine was prepared by hydrogenating terephthalonitrile in the presence of the Raney nickel under high pressure of hydrogen.<sup>6</sup> Bis-5-aminoamyl ether was prepared from bis-4-cyanobutyl ether<sup>7</sup> through catalytic hydrogenation. The characteristics of these diamines agreed with those in the literature.

### Methods

**Polymer Melting Points.** The melting point was measured by observing particles of the polymer between crossed nicol polarizers under an electrically heated hot-stage microscope. The melting point was taken as the temperature at which the last trace of birefringent crystallinity disappeared. Since the crystallinity of some polymers of bis-5-aminoamyl ether with unsymmetric  $\alpha,\omega$ -oxaalkanedioic acids remained poor after gradual cooling from the melts, the melting points of the polymers of this diamine were measured with the usual apparatus. The differences between the melting points obtained by these two methods were ascertained to be within 3°C. for polymers melting at below 200°C.

**Reduced Viscosities.** The polyamides were dissolved in *m*-cresol at temperatures of 60–80°C. for 2 hr. with the use of a magnetic stirrer. Solutions of 0.5% concentration at 25°C. were used for viscosity measurement.

**Preparation of Nylon Salts.** Equimolar ethanol solutions of diamine and dicarboxylic acid at a concentration of 10% were mixed together, and the solution was refluxed for 0.5 hr. After being cooled with ice water, the precipitated salt was filtered, washed with ether, and dried. As the precipitation of nylon salts was often incomplete in the cases of aliphatic diamines, ether was added to the alcoholic solution. The yields of the salts were in general quantitative.

**Polycondensation of Nylon Salts.** In a small-scale experiment, a few grams of the nylon salt was sealed in a glass tube under reduced pressure. The glass tube was heated in an oil bath at temperatures of 230–260°C. for 2 hr. The glass tube was opened and the contents heated at 250–270°C. for 1 hr. in a stream of nitrogen and then for an additional 0.5 hr. under reduced pressure of 1 mm. Hg. to complete the reaction. The obtained polymers are white (sometimes slightly yellow colored), hornlike solids, except those of bis-5-aminoamyl ether with the unsymmetric  $\alpha,\omega$ -oxaalkanedioic acids. In this case, the polymers are more transparent and sometimes amorphous.

## RESULTS AND DISCUSSION

Three series of polyamides have been prepared from three diamines (hexamethylenediamine, bis-5-aminoamyl ether and *p*-xylylenediamine) and the  $\alpha,\omega$ -oxaalkanedioic acids. Data on the nylon salts and the polyamides of each series are shown in Tables I–III.

In the polycondensation of 4-oxapimelic acid, marked decomposition is observed during the course of the reaction, and a part of the colored prod-

TABLE I  
Nylon Salts and Polyamides of Hexamethylenediamine with  
 $\text{HOOC}(\text{CH}_2)_m\text{O}(\text{CH}_2)_n\text{COOH}$

$m$	$n$	Nylon salt m.p., °C.	Polyamide m.p., °C.	$\eta_{sp}/c$
3	3	167-168	187	0.68
4	4	163-164	180	1.25
5	5	164-165	175	0.97
6	6	168-169	170	1.02
8	8	125-126	158	1.09
3	4	142-143	160	0.78
3	5	137-138	152	0.82
3	6	142-143	149	0.78
3	8	121-122	155	0.81
3	10	114-115	159	0.92
4	5	157-158	149	0.74
4	6	146-147	147	0.81
4	8	154-155	154	1.04
4	10	147-148	160	0.98

TABLE II  
Nylon Salts and Polyamides of Bis-5-aminoamyl Ether with  
 $\text{HOOC}(\text{CH}_2)_m\text{O}(\text{CH}_2)_n\text{COOH}$

$m$	$n$	Nylon salt m.p., °C.	Polyamide m.p., °C.	$\eta_{sp}/c$
3	3	126-127	136-138	0.57
4	4	134-135	133-134	0.98
5	5	144-145	126-128	1.16
6	6	135-136	126-129	1.04
8	8	138-139	127-129	1.08
3	4	120-121	125-127	0.76
3	5	124-125	105-108	0.83
3	6	125-126	99-102	0.79
3	8	116-117	114-118	0.97
3	10	119-120	120-122	1.07
4	5	110-111	97-100	0.92
4	6	115-116	103-106	1.00
4	8	120-121	114-117	0.83
4	10	143-144	125-128	1.07

uct remains insoluble in *m*-cresol. The analysis of the trapped distillate from the reaction mixture indicates the formation of  $\beta$ -propiolactone. This tendency for decomposition is also observed, but only slightly, in the polycondensation of 5-oxaazelaic acid. The reduced viscosities of these polyamides, as shown in the tables, are lower than others. When the reaction is carried out at temperatures above 280°C., the reduced viscosity is hardly above 0.5.

In another series of experiments in which the last stage of the polycondensation was carried out in a sealed glass tube in vacuo at temperatures



TABLE III  
Nylon Salts and Polyamides of *p*-Xylylenediamine  
with  $\text{HOOC}(\text{CH}_2)_m\text{O}(\text{CH}_2)_n\text{COOH}$

<i>m n</i>	Nylon salt m.p., °C.	Polyamide m.p., °C.	$\eta_{sp}/c$
3 3	196-197	241	0.58
4 4	173-174	243	1.20
5 5	177-178	234	1.01
6 6	173-174	229	1.25
8 8	177-178	215	1.12
3 4	182-183	234	0.78
3 5	161-162	190	0.87
3 6	164-165	200	0.79
3 8	163-164	215	0.88
3 10	167-168	220	1.02
4 5	168-169	206	0.71
4 6	153-154	207	0.83
4 8	164-165	217	0.95
4 10	170-171	223	1.01

of 250-270°C. for 2 hr., reduced viscosities above 1.4 were obtained for every selected nylon salt other than those of the above two dicarboxylic acids.

The melting points of the  $\alpha,\omega$ -oxaalkanedioic acids are plotted against the number of carbon atoms in the oxaalkylene groups in Fig. 1.<sup>5</sup> The melting points of the polyamides of these three series are plotted in the same manner in Figures 2-4. The plots of the melting points fall on three

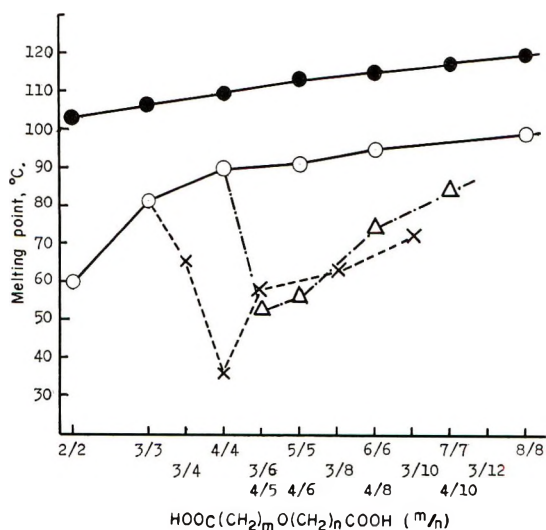


Fig. 1. Melting points of  $\alpha,\omega$ -oxaalkanedioic acids: (●) odd alkanedioic acid,  $\text{HOOC}(\text{CH}_2)_n\text{COOH}$ ; (○) symmetrical  $n/n$ ; (×) unsymmetrical  $3/n$ ; (Δ) unsymmetrical  $4/n$ .

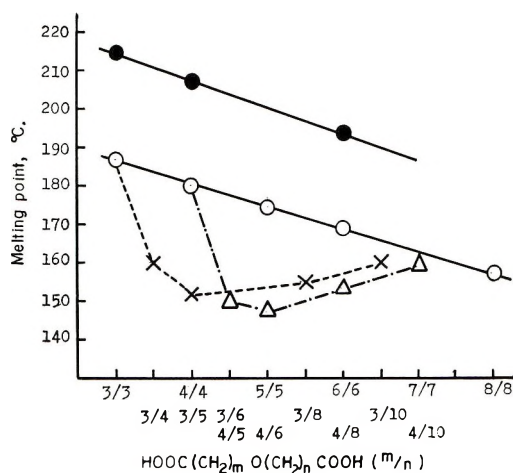


Fig. 2. Melting points of polyamides from hexamethylenediamine: (●) odd alkanedioic acid  $\text{HOOC}(\text{CH}_2)_n\text{COOH}$ ; (○) symmetrical  $n/n$ ; (×) unsymmetrical  $3/n$ ; (△) unsymmetrical  $4/n$ .

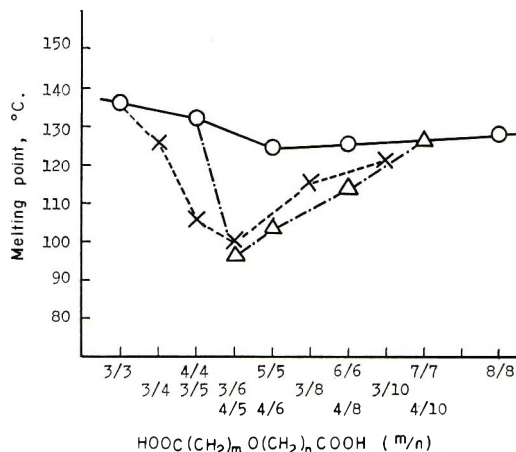


Fig. 3. Melting points of polyamides from bis-5-aminoamyl ether: (○) symmetrical  $n/n$ ; (×) unsymmetrical  $3/n$ ; (△) unsymmetrical  $4/n$ .

different curves for each diamine according to the structures of the oxalkylene groups; symmetric  $-(\text{CH}_2)_n\text{O}(\text{CH}_2)_n-$ , unsymmetric  $-(\text{CH}_2)_3\text{O}(\text{CH}_2)_n-$ , and unsymmetric  $-(\text{CH}_2)_4\text{O}(\text{CH}_2)_n-$ . It is of great interest that the shapes of these three curves for the polyamides of each series of diamine are much like with those of the free dicarboxylic acids, and sharp minima are found at around the same points ( $m = 3, n = 5, 6$  and  $m = 4, n = 5, 6$  respectively) in the cases of the unsymmetric structures. The polymer melting point of the symmetric dicarboxylic acids decreases linearly with increasing number of carbon atoms in the acid for every series of diamine. Furthermore, the polymer melting points of both unsymmetric

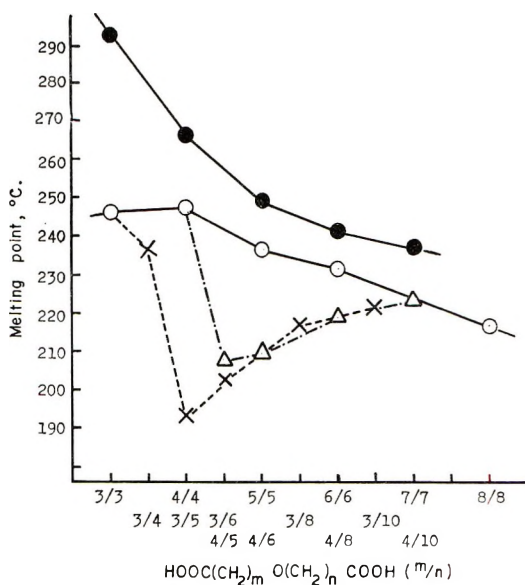


Fig. 4. Melting points of polyamides from *p*-xylylenediamine: (●) odd alkanedioic acid  $\text{HOOC}(\text{CH}_2)_n\text{COOH}$ ; (○) symmetrical  $n/n$ ; (×) unsymmetrical  $3/n$ ; (Δ) unsymmetrical  $4/n$ .

dicarboxylic acids coincide with those of the symmetric ones when the number of carbons in the acid molecule becomes as large as 16. A parallel relationship is also observed between the polymer melting points of the symmetric  $\alpha,\omega$ -oxaalkanedioic acids and of the odd-carbon-numbered  $\alpha,\omega$ -alkanedioic acids of the corresponding chain length.

The reason for the existence of minima in the melting point curves, both in the free unsymmetric acids and the polyamides from them, is considered attributable to the decrease of the symmetry of structures, in other words, the increase of the entropy of fusion  $[\Delta S_m]$ . As mentioned in the following paper<sup>8</sup> concerning isomorphism in polyamides having long repeating units, these polyamides excepting those of bis-5-aminoamyl ether, are highly crystalline, even for the unsymmetric  $\alpha,\omega$ -oxaalkanedioic acids. Therefore, the marked depression of the melting points around the minima indicates that the contribution of the entropy of fusion to the heat of fusion ( $\Delta H_m$ ) is quite large.

## References

1. R. Hill and E. E. Walker, *J. Polymer Sci.*, **3**, 609 (1948).
2. Imperial Chemical Industries Ltd., British Pat., 562,370 (1944); *Chem. Abstr.*, **40**, 769 (1946).
3. E. Ellery (Imperial Chemical Industries Ltd.), British Pat., 615,954 (1949); *Chem. Abstr.*, **43**, 5602 (1949).
4. W. Costain (Imperial Chemical Industries Ltd.), British Pat., 733,002 (1955); *Chem. Abstr.*, **49**, 16452 (1955).
5. K. Saotome and K. Sato, *Bull. Chem. Soc. Japan*, **39**, 480 (1966).

6. L. Kh. Freidlin et al., *Izv. Akad. Nauk SSSR, Otd. Khim. Nauk*, **1961**, 1713.
7. K. Alexander and L. E. Schniepp, *J. Am. Chem. Soc.*, **70**, 1839 (1948).
8. K. Saotome and H. Komoto, *J. Polymer Sci. A*, in press.

### Résumé

Trois séries de polyamides ont été préparés au départ de diamines (hexaméthylène diamine, l'éther bis-5-aminiamylé, la *p*-xylylènediamine) et des acides  $\alpha\text{-}\omega$  oxa-alkanedioïque de formule  $\text{COOH}(\text{CH}_2)_m\text{O}(\text{CH}_2)_n\text{COOH}$ , où  $m = n$  et varie de 3 à 10, dans des structures symétriques, mais  $m = 3$  ou 4 pour des structures asymétriques. Les points de fusion de ces polymères ont été portés en diagramme en fonction du nombre de carbones des groupes oxaalkylènes. Les points de fusion des polymères de chaque diamine se situent sur trois courbes différentes suivant la structure des acides dicarboxyliques; symétrique  $\text{—}(\text{CH}_2)_n\text{O}(\text{CH}_2)_n\text{—}$ , asymétrique  $\text{—}(\text{CH}_2)_3\text{O}(\text{CH}_2)_n\text{—}$ , et asymétrique  $\text{—}(\text{CH}_2)_4\text{O}(\text{CH}_2)_n\text{—}$ . Un point de fusion minimum est observé environ au même point de la structure de l'acide dans chaque courbe pour les acides dicarboxyliques asymétriques. La diminution marquée des points de fusion du polymère au voisinage de ce point minimum est attribuée à l'augmentation de l'entropie de fusion.

### Zusammenfassung

Drei Polyamidreihen wurden aus Diaminen (Hexamethyldiamin, Bis(5-aminiamyl)äther, *p*-Xylyldiamin) und  $\alpha,\omega$ -Oxaalkandicarbonsäuren der Formel  $\text{HOOC}(\text{CH}_2)_m\text{O}(\text{CH}_2)_n\text{COOH}$ , wo  $n = m = 3\text{--}10$  in symmetrischer Struktur, aber  $m = 3$  oder 4 in unsymmetrischer Struktur, dargestellt. Die Schmelzpunkte dieser Polymeren wurden gegen die Kohlenstoffanzahl der Oxaalkylengruppen aufgetragen. Die Polymerschmelzpunkte für jedes Diamin lagen je nach der Struktur der Dicarbonsäuren auf drei verschiedenen Kurven; symmetrische  $\text{—}(\text{CH}_2)_n\text{O}(\text{CH}_2)_n\text{—}$ , unsymmetrische  $\text{—}(\text{CH}_2)_3\text{O}(\text{CH}_2)_n\text{—}$  und unsymmetrische  $\text{—}(\text{CH}_2)_4\text{O}(\text{CH}_2)_n\text{—}$ . Ein Schmelzpunktminimum wird bei etwa dem gleichen Punkt für die Säurestruktur auf jeder Kurve der unsymmetrischen Dicarbonsäure gefunden. Die ausgeprägte Herabsetzung der Polymerschmelzpunkte um dieses Minimum wird auf eine Zunahme der Schmelzentropie zurückgeführt.

Received August 30, 1965

Revised October 20, 1965

Prod. No. 4958A

## NOTES

***Thiobenzophenone—A New Sensibilizer for the Photodegradation of Diene Polymers in Solutions by Visible and Ultraviolet Light***

Phenyl-, diphenyl- and naphthyl-thioketones,  $\begin{matrix} R_1 \\ \diagdown \\ C=S \\ \diagup \\ R_2 \end{matrix}$ , show an abnormal intense

blue coloration. According to Lewis and Kasha<sup>1</sup> the absorption of light quanta excites these thioketones from the basic singlet to the triplet state. Singlet-triplet absorption may give rise to noticeable color and may be shown to be the cause of the abnormal colors of thioketones. Photolysis of thioketone was investigated by several authors.<sup>2,3</sup> Oster

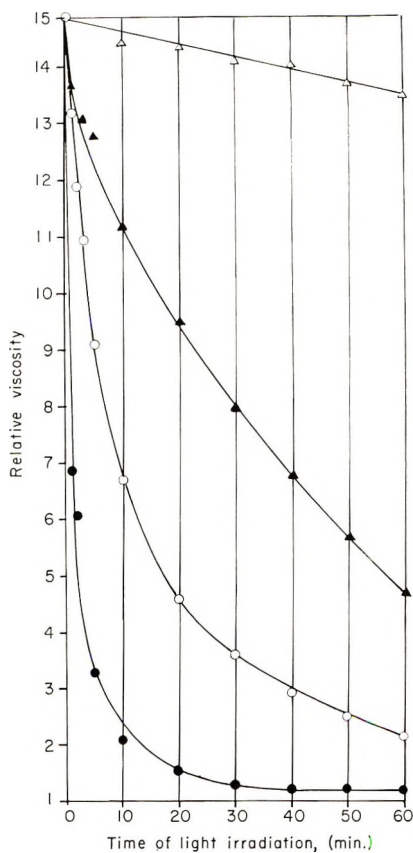


Fig. 1. *cis*-1,4-Polyisoprene (benzene solvent), with weight concentration of 0.65%. Molar ratio of thiobenzophenone (I):chloroprene was 1:6. (Δ) with visible light and without I, (O) with visible light and with I, (▲) with ultraviolet light and without I, (●) with ultraviolet light and with I.



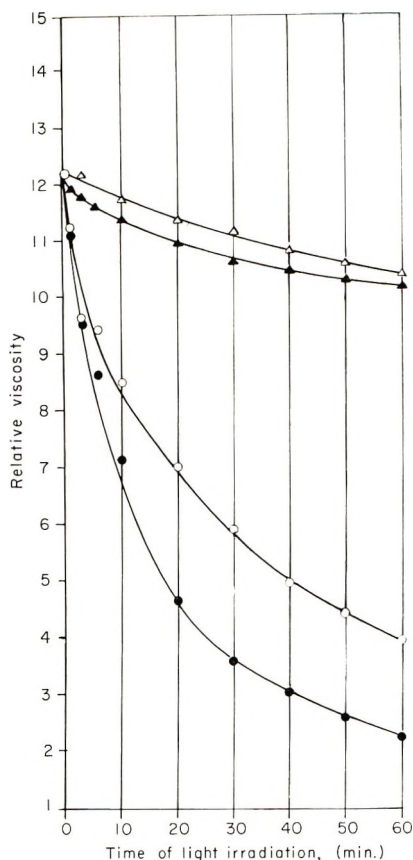


Fig. 2. *cis*-1,4-Polychloroprene (benzene solvent) with weight concentration of 2.1%. Molar ratio of thiobenzophenone (I): chloroprene was 1:6. ( $\Delta$ ) with visible light and without I, ( $\blacktriangle$ ) with visible light and with I, ( $\circ$ ) with ultraviolet light and without I, ( $\bullet$ ) with ultraviolet light and with I.

Citarel, and Goodman<sup>2</sup> found that the mechanism of thiobenzophenone decomposition depends not only upon the wavelength of incident light but also upon the presence of oxygen and the solvent used. The complicated reactions result in photooxidation, photoreduction, or photolysis.

During the investigations of the sensitized photodegradation of polymers, it was found that thiobenzophenone sensitizes the process of photochemical degradation of diene polymers in solutions.

The measurements of the decrease of relative viscosity in benzene solutions of *cis*-1,4-polyisoprene and *cis*-1,4-polychloroprene (Figs. 1 and 2) show that the sensitizing effects of thiobenzophenone are considerable in the case of photodegradation of *cis*-1,4-polyisoprene, whereas in the case of *cis*-1,4-polychloroprene they are distinctly less intense, which is probably due to the presence of the large chlorine atom in the vicinity of the double bond. The chlorine atom may inhibit the reaction of the excited sensitizer molecule with the polymer macromolecule.

The sensitizing effect of thiobenzophenone on photodegradation of examined diene polymers is higher in the ultraviolet range than in the visible range, and corresponds to the higher absorbing power of thiobenzophenone for the ultraviolet radiation. Detailed investigations of this effect are being carried on.

**References**

1. Lewis, N. G., and M. Kasha, *J. Am. Chem. Soc.*, **67**, 994 (1945).
2. Oster, G., L. Citarel, and M. Goodman, *J. Am. Chem. Soc.*, **84**, 703 (1962).
3. Schönberg, A., and A. Mustafa, *J. Chem. Soc.*, **1943**, 275.

JAN F. RABEK

Department of Plastic Technology  
Technical University of Wrocław  
Wrocław, Poland

Received July 8, 1965  
Revised October 28, 1965

## *Permeability of Polymer Membranes to Dissolved Oxygen*

### INTRODUCTION

The permeation of dissolved oxygen through membranes is an important phenomenon in many biological systems. However, methods of measuring the permeability of oxygen through polymer membranes, such as those which rely upon the pressure-volume relationship of the gas, are not applicable to some hydrophilic polymers and biological membranes since the membranes exist in a highly hydrated state and their morphological or topological structure depends on the degree of hydration.

The polarographic method of measuring oxygen provides a quick and accurate means of measuring the permeability of oxygen through many membranes, both in the gas phase and as dissolved oxygen. Accordingly, the oxygen permeability can be utilized as a means of estimating changes in the structure of hydrated membranes, especially hydrophilic polymer membranes and hydrated polymer gels.

Oxygen has a molecular size somewhat similar to that of water, and their diffusivities are also similar in many cases. For instance, the diffusion constant of oxygen in water at 25°C. is  $2.5 \times 10^{-5}$  cm.<sup>2</sup>/sec. and the self-diffusion constant of water is expected to be on the order of  $2.3\text{--}2.4 \times 10^{-5}$  cm.<sup>2</sup>/sec.<sup>1</sup> Diffusion constants of oxygen and water in some polymers are also somewhat similar.<sup>2</sup> For this reason, the oxygen permeability may be used as a means of investigating changes in the structure of a hydrated polymer membrane and also as a tool for comparing the ease of water movement through hydrated membranes.

The measurement of oxygen permeability may have advantages over the measurement of water movement, since oxygen flow can be created without causing appreciable change in the water activity and, consequently, it is possible to maintain the conditions of the hydrated membrane at the point of interest.

In order to compare the oxygen permeability of both hydrated and nonhydrated membranes by the same method, the polarographic method is applied for measurement of permeability both as the gas and as dissolved oxygen.

### EXPERIMENT AND RESULTS

A Beckman laboratory oxygen analyzer, model 777, was used in this experiment. The sensor is sealed into a stainless steel permeation cell, which was originally designed by Amicon Inc., Cambridge, Massachusetts, by means of a screw and O-ring. The rough sketch of the cell is presented in Figure 1.

Experiments which were done in the gas phase and with dissolved oxygen in water are represented schematically in Figure 2. All experiments were performed at room temperature.

#### A. Gas/Gas Measurement

Oxygen is supplied and detected in the gas phase. The air was used as the source of oxygen, and the air in the detection side of the cell was replaced by blowing nitrogen gas into the cell until the meter reading dropped to zero. In this type of measurement, the water jacket of the cell was removed and the air above the film was circulated by a fan.

#### B. Weight/Weight Measurement

Distilled water in which oxygen is purged by nitrogen gas was allowed to fill the cell and the water was stirred with a magnetic stirrer. The speed of the magnetic stirrer was adjusted prior to the measurement to obtain the required flow rate across the face of the sensor. This is done by filling the cell with oxygen-containing water and stirring it until there is no increase in the meter reading with increasing agitation.

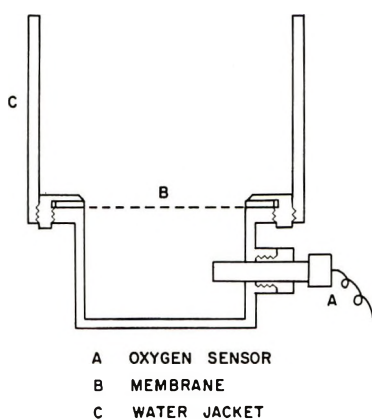


Fig. 1. Permeability cell.

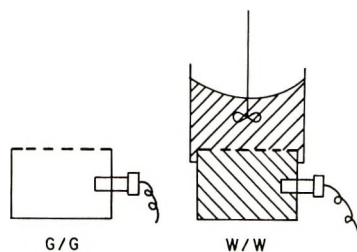


Fig. 2. Schematic representation of gas phase and dissolved oxygen in the permeability measurements.

The water jacket above the membrane was filled with air-saturated water, of which the oxygen partial pressure was measured by the sensor prior to the measurement. The water in the jacket was stirred with a propeller-type stirrer.

The polarographic oxygen sensor measures only the partial pressure of oxygen and does not measure the actual quantity of oxygen in a solution. Therefore, the meter reading can be treated just as the pressure reading of oxygen in a vacuum method, regardless of whether it is detected as gas or as dissolved oxygen. Before each measurement, the meter is calibrated using air as a standard (the partial pressure of oxygen is 159 mm. Hg at one atmosphere).

In measuring permeability, the meter reading is recorded against time, and the slope ( $\Delta p/\Delta t$ ) of the curve is calculated from the tangential line at a certain pressure reading (usually 30–40 mm. Hg). The difference of the partial pressure between the point where the slope is taken and the partial pressure on the high oxygen side is taken as the driving pressure.

The permeability coefficient,  $P$ , is calculated by the following relation.<sup>3</sup>

$$P = \left( \frac{\Delta p}{\Delta t} \right) \left( \frac{273}{273 + T} \right) \left( \frac{V}{A} \right) \left( \frac{l}{p} \right) \left( \frac{1}{760} \right)$$

where  $l$  is the thickness,  $A$  the area of the membrane,  $V$  the volume of the cell,  $p$  the driving pressure, and  $T$  the temperature in °C.

The results of the measurement are summarized in Table I.

The results indicate that higher oxygen permeability is usually observed with dissolved oxygen even for highly hydrophobic polymer membranes. This may be due to the

TABLE I  
Permeability of Gas and Dissolved Oxygen in Polymers

Polymer	$P \times 10^{10}$ , cc. STP (cm.) / cm. <sup>2</sup> sec. (cm. Hg)	
	G/G	W/W
Poly(dimethyl siloxane) <sup>a</sup>	665	4000
Polyethylene (low density)	2.34	50.0
Poly(fluorinated ethylene-propylene), (Teflon FEP)	3.86	105
Poly(tetrafluoroethylene)	23.7	91.0
(HEMA) Hydrogel <sup>b</sup>	—	180
Polyelectrolyte complex <sup>c</sup>	—	270

<sup>a</sup> Dow Corning "Medical Silastic," with SiO<sub>2</sub> fillers.

<sup>b</sup> Crosslinked poly(hydroxyethyl methacrylate); water content 38%.

<sup>c</sup> Poly(vinyl trimethylammonium)-poly(styrene sulfonate); water content 35% (Amicon Inc., Cambridge, Massachusetts).

fact that the solubilities of water in many polymers (including hydrophobic polymers) are much higher than those of oxygen in the same polymers, and also that the solubility of oxygen in water is much greater than in polymers. Consequently, oxygen may permeate through the preexisting water, which may exist as uniformly distributed single molecules and also as clusters of water in existing voids, in the polymer matrix.

The results also indicate that the permeability of oxygen (and possibly some other gases) in some hydrated membranes, which can only be measured accurately (without altering the structure of the membrane) with dissolved gas, cannot be compared directly with the reported permeability values of many polymers, which are mostly obtained by measurements in G/G condition. Factors of 4-30, found in polymers presented here, for permeability of dissolved oxygen over the gas phase oxygen, must be taken into account for proper comparison.

This study was supported in part by National Institutes of Health Grants, NB 06077, NB 06078, NB 06281; and by Office of Naval Research Contract, NONR 4800(00).

#### References

1. Wang, J. H., C. V. Robinson, and I. S. Edelman, *J. Am. Chem. Soc.*, **75**, 466 (1953).
2. Yasuda, H., and V. Stanett, *J. Polymer Sci.*, **57**, 907 (1962).
3. Rogers, C., J. A. Meyer, V. Stanett, and M. Szwarc, *Tappi*, **39**, 737 (1956).

H. YASUDA\*

WILLIAM STONE, JR.

Polymer Division  
Eye Research  
Cedars-Sinai Medical Center  
Los Angeles, California

Received August 27, 1965

Revised November 1, 1965

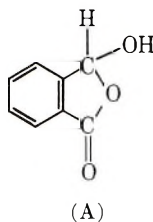
\* Present address: Department of Polymer Technology, Royal Institute of Technology, Stockholm, Sweden.



### *Phthalaldehydic Acid-Glycol Reactions\**

Phthalaldehydic acid (P acid) reacts with poly(vinyl alcohol) in aqueous solution in both uncatalyzed and mineral acid catalyzed reactions to yield an alkali soluble polymer. Films cast from aqueous ammonia are clear, tough, and water insoluble. Because of the reported structure and reactions of P acid with alcohols and glycols, it was decided to briefly investigate the structure of this polymer and to carry out some additional work on the reactions of P acid with glycols.

P acid (*o*-carboxybenzaldehyde) exists in the 3-hydroxyphthalide form (A) in both the solid state and in water solution.<sup>1</sup>



Its infrared spectrum (Fig. 1) shows an alcoholic OH at  $3.01 \mu$  and the typical COOH doublet present in terephthalaldehydic acid at  $3.73$  and  $3.93 \mu$  is absent. Carbonyl absorption at  $5.73 \mu$  is that of a lactone and not of an aldehyde or acid. Carbon-oxygen stretching vibrations of the phthalide ring account for bands at  $9.33$  and  $11.00 \mu$ . These latter bands are present in the spectra of derivatives of P acid in which the phthalide ring remains intact, except that they may be somewhat displaced. A strong band at  $8.90 \mu$  in P acid and alkoxyphthalides has been tentatively assigned to C—O stretch of the 3 oxygen.

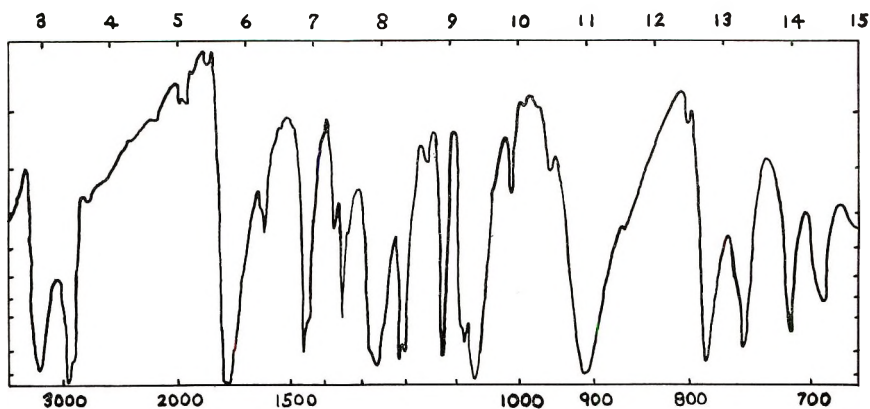
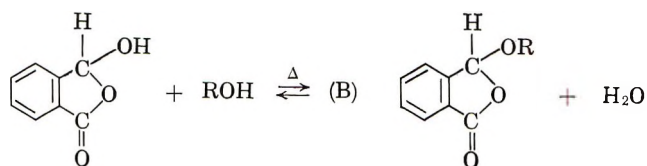


Fig. 1. Infrared spectrum of phthalaldehydic acid (oil mull).

Wheeler et al.<sup>1</sup> have studied uncatalyzed reactions of P acid. They report that the acid is very reactive and approaches in reactivity that of acid chlorides and anhydrides. Equilibrium is essentially reached in one or two hours when P acid is refluxed in a lower alcohol. The product is predominantly the 3-alkoxyphthalide (B) with only 10 to 15% of the open form derivative.

\* Contribution from the Research Laboratories of Polaroid Corporation.



Wheeler et al. obtained the 3,3'-alkylenedioxydiphthalides in high yield with glycols, using two moles of P acid to one of glycol.

We have found in our work that the course of the reaction between P acid and a glycol depends on the reaction conditions and also on the relative amounts of P acid and glycol present.

When 2,4-pentanediol, a low molecular weight analogue of poly(vinyl alcohol), is

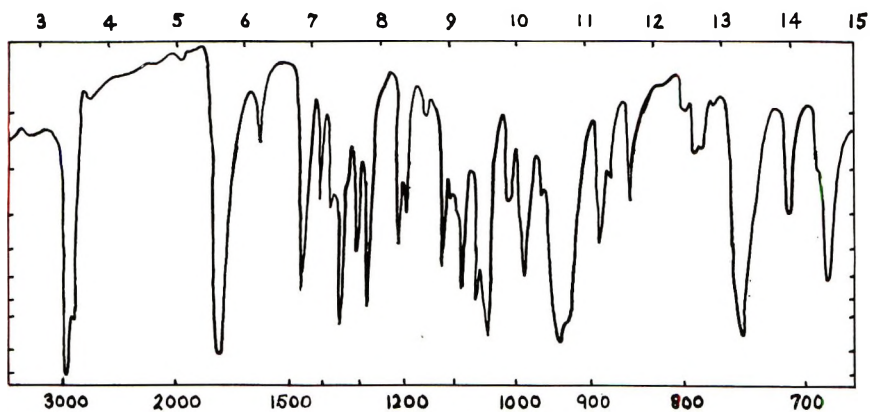


Fig. 2. Infrared spectrum of 3,3'-1,3-dimethylpropylenedioxydiphthalide (oil mull).

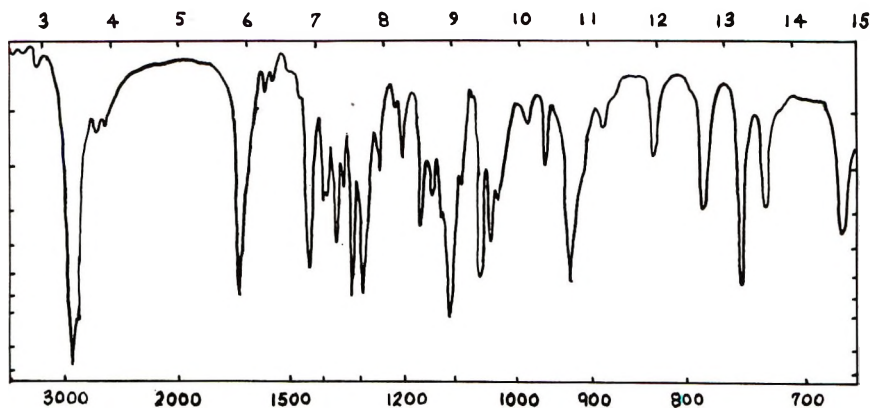
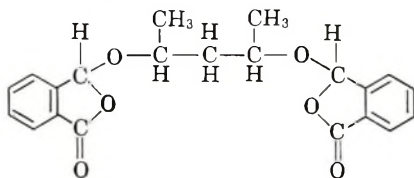


Fig. 3. Infrared spectrum of the 2,4-pentanediol cyclic acetal of *o*-carboxybenzaldehyde (oil mull).

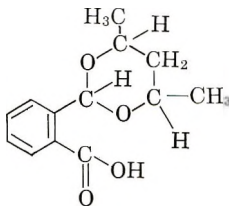
reacted with P acid at 140–160°C. in the ratio of 2 moles of acid to 1 mole of glycol, the product obtained is mainly the alkylenedioxydiphthalide (C)



(C)

whose infrared spectrum (Fig. 2) is consistent with the structure. Lactone carbonyl appears at 5.6  $\mu$ , C—O stretchings of the phthalide ring at 9.6 and 10.6  $\mu$ , and the 8.9  $\mu$  band for the C—O stretch of the 3 position oxygen is present.

When a large excess of 2,4-pentanediol is reacted with P acid in the same manner as described above, the phthalide ring opens and the cyclic acetal of P acid (D) is obtained in high yield.



(D)

The infrared spectrum of this product (Fig. 3) shows carbonyl stretching of the acid function at 5.9  $\mu$  and the COOH doublet at about 3.75 and 3.9  $\mu$ . Similarly, when P acid is reacted with excess 2,4-pentanediol in dilute aqueous solution, either mineral acid catalyzed or not, the predominant product is the cyclic acetal (D).

One mole of ethylene glycol reacted with 2 moles of P acid gives a 99% yield of 3,3'-ethylenedioxydiphthalide.<sup>1</sup> However, when excess ethylene glycol is employed, completely different results are again observed. Heating P acid with excess ethylene glycol at 160°C. stripping off the ethylene glycol under vacuum, washing the residue with water, and drying leaves an oil. This oil, which partially crystallizes on standing, is

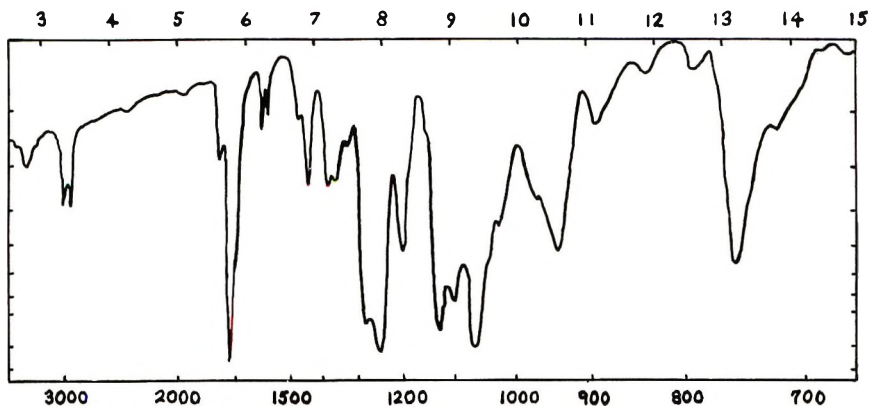


Fig. 4. Oil from the phthalaldehydic acid-ethylene glycol reaction.

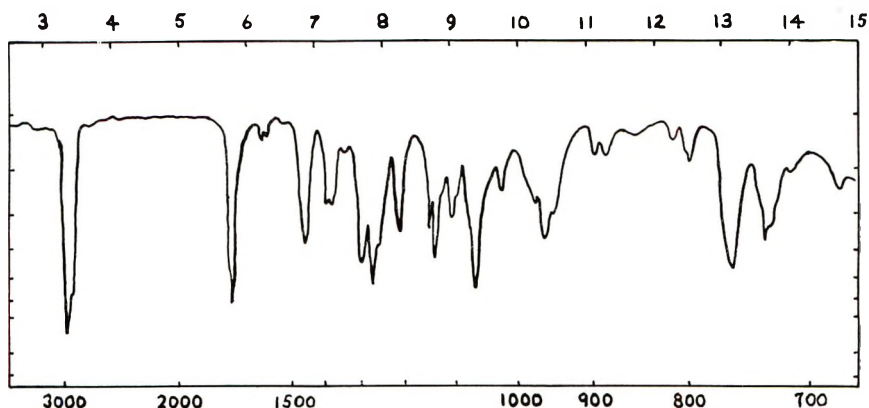


Fig. 5. Cyclic ethylene glycol acetal of the phthalaldehyde bisester of ethylene glycol (oil mull).

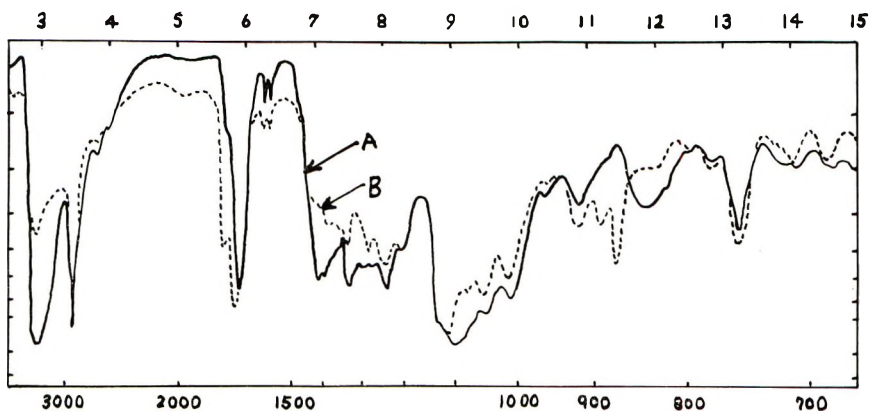
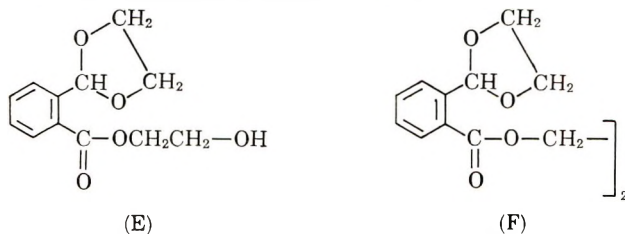


Fig. 6. (A) Infrared spectrum of the reaction products of PVA and phthalaldehyde acid (excess PVA); (B) Infrared spectrum of the reaction product of PVA and phthalaldehyde acid (excess P acid).

insoluble in aqueous alkali and has an average molecular weight (freezing point depression of benzene) of 335. NMR measurements indicate a mixture and also show that only a trace of aldehyde hydrogen is present. The infrared spectrum (Fig. 4) has the following features: a low intensity OH stretching band at  $2.8 \mu$ , low intensity phthalide carbonyl at  $5.6 \mu$ , and strong ester carbonyl at  $5.8 \mu$ . The band at  $10.5 \mu$  is too weak to be C—O stretching of the phthalide ring. A well defined doublet at  $6.25\text{--}6.35 \mu$  seems to be associated with compounds in which the phthalide ring has been opened (compare with Fig. 3, as opposed to Figs. 1 & 2). This oil appears to be a mixture of (E) and (F), contaminated with a small amount of mono or diphtalide.



High vacuum distillation of a portion of this oil and treatment of the distillate with ether caused crystallization of pure (F) (see Fig. 5). Since ethylene glycol is a primary alcohol, it is not surprising that esters are obtained, whereas with 2,4-pentanediol the cyclic acetal of the free acid results.

The infrared spectrum of the poly(vinyl alcohol)—P acid reaction product prepared in water (Fig. 6A) indicates it is predominantly the normal acetal. The COOH doublet between 3.5 and 4  $\mu$ , acid carbonyl at 5.9  $\mu$  and the doublet between 6.25 and 6.50  $\mu$  support this structure. The shoulder on the carbonyl absorption at 5.7  $\mu$  implies that a small percentage of the 3-alkoxyphthalide structure is also present in the polymer. If a large excess of P acid is employed, the phthalide content of the polymer is increased, but the acetal structure still predominates (Fig. 6B).

## EXPERIMENTAL

### Preparation of 3,3'-1,3-Dimethylpropylenedioxydiphthalide

P acid (m.p. 98°C., 30 g., 0.2 moles) and 2,4-pentanediol (b.p. 100°C./16 mm. 10.4 g., 0.1 moles) were heated together at 140–160°C. for several hours and then under vacuum (15 mm.) for several hours. The glassy material remaining was dissolved in dioxane and poured into H<sub>2</sub>O to remove any unreacted P acid or diol. The precipitated oil was dried under vacuum at 40°C. After several days it started to crystallize. The paste was treated with hot dioxane-hexane, cooled, and the crystals were filtered off, m.p. = 225°C.

ANAL. Calcd.: C, 68.5; H, 5.46. Found: C, 68.7; H, 5.3.\*

### Preparation of 2,4-Pentanediol Cyclic Acetal of P Acid

P acid (15 g., 0.1 moles) and 2,4-pentanediol (52.0 g., 0.5 moles) were heated at 140–160°C. for about 14 hr. and then under vacuum for several hours. After cooling, the reaction was poured into water. The solid that precipitated was recrystallized from water and dried (m.p. = 113–114°C. Neutral equivalent: Theory, 236; Found, 243).

ANAL. Calcd. (for cyclic acetal): C, 66.1; H, 6.82. Found: C, 66.5; H, 6.8.\*

P acid (15 g., 0.1 moles) and 2,4-pentanediol (26 g., 0.25 moles) were dissolved in 180 ml. of water. The solution was divided into two equal portions and 10 drops of concentrated H<sub>2</sub>SO<sub>4</sub> added to one portion. The solutions were heated on a steam cone for several hours. On cooling, crystals were obtained, which on recrystallization from water and drying, were found to be the pure cyclic acetal. An NMR spectrum integrates properly for this compound.

### Reaction of P Acid with Excess Ethylene Glycol

P acid (15 g., 0.1 moles) and ethylene glycol (32 g., 0.5 moles) were heated at 160°C. for 15 hr. and then under vacuum (15 mm.) for several hours. The reaction mixture was poured into water and the precipitated oil washed with water numerous times to remove unreacted P acid and glycol. The oil was finally dried at 40°C. under vacuum. On standing it became partially crystalline. An attempt was made to fractionate the mixture but this was not successful. Viscous distillate, which came over at 180–240°C./0.2 mm., yielded crystalline material on treatment with ether. This product upon recrystallization from diethyl ether gave pure ethylene glycol acetal ethylene glycol bisester of P acid, m.p. = 86°C.

ANAL. Calcd. (for product F): C, 63.70; H, 5.34; Found: C, 63.52; H, 5.03.\*

The NMR spectrum integrates properly for this product.

\* C and H analyses were carried out by C. K. Fitz, Needham Heights, Mass. and by Clark Microanalytical Laboratory, Urbana, Illinois.



### Reaction of P Acid with Poly(vinyl Alcohol)

Poly(vinyl alcohol) (Gelvaton 2/75, Shawinigan Resins Corp., 22 g., 0.5 moles) and P acid (15 g., 0.1 moles) were dissolved in 180 ml. of water. The solution was divided into two equal portions and 10 drops of concentrated  $\text{H}_2\text{SO}_4$  added to one portion. The solutions were heated on a steam cone. After a few minutes polymer started to separate from the acid catalyzed solution. After several hours of heating, the precipitated polymers were removed, washed with water, and reprecipitated from dioxane- $\text{H}_2\text{O}$  into a large excess of acetone. The polymers were then extracted with hot acetone and dried. Infrared spectra of the two polymers were identical.

### Spectra

Infrared spectra were taken on a Perkin-Elmer Infracord spectrophotometer. Spectra reproduced in Figures 1, 2, 3, and 5 were mineral oil mulls. Figure 4 was obtained by spreading the oil on a AgCl disc. The P acid derivative of poly(vinyl alcohol) was cast from dioxane- $\text{H}_2\text{O}$  on a AgCl disk to obtain Figure 6. NMR measurements were made on a Varian NMR Spectrophotometer, Model No. A-60.

### Reference

1. Wheeler, D. D., D. C. Young, and D. S. Erley, *J. Org. Chem.*, **22**, 547 (1957).

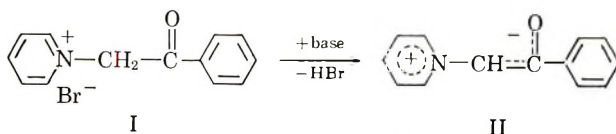
HOWARD C. HAAS

Polaroid Corporation  
Cambridge, Massachusetts

Received October 26, 1965

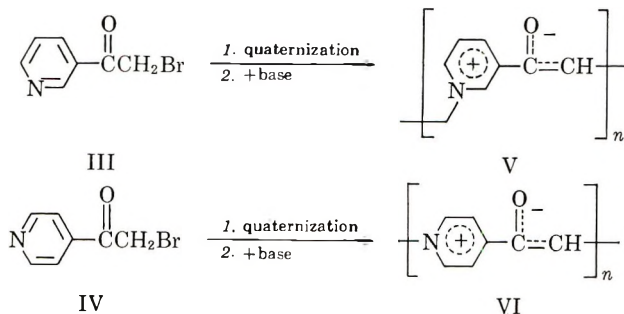
### The Synthesis of Polymeric Ylids

Kröhnke, in numerous publications<sup>1</sup> dating from 1935, described the preparation and properties of stable ylids (enolbetaines) by treatment of the pyridinium salts of  $\alpha$ -halo-ketones with base. For example, 1-(phenacyl)pyridinium bromide, I, treated with aqueous potassium carbonate, gave the charge delocalized enolbetaine, II.



The possibility that polymeric chains consisting of stable ylid structure II might possess unusual electrical properties prompted us to undertake the work reported here.

We felt that if the 3- and 4-(bromoacetyl)pyridines, III and IV, which incorporate both the  $\alpha$ -haloketone and the pyridine nucleus into a single molecule, could be prepared, purified, and quaternized to polymeric quaternary salts, polymeric ylids V and VI could be obtained by treating these salts with base.



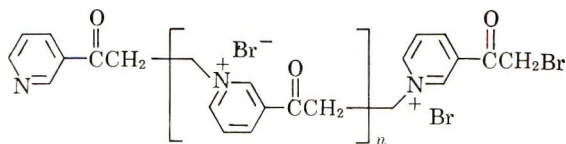
The known 3- and 4-(bromoacetyl)pyridinium bromides VII and VIII, (2,3) hydrobromide salts of monomers III and IV, were prepared by the HBr-catalyzed bromination



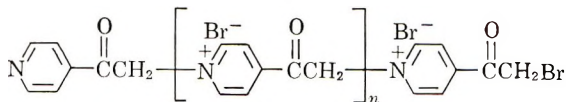
of 3- and 4-acetylpyridines in benzene-acetic acid. The same compounds were prepared from nicotinyll and isonicotinyll chlorides by the Arndt-Eistert synthesis.

Neutralization of VII and VIII in aqueous NaHCO<sub>3</sub> resulted in only tarry products. However, when a mixture of the dry hydrobromide and one equivalent of NaHCO<sub>3</sub> was stirred under cold benzene or ether, while enough water was added to dissolve the bicarbonate, the free 3- and 4-(bromoacetyl)pyridines, III and IV, were apparently formed and absorbed by the solvent to give clear, colorless solutions. Removal of the solvent by distillation or vacuum evaporation gave, rather than III or IV, crystalline, water soluble solids, which were highly colored, orange in the case of VII and purple from VIII. The same results were obtained regardless of the base, solvent or conditions used. Apparently III and IV quaternize too readily to be isolated. The colored solids were identified as the quaternary salts IX and X. Some control over the quaternization was exercised by refluxing the benzene solutions of the (bromoacetyl)pyridines overnight, during which time IX and X, formed and precipitated in 60% yield.

Molecular weights of IX and X were estimated by analysis of both ionic and total bromine content and comparison of the two values, assuming that each molecule of the



IX



X

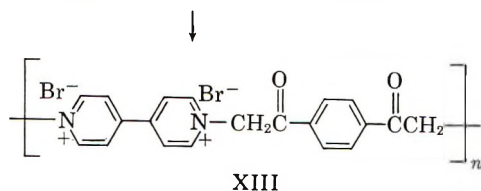
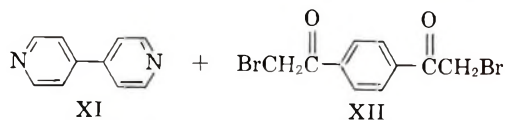
salt still contained one covalently bound bromine on an endgroup. The average D.P. of the two salts was thus found to be only 4-6 ( $n = 2-4$ ).

The unexpected brilliant colors of IX and X may be explained by the postulation that one ylid group per molecule is formed during the quaternization *via* extraction of HBr by the endgroup pyridine nucleus. Such ylid formation would be expected to cause color in the molecule.<sup>1</sup> The acidification of an aqueous solution of either salt caused the color to disappear completely while neutralization of the added acid regenerated the color. The regeneration of quaternary salts by addition of acid to ylids of this type is a known reaction.<sup>1</sup> The neutralization of the endgroup pyridine nuclei during the ylid formation postulated here would also explain the failure to obtain high molecular weight polymeric quaternary salts since these neutralized endgroups could undergo no further quaternization.

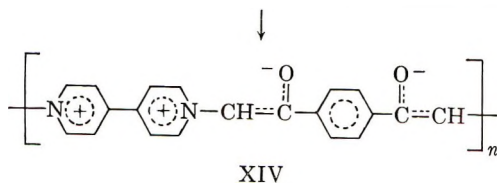
The quaternary salts, IX and X, were hygroscopic and decomposed to sticky substances at 235-240°C.

When aqueous solutions of IX and X were treated with aqueous potassium carbonate solution, the corresponding ylids III and IV precipitated immediately. Ylid III was brick-red in color and turned black at 280°C. without melting. Ylid IV was greenish-black and melted at 185-190°C. with decomposition. Both III and IV were hygroscopic, crystalline, and insoluble in common solvents. Both seemed to be very slowly soluble in water at room temperature. The infrared spectra had only very weak absorptions in the carbonyl and hydroxyl regions.

Similar results were obtained when 4,4'-bipyridyl (XI) was quaternized with *p*-bis(bromoacetyl)benzene (XII) in refluxing benzene, giving a 92% yield of the light blue-



XIII



XIV

green salt, XIII, which was a brilliant blue in aqueous solution. Potassium carbonate treatment of XIII gave the greenish-black ylid, XIV, which was similar in appearance and properties to VI.

#### References

1. (a) F. Kröhnke, *Ber.*, **68B**, 1177 (1935); (b) F. Kröhnke and E. Börner, *ibid.*, **69B**, 2006 (1936); (c) F. Kröhnke and H. Kübler, *ibid.*, **70B**, 538 (1937); (d) F. Kröhnke, *ibid.*, **70B**, 543, 1114 (1937); (e) F. Kröhnke and W. Heffe, *ibid.*, **70B**, 1720 (1937); (f) F. Kröhnke and H. Schmeiss, *ibid.*, **70B**, 1728 (1937).
2. A. Burger, R. W. Alfried, and A. J. Deinet, *J. Am. Chem. Soc.*, **66**, 1327 (1944).
3. A. R. Katritzky, *J. Chem. Soc.*, **1955**, 2586.

DANIEL E. GEORGE  
ROBERT E. PUTNAM  
STANLEY SELMAN

Plastics Department  
E. I. Du Pont de Nemours & Company  
Wilmington, Delaware

Received December 21, 1965

*A Note on the Capillary Flow of Polydimethylsiloxane*

The capillary viscometer is one of the most common apparatus to study flow properties of liquids. Analysis of the data is conventionally based on the assumption that the flow velocity is zero at the wall. If the material slips at the wall some modification must be required in the analysis. In such a case, the shear rate at the wall  $\dot{\gamma}_w$  is given by the following equation:

$$\dot{\gamma}_w = 4Q/\pi r^3 - 4V_w/r \quad (1)$$

where  $Q$  is the volume rate measured actually,  $r$  is the radius of the capillary, and  $V_w$  is the slip rate of the material at the wall. The shear rate  $\dot{\gamma}_w$  is equal to  $4Q/\pi r^3$  in the case of no slippage. This equation shows that the slippage leads to an apparent value of  $4Q/\pi r^3$  larger than the actual one. The difference is significant in the case of the smaller-radius capillary.

An attempt was made to clarify this point, using a nitrogen-gas-operated capillary viscometer. Three capillaries of different radii with almost the same length-to-radius ratio,  $l/r$ , were employed. They were made of stainless steel and had flat entries. Their dimensions are as follows:

No.	$r$ , mm.	$l$ , mm.	$l/r$
1	0.153	2.68	17.52
2	0.250	4.51	18.04
3	0.500	9.01	18.02

TABLE I

$Pr/2l \times 10^{-3}$ , dynes/cm. <sup>2</sup>	$4Q/\pi r^3 \times 10^{-4}$ , <sup>a</sup> sec. <sup>-1</sup>		
	Capillary no. 1	Capillary no. 2	Capillary no. 3
22	12.0	12.0	—
21	10.4	10.5	—
20	9.00	8.85	9.00
19	7.20	7.20	7.25
18	5.95	6.00	6.00
17	5.00	5.15	5.35
16	4.20	4.35	4.45
15	3.55	3.75	3.50
14	2.85	3.05	2.85
13	2.25	2.40	2.25
12	1.72	1.90	1.88
11	1.35	1.50	1.42
10	1.04	1.10	1.02
9.0	0.820	0.820	0.820
8.0	0.600	0.605	0.610
7.0	0.425	0.430	0.430
6.0	0.290	0.295	0.300
5.0	0.192	0.190	0.188
4.5	0.144	0.144	0.144
4.0	0.110	0.110	0.110
3.5	0.0800	0.0800	0.0780
3.0	0.0585	0.0560	0.0565

<sup>a</sup> These values were interpolated from measured values.



Polydimethylsiloxane which had a viscosity-average molecular weight of 140,000 was extruded through these capillaries at 30°C.

Results are shown in Table I. In this table,  $Pr/2l$  is the apparent shear stress at the wall. The pressure  $P$  was corrected for kinetic energy when this term was over 1% of the total pressure. The errors involved in the evaluation were  $\pm 4\%$  for the value of  $Pr/2l$  and less than  $\pm 6\%$  for the value of  $4Q/\pi r^3$ . Flow irregularities were observed above  $1.25 \times 10^6$  dynes/cm.<sup>2</sup>  $\times Pr/2l$  irrespective of the capillary radius.

As is shown in Table I, even in the case of the irregular flow,  $4Q/\pi r^3$  is not observed to increase with the decrease of the radius of the capillary. This means that the second term in the right hand of eq. (1) is negligible. We conclude, therefore, that polydimethylsiloxane does not slip appreciably when extruded through the stainless steel capillary, at least in the range of this investigation.

This is contrary to the observation that the slip of the material at the wall caused an irregular flow.<sup>1</sup> A more elaborate experiment must be carried out to clear up this point. Further studies are now in progress in our laboratory.

#### Reference

1. J. J. Benbow and P. Lamb, *SPE Trans.*, **3**, 7 (1963).

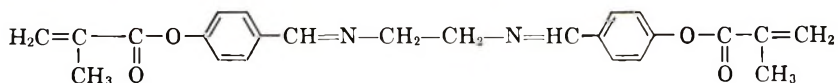
TADAO KATAOKA  
SHIGEYUKI UEDA

Textile Research Institute of the Japanese Government  
Kanagawa, Yokohama, Japan

Received June 1, 1965

### Crosslinking in Popcorn Polymers

In the early work on popcorn-polymer formation in the styrene-divinylbenzene system it was found that the degree of swelling of a popcorn polymer was very much lower than that of the glassy polymer formed in the same system.<sup>1</sup> It has been assumed that this behavior was due to a higher divinyl compound content in the popcorn polymer than in the glassy phase. On the other hand it seems possible that additional crosslinks are formed by chain transfer to the polymer and chain combination of the resulting branches. To be able to distinguish between these two possibilities we used a divinyl compound in the polymerizing system which could specifically and easily be destroyed in the polymer. Such compounds have been described by Ringsdorf and Greber.<sup>2</sup> They are divinyl Schiff bases where the  $\text{—N=C—}$  double bond can rapidly be split by acid hydrolysis in a predominantly organic medium at room temperature. We used the bis(4-methacryloxybenzylidene)ethylenediamine



and studied its ability to form popcorn polymers with styrene.

As in the case of *p*-divinylbenzene there exist optimum conditions for popcorn formation, with this crosslinking agent, e.g. without added initiator at 70°C., 0.015 moles of the Schiff base per mole styrene give a very high yield of popcorn polymer. This polymer has the typical optical anisotropy previously described for a great variety of popcorn polymers.\* It swells only to a very low degree in benzene. When a few drops of a 0.7*M* dichloroacetic acid solution in tetrahydrofuran are added to this system, most of the optical anisotropy of the polymer disappears indicating a decrease of the internal strains by a loss of crosslinks. However the polymer still remains insoluble after prolonged contact with the hydrolyzing agent. Under the same conditions a glasslike crosslinked polymer obtained from the same polymerization system was completely dissolved. Due to the loss of the crosslinks formed by the divinyl Schiff-base the degree of swelling of the popcorn polymers increased during hydrolysis. The remaining non-hydrolyzable crosslinks probably have been formed by the chain transfer-chain combination mechanism giving  $\text{—C—C—}$  crosslinks. This high content on crosslinks not formed by copolymerization of pendant double bonds of the divinyl compound seems to be an important new characteristic of popcorn polymerization. The formation of large amounts of insoluble popcorn material during the growth of a popcorn seed in a pure monovinyl compound is probably due to this crosslinking process.

A complete account of this work will be published elsewhere.

#### References

1. H. Staudinger and E. Husemann, *Ber. dtsch. chem. Ges.*, **68**, 1618 (1935).
2. H. Ringsdorf and G. Greber, *Makromol Chem.*, **31**, 50 (1959).

J. W. BREITENBACH  
H. DWORAK

Institut für physikalische Chemie  
der Universität Wien  
Wien, Austria

Received December 13, 1965

\* The highest optical anisotropy in microscopic dimensions has been found in *m*-bromostyrene and 2,5-dichlorostyrene popcorns, but all other nuclear substituted styrenes and the unsubstituted styrene show an easily observable anisotropy. This is also the case for butadiene and chloroprene popcorns and related substances. Low values of optical anisotropy are characteristic of acrylate and methacrylate popcorns including phenyl methacrylate.